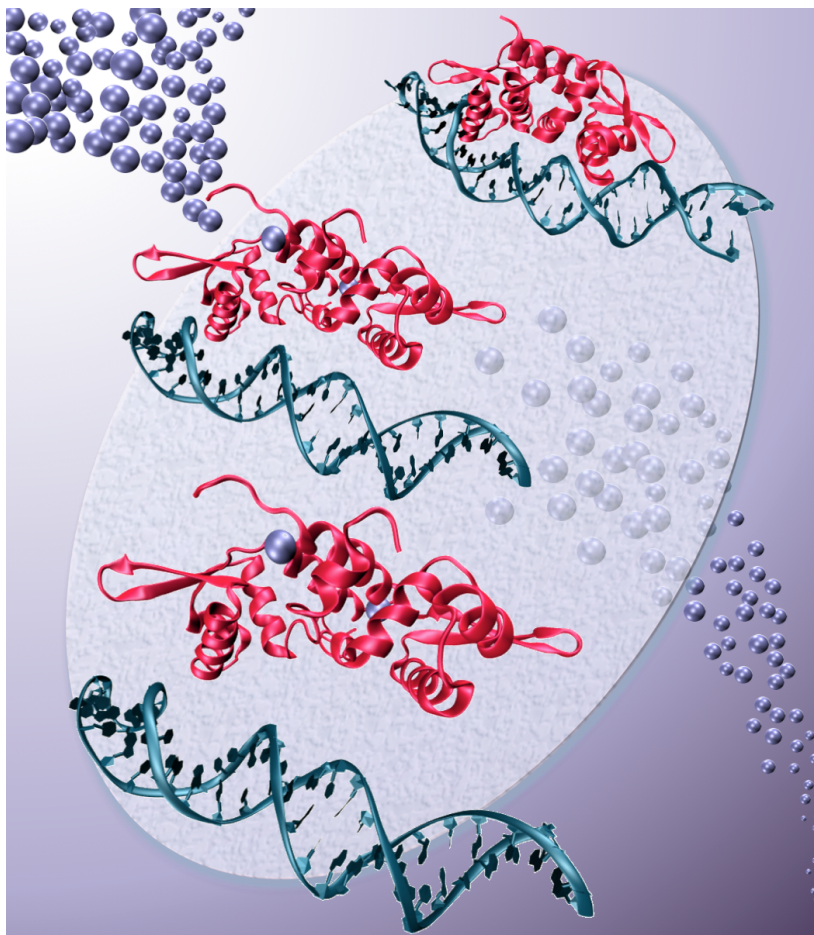


# Amber 12 Reference Manual





# Amber 12

## Reference Manual

### Principal contributors to the current codes:

David A. Case (Rutgers University)	Jian Liu (Berkeley)
Tom Darden (OpenEye)	Xiongwu Wu (NIH)
Thomas E. Cheatham III (Utah)	Scott R. Brozell (Rutgers)
Carlos Simmerling (Stony Brook)	Thomas Steinbrecher (Karlsruhe)
Junmei Wang (UT Southwestern Medical Center)	Holger Gohlke (Düsseldorf)
Robert E. Duke (NIEHS and UNC-Chapel Hill)	Qin Cai (UC Irvine)
Ray Luo (UC Irvine)	Xiang Ye (UC Irvine)
Ross C. Walker (SDSC, UCSD)	Jun Wang (UC Irvine)
Wei Zhang (UT Houston)	Meng-Juei Hsieh (UC Irvine)
Kenneth M. Merz (Florida)	Guanglei Cui (Stony Brook)
Benjamin P. Roberts (Florida)	Daniel R. Roe (Rutgers University)
Seth Hayik (Florida)	David H. Mathews (Rochester)
Adrian Roitberg (Florida)	Matthew G. Seetin (Rochester)
Gustavo Seabra (Recife, Brazil)	Romelia Salomon-Ferrer (SDSC, UCSD)
Jason Swails (Florida)	Celeste Sagui (North Carolina State)
Andreas W. Götz (SDSC, UCSD)	Volodymyr Babin (North Carolina State)
István Kolossváry (Budapest and D.E. Shaw)	Tyler Luchko (Rutgers University)
Kim F. Wong (Pitt)	Sergey Gusarov (NINT)
Francesco Paesani (UC San Diego)	Andriy Kovalenko (NINT)
Jiri Vanicek (EPL-Lausanne)	Peter A. Kollman (UC San Francisco)
Romain M. Wolf (Novartis)	

### Additional key contributors to earlier versions:

David A. Pearlman (UC San Francisco)	Bing Wang (Florida)
Robert V. Stanton (UC San Francisco)	Chunhu Tan (UC Irvine)
Jed Pitera (UC San Francisco)	Lijiang Yang (UC Irvine)
Irina Massova (UC San Francisco)	Christian Schafmeister (Pitt)
Ailan Cheng (Penn State)	Wilson S. Ross (UC San Francisco)
James J. Vincent (Penn State)	Randall Radmer (UC San Francisco)
Paul Beroza (Telik)	George L. Seibel (UC San Francisco)
Vickie Tsui (TSRI)	James W. Caldwell (UC San Francisco)
Mike Crowley (NREL)	U. Chandra Singh (UC San Francisco)
John Mongan (UC San Diego)	Paul Weiner (UC San Francisco)

For more information, please visit <http://ambermd.org/contributors>

### *Acknowledgments*

Research support from DARPA, NIH and NSF for Peter Kollman is gratefully acknowledged, as is support from NIH, NSF, ONR and DOE for David Case. Use of the facilities of the UCSF Computer Graphics Laboratory (Thomas Ferrin, PI) is appreciated. The pseudocontact shift code was provided by Ivano Bertini of the University of Florence. We thank Chris Bayly and Merck-Frosst, Canada for permission to include charge increments for the AM1-BCC charge scheme. Many people helped add features to various codes; these contributions are described in the documentation for the individual programs; see also <http://ambermd.org/contributors.html>.

### *Recommended Citations:*

- When citing Amber 12 in the literature, the following citation should be used:  
D.A. Case, T.A. Darden, T.E. Cheatham, III, C.L. Simmerling, J. Wang, R.E. Duke, R. Luo, R.C. Walker, W. Zhang, K.M. Merz, B. Roberts, S. Hayik, A. Roitberg, G. Seabra, J. Swails, A.W. Götz, I. Kolossváry, K.F. Wong, F. Paesani, J. Vanicek, R.M. Wolf, J. Liu, X. Wu, S.R. Brozell, T. Steinbrecher, H. Gohlke, Q. Cai, X. Ye, J. Wang, M.-J. Hsieh, G. Cui, D.R. Roe, D.H. Mathews, M.G. Seetin, R. Salomon-Ferrer, C. Sagui, V. Babin, T. Luchko, S. Gusarov, A. Kovalenko, and P.A. Kollman (2012), AMBER 12, University of California, San Francisco.

The history of the codes and a basic description of the methods can be found in two papers:

- D.A. Pearlman, D.A. Case, J.W. Caldwell, W.S. Ross, T.E. Cheatham, III, S. DeBolt, D. Ferguson, G. Seibel, and P. Kollman. AMBER, a package of computer programs for applying molecular mechanics, normal mode analysis, molecular dynamics and free energy calculations to simulate the structural and energetic properties of molecules. *Comp. Phys. Commun.* **91**, 1-41 (1995).
- D.A. Case, T. Cheatham, T. Darden, H. Gohlke, R. Luo, K.M. Merz, Jr., A. Onufriev, C. Simmerling, B. Wang and R. Woods. The Amber biomolecular simulation programs. *J. Computat. Chem.* **26**, 1668-1688 (2005).

Peter Kollman died unexpectedly in May, 2001. We dedicate Amber to his memory.

### *Cover Illustration*

The cover image represents the allosteric changes in the transcriptional repressor protein *Staphylococcus aureus* CzrA upon binding of Zn(II). As Zn(II) binds DNA bound apo-CzrA (upper right image) the DNA binding affinity is reduced by 4 orders of magnitude and the structure of CzrA switches from a +“closed” conformation to an “open” conformation facilitating its release from DNA (lower left image). See <http://pubs.acs.org/doi/abs/10.1021/ja208047b>. Image created by M. Nihan Ucisik, Dhruva Chakravorty and Kenneth M. Merz, Jr.

# Contents

<b>Contents</b>	<b>3</b>
<b>1. Introduction</b>	<b>9</b>
1.1. What to read next	9
1.2. Installation of Amber 12	10
1.3. Basic tutorials	10
<b>2. Sander basics</b>	<b>13</b>
2.1. Introduction	13
2.2. File usage	15
2.3. Example input files	16
2.4. Overview of the information in the input file	17
2.5. General minimization and dynamics parameters	17
2.5.1. General flags describing the calculation	17
2.5.2. Nature and format of the input	18
2.5.3. Nature and format of the output	19
2.5.4. Frozen or restrained atoms	21
2.5.5. Energy minimization	22
2.5.6. Molecular dynamics	22
2.5.7. Temperature regulation	23
2.5.8. Pressure regulation	25
2.5.9. SHAKE bond length constraints	26
2.5.10. Water cap	27
2.5.11. NMR refinement options	28
2.5.12. EMAP constraints	29
2.6. Potential function parameters	29
2.6.1. Generic parameters	29
2.6.2. Particle Mesh Ewald	31
2.6.3. Using IPS for the calculation of nonbonded interactions	33
2.6.4. Extra point options	35
2.6.5. Polarizable potentials	35
2.6.6. Dipole Printing	36
2.6.7. Detailed MPI Timings	37
2.7. Varying conditions	37
2.8. File redirection commands	42
2.9. Getting debugging information	43

## CONTENTS

<b>3. Force field modifications</b>	<b>47</b>
3.1. The Generalized Born/Surface Area Model	47
3.1.1. GB/SA input parameters	50
3.1.2. ALPB (Analytical Linearized Poisson-Boltzmann)	53
3.2. PBSA	54
3.3. Reference Interaction Site Model of Molecular Solvation	55
3.3.1. Multiple Time Step Methods for 3D-RISM	55
3.3.2. 3D-RISM in <code>sander</code>	57
3.4. Empirical Valence Bond	63
3.4.1. Introduction	63
3.4.2. General usage description	65
3.4.3. Biased sampling	67
3.4.4. Quantization of nuclear degrees of freedom	69
3.4.5. Distributed Gaussian EVB	70
3.4.6. EVB input variables and interdependencies	73
3.5. The AMOEBA force field	78
3.6. QM/MM calculations: Semi-empirical methods	80
3.6.1. The hybrid QM/MM potential	80
3.6.2. The QM/MM interface and link atoms	82
3.6.3. A reformulated QM/MM interface for PM3	83
3.6.4. Generalized Born implicit solvent	84
3.6.5. Ewald and PME	84
3.6.6. Hints for running successful QM/MM calculations	85
3.6.7. General QM/MM & qmmm Namelist Variables	86
3.6.8. Link Atom Specific QM/MM & qmmm Namelist Variables	90
3.7. QM/MM calculations: <i>ab initio</i> and DFT methods	91
3.7.1. Theory	92
3.7.2. General Remarks	94
3.7.3. Limitations	95
3.7.4. Performance Considerations	95
3.7.5. Parallelization	95
3.7.6. Usage	96
3.8. Charge Relocation	106
3.8.1. Preparing Input Files for Charge Relocation	107
<b>4. Sampling and free energies</b>	<b>113</b>
4.1. Thermodynamic integration	113
4.1.1. Basic inputs for thermodynamic integration	114
4.1.2. Softcore Potentials in Thermodynamic Integration	118
4.1.3. Collecting potential energy differences for FEP calculations	120
4.2. Umbrella sampling	121
4.3. Self-Guided Langevin dynamics	122
4.4. Targeted MD	124
4.5. Multiply-Targeted MD (MTMD)	126
4.5.1. Variables in the <code>&amp;tgt</code> namelist:	126

4.6. Steered Molecular Dynamics (SMD) and the Jarzynski Relationship . . . . .	128
4.6.1. Background . . . . .	128
4.6.2. Implementation and usage . . . . .	128
4.7. Replica Exchange Molecular Dynamics (REMD) . . . . .	130
4.7.1. Running REMD simulations . . . . .	130
4.7.2. Restarting REMD simulations . . . . .	132
4.7.3. Content of the output files . . . . .	132
4.7.4. Major changes from sander when using replica exchange . . . . .	133
4.7.5. Cautions when using replica exchange . . . . .	133
4.7.6. Replica exchange example . . . . .	134
4.7.7. Replica exchange using a hybrid solvent model . . . . .	136
4.7.8. Reservoir REMD . . . . .	137
4.7.9. Hamiltonian replica exchange . . . . .	139
4.7.10. RXSGLD: Replica exchange using Self-Guided Langevin Dynamics . . . . .	143
4.8. Adaptively biased MD, steered MD, and umbrella sampling with REMD . . . . .	144
4.8.1. Overview . . . . .	144
4.8.2. Reaction Coordinates . . . . .	145
4.8.3. Steered Molecular Dynamics . . . . .	148
4.8.4. Umbrella sampling . . . . .	149
4.8.5. Adaptively Biased Molecular Dynamics . . . . .	150
4.9. Nudged elastic band calculations . . . . .	154
4.9.1. Background . . . . .	154
4.9.2. Preparing input files for NEB . . . . .	156
4.9.3. Input Variables . . . . .	156
4.9.4. Important Considerations for NEB Simulations . . . . .	158
4.10. Accelerated Molecular Dynamics . . . . .	158
4.10.1. Background . . . . .	158
4.10.2. AMD implementation in Amber . . . . .	159
4.10.3. Preparing a system for AMD . . . . .	160
4.10.4. Sample input file for AMD . . . . .	160
4.10.5. Further information . . . . .	161
4.11. Constant pH calculations . . . . .	161
4.11.1. Background . . . . .	161
4.11.2. Preparing a system for constant pH . . . . .	161
4.11.3. Running at constant pH . . . . .	163
4.11.4. Analyzing constant pH simulations . . . . .	164
4.11.5. Extending constant pH to additional titratable groups . . . . .	166
4.12. Low-MODE (LMOD) methods . . . . .	167
4.12.1. XMIN . . . . .	168
4.12.2. LMOD . . . . .	169

## CONTENTS

<b>5. Quantum dynamics</b>	<b>173</b>
5.1. Path-Integral Molecular Dynamics	173
5.1.1. General theory	173
5.1.2. How PIMD works in Amber	175
5.2. Centroid Molecular Dynamics (CMD)	179
5.2.1. Implementation and input/output files	180
5.2.2. Examples	181
5.3. Ring Polymer Molecular Dynamics (RPMD)	182
5.3.1. Input parameters	182
5.3.2. Examples	182
5.4. Linearized semiclassical initial value representation	183
5.4.1. Experimental observables and thermal correlation functions	183
5.4.2. Linearized semiclassical initial value representation	183
5.4.3. Local Gaussian approximation	184
5.4.4. Input parameters for LSC-IVR in Amber	185
5.5. Reactive Dynamics	189
5.5.1. Path integral quantum transition state theory	189
5.5.2. Quantum Instanton	189
5.6. Isotope effects	193
5.6.1. Thermodynamic integration with respect to mass	193
5.6.2. Amber implementation	194
5.6.3. Equilibrium isotope effects	195
5.6.4. Kinetic isotope effects	195
5.6.5. Estimating the kinetic isotope effect using EVB/LES-PIMD	197
<b>6. NMR, X-ray, and cryo-EM/ET refinement</b>	<b>199</b>
6.1. Distance, angle and torsional restraints	200
6.1.1. Variables in the &rst namelist:	200
6.2. NOESY volume restraints	207
6.3. Chemical shift restraints	209
6.4. Pseudocontact shift restraints	210
6.5. Direct dipolar coupling restraints	212
6.6. Residual CSA or pseudo-CSA restraints	214
6.7. Preparing restraint files for Sander	215
6.7.1. Preparing distance restraints: makeDIST_RST	217
6.7.2. Preparing torsion angle restraints: makeANG_RST	219
6.7.3. Chirality restraints: makeCHIR_RST	221
6.7.4. Direct dipolar coupling restraints: makeDIP_RST	222
6.7.5. fantasian	222
6.8. Getting summaries of NMR violations	223
6.9. Time-averaged restraints	224
6.10. Multiple copies refinement using LES	225
6.11. Some sample input files	226
6.11.1. 1. Simulated annealing NMR refinement	226
6.11.2. Part of the RST.f file referred to above	227



6.11.3. 3. Sample NOESY intensity input file . . . . .	228
6.11.4. Residual dipolar restraints, prepared by makeDIP_RST: . . . . .	229
6.11.5. A more complicated constraint . . . . .	230
6.12. X-ray Crystallography Refinement using SANDER . . . . .	230
6.13. EMAP constraints using SANDER . . . . .	231
<b>7. PMEMD</b>	<b>235</b>
7.1. Introduction . . . . .	235
7.2. Functionality . . . . .	235
7.3. PMEMD-specific namelist variables . . . . .	237
7.4. Slightly changed functionality . . . . .	239
7.5. Parallel performance tuning and hints . . . . .	240
7.6. Installation . . . . .	241
7.7. GPU Accelerated PMEMD . . . . .	241
7.7.1. New Features in AMBER 12 . . . . .	242
7.7.2. Supported Features . . . . .	242
7.7.3. Supported GPUs . . . . .	243
7.7.4. Accuracy Considerations . . . . .	244
7.7.5. Installation and Testing . . . . .	245
7.7.6. Running GPU Accelerated Simulations . . . . .	247
7.7.7. Considerations for Maximizing GPU Performance . . . . .	247
7.8. Acknowledgements . . . . .	249
<b>8. LES</b>	<b>251</b>
8.1. Preparing to use LES with Amber . . . . .	251
8.2. Using the ADDLES program . . . . .	252
8.3. More information on the ADDLES commands and options . . . . .	255
8.4. Using the new topology/coordinate files with SANDER . . . . .	257
8.5. Using LES with the Generalized Born solvation model . . . . .	257
8.6. Case studies: Examples of application of LES . . . . .	258
8.6.1. Enhanced sampling for individual functional groups: Glucose . . . . .	258
8.6.2. Enhanced sampling for a small region: Application of LES to a nucleic acid loop . . . . .	259
8.6.3. Improving conformational sampling in a small peptide . . . . .	260
<b>Bibliography</b>	<b>263</b>
<b>Bibliography</b>	<b>263</b>
<b>Index</b>	<b>305</b>
<b>A. Namelist Input Syntax</b>	<b>313</b>
<b>B. GROUP Specification</b>	<b>315</b>
<b>C. ambmask</b>	<b>319</b>

## CONTENTS

<b>D. MM_PBSA</b>	<b>323</b>
D.1. General instructions . . . . .	324
D.2. Input explanations . . . . .	325
D.2.1. General . . . . .	325
D.2.2. Energy Decomposition Parameters . . . . .	326
D.2.3. Poisson-Boltzmann Parameters . . . . .	327
D.2.4. Molecular Mechanics Parameters . . . . .	329
D.2.5. Generalized Born Parameters . . . . .	329
D.2.6. Molsurf Parameters . . . . .	330
D.2.7. NMODE Parameters . . . . .	330
D.2.8. Parameters for Snapshot Generation . . . . .	330
D.2.9. Parameters for Alanine Scanning . . . . .	331
D.2.10. Trajectory Specification . . . . .	331
D.3. Auxiliary programs used by MM_PBSA . . . . .	332
D.4. APBS as an alternate PB solver in Sander . . . . .	332
<b>E. EVB output file specifications</b>	<b>335</b>
<b>F. Distributed Gaussian EVB format specifications</b>	<b>339</b>
F.1. Cartesian coordinate representation . . . . .	339
F.2. Internal coordinate representation . . . . .	341
<b>G. AMBER Trajectory NetCDF Format</b>	<b>343</b>
G.0.1. Program behavior . . . . .	343
G.0.2. NetCDF file encoding . . . . .	344
G.0.3. Global attributes . . . . .	344
G.0.4. Dimensions . . . . .	345
G.0.5. Label variables . . . . .	345
G.0.6. Data variables . . . . .	346
G.0.7. Example . . . . .	347

# 1. Introduction

*Amber* is the collective name for a suite of programs that allow users to carry out molecular dynamics simulations, particularly on biomolecules. None of the individual programs carries this name, but the various parts work reasonably well together, and provide a powerful framework for many common calculations.[1, 2] The term *amber* is also sometimes used to refer to the empirical force fields that are implemented here.[3, 4] It should be recognized however, that the code and force field are separate: several other computer packages have implemented the *amber* force fields, and other force fields can be implemented with the *amber* programs. Further, the force fields are in the public domain, whereas the codes are distributed under a license agreement.

The Amber software suite is divided into two parts: AmberTools12, a collection of freely available programs mostly under the GPL license, and Amber12, which is centered around the *sander* and *pmemd* simulation programs, and which continues to be licensed as before, under a more restrictive license. You need to install both parts, starting with AmberTools.

*Amber 12* (2012) represents a significant change from the most recent previous version, *Amber 11*, which was released in April, 2010. Please see <http://ambermd.org> for an overview of the most important changes.

## 1.1. What to read next

*Everyone should read (or at least skim) Section 1.1 of the AmberTools12 Reference Manual.* Even if you are an experienced Amber user, there may be things you have missed, or new features, that will help.

If you are installing this package see Section 1.2. New users should consult the tutorial information in Section 1.4. There are also tips and examples on the Amber Web pages at <http://ambermd.org>. Although Amber may appear dauntingly complex at first, it has become easier to use over the past few years, and overall is reasonably straightforward once you understand the basic architecture and option choices. In particular, we have worked hard on the tutorials to make them accessible to new users. Thousands of people have learned to use Amber; don't be easily discouraged.

If you want to learn more about basic biochemical simulation techniques, there are a variety of good books to consult, ranging from introductory descriptions,[5, 6] to standard works on liquid state simulation methods,[7, 8] to multi-author compilations that cover many important aspects of biomolecular modelling.[9–11] Looking for "paradigm" papers that report simulations similar to ones you may want to undertake is also generally a good idea.

## 1. Introduction

### 1.2. Installation of Amber 12

Installation instructions are given in Section 1.2 of the *AmberTools12 Reference Manual*. There is also a section in that manual about applying bug fixes, which applies to Amber 12 as well. The only specialized instructions for Amber 12 involve the GPU version of *pmemd*. Installation instructions for *pmemd.cuda* are outlined here [7.6](#).

### 1.3. Basic tutorials

Amber is a suite of programs for use in molecular modeling and molecular simulations. It consists of a substructure database, a force field parameter file, and a variety of useful programs. Here we give some commented sample runs to provide an overview of how things are carried out. The examples only cover a fraction of the things that it is possible to do with Amber. The formats of the example files shown are described in detail later in the manual, in the chapters pertaining to the programs. Tom Cheatham, Bernie Brooks and Peter Kollman have prepared some detailed information on simulation protocols that should also be consulted.[\[12\]](#)

Additional tutorial examples are available at <http://ambermd.org>. Because the web can provide a richer interface than one can get on the printed page (with screen shots, links to the actual input and output files, etc.), most of our recent efforts have been devoted to updating the tutorials on the web site.

As a basic example, we consider here the minimization of a protein in a simple solvent model. The procedure consists of three steps:

#### **Step 1. Generate some starting coordinates.**

The first step is to obtain starting coordinates. We begin with the bovine pancreatic trypsin inhibitor, and consider the file *6pti.pdb*, exactly as distributed by the Protein Data Bank. **This file (as with most PDB files) needs some editing before it can be used by Amber.** (See Section 5.8 of the *AmberTools Reference Manual* for a more detailed discussion.) First, alternate conformations are provided for residues 39 and 50, so we need to figure out which one we want. For this example, we choose the "A" conformation, and manually edit the file to remove the alternate conformers. Second, coordinates are provided for a phosphate group and a variety of water molecules. These are not needed for the calculation we are pursuing here, so we also edit the file to remove these. Third, the cysteine residues are involved in disulfide bonds, and need to have their residue names changed in an editor from CYS to CYX to reflect this. Finally, since we removed the phosphate groups, some of the CONECT records now refer to non-existent atoms; if you are not sure that the CONECT records are all correct then it may be safest to remove all of them, as we do for this example. Let's call this modified file *6pti.mod.pdb*.

Although Amber tries hard to interpret files in PDB formats, it is typical to have to do some manual editing before proceeding. A general prescription is: "keep running the *loadPdb* step in LEaP (see step 2, below), and editing the PDB file, until there are no error messages."

**Step 2. Run LEaP to generate the parameter and topology file.**

This is a fairly straightforward exercise in loading in the PDB file, adding the disulfide cross links, and saving the resulting files. Typing the following commands should work in either *tleap* or *xleap*:

```
source leaprc.ff03
bpti = loadPdb 6pti.mod.pdb
bond bpti.5.SG bpti.55.SG
bond bpti.14.SG bpti.38.SG
bond bpti.30.SG bpti.51.SG
saveAmberParm bpti prmtop prmcrd
quit
```

**Step 3. Perform some minimization.**

Use this script:

```
# Running minimization for BPTI
cat << eof > min.in
# 200 steps of minimization, generalized Born solvent model
&cntrl
maxcyc=200, imin=1, cut=12.0, igb=1, ntb=0, ntp=10,
/
eof
sander -i min.in -o 6pti.min1.out -c prmcrd -r 6pti.min1.xyz
/bin/rm min.in
```

This will perform minimization ( $imin=1$ ) for 200 steps ( $maxcyc$ ), using a nonbonded cutoff of 12 Å ( $cut$ ), a generalized Born solvent model ( $igb=1$ ), and no periodic boundary ( $ntb=0$ ); intermediate results will be printed every 10 steps ( $ntp$ ). Text output will go to file *6pti.min1.out*, and the final coordinates to file *6pti.min1.xyz*. The "out" file is intended to be read by humans, and gives a summary of the input parameters and a history of the progress of the minimization.

Of course, Amber can do much more than the above minimization. This example illustrates the basic information flow in Amber: Cartesian coordinate preparation (*Step 1.*), topology and force field selection (*Step 2.*), and simulation program command specification (*Step 3.*). Typically the subsequent steps are several stages of equilibration, production molecular dynamics runs, and analyses of trajectories. The tutorials in *amber12/tutorial* should be consulted for examples of these latter steps.



## 2. Sander basics

### 2.1. Introduction

This is a guide to *sander*, the Amber module which carries out energy minimization, molecular dynamics, and NMR refinements. The acronym stands for **S**imulated **A**nnealing with **N**M**R**-**D**erived **E**nergy **R**estraints, but this module is used for a variety of simulations that have nothing to do with NMR refinement. Some general features are outlined in the following paragraphs:

1. *Sander* provides direct support for several force fields for proteins and nucleic acids, and for several water models and other organic solvents. The basic force field implemented here has the following form, which is about the simplest functional form that preserves the essential nature of molecules in condensed phases:

$$\begin{aligned} V(\mathbf{r}) = & \sum_{bonds} K_b(b - b_0)^2 + \sum_{angles} K_\theta(\theta - \theta_0)^2 \\ & + \sum_{dihedrals} (V_n/2)(1 + \cos[n\phi - \delta]) \\ & + \sum_{nonbij} (A_{ij}/r_{ij}^{12}) - (B_{ij}/r_{ij}^6) + (q_i q_j / r_{ij}) \end{aligned}$$

"Non-additive" force fields based on atom-centered dipole polarizabilities can also be used. These add a "polarization" term to what was given above:

$$E_{pol} = -2 \sum_i \mu_i \cdot \mathbf{E}_{io}$$

where  $\mu_i$  is an induced atomic dipole. In addition, charges that are not centered on atoms, but are off-center (as for lone-pairs or "extra points") can be included in the force field.

2. The particle-mesh Ewald (PME) procedure (or, optionally, a "true" Ewald sum) is used to handle long-range electrostatic interactions. Long-range van der Waals interactions are estimated by a continuum model. Biomolecular simulations in the NVE ensemble (*i.e.* with Newtonian dynamics) conserve energy well over multi-nanosecond runs without modification of the equations of motion.
3. Two periodic imaging geometries are included: rectangular parallelepiped and truncated octahedron (box with corners chopped off). (*Sander* itself can handle many other periodically-replicating boxes, but input and output support in *LEaP* and *ptraj* is only available right

## 2. Sander basics

now for these two.) The size of the repeating unit can be coupled to a given external pressure, and velocities can be coupled to a given external temperature by several schemes. The external conditions and coupling constants can be varied over time, so various simulated annealing protocols can be specified in a simple and flexible manner.

4. It is also possible to carry out non-periodic simulations in which aqueous solvation effects are represented *implicitly* by a generalized Born/ surface area model by adding the following two terms to the "vacuum" potential function:

$$\Delta G_{sol} = \sum_{ij} \left(1 - \frac{1}{\epsilon}\right) (q_i q_j / f_{GB}(r_{ij})) + A \sum_i \sigma_i$$

The first term accounts for the polar part of solvation (free) energy, designed to provide an approximation for the reaction field potential, and the second represents the non-polar contribution which is taken to be proportional to the surface area of the molecule.

5. Users can define internal restraints on bonds, valence angles, and torsions, and the force constants and target values for the restraints can vary during the simulation. The relative weights of various terms in the force field can be varied over time, allowing one to implement a variety of simulated annealing protocols in a single run.
6. Internal restraints can be defined to be "time-averaged", that is, restraint forces are applied based on the averaged value of an internal coordinate over the course of the dynamics trajectory, not only on its current value. Alternatively, restraints can be "ensemble-averaged" using the locally-enhanced-sampling (LES) option.
7. Restraints can be directly defined in terms of NOESY intensities (calculated with a relaxation matrix technique), residual dipolar couplings, scalar coupling constants and proton chemical shifts. There are provisions for handling overlapping peaks or ambiguous assignments. In conjunction with distance and angle constraints, this provides a powerful and flexible approach to NMR structural refinements.
8. Replica exchange calculations can allow simultaneous sampling at a variety of conditions (such as temperature), and allow the user to construct Boltzmann samples in ways that converge more quickly than standard MD simulations. Other variants of biased MD simulations can also be used to improve sampling.
9. Restraints can also be defined in terms of the root-mean-square coordinate distance from some reference structure. This allows one to bias trajectories either towards or away from some target. Free energies can be estimated from non-equilibrium simulations based on targetting restraints.
10. Free energy calculations, using thermodynamic integration (TI) with a linear or non-linear mixing of the "unperturbed" and "perturbed" Hamiltonian, can be carried out. Alternatively, potentials of mean force can be computed using umbrella sampling.
11. The empirical valence bond (EVB) scheme can be used to mix "diabatic" states into a potential that can represent many types of chemical reactions that take place in enzymes.



12. QMMM Calculations where part of the system can be treated quantum mechanically allowing bond breaking and formation during a simulation. Semi-empirical and DFTB Hamiltonians are provided directly within *sander*. More advanced *ab initio* and DFT Hamiltonians are available via an interface to external QM software packages.
13. Nuclear quantum effects can be included through path-integral molecular dynamics (PIMD) simulations, and estimates of quantum time-correlation functions can be computed.

## 2.2. File usage

```
sander [-help] [-O] [-A] -i mdin -o mdout -p prmtop -c inpcrd -r restrt
-ref refc -mtmd mtmd -x mdcrd -y inptraj -v mdvel -e mden -inf mdinfo
-radii radii -cpin cpin -cpout cpout -cprestrt cprestrt -evbin evbin
-O Overwrite output files if they exist.
-A Append output files if they exist (used mainly for replica exchange).
```

Here is a brief description of the files referred to above; the first five files are used for every run, whereas the remainder are only used when certain options are chosen.

**mdin** *input* control data for the min/md run

**mdout** *output* user readable state info and diagnostics -o stdout will send output to stdout (to the terminal) instead of to a file.

**mdinfo** *output* latest mdout-format energy info

**prmtop** *input* molecular topology, force field, periodic box type, atom and residue names

**inpcrd** *input* initial coordinates and (optionally) velocities and periodic box size

**refc** *input* (optional) reference coords for position restraints; also used for targeted MD

**mtmd** *input* (optional) containing list of files and parameters for targeted MD to multiple targets

**mdcrd** *output* coordinate sets saved over trajectory

**inptraj** *input* input coordinate sets in trajectory format, when imin=5

**mdvel** *output* velocity sets saved over trajectory

**mden** *output* extensive energy data over trajectory

**restrt** *output* final coordinates, velocity, and box dimensions if any - for restarting run

**inp dip** *input* polarizable dipole file, when indmeth=3

**rst dip** *output* polarizable dipole file, when indmeth=3

## 2. Sander basics

**cpin** *input* protonation state definitions

**cprestrt** protonation state definitions, final protonation states for restart (same format as cpin)

**cpout** *output* protonation state data saved over trajectory

**evbin** *input* input for EVB potentials

## 2.3. Example input files

Here are a couple of sample files, just to establish a basic syntax and appearance. There are more examples of NMR-related files later in this chapter.

### 1. Simple restrained minimization

```
Minimization with Cartesian restraints
&cntrl
imin=1, maxcyc=200, (invoke minimization)
ntpr=5, (print frequency)
ntr=1, (turn on Cartesian restraints)
restraint_wt=1.0, (force constant for restraint)
restraintmask=':1-58', (atoms in residues 1-58 restrained)
/
```

### 2. "Plain" molecular dynamics run

```
molecular dynamics run
&cntrl
imin=0, irest=1, ntx=5, (restart MD)
ntt=3, temp0=300.0, gamma_ln=5.0, (temperature control)
ntp=1, taup=2.0, (pressure control)
ntb=2, ntc=2, ntf=2, (SHAKE, periodic bc.)
nstlim=500000, (run for 0.5 nsec)
ntwe=100, ntwx=1000, ntpr=200, (output frequency)
/
```

### 3. Self-guided Langevin dynamics run

```
Self-guided Langevin dynamics run
&cntrl
imin=0, irest=0, ntx=1, (start LD)
ntt=3, temp0=300.0, gamma_ln=1.0 (temperature control)
ntc=3, ntf=3, (SHAKE)
nstlim=500000, (run for 0.5 nsec)
ntwe=100, ntwx=1000, ntpr=200, (output frequency)
```

```
isgld=1, tsgavg=0.2, tempsg=400.0 (SGLD)
/
```

## 2.4. Overview of the information in the input file

### General minimization and dynamics input

One or more title lines, followed by the (required) `&cntrl` and (optional) `&pb`, `&ewald`, `&qmmm`, `&amoeba` or `&debugf` namelist blocks. Described in Sections 2.5 and 2.6.

### Varying conditions

Parameters for changing temperature, restraint weights, etc., during the MD run. Each parameter is specified by a separate `&wt` namelist block, ending with `&wt type='END'`, `/`. Described in Section 2.7.

### File redirection

`TYPE=filename` lines. Section ends with the first non-blank line which does not correspond to a recognized redirection. Described in Section 2.8.

### Group information

Read if `ntr`, `ibelly` or `idecomp` are set to non-zero values, and if some other conditions are satisfied; see sections on these variables, below. Described in Appendix B.

## 2.5. General minimization and dynamics parameters

Each of the variables listed below is input in a namelist statement with the namelist identifier `&cntrl`. You can enter the parameters in any order, using keyword identifiers. Variables that are not given in the namelist input retain their default values. Support for namelist input is included in almost all current Fortran compilers, and is a standard feature of Fortran 90. A detailed description of the namelist convention is given in Appendix A.

In general, namelist input consists of an arbitrary number of comment cards, followed by a record whose first seven characters after a `"&"` (e.g. `"&cntrl"`) name a group of variables that can be set by name. This is followed by statements of the form `" maxcyc=500, diel=2.0, ... "`, and is concluded by an `/"` token. The first line of input contains a title, which is then followed by the `&cntrl` namelist. Note that the first character on each line of a namelist block must be a blank.

Some of the options and variables are much more important, and commonly modified, than are others. We have denoted the "common" options by printing them in **boldface** below. In general, you can skip reading about the non-bold options on a first pass, and you should change these from their defaults only if you think you know what you are doing.

### 2.5.1. General flags describing the calculation

**imin**            Flag to run minimization

## 2. Sander basics

- = 0 (default) Run molecular dynamics without any minimization.
- = 1 Perform an energy minimization.
- = 5 Read in a trajectory for analysis.

Although sander will write energy information in the output files (using *ntpr*), it is often desirable to calculate the energies of a set of structures at a later point. In particular, one may wish to post-process a set of structures using a different energy function than was used to generate the structures. An example of this is MM-PBSA analysis, where the explicit water is removed and replaced with a continuum model.

If *imin* is set to 5, sander will expect to read a trajectory file (the “inpraj” argument, specified using *-y* on the command line), and will perform the functions described in the *mdin* file (e.g., an energy minimization) for each of the structures in this file. The final structure from each minimization will be written out to the normal *mdcrd* file. If you wish to read in a binary (i.e., NetCDF format) trajectory, be sure to set *ioutfm* to 1 (see below). Note that this will result in the output trajectory having NetCDF format as well.

For example, when *imin* = 5 and *maxcyc* = 1000, sander will minimize each structure in the trajectory for 1000 steps and write a minimized coordinate set for each frame to the *mdcrd* file. If *maxcyc* = 1, the output file can be used to extract the energies of each of the coordinate sets in the *inpraj* file.

Trajectories containing box coordinates can now be post-processed. In order to read trajectories with box coordinates, *ntb* should be greater than 0.

**IMPORTANT CAVEAT:** The input coordinate file used (*-c <inpcrd>*) should be the same as the input coordinate file used to generate the original trajectory. This is because sander sets up parameters for PME from the box coordinates in the input coordinate file.

### nmropt

- = 0 (default) No nmr-type analysis will be done.
- = 1 NMR restraints and weight changes will be read.
- = 2 NMR restraints, weight changes, NOESY volumes, chemical shifts and residual dipolar restraints will be read.

### 2.5.2. Nature and format of the input

**ntx** Option to read the initial coordinates, velocities and box size from the *inpcrd* file. Either 1 or 2 must be used when one is starting from minimized or model-built coordinates. If an MD restrt file is used as *inpcrd*, then options 4-7 may be used. Only options 1 and 5 are in common use.

- = 1 (default) Coordinates, but no velocities, will be read; a formatted (ASCII) coordinate file is expected.

## 2.5. General minimization and dynamics parameters

- = 2 Coordinates, but no velocities, will be read; an unformatted (binary) coordinate file is expected.
  - = 4 Coordinates and velocities will be read; an unformatted coordinate file is expected.
  - = 5 Coordinates and velocities will be read; a formatted (ASCII) coordinate file is expected. Box information will be read if  $ntb > 0$ . The velocity information will only be used if  $irest = 1$  (see below).
  - = 6 Coordinates, velocities and box information will be read; an unformatted coordinate file is expected.
- irest** Flag to restart a simulation.
- = 0 (default) Do not restart the simulation; instead, run as a new simulation. Velocities in the input coordinate file, if any, will be ignored, and the time step count will be set to 0 (unless overridden by  $t$ ; see below).
  - = 1 Restart the simulation, reading coordinates and velocities from a previously saved restart file. The velocity information is necessary when restarting, so  $ntx$  (see above) must be 4 or higher if  $irest = 1$ .
- nrxc** Format of the Cartesian coordinates for restraint from the `refc` file. Note: the program expects the `refc` file to contain coordinates for all the atoms in the system. The atoms that are to be restrained are specified by a `restraintmask` entry in the `&cntrl` namelist (see below).
- = 0 Unformatted (binary)
  - = 1 (default) Formatted (ASCII)

### 2.5.3. Nature and format of the output

- ntxo** Format of the final coordinates, velocities, and box size (if constant volume or pressure run) written to file "restrt".
- = 0 Unformatted (no longer recommended or allowed: please use formatted restart files)
  - = 1 (default) Formatted (ASCII)
- ntpr** Every  $ntpr$  steps, energy information will be printed in human-readable form to files "mdout" and "mdinfo". "mdinfo" is closed and reopened each time, so it always contains the most recent energy and temperature. Default 50.
- ntave** Every  $ntave$  steps of dynamics, running averages of average energies and fluctuations over the last  $ntave$  steps will be printed out. A value of 0 disables this printout. Setting  $ntave$  to a value 1/2 or 1/4 of  $nstlim$  provides a simple way to look at convergence during the simulation. Default = 0 (disabled).

## 2. Sander basics

- ntwr** Every *ntwr* steps during dynamics, the “restrt” file will be written, ensuring that recovery from a crash will not be so painful. No matter what the value of *ntwr*, a restrt file will be written at the end of the run, i.e., after *nstlim* steps (for dynamics) or *maxcyc* steps (for minimization). If *ntwr* < 0, a unique copy of the file, “restrt\_<nstep>”, is written every  $\text{abs}(ntwr)$  steps. This option is useful if for example one wants to run free energy perturbations from multiple starting points or save a series of restrt files for minimization. Default = 500.
- iwrap** If *iwrap* = 1, the coordinates written to the restart and trajectory files will be “wrapped” into a primary box. This means that for each molecule, its periodic image closest to the middle of the “primary box” (with x coordinates between 0 and a, y coordinates between 0 and b, and z coordinates between 0 and c) will be the one written to the output file. This often makes the resulting structures look better visually, but has no effect on the energy or forces. Performing such wrapping, however, can mess up diffusion and other calculations. If *iwrap* = 0, no wrapping will be performed, in which case it is typical to use ptraj as a post-processing program to translate molecules back to the primary box. For very long runs, setting *iwrap* = 1 may be required to keep the coordinate output from overflowing the trajectory and restart file formats, especially if trajectories are written in ASCII format instead of NetCDF (see also the *ioutfm* option). Default = 0.
- ntwx** Every *ntwx* steps, the coordinates will be written to the mdcrd file. If *ntwx* = 0, no coordinate trajectory file will be written. Default = 0.
- ntwv** Every *ntwv* steps, the velocities will be written to the mdvel file. If *ntwv* = 0, no velocity trajectory file will be written. If *ntwv* = -1, velocities will be written to mdcrd, which then becomes a combined coordinate/velocity trajectory file, at the interval defined by *ntwx*. This option is available only for binary NetCDF output (*ioutfm* = 1). Most users will have no need for a velocity trajectory file and so can safely leave *ntwv* at the default. Default = 0.
- ntwe** Every *ntwe* steps, the energies and temperatures will be written to file “mden” in a compact form. If *ntwe* = 0, no mden file will be written. Default = 0.
- ioutfm** The format of coordinate and velocity trajectory files (mdcrd, mdvel and inptraj). As of Amber 9, the binary format used in previous versions is no longer supported; binary output is now in NetCDF trajectory format. While not the default option, binary trajectory files have many advantages: they are smaller, higher precision, much faster to read and write, and able to accept a wider range of coordinate (or velocity) values than formatted trajectory files.
- = 0 (default) Formatted ASCII trajectory  
= 1 Binary NetCDF trajectory
- ntwpri** The number of atoms to include in trajectory files (mdcrd and mdvel). This flag can be used to decrease the size of these files, by including only the first part of the system, which is usually of greater interest (for instance, one might include only the solute and not the solvent). If *ntwpri* = 0, all atoms will be included.

- = 0 (default) Include all atoms of the system when writing trajectories.
- > 0 Include only atoms 1 to *ntwpvt* when writing trajectories.

**idecomp** Perform energy decomposition according to a chosen scheme. In former distributions this option was only really useful in conjunction with *mm\_pbsa*, where it is turned on automatically if required. Now, a decomposition of  $\langle \partial V / \partial \lambda \rangle$  on a per-residue basis in thermodynamic integration (TI) simulations is also possible.[13] The options are:

- = 0 (default) Do not decompose energies.
- = 1 Decompose energies on a per-residue basis; 1-4 EEL + 1-4 VDW are added to internal (bond, angle, dihedral) energies.
- = 2 Decompose energies on a per-residue basis; 1-4 EEL + 1-4 VDW are added to EEL and VDW.
- = 3 Decompose energies on a pairwise per-residue basis; otherwise equivalent to *idecomp* = 1. Not available in TI simulations.
- = 4 Decompose energies on a pairwise per-residue basis; otherwise equivalent to *idecomp* = 2. Not available in TI simulations.

If energy decomposition is requested, residues may be chosen by the RRES and/or LRES card. The RES card is used to select the residues about which information is written out. See chapters 4.1 or D for more information. Use of *idecomp* > 0 is incompatible with *ntr* > 0 or *ibelly* > 0.

#### 2.5.4. Frozen or restrained atoms

**ibelly** Flag for belly type dynamics. If set to 1, a subset of the atoms in the system will be allowed to move, and the coordinates of the rest will be frozen. The *moving* atoms are specified *bellymask*. This option is not available when *igb*>0. Note also that this option does *not* provide any significant speed advantage, and is maintained primarily for backwards compatibility with older version of Amber. Most applications should use the *ntr* variable instead to restrain parts of the system to stay close to some initial configuration. Default = 0.

**ntr** Flag for restraining specified atoms in Cartesian space using a harmonic potential, if *ntr* > 0. The restrained atoms are determined by the *restraintmask* string. The force constant is given by *restraint\_wt*. The coordinates are read in "restrt" format from the "refc" file (see NTRX, above). Default = 0.

**restraint\_wt** The weight (in *kcal/mol* – Å<sup>2</sup>) for the positional restraints. The restraint is of the form  $k(\Delta x)^2$ , where *k* is the value given by this variable, and  $\Delta x$  is the difference between one of the Cartesian coordinates of a restrained atom and its reference position. There is a term like this for each Cartesian coordinate of each restrained atom.

**restraintmask** String that specifies the *restrained* atoms when *ntr*=1.

## 2. Sander basics

**bellymask** String that specifies the *moving* atoms when *ibelly=1*.

The syntax for both *restraintmask* and *bellymask* is given in Section C. Note that these mask strings are limited to a maximum of 256 characters.

### 2.5.5. Energy minimization

**maxcyc** The maximum number of cycles of minimization. Default = 1.

**ncyc** If NTMIN is 1 then the method of minimization will be switched from steepest descent to conjugate gradient after NCYC cycles. Default 10.

**ntmin** Flag for the method of minimization.

= 0 Full conjugate gradient minimization. The first 4 cycles are steepest descent at the start of the run and after every nonbonded pairlist update.

= 1 For NCYC cycles the steepest descent method is used then conjugate gradient is switched on (default).

= 2 Only the steepest descent method is used.

= 3 The XMIN method is used, see Section 4.12.1.

= 4 The LMOD method is used, see Section 4.12.2.

**dx0** The initial step length. If the initial step length is too big then will give a huge energy; however the minimizer is smart enough to adjust itself. Default 0.01.

**drms** The convergence criterion for the energy gradient: minimization will halt when the root-mean-square of the Cartesian elements of the gradient is less than DRMS. Default 1.0E-4 kcal/mole-Å

### 2.5.6. Molecular dynamics

**nstlim** Number of MD-steps to be performed. Default 1.

**nscm** Flag for the removal of translational and rotational center-of-mass (COM) motion at regular intervals (default is 1000). For non-periodic simulations, after every NSCM steps, translational and rotational motion will be removed. For periodic systems, just the translational center-of-mass motion will be removed. This flag is ignored for belly simulations.

For Langevin dynamics, the *position* of the center-of-mass of the molecule is reset to zero every NSCM steps, but the velocities are not affected. Hence there is no change to either the translation or rotational components of the momenta. (Doing anything else would destroy the way in which temperature is regulated in a Langevin dynamics system.) The only reason to even reset the coordinates is to prevent the molecule from diffusing so far away from the origin that its coordinates overflow the format used in restart or trajectory files.



## 2.5. General minimization and dynamics parameters

- t** The time at the start (psec) this is for your own reference and is not critical. Start time is taken from the coordinate input file if IREST=1. Default 0.0.
- dt** The time step (psec). Recommended MAXIMUM is .002 if SHAKE is used, or .001 if it isn't. Note that for temperatures above 300K, the step size should be reduced since greater temperatures mean increased velocities and longer distance traveled between each force evaluation, which can lead to anomalously high energies and system blowup. Default 0.001.
- nrespa** This variable allows the user to evaluate slowly-varying terms in the force field less frequently. For PME, "slowly-varying" (now) means the reciprocal sum. For generalized Born runs, the "slowly-varying" forces are those involving derivatives with respect to the effective radii, and pair interactions whose distances are greater than the "inner" cutoff, currently hard-wired at 8 Å. If NRESPA>1 these slowly-varying forces are evaluated every *nrespa* steps. The forces are adjusted appropriately, leading to an impulse at that step. If *nrespa\*dt* is less than or equal to 4 fs the energy conservation is not seriously compromised. However if *nrespa\*dt* > 4 fs the simulation becomes less stable. Note that energies and related quantities are only accessible every *nrespa* steps, since the values at other times are meaningless.

### 2.5.7. Temperature regulation

- ntt** Switch for temperature scaling. Note that setting *ntt*=0 corresponds to the microcanonical (NVE) ensemble (which should approach the canonical one for large numbers of degrees of freedom). Some aspects of the "weak-coupling ensemble" (*ntt*=1) have been examined, and roughly interpolate between the microcanonical and canonical ensembles.[14, 15]The *ntt*=2 and 3 options correspond to the canonical (constant T) ensemble.
- = 0** Constant total energy classical dynamics (assuming that *ntb*<2, as should probably always be the case when *ntt*=0).
- = 1** Constant temperature, using the weak-coupling algorithm.[16] A single scaling factor is used for all atoms. Note that this algorithm just ensures that the total kinetic energy is appropriate for the desired temperature; it does nothing to ensure that the temperature is even over all parts of the molecule. Atomic collisions will tend to ensure an even temperature distribution, but this is not guaranteed, and there are many subtle problems that can arise with weak temperature coupling.[17] Using *ntt*=1 is especially dangerous for generalized Born simulations, where there are no collisions with solvent to aid in thermalization.) Other temperature coupling options (especially *ntt*=3) should be used instead.
- = 2** Andersen temperature coupling scheme,[18] in which imaginary "collisions" randomize the velocities to a distribution corresponding to *temp0* every *vrand* steps. Note that in between these "massive collisions", the dynamics is Newtonian. Hence, time correlation functions (etc.) can be computed in these sections, and the results averaged over an initial canonical distribution. Note

## 2. Sander basics

also that too high a collision rate (too small a value of *vrand*) will slow down the speed at which the molecules explore configuration space, whereas too low a rate means that the canonical distribution of energies will be sampled slowly. A discussion of this rate is given by Andersen.[19]

= 3 Use Langevin dynamics with the collision frequency  $\gamma$  given by *gamma\_In*, discussed below. Note that when  $\gamma$  has its default value of zero, this is the same as setting *ntt* = 0. Since Langevin simulations are highly susceptible to "synchronization" artifacts,[20, 21] you should explicitly set the *ig* variable (described below) to a different value at each restart of a given simulation.

**temp0** Reference temperature at which the system is to be kept, if *ntt* > 0. Note that for temperatures above 300K, the step size should be reduced since increased distance traveled between evaluations can lead to SHAKE and other problems. Default 300.

temp0les This is the target temperature for all LES particles (see Chapter 6). If *temp0les* < 0, a single temperature bath is used for all atoms, otherwise separate thermostats are used for LES and non-LES particles. Default is -1, corresponding to a single (weak-coupling) temperature bath.

tempi Initial temperature. For the initial dynamics run, (NTX .lt. 3) the velocities are assigned from a Maxwellian distribution at TEMPI K. If TEMPI = 0.0, the velocities will be calculated from the forces instead. TEMPI has no effect if NTX .gt. 3. Default 0.0.

ig The seed for the pseudo-random number generator. The MD starting velocity is dependent on the random number generator seed if NTX .lt. 3 .and. TEMPI .ne. 0.0. The value of this seed also affects the set of pseudo-random values used for Langevin dynamics or Andersen coupling, and hence should be set to a different value on each restart if *ntt* = 2 or 3. Default 71277. If *ig* = -1, the random seed will be based on the current date and time, and hence will be different for every run. It is recommended that, unless you specifically desire reproducibility, that you set *ig* = -1 for all runs involving *ntt* = 2 or 3.

**tautp** Time constant, in ps, for heat bath coupling for the system, if *ntt* = 1. Default is 1.0. Generally, values for TAUTP should be in the range of 0.5-5.0 ps, with a smaller value providing tighter coupling to the heat bath and, thus, faster heating and a less natural trajectory. Smaller values of TAUTP result in smaller fluctuations in kinetic energy, but larger fluctuations in the total energy. Values much larger than the length of the simulation result in a return to constant energy conditions.

**gamma\_In** The collision frequency  $\gamma$ , in  $\text{ps}^{-1}$ , when *ntt* = 3. A simple Leapfrog integrator is used to propagate the dynamics, with the kinetic energy adjusted to be correct for the harmonic oscillator case.[22, 23] Note that it is not necessary that  $\gamma$  approximate the physical collision frequency, which is about  $50 \text{ ps}^{-1}$  for liquid water. In fact, it is often advantageous, in terms of sampling or stability of integration, to use much smaller values, around 2 to  $5 \text{ ps}^{-1}$ . [23, 24] Default is 0.

## 2.5. General minimization and dynamics parameters

- vrand** If  $vrand > 0$  and  $ntt=2$ , the velocities will be randomized to temperature  $TEMP0$  every  $vrand$  steps.
- vlimit** If not equal to 0.0, then any component of the velocity that is greater than  $abs(VLIMIT)$  will be reduced to  $VLIMIT$  (preserving the sign). This can be used to avoid occasional instabilities in molecular dynamics runs.  $VLIMIT$  should generally be set to a value like 20 (the default), which is well above the most probable velocity in a Maxwell-Boltzmann distribution at room temperature. A warning message will be printed whenever the velocities are modified. Runs that have more than a few such warnings should be carefully examined.

### 2.5.8. Pressure regulation

In "constant pressure" dynamics, the volume of the unit cell is adjusted (by small amounts on each step) to make the computed pressure approach the target pressure,  $pres0$ . Equilibration with  $ntp > 0$  is generally necessary to adjust the density of the system to appropriate values. Note that fluctuations in the instantaneous pressure on each step will appear to be large (several hundred bar), but the average value over many steps should be close to the target pressure. Pressure regulation only applies when Constant Pressure periodic boundary conditions are used ( $ntb = 2$ ). Pressure coupling algorithms used in Amber are of the "weak-coupling" variety, analogous to temperature coupling.[16] Please note: in general you will need to equilibrate the temperature to something like the final temperature using constant volume ( $ntp=0$ ) before switching on constant pressure simulations to adjust the system to the correct density. If you fail to do this, the program will try to adjust the density too quickly, and bad things (such as SHAKE failures) are likely to happen.

- ntp** Flag for constant pressure dynamics. This option should be set to 1 or 2 when Constant Pressure periodic boundary conditions are used ( $NTB = 2$ ).
- = 0 No pressure scaling (Default)
  - = 1 md with isotropic position scaling
  - = 2 md with anisotropic (x-,y-,z-) pressure scaling: this should only be used with orthogonal boxes (i.e. with all angles set to 90 o ). Anisotropic scaling is primarily intended for non-isotropic systems, such as membrane simulations, where the surface tensions are different in different directions; it is generally not appropriate for solutes dissolved in water.
  - = 3 md with semiisotropic pressure scaling: this is only available with constant surface tension ( $csurfTEN > 0$ ) and orthogonal boxes. This links the pressure coupling in the two directions tangential to the interface.
- pres0** Reference pressure (in units of bars, where 1 bar  $\approx$  0.987 atm) at which the system is maintained ( when  $NTP > 0$ ). Default 1.0.
- comp** compressibility of the system when  $NTP > 0$ . The units are in  $1.0 \times 10^{-6} \text{ bar}^{-1}$ ; a value of 44.6 (default) is appropriate for water.

## 2. *Sander basics*

**taup** Pressure relaxation time (in ps), when  $NTP > 0$ . The recommended value is between 1.0 and 5.0 psec. Default value is 1.0, but larger values may sometimes be necessary (if your trajectories seem unstable).

### 2.5.8.1. Surface tension regulation

Constant surface tension is used in statistical ensembles for simulating liquid interfaces. This is primarily intended for lipid membrane simulations with two or more interfaces. Constant surface tension is only available for simulations with anisotropic pressure or semiisotropic scaling. This algorithm is an extension to the Berendsen pressure scaling algorithm that adjusts the tangential pressure evaluation in order to maintain a “constant” surface tension [25]. Since the surface tension is a function of the pressure tensor, fluctuations of the surface tension will be large.

In order to use constant surface tension, periodic boundary conditions ( $ntb = 2$ ), anisotropic or semiisotropic pressure scaling ( $ntp = 2$  or  $ntp = 3$ ), and an orthogonal box must be used.

**csurften** Flag for constant surface tension dynamics.

= 0 No constant surface tension (default)

= 1 Constant surface tension with interfaces in the yz plane

= 2 Constant surface tension with interfaces in the xz plane

= 3 Constant surface tension with interfaces in the xy plane

**gamma\_ten** Surface tension value in units of dyne/cm. Default value is 0.0 dyne/cm.

**ninterface** Number of interfaces in the periodic box. There must be at least two interfaces in the periodic box. Two interfaces is appropriate for a lipid bilayer system and is the default value.

### 2.5.9. SHAKE bond length constraints

**ntc** Flag for SHAKE to perform bond length constraints.[26] (See also NTF in the **Potential function** section. In particular, typically  $NTF = NTC$ .) The SHAKE option should be used for most MD calculations. The size of the MD timestep is determined by the fastest motions in the system. SHAKE removes the bond stretching freedom, which is the fastest motion, and consequently allows a larger timestep to be used. For water models, a special "three-point" algorithm is used.[27] Consequently, to employ TIP3P set  $NTF = NTC = 2$ .

Since SHAKE is an algorithm based on dynamics, the minimizer is not aware of what SHAKE is doing; for this reason, minimizations generally should be carried out without SHAKE. One exception is short minimizations whose purpose is to remove bad contacts before dynamics can begin.

For parallel versions of *sander* only intramolecular atoms can be constrained. Thus, such atoms must be in the same chain of the originating PDB file.

= 1 SHAKE is not performed (default)

## 2.5. General minimization and dynamics parameters

- = 2** bonds involving hydrogen are constrained  
**= 3** all bonds are constrained (not available for parallel or qmmm runs in *sander*)
- tol** Relative geometrical tolerance for coordinate resetting in shake. Recommended maximum: <0.00005 Angstrom Default 0.00001.
- jfastw** Fast water definition flag. By default, the system is searched for water residues, and special routines are used to SHAKE these systems.[27]
- = 0** Normal operation. Waters are identified by the default names (given below), unless they are redefined, as described below.  
**= 4** Do not use the fast SHAKE routines for waters.
- The following variables allow redefinition of the default residue and atom names used by the program to determine which residues are waters.
- WATNAM** The residue name the program expects for water. Default 'WAT'.
- OWTNM** The atom name the program expects for the oxygen of water. Default 'O'.
- HWTNM1** The atom name the program expects for the 1st H of water. Default 'H1'.
- HWTNM2** The atom name the program expects for the 2nd H of water. Default 'H2'.
- noshakemask** String that specifies atoms that are not to be shaken (assuming that *ntc*>1). Any bond that would otherwise be shaken by virtue of the *ntc* flag, but which involves an atom flagged here, will \*not\* be shaken. The syntax for this string is given in Chap. 13.5. Default is an empty string, which matches nothing. A typical use would be to remove SHAKE constraints from all or part of a solute, while still shaking rigid water models like TIPnP or SPC/E. Another use would be to turn off SHAKE constraints for the parts of the system that are being changed with thermodynamic integration, or which are the EVB or quantum regions of the system.
- If this option is invoked, then all parts of the potential must be evaluated, that is, *ntf* must be one. The code enforces this by setting *ntf* to 1 when a *noshakemask* string is present in the input.
- If you want the *noshakemask* to apply to all or part of the water molecules, you must also set *jfastw*=4, to turn off the special code for water SHAKE. (If you are not shaking waters, you presumably also want to issue the "set default FlexibleWater on" command in LEaP; see that chapter for more information.)

### 2.5.10. Water cap

- ivcap** Flag to control cap option. The "cap" refers to a spherical portion of water centered on a point in the solute and restrained by a soft half-harmonic potential. For the best physical realism, this option should be combined with *igb*=10, in order to include the reaction field of waters that are beyond the cap radius.

## 2. Sander basics

- = 0 Cap will be in effect if it is in the *prmtop* file (default).
- = 1 With this option, a cap can be excised from a larger box of water. For this, *cutcap* (i.e., the radius of the cap), *xcap*, *ycap*, and *zcap* (i.e., the location of the center of the cap) need to be specified in the *&cntrl* namelist. Note that the cap parameters must be chosen such that the whole solute is covered by solvent. Solvent molecules (and counterions) located outside the cap are ignored. Although this option also works for minimization and dynamics calculations in general, it is intended to post-process snapshots in the realm of MM-PBSA to get a linear-response approximation of the solvation free energy, output as 'Protein-solvent interactions'.
- = 2 Cap will be inactivated, even if parameters are present in the *prmtop* file.
- = 5 With this option, a shell of water around a solute can be excised from a larger box of water. For this, *cutcap* (i.e., the thickness of the shell) needs to be specified in the *&cntrl* namelist. Solvent molecules (and counterions) located outside the cap are ignored. This option only works for a single-step minimization. It is intended to post-process snapshots in the realm of MM-PBSA to get a linear-response approximation of the solvation free energy, output as 'Protein-solvent interactions'.

*fcap*            The force constant for the cap restraint potential.

*cutcap*        Radius of the cap, if *ivcap=1* is used.

*xcap,ycap,zcap* Location of the cap center, if *ivcap=1* is used.

### 2.5.11. NMR refinement options

(Users should consult the section NMR refinement to see the context of how the following parameters would be used.)

*iscale*        Number of additional variables to optimize beyond the 3N structural parameters. (Default = 0). At present, this is only used with residual dipolar coupling and CSA or pseudo-CSA restraints.

*noeskp*        The NOESY volumes will only be evaluated if  $\text{mod}(\text{nstep}, \text{noeskp}) = 0$ ; otherwise the last computed values for intensities and derivatives will be used. (default = 1, i.e. evaluate volumes at every step)

*ipnlty*        This parameter determines the functional form of the penalty function for NOESY volume and chemical shift restraints.

= 1 the program will minimize the sum of the absolute values of the errors; this is akin to minimizing the crystallographic R-factor (default).

= 2 the program will optimize the sum of the squares of the errors.

= 3 For NOESY intensities, the penalty will be of the form  $awt[I_c^{1/6} - I_o^{1/6}]^2$ . Chemical shift penalties will be as for *ipnlty=1*.

## 2.6. Potential function parameters

mxsub	Maximum number of submolecules that will be used. This is used to determine how much space to allocate for the NOESY calculations. Default 1.
scalm	"Mass" for the additional scaling parameters. Right now they are restricted to all have the same value. The larger this value, the slower these extra variables will respond to their environment. Default 100 amu.
pencut	In the summaries of the constraint deviations, entries will only be made if the penalty for that term is greater than PENCUT. Default 0.1.
tausw	For noesy volume calculations ( <i>NMROPT</i> = 2), intensities with mixing times less than TAUSW (in seconds) will be computed using perturbation theory, whereas those greater than TAUSW will use a more exact theory. See the theory section (below) for details. To always use the "exact" intensities and derivatives, set TAUSW = 0.0; to always use perturbation theory, set TAUSW to a value larger than the largest mixing time in the input. Default is TAUSW of 0.1 second, which should work pretty well for most systems.

### 2.5.12. EMAP constraints

EMAP constraints are used to perform targeted conformational search(TCS). EMAP uses maps to define conformation targets and induce simulation systems to the target conformations. The constraint map can be either obtained from electron microscopy experiments or from known protein structures, or from initial simulation coordinates. EMAP can be used to do rigid docking of molecules into maps and to do flexible fitting to obtain conformations defined by experimental maps. EMAP can also be used to maintain internal conformations of protein domains when studying large scale conformational change. Users should consult the section [6.13](#) to see how to define EMAP constraints.

iemap	Turn on EMAP constrained simulation when <i>iemap</i> >0. (Default = 0). EMAP constraint information need be input from <i>emap</i> namelists in the input file.
-------	--

## 2.6. Potential function parameters

The parameters in this section generally control what sort of force field (or potential function) is used for the simulation.

### 2.6.1. Generic parameters

ntf	Force evaluation. Note: If SHAKE is used (see NTC), it is not necessary to calculate forces for the constrained bonds.  = 1 complete interaction is calculated (default) = 2 bond interactions involving H-atoms omitted (use with NTC=2) = 3 all the bond interactions are omitted (use with NTC=3)
-----	--

## 2. Sander basics

- = 4 angle involving H-atoms and all bonds are omitted
- = 5 all bond and angle interactions are omitted
- = 6 dihedrals involving H-atoms and all bonds and all angle interactions are omitted
- = 7 all bond, angle and dihedral interactions are omitted
- = 8 all bond, angle, dihedral and non-bonded interactions are omitted

**ntb** This variable controls whether or not periodic boundaries are imposed on the system during the calculation of non-bonded interactions. Bonds spanning periodic boundaries are not yet supported. There is no longer any need to set this variable, since it can be determined from *igb* and *ntp* parameters. The “proper” default for *ntb* is chosen (*ntb*=0 when *igb* > 0, *ntb*=2 when *ntp* > 0, and *ntb*=1 otherwise). This behavior can be overridden by supplying an explicit value, although this is discouraged to prevent errors. The allowed values for *NTB* are

- = 0 no periodicity is applied and PME is off (default when *igb* > 0)
- = 1 constant volume (default when *igb* and *ntp* are both 0)
- = 2 constant pressure (default when *ntp* > 0)

If *NTB* .NE. 0, there must be a periodic boundary in the topology file. Constant pressure is not used in minimization (*IMIN*=1, above).

For a periodic system, constant pressure is the only way to equilibrate density if the starting state is not correct. For example, the solvent packing scheme used in LEaP can result in a net void when solvent molecules are subtracted which can aggregate into "vacuum bubbles" in a constant volume run. Another potential problem are small gaps at the edges of the box. The upshot is that almost every system needs to be equilibrated at constant pressure (*ntb*=2, *ntp*>0) to get to a proper density. But be sure to equilibrate first (at constant volume) to something close to the final temperature, before turning on constant pressure.

**dielc** Dielectric multiplicative constant for the electrostatic interactions. Default is 1.0. Please note this is NOT related to dielectric constants for generalized Born or Poisson-Boltzmann calculations. It should only be used for quasi-vacuum simulations, e.g. where one wants  $\epsilon = 4\epsilon_r$ ; in this case you would also set the *eedmeth* variable as well.

**cut** This is used to specify the nonbonded cutoff, in Angstroms. For PME, the cutoff is used to limit direct space sum, and 8.0 is usually a good value. When *igb*>0, the cutoff is used to truncate nonbonded pairs (on an atom-by-atom basis); here a larger value than the default is generally required. A separate parameter (**RGBMAX**) controls the maximum distance between atom pairs that will be considered in carrying out the pairwise summation involved in calculating the effective Born radii, see the generalized Born section below.

When *igb* > 0, the default is 9999.0 (effectively infinite)

When *igb*=0, the default is 8.0.



<b>nsnb</b>	Determines the frequency of nonbonded list updates when <i>igb=0</i> and <i>nbflag=0</i> ; see the description of <i>nbflag</i> for more information. Default is 25.
<b>ipol</b>	When set to 1, use a polarizable force field. See Section 2.6.5 for more information. Default is 0.
<b>ifqnt</b>	Flag for QM/MM run; if set to 1, you must also include a <i>&amp;qmmm</i> namelist. See Section 6.4 for details on this option. Default is 0.
<b>igb</b>	Flag for using the generalized Born or Poisson-Boltzmann implicit solvent models. See Section 3.1 for information about using this option. Default is 0.
<b>irism</b>	Flag for 3D-reference interaction site model (RISM) molecular solvation method. See Section 3.3 for information about this option. Default is 0.
<b>ievb</b>	If set to 1, use the empirical valence bond method to compute energies and forces. See Section 6.3 for information about this option. Default is 0.
<b>iamoeba</b>	Flag for using the <i>amoeba</i> polarizable potentials of Ren and Ponder.[28, 29] When this option is set to 1, you need to prepare an <i>amoeba</i> namelist with additional parameters. Also, the <i>prmtop</i> file is built in a special way. See Section 3.5 for more information about this option. Default is 0.

### 2.6.2. Particle Mesh Ewald

The Particle Mesh Ewald (PME) method is always "on", unless *ntb* = 0. PME is a fast implementation of the Ewald summation method for calculating the full electrostatic energy of a unit cell (periodic box) in a macroscopic lattice of repeating images. The PME method is fast since the reciprocal space Ewald sums are B-spline interpolated on a grid and since the convolutions necessary to evaluate the sums are calculated via fast Fourier transforms. Note that the accuracy of the PME is related to the density of the charge grid (NFFT1, NFFT2, and NFFT3), the spline interpolation order (ORDER), and the direct sum tolerance (DSUM\_TOL); see the descriptions below for more information.

The particle mesh Ewald (PME) method was implemented originally in Amber 3a by Tom Darden, and has been developed in subsequent versions of Amber by many people, in particular by Tom Darden, Celeste Sagui, Tom Cheatham and Mike Crowley.[30–33] Generalizations of this method to systems with polarizable dipoles and electrostatic multipoles is described in Refs. [34, 35].

The *&ewald* namelist is read immediately after the *&cntrl* namelist. We have tried hard to make the defaults for these parameters appropriate for solvated simulations. *Please take care in changing any values from their defaults.* The *&ewald* namelist has the following variables:

**nfft1, nfft2, nfft3** These give the size of the charge grid (upon which the reciprocal sums are interpolated) in each dimension. Higher values lead to higher accuracy (when the DSUM\_TOL is also lowered) but considerably slow the calculation. Generally it has been found that reasonable results are obtained when NFFT1, NFFT2 and NFFT3 are approximately equal to A, B and C, respectively, leading to a grid

## 2. Sander basics

spacing ( $A/NFFT1$ , etc.) of  $1.0 \text{ \AA}$ . Significant performance enhancement in the calculation of the fast Fourier transform is obtained by having each of the integer  $NFFT1$ ,  $NFFT2$  and  $NFFT3$  values be a *product of powers* of 2, 3, and/or 5. If the values are not given, the program will chose values to meet these criteria.

- order      The order of the B-spline interpolation. The higher the order, the better the accuracy (unless the charge grid is too coarse). The minimum order is 3. An order of 4 (the default) implies a cubic spline approximation which is a good standard value. Note that the cost of the PME goes as roughly the order to the third power.
- verbose    Standard use is to have  $VERBOSE = 0$ . Setting  $VERBOSE$  to higher values (up to a maximum of 3) leads to voluminous output of information about the PME run.
- ew\_type    Standard use is to have  $EW\_TYPE = 0$  which turns on the particle mesh ewald (PME) method. When  $EW\_TYPE = 1$ , instead of the approximate, interpolated PME, a *regular* Ewald calculation is run. The number of reciprocal vectors used depends upon  $RSUM\_TOL$ , or can be set by the user. The exact Ewald summation is present mainly to serve as an accuracy check allowing users to determine if the PME grid spacing, order and direct sum tolerance lead to acceptable results. Although the cost of the exact Ewald method formally increases with system size at a much higher rate than the PME, it may be faster for small numbers of atoms ( $< 500$ ). For larger, macromolecular systems, with  $> 500$  atoms, the PME method is significantly faster.
- dsum\_tol   This relates to the width of the direct sum part of the Ewald sum, requiring that the value of the direct sum at the Lennard-Jones cutoff value (specified in  $CUT$  as during standard dynamics) be less than  $DSUM\_TOL$ . In practice it has been found that the relative error in the Ewald forces (RMS) due to cutting off the direct sum at  $CUT$  is between 10.0 and 50.0 times  $DSUM\_TOL$ . Standard values for  $DSUM\_TOL$  are in the range of  $10^{-6}$  to  $10^{-5}$ , leading to estimated RMS deviation force errors of 0.00001 to 0.0005. Default is  $10^{-5}$ .
- rsum\_tol   This serves as a way to generate the number of reciprocal vectors used in an Ewald sum. Typically the relative RMS reciprocal sum error is about 5-10 times  $RSUM\_TOL$ . Default is  $5 \times 10^{-5}$ .
- mlimit(1,2,3) This allows the user to explicitly set the number of reciprocal vectors used in a regular Ewald run. Note that the sum goes from  $-MLIMIT(2)$  to  $MLIMIT(2)$  and  $-MLIMIT(3)$  to  $MLIMIT(3)$  with symmetry being used in first dimension. Note also the sum is truncated outside an automatically chosen sphere.
- ew\_coeff    Ewald coefficient, in  $\text{\AA}^{-1}$ . Default is determined by  $dsum\_tol$  and  $cutoff$ . If it is explicitly inputted then that value is used, and  $dsum\_tol$  is computed from  $ew\_coeff$  and  $cutoff$ .
- nbflag     If  $nbflag = 0$ , construct the direct sum nonbonded list in the "old" way, *i.e.* update the list every  $nsnb$  steps. If  $nbflag = 1$  (the default when  $imin = 0$  or  $ntb > 0$ ),

- nsnb* is ignored, and the list is updated whenever any atom has moved more than  $1/2$  *skinb* since the last list update.
- skinb** Width of the nonbonded "skin". The direct sum nonbonded list is extended to *cut* + *skinb*, and the van der Waals and direct electrostatic interactions are truncated at *cut*. Default is 2.0 Å. Use of this parameter is required for energy conservation, and recommended for all PME runs.
- nbtell** If *nbtell* = 1, a message is printed when any atom has moved far enough to trigger a list update. Use only for debugging or analysis. Default of 0 inhibits the message.
- netfrc** The basic "smooth" PME implementation used here does not necessarily conserve momentum. If *netfrc* = 1, (the default) the total force on the system is artificially removed at every step. This parameter is set to 0 if minimization is requested, which implies that the gradient is an accurate derivative of the energy. You should only change this parameter if you really know what you are doing.
- vdwmeth** Determines the method used for van der Waals interactions beyond those included in the direct sum. A value of 0 includes no correction; the default value of 1 uses a continuum model correction for energy and pressure.
- eedmeth** Determines how the switch function for the direct sum Coulomb interaction is evaluated. The default value of 1 uses a cubic spline. A value of 2 implies a linear table lookup. A value of three implies use of an "exact" subroutine call. When *eedmeth*=4, no switch is used (*i.e.* the bare Coulomb potential is evaluated in the direct sum, cut off sharply at CUT). When *eedmeth*=5, there is no switch, and a distance-dependent dielectric is used (*i.e.* the distance dependence is  $1/r^2$  rather than  $1/r$ ). The last two options are intended for non-periodic calculations, where no reciprocal term is computed.
- eedtdbns** Density of spline or linear lookup table, if *eedmeth* is 1 or 2. Default is 500 points per unit.
- column\_fft** 1 or 0 flag to turn on or off, respectively, column-mode fft for parallel runs. The default mode is slab mode which is efficient for low processor counts. The column method can be faster for larger processor counts since there can be more columns than slabs and the communications pattern is less congested. This flag has no effect on non-parallel runs. Users should test the efficiency of the method in comparison to the default method before performing long calculations. Default is 0 (off).

### 2.6.3. Using IPS for the calculation of nonbonded interactions

Isotropic Periodic Sum (IPS) is a method for long-range interaction calculation.[36–41] Unlike Ewald method, which uses periodic boundary images to calculate long range interactions, IPS uses isotropic periodic images of a local region to calculate the long-range contributions.

The IPS method in the current version is different from that implemented in Amber10. All IPS potentials use rationalized polynomial forms and the electrostatic interaction is calculated

## 2. Sander basics

using the polar IPS potential [Wu09]. In addition, 3D IPS/DFFT algorithm [Wu08] is implemented to handle heterogeneous systems as well as finite systems. A homogeneous system is defined as the one where a cutoff region (with *cut* as its radius) has similar composition throughout the system, such as small molecular solutions. Otherwise, a system is defined as a heterogeneous system, such as interfacial systems or finite systems. For heterogeneous systems, a local region larger than the cutoff region, normally equal or larger than the periodic boundary box, must be used to produce accurate long range interactions. For homogeneous systems, it is recommended to use the 3D IPS method ( $ips \leq 3$ ), which uses the cutoff distance, *cut*, to define the local region radius. *cut* is typically around 10 Å. The 3D IPS/DFFT method ( $ips \geq 4$ ) can be used for any type of systems, but is recommended for heterogeneous systems due to extra discrete fast Fourier transform (DFFT) expense.

**ips** Flag to control nonbonded interaction calculation method. The *cut* value will be used to define the local region radius for  $ips \leq 3$ . When IPS is used for electrostatic interaction, PME will be turned off.

= 0 IPS will not be used (default).

= 1 3D IPS will be used for both electrostatic and L-J interactions.

= 2 3D IPS will be used only for electrostatic interactions.

= 3 3D IPS will be used only for L-J interactions.

= 4 3D IPS/DFFT will be used for both electrostatic and L-J interactions.

= 5 3D IPS/DFFT will be used only for electrostatic interactions.

= 6 3D IPS/DFFT will be used only for L-J interactions.

**raips** Local region radius. *raips* is automatically set to *cut* for 3D IPS calculations ( $ips \leq 3$ ) and should be set larger than *cut* for 3D IPS/DFFT calculations ( $ips \geq 4$ ). A negative value indicates that it is set to the longest box side of a simulation system. For finite systems, i.e., system without periodic boundary conditions, *raips*=∞, which corresponding no image interaction. The default value is -1 Å.

**mipxs,mipsy,mipsz** Number of grids along three periodic boundary sides when using 3D IPS/DFFT method ( $ips \geq 4$ ). Negative values indicate they are calculated based on the grid size, *gridips*. Typical numbers are the lengths of box sides (in Å) divided by 2 Å. Default values are -1. When  $ips=6$  and PME is used for electrostatic interaction, they are set to *nfft1*, *nfft2*, and *nfft3* defined for PME, respectively.

**mipso** The order of the B-spline interpolation ( $ips \geq 4$ ). The higher the order, the better the accuracy (unless the charge grid is too coarse). The minimum order is 3. An order of 4 (the default) implies a cubic spline approximation which is a good standard value. The cost for the DFFT calculation goes as roughly the order to the third power. For  $ips=6$  and PME is used to electrostatic interaction, it is set to *order* defined for PME.

**gridips** Grid size for 3D IPS/DFFT calculation ( $ips \geq 4$ ). The default value is 2 Å.

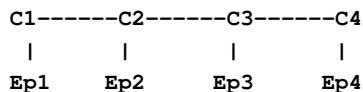
**dvbips** Volume tolerance for updating IPS function grids ( $ips \geq 4$ ). When volume changes like in *NPT* simulations, the grid size changes and IPS function on grid points need be updated. The updating only happens when the volume change ratio is more than *dvbips*. The default value is  $1 \times 10^{-8}$ .

#### 2.6.4. Extra point options

Several parameters deal with "extra-points" (sometimes called lone-pairs), which are force centers that are not at atomic positions. These are currently defined as atoms with "EP" in their names. These input variables are really only for the convenience of force-field developers; *do not change the defaults unless you know what you are doing, and have read the code*. These variables are set in the &ewald namelist.

**frameon** If *frameon* is set to 1, (default) the bonds, angles and dihedral interactions involving the lone pairs/extra points are removed except for constraints added during parm. The lone pairs are kept in ideal geometry relative to local atoms, and resulting torques are transferred to these atoms. To treat extra points as regular atoms, set *frameon*=0.

**chnghmask** If *chnghmask*=1 (default), new 1-1, 1-2, 1-3 and 1-4 interactions are calculated. An extra point belonging to an atom has a 1-1 interaction with it, and participates in any 1-2, 1-3 or 1-4 interaction that atom has. For example, suppose (excusing the geometry) C1,C2,C3,C4 form a dihedral and each has 1 extra point attached as below



The 1-4 interactions include C1-C4, Ep1-C4, C1-Ep4, and Ep1-Ep4. (To see a printout of all 1-1, 1-2, 1-3 and 1-4 interactions set *verbose*=1.) These interactions are masked out of nonbonds. Thus the amber mask list is rebuilt from these 1-1, 1-2, 1-3 and 1-4 pairs. A separate list of 1-4 nonbonds is then compiled. This list does not agree in general with the above 1-4, since a 1-4 could also be a 1-3 if its in a ring. See the *ephi()* routine for the precise algorithm involved here. The list of 1-4 nonbonds is printed if *verbose*=1.

#### 2.6.5. Polarizable potentials

The following parameters are relevant for *polarizable potentials*, that is, when *ipol* is set to 1 in the &cntrl namelist. These variables are set in the &ewald namelist.

**indmeth** If *indmeth* is 0, 1, or 2 then the nonbond force is called iteratively until successive estimates of the induced dipoles agree to within DIPTOL (default 0.0001 debye) in the root mean square sense. The difference between *indmeth* = 0, 1, or 2 have to do with the level of extrapolation (1st, 2nd or 3rd-order) used from previous time steps for the initial guess for dipoles to begin the iterative loop. So far 2nd order (*indmeth*=1) seems to work best.

## 2. Sander basics

	If <code>indmeth = 3</code> , use a Car-Parinello scheme wherein dipoles are assigned a fictitious mass and integrated each time step. This is much more efficient and is the current default. Note that this method is unstable for $dt > 1$ fs.
<code>diptol</code>	Convergence criterion for dipoles in the iterative methods. Default is 0.0001 Debye.
<code>maxiter</code>	For iterative methods ( <code>indmeth &lt; 3</code> ), this is the maximum number of iterations allowed per time step. Default is 20.
<code>dipmass</code>	The fictitious mass assigned to dipoles. Default value is 0.33, which works well for 1fs time steps. If <code>dipmass</code> is set much below this, the dynamics are rapidly unstable. If set much above this the dynamics of the system are affected.
<code>diptau</code>	This is used for temperature control of the dipoles (for <code>indmeth=3</code> ). If <code>diptau</code> is greater than 10 (ps units) temperature control of dipoles is turned off. Experiments so far indicate that running the system in NVE with no temperature control on induced dipoles leads to a slow heating, barely noticeable on the 100ps time scale. For runs of length 10ps, the energy conservation with this method rivals that of SPME for standard fixed charge systems. For long runs, we recommend setting a weak temperature control (e.g. 9.99 ps) on dipoles as well as on the atoms. Note that to achieve good energy conservation with iterative method, the <code>diptol</code> must be below $10^{-7}$ debye, which is much more expensive. Default is 11 ps ( <i>i.e.</i> default is turned off).
<code>irstdip</code>	If <code>indmeth=3</code> , a restart file for dipole positions and velocities is written along with the restart for atomic coordinates and velocities. If <code>irstdip=1</code> , the dipolar positions and velocities from the <code>inpdip</code> file are read in. If <code>irstdip=0</code> , an iterative method is used for step 1, after which Car-Parrinello is used.
<code>scaldip</code>	To scale 1-4 charge-dipole and dipole-dipole interactions the same as 1-4 charge-charge ( <i>i.e.</i> divided by <code>scee</code> ) set <code>scaldip=1</code> (default). If <code>scaldip=0</code> the 1-4 charge-dipole and dipole-dipole interactions are treated the same as other dipolar interactions ( <i>i.e.</i> divided by 1).

### 2.6.6. Dipole Printing

By including a `&dipoles` namelist containing a series of groups, at the end of the input file, the printing of permanent, induced and total dipoles is enabled.

The X, Y and Z components of the dipole (in debye) for each group will be written to `mdout` every NTPR steps. In order to avoid ambiguity with charged groups all of the dipoles for a given group are calculated with respect to the centre of mass of that group.

It should be noted that the permanent, inducible and total dipoles will be printed regardless of whether a *polarizable potential* is in use. However, only the permanent dipole will have any physical meaning when *non-polarizable potentials* are in use.

It should also be noted that the groups used in the dipole printing routines are not exclusive to these routines and so the dipole printing procedure can only be used when group input is *not* in use for something else (*i.e.* restraints).

### 2.6.7. Detailed MPI Timings

`profile_mpi` Adjusts whether detailed per thread timings should be written to a file called `profile_mpi` when running `sander` in parallel. By default only average timings are printed to the output file. This is done for performance reasons, especially when running multisander runs. However for development it is useful to know the individual timings for each mpi thread. When running in serial the value of `profile_mpi` is ignored.

= 0 No detailed MPI timings will be written (default).

= 1 A detailed breakdown of the timings for each MPI thread will be written to the file: `profile_mpi`.

## 2.7. Varying conditions

This section of information is read (if `NMROPT > 0`) as a series of namelist specifications, with name "&wt". This namelist is read repeatedly until a namelist &wt statement is found with `TYPE=END`.

`TYPE` Defines quantity being varied; valid options are listed below.

`ISTEP1,ISTEP2` This change is applied over steps/iterations `ISTEP1` through `ISTEP2`. If `ISTEP2 = 0`, this change will remain in effect from step `ISTEP1` to the end of the run at a value of `VALUE1` (`VALUE2` is ignored in this case). (*default= both 0*)

`VALUE1,VALUE2` Values of the change corresponding to `ISTEP1` and `ISTEP2`, respectively. If `ISTEP2=0`, the change is fixed at `VALUE1` for the remainder of the run, once step `ISTEP1` is reached.

`IINC` If `IINC > 0`, then the change is applied as a step function, with `IINC` steps/iterations between each change in the target `VALUE` (ignored if `ISTEP2=0`). If `IINC =0`, the change is done continuously. (*default=0*)

`IMULT` If `IMULT=0`, then the change will be linearly interpolated from `VALUE1` to `VALUE2` as the step number increases from `ISTEP1` to `ISTEP2`. (*default*) If `IMULT=1`, then the change will be effected by a series of multiplicative scalings, using a single factor, `R`, for all scalings. i.e.

$$\text{VALUE2} = (\text{R}^{**}\text{INCREMENTS}) * \text{VALUE1}.$$

`INCREMENTS` is the number of times the target value changes, which is determined by `ISTEP1`, `ISTEP2`, and `IINC`.

The remainder of this section describes the options for the `TYPE` parameter. For a few types of cards, the meanings of the other variables differ from that described above; such differences are noted below. Valid Options for `TYPE` (you must use uppercase) are:

## 2. Sander basics

BOND	Varies the relative weighting of bond energy terms.
ANGLE	Varies the relative weighting of valence angle energy terms.
TORSION	Varies the relative weighting of torsion (and J-coupling) energy terms. Note that any restraints defined in the input to the PARM program are included in the above. Improper torsions are handled separately (IMPROP).
IMPROP	Varies the relative weighting of the "improper" torsional terms. These are not included in TORSION.
VDW	Varies the relative weighting of van der Waals energy terms. This is equivalent to changing the well depth (epsilon) by the given factor.
HB	Varies the relative weighting of hydrogen-bonding energy terms.
ELEC	Varies the relative weighting of electrostatic energy terms.
NB	Varies the relative weights of the non-bonded (VDW, HB, and ELEC) terms.
ATTRACT	Varies the relative weights of the attractive parts of the van der waals and h-bond terms.
REPULSE	Varies the relative weights of the repulsive parts of the van der waals and h-bond terms.
RSTAR	Varies the effective van der Waals radii for the van der Waals (VDW) interactions by the given factor. Note that this is done by changing the relative attractive and repulsive coefficients, so ATTRACT/REPULSE should not be used over the same step range as RSTAR.
INTERN	Varies the relative weights of the BOND, ANGLE and TORSION terms. "Improper" torsions (IMPROP) must be varied separately.
ALL	Varies the relative weights of all the energy terms above (BOND, ANGLE, TORSION, VDW, HB, and ELEC; does not affect RSTAR or IMPROP).
REST	Varies the relative weights of *all* the NMR restraint energy terms.
RESTS	Varies the weights of the "short-range" NMR restraints. Short-range restraints are defined by the SHORT instruction (see below).
RESTL	Varies the weights of any NMR restraints which are not defined as "short range" by the SHORT instruction (see below). When no SHORT instruction is given, RESTL is equivalent to REST.
NOESY	Varies the overall weight for NOESY volume restraints. Note that this value multiplies the individual weights read into the "awt" array. (Only if NMROPT=2; see Section 4 below).



**SHIFTS** Varies the overall weight for chemical shift restraints. Note that this value multiplies the individual weights read into the "wt" array. (Only if NMROPT=2; see section 4 below).

**SHORT** Defines the short-range restraints. For this instruction, ISTEP1, ISTEP2, VALUE1, and VALUE2 have different meanings. A short-range restraint can be defined in two ways.

(1) If the residues containing each pair of bonded atoms comprising the restraint are close enough in the primary sequence:

$$\text{ISTEP1} \leq \text{ABS}(\text{delta\_residue}) \leq \text{ISTEP2},$$

where delta\_residue is the difference in the numbers of the residues containing the pair of bonded atoms.

(2) If the distances between each pair of bonded atoms in the restraint fall within a prescribed range:

$$\text{VALUE1} \leq \text{distance} \leq \text{VALUE2}.$$

Only one SHORT command can be issued, and the values of ISTEP1, ISTEP2, VALUE1, and VALUE2 remain fixed throughout the run. However, if IINC>0, then the short-range interaction list will be re-evaluated every IINC steps.

**TGTRMSD** Varies the RMSD target value for targeted MD.

**TEMP0** Varies the target temperature TEMP0.

**TEMP0LES** Varies the LES target temperature TEMP0LES.

**TAUTP** Varies the coupling parameter, TAUTP, used in temperature scaling when temperature coupling options NTT=1 is used.

**CUT** Varies the non-bonded cutoff distance.

**NSTEP0** If present, this instruction will reset the initial value of the step counter (against which ISTEP1/ISTEP2 and NSTEP1/NSTEP2 are compared) to the value ISTEP1. This only affects the way in which NMR weight restraints are calculated. It does not affect the value of NSTEP that is printed as part of the dynamics output. An NSTEP0 instruction only has an effect at the beginning of a run. For this card (only) ISTEP2, VALUE1, VALUE2 and IINC are ignored. If this card is omitted, NSTEP0 = 0. This card can be useful for simulation restarts, where NSTEP0 is set to the final step on the previous run.

**STPMLT** If present, the NMR step counter will be changed in increments of STPMLT for each actual dynamics step. For this card, only VALUE1 is read. ISTEP1, ISTEP2, VALUE2, IINC, and IMULT are ignored. Default = 1.0.

## 2. Sander basics

DISAVE, ANGAVE, TORAVE If present, then by default time-averaged values (rather than instantaneous values) for the appropriate set of restraints will be used. DISAVE controls distance data, ANGAVE controls angle data, TORAVE controls torsion data. See below for the functional form used in generating time-averaged data.

For these cards: VALUE1 =  $\tau$  (characteristic time for exponential decay) VALUE2 = POWER (power used in averaging; the nearest integer of value2 is used) Note that the range (ISTEP1→ISTEP2) applies only to TAU; The value of POWER is not changed by subsequent cards with the same ITYPE field, and time-averaging will always be turned on for the entire run if one of these cards appears.

Note also that, due to the way that the time averaged internals are calculated, changing  $\tau$  at any time after the start of the run will only affect the relative weighting of steps occurring after the change in  $\tau$ . Separate values for  $\tau$  and POWER are used for bond, angle, and torsion averaging.

The default value of  $\tau$  (if it is 0.0 here) is 1.0D+6, which results in no exponential decay weighting. Any value of  $\tau \geq 1.0D+6$  will result in no exponential decay.

If DISAVE, ANGAVE, or TORAVE is chosen, one can still force use of an instantaneous value for specific restraints of the particular type (bond, angle, or torsion) by setting the IFNTYP field to "1" when the restraint is defined (IFNTYP is defined in the DISANG file).

If time-averaging for a particular class of restraints is being performed, all restraints of that class that are being averaged (that is, all restraints of that class except those for which IFNTYP=1) *must* have the same values of NSTEP1 and NSTEP2 (NSTEP1 and NSTEP2 are defined below). (For these cards, IINC and IMULT are ignored) See the discussion of time-averaged restraints following the input descriptions.

### DISAVI, ANGAVI, TORAVI

**ISTEP1:** Ignored.

**ISTEP2:** Sets IDMPAV. If IDMPAV > 0, *and* a dump file has been specified (DUMPAVE is set in the file redirection section below), then the time-averaged values of the restraints will be written every IDMPAV steps. Only one value of IDMPAV can be set (corresponding to the first DISAVI/ANGAVI/TORAVI card with ISTEP2 > 0), and *all* restraints (even those with IFNTYP=1) will be "dumped" to this file every IDMPAV steps. The values reported reflect the current value of  $\tau$ .

**VALUE1:** The integral which gives the time-averaged values is undefined for the first step. By default, for each time-averaged internal, the integral is assigned the current value of the internal on the first step. If VALUE1 $\neq$ 0, this initial value of internal r is reset as follows:

```
-1000. < VALUE1 < 1000.: Initial value = r_initial + VALUE1
VALUE1 <= -1000.: Initial value = r_target + 1000.
1000. <= VALUE1 : Initial value = r_target - 1000.
```

$r\_target$  is the target value of the internal, given by R2+R3 (or just R3, if R2 is 0). VALUE1 is in angstroms for bonds, in degrees for angles.

**VALUE2:** This field can be used to set the value of  $\tau$  used in calculating the time-averaged values of the internal restraints reported at the end of a simulation (if LISTOUT is specified in the redirection section below). By default, no exponential decay weighting is used in calculating the final reported values, regardless of what value of  $\tau$  was used during the simulation. If VALUE2>0, then  $\tau = \text{VALUE2}$  will be used in calculating these final reported averages. Note that the value of VALUE2 =  $\tau$  specified here only affects the reported averaged values in at the end of a simulation. It does not affect the time-averaged values used during the simulation (those are changed by the VALUE1 field of DISAVE, ANGAVE and TORAVE instructions).

**IINC:** If IINC = 0, then forces for the class of time-averaged restraints will be calculated exactly as  $(dE/dr\_ave)$   $(dr\_ave/dx)$ . If IINC = 1, then then forces for the class of time-averaged restraints will be calculated as  $(dE/dr\_ave)$   $(dr(t)/dx)$ . Note that this latter method results in a non-conservative force, and does not integrate to a standard form. But this latter formulation helps avoid the large forces due to the  $(1+i)$  term in the exact derivative calculation—and may avert instabilities in the molecular dynamics trajectory for some systems. See the discussion of time-averaged restraints following the input description. Note that the DISAVI, ANGAVI, and TORAVI instructions will have no affect unless the corresponding time average request card (DISAVE, ANGAVE or TORAVE, respectively) is also present.

DUMPFREQ Istep1 is the only parameter read, and it sets the frequency at which the coordinates in the distance or angle restraints are dumped to the file specified by the DUMPAVE command in the I/O redirection section. (For these cards, ISTEP1 and IMULT are ignored).

END        END of this section.

**NOTES:**

1. All weights are relative to a default of 1.0 in the standard force field.
2. Weights are not cumulative.
3. For any range where the weight of a term is not modified by the above, the weight reverts to 1.0. For any range where TEMPO, SOFTR or CUTOFF is not specified, the value of the relevant constant is set to that specified in the input file.
4. If a weight is set to 0.0, it is set internally to 1.0D-7. This can be overridden by setting the weight to a negative number. In this case, a weight of exactly 0.0 will be used. *However*, if any weight is set to exactly 0.0, it cannot be changed again during this run of the program.
5. If two (or more) cards change a particular weight over the same range, the weight given on the last applicable card will be the one used.

## 2. Sander basics

6. Once any weight change for which NSTEP2=0 becomes active (i.e. one which will be effective for the remainder of the run), the weight of this term cannot be further modified by other instructions.
7. Changes to RSTAR result in exponential weighting changes to the attractive and repulsive terms (proportional to the scale factor\*\*6 and \*\*12, respectively). For this reason, scaling RSTAR to a very small value (e.g.  $\leq 0.1$ ) may result in a zeroing-out of the vdw term.

## 2.8. File redirection commands

Input/output redirection information can be read as described here. Redirection cards must follow the end of the weight change information. Redirection card input is terminated by the first non-blank line which does not start with a recognized redirection TYPE (e.g. LISTIN, LISTOUT, etc.).

The format of the redirection cards is

TYPE = filename

where TYPE is any valid redirection keyword (see below), and filename is any character string. The equals sign ("=") is required, and TYPE must be given in *uppercase* letters.

Valid redirection keywords are:

- LISTIN     An output listing of the restraints which have been read, and their deviations from the target distances *before* the simulation has been run. By default, this listing is not printed. If POUT is used for the filename, these deviations will be printed in the normal output file.
- LISTOUT    An output listing of the restraints which have been read, and their deviations from the target distances *\_after* the simulation has finished. By default, this listing is not printed. If POUT is used for the filename, these deviations will be printed in the normal output file.
- DISANG     The file from which the distance and angle restraint information described below (Section 6.1) will be read.
- NOESY     File from which NOESY volume information (Section 6.2) will be read.
- SHIFTS     File from which chemical shift information (Section 6.3) will be read.
- PCSHIFT    File from which paramagnetic shift information (Section 6.3) will be read.
- DIPOLE     File from which residual dipolar couplings (Section 6.5) will be read.
- CSA        File from which CSA or pseduo-CSA restraints (Section 6.6) will be read.
- DUMPAVE    File to which the time-averaged values of all restraints will be written. If DISAVI / ANGAVI / TORAVI has been used to set IDMPAV $\neq$ 0, then averaged values will be output. If the DUMPFREQ command has been used, the instantaneous values will be output.

## 2.9. Getting debugging information

The debug options in *sander* are there principally to help developers test new options or to test results between two machines or versions of code, but can also be useful to users who want to test the effect of parameters on the accuracy of their ewald or pme calculations. If the debug options are set, *sander* will exit after performing the debug tasks set by the user.

To access the debug options, include a `&debugf` namelist. Input parameters are:

`do_debugf` Flag to perform this module. Possible values are zero or one. Default is zero. Set to one to turn on debug options.

One set of options is to test that the atomic forces agree with numerical differentiation of energy.

`atomn` Array of atom numbers to test atomic forces on. Up to 25 atom numbers can be specified, separated by commas.

`nranatm` number of random atoms to test atomic forces on. Atom numbers are generated via a random number generator.

`ransed` seed of random number generator used in generating atom numbers default is 71277

`neglghdel` negative log of delta used in numerical differentiating; e.g. 4 means delta is  $10^{-4}$  Angstroms. Default is 5. *Note:* In general it does no good to set `neglghdel` larger than about 6. This is because the relative force error is at best the square root of the numerical error in the energy, which ranges from  $10^{-15}$  up to  $10^{-12}$  for energies involving a large number of terms.

`chkvir` Flag to test the atomic and molecular virials numerically. Default is zero. Set to one to test virials.

`dumpfrfc` Flag to dump energies, forces and virials, as well as components of forces (bond, angle forces etc.) to the file "forcedump.dat" This produces an ascii file. Default is zero. Set to one to dump forces.

`rmsfrfc` Flag to compare energies forces and virials as well as components of forces (bond, angle forces etc.) to those in the file "forcedump.dat". Default is zero. Set to one to compare forces.

Several other options are also possible to modify the calculated forces.

`zerochg` Flag to zero all charges before calculating forces. Default zero. Set to one to remove charges.

`zerovdw` Flag to remove all van der Waals interactions before calculating forces. Default zero. Set to one to remove van der Waals.

`zerodip` Flag to remove all atomic dipoles before calculating forces. Only relevant when polarizability is invoked.

## 2. Sander basics

do\_dir, do\_rec, do\_adj, do\_self, do\_bond, do\_cbond, do\_angle, do\_ephi, do\_xconst, do\_cap These are flags which turn on or off the subroutines they refer to. The defaults are one. Set to zero to prevent a subroutine from running. For example, set do\_dir=0 to turn off the direct sum interactions (van der Waals as well as electrostatic). These options, as well as the zerochg, zerovdw, zerodip flags, can be used to fine tune a test of forces, accuracy, etc.

### EXAMPLES:

This input list tests the reciprocal sum forces on atom 14 numerically, using a delta of  $10^{-4}$ .

```
&debugf
neglgdel=4, nranatm = 0, atomn = 14,
do_debugf = 1, do_dir = 0, do_adj = 0, do_rec = 1, do_self = 0,
do_bond = 1, do_angle = 0, do_ephi = 0, zerovdw = 0, zerochg = 0,
chkvir = 0,
dumpfrc = 0,
rmsfrc = 0,
/
```

This input list causes a dump of force components to "forcedump.dat". The bond, angle and dihedral forces are not calculated, and van der Waals interactions are removed, so the total force is the Ewald electrostatic force, and the only non-zero force components calculated are electrostatic.

```
&debugf
neglgdel=4, nranatm = 0, atomn = 0,
do_debugf = 1, do_dir = 1, do_adj = 1, do_rec = 1, do_self = 1,
do_bond = 0, do_angle = 0, do_ephi = 0, zerovdw = 1, zerochg = 0,
chkvir = 0,
dumpfrc = 1,
rmsfrc = 0,
/
```

In this case the same force components as above are calculated, and compared to those in "forcedump.dat". Typically this is used to get an RMS force error for the Ewald method in use. To do this, when doing the force dump use ewald or pme parameters to get high accuracy, and then normal parameters for the force compare:

```
&debugf
neglgdel=4, nranatm = 0, atomn = 0,
do_debugf = 1, do_dir = 1, do_adj = 1, do_rec = 1, do_self = 1,
do_bond = 0, do_angle = 0, do_ephi = 0, zerovdw = 1, zerochg = 0,
chkvir = 0,
dumpfrc = 0,
rmsfrc = 1,
/
```

## 2.9. Getting debugging information

For example, if you have a 40x40x40 unit cell and want to see the error for default pme options (cubic spline, 40x40x40 grid), run 2 jobs—— (assume box params on last line of inpcrd file)

Sample input for 1st job:

```
&cntrl
dielc =1.0,
cut = 11.0, nsnb = 5, ibelly = 0,
ntx = 7, irest = 1,
ntf = 2, ntc = 2, tol = 0.0000005,
ntb = 1, ntp = 0, temp0 = 300.0, tautp = 1.0,
nstlim = 1, dt = 0.002, maxcyc = 5, imin = 0, ntmin = 2,
ntpr = 1, ntwx = 0, ntt = 0, ntr = 0,
jfastw = 0, nmrmax=0, ntave = 25,
/
&debugf
do_debugf = 1,do_dir = 1,do_adj = 1,do_rec = 1, do_self = 1,
do_bond = 0,do_angle = 0,do_ephi = 0, zerovdw = 1, zerochg = 0,
chkvir = 0,
dumpfrc = 1,
rmsfrc = 0,
/
&ewald
nfft1=60,nfft2=60,nfft3=60,order=6, ew_coeff=0.35,
/
```

Sample input for 2nd job:

```
&cntrl
dielc =1.0,
cut = 8.0, nsnb = 5, ibelly = 0,
ntx = 7, irest = 1,
ntf = 2, ntc = 2, tol = 0.0000005,
ntb = 1, ntp = 0, temp0 = 300.0, tautp = 1.0,
nstlim = 1, dt = 0.002, maxcyc = 5, imin = 0, ntmin = 2,
ntpr = 1, ntwx = 0, ntt = 0, ntr = 0,
jfastw = 0, nmrmax=0, ntave = 25,
/
&debugf
do_debugf = 1,do_dir = 1,do_adj = 1,do_rec = 1, do_self = 1,
do_bond = 0,do_angle = 0,do_ephi = 0, zerovdw = 1, zerochg = 0,
chkvir = 0,
dumpfrc = 0,
rmsfrc = 1,
/
&ewald
ew_coeff=0.35,
/
```

## 2. *Sander basics*

Note that an Ewald coefficient of 0.35 is close to the default error for an 8 Angstrom cutoff. However, the first job used an 11 Angstrom cutoff. The direct sum forces calculated in the 2nd job are compared to these, giving the RMS error due to an 8 Angstrom cutoff, with this value of `ew_coeff`. The reciprocal sum error calculated in the 2nd job is with respect to the pme reciprocal forces in the 1st job considered as "exact".

Note further that if in these two jobs you had not specified "`ew_coeff`" *sander* would have calculated `ew_coeff` according to the cutoff and the direct sum tolerance, defaulted to  $10^{-5}$ . This would give two different ewald coefficients. Under these circumstances the direct, reciprocal and adjust energies and forces would not agree well between the two jobs. However the total energy and forces should agree reasonably, (forces to within about  $5 \times 10^{-4}$  relative RMS force error) Since the totals are invariant to the coefficient.

Finally, note that if other force components are calculated, such as van der Waals, bond, angle, etc., then the total force will include these, and the relative RMS force errors will be with respect to this total force in the denominator.



## 3. Force field modifications

This chapter provides a number of sections describing how to use *sander* for particular types of problems. It should be read in conjunction with the previous chapter.

### 3.1. The Generalized Born/Surface Area Model

The generalized Born solvation model can be used instead of explicit water for non-polarizable force fields; it has been most widely tested on ff99SB, but in principle could be used with other non-polarizable force fields, such as ff03. To estimate the total solvation free energy of a molecule,  $\Delta G_{solv}$ , one typically assumes that it can be decomposed into the "electrostatic" and "non-electrostatic" parts:

$$\Delta G_{solv} = \Delta G_{el} + \Delta G_{nonel} \quad (3.1)$$

where  $\Delta G_{nonel}$  is the free energy of solvating a molecule from which all charges have been removed (i.e. partial charges of every atom are set to zero), and  $\Delta G_{el}$  is the free energy of first removing all charges in the vacuum, and then adding them back in the presence of a continuum solvent environment. Generally speaking,  $\Delta G_{nonel}$  comes from the combined effect of two types of interaction: the favorable van der Waals attraction between the solute and solvent molecules, and the unfavorable cost of breaking the structure of the solvent (water) around the solute. In the current Amber codes, this is taken to be proportional to the total solvent accessible surface area (SA) of the molecule, with a proportionality constant derived from experimental solvation energies of small non-polar molecules, and uses a fast LCPO algorithm [42] to compute an analytical approximation to the solvent accessible area of the molecule.

The Poisson-Boltzmann approach described in the next section has traditionally been used in calculating  $\Delta G_{el}$ . However, in molecular dynamics applications, the associated computational costs are often very high, as the Poisson-Boltzmann equation needs to be solved every time the conformation of the molecule changes. Amber developers have pursued an alternative approach, the analytic generalized Born (GB) method, to obtain a reasonable, computationally efficient estimate to be used in molecular dynamics simulations. The methodology has become popular,[43–50] especially in molecular dynamics applications,[51–54] due to its relative simplicity and computational efficiency, compared to the more standard numerical solution of the Poisson-Boltzmann equation. Within Amber GB models, each atom in a molecule is represented as a sphere of radius  $R_i$  with a charge  $q_i$  at its center; the interior of the atom is assumed to be filled uniformly with a material of dielectric constant 1. The molecule is surrounded by a solvent of a high dielectric  $\epsilon$  (80 for water at 300 K). The GB model approximates  $\Delta G_{el}$  by an analytical formula,[43, 55]

### 3. Force field modifications

$$\Delta G_{el} = -\frac{1}{2} \sum_{ij} \frac{q_i q_j}{f_{GB}(r_{ij}, R_i, R_j)} \left( 1 - \frac{\exp[-\kappa f_{GB}]}{\epsilon} \right) \quad (3.2)$$

where  $r_{ij}$  is the distance between atoms  $i$  and  $j$ , the  $R_i$  are the so-called *effective Born radii*, and  $f_{GB}()$  is a certain smooth function of its arguments. The electrostatic screening effects of (monovalent) salt are incorporated [55] via the Debye-Huckel screening parameter  $\kappa$ .

A common choice [43] of  $f_{GB}$  is

$$f_{GB} = [r_{ij}^2 + R_i R_j \exp(-r_{ij}^2/4R_i R_j)]^{1/2} \quad (3.3)$$

although other expressions have been tried.[46, 56] The effective Born radius of an atom reflects the degree of its burial inside the molecule: for an isolated ion, it is equal to its van der Waals (VDW) radius  $\rho_i$ . Then one obtains the particularly simple form:

$$\Delta G_{el} = -\frac{q_i^2}{2\rho_i} \left( 1 - \frac{1}{\epsilon} \right) \quad (3.4)$$

where we assumed  $\kappa = 0$  (pure water). This is the famous expression due to Born for the solvation energy of a single ion. The function  $f_{GB}()$  is designed to interpolate, in a clever manner, between the limit  $r_{ij} \rightarrow 0$ , when atomic spheres merge into one, and the opposite extreme  $r_{ij} \rightarrow \infty$ , when the ions can be treated as point charges obeying the Coulomb's law.[49] For deeply buried atoms, the effective radii are large,  $R_i \gg \rho_i$ , and for such atoms one can use a rough estimate  $R_i \approx L_i$ , where  $L_i$  is the distance from the atom to the molecular surface. Closer to the surface, the effective radii become smaller, and for a completely solvent exposed side-chain one can expect  $R_i$  to approach  $\rho_i$ .

The effective radii depend on the molecule's conformation, and so have to be re-computed every time the conformation changes. This makes the computational efficiency a critical issue, and various approximations are normally made that facilitate an effective estimate of  $R_i$ . In particular, the so-called *Coulomb field approximation*, or *CFA*, is often used, which replaces the true electric displacement around the atom by the Coulomb field. Within this assumption, the following expression can be derived:[49]

$$R_i^{-1} = \rho_i^{-1} - \frac{1}{4\pi} \int \theta(|\mathbf{r}| - \rho_i) r^{-4} d\mathbf{r} \quad (3.5)$$

where the integral is over the solute volume surrounding atom  $i$ . For a realistic molecule, the solute boundary (molecular surface) is anything but trivial, and so further approximations are made to obtain a closed-form analytical expression for the above equation, *e.g.* the so-called pairwise de-screening approach of Hawkins, Cramer and Truhlar,[57] which leads to a GB model implemented in Amber with  $igb=1$ . The 3D integral used in the estimation of the effective radii is performed over the van der Waals (VDW) spheres of solute atoms, which implies a definition of the solute volume in terms of a set of spheres, rather than the complex molecular surface,[58] commonly used in the PB calculations. For macromolecules, this approach tends to underestimate the effective radii for buried atoms,[49] arguably because the standard integration procedure treats the small vacuum-filled crevices between the van der Waals (VDW) spheres of protein atoms as being filled with water, even for structures with large interior.[56]

This error is expected to be greatest for deeply buried atoms characterized by large effective radii, while for the surface atoms it is largely canceled by the opposing error arising from the Coulomb approximation, which tends [44, 48, 59] to overestimate  $R_i$ .

The deficiency of the model described above can, to some extent, be corrected by noticing that even the optimal packing of hard spheres, which is a reasonable assumption for biomolecules, still occupies only about three quarters of the space, and so "scaling-up" of the integral by a factor of four thirds should effectively increase the underestimated radii by about the right amount, without any loss of computational efficiency. This idea was developed and applied in the context of pH titration,[49] where it was shown to improve the performance of the GB approximation in calculating pKa values of protein sidechains. However, the one-parameter correction introduced in Ref. [49] was not optimal in keeping the model's established performance on small molecules. It was therefore proposed [54] to re-scale the effective radii with the re-scaling parameters being proportional to the degree of the atom's burial, as quantified by the value  $I_i$  of the 3D integral. The latter is large for the deeply buried atoms and small for exposed ones. Consequently, one seeks a well-behaved re-scaling function, such that  $R_i \approx (\rho_i^{-1} - I_i)^{-1}$  for small  $I_i$ , and  $R_i > (\rho_i^{-1} - I_i)^{-1}$  when  $I_i$  becomes large. The following simple, infinitely differentiable re-scaling function was chosen to replace the model's original expression for the effective radii:

$$R_i^{-1} = \tilde{\rho}_i^{-1} - \rho_i^{-1} \tanh(\alpha\Psi - \beta\Psi^2 + \gamma\Psi^3) \quad (3.6)$$

where  $\Psi = I_i\tilde{\rho}_i$ , and  $\alpha$ ,  $\beta$ ,  $\gamma$  are treated as adjustable dimensionless parameters which were optimized using the guidelines mentioned earlier (primarily agreement with the PB). Currently, Amber supports two GB models ( termed OBC ) based on this idea. These differ by the values of  $\alpha$ ,  $\beta$ ,  $\gamma$ , and are invoked by setting `igb` to either `igb=2` or `igb=5`. The details of the optimization procedure and the performance of the OBC model relative to the PB treatment and in MD simulations on proteins is described in Ref. [54]; an independent comparison to the PB in calculating the electrostatic part of solvation free energy on a large data set of proteins can be found in Ref. [60].

Our experience with generalized Born simulations is mainly with `ff12` or `ff03`; the current GB models are not compatible with polarizable force fields. Replacing explicit water with a GB model is equivalent to specifying a different force field, and users should be aware that none of the GB options (in Amber or elsewhere) is as mature as simulations with explicit solvent; user discretion is advised! For example, it was shown that salt bridges are too strong in some of these models [61, 62] and some of them provide secondary structure distributions that differ significantly from those obtained using the same protein parameters in explicit solvent, with GB having too much  $\alpha$ -helix present.[63, 64] The combination of the `ff12SB` force field with `igb=8` gives the best results for proteins; `ff12SB` and `igb=1` is recommended for nucleic acids(see[65]for an evaluation of GB models for DNA).

The generalized Born models used here are based on the "pairwise" model introduced by Hawkins, Cramer and Truhlar,[57, 66] which in turn is based on earlier ideas by Still and others.[43, 48, 59, 67] The so-called overlap parameters for most models are taken from the TINKER molecular modeling package (<http://tinker.wustl.edu>). The effects of added monovalent salt are included at a level that approximates the solutions of the linearized Poisson-Boltzmann equation.[55] The original implementation was by David Case, who thanks Charlie Brooks for inspiration. Details of our implementation of generalized Born models can be found

### 3. Force field modifications

in Refs. [68, 69].

#### 3.1.1. GB/SA input parameters

As outlined above, there are several "flavors" of GB available, depending upon the value of *igb*. The version that has been most extensively tested corresponds to *igb*=1; the "OBC" models (*igb*=2 and 5) are newer, but appear to give significant improvements and are recommended for most projects (certainly for peptides or proteins). The newest, most advanced, and least extensively tested model, *GBn* (*igb*=7), yields results in considerably better agreement with molecular surface Poisson-Boltzmann and explicit solvent results than the "OBC" models under many circumstances.[64] The *GBn* model was parameterized for peptide and protein systems and is not recommended for use with nucleic acids. Users should understand that all (current) GB models have limitations and should proceed with caution. Generalized Born simulations can only be run for non-periodic systems, *i.e.* where *ntb*=0. The nonbonded cutoff for GB calculations should be greater than that for PME calculations, perhaps *cut*=16. The slowly-varying forces generally do not have to be evaluated at every step for GB, either *nrespa*=2 or 4.

#### **igb**

- = 0 No generalized Born term is used. (Default)
- = 1 The Hawkins, Cramer, Truhlar[57, 66] pairwise generalized Born model is used, with parameters described by Tsui and Case.[68] This model uses the default radii set up by LEaP. It is slightly different from the GB model that was included in Amber6. If you want to compare to Amber 6, or need to continue an ongoing simulation, you should use the command "set default PBradii amber6" in LEaP, and set *igb*=1 in *sander*. For reference, the Amber6 values are those used by an earlier Tsui and Case paper.[52] Note that most nucleic acid simulations have used this model, so you take care when using other values. Also note that Tsui and Case used an offset (see below) of 0.13 Å, which is different from its default value.
- = 2 Use a modified GB model developed by A. Onufriev, D. Bashford and D.A. Case; the main idea was published earlier,[49] but the actual implementation here[54] is an elaboration of this initial idea. Within this model, the effective Born radii are re-scaled to account for the interstitial spaces between atom spheres missed by the  $GB^{HCT}$  approximation. In that sense,  $GB^{OBC}$  is intended to be a closer approximation to true molecular volume, albeit in an average sense. With *igb*=2, the inverse of the effective Born radius is given by:

$$R_i^{-1} = \bar{\rho}_i^{-1} - \tanh(\alpha\Psi - \beta\Psi^2 + \gamma\Psi^3) / \rho_i$$

where  $\bar{\rho}_i = \rho_i - offset$ , and  $\Psi = I\rho_i$ , with *I* given in our earlier paper. The parameters  $\alpha$ ,  $\beta$ , and  $\gamma$  were determined by empirical fits, and have the values 0.8, 0.0, and 2.909125. This corresponds to model I in Ref [54]. With this option, you should use the LEaP command "set default PBradii mbondi2" or "set default PBradii bondi" to prepare the *prmtop* file.

### 3.1. The Generalized Born/Surface Area Model

- = **3 or 4** These values are unused; they were used in Amber 7 for parameter sets that are no longer supported.
- = **5** Same as  $igb=2$ , except that now  $\alpha, \beta, \gamma$  are 1.0, 0.8, and 4.85. This corresponds to model II in Ref [54]. With this option, you should use the command "set default PBradii mbondi2" in setting up the *prmtop* file, although "set default PBradii bondi" is also OK. When tested in MD simulations of several proteins,[54] both of the above parameterizations of the "OBC" model showed equal performance, although further tests [60] on an extensive set of protein structures revealed that the  $igb=5$  variant agrees better with the Poisson-Boltzmann treatment in calculating the electrostatic part of the solvation free energy.
- = **6** With this option, there is no continuum solvent model used at all; this corresponds to a non-periodic, "vacuum", model where the non-bonded interactions are just Lennard-Jones and Coulomb interactions. This option is logically equivalent to setting  $igb=0$  and  $eedmeth=4$ , although the implementation (and computational efficiency) is not the same.
- = **7** The *GBn* model described by Mongan, Simmerling, McCammon, Case and Onufriev[70] is employed. This model uses a pairwise correction term to  $GB^{HCT}$  to approximate a molecular surface dielectric boundary; that is to eliminate interstitial regions of high dielectric smaller than a solvent molecule. This correction affects all atoms and is geometry-specific, going beyond the geometry-free, "average" re-scaling approach of  $GB^{OBC}$ , which mostly affects buried atoms. With this method, you should use the bondi radii set. The overlap or screening parameters in the *prmtop* file are ignored, and the model-specific *GBn* optimized values are substituted. The model carries little additional computational overhead relative to the other GB models described above.[70] This method is not recommended for systems involving nucleic acids.
- = **8** Same GB functional form as the *GBn* model ( $igb=7$ ), but with different parameters (Nguyen and Simmerling, in preparation). The offset, overlap screening parameters, and  $gbneckscale$  are changed. In addition, individual  $\alpha, \beta$ , and  $\gamma$  parameters are introduced for each of the elements H, C, N, O, S. Parameters for other elements have not been optimized, and the values used are those from  $igb=5$ . An option is given to specify individual parameters for P, though these are not included by default.

The following are the default parameters sander uses with  $igb=8$ , but they can also be changed in the *mdin* file:  $Sh=1.425952$ ,  $Sc=1.058554$ ,  $Sn=0.733599$ ,  $So=1.061039$ ,  $Ss=-0.703469$ ,  $Sp=0.5$ ,  $offset=0.195141$ ,  $gbneckscale=0.826836$ ,  $galphaH=0.788440$ ,  $gbetaH=0.798699$ ,  $ggammaH=0.437334$ ,  $galphaC=0.733756$ ,  $gbetaC=0.506378$ ,  $ggammaC=0.205844$ ,  $galphaN=0.503364$ ,  $gbetaN=0.316828$ ,  $ggammaN=0.192915$ ,  $galphaOS=0.867814$ ,  $gbetaOS=0.876635$ ,  $ggammaOS=0.387882$ ,  $galphaP=1.0$ ,  $gbetaP=0.8$ ,  $ggammaP=4.851$  (using OBC parameters for P)

### 3. Force field modifications

where  $Sh$ ,  $Sc$ ,  $Sn$ ,  $So$ ,  $Ss$  and  $Sp$  are scaling parameters,  $g\alpha X$ ,  $g\beta X$ ,  $g\gamma X$  are the  $\alpha$ ,  $\beta$ ,  $\gamma$  set for element  $X$ .  $g\alpha OS$ ,  $g\beta OS$ ,  $g\gamma OS$  is the  $\alpha$ ,  $\beta$ ,  $\gamma$  set for O and S.  $mbondi3$  radii are recommended with  $igb=8$  and can be employed with the LEaP command "set default PBradii mbondi3".

- =10** Calculate the reaction field and nonbonded interactions using a numerical Poisson-Boltzmann solver. This option is described in the *AmberTools* manual. Note that this is *not* a generalized Born simulation, in spite of its use of *igb*; it is rather an alternative continuum solvent model.
- intdiel** Sets the interior dielectric constant of the molecule of interest. Default is 1.0. Other values have not been extensively tested.
- extdiel** Sets the exterior or solvent dielectric constant. Default is 78.5.
- saltcon** Sets the concentration (M) of 1-1 mobile counterions in solution, using a modified generalized Born theory based on the Debye-Hückel limiting law for ion screening of interactions.[\[55\]](#) Default is 0.0 M (*i.e.* no Debye-Hückel screening.) Setting *saltcon* to a non-zero value does result in some increase in computation time.
- rgbmax** This parameter controls the maximum distance between atom pairs that will be considered in carrying out the pairwise summation involved in calculating the effective Born radii. Atoms whose associated spheres are farther away than *rgbmax* from given atom will not contribute to that atom's effective Born radius. This is implemented in a "smooth" fashion (thanks mainly to W.A. Svrcek-Seiler), so that when part of an atom's atomic sphere lies inside *rgbmax* cutoff, that part contributes to the low-dielectric region that determines the effective Born radius. The default is 25 Å, which is usually plenty for single-domain proteins of a few hundred residues. Even smaller values (of 10-15 Å) are reasonable, changing the functional form of the generalized Born theory a little bit, in exchange for a considerable speed-up in efficiency, and without introducing the usual cut-off artifacts such as drifts in the total energy.
- The *rgbmax* parameter affects only the effective Born radii (and the derivatives of these values with respect to atomic coordinates). The *cut* parameter, on the other hand, determines the maximum distance for the electrostatic, van der Waals and "off-diagonal" terms of the generalized Born interaction. The value of *rgbmax* might be either greater or smaller than that of *cut*: these two parameters are independent of each other. However, values of *cut* that are too small are more likely to lead to artifacts than are small values of *rgbmax*; therefore one typically sets  $rgbmax \leq cut$ .
- rbornstat** If *rbornstat* = 1, the statistics of the effective Born radii for each atom of the molecule throughout the molecular dynamics simulation are reported in the output file. Default is 0.
- offset** The dielectric radii for generalized Born calculations are decreased by a uniform

### 3.1. The Generalized Born/Surface Area Model

value "offset" to give the "intrinsic radii" used to obtain effective Born radii. Default is 0.09 Å.

- gbsa** Option to carry out GB/SA (generalized Born/surface area) simulations. For the default value of 0, surface area will not be computed and will not be included in the solvation term. If  $gbsa = 1$ , surface area will be computed using the LCPO model.[42] If  $gbsa = 2$ , surface area will be computed by recursively approximating a sphere around an atom, starting from an icosahedra. Note that no forces are generated in this case, hence,  $gbsa = 2$  only works for a single point energy calculation and is mainly intended for energy decomposition in the realm of MM\_GBSA.
- surften** Surface tension used to calculate the nonpolar contribution to the free energy of solvation (when  $gbsa = 1$ ), as  $Enp = surften * SA$ . The default is 0.005 kcal/mol/Å<sup>2</sup>. [71]
- rdt** This parameter is only used for GB simulations with LES (Locally Enhanced Sampling). In GB+LES simulations, non-LES atoms require multiple effective Born radii due to alternate descreening effects of different LES copies. When the multiple radii for a non-LES atom differ by less than RDT, only a single radius will be used for that atom. See the LES portion of the manual for more details. Default is 0.0 Å.

#### 3.1.2. ALPB (Analytical Linearized Poisson-Boltzmann)

Like the GB model, the ALPB approximation [72, 73] can be used to replace the need for explicit solvent, with similar benefits (such as enhanced conformational sampling) and caveats. The basic ALPB equation that approximates the electrostatic part of the solvation free energy is

$$\Delta G_{el} \approx \Delta G_{alpb} = -\frac{1}{2} \left( \frac{1}{\epsilon_{in}} - \frac{1}{\epsilon_{ex}} \right) \frac{1}{1 + \alpha\beta} \sum_{ij} q_i q_j \left( \frac{1}{f_{GB}} + \frac{\alpha\beta}{A} \right)$$

where  $\beta = \epsilon_{in}/\epsilon_{ex}$  is the ratio of the internal and external dielectrics,  $\alpha=0.571412$ , and  $A$  is the so-called *effective electrostatic size* of the molecule, see the definition of  $Arad$  below. Here  $f_{GB}$  is the same smooth function as in the GB model. The GB approximation is then just the special case of ALPB when the solvent dielectric is infinite; however, for finite values of solvent dielectric the ALPB tends to be more accurate. For aqueous solvation, the accuracy advantage offered by the ALPB is still noticeable, and becomes more pronounced for less polar solvents. Statistically significant tests on macromolecular structures [73] have shown that ALPB is more likely to be a better approximation to PB than GB. At the same time, ALPB has virtually no additional computational overhead relative to GB. However, users should realize that at this point the new model has not yet been tested nearly as extensively as the GB model, and is therefore in its experimental stage. The model can potentially replace GB in the energy analysis of snapshots via the MM-GB/SA scheme. The electrostatic screening effects of monovalent salt are currently introduced into the ALPB in the same manner as in the GB, and are determined by the parameter *saltcon*.

- alpb** Flag for using ALPB to handle electrostatic interactions within the implicit solvent model.



### 3. Force field modifications

= 0 No ALPB (default).

= 1 ALPB is turned on. Requires that one of the GB models is also used to compute the effective Born radii, that is one must set  $igb=1,2,5$ , or 7. The ALPB uses the same sets of radii as required by the particular GB model.

**arad** Effective electrostatic size (radius) of the molecule. Characterizes its over-all dimensions and global shape, and is not to be confused with the effective Born radius of an atom. An appropriate value of *Arad* must be set if  $alpb=1$ : this can be conveniently estimated for your input structure with the utility *elsize* that comes with the main distribution. The default is 15 Å. While *Arad* may change during the course of a simulation, these changes are usually not very large; the accuracy of the ALPB is found to be rather insensitive to these variations. In the current version of Amber *Arad* is treated as constant throughout the simulation, the validity of this assumption is discussed in Ref. [73]. Currently, the effective electrostatic size is only defined for "single-connected" molecules. However, the ALPB model can still be used to treat the important case of complex formation. In the docked state, the compound is considered as one, with its electrostatic size well defined. When the ligand and receptor become infinitely separated, each can be assigned its own value of *Arad*.

## 3.2. PBSA

Several efficient finite-difference numerical solvers, both linear [74, 75] and nonlinear,[76] are implemented in *pbsa* and *sander* for various applications of the Poisson-Boltzmann (PB) method. For more background information and how to use the PB method, please consult the chapter on PBSA in the AmberTools manual, cited references, and online *Amber* tutorial pages.

The keywords for PBSA in *sander* are put in the the namelist of `&cntrl` for basic controls and `&pb` for more detailed manipulation of the numerical procedures. Here we only describe the usage of basic input options inside `&cntrl`. The numerical electrostatic procedures can be turned on by setting `IPB` to either 1 or 2. The backward compatible flag `IGB=10` is equivalent to `IPB=1` and will be phased out in future releases. The numerical non-polar procedures can be turned on by setting `INP` to either 1 or 2. The backward compatible flag `NPOPT` will be phased out in future releases.

**ipb** Option to set up a dielectric model for all numerical PB procedures.

= 0 No electrostatic solvation free energy is computed. **Default.**

= 1 The dielectric interface between solvent and solute is defined to be the numerical solvent excluded surface.

= 2 The dielectric interface is also the solvent excluded surface, but it is implemented with the level set function, which is the signed distance from the numerical solvent accessible surface. The solvent excluded surface is the isosurface where the function value equals to negative solvent probe radius. [Wang and Luo, Manuscript in preparation] Use of a level set function simplifies the calculation of the intersection points of the solvent excluded surface



### 3.3. Reference Interaction Site Model of Molecular Solvation

and grid edges (when SMOOTHOPT=1 in the &pb namelist) and leads to more stable numerical calculations.

- igb      When set to 10, it instructs *sander* to set up PBSA calculations, equivalent to the IPB=1 option. This will be over-written by IPB if inconsistency between the two is detected except IPB=0.
- inp      Option to select different methods to compute non-polar solvation free energy.
- = 0 No non-polar solvation free energy is computed.
  - = 1 The total non-polar solvation free energy is modeled as a single term linearly proportional to the solvent accessible surface area, as in the PARSE parameter set. **Default** for backward-compatibility.
  - = 2 The total non-polar solvation free energy is modeled as two terms: the cavity term and the dispersion term. The dispersion term is computed with a surface-based integration method [77] closely related to the PCM solvent for quantum chemical programs.[78] Under this framework, the cavity term is still computed as a term linearly proportional to the molecular solvent-accessible-surface area (SASA) or the molecular volume enclosed by SASA. With this option, please do not use RADIOPT=0, i.e. the radii in the prmtop file. Otherwise, a warning will be issued in the output file.

Once the above basic options are specified, *sander* can proceed with the default options to compute the solvation free energies with the input coordinates. Of course, this means that you only want to use default options for default applications.

More PB options can be defined in the &pb namelist, which is read immediately after the &cntrl namelist. We have tried hard to make the defaults for these parameters appropriate for calculations of solvated molecular systems. Please use caution when changing any default options. For more information about detail options in the &pb namelist, please refer to the PBSA chapter of the AmberTools manual.

## 3.3. Reference Interaction Site Model of Molecular Solvation

In addition to explicit and continuum implicit solvation models, Amber has a third type of solvation model for molecular mechanics simulations, the reference interaction site model (RISM) of molecular solvation[79–93]. In AmberTools, 1D-RISM is available as *rism1d*. 3D-RISM is available as an option in NAB, MMPBSA.py and *sander*. *rism3d.snglpnt* is a simplified, standalone interface, ideal for calculating solvation thermodynamics on individual structures and trajectories. General information about RISM and detailed information specific to using *rism1d*, NAB, MMPBSA.py and *rism3d.snglpnt* can be found in the AmberTools manual.

### 3.3.1. Multiple Time Step Methods for 3D-RISM

At this time, the computational cost of 3D-RISM is still prohibitive for performing calculations at each step of molecular dynamics calculations. One of the most effective ways to reduce

### 3. Force field modifications

this computational burden is to reduce the number of solutions calculated by using multiple time step (MTS) methods. Two MTS methods, r-RESPA and force-coordinate extrapolation (FCE), are implemented for 3D-RISM and can be combined such that solutions are only calculated once every 10 or 20 fs. At this time, these methods are only available for `sander` and not `NAB`.

r-RESPA[94, 95] and I-Verlet[96] impulse MTS algorithms are widely used methods to reduce the computational load of long-range interactions while maintaining the desirable properties of energy conservation and time reversibility. Impulse MTS can be invoked for 3D-RISM independent of the existing r-RESPA implementation using the `RISMnRESPA` variable. For typical biomolecular simulations, impulse MTS is limited to a maximum step size of 5 fs[97]. Since the computational load of calculating all internal interactions of the solute is small compared to the 3D-RISM calculation, it is recommend to use `dt=0.001`, `nrespa=1` and `RISMnRESPA=5`.

To overcome the stability limitation of impulse MTS, FCE uses an efficient extrapolation method to predict the forces for some time steps rather than computing a full 3D-RISM solution[79]. In this method, forces,  $\{\mathbf{F}\}$ , on  $N^U$  solute atoms for the current time step  $t_k$  are approximated as a linear combination of forces from the  $n$  previous time steps obtained from 3D-RISM calculations,

$$\{\mathbf{F}\}^{(k)} = \sum_{l=1}^n a_{kl} \{\mathbf{F}\}^{(l)}, \quad l \in \text{3D-RISM steps.} \quad (3.7)$$

The weight coefficients  $a_{kl}$  are obtained by expressing the current set of coordinates,  $\{\mathbf{R}\}^{(k)}$ , as a linear combination of coordinates from the  $n$  previous time steps for which 3D-RISM calculations were performed. That is, the current set of coordinates is projected onto the basis of  $n$  previous solute arrangements by minimizing the norm of the difference between the current  $3 \times N^U$  matrix of coordinates  $\{\mathbf{R}\}^{(k)}$  and the corresponding linear combination of the previous ones  $\{\mathbf{R}\}^{(l)}$ ,

$$\text{minimize} \left| \{\mathbf{R}\}^{(k)} - \sum_{l=1}^n a_{kl} \{\mathbf{R}\}^{(l)} \right|^2.$$

Coefficients  $a_{kl}$  are then used in Equation (3.7) to extrapolate forces at the current intermediate time step. Similarly, the known coordinates for the current time step can be approximated from previous time steps as

$$\{\mathbf{R}\}^{(k)} = \sum_{l=1}^N a_{kl} \{\mathbf{R}\}^{(l)}.$$

FCE MTS does not conserve energy and is not time reversible. However, 3D-RISM calculations can be reduced to a frequency of once every 10 to 20 fs and stable dynamics achieved by using a Langevin thermostat with `gamma_ln=10 to 20 ps-1`. Combined impulse FCE MTS calculations (see Figure 3.1) start the simulation using impulse MTS until the requested size for the basis set, `FCEnbasis`, is achieved. After a large enough basis set is collected, 3D-RISM calculations are only performed once every `FCEstride × RISMnRESPA` time steps.

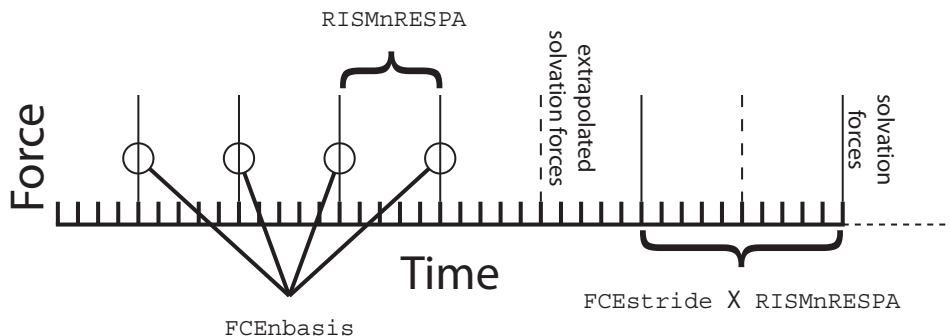


Figure 3.1.: Multiple time step methods in 3D-RISM.  $RISMnRESPA(= 5)$  is the number of base time steps between application of solvation forces (exact or extrapolated).  $FCEnbasis(= 4)$  is the number of previous solutions used to extrapolate forces, in this case four previous solutions. Once  $FCEnbasis$  solutions have been calculated, exact 3D-RISM forces are calculated every  $FCEstride(= 2) \times RISMnRESPA$  time steps; solvation forces are otherwise obtained through extrapolation.

### 3.3.2. 3D-RISM in sander

At the time of release, 3D-RISM is not available as part of `sander` but this functionality will be added later via a patch. Even with the patch, 3D-RISM will *only* be built if the Intel Math Kernel Library (MKL) is available during the build process. That is, `MKL_HOME` must be appropriately set at compile time.

With MKL, full 3D-RISM functionality will be available in `sander` as part of the standard install procedure. However, some methods available in `sander` are not compatible with 3D-RISM, such as QM/MM simulations. At this time, only standard molecular dynamics, minimization and trajectory post-processing with non-polarizable force fields are supported. With the exception of multiple time step features, 3D-RISM keywords in `sander` are identical to those in NAB, `rism3d.snglpt` and `MMPBSA.py`.

3D-RISM specific command line options for `sander` are

```
sander [standard options] -xvv xvfile -guv guvroot -huv huvroot
    -cuv cuvroot -uuv uuvroot -asympt asympfile
    -quv quvroot -chgdist chgdistroot
```

**xvfile** *input* description of bulk solvent properties, required for 3D-RISM calculations. Produced by `rismld`.

**guvroot** *output* rootname for solute-solvent 3D pair distribution function,  $G^{UV}(\mathbf{R})$ . This will produce one file for each solvent atom type for each frame requested.

**huvroot** *output* rootname for solute-solvent 3D total correlation function,  $H^{UV}(\mathbf{R})$ . This will produce one file for each solvent atom type for each frame requested.

### 3. Force field modifications

**cuvroot** *output* rootname for solute-solvent 3D total correlation function,  $C^{UV}(\mathbf{R})$ . This will produce one file for each solvent atom type for each frame requested.

**uuvroot** *output* rootname for solute-solvent 3D potential energy function,  $U^{UV}(\mathbf{R})$ , in units of  $kT$ . This will produce one file for each solvent atom type for each frame requested.

**asymptfile** *output* rootname for solute-solvent 3D long-range real-space asymptotics for  $C$  and  $H$ . This will produce one file for each of  $C$  and  $H$  for each frame requested and does not include the solvent site charge. Multiply the distribution by the solvent site charge to obtain the long-range asymptotics for that site.

**quvroot** *output* rootname for solute-solvent 3D charge density distribution [ $e/\text{\AA}$ ]. This will produce one file that combines contributions from all solvent atom types for each frame requested.

**chgdist** *output* rootname for solute-solvent 3D charge distribution [ $e$ ]. This will produce one file that combines contributions from all solvent atom types for each frame requested.

Generated output files can be large and numerous. For each type of correlation, a separate file is produced for each solvent atom type. The frequency that files are produced is controlled by the `ntwrism` parameter. Every time step that output is produced, a new set of files is written with the time step number in the file name. For example, a molecular dynamics calculation using an SPC/E water model with `ntwrism=2` and `-guv guv` on the command line will produce two files on time step ten: `guv.O.10.dx` and `guv.H1.10.dx`.

#### 3.3.2.1. Keywords

With the exception of `irism`, which is found in the `&cntrl` name list, all 3D-RISM options are specified in the `&rism` name list.

**irism** [0] Use 3D-RISM. Found in `&cntrl` name list.

= 0 Off.

= 1 On.

#### Closure Approximation

**closure** [KH] Select closure approximation.

= **KH** Kovalenko-Hirata (KH).

= **HNC** Hyper-netted chain equation (HNC).

= **PSE $n$**  Partial series expansion of order- $n$  (PSE- $n$ ), where “ $n$ ” is a positive integer.

### 3.3. Reference Interaction Site Model of Molecular Solvation

**Long-range asymptotics** Long-range asymptotics are used to analytically account for solvent distribution beyond the solvent box. Long-range asymptotics are always used to when calculating solution but can be omitted for the subsequent thermodynamic calculations, though it is not recommended.

asymcorr [T] Use long-range asymptotic corrections for thermodynamic calculations.

= T Use the long-range corrections.

= F Do not use long-range corrections.

**Solvation Box** The non-periodic solvation box super-cell can be defined as variable or fixed in size. When a variable box size is used, the box size will be adjusted to maintain a minimum buffer distance between the atoms of the solute and the box boundary. This has the advantage of maintaining the smallest possible box size while adapting to changes of solute shape and orientation. Alternatively, the box size can be specified at run-time. This box size will be used for the duration of the sander calculation.

**solvcut** [buffer] Cut-off distance for solvent-solute potential and force calculations. If `buffer < 0` and `solvcut` is not explicitly set, `solvcut = |buffer|`. For minimization it is recommended to not use a cut-off (e.g. `solvcut=9999`).

#### Variable Box Size

**buffer** [14] Minimum distance in Å between the solute and the edge of the solvent box.

< 0 Use fixed box size (`ng3` and `solvbox`).

>= 0 Buffer distance.

**grdspc** [0.5,0.5,0.5] Linear grid spacing in Å.

#### Fixed Box Size

**ng3** [] Sets the number of grid points for a fixed size solvation box. This is only used if `buffer < 0`.

`nx,ny,nz` Points for *x*, *y* and *z* dimensions.

**solvbox** [] Sets the size in Å of the fixed size solvation box. This is only used if `buffer < 0`.

`lx,ly,lz` Box length in *x*, *y* and *z* dimensions.

#### Solution Convergence

**tolerance** [1e-5] Maximum residual tolerance required for convergence. For minimization a tolerance of 1e-11 or lower is recommended.

**mdiis\_del** [0.7] “Step size” in MDIIS.

### 3. Force field modifications

**mdiis\_nvec** [5] Number of vectors used by the MDIIS method. Higher values for this parameter can greatly increase memory requirements but may also accelerate convergence.

**mdiis\_method** [2] Specify implementation of the MDIIS routine.

= 0 Original. For small systems (e.g.  $< 64^3$  grid points) this implementation may be faster than the BLAS optimized version.

= 1 BLAS optimized.

= 2 BLAS and memory optimized.

**maxstep** [10000] Maximum number of iterations allowed to converge on a solution.

**npropagate** [5] Number of previous solutions propagated forward to create an initial guess for this solute atom configuration.

= 0 Do not use any previous solutions

= 1..5 Values greater than 0 but less than 4 or 5 will use less system memory but may introduce artifacts to the solution (e.g., energy drift).

### Minimization and Molecular Dynamics

**centering** [1] Controls how the solute is centered/re-centered in the solvent box.

= -2 Center of geometry. Center on first step only.

= -1 Center of mass. Center on first step only.

= 0 No centering. Dangerous.

= 1 Center of mass. Center on every step. Recommended for molecular dynamics.

= 2 Center of geometry. Center on every step. Recommended for minimization.

**zerofric** [1] Redistribute solvent forces across the solute such that the net solvation force on the solute is zero.

= 0 Unmodified forces.

= 1 Zero net force.

### Trajectory Post-Processing

**apply\_rism\_force** [1] Calculate and use solvation forces from 3D-RISM. Not calculating these forces can save computation time and is useful for trajectory post-processing.

= 0 Do not calculate forces.

= 1 Calculate forces.

**Multiple Time Steps** Multiple time step features are only available in `sander`.

**rismnrespa** [1]  $\text{rismnrespa} \times \text{dt}$  = RISM RESPA multiple time step size. 5 fs is the maximum time step. “1” corresponds to no multiple time stepping.

**fcestride** [0]  $\text{fcestride} \times \text{rismnrespa} \times \text{dt}$  = FCE multiple time step size. I.e., full 3D-RISM solutions are performed every  $\text{fcestride} \times \text{rismnrespa}$  steps. In between full solutions extrapolated force impulses are applied every  $\text{rismnrespa}$  steps. Maximum step size for stable dynamics depends on damping coefficient for Langevin dynamics. “1” corresponds to no multiple time stepping.

= 0 No FCE multiple time stepping.

= 1 Invokes the FCE code but yields the same trajectories as 0.

>= 1 Invoke FCE with 3D-RISM solutions every  $\text{fcestride} \times \text{rismnrespa}$  steps.

**fcenbasis** [10] Number of previous full solutions used to extrapolate new forces. If FCE is not used this can be set to 1 to reduce memory usage.

**fcecrd** [0] The coordinates used for the FCE method.

= 0 The absolute x, y, z position of each neighbour atom (with translations due to centering).

= 1 For predicting the forces on atom  $i$ , use the distance of each neighbour atom as the “coordinate”. This has one third the number of coordinates to use in the prediction. Also, directional information is lost.

= 2 For predicting the forces on atom  $i$ , use the x, y, z position of each neighbour atom with atom  $i$  as the origin. Recommended.

## Output

**ntwrism** [0] Indicates that solvent density grid should be written to file every `ntwrism` iterations.

= 0 No files written.

>= 1 Output every `ntwrism` time steps.

**volfmt** ['DX'] Format of volumetric data files. May be 'dx' for DX files or 'xyzv' for XYZV format. See the AmberTools manual for more information.

**verbose** [0] Indicates level of diagnostic detail about the calculation written to the log file.

= 0 No output.

= 1 Print the number of iterations used to converge.

= 2 Print details for each iteration and information about what FCE is doing every `progress` iterations.

**write\_thermo** [1] Print solvation thermodynamics in addition to standard `sander` output. The format is the same as that found in NAB and `rism3d.snglpnt`.

### 3. Force field modifications

**polarDecomp** [0] Decomposes solvation free energy into polar and non-polar components. Note that this typically requires 80% more computation time.

= 0 No polar/non-polar decomposition.

= 1 Polar/non-polar decomposition.

**progress** [1] Display progress of the 3D-RISM solution every `kshow` iterations. 0 indicates this information will not be displayed. Must be used with `verbose > 1`.

#### 3.3.2.2. Example

##### Molecular Dynamics (`imin=0`)

```
molecular dynamics with 3D-RISM and impulse MTS
&cntrl
  ntx=1, ntp=100, ntwx=1000,ntwr=1000,
  nstlim=10000,dt=0.001,                !No shake or r-RESPA
  ntt=3, temp0=300, gamma_ln=20,        !Langevin dynamics
  ntb=0,                                  !Non-periodic
  cut=999.,                               !Calculate all
                                           !solute-solute
                                           !interactions

  irism=1,
/
&risp
  rispnr=5,                               !r-RESPA MTS
  fcenbasis=10,fcstride=2,fcscr=2        !FCE MTS
/
```

##### Minimization (`imin=1`)

```
Default XMIN minimization with 3D-RISM
&cntrl
  imin=1, maxcyc=200,
  drms=1e-3,                             !RMS force. Can be as low as 1e-4
  ntmin=3,                                !XMIN
  ntp=5,
  ntb=0,                                  !Non-periodic
  cut=999.,                               !Calculate all
                                           !solute-solute interactions

  irism=1
/
&risp
  tolerance=1e-11,                       !Low tolerance
  solvcut=9999,                          !No cut-off for
                                           !solute-solvent interactions
```



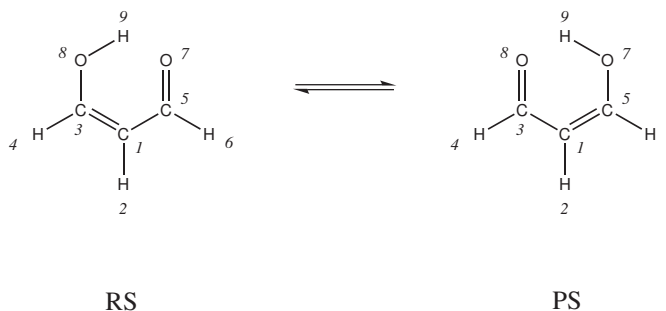


Figure 3.2.: Intramolecular proton transfer in malonaldehyde.

```

centering=2          !Solvation box centering
                    !using center-of-geometry
/

Trajectory Post-Processing (imin=5)

Trajectory post-processing with 3D-RISM
&cntrl
  ntx=1, ntpr=1, ntwx=1,
  imin=5,maxcyc=1,      !Single-point energy calculation
                      !on each frame
  ntb=0,                !Non-periodic
  cut=9999.,            !Calculate all
                      !solute-solute interactions

  irism=1

/
&rism
  tolerance=1e-4,      !Saves some time compared to 1e-5
  apply_rism_force=0,  !Saves some time. Forces are not used.
  npropagate=1         !Saves some time and 4*8*Nbox bytes
                      !of memory compared to npropagate=5.
/

```

## 3.4. Empirical Valence Bond

### 3.4.1. Introduction

Chemical reactivity can be formulated within the empirical valence bond (EVB) model[98, 99], whereby the reactive surface is defined as the lowest adiabatic surface obtained by diagonalization of the potential energy matrix in the representation of non-reactive diabatic states. These diabatic states can be described by a force field approach, such as Amber, or by a pre-

### 3. Force field modifications

scription incorporating information from ab initio calculations. The coupling elements in the matrix embody all the physics needed for describing transitions between the diabatic states.

As an example, the intramolecular proton transfer reaction in malonaldehyde (Figure 3.2) can be described by a two-state EVB matrix

$$\mathbf{V} = \begin{bmatrix} V_{11} & V_{12} \\ V_{21} & V_{22} \end{bmatrix} \quad (3.8)$$

where valence bond state 1 represents the reactant state (RS) with the proton  $\text{H}_9$  bonded to  $\text{O}_8$  and valence bond state 2 represents the product state (PS) with the proton bonded to  $\text{O}_7$ . The matrix elements  $V_{11}$  and  $V_{22}$  are simply the energies of the reactant and product systems. The off-diagonal elements of this symmetric matrix, i.e.  $V_{12} = V_{21}$ , couple these diabatic states.

Amber provides several options for computing the  $V_{12}$  resonance integrals. In its simplest form,  $V_{12}$  is set to a constant value which provides an EVB surface that reproduces experimental or ab initio barrier heights. More flexibility can be introduced into  $V_{12}$  by employing an exponential or Gaussian function of the coordinates. It has recently been shown [100, 101] that a linear combination of distributed Gaussian functions is the most accurate and flexible form for  $V_{12}$ . With a set of distributed Gaussians,  $V_{12}$  can be fit to high-level electronic structure data using the following form,

$$V_{12}^2(\mathbf{q}) = \sum_K \sum_{i \geq j \geq 0}^{NDim} B_{ijk} g(\mathbf{q}, \mathbf{q}_K, i, j, \alpha_K) \quad (3.9)$$

$$V_{12}^2(\mathbf{q}) = [V_{11}(\mathbf{q}) - V(\mathbf{q})][V_{22}(\mathbf{q}) - V(\mathbf{q})] \quad (3.10)$$

$$g(\mathbf{q}, \mathbf{q}_K, 0, 0, \alpha_K) = \left(1 + \frac{1}{2} \alpha_K |\mathbf{q} - \mathbf{q}_K|^2\right) \exp\left[-\frac{1}{2} \alpha_K |\mathbf{q} - \mathbf{q}_K|^2\right] \quad (3.11)$$

$$g(\mathbf{q}, \mathbf{q}_K, i, 0, \alpha_K) = (\mathbf{q} - \mathbf{q}_K)_i \exp\left[-\frac{1}{2} \alpha_K |\mathbf{q} - \mathbf{q}_K|^2\right] \quad (3.12)$$

$$g(\mathbf{q}, \mathbf{q}_K, i, j, \alpha_K) = (\mathbf{q} - \mathbf{q}_K)_i (\mathbf{q} - \mathbf{q}_K)_j \exp\left[-\frac{1}{2} \alpha_K |\mathbf{q} - \mathbf{q}_K|^2\right] \quad (3.13)$$

where  $g(\mathbf{q}, \mathbf{q}_K, i, j, \alpha_K)$  are s-, p-, and d-type Gaussians at a number of points,  $\mathbf{q}_K$ , on the potential energy surface,  $NDim$  is the total number of internal coordinates,  $V$  is the ab initio energy and  $\mathbf{B}$  is a vector of coefficients. It is important to note that a nonstandard s-type Gaussian is employed to precondition the resulting set of linear equations that is passed to a GMRES[102] (aka DIIS[103, 104]) solver. For a more exhaustive discussion of the DG EVB method please see reference [101]. Additionally, the EVB facility in Amber can perform MD or energy optimization on the EVB ground-state surface and biased sampling along a predefined reaction coordinate (RC). Nuclear quantization based on the Feynman path integral formalism [105–107] is also possible.

### 3.4.2. General usage description

The EVB facility is built on top of the *multisander* infrastructure in Amber. As such, the user will need to build the parallel version of *sander* in order to utilize the EVB feature. Information for each EVB diabatic state is obtained from separate (simultaneous) instances of *sander*. The energies and forces of all the states are communicated via MPI to the master node, which is responsible for computing the EVB energy and forces and broadcasting these to the other nodes for the next MD step.

The required input files are (1) an EVB *multisander* group file containing per line all the command line options for each *sander* job, (2) the *mdin*, coordinate, and parmtop files specified in the group file, and (3) the EVB input files. At the top level, an EVB calculation is invoked as follows:

```
mpirun -np <# procs> sander.MPI -ng <# groups> -groupfile <EVB group file>
```

The contents of the EVB group file is similar to that for a conventional *multisander* execution, with the addition of a command line flag *-evbin* for specifying the name of the EVB input file. Below is an example of an EVB group file:

```
# Malonaldehyde RS: H9 bonded to O8
-O -i mdin -p mr.top -c mr.crd -o mr.out -r mr.rst -evbin input.mr
# Malonaldehyde PS: H9 bonded to O7
-O -i mdin -p mp.top -c mr.crd -o mp.out -r mp.rst -evbin input.mp
```

Each line corresponds to a diabatic state, and comments are preceded by a # symbol in the first column of a line. Now, it is important to notice in the above example that the starting configurations for both *sander* jobs are the same, although the topology files are different. This constraint guarantees that the system starts in a physically meaningful part of configuration space. Furthermore, it is critical that the atom numbers (delineating the atom locations in the coordinate and parmtop files) are identical among the EVB diabatic states. In Figure 3.2, for example, the atom numbers of the RS and PS malonaldehydes are identical. The only additional flag in the **&cntrl** namelist of the *mdin* file is **ievb**, which has the following values

<b>ievb</b>	Flag to run EVB
= 0	No effect (default)
= 1	Enable EVB. The value of <b>imin</b> specifies if the <i>sander</i> calculation is a molecular dynamics ( <b>imin=0</b> ) or an energy minimization ( <b>imin=1</b> ). The variable <b>evb_dyn</b> in the <b>&amp;evb</b> namelist of the EVB input file refines this choice to specify if the calculation type is on the EVB ground-state surface, on a mapping potential, or on a biased potential.

The argument of the command line flag *-evbin* provides the name of the EVB input file. Corresponding to the above group file example, the inputs for EVB state 1 are provided in the file *input.mr* and those for EVB state 2 are provided in *input.mp*. For the case of constant coupling between the EVB states, the file *input.mr* may look like the following:

### 3. Force field modifications

```
# Malonaldehyde RS: proton (H9) bound to O8
&evb nevb = 2, nbias = 1, nmorse = 1, nmodvdw = 1, ntw_evb = 50,
xch_type      = "constant",
evb_dyn       = "egap_umb",
dia_shift(1)%st = 1, dia_shift(1)%nrg_offset = 0.0,
dia_shift(2)%st = 2, dia_shift(2)%nrg_offset = 0.0,
xch_cnst(1)%ist = 1, xch_cnst(1)%jst = 2,
xch_cnst(1)%xcnst = 12.5,
egap_umb(1)%ist = 1, egap_umb(1)%jst = 2,
egap_umb(1)%k = 0.005, egap_umb(1)%ezero = 0.0,
morsify(1)%iatom = 8, morsify(1)%jatom = 9, morsify(1)%D = 356.570,
morsify(1)%a = 1.046, morsify(1)%r0 = 1.000,
modvdw(1)%iatom = 9, modvdw(1)%jatom = 7,
/
```

and the file *input.mp* may appear as follows:

```
# Malonaldehyde PS: proton (H9) bound to O7
&evb nevb = 2, nbias = 1, nmorse = 1, nmodvdw = 1, ntw_evb = 50,
xch_type      = "constant",
evb_dyn       = "egap_umb",
dia_shift(1)%st = 1, dia_shift(1)%nrg_offset = 0.0,
dia_shift(2)%st = 2, dia_shift(2)%nrg_offset = 0.0,
xch_cnst(1)%ist = 1, xch_cnst(1)%jst = 2,
xch_cnst(1)%xcnst = 12.5,
egap_umb(1)%ist = 1, egap_umb(1)%jst = 2,
egap_umb(1)%k = 0.005, egap_umb(1)%ezero = 0.0,
morsify(1)%iatom = 7, morsify(1)%jatom = 9, morsify(1)%D = 356.570,
morsify(1)%a = 1.046, morsify(1)%r0 = 1.000,
modvdw(1)%iatom = 9, modvdw(1)%jatom = 8,
/
```

The above EVB files specify that the system is described by a two-state model, the coupling between the two-states is a constant, and the dynamics is umbrella sampling along an energy gap RC. Since the reactant and product states are identical by symmetry, no adjustments of the relative energies of the diabatic states are performed. The constant value coupling between the two states is parameterized such that the EVB barrier reproduces the ab initio barrier of ~ 3 kcal/mol (RMP2/cc-pVTZ level). Lastly, the standard Amber harmonic bond interactions involving the proton with the donor and acceptor oxygens are replaced by Morse functions and certain van der Waals interactions are excluded.

This parameterization of the EVB surface to provide observables that match either results from high-level quantum chemistry calculations or experimental measurements is the trickiest aspect of the EVB model. However, after the EVB surface has been calibrated, the user has access to reactive chemical dynamics simulation timescales and lengthscales which would be otherwise inaccessible using conventional ab initio MD approaches. The distributed Gaussian EVB framework provides a systematic procedure for computing  $V_{12}$  from ab initio data.

Now, let us suppose that the constant coupling prescription does not provide the detailed features needed to describe the reaction pathway. Furthermore, we find that the coupling as a function of the coordinates can be described adequately (from comparison to ab initio data) using a Gaussian functional form. How should one modify the above EVB input files to obtain a more accurate reactive surface? We need to change the `xch_type` variable from “**constant**” to “**gauss**” as well as replace the variable `xch_cnst` by the variable `xch_gauss(:)`, which contains the parameters for the Gaussian functional form. Of course, these parameters need to be optimized to provide the more accurate surface. The modifications to the EVB input files look something like the following,

```

:
xch_type = "constant",
xch_type = "gauss",
:
:
xch_cnst(1)%ist = 1, xch_cnst(1)%jst = 2,
xch_cnst(1)%xcnst = 12.5,
xch_gauss(1)%ist = 1, xch_gauss(1)%jst = 2,
xch_gauss(1)%iatom = 8, xch_gauss(1)%jatom = 7,
xch_gauss(1)%a = 11.0, xch_gauss(1)%sigma = 0.0447,
xch_gauss(1)%r0 = 2.3,
:
:

```

where the cross-through lines have been replaced by those below them. Access to the exponential functional form or the distributed Gaussian approximation to  $V_{12}$  entails similar changes to the input files. Please see \$AMBERHOME/test/evb for examples.

### 3.4.3. Biased sampling

When a reactive event is described by an intrinsic high free energy barrier, molecular dynamics on the EVB ground-state surface will not adequately sample the important transition state region. Under these conditions, chemical reactions are rare events and sampling on the EVB surface effectively reduces to sampling on a diabatic surface. One framework for enhancing the sampling of rare events is through modification of the system Hamiltonian with the addition of biasing potentials. The EVB facility in Amber offers several options for biased sampling: (1) Ariel Warshel’s mapping potential approach[98] (2) Dave Case’s umbrella sampling on an energy gap RC (3) umbrella sampling on a distance RC and (4) umbrella sampling on a difference of distances RC.

In the mapping potential framework, the system Hamiltonian (and hence, the molecular dynamics) is described by the modified potential

$$V_{\lambda} = (1 - \lambda)V_{ii} + \lambda V_{ff} \quad (3.14)$$

where  $V_{ii}$  is the EVB matrix element for the *initial* state and  $V_{ff}$  is the EVB matrix element for the *final* state. As the value of the mapping potential parameter  $\lambda$  changes from 0 to 1, the system *evolves* from the initial state to the final state. As an example, for  $\lambda = 0.50$ , the

### 3. Force field modifications

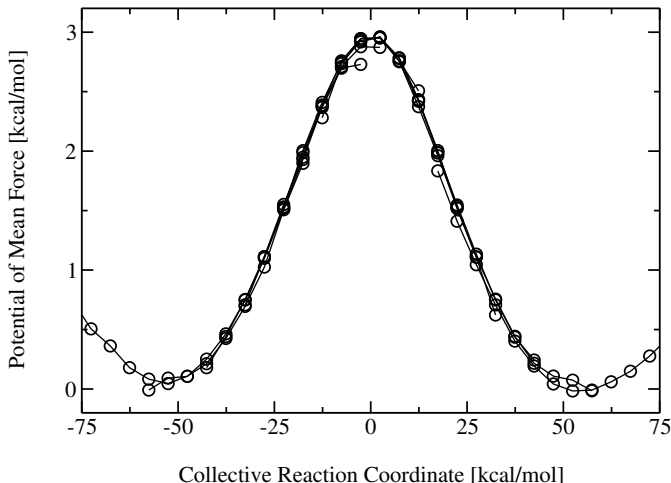


Figure 3.3.: *Potential of mean force along an energy gap RC for the intramolecular proton transfer in malonaldehyde as obtained from a series of mapping potential simulations.*

system Hamiltonian is an equal linear combination of the initial and final states and molecular dynamics sample the region in the vicinity of the transition state. Each mapping potential  $V_\lambda$  samples only a portion of the reaction coordinate. In practice, a series of mapping potentials are used to bias the sampling across the entire range of the RC. The average distribution of the RC for each mapping potential is then *unbiased* and the set of unbiased distributions are combined to give the potential of mean force (PMF) on the EVB ground-state surface. Figure 3.3 shows a PMF for the malonaldehyde intramolecular proton transfer reaction as obtained from 9 mapping potential simulations with  $\lambda$  ranging from 0.10 to 0.90 at 0.10 intervals.

In the umbrella sampling framework, the system Hamiltonian is described by the modified potential

$$\begin{aligned} V_{\text{biased}}^{(n)}(\mathbf{q}) &= V_{\text{el0}}(\mathbf{q}) + V_{\text{umb}}^{(n)}(\mathbf{q}) \\ &= V_{\text{el0}}(\mathbf{q}) + \frac{1}{2}k^{(n)} \left[ \text{RC}(\mathbf{q}) - \text{RC}_0^{(n)} \right]^2 \end{aligned} \quad (3.15)$$

where  $\mathbf{q}$  is the set of system coordinates,  $k$  is the *harmonic force constant* parameter, and  $V_{\text{umb}}^{(n)}$  is an umbrella potential that is added to the original system potential  $V_{\text{el0}}$  (obtained from diagonalization of the EVB matrix) to bias the sampling towards a particular value of the reaction coordinate  $\text{RC}_0^{(n)}$ . The superscript  $(n)$  denotes that a series of biased simulations, each enhancing the sampling of a particular window of the RC, is required to map out the entire PMF. The number of umbrella sampling windows as well as the choice of values for the force constant parameter and the RC equilibrium position will depend ultimately on the nature of the free energy landscape of the system in question.

Results from the biased samplings then can be unbiased and combined using the weighted histogram analysis method (WHAM)[108–110] to generate the PMF describing chemistry on the physically relevant EVB ground-state potential energy surface,  $V_{\text{el0}}$ . Figure 3.4 depicts the PMF for the malonaldehyde intramolecular proton transfer that is obtained from 13 umbrella sampling simulations with  $\text{RC}_0^{(n)}$  spanning the range -60 kcal/mol to +60 kcal/mol at 10 kcal/mol intervals. The supporting program to generate the PMF from a set of mapping poten-

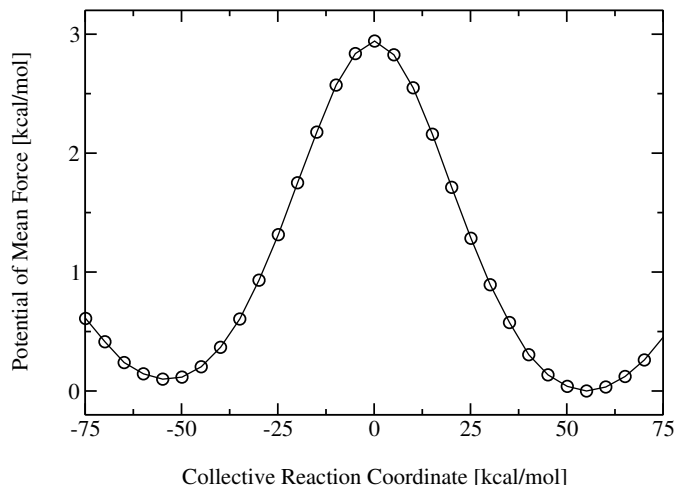


Figure 3.4.: *Potential of mean force for the intramolecular proton transfer in malonaldehyde as obtained from a series of umbrella sampling simulations along an energy gap RC. The distributions of the RC from all the windows are combined using the WHAM procedure.*

tial or from a set of umbrella sampling simulations can be obtained from the Amber website, <http://ambermd.org>.

Biased sampling is accessed through the **nbias** and **evb\_dyn** variables in the EVB input file. The variable **nbias** specifies the number of biasing potentials to include in the system Hamiltonian. Mapping potential dynamics is invoked using the assignment **evb\_dyn="evb\_map"**. Biased sampling via umbrella potentials is invoked with the assignment **evb\_dyn="egap\_umb"**, **evb\_dyn="bond\_umb"** or **evb\_dyn="dbonds\_umb"**. Associated with each choice of biased sampling approach is a derived type variable that provides the required parameters, as shown in Table 3.2. Please see Section 3.4.6 for more details about the variable dependencies.

#### 3.4.4. Quantization of nuclear degrees of freedom

The EVB framework provides a computationally practical approximation to the *electronic* surface for modeling chemical reactions involving classical atoms. The full Schrödinger equation, nevertheless, describes not only the electrons but also the nuclei as a wave function. This quantum mechanical description of nuclei is particularly important for capturing the nuclear dispersion of light particles, such as hydrogen. We provide quantization of the nuclear degrees of freedom via coupling of the EVB facility with the Feynman Path-Integral Molecular Dynamics function in Amber [105–107]. The current implementation utilizes the PIMD engine that is built on top of the locally enhanced sampling (LES) infrastructure. As such, the user will need to build the parallel version of LES *sander* in order to utilize EVB/LES-PIMD.

PIMD is invoked using the **ipimd** variable (and associated dependencies) in the **&cntrl** namelist of the *mdin* input file (please consult Section 5.1.2). The requirements for EVB

### 3. Force field modifications

within the EVB/LES-PIMD context are similar to those described for classical EVB but with the coordinate and parmtop files modified for a LES-type calculation, where the number of LES copies correspond to the number of path integral slices. For example, a classical EVB umbrella sampling on a difference of distances RC will have EVB input files similar to the above examples but with the following modifications

```
:
evb_dyn      = "dbonds_umb",
:
dbonds_umb(1)%iatom = 8, dbonds_umb(1)%jatom = 9, dbonds_umb(1)%katom = 7,
dbonds_umb(1)%k = 100.000, dbonds_umb(1)%zero = -.20,
:
```

EVB/LES-PIMD utilizes these same EVB input files. The EVB group file *evb.grpfile*, however, has been modified to point to the LES coordinate and parmtop files

```
# 32-bead Malonaldehyde RS: H9 bonded to O8
-O -i mdin -p mr_les.top -c mr_les.crd -o mr_les.out -r mr_les.rst \
  -evbin input.mr
# 32-bead Malonaldehyde PS: H9 bonded to O7
-O -i mdin -p mp_les.top -c mr_les.crd -o mp_les.out -r mp_les.rst \
  -evbin input.mp
```

Additionally, the *-nslice <# PIMD slices>* variable must be passed to the *sander* executable:

```
mpirun -np 2 sander.LES.MPI -ng 2 -nslice 32 -groupfile evb.grpfile
```

Here, the atoms of the malonaldehyde system have been replicated into 32 copies using the *addles* utility (see Section 5.1.2) and each of the EVB diabatic states now use the corresponding LES coordinate and parmtop files. Nuclear quantization lowers the free energy barrier due to quantum mechanical effects, such as zero point motion and tunneling. Figure 3.5 compares the PMFs for the malonaldehyde proton transfer reaction along a difference of distances RC from classical EVB and EVB/PIMD umbrella sampling simulations. Currently, only the distance and difference of distances RCs are supported in EVB/PIMD. The energy gap RC is not supported because the theoretical formulation of quantum transition state theory based on an energy gap RC has not yet been worked out.

#### 3.4.5. Distributed Gaussian EVB

As briefly mentioned in the Introduction to EVB,  $V_{12}$  can be fit to high-level electronic structure data using a set of s-, p-, and d-type Gaussians as the fitting basis functions. The current incarnation of DG EVB is limited to two-state gas-phase systems. Current efforts to extend this approach to the condensed phase will provide a practical systematic procedure for constructing a reactive surface from ab initio information. The curious student is encouraged to read the original papers on this method for the theoretical formulation[100, 101]. Here, we



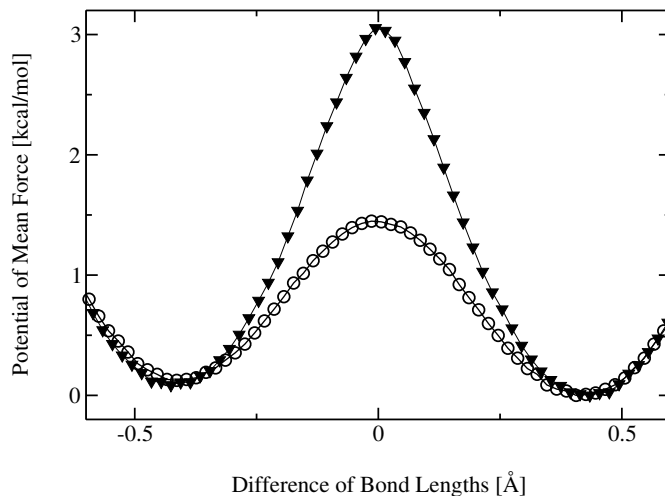


Figure 3.5.: PMFs as a function of the difference of bond lengths involving the proton with the donor and acceptor oxygens in malonaldehyde. The ▼ curve is from classical EVB, while the ⊙ curve is from EVB/PIMD.

only provide an example of this approach for constructing an ab initio-inspired surface describing the proton transfer reaction in malonaldehyde. All the previously described EVB functionalities are accessible to this method. For example, the key elements of the *RS input.mr* file for biased sampling along a distance RC on the DG EVB surface may look something like the following:

```

:
:
nUFF = 1, nbias = 1,
dia_type = "ab_initio",
xch_type = "dist_gauss",
evb_dyn = "bond_umb",
bond_umb(1)%iatom = 7, bond_umb(1)%jatom = 9,
bond_umb(1)%k = 400.000, bond_umb(1)%zero = 1.20,
dist_gauss%stype = "no_dihedrals",
dist_gauss%lin_solve = "diis",
dist_gauss%xfile_type = "gaussian_fchk",
ts_xfile(1) = "malonaldehydeTS_35.fchk",
min_xfile(1) = "malonaldehydeR_35.fchk",
min_xfile(2) = "malonaldehydeP_35.fchk",
dgpt_alpha(1) = 0.72,
dgpt_alpha(2) = 0.72,
dgpt_alpha(3) = 0.72,
UFF(1)%iatom = 7, UFF(1)%jatom = 9

```

### 3. Force field modifications

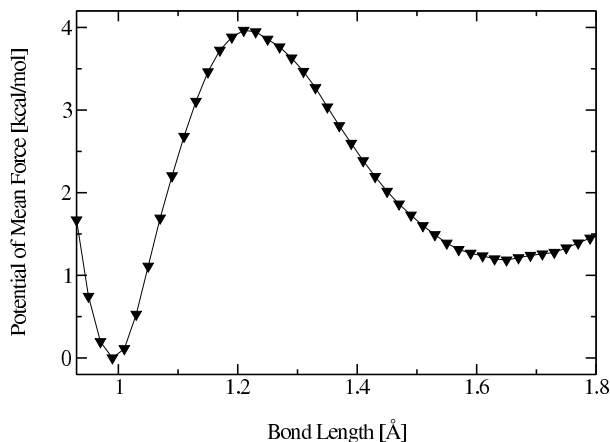


Figure 3.6.: PMF as a function of the distance between atoms  $H_9$  and  $O_7$  in malonaldehyde. The potential energy surface was constructed from *ab initio* data using the DG EVB approach.

⋮

These variables are described in Section 3.4.6. DG EVB is invoked through the `xch_type` variable, with dependencies on `dist_gauss`, `ts_xfile(:)`, `min_xfile(:)`, `dgpt_alpha(:)`, and `UFF(:)`. The *ab initio* data for the RS minimum are contained in the file `malonaldehydeR_35.fchk`, those for the PS minimum are contained in `malonaldehydeP_35.fchk`, and those for the transition state are contained in `malonaldehydeTS_35.fchk`. These files are in the *Gaussian* [111] formatted checkpoint file format (`gaussian_fchk`). The  $\alpha$  parameter [see Eqs. (3.11-3.13)] associated with each of these configuration space points is specified in the variable `dgpt_alpha(:)`. If we wish to include additional *ab initio* data points along the reaction path, we can specify the file names for those points in the variable `xdg_xfile(:)`. The  $\alpha$  parameters associated with these points can be specified in `dgpt_alpha(:)`. It is important to keep in mind that the  $\alpha$  parameters are ordered as follows: `dgpt_alpha(ts_xfile(1), min_xfile(1), min_xfile(2), xdg_xfile(:))`. Lastly, the `UFF` variable requests the inclusion of a Universal Force Field [112] repulsive term in  $V_{11}$  between the transferred proton ( $H_9$ ) and the acceptor ( $O_7$ ). The *input.mp* file for the PS  $V_{22}$  is identical to the above, but with the `UFF` variable changed to reflect the identity of the acceptor atom from the perspective of the product state topology: `UFF(1)%iatom = 8, UFF(1)%jatom = 9`. In practice, the inclusion of this term to  $V_{ii}$  provides a more optimal DG EVB surface for molecular dynamics sampling. Figure 3.6 shows the PMF for shortening the  $r_{H_9-O_7}$  distance of the malonaldehyde RS from 1.8 Å to 1.0 Å using umbrella sampling of this RC. Note that the PMF is not symmetric because this choice of RC breaks the intrinsic symmetry of the reaction. The difference of distances RC involving atoms  $O_8$ ,  $H_9$  and  $O_7$  does provide a symmetric PMF and this is shown in Figure 5.2 within the context of kinetic isotope effect (Section 5.6.5).

### 3.4.6. EVB input variables and interdependencies

The variables in the **&evb** namelist of the EVB input file are described below. The style of the input file is similar to the traditional *mdin* used in a *sander* run. Assignment to character type variables need to be encapsulated within quotation marks (for example, **evb\_dyn**="groundstate"). Array variables are denoted below by a colon enclosed within parentheses [for example, **dia\_shift**(:)]. Derived type variables can be assigned element-wise, i.e., **dia\_shift**(1)%st = 1, **dia\_shift**(1)%nrg\_offset = 0.0. In the specifications below, the data type of each variable is enclosed in {...}, while the size of each array variable is enclosed in [...].

- ntw\_evb** {integer}. MD step interval for writing to the EVB output file *evbout*.
- nevb** {integer}. Number of EVB states. For example, **nevb** = 3 specifies that the system is described by a  $3 \times 3$  EVB matrix in the representation of three diabatic states. The EVB group file will contain three lines of *sander* command line options specifying the *mdin*, coordinate, parmtop, and EVB input files.
- nmorse** {integer}. Number of Amber harmonic bond interactions that will be changed to a Morse type interaction. Requires additional inputs from the variable **morsify**(:).
- nbias** {integer}. Number of biasing potentials to include in the system Hamiltonian. The supported biased sampling approaches include (1) mapping potential, (2) umbrella sampling along an energy gap RC, (3) umbrella sampling along a distance RC, and (4) umbrella sampling along a difference of distances RC. See **evb\_dyn** for associated dependencies.
- nmodvdw** {integer}. Number of van der Waals terms to exclude in the calculation of  $V_{ij}$ . Requires additional inputs from the variable **modvdw**(:).
- nuff** {integer}. Number of Universal Force Field [112] repulsive terms to include in the harmonic expansion of  $V_{ii}$  about the ab initio minimum. Requires additional inputs from the variable **uff**(:).
- xch\_type** {character\*512}. Coupling element type.
- = "constant"  $V_{ij}$  is a constant. Requires additional inputs from the variable **xch\_cnst**(:).
- = "exp"  $V_{ij}(r_{kl}) = A_{ij} \exp \left[ -u_{ij} \left( r_{kl} - r_{kl}^{(0,ij)} \right) \right]$ . Requires additional inputs from the variable **xch\_exp**(:).

### 3. Force field modifications

- = “*gauss*”  $V_{ij}(r_{kl}) = A_{ij} \exp \left[ -\frac{1}{\sigma_{ij}^2} \left( r_{kl} - r_{kl}^{(0,ij)} \right)^2 \right]$ . Requires additional inputs from the variable **xch\_gauss(:)**.
- = “*dist\_gauss*”  $V_{ij}$  is described by the Schlegel-Sonnenberg distributed Gaussian approach. Requires additional inputs from the variables **dist\_gauss**, **ts\_xfile(:)**, **min\_xfile(:)**, **xdg\_xfile(:)**, **dgpt\_alpha(:)**, **uff(:)**.

**evb\_dyn** {character\*512}. EVB dynamics type.

- = “*groundstate*” Dynamics on the EVB ground-state potential energy surface.
- = “*evb\_map*” Biased sampling based on Ariel Warshel’s mapping potential approach. Requires additional inputs from the variable **emap(:)**.
- = “*egap\_umb*” Umbrella sampling along an energy gap reaction coordinate. Requires additional inputs from the variable **egap\_umb(:)**.
- = “*bond\_umb*” Umbrella sampling along a distance reaction coordinate. Requires additional inputs from the variable **bond\_umb(:)**.
- = “*dbonds\_umb*” Umbrella sampling along a difference of two distances reaction coordinate. Requires additional inputs from the variable **dbonds\_umb(:)**.
- = “*qi\_bond\_pmf*” For generating the QI joint distribution function along the distance RCs of the  $P$  and  $P/2$  slices (see Section 5.5.2). Requires additional inputs from the variable **bond\_umb(:)**.
- = “*qi\_bond\_dyn*” For sampling of the QI  $f_v$ ,  $F$  and  $G$  factors with the  $P$  and  $P/2$  slices constrained to the dividing surfaces along the distance RCs (see Section 5.5.2). Requires additional inputs from the variable **bond\_umb(:)**.
- = “*qi\_dbonds\_pmf*” For generating the QI joint distribution function along the difference of distances RCs of the  $P$  and  $P/2$  slices (see Section 5.5.2). Requires additional inputs from the variable **dbonds\_umb(:)**.
- = “*qi\_dbonds\_dyn*” For sampling of the QI  $f_v$ ,  $F$  and  $G$  factors with the  $P$  and  $P/2$  slices constrained to the dividing surfaces along the difference of distances RCs (see Section 5.5.2). Requires additional inputs from the variable **dbonds\_umb(:)**.

**dia\_shift(:)** {derived type}, [nevb]. Diabatic state energy shift.

*%st* {integer}. Diabatic state index.

*%nrg\_offset* {real}. Energy offset for EVB state.

**xch\_cnst(:)** {derived type}, [nxch]. Constant coupling. The size of this derived type array is *nxch*, which is calculated internally as  $nevb(nevb - 1)/2$ .

*%ist* {integer}. Diabatic state index involved in the coupling.  
*%jst* {integer}. Diabatic state index involved in the coupling.  
*%xcnst* {real}. Constant exchange parameter.

**xch\_exp(:)** {derived type}, [nxch]. Parameters for the exponential functional form of the coupling term,  $V_{ij}(r_{kl}) = A_{ij} \exp \left[ -u_{ij} \left( r_{kl} - r_{kl}^{(0,ij)} \right) \right]$ . The size of this derived type array is *nxch*, which is calculated internally as  $nevb(nevb - 1)/2$ .

*%ist* {integer}. Diabatic state index involved in the coupling.  
*%jst* {integer}. Diabatic state index involved in the coupling.  
*%iatom* {integer}. Index of atom involved in  $r_{kl}$ .  
*%jatom* {integer}. Index of atom involved in  $r_{kl}$ .  
*%a* {real}.  $A_{ij}$ .  
*%u* {real}.  $u_{ij}$ .  
*%r0* {real}.  $r_{kl}^{(0,ij)}$ .

**xch\_gauss(:)** {derived type}, [nxch]. Parameters for the Gaussian functional form of the coupling term,  $V_{ij}(r_{kl}) = A_{ij} \exp \left[ -\frac{1}{\sigma_{ij}^2} \left( r_{kl} - r_{kl}^{(0,ij)} \right)^2 \right]$ . The size of this derived type array is *nxch*, which is calculated internally as  $nevb(nevb - 1)/2$ .

*%ist* {integer}. Diabatic state index involved in the coupling.  
*%jst* {integer}. Diabatic state index involved in the coupling.  
*%iatom* {integer}. Index of atom involved in  $r_{kl}$ .  
*%jatom* {integer}. Index of atom involved in  $r_{kl}$ .  
*%a* {real}.  $A_{ij}$ .  
*%sigma* {real}.  $\sigma_{ij}$ .  
*%r0* {real}.  $r_{kl}^{(0,ij)}$ .

**morsify(:)** {derived type}, [nmorse]. Parameters used for converting the Amber harmonic bond interactions to the Morse type,  $V_{\text{Morse}}(r_{ij}) = D_e \left[ 1 - e^{-\alpha(r_{ij} - r_{ij}^0)} \right]^2$ . The components in the derived type are

*%iatom* {integer}. Index of atom involved in  $r_{ij}$ .  
*%jatom* {integer}. Index of atom involved in  $r_{ij}$ .

### 3. Force field modifications

*%d* {real}.  $D_e$ .

*%a* {real}.  $\alpha$ .

*%r0* {real}.  $r_{ij}^0$ .

**emap(:)** {derived type}, [nbias]. Mapping potential parameters required for the function  $V_\lambda = (1 - \lambda)V_{ii} + \lambda V_{ff}$ .

*%ist* {integer}. Diabatic state index for the initial state.

*%jst* {integer}. Diabatic state index for the final state.

*%lambda* {real}.  $\lambda$ .

**egap\_umb(:)** {derived type}, [nbias]. Umbrella potential parameters required for the function  $V_{\text{umb}}(\text{RC}) = \frac{1}{2}k[\text{RC} - \text{RC}_0]^2$ , where  $\text{RC} = V_{ii} - V_{ff}$ .

*%ist* {integer}. Diabatic state index for the initial state.

*%jst* {integer}. Diabatic state index for the final state.

*%k* {real}.  $k$ .

*%ezero* {real}.  $\text{RC}_0$ .

**modvdw(:)** {derived type}, [nmodvdw]. Exclude the van der Waals interactions between the specified atom pairs.

*%iatom* {integer}. Index of atom involved in the non-bonded interaction.

*%jatom* {integer}. Index of atom involved in the non-bonded interaction.

**bond\_umb(:)** {derived type}, [nbias]. Umbrella potential parameters for the function  $V_{\text{umb}}(\text{RC}) = \frac{1}{2}k[\text{RC} - \text{RC}_0]^2$ , where  $\text{RC} = r_{ij}$ .

*%iatom* {integer}. Index of atom involved in a distance.

*%jatom* {integer}. Index of atom involved in a distance.

*%k* {real}.  $k$ .

*%ezero* {real}.  $\text{RC}_0$ .

**dbonds\_umb(:)** {derived type}, [nbias]. Umbrella potential parameters for the difference of two distances  $\text{RC}$  where one of the atoms is common to both distances.  $V_{\text{umb}}(\text{RC}) = \frac{1}{2}k[\text{RC} - \text{RC}_0]^2$ , where  $\text{RC} = r_{ij} - r_{kj}$ .

*%iatom* {integer}. Index of atom involved in a distance.  
*%jatom* {integer}. Index of the atom common to both distances.  
*%katom* {integer}. Index of atom involved in a distance.  
*%k* {real}.  $k$ .  
*%ezero* {real}.  $RC_0$ .

**out\_RCdot** {logical}. Output the velocity of a free particle along the RC direction to the file *evbout*.

**dist\_gauss** {derived type}. Schlegel-Sonnenberg distributed Gaussian specifications.

*%stype* {character\*512}. Coordinate selection type. Supported coordinate selection types include “*all\_coords*”, “*bonds\_only*”, “*no\_dihedrals*”, “*react-product*”, “*react-ts-product*”.

*%stol* {real}. Coordinate selection tolerance for *stype*=“*react-product*” or *stype*=“*react-ts-product*”. For *stype*=“*react-product*”, a particular internal coordinate is used in the DG EVB procedure if the difference between the reactant and product structures is  $> stol$ . For the case of *stype*=“*react-ts-product*”, the intersection of the selected set of coordinates from *react-ts*  $> stol$  and *product-ts*  $> stol$  will be used for the DG EVB procedure.

*%xfile\_type* {character\*512}. File type of external ab initio data. Supported file types are “*gaussian\_fchk*” and “*EVB*” (see Section F).

**ts\_xfile(:)** {character\*512}, [\*]. Name of the file containing the ab initio data corresponding to the transition state.

**min\_xfile(:)** {character\*512}, [\*]. Name of the file containing the ab initio data corresponding to the minimum, i.e.  $V_{11}$  and  $V_{22}$ .

**xdg\_xfile(:)** {character\*512}, [\*]. Name of the file containing the ab initio data corresponding to additional points along the IRC.

**dgpt\_alpha(:)** {real}, [\*]. Optimized  $\alpha$  parameters associated with the distributed Gaussian data points.

### 3. Force field modifications

**uff(:)** {derived type}, [nuff]. Include a UFF repulsive term between the specified atom pairs in the harmonic expansion of  $V_{ij}$  about the ab initio minimum.

*%iatom* {integer}. Index of atom involved in the non-bonded interaction.

*%jatom* {integer}. Index of atom involved in the non-bonded interaction.

## 3.5. The AMOEBA force field

The Amoeba force field is a recently developed polarizable force field with parameters for water, univalent ions, small organic molecules and proteins.[28, 29, 113, 114] Differences from the current amber force fields include more complex valence terms including anharmonic bond and angle corrections and bond angle and bond dihedral cross terms, and a two dimensional spline fit for the phi-psi bitorsional energy. The differences in the nonbond treatment include the use of atomic multipoles up to quadrupole order, induced dipoles using a Tholé screening model, and the use of the Halgren buffered 7-14 functional form for van der Waals interactions. The PME implementation used here, as well as a multigrid approach for atomic multipoles, is described in Ref. [35].

Preparation of the necessary coordinate and parameter files for performing simulations using the amoeba forcefield is now very simple (unlike in Amber 9), but does require that you use *slap* in place of *tleap*. The procedure is now almost like any other force field: you load *leaprc.amoeba* in place of other leaprc files at the beginning; at the end, use *saveamoebaparm* in place of *saveamberparm*.

With the use of Amoeba, minimization as well as usual *sander* methods of molecular dynamics can be used, including constant temperature and pressure simulations. In addition, with the amoeba implementation it is possible to use the Beeman dynamics integrator, which is helpful in making detailed comparisons to Tinker results. Note that the Amoeba forcefield is parametrized for fully flexible molecules. At this time it is not possible to use SHAKE with this forcefield.

The parameters *ew\_coeff*, *nfft1*, *nfft2*, *nfft3*, and *order* from the *&ewald* section of input all relate to the accuracy of the PME method, which is used in the Amoeba implementation in *sander*. Due to the use of atomic quadrupoles, *order* (i.e. the B-spline polynomial degree plus one) needs to be at least 5 since the B-spline needs 3 continuous derivatives. The *ew\_coeff* together with the direct sum cutoff (see below) controls the accuracy in the Ewald direct sum, and *ew\_coeff* together with the PME grid dimensions *nfft1,2,3* and *order* controls the accuracy in the reciprocal sum. Since Amoeba atomic multipoles are typically dominated by the charges, experience gained in the usual use of PME is pertinent. Typical values we have used for a good cost vs. accuracy balance are *ew\_coeff*=0.45, *order*=5, and *nfft1,2,3* approximately 1.25 times the cell length in that direction.

Some specific amoeba-related input parameters are given here. They should be placed in the *&amoeba* namelist, following the *&cntrl* namelist where *iamoeba* has been set to 1.

*beeman\_integrator* Setting this to be one turns on the Beeman integrator. This is the default integrator for Amoeba in Tinker. In *sander* this integrator can be used for NVE



simulations, or for NVT or NTP simulations using the Berendsen coupling scheme. (This means that you must set *ntt* to 0 or 1 if you use the Beeman integrator.) By default, *beeman\_integrator*=0, and the usual velocity Verlet integration scheme is used instead.

- amoeba\_verbose* In addition to the usual sander output, by setting *amoeba\_verbose*=1, energy and virial components can be output. By default, *amoeba\_verbose*=0.
- ee\_dsum\_cut* This is the ewald direct sum cutoff. In the amoeba implementation this is allowed to be different from the nonbond cutoff specified by *cut*. It should be less than or equal to the latter. (Note, this feature does not apply to the direct sum for standard amber force fields, which use the nonbond cutoff for the Ewald direct sum as well as van der Waals interactions. The default is 7.0 Angstroms, which is conservative for energy conservation with *ew\_coeff*=0.45.
- dipole\_scf\_tol* The induced dipoles in the amoeba force field are solutions to a set of linear equations (like the Applequist model but modified by Thol  damping for close dipole-dipole interactions). These equations are solved iteratively by the method of successive over-relaxation. *dipole\_scf\_tol* is the convergence criterion for the iterative solution to the linear equations. The iterations towards convergence stop when the RMS difference between successive sets of induced dipoles is less than this tolerance in Debye. The default is set to 0.01 Debye, which has been seen to give reasonable energetics and dynamics, but requires mild temperature restraints. Good energy conservation in NVE simulations requires a tolerance of about  $10^{-6}$  Debye tolerance.
- sor\_coefficient* This is the successive over-relaxation parameter. This can be adjusted to optimize the number of iterations needed to achieve convergence. Default value is 0.75. Productive values seem to be in the range 0.6-0.8. The optimal values seem to depend on the polarizabilities of the system atoms.
- dipole\_scf\_iter\_max* This prevents infinite iterations when the polarization equations are somehow not converging. A possible reason for this is a bad *sor\_coefficient*, exacerbated by a close contact. Default is 50. For comparison, with typical *sor\_coefficient* values and an equilibrated system it should take 4-7 iterations to achieve 0.01 Debye convergence and 18-25 iterations to achieve  $10^{-6}$  Debye.
- ee\_damped\_cut* This is used to cutoff the Thol  damping interactions. The default value is 4.5 Angstroms, which should work for the typical sized polarizabilities encountered, and the default Thol  screening parameter (0.39).
- do\_vdw\_taper* Amoeba uses a Halgren buffered 7-14 form for the van der Waals interactions. In the Tinker code these are typically evaluated out to 12 Angstroms, with a taper turned on and no long-range isotropic continuum corrections to the energy and virial. In the sander implementation, the usual nonbond cutoff from the *&cntrl* namelist is used for van der Waals interactions. The long range correction is available to allow for shorter cutoffs. Setting *do\_vdw\_taper* to one causes VDW interactions to be tapered to zero beginning at 0.9 times the van der waals cutoff. The

### 3. Force field modifications

taper is a 5th order polynomial switch on the energy term, which gets differentiated for the forces (atom based switching). Its turned on by default.

do\_vdw\_longrange Setting this to one causes the long-range isotropic continuum correction to be turned on. This adjusts the energy and virial, and in most cases will result in energies and virials that are fairly invariant to van der Waals cutoff, with or without the above taper function. The integrals involved in this correction are done numerically.

## 3.6. QM/MM calculations: Semi-empirical methods

*Sander* supports the option of describing part of the system quantum mechanically in an approach known as a hybrid (or coupled potential) QM/MM simulation. Semi-empirical neglect of diatomic overlap (NDDO)-type and density functional tight binding (DFTB) Hamiltonians are supported natively by *sander* and the basic documentation (e.g. what Hamiltonians are implemented, description of the input parameters) can be found in Chapter 5 of the *AmberTools Users' Manual*. Here we limit our description to those features that are unique to the QM/MM interface implemented in *sander*. More advanced Hamiltonians based on *ab initio* wave function theory (WFT) and density functional theory (DFT) are supported via an interface to external QM software packages the use of which is described in section 3.7.

The built-in semi-empirical QM/MM support was written by Ross Walker and Mike Crowley, [115] based originally on public-domain MOPAC codes of J.J.P. Stewart. The QM/MM Generalised Born implementation uses the model described by Pellegrini and Field[116] while regular QM/MM Ewald support is based on the work of Nam *et al.*[117] with QM/MM PME support based on the work of Walker *et al.*[115]. SCC-DFTB support was written by Gustavo Seabra, Ross Walker and Adrian Roitberg,[118] and is based on earlier work of Marcus Elstner.[119, 120] Support for third-order SCC-DFTB was written by Gustavo Seabra and Josh McClellan.

### 3.6.1. The hybrid QM/MM potential

When running a QM/MM simulation in *Sander* the system is partitioned into two regions, a QM region consisting of the atoms defined by either the *qmmask* or *iqmatoms* keyword, and a MM region consisting of all the atoms that are not part of the QM region. For a typical protein simulation in explicit solvent the number of MM atoms will be much greater than the number of QM atoms. Either region can contain zero atoms, giving either a pure QM simulation or a standard classical simulation. For periodic simulations, the quantum region must be *compact*, so that the extent (or diameter) of the QM region (in any direction) plus twice the QM/MM cutoff must be less than the box size. Hence, you can define an "active site" to be the QM region, but in most cases could not ask that all cysteine residues (for example) be quantum objects. The restrictions are looser for non-periodic (gas-phase or generalized Born) simulations, but the codes are written and tested for the case of a single, compact quantum region.

The partitioned system is characterized by an effective Hamiltonian which operates on the system's wavefunction  $\Psi$ , which is dependent on the position of the MM and QM nuclei, to yield the system energy  $E_{eff}$ :

### 3.6. QM/MM calculations: Semi-empirical methods

$$H_{eff}\Psi(x_e, x_{QM}, x_{MM}) = E(x_{QM}, x_{MM})\Psi(x_e, x_{QM}, x_{MM}) \quad (3.16)$$

The effective Hamiltonian consists of three components - one for the QM region, one for the MM region and a term that describes the interaction of the QM and MM regions, implying that likewise the energy of the system can be divided into three components. If the total energy of the system is re-written as the expectation value of  $H_{eff}$  then the MM term can be removed from the integral since it is independent of the position of the electrons:

$$E_{eff} = \langle \Psi | H_{QM} + H_{QM/MM} | \Psi \rangle + E_{MM} \quad (3.17)$$

In the QM/MM implementation in *sander*,  $E_{MM}$  is calculated classically from the MM atom positions using the Amber or CHARMM force field equation and parameters, whereas  $H_{QM}$  is evaluated using the chosen QM method.

The interaction term  $H_{QM/MM}$  is more complicated. By default, *sander* uses an electrostatic embedding scheme (also referred to as additive scheme) in which the interaction of the MM point charges with the electrons of the QM system as well as the interaction between the MM point charges and the QM nuclei (atomic cores for semi-empirical methods) is explicitly taken into account. In other words, the MM region polarizes the QM electron density. For the case where there are no covalent bonds between the atoms of the QM and MM regions the interaction Hamiltonian is thus the sum of an electrostatic term and a Lennard-Jones (VDW) term and can be written as

$$H_{QM/MM} = \sum_q \sum_m \left[ Q_m h_{electron}(x_e, x_{MM}) - Q_m Z_q h_{core}(x_{QM}, x_{MM}) + \left( \frac{A}{r_{qm}^{12}} - \frac{B}{r_{qm}^6} \right) \right] \quad (3.18)$$

where the subscripts  $e$ ,  $m$  and  $q$  refer to the electrons, the MM nuclei and the QM nuclei respectively. Here  $Q_m$  is the charge on MM atom  $m$ ,  $Z_q$  is the core charge (nucleus minus core electrons) on QM atom  $q$ ,  $r_{qm}$  is the distance between atoms  $q$  and  $m$ , and A and B are Lennard-Jones interaction parameters. For systems that have covalent bonds between the QM and MM regions, the situation is more complicated, as discussed later.

A more approximate form of the interaction term  $H_{QM/MM}$  is referred to as mechanical embedding (or subtractive QM/MM scheme). In this case the interactions between the QM and the MM region are obtained within the same classical approximation that is used for the MM region, that is

$$H_{QM/MM} = \sum_q \sum_m \left[ \frac{Q_m Q_q}{r_{qm}} + \left( \frac{A}{r_{qm}^{12}} - \frac{B}{r_{qm}^6} \right) \right] \quad (3.19)$$

where  $Q_q$  is the classical MM point charge assigned to an atom in the QM region. Mechanical embedding is useful to impose steric constraints on the embedded QM system, however, the electron density is not polarized by the MM environment. An additional complication of this approach is that the point charges that are assigned to the atoms in the QM region have to represent the electrostatic potential of the QM region during the whole course of a QM/MM simulation.

### 3. Force field modifications

If one evaluates the expectation values in Eq. 3.17 over a single determinant built from molecular orbitals

$$\phi_i = \sum_j c_{ij} \chi_j \quad (3.20)$$

where the  $c_{ij}$  are molecular orbital coefficients and the  $\chi_j$  are atomic basis functions, the total energy depends upon the  $c_{ij}$  and on the positions  $x_{MM}$  and  $x_{QM}$  of the atoms. The energy is obtained by setting  $\partial E_{eff}/\partial c_{ij}$  to zero which leads to a self-consistent (SCF) procedure to determine the  $c_{ij}$ , (with a modified Fock matrix that contains the electric field arising from the MM charges in the case of electrostatic embedding). Once the energy is known, the forces on the atoms can be obtained by taking the derivative of the energy expression with respect to the positions of the QM and MM atoms.

The main subtlety that arises in the case of electrostatic embedding is that, for a periodic system, there are formally an infinite number of QM/MM interactions; even for a non-periodic system, the (finite) number of such interactions may be prohibitively large. These problems are addressed in a manner analogous to that used for pure MM systems: a PME approach is used for periodic systems, and a (large) cutoff may be invoked for non-periodic systems. Some details are discussed below.

#### 3.6.2. The QM/MM interface and link atoms

The sections above dealt with situations where there are no covalent bonds between the QM and MM regions. In many protein simulations, however, it is necessary to have the QM/MM boundary cut covalent bonds, and a number of additional approximations have to be made. There are a variety of approaches to this problem, including hybrid orbitals, capping potentials, and explicit link atoms. The last option is the method available in *sander*.

There are a number of ways to implement a link atom approach that deal with the way the link atom is positioned, the way the forces on the link atom are propagated, and the way non-bonding interactions around the link atom are treated. Each time an energy or gradient calculation is to be done, the link atom coordinates are re-generated from the current coordinates of the QM and MM atoms making up the QM-MM covalent pair. The link atom is placed along the bond vector joining the QM and MM atom, at a distance  $d_{L-QM}$  from the QM atom. By default  $d_{L-QM}$  is set to the equilibrium distance of a methyl C-H atom pair (1.09 Å) but this can be set in the input file. The default link atom type is hydrogen, but this can also be specified as an input.

Since the link atom position is a function of the coordinates of the "real" atoms, it does not introduce any new degrees of freedom into the system. The chain rule is used to re-write forces on the link atom itself in terms of forces on the two real atoms that define its position. This is analogous to the way in which "extra points" or "lone-pairs" are handled in MM force fields.

The remaining details of how the QM-MM boundary is treated are as follows: for the interactions surrounding the link atom, the MM bond term between the QM and MM atoms is calculated classically using the classical force field parameters, as are any angle or dihedral terms that include at least one MM atom. The Lennard-Jones interactions between QM-MM atom pairs are calculated in the same way as described in the section above with exclusion of 1-2 and 1-3 interactions and scaling of 1-4 interactions. What remains is to specify the electrostatic interactions between QM and MM atoms around the region of the link atom.

A number of different schemes have been proposed for handling link-atom electrostatics. Many of these have been tested or calibrated on (small) gas-phase systems, but such testing can neglect some considerations that are very important for more extended, condensed-phase simulations. In choosing our scheme, we wanted to ensure that the total charge of the system is rigorously conserved (at the correct value) during an MD simulation. Further, we strove to have the Mulliken charge on the link atom (and the polarity of its bond to the nearest QM atom) adopt reasonable values and to exhibit only small fluctuations during MD simulations. Link atoms interact with the MM field in exactly the same way as regular QM atoms. That is they interact with the electrostatic field due to all the MM atoms that are within the cutoff, with the exception of the MM link pair atoms (MM atoms that are bound directly to QM atoms). VDW interactions are not calculated for link atoms. These are calculated between all real QM atoms and all MM atoms, including the MM link pair atoms. For Generalized Born simulations the effective Born radii for the link atoms are calculated using the intrinsic radii for the MM link pair atoms that they are replacing.

In the case of electrostatic embedding the atoms that make up the QM region (including the MM link pair atom) have their charges from the prmtop file essentially replaced with Mulliken charges. Hence it is important to consider the issue of charge conservation. The QM region (including the link atoms) by definition must have an integer charge. This is defined by the &qmmm namelist variable *qmcharge*. If the MM atoms (including the MM link pair atoms) that make up the QM region have prmtop charges that sum to the value of *qmcharge* then there is no problem. If not, there are two options for dealing with this charge, defined by the namelist variable *adjust\_q*. A value of 1 will distribute the difference in charge equally between the nearest *nlink* MM atoms to the MM link pair atoms. A value of 2 will distribute this charge equally over all of the MM atoms in the simulation (excluding MM link pair atoms).

### 3.6.3. A reformulated QM/MM interface for PM3

In the current version of Amber, a reformulated QM-MM core-charge potential (denoted as PM3/MM\*) has been implemented. This reformulated potential scales the interaction between a QM core and a MM charge for the purpose of better description of the geometry and energy at the QM-MM interface:[121]

$$E_{QM/MM}^{core} = Z_a q_m (s_a s_a, s_m s_m) \left[ 1 + \frac{|q_m|}{q_m} \cdot \left( -e^{-f_1^a \cdot R_{am}} + e^{-f_2^a \cdot R_{am}} \right) \right] \quad (3.21)$$

where  $Z_a$  is the effective core charge of QM atom  $a$ ,  $q_m$  is the partial charge on MM atom  $m$ ,  $s_a$  is an  $s$  orbital on the QM atom,  $s_m$  is a notional  $s$  orbital on the MM atom,  $R_{am}$  is the QM-MM interatomic distance, and  $f_1^a$  and  $f_2^a$  are exponential scale factors which depend on the QM atom only. Optimal values for  $f_1^a$  and  $f_2^a$  were determined based on the PM3 Hamiltonian, and are available for H, C, N and O atoms (so the QM region is limited to these four atoms; but the MM region is not restricted). Application of this reformulated potential shows improved prediction of geometry and interaction energy at the QM-MM interface for hydrogen bonded small molecule complexes typical of biomolecular interactions, without significantly impacting the modeling of other interaction types, such as dispersion dominant complexes.[121] In a QM/MM calculation, giving *qmmm\_int=3* along with *qm\_theory=PM3* will invoke this potential.

### 3. Force field modifications

Based on PM3/MM\*, further developments to semi-empirical QM/MM coupling method have been introduced – PM3/MMX2 (*qmmm\_int=4* and *qm\_theory=PM3*) – which shares same QM core-MM charge equation with PM3/MM\* model. In addition, a QM parameter,  $\rho_{mm}$ , is introduced to each type of QM atoms in order to “fine-tune” the QM electron-MM charge interaction (Eq. 3.22). Although  $\rho_{mm}$  is a parameter for QM atom, the subscript *mm* emphasizes that it is a MM-related property (eqn 3.xx). Parameters are currently available for H, C, N, O and S QM atoms (manuscript in preparation).

$$E_{QM/MM}^{electron} = -q_m(\mu_a v_a, s_m s_m) = \sum_{\ell_a} \sum_{\ell_m} [M_{\ell_a k}^a M_{\ell_m k}^m] \quad (3.22)$$

where

$$[M_{\ell_a k}^a M_{\ell_m k}^m] = \frac{e^2}{2^{l_a+l_m}} \sum_{i=1}^{2^{l_a}} \sum_{j=1}^l [r_{ij}^2 + (\rho_{l_a}^a + \rho_{mm}^a)^2]^{-1/2} \quad (3.23)$$

#### 3.6.4. Generalized Born implicit solvent

The implementation of Generalized Born (GB) for QM/MM calculations is based on the method described by Pellegrini and Field.[116] Here, the total energy is taken to be  $E_{eff}$  from Eq. 3.17 plus  $E_{gb}$  from Eq. 3.2. In  $E_{gb}$ , charges on the QM atoms are taken to be the Mulliken charges determined from the quantum calculation; hence these charges depend upon the molecular orbital coefficients  $c_{ij}$  as well as the positions of the atoms.

As with conventional QM/MM simulations, one then solves for the  $c_{ij}$  by setting  $\partial E_{eff} / \partial c_{ij} = 0$ . This leads to a set of SCF equations with a Fock matrix modified not only by the presence of MM atoms (as in "ordinary" QM/MM simulations), but also modified by the presence of the GB polarization terms. Once self-consistency is achieved, the resulting Mulliken charges can be used in the ordinary way to compute the GB contribution to the total energy and forces on the atoms.

#### 3.6.5. Ewald and PME

The support for long range electrostatics in QM/MM calculations using electrostatic embedding is based on a modification of the Nam, Gao and York Ewald method for QM/MM calculations.[117] This approach works in a similar fashion to GB in that Mulliken charges are used to represent long range interactions. Within the cut off, interactions between QM and MM atoms are calculated using a full multipole treatment. Outside of the cut off the interaction is based on pairwise point charge interactions. This leads to a slight discontinuity at the QM/MM cut off boundary and thus a small energy drift during QM/MM MD simulations in the NVE ensemble. This energy drift can be avoided by using a switching function at the cutoff (see below).

The implementation in Ref [117] uses an Ewald sum for both QM/QM and QM/MM electrostatic interactions. This can be expensive for large MM regions, and thus *sander* uses a modification of this method by Walker and Crowley[115] that uses a PME model (rather than an Ewald sum) for QM/MM interactions. This is controlled by the *qm\_pme* variable discussed below.

### 3.6. QM/MM calculations: Semi-empirical methods

When running QM/MM Ewald or PME simulations in Sander, if QM multipoles are involved in QM-MM interaction, a discontinuity in the QM-MM electrostatic potential may occur at the cut-off distance due to the sudden change in the potential function (the difference between Eqs. 3.24 and 3.25), thus resulting in energy conservation problems in the simulation.

$$E_{QM/MM}^{r < cutoff} = -q_m(\mu_a \nu_a, s_m s_m) + Z_a q_m(s_a s_a, s_m s_m)(1 + scale) \quad (3.24)$$

$$E_{QM/MM}^{r > cutoff} = \frac{q_m(Z_a - \sum c_{\mu\mu})}{r} \quad (3.25)$$

This problem can be avoided by applying a switching function to smoothly connect the two different potentials. The QM/MM electrostatic potential using a switching function can thus be written as:

$$E_{QM/MM} = E_{QM/MM}^{r < cutoff} s(r) + E_{QM/MM}^{r > cutoff} (1 - s(r))$$

The switching function can be turned on or off via setting `&qmmm` namelist variable `qmmm_switch`, for details see section 3.6.7 below.

#### 3.6.6. Hints for running successful QM/MM calculations

##### **Required Parameters and Prmtop Creation**

QM/MM calculations without link atoms require mass, charges, van der Waals and GB radii in the `prmtop` file. All bonds, angles, and dihedrals parameters involving QM atoms are neglected. In the case of electrostatic embedding the charges are also neglected. (Note that when SHAKE is applied, the bonds are constrained to the ideal MM values, even when these are part of a QM region; hence, for this case, it is important to have correct bond parameters in the QM region.) The simplest general prescription for setting things up is to use `antechamber` and `LEaP` to create a reference force field, since "placeholders" are required in the `prmtop` file even for things that will be neglected. This also allows you to run comparison simulations between pure MM and QM/MM simulations, which can be helpful if problems are encountered in the QM/MM calculations.

The use of `antechamber` to construct a pure MM reference system is even more useful when there are link atoms, since here MM parameters for bonds, angles and dihedrals that cross the QM/MM boundary are also needed.

##### **Choosing the QM region**

There are no good universal rules here. Generally, one might want to have as large a QM region as possible, but having more than 80-100 atoms in the QM region will lead to simulations that are very expensive. One should also remember that for many features of conformational analysis, a good MM force field may be better than a semiempirical or DFTB quantum description. In choosing the QM/MM boundary, it is better to cut non-polar bonds (such as C-C single bonds) than to cut unsaturated or polar bonds. Link atoms are not placed between bonds to hydrogen. Thus cutting across a C-H bond will NOT give you a link atom across that bond.

### 3. Force field modifications

(This is not currently tested for in the code and so it is up to the user to avoid such a situation.) Furthermore, link atoms are restricted to one per MM link pair atom. This is tested for during the detection of link atoms and an error is generated if this requirement is violated. This would seem to be a sensible policy otherwise you could have two link atoms too close together. See the comments in *qm\_link\_atoms.f* for a more in-depth discussion of this limitation.

#### **Choice of electrostatic cutoff**

The implementation of the non-bonded cut off in QM/MM simulations is slightly different than in regular MM simulations. The cut off between MM-MM atoms is still handled in a pairwise fashion. However, for QM atoms any MM atom that is within *qmcut* of ANY QM atom is included in the interaction list for all QM atoms. This means that the value of *qmcut* essentially specifies a shell around the QM region rather than a spherical shell around each individual QM atom. Ideally the cut off should be large enough that the energy as a function of the cutoff has converged. For non-periodic, generalized Born simulations, a cutoff of 15 to 20 Å seems sufficient in some tests. (Remember that long-range electrostatic interactions are reduced by a factor of 80 from their gas-phase counterparts, and by more if a non-zero salt concentration is used.) For periodic simulations, the cutoff only serves to divide the interactions between "direct" and "reciprocal" parts; as with pure MM calculations, a cutoff of 8 or 9 Å is sufficient here.

#### **Parallel simulations**

The built-in QM/MM implementation currently supports execution in parallel via the message passing interface (MPI), however, the implementation is not fully parallel. At present all parts of the QM simulation are parallel except the density matrix build and the matrix diagonalization. For small QM systems these two operations do not take a large percentage of time and so acceptable scaling can be seen to around 8 CPU cores (depending on type of CPU and/or interconnect speed between compute nodes). For large QM systems the matrix diagonalization time will dominate and so the scaling will not be as good. In this case it may be beneficial to choose a LAPACK diagonalization routine in combination with a threaded library such as the Intel Math Kernel Library (MKL). For details on how to choose the diagonalization routine see the *sqm* section of the AmberTools manual. The number of threads to be used for the diagonalization is set via an environment variable of the operating system (typically OMP\_NUM\_THREADS).

### 3.6.7. General QM/MM &qmmm Namelist Variables

An example input file for running a simple QM/MM MD simulation is shown here:

```
&cntrl
  imin=0, nstlim=10000,           ! Perform MD for 10,000 steps
  dt=0.002,                       ! 2 fs time step
  ntt=1, tempi=0.1, temp0=300.0,  ! Berendsen temperature control
  ntb=1,                           ! Constant volume periodic boundaries
  ntf=2, ntc=2,                   ! Shake hydrogen atoms
  cut=8.0,                         ! 8 angstrom classical non-bond cut off
```



### 3.6. QM/MM calculations: Semi-empirical methods

```
    ifqnt=1                                ! Switch on QM/MM coupled potential
  /
  &qmmm
    qmmask=':753',      ! Residue 753 should be treated using QM
    qmcharge=-2,       ! Charge on QM region is -2
    qm_theory='PM3',   ! Use the PM3 semi-empirical Hamiltonian
    qmcut=8.0          ! Use 8 angstrom cut off for QM region
  /
```

The `&qmmm` namelist contains variables that allow you to control the options used for a QM/MM simulation. This namelist must be present when running QM/MM simulations and at the very least must contain either the `iqmatoms` or `qmmask` variable which define the region to be treated quantum mechanically. If `ifqnt` is set to zero then the contents of this namelist are ignored.

For the QM region definition specify one of either `iqmatoms` or `qmmask`. Link atoms will be added automatically along bonds (as defined in the `prmtop` file) that cross the QM/MM boundary.

- `iqmatoms` comma-separated integer list containing the atom numbers (from the `prmtop` file) of the atoms to be treated quantum mechanically.
- `qmmask` Mask specifying the quantum atoms. E.g. `:1-2,` = residues 1 and 2. See mask documentation for more info.
- `qmcut` Specifies the size of the electrostatic cutoff in Angstroms for QM/MM electrostatic interactions. By default this is the same as the value of `cut` chosen for the classical region, and the default generally does not need to be changed. Any classical atom that is within `qmcut` of *any* QM atom is included in the pair list. For PME calculations, this parameter just affects the division of forces between direct and reciprocal space. *Note:* this option only effects the electrostatic interactions between the QM and MM regions. Within the QM region all QM atoms see all other QM atoms regardless of their separation. QM-MM van der Waals interactions are handled classically, using the cutoff value specified by `cut`.
- `qm_ewald` This option specifies how long range electrostatics for the QM region should be treated.
- = 0** Use a real-space cutoff for QM-QM and QM-MM long range interactions. In this situation QM atoms do not see their images and QM-MM interactions are truncated at the cutoff. This is the default for non-periodic simulations.
  - = 1** (default) Use PME or an Ewald sum to calculate long range QM-QM and QM-MM electrostatic interactions. This is the default when running QM/MM with periodic boundaries and PME.
  - = 2** This option is similar to option 1 but instead of varying the charges on the QM images as the central QM region changes the QM image charges are fixed at the Mulliken charges obtained from the previous MD step. This approach

### 3. Force field modifications

offers a speed improvement over  $qm\_ewald=1$ , since the SCF typically converges in fewer steps, with only a minor loss of accuracy in the long range electrostatics. This option has not been extensively tested, although it becomes increasingly accurate as the box size gets larger.

- kmaxqx,y,z** Specifies the maximum number of kspace vectors to use in the x, y and z dimensions respectively when doing an Ewald sum for QM-MM and QM-QM interactions. Higher values give greater accuracy in the long range electrostatics but at the expense of calculation speed. The default value of 5 should be optimal for most systems.
- ksqmaxq** Specifies the maximum number of K squared values for the spherical cut off in reciprocal space when doing a QM-MM Ewald sum. The default value of 27 should be optimal for most systems.
- qm\_pme** Specifies whether a PME approach or regular Ewald approach should be used for calculating the long range QM-QM and QM-MM electrostatic interactions.
- = 0** Use a regular Ewald approach for calculating QM-MM and QM-QM long range electrostatics. Note this option is often much slower than a pme approach and typically requires very large amounts of memory. It is recommended only for testing purposes.
  - = 1 (default)** Use a QM compatible PME approach to calculate the long range QM-MM electrostatic energies and forces and the long range QM-QM forces. The long range QM-QM energies are calculated using a regular Ewald approach.
- qmmm\_switch** Specifies whether a switching function shall be used at the cutoff for long range electrostatics. The lower and higher boundaries of the switching function are user definable, see *r\_switch\_lo* and *r\_switch\_hi*.
- = 0 (default)**. Do not use a switching function. This leads to slight discontinuities in the potential at the cut off and thus an energy drift in NVE simulations.
  - = 1** Use a switching function. See also variables *r\_switch\_hi* and *r\_switch\_lo*.
- r\_switch\_hi** Specifies the upper boundary of the switching function in Å (see *qmmm\_switch*). Defaults to *qmcut*.
- r\_switch\_lo** Specifies lower boundary of the switching function in Å (see *qmmm\_switch*). Defaults to *r\_switch\_hi* - 2.
- qmgb** Specifies how the QM region should be treated with generalized Born.
- = 2 (default)** As described above, the electrostatic and "polarization" fields from the MM charges and the exterior dielectric (respectively) are included in the Fock matrix for the QM Hamiltonian.
  - = 3** This is intended as a debugging option and should only be used for single point calculations. With this option the GB energy is calculated using the Mulliken charges as with option 2 above but the fock matrix is NOT modified by the

### 3.6. QM/MM calculations: Semi-empirical methods

GB field. This allows one to calculate what the GB energy would be for a given structure using the gas phase quantum charges. When combined with a simulation using *qmg*=2, this allows the strain energy from solvation to be calculated.

**qm\_theory** Level of theory to use for the QM region of the simulation. (Hamiltonian). Default is to use the semi-empirical hamiltonian PM3. See the *AmberTools Users' Manual* for details.

**qmmm\_int** Controls the way in which QM/MM interactions are handled in the direct space QMMM sum. This controls only the electrostatic interactions. VDW interactions are always calculated classically using the standard 6-12 potential. Note: with the exception of *qmmm\_int*=0 DFTB calculations (*qm\_theory*=DFTB) always use a simple mulliken charge - resp charge interaction and the value of *qmmm\_int* has no influence.

**= 0** This turns off all electrostatic interaction between QM and MM atoms in the direct space sum. Note QM-MM VDW interactions will still be calculated classically.

**= 1** (default) QM-MM interactions in direct space are calculated in the same way for all of the various semi-empirical hamiltonians. The interaction is calculated in an analogous way to the the core-core interaction between QM atoms. The MM resp charges are included in the one electron hamiltonian so that QMcore-MMResp and QMelectron-MMResp interactions are calculated.

**= 2** This is the same as for 1 above except that when AM1, PM3 or Hamiltonians derived from these are in use the extra Gaussian terms that are introduced in these methods to improve the core-core repulsion term in QM-QM interactions are also included for the QM-MM interactions. This is the equivalent to the QM-MM interaction method used in CHARMM and DYNAMO. It tends to slightly reduce the repulsion between QM and MM atoms at small distances. For distances above approximately 3.5 angstroms it makes almost no difference.

**= 3** Using this along with *qm\_theory*=PM3 invokes a reformulated QM core-MM charge potential at the QM-MM interface (Eq. 3.21). Current parametrization limits the QM region to H, C, N and O atoms only; MM region is not restricted.[121]

**= 4** Currently not in use.

**= 5** Mechanical embedding: The electrostatic interaction between QM and MM atoms is treated on the same level as within the MM region using the classical force field point charges also for the QM atoms. The electronic Hamiltonian does not contain the field generated by the MM region point charges and thus the electron density is not polarized by the MM environment. Does not work with GB. Not extensively tested in presence of link atoms.

### 3. Force field modifications

**qmshake** Controls whether shake is applied to QM atoms. Using shake on the QM region will allow you to use larger time steps such as 2 fs with NTC=2. If, however, you expect bonds involving hydrogen to be broken during a simulation you should not SHAKE for the QM region. **WARNING:** the shake routine uses the equilibrium bond lengths as specified in the prmtop file to reset the atom positions. Thus while bond force constants and equilibrium distances are not used in the energy calculation for QM atoms the equilibrium bond length is still required if QM shake is on.

= 0 Do not shake QM H atoms.

= 1 Shake QM H atoms if shake is turned on (NTC>1) (default).

**printdipole** Controls whether the dipole moment shall be printed every *npr* steps.

= 0 Do not print the dipole moment (default).

= 1 Print the dipole moment of the QM region.

= 2 Print the total dipole moment of the QM and MM region.

**writpdb**

= 0 Do not write a PDB file of the selected QM region. (default).

= 1 Write a PDB file of the QM region. This option is designed to act as an aid to the user to allow easy checking of what atoms were included in the QM region. When this option is set a crude PDB file of the atoms in the QM region will be written on the very first step to the file *qmmm\_region.pdb*.

In addition to the above parameters, the following variables may be set, as described in the *AmberTools Users' Manual*:

qm\_theory, dftb\_disper, dftb\_3rd\_order, dftb\_chg, dftb\_telec, dftb\_maxiter, qm-charge, spin, qmqmdx, verbosity, tight\_p\_conv, scfconv, pseudo\_diag, pseudo\_diag\_criteria, diag\_routine, printcharges, qxd, parameter\_file, peptide\_corr, and itrmax.

#### 3.6.8. Link Atom Specific QM/MM &qmmm Namelist Variables

The following options go in the *&qmmm* namelist and control the link atom behaviour.

**lnk\_dis** Distance in Å from the QM atom to its link atom. Currently all link atoms must be placed at the same distance. A negative value of *lnk\_dis* specifies that the link atom should be placed directly on top of the MM link pair atom. In this case the distance of the link atom from the QM region changes as a function of time and the actual value of *lnk\_dis* is ignored. Additionally this means that not all link atoms will be placed at the same distance. Negative values of *lnk\_dis* will work with regular link atoms, such as hydrogen, but are really intended for use with pseudo atom / capping approaches. Default = 1.09Å.

**lnk\_method** This defines how classical valence terms that cross the QM/MM boundary are dealt with.

### 3.7. QM/MM calculations: *ab initio* and DFT methods

**=1** (Default) in this case any bond, angle or dihedral that involves at least one MM atom, including the MM link pair atom is included. This means the following (where QM = QM atom, MM = MM atom, MML = MM link pair atom.):

**Bonds** = MM-MM, MM-MML, MML-QM

**Angles** = MM-MM-MM, MM-MM-MML, MM-MML-QM, MML-QM-QM

**Dihedrals** = MM-MM-MM-MM, MM-MM-MM-MML, MM-MM-MM-MML-QM, MM-MML-QM-QM, MML-QM-QM-QM

**=2** Only include valence terms that include a full MM atom, that is, count the MM link pair atom as effectively being a QM atom. This option is designed to be used in conjunction with a pseudo atom / capping type approach where the link atom is parameterized specifically to behave like a uni-valent version of the MM atom it replaces. This option gives the following interactions:

**Bonds** = MM-MM, MM-MML

**Angles** = MM-MM-MM, MM-MM-MML, MM-MML-QM

**Dihedrals** = MM-MM-MM-MM, MM-MM-MM-MML, MM-MM-MML-QM, MM-MML-QM-QM

**lnk\_atomic\_no** The atomic number of the link atoms. This selects what element the link atoms are to be. Default = 1 (Hydrogen). Note this must be an integer and an atomic number supported by the chosen QM theory.

**adjust\_q** This controls how charge is conserved during a QMMM calculation involving link atoms. When the QM region is defined the QM atoms and any MM atoms involved in link bonds have their RESP charges zeroed. If the sum of these RESP charges does not exactly match the value of *qmcharge* then the total charge of the system will not be correct.

**= 0** No adjustment of the charge is done.

**= 1** The charge correction is applied to the nearest *nlink* MM atoms to MM atoms that form link pairs. Typically this will be any MM atom that is bonded to a MM link pair atom (a MM atom that is part of a QM-MM bond). This results in the total charge of QM+QMlink+MM equaling the original total system charge from the *prmtop* file. Requires *natom-nquant-nlink*  $\geq$  *nlink* and *nlink*  $>$  0.

**= 2** (default) - This option is similar to option 1 but instead the correction is divided among all MM atoms (except for those adjacent to link atoms). As with option 1 this ensures that the total charge of the QM/MM system is the same as that in the *prmtop* file. Requires *natom-nquant-nlink*  $\geq$  *nlink*.

### 3.7. QM/MM calculations: *ab initio* and DFT methods

In addition to the built-in semi-empirical methods *sander* also supports QM/MM simulations with *ab initio* wave function theory (WFT) and density functional theory (DFT) potentials

### 3. Force field modifications

via an interface to external QM software packages. The implementation makes use of the existing QM/MM infrastructure that has been developed earlier for the semi-empirical methods. Thus, much of AMBER's previous QM/MM functionality such as the user-friendly link atom approach are available and the implementation remains simple and transparent to use without any significant additional steps in the simulation setup as compared to semi-empirical QM/MM simulations. At present the interface supports several well-known and widely used QM software packages. Mechanical embedding is available for

- ADF (Amsterdam Density Functional) [122, 123]
- GAMESS-US [124, 125]
- NWChem [126]

Mechanical and electrostatic embedding is available for

- Gaussian [111, 127]
- Orca [128]
- TeraChem [129]

While ADF, Gaussian and TeraChem are commercial programs, GAMESS-US, NWChem and Orca are available at no cost for academic research. The interface has been written in a modular fashion and is easily extensible to support other QM software packages. It is our intention to keep adding support for other software packages. If you are interested in interfacing a specific program, please do not hesitate to contact us.

The interface was developed by Andreas Goetz (SDSC, UCSD) with help of Matthew Clark (SDSC) and support by Ross Walker (SDSC, UCSD). Thanks are due to Christine Isborn and Todd Martinez (Stanford University) for modifications to the TeraChem code to support this interface and to Mark Williamson (University of Cambridge) for adding the module that supports NWChem. If you make use of this interface, please cite the following work:

- A.W. Götz, M. Clark, R.C. Walker, *An extensible QM/MM interface for ab initio and DFT calculations with AMBER*, in preparation (2012).

Access to QM methods not available within Amber is also possible via the Amber interface to the PUPIL simulation framework. For details, see refs. 130, 131. In what follows we will describe the new interface that is native to *sander*.

#### 3.7.1. Theory

As described in section 3.6, the Hamiltonian of a system that is partitioned into a QM region that is treated with WFT and a classical region that is treated with MM consists of three components and the energy associated with this Hamiltonian is obtained as the corresponding expectation value

$$E = \langle \Psi | \mathcal{H}_{\text{QM}} + \mathcal{H}_{\text{QM/MM}} | \Psi \rangle + E_{\text{MM}}. \quad (3.26)$$

### 3.7. QM/MM calculations: ab initio and DFT methods

A QM/MM calculation therefore requires not only to choose the WFT used in the QM region and the MM model used for the MM region, but in addition also the form of the QM/MM Hamiltonian which describes the interaction between the quantum and the classical region. The most simple approach is to neglect any electronic coupling between the QM and the MM system and include only the classical non-bonded van der Waals (vdW) and electrostatic interactions between the QM and the MM atoms. This is useful to impose steric constraints on the embedded QM system and commonly referred to as mechanical embedding. In most cases, however, it is better to allow for an explicit polarization of the QM system due to the presence of the point charges on the MM atoms. This is referred to as electronic embedding and the resulting interaction energy becomes

$$E_{\text{QM/MM}}^{\text{electronic}} = \sum_{A \in \text{MM}} \int \rho(\mathbf{r}) \frac{Q_A}{|\mathbf{r} - \mathbf{R}_A|} d\mathbf{r} + \sum_{A \in \text{QM}, B \in \text{MM}} \frac{Z_A Q_B}{R_{AB}} + \sum_{A \in \text{QM}, B \in \text{MM}} \epsilon_{AB} \left[ \left( \frac{\sigma_{AB}}{R_{AB}} \right)^{12} - \left( \frac{\sigma_{AB}}{R_{AB}} \right)^6 \right]. \quad (3.27)$$

This QM/MM energy expression also holds for DFT and the terms represent, in order, the electrostatic interaction between the QM electron density and the MM point charges, the electrostatic interaction between the QM point charge nuclei and the MM point charges, and the van der Waals repulsion between the QM and MM atoms.

The forces acting on an atom  $A$  in a QM/MM calculation are given in terms of derivatives of the total energy expression (3.26) with respect to the Cartesian coordinates of the atom,

$$\mathbf{F}_A = -\nabla_A E_{\text{QM}} - \nabla_A E_{\text{QM/MM}} - \nabla_A E_{\text{MM}}, \quad (3.28)$$

where  $\nabla_A = \partial/\partial \mathbf{R}_A = (\partial/\partial R_A^x, \partial/\partial R_A^y, \partial/\partial R_A^z)$ . If a QM and an MM program are coupled for QM/MM calculations, the QM program will calculate the QM forces  $-\nabla_A E_{\text{QM}}$  acting on QM atoms and the MM program the MM forces  $-\nabla_A E_{\text{MM}}$  acting on the MM atoms. All that remains, is to calculate the forces acting on QM and MM atoms due to the QM/MM interaction energy,  $-\nabla_A E_{\text{QM/MM}}$ . For mechanical embedding this will be entirely handled by the MM program. For electronic embedding the forces are given as

$$\begin{aligned} \nabla_A E_{\text{QM/MM}}^{\text{electronic}} &= Z_A \sum_{B \in \text{MM}} \frac{Q_B (\mathbf{R}_A - \mathbf{R}_B)}{R_{AB}^3} + \sum_{B \in \text{MM}} \int \frac{\partial \rho(\mathbf{r})}{\partial \mathbf{R}_A} \frac{Q_B}{|\mathbf{r} - \mathbf{R}_B|} d\mathbf{r} + \sum_{B \in \text{MM}} \nabla_A V_{AB}^{\text{LJ}} \\ &= -Z_A \mathbf{E}_{\text{MM}}(\mathbf{R}_A) - \int \rho(\mathbf{r}) \mathbf{E}_{\text{MM}}(\mathbf{r}) d\mathbf{r} + \sum_{B \in \text{MM}} \nabla_A V_{AB}^{\text{LJ}} \end{aligned} \quad (3.29)$$

for the derivatives with respect to the positions of the QM atoms  $A$  where  $\mathbf{E}_{\text{MM}}$  is the electric field generated by the MM point charges and  $V_{AB}^{\text{LJ}}$  is the Lennard-Jones potential from (3.27) and

### 3. Force field modifications

$$\begin{aligned}\nabla_B E_{\text{QM/MM}}^{\text{electronic}} &= Q_B \sum_{A \in \text{QM}} \frac{Z_A(\mathbf{R}_B - \mathbf{R}_A)}{R_{AB}^3} + \int \rho(\mathbf{r}) \frac{Q_B(\mathbf{R}_B - \mathbf{r})}{|\mathbf{r} - \mathbf{R}_B|^3} d\mathbf{r} + \nabla_B E_{\text{QM/MM}}^{\text{mechanic}} \\ &= -Q_B \mathbf{E}_{\text{QM}}(\mathbf{R}_B) + \sum_{A \in \text{QM}} \nabla_B V_{AB}^{\text{LJ}}\end{aligned}\quad (3.30)$$

for the derivatives with respect to the positions of the MM atoms  $B$  where  $\mathbf{E}_{\text{QM}}$  is the electric field due to the QM charge distribution. The contributions to the gradient due to the point charge interactions and due to the interaction between the MM point charges and the QM electrons is evaluated by the QM program. Some QM programs do not calculate the forces acting on the MM atoms (point charges) due to the presence of the QM system but in general are able to return the electric field  $\mathbf{E}_{\text{QM}}$  at arbitrary points in space which is then used to obtain these forces. The van der Waals repulsion (Lennard-Jones interaction) between QM and MM atoms is treated by AMBER in the same way as for semiempirical NDDO-type and DFTB methods.

#### 3.7.2. General Remarks

When using the AMBER interface to external QM software packages for performing WFT or DFT based QM or QM/MM MD simulations, it is absolutely critical to be aware of the capabilities and limitations of the QM method to be employed. In particular, QM based MD can be more tricky than MM based MD in the sense that it is more likely that the QM program can fail for example due to SCF convergence problems. This can be the case if the geometry of the QM region is far from its ground state equilibrium, for example because a simulation is started from a bad geometry or performed at high temperature.

We have gone to large efforts and analyzed a large set of test simulations to provide the best default parameters for the supported QM programs such that forces are computed with sufficient accuracy to guarantee energy conservation for constant energy MD simulations. Of particular importance are SCF convergence and associated integral neglect thresholds and the size of the grid used for the numerical quadrature of the exchange-correlation (XC) potential and energy for DFT calculations. However, other than providing appropriate input parameters, AMBER does not have any control over the external program and it is at the user's discretion to employ sensible input parameters for the QM program and to prepare the system such that the simulations are started at a reasonable starting structure.

In any case we highly recommend to write restart files frequently so that a simulation can be restarted without loss of much computational time in the case that a simulation should crash. The interface also stores the last in- and output files of the external QM program during each MD step. Should there be any problems with the QM program, it is therefore possible to analyze the reasons and take appropriate countermeasures.

The interface requires data to be exchanged between *sander* and the QM program. The interface is based on file exchange and system calls and, during each step of a geometry optimization or an MD simulation, writes an input file for the external program, starts a single point gradient calculation with the external program, and reads the energy and forces from the external program's output file (binary ADF checkpoint or formatted GAMESS, Gaussian, ORCA and TeraChem output file).



### 3.7.3. Limitations

In principle, all types of simulations that are possible with *sander* are supported. There are, however, some restrictions for simulations that require *sander* to run in parallel, in particular path integral molecular dynamics (PIMD) and replica exchange molecular dynamics (REMD), see the discussion of Parallelization below. The interface to external QM programs also lacks some critical features regarding solvent models in comparison to the semiempirical MNDO and DFTB QM/MM implementation that is available in AMBER, the most critical ones are listed here.

**Generalized Born** Generalized Born (GB) implicit solvent models are not supported if external QM programs are used for the QM region.

**Particle Mesh Ewald (PME) and Periodic Boundary Conditions** The PME approach for treating long-range electrostatic QM/MM and QM/QM interactions in periodic systems is currently not supported. It is possible to use periodic boundary conditions but a cutoff is used for the point charges to be included in the QM Hamiltonian (determined by *&qmmm* namelist variable *qmcut*) thus truncating the long-range QM/MM electrostatic interactions in (3.27). This leads to discontinuities in the potential energy surface and poor energy conservation for MD runs in the NVE ensemble. The user may consider running non-periodic simulations with a cutoff that is larger than the system size thus effectively including all interactions.

### 3.7.4. Performance Considerations

The computational cost of DFT is comparable to Hartree–Fock (HF) theory which is the simplest WFT method that serves as zeroth order approximation for more elaborate correlated WFT methods such as Møller–Plesset perturbation theory, configuration interaction theory and coupled cluster theory. The calculations can be accelerated by using density fitting approaches, sometimes called resolution-of identity (RI) approximation, which in the case of DFT with exchange–correlation (XC) functionals that do not require admixture of exact HF-exchange, leads to speedups of roughly one order of magnitude without compromising the accuracy of the results. Nevertheless, the computational cost of DFT is in general two to three orders of magnitude higher than that of semiempirical QM models. We recommend to carefully test the performance of the QM program to choose an optimal number of processor counts for parallelized QM calculations. Typical simulation performance for typical QM system sizes of tens of atoms will be on the order of a few picoseconds per day, depending on the underlying QM model chosen.

### 3.7.5. Parallelization

At present only the serial version of *sander* can be used for all QM and QM/MM MD simulations with external QM software, unless a simulation requires multiple energy and force evaluations for each time step as, for example, in PIMD and REMD simulations. This is not a limitation since typically the computational cost of the MM part is negligible compared to the cost of the QM part and parallelism is dealt with by the external QM program.

### 3. Force field modifications

In the case of PIMD or REMD simulations, the parallelized executable *sander.MPI* has to be used. However, only one thread per group can be launched and special care has to be taken to choose the right number of parallel threads in the external QM program. For example, on a machine with 32 cores, a simulation with 16 beads or replicas can run the external QM program with 2 threads in parallel to make maximum use of the available processing cores. If the available processors are spread over multiple nodes, special care has to be taken to ensure that the different instances of the external QM program are launched on the correct nodes.

#### 3.7.6. Usage

All that is required to use the interface is a working installation of AMBER and one or more of the supported QM programs. In order to use the external program from within *sander*, the *&cntrl* namelist variable *ifqnt = 1* must be set to enable QM calculations and the *&qmmm* namelist variable *qm\_theory = 'EXTERN'* must be set to enable the external interface. The *&qmmm* namelist variable *qmmask* is used for selecting the QM region just as for QM/MM calculations with the semiempirical NDDO-type and DFTB approaches that are natively available in AMBER. For a QM MD simulation, the *sander* input file therefore needs to contain

```
&cntrl
  ...
  ifqnt = 1,
/
&qmmm
  qmmask = '@*',
  qm_theory = 'EXTERN',
/
```

For QM/MM simulations with electronic embedding it is mandatory to specify the charge of the QM region in the *&qmmm* namelist with variable *qmcharge* in addition to specifying the charge in the namelist that is specific for the external QM program (see below). We also recommend to include all MM point charges as external electric field in the QM Hamiltonian to avoid problems with energy conservation. For non-periodic simulations this can be achieved by setting the *&qmmm* namelist variable *qmcut* to a value larger than the system size.

In addition either the *&adf*, *&gms*, *&nw*, *&gau*, *&orc* or *&tc* namelist must be present to use either ADF, GAMESS, NWChem, Gaussian, ORCA or TeraChem, respectively, and to assign parameters for the external QM program. Please refer to the ADF, GAMESS, NWChem, Gaussian, ORCA or TeraChem user manual for details on settings for the *ab initio* or DFT calculations. A list of namelist variables and their default setting is given below. The defaults have been chosen such that energy conserving MD simulations in the NVE ensemble are possible. An exception is ADF for which satisfactory energy conservation cannot be reached at present, in particular with the DZ basis set. NWChem has not been extensively tested.

Properties that are calculated along the trajectory are printed to property files with names *adf\_job.ext*, *gms\_job.ext*, *gau\_job.ext*, *orc\_job.ext* and *tc\_job.ext*, where *ext* is either *dip* for dipole moment (x, y, z component and absolute value) or *chg* for atomic charges, where supported. The dipole moment is always stored while the charges only if requested.

These property files will be deleted at the beginning of a run, so back them up in case a trajectory needs to be restarted.

All calculations with a spin multiplicity larger than one will automatically be performed in the framework of an unrestricted formalism (as opposed to restricted open shell), that is with unrestricted HF (UHF), unrestricted DFT (UDFT) and MP2 with a UHF reference wave function (UMP2).

In addition to controlling the external programs via the sander input file, you may supply a template input file for the external program in order to provide additional input which is not supported by the external interface. The format, name, and input requirements for the template file vary with the external program as detailed in the corresponding program's documentation below. If you are using your own template, please make sure that the parameters of the QM method (like SCF convergence threshold and XC quadrature grid size) are chosen such that energy is conserved during MD simulations.

### 3.7.6.1. AMBER/ADF

To use ADF with the external interface, ADF must be installed on the working machine and the `$ADFBIN` environment variable must be pointing to the directory in which the ADF executables reside. If you wish to perform DFTB calculations with ADF then `$ADFBIN/dftb` must be present. Please note that by default the ZORA/QZ4P fit basis will be used for all basis sets to maximize the accuracy of the gradients calculated by ADF and thus obtain the best possible energy conservation.

**Limitations** At present only mechanical embedding is supported.

#### **&adf** Namelist variables

basis	Basis set type to be used in the DFT calculation. Valid standard basis set types are: SZ, DZ, DZP, TZP, TZ2P, TZ2P+ and ZORA/QZ4P. (Default: basis = 'DZP')
fit_type	Fit basis set type to be used for density fitting. Valid values are identical to the available basis sets (SZ, DZ etc) in which case the fit basis corresponding to the AO Basis will be used; "standard" will choose the fit basis that by default corresponds to the basis set chosen with the <i>basis</i> namelist variable. (Default: fit_type = 'ZORA/QZ4P')
core	Type of frozen core to use. Allowed values are: None, Small, Medium, Large. (Default: core = 'None')
xc	Exchange-correlation functional to be used. Popular choices are 'LDA VWN', 'GGA BLYP', 'GGA PBE', 'HYBRID B3LYP' and 'HYBRID PBE0'. Consult the ADF manual for all available options. (Default: xc = 'GGA BLYP')
charge	Net total charge of the QM region. (Default: charge = 0)
spin	Net total spin polarization of the QM region (number of spin $\alpha$ electrons in excess of spin $\beta$ electrons). Spin-polarized calculations will be performed with the unrestricted KS formalism. (Default: spin = 0)

### 3. Force field modifications

- `scf_iter` Maximum number of SCF cycles allowed. (Default: `scf_iter = 50`)
- `scf_conv` Threshold upon which to stop the SCF procedure. The tested error is the commutator of the Fock matrix and the density matrix. Convergence is considered to be achieved if the maximum element of the commutator (which is zero for an optimized wave function) is smaller than `scf_conv`. (Default: `scf_conv = 1.0d-06`)
- `integration` Numerical integration accuracy. (Default: `integration = 5.0`)
- `num_threads` Number of threads (and thus CPU cores) for ADF to use. Note that this is not required if you are running in a queuing system as ADF will automatically use the full number of reserved cores. (Default: `num_threads = 0` [this causes ADF to use all available cores on a machine])
- `use_dftb` Specifies whether DFTB shall be used with ADF's DFTB program `dftb`. If `use_dftb = 1` then DFTB will be used and only variables `charge` and `scf_conv` will be considered. (Default: `use_dftb = 0` [do not use DFTB, regular DFT calculation])
- `exactdensity` The exact (as opposed to fitted) electron density is used for the evaluation of the exchange-correlation potential if `exactdensity = 1`. (Default: `exactdensity = 0`)
- `use_template` Determine whether or not to use a user-provided template file for running external programs. (Default: `use_template = 0`)
- `ntpr` Controls frequency of printing for dipole moment and atomic charges to files `adf_job.ext`. (Defaults to `&cntrl` namelist variable `ntpr`)
- `dipole` Toggles reading/printing for dipole moment. (Default: `dipole = 0`)

**Example** An input file for QM MD with ADF using the PBE functional and the TZP basis set and a QM region with charge +2 therefore would have to contain

```
&adf
  xc = 'GGA PBE',
  basis = 'TZP',
  charge = 2,
/
```

**Template input file** The template file for ADF should be named `adf_job.tpl` and must contain the following keywords:

```
BASIS ... END
SAVE TAPE21
```

You should not include the following (block) keywords in the template file as these are taken care of by *sander*:

```

UNITS
FRAGMENTS ... END
RESTART
GRADIENT
ATOMS ... END

```

### 3.7.6.2. AMBER/GAMESS-US

To use GAMESS with the external interface, GAMESS must be compiled on the target system. Make note of the version number you specify during the GAMESS compilation process (default is 00 which makes the GAMESS execution script `runqms` look for the executable `gamess.00.x`). If you use a different version number you must specify it with the `gms_version` namelist variable. `$GMS_PATH` should be set to the path where the script `runqms` is located (for example `/opt/gamess/`). We assume that the `runqms` script copies the output `.dat` files to the directory from which GAMESS is invoked. If this is not the case, please modify the script `runqms` accordingly.

**Limitations** Only mechanical embedding is supported with GAMESS. The available QM models are limited to HF, DFT and MP2 since only for these analytical gradients are available in GAMESS.

#### **&gms** Namelist variables

basis	Basis set type to be used in the calculation. Presently supported are the Pople type basis sets STO-3G, 6-31G, 6-31G*, 6-31G**, 6-31+G*, 6-31++G*, 6-311G, 6-311G* and 6-311G**. Also supported are the Karlsruhe valence triple zeta basis sets KTZV, KTZVP and KTZVPP (with none, one and two polarization functions, respectively) and the Dunning-type correlation consistent basis sets CCn (n = D, T, Q, 5, 6; officially called cc-pVnZ) and ACCn (as CCn but augmented with a set of diffuse function, officially called aug-cc-pVnZ). (Default: basis = '6-31G**')
method	QM method to be used. At present, we support 'HF' for Hartree-Fock, 'MP2' for second order Møller-Plesset perturbation theory and any of the supported DFT functionals. Popular choices for for DFT functionals include 'BP86', 'BLYP', 'PBE', 'B3LYP' or 'PBE0'. (Default: method = 'BP86')
charge	Net total charge of the QM region. (Default: charge = 0)
spinmult	Net total spin multiplicity of the QM region. Open shell systems (spin multiplicity larger than 1) are treated with unrestricted HF or KS approaches. MP2 uses an unrestricted HF reference wavefunction. (Default: spinmult = 1)
chelpg	CHELPG charges are calculated if <code>chelpg = 1</code> . These charges are stored in the file <code>gms_prop.chg</code> . (Default: <code>chelpg = 0</code> )
nrad	Number of radial points in the Euler-MacLaurin quadrature of the XC potential and energy density. (Default: nrad = 96)

### 3. Force field modifications

- nleb** Number of angular points in the Lebedev grids for the numerical quadrature of the XC potential and energy density. (Default: `nleb = 590` [The GAMESS default of 302 is not accurate enough to conserve energy])
- scf\_conv** SCF convergence threshold. Convergence is reached when the absolute density change between two consecutive SCF cycles is less than `scf_conv`. (Default: `scf_conv = 1.0D-06`)
- maxit** Maximum number of SCF iterations. (Default: `maxit = 50`)
- gms\_version** This is the version number specified when building GAMESS. (Default: `gms_version = 00`)
- num\_threads** Number of threads (and thus CPU cores) for GAMESS to use. Note that GAMESS may require a special setup in the `runngms` script to be able to run using multiple threads. Unless `num_threads` is explicitly specified, GAMESS will only use one thread (run on one core). (Default: `num_threads = 1`)
- mwords** The maximum replicated memory which your job can use, on every node. This is given in units of 1,000,000 words (as opposed to 1024\*1024 words), where a word is defined as 64 bits. You may need to increase this value if GAMESS crashes due to not having enough memory allocated. (Default: `mwords = 50`)
- use\_template** Determine whether or not to use a user-provided template file for running external programs. (Default: `use_template = 0`)
- npr** Controls frequency of printing for dipole moment and atomic charges to files `gms_job.ext`. (Defaults to `&cntrl` namelist variable `npr`)
- dipole** Toggles reading/printing for dipole moment. (Default: `dipole = 0`)

**Example** An input file for QM MD with GAMESS using the PBE functional and the 6-31G\*\* basis set and a QM region with charge +2 that should run on 16 CPU cores therefore would have to contain

```
&gms
  method = 'DFT',
  dfttyp = 'PBE',
  basis = '6-31G**',
  charge = 2,
  num_threads = 16,
/
```

**Template input file** The template file for GAMESS should be named `gms_job.tpl` and the `$CONTRL` card must contain the following keywords:

```
RUNTYP=GRADIENT
UNIT=ANGS
COORD=UNIQUE
```

You should not include the \$DATA card in the template file as it is taken care of by *sander*.

### 3.7.6.3. AMBER/Gaussian

To use Gaussian with the interface, Gaussian03 or Gaussian09 must be properly installed on the system and the g03 or g09 executable must be in the path.

**Limitations** A cutoff is applied to QM/MM interactions in QM/MM simulations using electrostatic embedding with and without PBCs. This leads to discontinuities in the potential energy surface and poor energy conservation. In the case of QM/MM simulations without PBCs, this cutoff (*qmcut* variable in the *&qmmm* namelist) can be set to a number that is larger than the simulated system, thus effectively not applying a cutoff. This is highly recommended.

#### **&gau** Namelist variables

basis	Basis set type to be used in the calculation. Any basis set that is natively supported by Gaussian can be used. Examples are the single zeta, split valence or triple zeta Pople type basis sets 'STO-3G', '3-21G', '6-31G' and '6-311G'. The split-valence or triple zeta basis sets can be augmented with diffuse functions on heavy atoms or additionally hydrogen by adding one or two plus signs, respectively, as in '6-31++G'. Polarization functions on heavy atoms or additionally hydrogens are used by adding one or two stars, respectively, as in '6-31G**'. (Default: basis = '6-31G*')
method	Method to be used in the calculation. Can either be one of the WFT models for which Gaussian supports gradients, for example 'RHF' or 'MP2', or some supported DFT functional. Popular choices are 'BLYP', 'PBE' and 'B3LYP'. (Default: method = 'BLYP')
scf_conv	Threshold upon which to stop the SCF procedure. The tested error is the commutator of the Fock matrix and the density matrix. Convergence is considered to be achieved if the maximum element of the commutator (which is zero for an optimized wave function) is smaller than scf_conv}. Set in the form of $10^{-N}$ . (Default: scf_conv = 8)
charge	Net total charge of the QM region. (Default: charge = 0)
spinmult	Net total spin multiplicity of the QM region. Open shell systems (spin multiplicity larger than 1) are treated with unrestricted HF, MP2, or KS approaches. (Default: spinmult = 1)
num_threads	Number of threads (and thus CPU cores) for Gaussian to use. Unless num_threads is explicitly specified, Gaussian will only use one thread (run on one core). (Default: num_threads = 1)
use_template	Determine whether or not to use a user-provided template file for running external programs. (Default: use_template = 0)

### 3. Force field modifications

- `npr` Controls frequency of printing for dipole moment and atomic charges to files `gau_job.ext.` (Defaults to `&cntrl` namelist variable `npr`)
- `dipole` Toggles reading/printing for dipole moment. (Default: `dipole = 0`)

**Example** An input file for QM MD with Gaussian using the BP86 functional and the 6-31G\*\* basis set and a QM region with charge +2 therefore would have to contain

```
&gau
  method = 'BP86',
  basis   = '6-31G**',
  charge  = 2,
/
```

**Template input file** The template file for Gaussian should be named `gau_job.tpl` and should contain the content of a Gaussian input file up to and including charge and spin multiplicity. That is, the full route section defining the method to be used and SCF convergence criteria, a comment line and charge and spin multiplicity, for example for a B3LYP calculation with 6-31G\* basis set of an uncharged system in triplet state:

```
#P B3LYP/6-31G* SCF=(Conver=8)
Test calculation
0 3
```

Do not include any information about coordinates or point charge treatment since this will all be handled by *sander*. Also, do not include any *Link 0 Commands* (line starting with %) since these are handled by *sander*. If you want to run Gaussian in parallel, specify the number of processors via the `num_threads` variable in the `&gau` namelist.

#### 3.7.6.4. AMBER/Orca

To use Orca with the interface, Orca must be properly installed on the system and the `$ORCAHOME` environment variable needs to point to the directory where the Orca executables reside. For convenience of use, namelist parameters in general correspond to Orca keywords, see the Orca manual for details.

**Limitations** A cutoff is applied to QM/MM interactions in QM/MM simulations with and without PBCs. This leads to discontinuities in the potential energy surface and poor energy conservation. In the case of QM/MM simulations without PBCs, this cutoff (`qmcut` variable in the `qmnm` namelist) can be set to a number that is larger than the simulated system, thus effectively not applying a cutoff. This is highly recommended.

Also note that ORCA only supports OpenMPI for parallel calculations.



**&orc Namelist variables**

basis	Basis set type to be used in the calculation. Possible choices include 'svp', '6-31g', etc. See Orca manual for a complete list. (Default: basis = 'SV(P)')
cbasis	Auxillary basis set for correlation fitting. See Orca manual for a complete list. (Default: basis = 'NONE')
jbasis	Auxillary basis set for Coulomb fitting. See Orca manual for a complete list. (Default: basis = 'NONE')
method	Method to be used in the calculation. Popular choices include 'hf', 'pm3', 'blyp', and 'mp2'. (Default: method = 'blyp')
convkey	General SCF convergence setting for simplified Orca input. Can take values 'TIGHTSCF', 'VERYTIGHTSCF', etc. (Default: convkey='VERYTIGHTSCF')
scfconv	SCF convergence threshold for the energy. (Default: scfconv = -1, that is, not in use since we use the general convergence settings keyword <i>convkey</i> . Otherwise this would lead to SCF energy convergence of $10^{-N}$ au, if set to N.)
grid	Grid type used during the SCF for the XC quadrature in DFT. (Default: grid = 4, this corresponds to Intacc = 4.34 for the radial grid and an angular Lebedev grid with 302 points. Conservatively chosen together with finalgrid to conserve energy.)
finalgrid	Grid type used for the energy and gradient calculation after the SCF for the XC quadrature in DFT. (Default: finalgrid = 6, this corresponds to Intacc = 5.34 for the radial grid and an angular Lebedev grid with 590 points. Conservatively chosen together with <i>grid</i> to conserve energy.)
charge	Net total charge of the QM region. (Default: charge = 0)
spinmult	Net total spin multiplicity of the QM region. Open shell systems (spin multiplicity larger than 1) are treated with unrestricted HF. (Default: spinmult = 1)
maxiter	Maximum number of SCF iterations. (Default maxiter = 100)
maxcore	Global scratch memory (in MB) used by Orca. You may need to increase this when running larger jobs. See Orca manual for more information. (Default maxcore = 1024)
num_threads	Number of threads (and thus CPU cores) for Orca to use. Note that Orca only supports OpenMPI. (Default: num_threads = 1)
use_template	Determine whether or not to use a user-provided template file for running external programs. (Default: use_template = 0)
ntr	Controls frequency of printing for dipole moment and atomic charges to files <i>orc_job.ext</i> . (Defaults to &cntrl namelist variable ntr)
dipole	Toggles reading/printing for dipole moment. (Default: dipole = 0)

### 3. Force field modifications

**Example** An input file for QM MD with Orca using the BLYP functional, the SVP basis set and a QM region with charge +2 therefore would have to contain

```
&orca
  method = 'blyp',
  basis   = 'svp',
  charge  = 2,
/
```

**Template input file** The template file for Orca should be named `orca_job.tpl` and must at least contain keywords specifying the method and basis set to be used in the calculation, for example:

```
# ORCA input file for BLYP/SVP simulation
! BLYP SVP
```

You should not include the following keywords in the template file as these are taken care of by sander (like setting the runtime and adding coordinates):

```
# NOT to be included in ORCA input file
!engrad
!energy # (or any run type)
%pointcharges
*xyzfile # (or any coordinates)
```

#### 3.7.6.5. AMBER/TeraChem

To use TeraChem with the interface, TeraChem must be properly installed on the system. In particular, the environment variable `$TeraChem` needs to point to the directory of the TeraChem executable which must be named `terachem` (alternatively the name can be specified via the input). Namelist parameters correspond to TeraChem keywords, see the TeraChem manual for details.

**Limitations** A cutoff is applied to QM/MM interactions in QM/MM simulations with and without PBCs. This leads to discontinuities in the potential energy surface and poor energy conservation. In the case of QM/MM simulations without PBCs, this cutoff (`qmcut` variable in the `&qmmm` namelist) can be set to a number that is larger than the simulated system, thus effectively not applying a cutoff. This is highly recommended.

#### **&tc** Namelist variables

basis	Basis set type to be used in the calculation. Possible choices presently (TeraChem version 1.4) are 'STO-3G', '3-21G', '6-31G' and '6-311G', '3-21++G' and '6-31++G' (Default: basis = '6-31G')
method	Method to be used in the calculation, can be either 'RHF' or some supported DFT functional. Popular choices are 'BLYP', 'PBE' and 'B3LYP'. (Default: method = 'BLYP')

### 3.7. QM/MM calculations: ab initio and DFT methods

dftd	Determines whether dispersion corrections are applied in the case of DFT calculations. (Default: dftd = 'no')
charge	Net total charge in the QM region. (Default: charge = 0)
spinmult	Net total spin multiplicity of the QM region. Open shell systems (spin multiplicity larger than 1) are treated with unrestricted HF or KS approaches. (Default: spinmult = 1)
precision	Precision model setting (single vs double precision). (Default: precision = 'mixed')
dynamicgrid	Use coarse grid during early SCF iterations. (Default: dynamicgrid = 'yes')
threall	Determines a variety of thresholds. (Default: threall = 1.0E-11)
convthre	SCF convergence threshold for the wavefunction. (Default: convthre = 3.0E-05, which leads to SCF energy convergence of approximately $10^{-7}$ au or $10^{-4}$ kcal/mol)
maxit	Maximum number of SCF iterations. (Default: maxit = 100)
dftgrid	DFT grid to be employed for the numerical XC quadrature in DFT calculations. (Default: dftgrid = 1)
ngpus	Determines how many GPUs are to be used. (Default: ngpus = 0, which uses all available GPUs)
gpuids	If <i>ngpus</i> has a value other than zero, this determines the IDs of the GPUs to be used for the calculation. (Default: gpuids = 0, 1, 2, etc.)
executable	Name of the TeraChem executable. (Default: executable = terachem)
use_template	Determine whether or not to use a user-provided template file for running external programs. (Default: use_template = 0)
ntr	Controls frequency of printing for dipole moment and atomic charges to files <i>tc_job.ext</i> . (Defaults to &cntrl namelist variable ntr)
dipole	Toggles reading/printing for dipole moment. (Default: dipole = 0)

**Example** An input file for QM MD with TeraChem using the PBE functional and the 3-21G basis set and a QM region with charge +2 therefore would have to contain

```
&tc
  method = 'PBE',
  basis   = '3-21G',
  charge  = 2,
/
```

### 3. Force field modifications

**Template input file** The template file for Terachem should be named `tc_job.tpl` and must at least contain the following keywords:

```
basis
method
```

Any occurrence of the `end` keyword will be ignored.

You should not include the following keywords in the template file as these are taken care of by *sander*:

```
run
coordinates
pointcharges
amber
```

## 3.8. Charge Relocation

The charges of atoms can be modified as a function of atomic distances and angles. The modification of charges can be interpreted as charge transfer, polarization and other effects. This feature was designed to improve fixed-charge force fields regarding the localized charge relocation.

As an example, a water molecule polarizes as a positive ion approaches towards the oxygen atom. The polarization can be achieved by separating more charges between the oxygen and hydrogen atoms. In a simple case, the amount of the extra-charge ( $q_{\text{extra}}$ ) can be assumed to be a function of the distance ( $r$ ) between the ion and the oxygen atom. As a result, the charges of the oxygen atom and hydrogen atoms become  $q_{\text{O}} = q_{\text{O},0} - q_{\text{extra}}(r)$  and  $q_{\text{H}} = q_{\text{H},0} + q_{\text{extra}}(r)/2$ , where the subscript 0 denotes their original charges. The model can be improved if you introduce the dependency of the angle ( $\theta$ ) of Ion-O-H. You can build two empirical quantities ( $q_1$  and  $q_2$ ) as functions of  $r$  and  $\theta$ , the new charge equations can be  $q_{\text{O}} = q_{\text{O}}^0 - q_1(r)q_2(\theta)$  and  $q_{\text{H}} = q_{\text{H}}^0 + q_1(r)q_2(\theta)/2$ .

As shown in the example above, you can add, multiply, divide and reassign an arbitrary quantity to the charge of any atom. However, there are limitations in designing the functions. They should be the form of a cubic-spline curve and should be dependent on only one variable.

The charge modification results in the energy of charge relocation, which can be an empirical form of quadratic equation,  $E_{\text{CRG}} = c_1\Delta q + c_2\Delta q^2$ . For the details about  $E_{\text{CRG}}$ , refer to the section [3.8.1](#).

Following parameters can be put in “cntrl” namelist in the input file of *sander* to control the charge relocation.

<code>ifcr</code>	Flag for the charge relocation.  <code>= 0</code> Charge relocation is not used (default) <code>= 1</code> Charge relocation is used. The input file for the charge relocation should be specified.
<code>crin</code>	The input file for charge relocation.

- crkut** The cut-off distance of charge relocation. Charge relocation rules are applied only when the distances of the first two atoms (*at1* and *at2* in the input file for charge relocation) are within the cut-off distance. The default is 3 (Å).
- crskin** The pair list for charge relocation is extended to *crkut* + *crskin*. The pair list is updated when a pair in the list changes more than half of the *crskin* distance. The default is 2 (Å).
- crprintcharges** If this is turned on, the modified charges are printed in the output file of sander.  
 = 0 Charges are not printed (default)  
 = 1 Charges are printed
- cropt** This controls the electrostatic energy.  
 = 0 1-4 elec is calculated using the original charges (default)  
 = 1 1-4 elec is calculated using the modified charges

### 3.8.1. Preparing Input Files for Charge Relocation

Detailed rules about charge modification are assigned in the input file for charge relocation. Following parameters need to be specified in the namelist “crset”. The namelist can be repeated.

- mode** This controls the input mode.  
 = 0 The mode for specifying atoms. This requires the parameters: *at1*, *at2*, *at3*, (*at4*), and *cect* (default)  
 = 1 The mode for defining a function. This requires the parameters: *type*, *r*, *c*, *pi1*, *pi2*, *pr1*, *pr2* and *npts*
- r** This is the list of numbers in the domain of the defined function. The numbers should be in an increasing order. The smallest and the biggest numbers determine the boundary of the domain. Possible numbers are either distances ( $0 - \infty$ ) or (radian) angles ( $0 - \pi$ ).
- c** This is the list of numbers in the codomain of the defined function,  $f(r)$ . The numbers should match the numbers in *r*. For example, if  $r = 0, 1, 2, 3$ , then  $c = f(0), f(1), f(2), f(3)$ . The finally defined function will be the cubic-spline curve linking the discrete data points.
- npts** The number of data points in *r* or *c*. ( $npts \geq 4$ )
- pi1** This determines the left-boundary condition of the defined function.  
 = 1 The first derivative of the left boundary of the function becomes *pr1*  
 = 2 The second derivative of the left boundary of the function becomes *pr1* (default)
- pi2** This determines the right-boundary condition of the defined function.

### 3. Force field modifications

- = 1 The first derivative of the right boundary of the function becomes *pr2*
- = 2 The second derivative of the right boundary of the function becomes *pr2* (default)
- pr1 This determines the left-boundary condition together with *pi1*. (default=0)
- pr2 This determines the right-boundary condition together with *pi2*. (default=0)
- type This determines how the defined function operate on the charge that will be modified. If the charge before the modification is  $q_{\text{prev}}$  and the function is  $f$ , the new charge  $q_{\text{cur}}$  after the modification is defined depending on the type.  $q_{\text{hold}}$  is the charge that is allocated when the type greater than 5 is first seen. Initially it is set to be the same as the currently defined function ( $q_{\text{hold}} = f$ ).  $q_{\text{hold}}$  combines with  $q_{\text{prev}}$  when the type smaller than 5 is seen or there is no more rule for the charge modification. The charge modification results in the empirical charge relocation energy  $E_{\text{CRG}} = c_1\Delta q + c_2\Delta q^2$ . The two coefficients,  $c_1$  and  $c_2$  can be defined by *cect*.
  - = 1 Plus operator.  $q_{\text{cur}} = q_{\text{prev}} + f$  and therefore  $\Delta q = f$ .
  - = 2 Minus operator.  $q_{\text{cur}} = q_{\text{prev}} - f$  and therefore  $\Delta q = -f$ .
  - = 3 Multiplication operator.  $q_{\text{cur}} = q_{\text{prev}} \cdot f$  and therefore  $\Delta q = q_{\text{prev}} \cdot (f - 1)$ .
  - = 4 Division operator.  $q_{\text{cur}} = q_{\text{prev}}/f$  and therefore  $\Delta q = q_{\text{prev}} \cdot (1/f - 1)$ .
  - = 5 Replace  $q_{\text{prev}}$  with  $f$ .  $q_{\text{cur}} = f$  and therefore  $\Delta q = f - q_{\text{prev}}$ .
  - = 6 Plus operator but the function combines first with the modification that will occur later. If this is the beginning of the hold,  $q_{\text{cur\_hold}} = f$  and  $\Delta q = f$ , otherwise  $q_{\text{cur\_hold}} = q_{\text{prev\_hold}} + f$  and  $\Delta q = f$ .
  - = 7 Minus operator but the function combines first with the modification that will occur later. If this is the beginning of the hold,  $q_{\text{cur\_hold}} = f$  and  $\Delta q = f$ , otherwise  $q_{\text{cur\_hold}} = q_{\text{prev\_hold}} - f$  and  $\Delta q = -f$ .
  - = 8 Multiplication operator but the function combines first with the modification that will occur later. If this is the beginning of the hold,  $q_{\text{cur\_hold}} = f$  and  $\Delta q = f$ , otherwise  $q_{\text{cur\_hold}} = q_{\text{prev\_hold}} \cdot f$  and  $\Delta q = q_{\text{prev\_hold}}(f - 1)$ .
  - = 9 Division operator but the function combines first with the modification that will occur later. If this is the beginning of the hold,  $q_{\text{cur\_hold}} = f$  and  $\Delta q = f$ , otherwise  $q_{\text{cur\_hold}} = q_{\text{prev\_hold}}/f$  and  $\Delta q = q_{\text{prev\_hold}}(1/f - 1)$  and  $\Delta q = q_{\text{prev\_hold}} \cdot (1/f - 1)$ .
- at1-at4 Atomic orders are assigned to the parameters. Defaults are 0. When  $at4 = 0$ , the variable for the previously defined function is the distance between the atom *at1* and *at2*. And the charge of the atom *at3* will be modified. When  $at4 \neq 0$ , the variable for the previously defined function is the angle of atom *at1*, *at2*, and *at3*. And the charge of the atom *at4* will be modified.
- cect It takes the two coefficients of the charge relocation energy. Charge relocation energy is  $E_{\text{CRG}} = c_1\Delta q + c_2\Delta q^2$  and the two coefficients correspond to  $c_1$  and  $c_2$ .

This example #1 below shows a simple distance-based charge modification.

```

&crset
  ! This defines a function, f with type=2
  mode=1, npts=7, type=2, pi1=2, pi2=1, pr1=0.0, pr2=0.0,
  r = 0.3, 0.5, 1.0, 1.5, 2.0, 2.5, 3.0
  c = 7.401, 3.825, 1.419, 0.751, 0.467, 0.319, 0.0
/
&crset
  ! The charge of atom 2 is subtracted by 'f(r)'
  ! r is the distance between atom 1 and atom 2.
  ! E_crg = 0.0 * -f(r) + 113.69 * (-f(r))**2
  at1=1, at2=2, at3=2, cect=0.0,113.69
/
&crset
  ! This defines another function, g with type=1
  mode=1, npts=7, type=1, pi1=2, pi2=1, pr1=0.0, pr2=0.0,
  r = 0.3, 0.5, 1.0, 1.5, 2.0, 2.5, 3.0
  c = 3.701, 1.913, 0.709, 0.376, 0.234, 0.160, 0.0
/
&crset
  ! The charge of atom 3 is added by 'g(x)'
  ! r is the distance between atom 1 and atom 2.
  ! E_crg = 0.0 * g(x) + 0.0 * (g(x))**2
  at1=1, at2=2, at3=3, cect=0.0,0.0
/
&crset
  ! The charge of atom 4 is added by 'g(x)'
  ! r is the distance between atom 1 and atom 2.
  ! The same function can be repeatedly applied to other atoms
  at1=1, at2=2, at3=4, cect=0.0,0.0
/

```

As a result, the charges of atom 2, 3, and 4 are modified based on the distance between atom 1 and atom 2 ( $r_{12}$ ):  $q_2 = q_{2,0} - f(r_{12})$ ,  $q_3 = q_{3,0} + g(r_{12})$  and  $q_4 = q_{4,0} + g(r_{12})$ . The total charge relocation energy is  $E_{CRG} = c_{1,f}(-f(r_{12})) + c_{2,f}(-f(r_{12}))^2 + c_{1,g}g(r_{12}) + c_{2,g}(g(r_{12}))^2$ , where  $c_{1,f} = 0.0$ ,  $c_{2,f} = 113.69$ ,  $c_{1,g} = 0.0$  and  $c_{2,g} = 0.0$ .

This example #2 below shows charge modification based on both distance and angle.

```

&crset
  ! This defines function, f with type=1
  mode=1, npts=7, type=6, pi1=2, pi2=2, pr1=0.0, pr2=0.0,
  r=0, 0.5, 1.0, 1.5, 2.0, 2.5, 3.0,
  c=-7.506, -3.336, -1.946, -1.251, -0.834, -0.556, 0.0
/
&crset

```

### 3. Force field modifications

```

! The charge of atom 2 is added by f(r)
! r is the distance between atom 1 and atom 2
at1=1, at2=2, at3=2, cect=0.0,50.0
/
&crset
! This defines function, g with type=3
mode=1, npts=6, type=3, pi1=1, pi2=1, pr1=0.0, pr2=0.0,
r=0, 0.6283186, 1.2566372, 1.8849558, 2.5132744, 3.141593,
c=1.0, 1.5995, 2.1990, 2.1990, 1.5995, 1.0,
/
&crset
! Then, the charge of atom 2 is multiplied by g(theta)
! theta is the angle of atom1-atom2-atom3
at1=1, at2=2, at3=3, at4=2, cect=0.0,100.0
/
&crset

```

The example above defines charge modification rules for atom 2,  $q_2 = (q_{2,0} + f(r_{12}))g(\theta_{123})$ . The charge relocation energy is  $E_{CRG} = c_{1,f}f(r_{12}) + c_{2,f}(f(r_{12}))^2 + c_{1,g}\Delta q_g + c_{2,g}(\Delta q_g)^2$ , where  $\Delta q_g = (q_{2,0} + f(r_{12}))(g(\theta_{123}) - 1)$ ,  $c_{1,f} = 0.0$ ,  $c_{2,f} = 50.0$ ,  $c_{1,g} = 0.0$ , and  $c_{2,g} = 100.0$ . This example #3 shows another charge modification based on both distance and angle.

```

&crset
! This defines function, f with type=6
mode=1, npts=7, type=6, pi1=2, pi2=2, pr1=0.0, pr2=0.0,
r=0, 0.5, 1.0, 1.5, 2.0, 2.5, 3.0,
c=-7.506, -3.336, -1.946, -1.251, -0.834, -0.556, 0.0
/
&crset
! The charge of atom 2 is added by q_hold=f(r) but it
! will be done after the rest of the modification rules
! are applied because type > 5.
at1=1, at2=2, at3=2, cect=0.0,50.0
/
&crset
! This defines function, g with type=3
mode=1, npts=6, type=3, pi1=1, pi2=1, pr1=0.0, pr2=0.0,
r=0, 0.6283186, 1.2566372, 1.8849558, 2.5132744, 3.141593,
c=1.0, 1.5995, 2.1990, 2.1990, 1.5995, 1.0,
/
&crset
! q_hold for atom 2 is multiplied by g(theta)
! Since type < 5, q_hold is added back to q_2,0
! after this multiplication.
at1=1, at2=2, at3=3, at4=2, cect=0.0,100.0
/

```



```
&crset
```

The example defines charge modification rules:  $q_2 = q_{2,0} + f(r_{12})g(\theta_{123})$ . The charge relocation energy is  $E_{CRG} = c_{1,f}f(r_{12}) + c_{2,f}(f(r_{12}))^2 + c_{1,g}\Delta q_g + c_{2,g}(\Delta q_g)^2$ , where  $\Delta q_g = f(r_{12})(g(\theta_{123}) - 1)$ ,  $c_{1,f} = 0.0$ ,  $c_{2,f} = 50.0$ ,  $c_{1,g} = 0.0$ , and  $c_{2,g} = 100.0$ . Compare example #3 with example #2.

This example #4 below is slightly different from example #3.

```
&crset
  mode=1, npts=7, type=6, pi1=2, pi2=2, pr1=0.0, pr2=0.0,
  r=0, 0.5, 1.0, 1.5, 2.0, 2.5, 3.0,
  c=-7.506, -3.336, -1.946, -1.251, -0.834, -0.556, 0.0
/
&crset
  at1=1, at2=2, at3=2, cect=0.0,50.0
/
&crset
  ! This defines function, g with type=8
  ! The difference between example #3 and this is the type of
  ! the function g.
  ! q_hold for atom 2 should not be added to q_2,0 until
  ! the end of the modification rule.
  ! Therefore, type > 5.
  mode=1, npts=6, type=8, pi1=1, pi2=1, pr1=0.0, pr2=0.0,
  r=0, 0.6283186, 1.2566372, 1.8849558, 2.5132744, 3.141593,
  c=1.0, 1.5995, 2.1990, 2.1990, 1.5995, 1.0,
/
&crset
  ! q_hold for atom 2 is multiplied by g(theta)
  ! theta is the angle of atom1-atom2-atom3
  at1=1, at2=2, at3=3, at4=2, cect=0.0,100.0
/
&crset
  ! q_hold for atom 2 is multiplied by g(theta)
  ! theta is the angle of atom1-atom2-atom4
  at1=1, at2=2, at3=4, at4=2, cect=0.0,80.0
/
! Since there is no more rule, q_hold for atom 2
! is added back to q_2,0 finally.
```

The defined charge modification rule is  $q_2 = q_{2,0} + f(r_{12})g(\theta_{123})g(\theta_{124})$ . The charge relocation energy is  $E_{CRG} = c_{1,f}f(r_{12}) + c_{2,f}(f(r_{12}))^2 + c_{1,g}\Delta q_g + c_{2,g}(\Delta q_g)^2 + c_{1,g'}\Delta q_{g'} + c_{2,g'}(\Delta q_{g'})^2$ , where  $\Delta q_g = f(r_{12})(g(\theta_{123}) - 1)$ ,  $\Delta q_{g'} = f(r_{12})g(\theta_{123})(g(\theta_{124}) - 1)$ ,  $c_{1,f} = 0.0$ ,  $c_{2,f} = 50.0$ ,  $c_{1,g} = 0.0$ ,  $c_{2,g} = 100.0$ ,  $c_{1,g'} = 0.0$ , and  $c_{2,g'} = 80.0$ .



## 4. Sampling and free energies

This chapter collects information about a variety of ways to perform or accelerate molecular sampling (ideally in the canonical distribution) and to estimate free energies of either conformational or “alchemical” changes.

### 4.1. Thermodynamic integration

*Sander* has the capability of doing simple thermodynamic free energy calculations, using either PME or generalized Born potentials. When *icfe* is set to 1, information useful for doing thermodynamic integration estimates of free energy changes will be computed. You must use the "multisander" capability to create two groups, one corresponding to the starting state, and a second corresponding to the ending state; you will need a *prmtop* file for each of these two end points. Then a mixing parameter  $\lambda$  is used to interpolate between the "unperturbed" and "perturbed" potential functions.

There are now two different ways to prepare a thermodynamic integration free energy calculation. The first is unchanged from previous versions of Amber: Here, the two *prmtop* files that you create must have the same number of atoms, and the atoms must appear *in the same order* in the two files. This is because there is only one set of coordinates that are propagated in the molecular dynamics algorithm. If there are more atoms in the initial state than in the final, "dummy" atoms must be introduced into the final state to make up the difference. Although there is quite a bit of flexibility in choosing the initial and final states, it is important in general that the system be able to morph "smoothly" from the initial to the final state. Alternatively, you can set up your system to use the softcore potential algorithm described below. This will remove the requirement to prepare "dummy" atoms and allows the two *prmtop* files to have different numbers of atoms.

In a free energy calculation, the system evolves according to a mixed potential (such as in Eqs. 4.3 or 4.4, below). The essence of free energy calculations is to record and analyze the fluctuations in the values of  $V_0$  and  $V_1$  (that is, what the energies *would have been* with the endpoint potentials) as the simulation progresses. For thermodynamic integration (which is a very straightforward form of analysis) the required averages can be computed "on-the-fly" (as the simulation progresses), and printed out at the end of a run. For more complex analyses (such as the Bennett acceptance ratio scheme), one needs to write out the history of the values of  $V_0$  and  $V_1$  to a file, and later post-process this file to obtain the final free energy estimates.

There is not room here to discuss the theory of free energy simulations, and there are many excellent discussions elsewhere.[8, 132, 133] There are also plenty of recent examples to consult. [134, 135] Such calculations are demanding, both in terms of computer time, and in a level of sophistication to avoid pitfalls that can lead to poor convergence. Since there is no one "best way" to estimate free energies, *sander* primarily provides the tools to collect the statistics

#### 4. Sampling and free energies

that are needed. Assembling these into a final answer, and assessing the accuracy and significance of the results, generally requires some calculations outside of what Amber provides, *per se*. The discussion here will assume a certain level of familiarity with the basis of free energy calculations.

The basics of the multisander functionality are given below, but the mechanics are really quite simple. You start a free energy calculation as follows:

```
mpirun -np 4 sander.MPI -ng 2 -groupfile <filename>
```

Since there are 4 total cpu's in this example, each of the two groups will run in parallel with 2 cpu's each. The number of processors must be a multiple of two. The *groups* file might look like this:

```
-O -i mdin -p prmtop.0 -c eq1.x -o md1.o -r md1.x -inf mdinfo  
-O -i mdin -p prmtop.1 -c eq1.x -o md1b.o -r md1b.x -inf mdinfob
```

The input (*mdin*) and starting coordinate files must be the same for the two groups. Furthermore, the two *prmtop* files must have the same number of atoms, in the same order (since one common set of coordinates will be used for both.) The simulation will use the masses found in the first *prmtop* file; in classical statistical mechanics, the Boltzmann distribution in coordinates is independent of the masses so this should not represent any real restriction.

On output, the two restart files should be identical, and the two output files should differ only in trivial ways such as timings; there should be no differences in any energy-related quantities, except if energy decomposition is turned on (*idecomp* > 0; then only the output file of the first group contains the per residue contributions to  $\langle \partial V / \partial \lambda \rangle$ ). For our example, this means that one could delete the *md1b.o* and *md1b.x* files, since the information they contain is also in *md1.o* and *md1.x*. (It is a good practice, however, to check these file identities, to make sure that nothing has gone wrong.)

##### 4.1.1. Basic inputs for thermodynamic integration

- icfe**        The basic flag for free energy calculations. The default value of 0 skips such calculations. Setting this flag to 1 turns them on, using the mixing rules in Eq. (5), below.
- clambda**    The value of  $\lambda$  for this run, as in Eqs. (6.21) and (6.22), below. Zero corresponds to the unperturbed Hamiltonian (or the first of the two multisander groups)  $\lambda=1$  corresponds to the perturbed Hamiltonian, or the second of the two multisander groups.
- klambda    The exponent in Eq. (6.22), below.
- idecomp    Flag that turns on/off decomposition of  $\langle \partial V / \partial \lambda \rangle$  on a per-residue level. The default value of 0 turns off energy decomposition. A value of 1 turns the decomposition on, and 1-4 nonbonded energies are added to internal energies (bond, angle, torsional). A value of 2 turns the decomposition on, and 1-4 nonbonded energies are added to EEL and VDW energies, respectively. The frequency by which values of  $\langle \partial V / \partial \lambda \rangle$  are included into the decomposition is determined by the NTPR

flag. This ensures that the sum of all contributions equals the average of all total  $\langle \partial V / \partial \lambda \rangle$  values output every NTPR steps. All residues, including solvent molecules, have to be chosen by the RRES card to be considered for decomposition. The RES card determines which residue information is finally output. The output comes at the end of the *mdout* file. For each residue contributions of internal -, VdW-, and electrostatic energies to  $\langle \partial V / \partial \lambda \rangle$  are given as an average over all (NSTLIM/NTPR) steps. In a first section total per residue values are output followed below by further decomposed values from backbone and sidechain atoms.

The *sander* program itself does not compute free energies; it is up to the user to combine the output of several runs (at different values of  $\lambda$ ) and to numerically estimate the integral:

$$\Delta A = A(\lambda = 1) - A(\lambda = 0) = \int_0^1 \langle \partial V / \partial \lambda \rangle_\lambda d\lambda \quad (4.1)$$

If you understand how free energies work, this should not be at all difficult. However, since the actual values of  $\lambda$  that are needed, and the exact method of numerical integration, depend upon the problem and upon the precision desired, we have not tried to pre-code these into the program.

The simplest numerical integration is to evaluate the integrand at the midpoint:

$$\Delta A \simeq \langle \partial V / \partial \lambda \rangle_{1/2}$$

This might be a good first thing to do to get some picture of what is going on, but is only expected to be accurate for very smooth or small changes, such as changing just the charges on some atoms. Gaussian quadrature formulas of higher order are generally more useful:

$$\Delta A = \sum_i w_i \langle \partial V / \partial \lambda \rangle_i \quad (4.2)$$

Some weights and quadrature points are given in the accompanying table; other formulas are possible,[136] but the Gaussian ones listed there are probably the most useful. The formulas are always symmetrical about  $\lambda = 0.5$ , so that  $\lambda$  and  $(1 - \lambda)$  both have the same weight. For example, if you wanted to use 5-point quadrature, you would need to run five *sander* jobs, setting  $\lambda$  to 0.04691, 0.23076, 0.5, 0.76923, and 0.95308 in turn. (Each value of  $\lambda$  should have an equilibration period as well as a sampling period; this can be achieved by setting the *ntave* parameter.) You would then multiply the values of  $\langle \partial V / \partial \lambda \rangle_i$  by the weights listed in the Table, and compute the sum.

When *icfe=1* and *klambda* has its default value of 1, the simulation uses the mixed potential function:

$$V(\lambda) = (1 - \lambda)V_0 + \lambda V_1 \quad (4.3)$$

where  $V_0$  is the potential with the original Hamiltonian, and  $V_1$  is the potential with the perturbed Hamiltonian. The program also computes and prints  $\langle \partial V / \partial \lambda \rangle$  and its averages; note that in this case,  $\langle \partial V / \partial \lambda \rangle = V_1 - V_0$ . This is referred to as linear mixing, and is often what you want unless you are making atoms appear or disappear. If some of the perturbed atoms are "dummy" atoms (with no van der Waals terms, so that you are making these atoms

#### 4. Sampling and free energies

"disappear" in the perturbed state), the integrand in Eq. 4.1 diverges at  $\lambda = 1$ ; this is a mild enough divergence that the overall integral remains finite, but it still requires special numerical integration techniques to obtain a good estimate of the integral.[133] *Sander* implements one simple way of handling this problem: if you set *klambda* > 1, the mixing rules are:

$$V(\lambda) = (1 - \lambda)^k V_0 + [1 - (1 - \lambda)^k] V_1 \quad (4.4)$$

where *k* is given by *klambda*. Note that this reduces to Eq. 4.3 when *k* = 1, which is the default. If *k* ≥ 4, the integrand remains finite as  $\lambda \rightarrow 1$ . [133] We have found that setting *k* = 6 with disappearing groups as large as tryptophan works, but using the softcore option (*ifsc* > 0) instead is generally preferred.[137] Note that the behavior of  $\langle \partial V / \partial \lambda \rangle$  as a function of  $\lambda$  is not monotonic when *klambda* > 1. You may need a fairly fine quadrature to get converged results for the integral, and you may want to sample more carefully in regions where  $\langle \partial V / \partial \lambda \rangle$  is changing rapidly.

Notes:

1. This capability in *sander* is implemented by calling the *force()* routine twice on each step, once for  $V_0$  and once for  $V_1$ . This increases the cost of the simulation, but involves extremely simple coding.
2. It is rather easy to make mistakes when running TI calculations. It is generally good to carry out a short run (say 50 steps) setting *ntpr*=1. The check the following; if either test fails, be sure to fix the problem before proceeding.
  - a) The restart files from  $V_0$  and  $V_1$  should be identical.
  - b) If you diff the output files, there should only be simple differences. All energies, temperatures, pressures, etc. must be the same in the two files. Simulations using the QM/MM facility may show differences in the SCF energies, but be sure that the total energies, and all the MM components, are the same.
3. Eq. 4.4 is designed for having dummy atoms in the perturbed Hamiltonian, and "real" atoms in the regular Hamiltonian. You must ensure that this is the case when you set up the system in LEaP. (See the softcore section, below, for a more general way to handle disappearing atoms, which does not require dummy atoms at all.)
4. One common application of this model is to pKa calculations, where the charges are mutated from the protonated to the deprotonated form. Since H atoms bonded to oxygen already have zero van der Waals radii (in the Amber force fields and in TIP3P water), once their charge is removed (in the deprotonated form) they are really then like dummy atoms. For this special situation, there is no need to use *klambda* > 1: since the van der Waals terms are missing from both the perturbed and unperturbed states, the proton's position can never lead to the large contributions to  $\langle \partial V / \partial \lambda \rangle$  that can occur when one is changing from a zero van der Waals term to a finite one.
5. The implementation requires that the masses of all atoms be the same on all threads. To enforce this, the masses found in the first *prmtop* file (for  $V_0$ ) are used for  $V_1$  as well. In classical statistical mechanics, the canonical distribution of configurations (and hence

$n$	$\lambda_i$	$1 - \lambda_i$	$w_i$
1	0.5		1.0
2	0.21132	0.78867	0.5
3	0.1127 0.5	0.88729	0.27777 0.44444
5	0.04691 0.23076 0.5	0.95308 0.76923	0.11846 0.23931 0.28444
7	0.02544 0.12923 0.29707 0.5	0.97455 0.87076 0.70292	0.06474 0.13985 0.19091 0.20897
9	0.01592 0.08198 0.19331 0.33787 0.5	0.98408 0.91802 0.80669 0.66213	0.04064 0.09032 0.13031 0.15617 0.16512
12	0.00922 0.04794 0.11505 0.20634 0.31608 0.43738	0.99078 0.95206 0.88495 0.79366 0.68392 0.56262	0.02359 0.05347 0.08004 0.10158 0.11675 0.12457

Table 4.1.: Abscissas and weights for Gaussian integration.

of potential energies) is unaffected by changes in the masses, so this should not pose a limitation. Since the masses in the second *prmtop* file are ignored, they do not have to match those in the first *prmtop* file.

- Special care needs to be taken when using SHAKE for atoms whose force field parameters differ in the two end points. The same bonds must be SHAKEN in both cases, and the equilibrium bond lengths must also be the same. The easiest way to ensure this is to use the *noshakemask* input to remove SHAKE from the regions that are being perturbed. You must do this manually, as the current code does not have any internal idea of "perturbed" and "unperturbed" atoms.

In particular, special care needs to be taken when water molecules are part of the region that is changing. You need to make sure that the "number of 3-point waters" is the same in both  $V_0$  and  $V_1$ . This may require setting *jfastw* and/or building the structure so that *sander* does not think that the water molecules involved are actually rigid waters. Also, just setting *noshakemask* might not be enough, since this flag does not affect the *settle* routine that handles rigid waters.

### 4.1.2. Softcore Potentials in Thermodynamic Integration

Softcore potentials provide an additional way to perform thermodynamic integration calculations in Amber. The system setup has been simplified so that appearing and disappearing atoms can be present at the same time and no dummy atoms need to be introduced. Two prmtop files, corresponding to the start and end states ( $V_0$  and  $V_1$ ) of the desired transformation need to be used. The common atoms that are present in both states need to appear in the same order in both prmtop files and must have identical starting positions. In addition to the common atoms, each process can have any number of unique soft core atoms, as specified by scmask. A modified version of the vdW equation is used to smoothly switch off non-bonded interactions of these atoms with their common atom neighbors:

$$V_{V_0,disappearing} = 4\epsilon(1-\lambda) \left[ \frac{1}{\left[\alpha\lambda + \left(\frac{r_{ij}}{\sigma}\right)^6\right]^2} - \frac{1}{\alpha\lambda + \left(\frac{r_{ij}}{\sigma}\right)^6} \right] \quad (4.5)$$

$$V_{V_1,appearing} = 4\epsilon\lambda \left[ \frac{1}{\left[\alpha(1-\lambda) + \left(\frac{r_{ij}}{\sigma}\right)^6\right]^2} - \frac{1}{\alpha(1-\lambda) + \left(\frac{r_{ij}}{\sigma}\right)^6} \right] \quad (4.6)$$

Please refer to Ref [137] for a description of the implementation and performance testing when compared to the TI methods described above. Note that the term “disappearing” is used here, but it would probably be better to say that atoms present in  $V_0$  but not in  $V_1$  are “decoupled” from their environment: the interactions among the “disappearing” atoms are not changed, and do not contribute to  $\langle \partial V / \partial \lambda \rangle$ . If the disappearing atoms are a separate molecule (say a non-covalently-bound ligand), this can be viewed as a transfer to the gas-phase.

All bonded interactions of the unique atoms are recorded separately in the output file (see below). Any bond, angle, dihedral or 1-4 term that involves at least one appearing or disappearing atom is not scaled by  $\lambda$  and does not contribute to  $\langle \partial V / \partial \lambda \rangle$ . Therefore, output from both processes will not be identical when soft core potentials are used. Softcore transformations avoid the origin singularity effect and therefore linear mixing can (and should) always be used with them. Since the unique atoms become decoupled from their surroundings at high or low lambdas and energy exchange between them and surrounding solvent becomes inefficient, a Berendsen type thermostat should not be used for SC calculations. Any SHAKE constraints applying to bonds between common and unique atoms will be removed before the simulation, but SHAKE constraints for bonds between unique atoms are unchanged. The icfe and klambda parameters should be set to 1 for a soft core run and the desired lambda value will be specified by clambda. When using softcore potentials,  $\lambda$  values should be picked so that  $0.01 < \text{clambda} < 0.99$ . Additionally, the following parameters are available to control the TI calculation:

ifsc            Flag for soft core potentials  
                   = 0 SC potentials are not used (default)  
                   = 1 SC potentials are used. Note that a different setup is required, so prmtop files for non soft core simulations cannot be used with soft core potentials and vice versa.



- scalpha The  $\alpha$  parameter in 4.5 and 4.6, its default value is 0.5. Other values have not been extensively tested
- scmask Specifies the unique atoms for this process in ambmask format. This, along with crgmask, is the only parameter that will frequently be different in the two mdin files for  $V_0$  and  $V_1$ . It is valid to set scmask to an empty string. A summary of the atoms in scmask is printed at the end of mdout.
- logdvdl If set to .ne. 0, a summary of all  $\partial V/\partial\lambda$  values calculated during every step of the run will be printed out at the end of the simulation for postprocessing.
- dvdlnorest If set to .ne. 0, the potential energy from positional restraints set by the &wt namelists will not be counted into  $\langle\partial V/\partial\lambda\rangle$ . This can be convenient in calculations of absolute binding free energies as in Ref .[138] Please note that the force constants of restraints are divided by lambda if soft core potentials are switched on. This results in the restraint being applied in full to the disappearing atoms at any lambda.
- dynlmb If set to a value .gt. zero, clambda is increased by dynlmb every ntime steps. This can be used to perform simulations with dynamically changing lambdas.
- crgmask Specifies a number of atoms (in ambmask format) that will have their atomic partial charges set to zero. This is mainly for convenience because it removes the need to build additional prmtop files with uncharged atoms for TI calculations involving the removal of partial charges.

The force field potential energy contributions for the unique atoms in each process will be evaluated separately during the simulation and are recorded after the complete system energy is given:

```
Softcore part of the system: 15 atoms, TEMP (K) = 459.76
SC_BOND = 2.0634   SC_ANGLE = 7.0386   SC_DIHED = 4.2087
SC_14NB = 3.3948   SC_14EEL = 0.0000   SC_EKIN  = 16.9021
SC_VDW  = -0.3269   SC_EEL   = 0.0000   SC_DERIV = -9.9847
```

The temperatures reported are calculated for the SC atoms only and fluctuate strongly for small numbers of unique atoms. The energies in the first two lines include all terms that involve at least one unique atom, but SC\_VDW gives the vdW energy for pairs of unique atoms only which are subject to the standard 12-6 LJ potential. The vdW potential between soft core / non soft core atoms (as given by equation 4.5) is part of the regular VDWAALS term and is counted for dV/dl. The same applies to SC\_EEL, which gives only the electrostatic interactions between unique atoms, since electrostatics between soft core / non soft core atoms (for which equation 4.7 is used) are part of regular EEL-energy.

SC\_DERIV is an additional  $\lambda$ -dependent contribution to  $\langle\partial V/\partial\lambda\rangle$  that arises from the form of the SC-potential. For more information on how to perform and setup calculations, please consult the tutorial written by Thomas Steinbrecher at <http://ambermd.org>.

## 4. Sampling and free energies

### 4.1.2.1. One step transformations using soft core electrostatics

Alternatively to the two-step process of removing charges from atoms first and then changing the vdW parameters of chargeless atoms in a second TI calculation, *sander* also has a soft core version of the Coulomb equation implemented for single step transformations under periodic boundary conditions. This is automatically applied to all atoms in *scmask* and their interactions with common atoms are given by:

$$V_{V_0,disappearing} = (1 - \lambda) \frac{q_i q_j}{4\pi\epsilon_o \sqrt{\beta\lambda + r_{ij}^2}} \quad (4.7)$$

for disappearing atoms. Replace  $\lambda$  by  $(1 - \lambda)$  and vice versa for the form for appearing atoms. This introduces a new parameter  $\beta$  which controls the 'softness' of the potential. This is set in the input file via:

scbeta      The parameter  $\beta$  in 4.7. Default value is  $12\text{\AA}^2$ , other values have not been extensively tested.

With the use of soft core vdW and electrostatics interactions, arbitrary changes between systems are possible in single TI calculations. However, due to the unusual potential function forms introduced, it is not always clear that a single-step calculation will converge faster than one broken down into several steps. Ref. [139] contains detailed information on the performance of such single step TI calculations.

### 4.1.3. Collecting potential energy differences for FEP calculations

In addition to the Thermodynamic Integration capabilities described above, *sander* can also collect potential energy values during free energy simulation runs for postprocessing by e.g. the Bennett acceptance ratio scheme. This will make *sander* calculate at given points during the simulation the total potential energy of the system as it would be for different  $\lambda$ -values at this conformation. This functionality is controlled by:

ifmbar      If set to 1 (Default = 0), additional output is generated for later postprocessing.

bar\_intervall    Compute potential energies every *bar\_intervall* steps (Default = 100)

bar\_l\_min    Minimum  $\lambda$ -value (Default = 0.1)

bar\_l\_max    Maximum  $\lambda$ -value (Default = 0.9)

bar\_l\_incr    The increment to increase  $\lambda$  by between the minimum and maximum (Default = 0.1)

Such energy collection will normally be part of a regular free energy calculation (using *icfe=1* and *ifsc=1*) involving simulations at various  $\lambda$ -values. Activating this functionality will not have any influence on the simulation trajectory which will evolve according to the preset *clambda* value, it is merely a bookkeeping scheme that removes the necessity of postprocessing output files later.

## 4.2. Umbrella sampling

Another free energy quantity that is accessible within *sander* is the ability to compute potentials of mean force (at least for simple distance, angle, or torsion variables) using umbrella sampling. The basic idea is as follows. You add an artificial restraint to the system to bias it to sample some coordinate in a certain range of values, and you keep track of the distribution of values of this coordinate during the simulation. Then, you repeatedly move the minimum of the biasing potential to different ranges of the coordinate of interest, and carry out more simulations. These different simulations (often called "windows") must have some overlap; that is, any particular value of the coordinate must be sampled to a significant extent in more than one window. After the fact, you can remove the effect of the biasing potential, and construct a potential of mean force, which is the free energy profile along the chosen coordinate.

The basic ideas have been presented in many places,[108–110, 140, 141] and will not be repeated here. The implementation in *sander* follows two main steps. First, restraints are set up (using the distance and angle restraint files) and the DUMPFREQ parameter is used to create "history" files that contain sampled values of the restraint coordinate. Second, a collection of these history files is analyzed (using the so-called "weighted histogram" or WHAM method [108–110]) to generate the potentials of mean force. As with thermodynamic integration, the *sander* program itself does not compute these free energies; it is up to the user to combine the output of several windows into a final result. For many problems, the programs prepared by Alan Grossfield (<http://membrane.urmc.rochester.edu/>) are very convenient, and the *sander* output files are compatible with these codes. Other methods of analysis, besides WHAM, may also be used.[142]

*A simple example.* The input below shows how one window of a potential of mean force might be carried out. The coordinate of interest here is the chi angle of a base in an RNA duplex. Here is the *mdin* file:

```
test of umbrella sampling of a chi torsion angle
&cntrl
  nstlim=50000, cut=20.0, igb=1, saltcon=0.1,
  ntp=1, ntwr=100000, ntt=3, gamma_ln=0.2,
  ntx=5, irect=1,
  ntc=2, ntf=2, tol=0.000001,
  dt=0.001, ntb=0,
  nmropt=1,
/
&wt type='DUMPFREQ', istep1=10 /
&wt type='END' /
DISANG=chi.RST
DUMPAVE=chi_vs_t.170
```

The items in the *&cntrl* namelist are pretty standard, and not important here, except for specifying *nmropt=1*, which allows restraints to be defined. (The name of this variable is an historical artifact: distance and angle restraints were originally introduced to allow NMR-related structure calculations to be carried out. But they are also very useful for cases, like this one, that have nothing to do with NMR.) The DUMPFREQ command is used to request a separate file

#### 4. Sampling and free energies

be created to hold values of the torsion angle; this will have the name *chi\_vs\_t.170* given in the DUMPAVE file redirection command.

The torsion angle restraint itself is given in the *chi.RST* file:

```
# torsion restraint for chi of residue 2
&r1 iat=39,40,42,43, r1=0., r2=170., r3=170., r4=360., rk2 = 30.,
rk3 = 30., /
```

The *iat* variable gives the atom numbers of the four atoms that define the torsion of interest. We set  $r2 = r3$  and  $rk2 = rk3$  to obtain a harmonic bias sing potential, with a minimum at 170 o . The values  $r1$  and  $r4$  should be far away from 170, so that the potential is essentially harmonic everywhere. (It is not required that bias sing potentials be harmonic, but Dr. Grossfield's programs assume that they are, so we enforce that here.) Subsequent runs would change the minimum in the potential to values other than 170, creating other *chi\_vs\_t* files. These files would then be used to create potentials of mean force. Note that the conventionally defined "force constant" is twice the value  $rk2$ , and that the Grossfield program uses force constants measured in degrees, rather than radians. So you must perform a unit conversion in using those programs, multiplying  $rk2$  by  $0.0006092$  ( $= 2(\pi/180)^2$ ) to get a equivalent force constant for a torsional restraint.

### 4.3. Self-Guided Langevin dynamics

Self-guided Langevin dynamics (SGLD) is designed to enhance conformational search efficiency in either a molecular dynamics (MD) simulation (when  $\gamma_{ln}=0$ ) or Langevin dynamics (LD) simulation (when  $\gamma_{ln}>0$ ). This method applies a guiding force calculated during a simulation to accelerate the systematic motion for more efficient conformational sampling.[143][144] The conformational distribution of SGLD can be reweighted to produce canonical ensemble averages[145, 146][144]. The guiding force can be applied to a part of a simulation system starting from atom *isgsta* to atom *isgend*. The strength of the guiding force is defined by either *tempsg* or *sgft*. A smaller *sgft* will produce results closer to a normal MD or LD simulation. Starting with AMBER 12, *tempsg* is redefined as a conformational search ability that is comparable to a high temperature simulation at  $temp0=tempsg$ . Normally, *tempsg* or *sgft* is set to the limit that accelerates slow events to an affordable time scale. The conformational distribution of a SGLD simulation can be converted to a canonical ensemble distribution through reweighting. The reweighting information is printed out from the simulation output. In addition, a force-momentum based SGLD algorithm (SGLDfp) [146] allows conformational search be accelerated while the canonical ensemble distribution be maintained.

SGLD can be used for replica exchange simulation (RXSGLD) to achieve enhance sampling without elevating temperature. Instead, *sgft* or *tempsg* is different for different replicas. See 4.6.12 for a detailed description of RXSGLD.

- |        |  |
|--------|--|
| isgld  | The default value of zero disables self-guiding; isgld=1 will turn on SGMD/SGLD method for accelerated conformational search and isgld=2 will turn on the SGLDfp method [146] to maintain a ensemble distribution. |
| tsgavg | Local averaging time ( <i>psec</i> ) for the guiding force calculation. Default 0.2 <i>psec</i> . A larger value defines a slower motion to be enhanced.   |

### 4.3. Self-Guided Langevin dynamics

sgft	Guiding factor. Defines the strength of the guiding force when $tempsg=0$ . Default 1.0 when $gamma\_ln>0$ and 0.2 when $gamma\_ln=0$ . $tempsg>0$ will override $sgft$ .
tempsg	Guiding temperature (K). This parameter is refined since Amber 12 as a conformational search ability which is comparable to a high temperature simulation with $temp0=tempsg$ . For example, by setting $tempsg=500K$ , a SGMD/SGLD simulation will accelerate conformational search as much as rising the simulation temperature to 500K. Default 0.0 K. $tempsg$ will not be used to control the guiding effect. $tempsg>temp0$ will accelerate conformational search and $tempsg<temp0$ will slow down conformational search. Once $tempsg$ is set, $sgft$ will fluctuate to reach the conformational search ability.
isgsta	The first atom index of SGLD region. Default 1.
isgend	The last atom index of SGLD region. Default is $natom$ .
treff	Reference low frequency temperature. Default 0.0. $treff$ is the low frequency temperature when no guiding force is applied to a simulation system ( $sgft=0$ ). $treff$ is required for the weighting factor calculation in SGMD/SGLD simulation ( $isgld=1$ ) or for the guiding force calculation in SGMDfp/SGLDfp simulations ( $isgld=2$ ). When $treff=0$ , $treff$ will be estimated during a simulation. An actual value of $treff$ can increase the accuracy in the weighting factor calculation or in SGMDfp/SGLDfp simulations.
fixcom	Option to remove the net translation of the center of mass. For finite systems it is often more convenient to have the center of mass fixed. Default 0. When $fixcom>0$ , the center of mass is allowed to translation.

The output of SGMD/SGLD simulations contains following properties related to the enhancement in conformational search and reweighting of conformational distribution:

SGLF = SGFT TEMPSG TEMPLF TREFLF FRCLF EPOTLF SGWT  
SGHF = SGFF SGFD TEMPHF TREFHF FRCHF EPOTHF VIRSG

These quantities are instantaneous values defined as below:

SGFT: Momentum guiding factor,  
SGFF: Force guiding factor. Adjusted in SGLDfp simulations ( $isgld=2$ )  
SGFD: Force dumping factor. Adjusted in SGLDfp simulations ( $isgld=2$ )  
TEMPSG: Guiding temperature.  
SGWT: Weighting free energy.  $\exp(SGWT)$  is the weighting factor of current frame.  
VIRSG: Virial of the guiding force.  
TEMPLF: low frequency temperature  
TEMPHF: high frequency temperature  
TREFLF: reference low frequency temperature. It is the TEMPLF at  $SGFT=0$  and  $TEMPSG=0$ .  
TREFHF: reference high frequency temperature. It is the TEMPHF at  $SGFT=0$  and  $TEMPSG=0$ .  
FRCLF: low frequency force factor  
FRCHF: high frequency force factor

#### 4. Sampling and free energies

EPOTLF: low frequency potential energy  
EPOTHF: high frequency potential energy

The weight of a conformation is calculated by

Weight= $\exp(\text{SGWT}) = \exp(((\text{FRCLF} * \text{TREFLF} / \text{TEMPLF} - 1) * \text{EPOTLF} + (\text{FRCHF} * \text{TREFHF} / \text{TEMPHF} - 1) * \text{EPOTHF} + \text{VIRSG}) / (\text{KBOLTZ} * \text{Temp}))$

$$w_i = \exp \left( \left( \lambda_{LF} \frac{T_{LF}^0}{T_{LF}} - 1 \right) \frac{E_{LF}}{kT} + \left( \lambda_{HF} \frac{T_{HF}^0}{T_{HF}} - 1 \right) \frac{E_{HF}}{kT} + \frac{W_{sg}}{kT} \right)$$

For convenience, two scripts, *sgldinfo.sh* and *sgldwt.sh*, are provided in the AMBERHOME/bin directory to extract SGLD properties and weighting factors from sander output files. For example, one can run:

```
sgldinfo.sh mdout
```

to examine the SGLD properties, and run:

```
sgldwt.sh mdout
```

to print weighting factors at each print time frame. One may specify TREFLF, e.g., 23.5 K, and/or TREFHF, e.g., 278.2 K, for more accurate weighting factors:

```
sgldwt.sh mdout 23.5 278.2
```

TREFLF and TREFHF can be obtained with *sgldinfo.sh* from a SGLD simulation at the same condition except SGFT=0 and TEMPSG=0. Without specifying TREFLF and TREFHF, they will be estimated for the calculation. Ensemble average properties are calculated through reweighting:

$$\langle P \rangle = \frac{\sum_{i=N_0}^N w_i P_i}{\sum_{i=N_0}^N w_i}$$

For SGLDfp (isgld=2) simulations, no reweighting is needed.

### 4.4. Targeted MD

The targeted MD option adds an additional term to the energy function based on the mass-weighted root mean square deviation of a set of atoms in the current structure compared to a reference structure. The reference structure is specified using the *-ref* flag in the same manner as is used for Cartesian coordinate restraints (NTR=1). Targeted MD can be used with or without positional restraints. If positional restraints are not applied (ntr=0), *sander* performs a best-fit of the reference structure to the simulation structure based on selection in *tgfitmask* and calculates the RMSD for the atoms selected by *tgtrmsmask*. The two masks can be identical or different. This way, fitting to one part of the structure but calculating the RMSD (and thus restraint force) for another part of the structure is possible. If targeted MD is used in conjunction with positional restraints (ntr=1), only *tgtrmsmask* should be given in the control input because the molecule is 'fitted' implicitly by applying positional restraints to atoms specified in *restraintmask*.

The energy term has the form:

$$E = 0.5 * \text{TGMTDFRC} * \text{NATTGTRMS} * (\text{RMSD} - \text{TGTRMSD}) ** 2$$

The energy will be added to the RESTRAINT term. Note that the energy is weighted by the number of atoms that were specified in the *tgtrmsmask* (NATTGTRMS). The RMSD is the root mean square deviation and is mass weighted. The force constant is defined using the *tgmdfrc* variable (see below). This option can be used with molecular dynamics or minimization. When targeted MD is used, *sander* will print the current values for the actual and target RMSD to the energy summary in the output file.

itgtmd

= 0 no targeted MD (default)

= 1 use targeted MD

= 2 use targeted MD to multiple targets (Multiply-targeted MD, or MTMD, see next section below)

tgtrmsd Value of the target RMSD. The default value is 0. This value can be changed during the simulation by using the weight change option.

tgmdfrc This is the force constant for targeted MD. The default value is 0, which will result in no penalty for structure deviations regardless of the RMSD value. Note that this value can be negative, which would force the coordinates AWAY from the reference structure.

tgfitmask Define the atoms that will be used for the rms superposition between the current structure and the reference structure. Syntax is in Chapter C.

tgtrmsmask Define the atoms that will be used for the rms difference calculation (and hence the restraint force), as outlined above. Syntax is in Chapter C.

One can imagine many uses for this option, but a few things should be kept in mind. In this implementation of targeted MD, there is currently only one reference coordinate set, so there is no way to force the coordinates to any specific structure other than the one reference. To move a structure toward a reference coordinate set, one might use an initial *tgtrmsd* value corresponding to the actual RMSD between the input and reference (*inpcrd* and *refc*). Then the weight change option could be used to decrease this value to 0 during the simulation. To move a structure away from the reference, one can increase *tgtrmsd* to values larger than zero. The minimum for this energy term will then be at structures with an RMSD value that matches *tgtrmsd*. Keep in mind that many different structures may have similar RMSD values to the reference, and therefore one cannot be sure that increasing *tgtrmsd* to a given value will result in a particular structure that has that RMSD value. In this case it is probably wiser to use the final structure, rather than the initial structure, as the reference coordinate set, and decrease *tgtrmsd* during the simulation. To address this, multiply-targeted MD is now available in Amber (*sander only*), and is described in the next section. As an additional note, a negative force constant *tgmdfrc* can be used, but this can cause problems since the energy will continue to decrease as the RMSD to the reference increases.

Also keep in mind that phase space for molecular systems can be quite complex, and this method does not guarantee that a low energy path between initial and target structures will be

#### 4. Sampling and free energies

followed. It is possible for the simulation to become unstable if the restraint energies become too large if a low-energy path between a simulated structure and the reference is not accessible.

Note also that the input and reference coordinates are expected to match the *prmtop* file and have atoms in the same sequence. No provision is made for symmetry; rotation of a methyl group by 120° would result in a non-zero RMSD value.

### 4.5. Multiply-Targeted MD (MTMD)

In Amber (*sander only*), the user may perform targeted MD calculations using multiple reference structures. Each reference may have its own associated target RMSD value and force constant, each of which can evolve independently in time. Additionally, the masks for each defined target may differ, and targeting to any given reference structure can be activated for some or part of the simulation. The energy term for MTMD is simply the sum of the energies that would be calculated for the molecule calculated relative to each target given the target RMSD and force constant for that target. The energy will then be added to the RESTRAINT term.

To use MTMD, the MTMD input file is specified using the *-mtmd* flag in the command line arguments for *sander*. The MTMD input file will contain one instance of the *tgt* namelist (“&tgt”) for each reference structure used. The user may specify any number of reference structures.

#### 4.5.1. Variables in the &tgt namelist:

- refin* The file name of the reference structure used. The input and reference coordinates are expected to match the *prmtop* file and have atoms in the same sequence. *Default for refin is “”, no reference structure given.*
- mtmdform* If *MTMDFORM* > 0, then the reference coordinate file is formatted. Otherwise, the reference coordinate file is an unformatted (binary) file. *Default for MTMDFORM is the value assigned to MTMDFORM in the most recent namelist where MTMDFORM was specified. If MTMDFORM has not been specified in any namelist, it defaults to 1.*
- mtmdstep1, mtmdstep2* Targeted MD for this structure is run for steps/iterations *MTMDSTEP1* through *MTMDSTEP2*. If *MTMDSTEP2* = 0, then TMD will be run through the end of the run, and the values of the target RMSD and the force constant will not change with time. Note that the first step/iteration is considered step 0. *Defaults for MTMDSTEP1 and MTMDSTEP2 are the values assigned to them in the most recent namelist where MTMDSTEP1 and MTMDSTEP2 were specified. If MTMDSTEP1 and MTMDSTEP2 have not been specified in any namelist, they default to 0.*
- mtmdvari* If *MTMDVARI* > 0, then the force constant and target RMSD will vary with step number. Otherwise, they are constant throughout the run. If *MTMDVARI* > 0, then the values *MTMDSTEP2*, *MTMDRMSD2*, and *MTMDFORCE2* must be specified (see below). *Default for MTMDVARI is the value assigned to MTMDVARI in the most recent namelist where MTMDVARI was specified. If MTMDVARI has not been specified in any namelist, it defaults to 0.*



#### 4.5. Multiply-Targeted MD (MTMD)

mtmdrmsd, mtmdrmsd2 The target RMSD for this reference. If MTMDVARI >0, then the value of MTMDRMSD will vary between MTMDSTEP1 and MTMDSTEP2, so that, e.g.  $MTMDRMSD(MTMDSTEP1) = MTMDRMSD$  and  $MTMDRMSD(MTMDSTEP2) = MTMDRMSD2$ . *Defaults for MTMDRMSD and MTMDRMSD2 are the values assigned to them in the most recent namelist where MTMDRMSD and MTMDRMSD2 were specified. If MTMDRMSD and MTMDRMSD2 have not been specified in any namelist, they default to 0.0.*

mtmdforce, mtmdforce2 The force constant for this reference. If MTMDVARI >0, then the value of MTMDFORCE will vary between MTMDSTEP1 and MTMDSTEP2, so that, e.g.  $MTMDFORCE(MTMDSTEP1) = MTMDFORCE$  and  $MTMDFORCE(MTMDSTEP2) = MTMDFORCE2$ . *Defaults for MTMDFORCE and MTMDFORCE2 are the values assigned to them in the most recent namelist where MTMDFORCE and MTMDFORCE2 were specified. If MTMDFORCE and MTMDFORCE2 have not been specified in any namelist, they default to 0.0.*

mtmdninc If MTMDVARI >0 and MTMDNINC > 0, then the changes in the values of of MTMDRMSD and MTMDFORCE are applied as a step function, with NINC steps/iterations between each change in the target values. If MTMDNINC = 0, the change is effected continuously (at every step). *Default for MTMDNINC is the value assigned to MTMDNINC in the most recent namelist where MTMDNINC was specified. If MTMDNINC has not been specified in any namelist, it defaults to 0.*

mtmdmult If MTMDMULT=0, and the values of MTMDFORCE changes with step number, then the changes in the force constant will be linearly interpolated from MTMDFORCE→MTMDFORCE2 as the step number changes. If MTMDMULT=1 and the force constant is changing with step number, then the changes in the force constant will be effected by a series of multiplicative scalings, using a single factor, R, for all scalings. *i.e.*

$$MTMDFORCE2 = R^{**INCREMENTS} * MTMDFORCE$$

INCREMENTS is the number of times the target value changes, which is determined by MTMDSTEP1, MTMDSTEP2, and MTMDNINC. *Default for MTMDMULT is the value assigned to MTMDMULT in the most recent namelist where MTMDMULT was specified. If MTMDMULT has not been specified in any namelist, it defaults to 0.*

mtmdmask Define the atoms that will be used for both the rms superposition between the current structure and the reference structure and the rms difference calculation (and hence the restraint force), as outlined above. Syntax is in Chapter C. *Default for MTMDMASK is the value assigned to MTMDMASK in the most recent namelist where MTMDMASK was specified. If MTMDMASK has not been specified in any namelist, it defaults to '\*', use all atoms in the fit and force calculations. \*

Namelist &tgt is read for each reference structure. Input ends when a namelist statement with refin = '' (or refin not specified) is found. Note that comments can precede or follow any namelist statement, allowing comments and reference definitions to be freely mixed.

## 4.6. Steered Molecular Dynamics (SMD) and the Jarzynski Relationship

### 4.6.1. Background

SMD applies an external force onto a physical system, and drives a change in coordinates within a certain time. Several applications have come from Klaus Schulten's group.[147] An implementation where the coordinate in question changes in time at constant velocity is coded in this version of Amber. The present implementation has been done by the group of Prof. Dario Estrin in Buenos Aires <dario@q1.fcen.uba.ar> by Marcelo Marti <marcelomarti@yahoo.com> and Alejandro Crespo <alec@qi.fcen.uba.ar>, and in the group of Prof. Adrian Roitberg at the University of Florida <roitberg@ufl.edu>.[148]

The method should be thought of as an umbrella sampling where the center of the restraint is time-dependent as in:

$$V_{rest}(t) = (1/2)k[x - x_0(t)]^2$$

where  $x$  could be a distance, an angle, or a torsion between atoms or groups of atoms.

This methodology can be used then to drive a physical process such as ion diffusion, conformational changes and many other applications. By integrating the force over time (or distance), a generalized work can be computed. This work can be used to compute free energy differences using the so-called Jarzynski relationship.[149–151] This method states that the free energy difference between two states A and B (differing in their values of the generalized coordinate  $x$ ) can be calculated as

$$\exp(-\Delta G/k_B T) = \langle \exp(-W/k_B T) \rangle_A \quad (4.8)$$

This means that by computing the work between the two states in question, and averaging over the initial state, equilibrium free energies can be extracted from non-equilibrium calculations. In order to make use of this feature, SMD calculations should be done, with different starting coordinates taken from equilibrium simulations. This can be done by running `sander` multiple times, or by running `multisander`. There are examples of the various modes of action under the `test/jar` directories in the Amber distribution.

### 4.6.2. Implementation and usage

To set up a SMD run, set the `jar` variable in the `&cntrl` namelist to 1. The change in coordinates is performed from a starting to an end value in `nstlim` steps.

To specify the type and conditions of the restraint an additional ".RST" file is used as in `nmropt=1`. (Note that `jar=1` internally sets `nmropt=1`.) The restraint file is similar to that of NMR restraints (see Section 6.1), but fewer parameters are required. For instance, the following RST file could be used:

```
# Change distance between atoms 485 and 134 from 15 A to 20 A
&rst iat=485,134, r2=15., rk2 = 5000., r2a=20. /
```

#### 4.6. Steered Molecular Dynamics (SMD) and the Jarzynski Relationship

Note that only  $r2$ ,  $r2a$  and  $rk2$  are required;  $rk3$  and  $r3$  are set equal to these so that the harmonic restraint is always symmetric, and  $r1$  and  $r4$  are internally set so that the restraint is always operative. An SMD run changing an angle, would use three *iat* entries, and one changing a torsion needs four. As in the case of NMR restraints, group inputs can also be used, using  $iat < 0$  and defining the corresponding groups using the *igr* flag.

The output file differs substantially from that used in the case of nmr restraints. It contains 4 columns:  $x_0(t)$ ,  $x$ , force, work. Here work is computed as the integrated force over distances (or angle, or torsion). These files can be used for later processing in order to obtain the free energy along the selected reaction coordinate using Jarzynski's equality.

##### Example

The following example changes the distance between two atoms along 1000 steps:

```
Sample pulling input
&cntrl
nstim=1000, cut=99.0, igb=1, saltcon=0.1,
ntpr=100, ntwr=100000, ntt=3, gamma_ln=5.0,
ntx=5, irect=1, ig = 256251,
ntc=2, ntf=2, tol=0.000001,
dt=0.002, ntb=0, tempi=300., temp0=300.,
jar=1,
/
&wt type='DUMPFREQ', istep1=1, /
&wt type='END', /
DISANG=dist.RST
DUMPAVE=dist_vs_t
LISTIN=POUT
LISTOUT=POUT
```

Note that the flag *jar* is set to 1, and redirections to the *dist.RST* file are given. In this example the values in the output file *dist\_vs\_t* are written every *istep=1* steps.

The restraint file *dist.RST* in this example is:

```
# Change distance between atoms 485 and 134 from 15 A to 20.0 A
&rst iat=485,134, r2=15., rk2 = 5000., r2a=20.0, /
```

and the output *dist\_vs\_t* file might contain:

```
15.00000 15.12396 -1239.55482 0.00000
15.00500 14.75768 2470.68119 3.07782
15.01000 15.13490 -1246.46571 6.13835
15.01500 15.15041 -1350.03026 -0.35289
15.02000 14.77085 2481.56731 2.47596
15.02500 15.12423 -987.34073 6.21152
15.03000 15.18296 -1520.41603 -0.05787
15.03500 14.79016 2431.22399 2.21915
.....
19.97000 19.89329 4.60255 67.01305
```

#### 4. Sampling and free energies

```
19.97500 19.87926 4.78696 67.03652
19.98000 19.86629 4.54839 67.05986
19.98500 19.85980 3.75589 67.08062
19.99000 19.86077 2.58457 67.09647
19.99500 19.86732 1.27678 67.10612
```

In this example, the work of pulling from 15.0 to 20.0 (over 2 ps) was 67.1 kcal/mol. One would need to repeat this calculation many times, starting from different snapshots from an equilibrium trajectory constrained at the initial distance value. This could be done with a long MD or a REMD simulation, and postprocessing with `ptraj` to extract snapshots. Once the work is computed, it should be averaged using Eq. (6.27) to get the final estimate of the free energy difference. The number of simulations, the strength of the constraint, and the rate of change are all important factors. The user should read the appropriate literature before using this method. It is recommended that the width of the work distribution do not exceed 5-10% for faster convergence. An example using `multisander` to run two of these simulations at the same time is presented under `$AMBERHOME/test`. In many cases, umbrella sampling (see Section 4.2) may be a better way to estimate the free energy of a conformational change.

### 4.7. Replica Exchange Molecular Dynamics (REMD)

In the replica-exchange method, noninteracting copies of the system (replicas) are simulated concurrently at different values of some independent variable, such as temperature. Replicas are subjected to Monte Carlo move evaluation periodically, thus effecting exchange between values of the independent variable. The replica-exchange method enables simulation in a generalized ensemble — one in which states may be weighted by non-Boltzmann probabilities. (However, one advantage of replica-exchange is the simplicity inherent in its use of Boltzmann factors.) Consequently, local potential energy wells may not dominate traversal through phase space because a replica trapped in a local minimum can escape via exchange to a different value of the independent variable.[152] The *multisander* approach runs multiple *sander* jobs concurrently under a single MPI program. This can be used to just run unconnected parallel jobs, but it is more useful to use this as a platform for the *replica exchange method*.

The replica exchange method in temperature space for molecular dynamics (REMD) [152–154] has been implemented on top of the framework that *multisander* provides.  $N$  non-interacting replicas are simultaneously simulated in  $N$  separate MPI groups, each of which has its own set of input and output files. One process from each MPI group is chosen to form another MPI group (called the master group), in which exchanges are attempted.

#### 4.7.1. Running REMD simulations

The  $N$  replicas are first sorted in an array by their target temperatures. Half of the  $N$  replicas (replicas with even array indices) are chosen to be exchange initiators. These initiators pair with their right and left neighbors alternatively after each *runmd* call. Topologically, the  $N$  temperature-sorted replicas form a loop, in which the first and the last replicas are neighbors. Therefore,  $N/2$  exchanges are attempted in each iteration. The current potential energies and

## 4.7. Replica Exchange Molecular Dynamics (REMD)

target (*temp0*) temperatures are used in a Metropolis-type calculation to determine the probability of making the exchange. If the exchange is allowed between the pair, the target temperatures for the two replicas are swapped before the next *runmd* call. The velocities of each replica involved in successful exchange are then adjusted by a scaling factor related to the previous and new target temperatures. After the exchange calculation, *runmd* is called to perform MD following the *mdin* file. After this *runmd* run, the exchange probability is calculated again, and so on.

Before starting a replica exchange simulation, an optimal set of target temperatures should be determined so that the exchange ratio is roughly a constant. These target temperatures determine the probability of exchange among the replicas, and the user is referred to the literature for a more complete description of the influence of various factors on the exchange probability.

Each replica requires (for input files) or generates (for output files) its own *mdin*, *inpcrd*, *mdout*, *mdcrd*, *restrt*, *mdinfo*, and associated files. The names are provided through the specification of a *groupfile* on the command line with the *-groupfile groupfile* option. The *groupfile* file contains a separate command line for each of the replicas or multisander instances, one per line (with no extra lines except for comments, which must have a '#' in the first column). To choose the number of replicas or multisander instances, the *-ng N* command line option is used (in this case to specify *N* separate instances.) If the number of processors (for the MPI run) is larger than *N* (and also a multiple of *N*), each replica or multisander instance will run on a number of processors equal to the total specified on the command line divided by *N*. Note that in the *groupfile*, the *-np* option is currently ignored, *i.e.* each replica or multisander instance is currently hardcoded to run on an equivalent number of processors.

For example, an 4-replica REMD job will need 4 *mdin* and 4 *inpcrd* files. Then, the *groupfile* might look like this:

```
#
# multisander or replica exchange group file
#
-O -i mdin.rep1 -o mdout.rep1 -c inpcrd.rep1 -r restrt.rep1 -x mdcrd.rep1
-O -i mdin.rep2 -o mdout.rep2 -c inpcrd.rep2 -r restrt.rep2 -x mdcrd.rep2
-O -i mdin.rep3 -o mdout.rep3 -c inpcrd.rep3 -r restrt.rep3 -x mdcrd.rep3
-O -i mdin.rep4 -o mdout.rep4 -c inpcrd.rep4 -r restrt.rep4 -x mdcrd.rep4
```

Note that the *mdin* and *inpcrd* files are *not* required to be ordered by their target temperatures since the temperatures of the replicas will not remain sorted during the simulation. Sorting is performed automatically at each REMD iteration as described above. Thus one can restart REMD simulations without modifying the restart files from the previous REMD run (see below for more information about restarting REMD).

It is important to ensure that the target temperature (specified using *temp0*) is the only difference among the *mdin* files for the replicas, otherwise the outcome of an REMD simulation may be unpredictable since each replica may be performing a different type of simulation. However, in order to accommodate advanced users, the input files are not explicitly compared.

## 4. Sampling and free energies

### 4.7.2. Restarting REMD simulations

It is recommended that each REMD run generate a new set of output files (such as mdcrd), but for convenience one may use `-A` in the command line in order to append output to existing output files. This can be a useful option when restarting REMD simulations. If `-A` is used, files that were present before starting the REMD simulation are appended to throughout the new simulation. Note that this can seriously affect performance on systems where the file writing becomes rate limiting, although the new implementation of REMD should help with this somewhat. If `-O` is used, any files present are overwritten during the first iteration, and then subsequent iterations append to these new files.

At the end of a REMD simulation, the target temperature of each replica is most likely not the same as it was at the start of the simulation (due to exchanges). If one wishes to continue this simulation, sander will need to know that the target temperatures have changed. Since the target temperature is normally specified in the mdin file (using `temp0`), the previous mdin files would all need to be modified to reflect changes in target temperature of each replica. In order to simplify this process, the program will write the current target temperature as additional information in the restart files during an REMD simulation. When an REMD simulation is started, the program will check to see if the target temperature is present in the restart file. If it is present, this value will override the target temperature specified using `temp0` in the mdin file. In this manner, one can restart the simulation from the set of restart files and the program will automatically update the target temperature of each replica to correspond to the final target temperature from the previous run. If the target temperature is not present (as would be the case for the first REMD run), the correct values should be present in the mdin files.

### 4.7.3. Content of the output files

As noted above, the current implementation of REMD restores the normal behavior of output and info (MDOUT and MDINFO) files. Again, it is important to note that in the current implementation of REMD *all output is currently BY REPLICA ONLY, NOT BY TEMPERATURE!* This is equivalent to the `repcrd &cntrl` namelist variable being set to 1. Setting `repcrd = 0` currently has no effect and will generate a warning message in the output file. To facilitate post processing of trajectory data by temperature, a header line is written to each frame just before the coordinates. This header line has the format:

```
REMD <replica#> <exchange#> <step#> <Temperature>
```

PTRAJ will be able to read trajectories with this new format.

One thing that has changed from Amber 11 is that the following output is no longer contained in the mdout files by default:

```
=====REMD EXCHANGE CALCULATION=====
Exch= 5 RREMD= 0
Replica Temp= 386.40 Indx= 2 Rep#= 1 EPot= -1518.88
Partner Temp= 393.50 Indx= 3 Rep#= 3 EPot= -1485.53
Metrop= 0.456848E+00 delta= 0.783404E+00 o_scaling= 0.99
Rand= 0.191995E+00 MyScaling= 1.01 Success= T
```

## 4.7. Replica Exchange Molecular Dynamics (REMD)

=====END REMD EXCHANGE CALCULATION=====

This has been disabled because for very frequent exchange attempts, which has been shown to improve Temperature space mixing, the mdout files quickly become very large, and the frequent output slows down the calculation. Furthermore, this section does not provide more valuable information than that found in the remlog file. If you wish to force printing of this section in the output files, you must recompile sander.MPI after setting the environment variable *AMBERBUILDFLAGS* to *-DVERBOSE\_REMD*.

### 4.7.4. Major changes from sander when using replica exchange

Within an MPI job, as discussed above, it is now possible to run multiple sander jobs at once, such that each job gets a subset of the total processors. To run multisander and replica exchange, there are three command-line arguments:

- ng** specifies the number of sander runs (replicas) to perform concurrently. Note that at present, the number of replicas must be a divisor of the total number of processors (specified by the MPI run command). The input and output file information must be provided in a groupfile (as described earlier in this section).
- rem** specifies the type of replica exchange simulation. Only two options are currently available. 0, no replica exchange (standard MD) (default behavior if -rem is not specified on command line); 1, regular replica exchange (requires -ng). 3, Hamiltonian replica exchange (requires -ng)
- remlog** specifies the filename of a log file. This file records from left to right, for every replica and every exchange attempt, the velocity scaling factor (negative if the exchange attempt failed), current actual temperature, current potential energy, current target temperature, and the new target temperature. The default value is *rem.log*.
- remtype** specifies a filename for the remtype file; this file provides helpful information about the current replica run. For reservoir REMD runs it also prints reservoir information. Default is "rem.type"

Next, there are new variables in the &cntrl namelist:

- repcrd      This variable is temporarily disabled.
- numexchg   The number of exchange attempts, default 0.
- nstlim      the number of MD steps \*between exchange attempts\*. Note that NSTLIM is not a new variable for REMD, but the meaning is somewhat different. The total length of the REMD simulation will be nstlim\*numexchg steps long.

### 4.7.5. Cautions when using replica exchange

While many variations of replica exchange have been tested with sander, all possible variations have not been tested and the option is intended for use by advanced researchers that

#### 4. Sampling and free energies

already have a comprehensive understanding of standard molecular dynamics simulations. Caution should be used when creating REMD input files. Amber will check for the most obvious errors but due to the nature of the multiple output files the reason for the error may not be readily apparent. The following is only a subset of things that users should keep in mind:

1. The number of replicas must be an even number (so that all replicas have a partner for exchange).
2. Temp0 values for each replica must be unique.
3. Other than temp0, mdin files should normally be identical.
4. Temp0 values should not be changed in the nmropt=1 weight change section.
5. As of Amber 10 the value of irect does not have to be 1. If irect is 1, the replica temperatures will be read from the restart files. If irect is 0, the replica temperatures will be read from the input files. This means that it is no longer necessary for inpcrd files to have velocities.
6. A groupfile is required (this was not the case in Amber 8).
7. If high temperatures are used, it may be necessary to use a smaller time step and possibly restraints to prevent cis/trans isomerization or chirality inversion.
8. Due to increased diffusion rates at high temperature, it may be good to use iwrap=1 to prevent coordinates from becoming too large to fit in the restart format.
9. Note that the optimal temperature range and spacing will depend on the system. The user is strongly recommended to read the literature in this area.
10. Constant pressure is not supported for REMD simulations. This means NTB must be 0 or 1.

#### 4.7.6. Replica exchange example

Below is an example of an 8-replica REMD run on 16 processors, assuming that relevant environment variables have been properly set.

```
$MPIRUN -np 16 sander.MPI -ng 8 -groupfile groupfile
```

Here is the groupfile:

```
#  
# multisander or replica exchange group file  
#  
-O -rem 1 -i mdin.rep1 -o mdout.rep1 -c inpcrd.rep1 -r restrt.rep1 -x mdcrd.rep1  
-O -rem 1 -i mdin.rep2 -o mdout.rep2 -c inpcrd.rep2 -r restrt.rep2 -x mdcrd.rep2  
-O -rem 1 -i mdin.rep3 -o mdout.rep3 -c inpcrd.rep3 -r restrt.rep3 -x mdcrd.rep3  
-O -rem 1 -i mdin.rep4 -o mdout.rep4 -c inpcrd.rep4 -r restrt.rep4 -x mdcrd.rep4  
-O -rem 1 -i mdin.rep5 -o mdout.rep5 -c inpcrd.rep5 -r restrt.rep5 -x mdcrd.rep5
```



#### 4.7. Replica Exchange Molecular Dynamics (REMD)

```
-O -rem 1 -i mdin.rep6 -o mdout.rep6 -c inpcrd.rep6 -r restrt.rep6 -x mdcrd.rep6
-O -rem 1 -i mdin.rep7 -o mdout.rep7 -c inpcrd.rep7 -r restrt.rep7 -x mdcrd.rep7
-O -rem 1 -i mdin.rep8 -o mdout.rep8 -c inpcrd.rep8 -r restrt.rep8 -x mdcrd.rep8
```

This input specifies that REMD should be used (-rem 1), with 8 replicas (-ng 8) and 2 processors per replica (-np 16). Note that the total number of processors should always be a multiple of the number of replicas.

Here is a section of a sample rem.log file produced by Amber:

```
# replica exchange log file
# Replica #, Velocity Scaling, T, Eptot, Temp0, NewTemp0, Success rate (i,i+1)
# exchange 1
1 1.46 0.00 -541.20 269.50 570.90 0.00
2 1.06 0.00 -541.20 300.00 334.00 2.00
3 0.95 0.00 -541.20 334.00 300.00 0.00
4 1.06 0.00 -541.20 371.80 413.90 2.00
5 0.95 0.00 -541.20 413.90 371.80 0.00
6 1.06 0.00 -541.20 460.70 512.90 2.00
7 0.95 0.00 -541.20 512.90 460.70 0.00
8 0.69 0.00 -541.20 570.90 269.50 2.00
# exchange 2
1 -1.00 0.00 -491.39 570.90 570.90 1.00
2 -1.00 0.00 -547.98 334.00 334.00 0.00
3 -1.00 0.00 -553.87 300.00 300.00 1.00
4 -1.00 0.00 -518.92 413.90 413.90 0.00
5 -1.00 0.00 -538.17 371.80 371.80 1.00
6 -1.00 0.00 -494.00 512.90 512.90 0.00
7 -1.00 0.00 -498.12 460.70 460.70 1.00
8 -1.00 0.00 -567.18 269.50 269.50 0.00
# exchange 3
1 -1.00 0.00 -462.14 570.90 570.90 0.67
2 0.95 0.00 -539.83 334.00 300.00 0.00
3 1.06 0.00 -537.76 300.00 334.00 1.33
4 -1.00 0.00 -510.33 413.90 413.90 0.00
5 -1.00 0.00 -540.74 371.80 371.80 0.67
6 -1.00 0.00 -491.99 512.90 512.90 0.00
7 -1.00 0.00 -522.01 460.70 460.70 0.67
8 -1.00 0.00 -568.87 269.50 269.50 0.00
```

Note that a section of the log file is written for each exchange attempt. For each exchange, the log contains a line for each replica. This line lists the replica number, the velocity scaling factor, the actual instantaneous temperature, the potential energy, the old and new target temperatures, and the current overall success rate for exchange between this temperature and the next higher temperature. Note that the velocity scaling factor will be -1.0 if the exchange was not successful. In that case, the old and new target temperatures will be identical.

In this particular example, all of the inpcrd files were identical, and thus the potential energies listed for exchange 1 are identical. For this reason, all of the exchanges are successful. After

#### 4. Sampling and free energies

this exchange, MD is performed for `nstlim` steps, and so the potential energies are no longer identical at exchange #2.

Note that the exchange success rate may be larger than 1.0 during the first few attempts, since each particular pair is considered only every other attempt. The success rate is the number of accepted exchanges for the pair divided by the total number of exchange attempts, multiplied by 2 to account for the alternating neighbors.

##### 4.7.7. Replica exchange using a hybrid solvent model

This section describes an advanced feature of Amber that is currently under development.[62, 63] Users that are not already comfortable with standard replica exchange simulations should likely get more experience with them before attempting hybrid solvent REMD calculations.

For large systems, REMD becomes intractable since the number of replicas needed to span a given temperature range increases roughly with the square root of the number of degrees of freedom in the system. Recognizing that the main difficulty in applying REMD with explicit solvent lies in the number of simulations required, rather than just the complexity of each simulation, we recently developed a new approach in which each replica is simulated in explicit solvent using standard methods such as periodic boundary conditions and inclusion of long-range electrostatic interactions using PME. However, the calculation of exchange probabilities (which determines the temperature spacing and thus the number of replicas) is handled differently. Only a subset of closest water molecules is retained, with the remainder temporarily replaced by a continuum representation. The energy is calculated using the hybrid model, and the exchange probability is determined. The original solvent coordinates are then restored and the simulation proceeds as a continuous trajectory with fully explicit solvation. This way the perceived system size for evaluation of exchange probability is dramatically reduced and fewer replicas are needed.

An important difference from existing hybrid solvent models is that the system is fully solvated throughout the entire MD simulation, and thus the distribution functions and solvent properties should not be affected by the use of the hybrid model in the exchange calculation. In addition, no restraints of any type are needed for the solvent, and the solute shape and volume may change since the solvation shells are generated for each replica on the fly at every exchange calculation. Nearly no computational overhead is involved since the calculation is performed infrequently as compared to the normal force evaluations. Thus the hybrid REMD approach can employ more accurate continuum models that are too computationally demanding for use in each time step of a standard molecular dynamics simulation. However, since the Hamiltonian used for the exchange differs from that employed during dynamics, these simulations are approximate and are not guaranteed to provide correct canonical ensembles.

At each exchange calculation `sander` will create the hybrid system based on the current coordinates for the fully solvated system. This is done by calculating the distance of each water oxygen to the nearest solute atom, and sorting the water by increasing shortest distance. The closest `numwatkeep` are retained and the potential energy is calculated using the GB model specified by `hybridgb`. After the energy calculation the fully solvated system is restored.

For a more complete example, users are directed to the hybridREMD test case (in the `rem_hybrid` subdirectory) in the Amber test directory.

#### 4.7. Replica Exchange Molecular Dynamics (REMD)

- numwatkeep** The number of explicit waters that should be retained for the calculation of potential energy to be used for the exchange calculation. Before each exchange attempt, the closest *numwatkeep* waters will be retained (closest to the solute) and the rest will be temporarily removed and then replaced after the exchange probability has been calculated. The default value is -1, indicating that all waters should be retained (standard REMD). A value of 0 would direct Amber to remove all of the explicit water (as in MM-PBSA) while a non-zero value will result in some water close to the solute being retained while the rest is removed. Currently it is not possible to select a subset of solute atoms for determining which waters are "close". Determining the optimal *numwatkeep* value is a topic of current research.
- hybridgb** Specifies which GB model should be used for calculating the PE of the stripped coordinates, equivalent to the *igb* variable. Currently only *hybridgb* values of 1, 2, and 5 are supported.

**Cautions:** This option has not been extensively tested. The following would not be expected to work without further modification of the code:

1. Only the water is imaged for the creation of the stripped system. Care should be taken with dimers (such as DNA duplexes) to ensure that the imaging is correct.
2. Explicit counterions should probably not be used.
3. The choice of implicit solvent model will likely have a large effect on the resulting ensemble.

##### 4.7.8. Reservoir REMD

The ability to perform REMD with a structure reservoir [155, 156] has been implemented in Amber as of version 10. Although REMD can significantly increase the efficiency of conformational sampling, obtaining converged data can still be challenging. This is particularly true for larger systems, as the number of replicas needed to span a given temperature range increases with the square root of the number of degrees of freedom in the system. Another consideration is that the folding rate of a peptide tends not to be as dependent on temperature as the unfolding rate, making the search for native peptide structures in higher temperature replicas more problematic; in the case where a native-like structure is found it will almost always be exchanged to a lower temperature replica, requiring a repeat of the search process. In addition, the exchange criterion in REMD assumes a Boltzmann-weighted ensemble of structures, which is typically not the case at the start of a REMD simulation. Although the exchange criterion will eventually drive each replica toward a Boltzmann-weighted ensemble of structures, this essentially means that until all of the replicas are converged, none of the replicas are converged.

Reservoir REMD is a method which can significantly enhance the rate of convergence and reduce the high computational expense of standard REMD simulations. An ensemble of structures (or reservoir) is generated at high temperature, then linked to lower temperatures via REMD. Periodic exchanges are attempted between randomly chosen structures in the reservoir and the highest temperature replica. If the structure reservoir is already Boltzmann-weighted, [155] convergence is significantly enhanced as the lower temperature replicas simply act to re-weight the

#### 4. Sampling and free energies

reservoir ensemble - in essence all of the searching has been accomplished from the start. This is in contrast to standard REMD where all the replicas are run simultaneously, and the computational expense for running long simulations must be paid for each of the replicas even though only a few high-temperature ones may be contributing to sampling of new basins.

One major advantage of this approach is that a converged ensemble of conformations needs to be generated only once and only for one temperature. Typically this temperature should be high enough to facilitate crossing of energy barriers, but low enough that there is still a measureable fraction of native structure present. Another advantage is that exchanges with the reservoir do not need to be time-correlated with the replica simulations; folding events sampled during reservoir generation can provide multiple native structures for the other replicas.

It may not always be possible however to generate a Boltzmann-weighted ensemble of structures (e.g. for a large molecule in explicit solvent). In such cases it is possible to use a non-Boltzmann weighted reservoir by modifying only the exchange criterion between the reservoir and the highest temperature replica (see Ref. ? for further details). If the weight of all structures in the reservoir is set to 1, this corresponds to a completely flat distribution across the free energy landscape. Alternatively, weights can be assigned to structures based on various structural properties. In the current implementation, weights are assigned to structures via dihedral bin clustering, wherein clusters are identified by unique configurations of user-defined dihedral angles.

There are several new command line arguments that pertain to Reservoir REMD:

**-rremd** Type of reservoir to use.

= 0 No reservoir (Default)

= 1 Boltzmann-weighted reservoir

= 2 Non-Boltzmann weighted reservoir where the weight of each structure in the reservoir is assumed to be 1/N

= 3 Non-Boltzmann weighted reservoir with weights defined by dihedral angle binning.

**-reservoir** Specifies the file name prefix for reservoir structures. Reservoir structure files should be in the restart file format *MDRESTRT*, and are expected to be named according to the format <name>.XXXXXX, where XXXXXX is a 6 digit integer, e.g. frame.000001. Default is "reserv/frame". **IMPORTANT NOTE:** Structure numbering should begin at 1.

**-saveene** specifies the file containing energies of the structures in the reservoir (default filename is "saveene"). This file must contain a header line with format:

```
<# reservoir structures> <reservoir T> <#atoms>  
<random seed> <velocity flag>
```

If the velocity flag =1 then velocity information will be read from the reservoir structure files, otherwise (if velocity flag =0) velocities will be assigned to the structure based on the reservoir temperature. After the header line there should be a line containing the potential energy of each reservoir structure. **IMPORTANT NOTE:** For reservoir REMD with dihedral bin clustering (rremd==3) each potential energy should be followed by the cluster # that reservoir structure belongs to.

**-clusterinfo** For reservoir REMD with dihedral bin clustering (`rremd==3`) this file specifies what dihedrals are used and the bin size, as well as what cluster each reservoir structure belongs to. Default is "cluster.info". File has the following format:

```
<# Dihedral Angles>
<atom# 1> <atom# 2> <atom# 3> <atom# 4> [Dihedral 1]
. .
. .
. .
<atom# 1> <atom# 2> <atom# 3>
<atom# 4> [# Dihedral Angles]
<Total # Clusters>
<Cluster #> <Weight>
<Bin1><Bin2>...<Bin #Dihedral Angles> [Cluster 1]
. .
. .
. .
<Cluster #> <Weight>
<Bin1><Bin2>...<Bin #Dihedral Angles> [# Clusters]
```

The first line is the number of dihedral angles that will be binned, following the definition of those dihedral angles (4 atoms using sander atom #s, starting from 1) and the bin size for each dihedral angle. Next is the total # of clusters followed by lines providing information about each cluster: the cluster number, weight and ID as defined by dihedral binning. The ID is composed of consecutive 3 digit integers, 1 for each dihedral angle. For example, a structure belonging to cluster 7 with a weight of 2 with 2 dihedral angles that fall in bins 3 and 8 would look like:

```
7 2 003008
```

#### 4.7.9. Hamiltonian replica exchange

Instead of spacing replicas throughout temperature space, you can also space replicas throughout "Hamiltonian space." That is, every replica has a different Hamiltonian, or energy function, and exchange attempts occur between adjacent Hamiltonians. There are a number of ways of carrying out these exchange attempts, and each one has a different exchange success probability. With *sander* and *pmemd*, Hamiltonian replica exchange is enabled with using `-rem 3` on the command-lines in the groupfile. The code was initially written by Yilin Meng and was integrated into *sander* and *pmemd* by Jason Swails and Danial Dashti from the research group of Adrian Roitberg.

This exchange attempt is performed by exchanging coordinates, leading to the detailed balance equation

$$P_{i \rightarrow j} = \min\{1, \exp(-\beta_1 [H_1(x_2) - H_1(x_1)] - \beta_2 [H_2(x_1) - H_2(x_2)])\} \quad (4.9)$$

Here, state  $i$  refers to the combination  $[\beta_1 H_1(x_1), \beta_2 H_2(x_2)]$  and state  $j$  refers to the combination  $[\beta_1 H_1(x_2), \beta_2 H_2(x_1)]$ . This equation assumes that only coordinates are traded between

## 4. Sampling and free energies

exchanging replicas, and allows for the temperatures to differ, but the temperature does not exchange upon a successful attempt. Because the temperature does not exchange, velocities are never scaled after a successful exchange attempt like they are with T-REMD.

### 4.7.9.1. Free Energy Perturbation

Upon closer inspection of 4.9, we can see a close resemblance to Free Energy Perturbation[157, 158]

$$\Delta G_{a \rightarrow b} = -K_B T \ln [\exp(-\beta(E_b - E_a))] \quad (4.10)$$

We can see that for every exchange attempt, the required  $\Delta E$  is calculated in both directions. The value for the free energy (in both directions) is accumulated and reported in the `rem.log` file each time an exchange is attempted.

For replica exchange free energy perturbation (REFEP), multiple topology files are often needed that correspond to a value of an alchemical parameter,  $\lambda$ , similar to thermodynamic integration. The ParmEd program included with AmberTools can be used to generate the intermediate topology files by scaling charges and/or van der Waals parameters. In this case, because coordinates are exchanged, each replica tracks a particular Hamiltonian and set of control variables, rather than a sequence of configurations. Note this is the opposite behavior of T-REMD in which replicas change temperatures but keep the same sequence of configurations.

### 4.7.9.2. Umbrella Sampling

Hamiltonian exchange can be used to perform replica exchange umbrella sampling [159] using the NMR flat well restraints. In this case, every line of the group file needs a different restraint file in which the center of the biasing umbrella changes. In this case, each replica tracks a particular umbrella location rather than a sequence of configurations. Note this is the opposite behavior of T-REMD in which replicas change temperatures but keep the same sequence of configurations.

### 4.7.9.3. Steps for running H-REMD simulations

Note: before running Hamiltonian replica exchange (H-REMD), you should be familiar with Temperature replica exchange (T-REMD) simulations. H-REMD simulations are set up similarly to T-REMD simulations. Each replica is specified on a line of a groupfile and is run with *multisander*. Each replica differs either by simulation control parameters in the input file (e.g. for constant pH replica exchange [160, 161] or umbrella sampling replica exchange[159]) or parameters in the topology file (e.g. REFEP).

- The majority of HREMD settings are similar to regular Replica Exchange MD (i.e., TREMD). A groupfile is needed. The number of replicas must be an even number (so that all replicas have a partner for exchange). Constant pressure is not supported for REMD simulations. This means NTB must be 0 or 1.
- Depending on the type of HREMD, all replicas may have different/similar force fields/-control variables

#### 4.7. Replica Exchange Molecular Dynamics (REMD)

- The order of the replicas in the groupfile is very important. As a general rule in all HREMD simulations, the least different Hamiltonians (replicas) should be neighbors. Because this method is relatively new, there are very limited discussions in the literature about the optimum positions of replicas in the Hamiltonian ladder [162, 163]. Exchange neighbors are defined by adjacent lines in the groupfile (i.e., each replica exchanges 'left' or 'up' with the replica defined by the line above and exchanges 'right' or 'down' with the replica defined by the line below in the groupfile).
- For editing the prmtop, e.g., in the case of FEREP, there is a python script in AmberTools, *parmed.py*, which facilitates the modifications of amber topology files. See the *AmberTools 12 Manual* for details.
- Although, the implementations of H-REMD in *sander* and *pmemd* are slightly different, the settings, format of outputs, and results are the same.
- In H-REMD, each replica has a different Hamiltonian. In contrast to T-REMD, neighbor replicas exchange their conformations, which means each replica keeps its initial Hamiltonian and there is no need for post-processing (i.e., using *ptraj* or *cpptraj*).

To enable H-REMD the *-rem* flag on the command-line or on each line of the groupfile must be given the value 3 (i.e., *-rem 3*). Like T-REMD, each H-REMD simulation takes the same input files (for constant pH REMD, you must also supply a *cpin* file) and provides the same output files, including REMD information found in the *rem.log* file.

The output printed in the remlog file differs significantly from that found in the remlog file for T-REMD. Example remlog output for H-REMD is shown below:

```
# Replica Exchange log file
# numexchg is 10000
# REMD filenames:
#  remlog= remlog
#  remtype= rem.type
# Rep#, Neibr#, Temp0, PotE(x_1), PotE(x_2), left_fe, right_fe, Success, Success rat
# exchange      1
   1   8   300.00 -12783.23 -12755.40   -16.39    0.00    F    0.00
   2   3   300.00 -12839.84 -12802.56    0.00   -0.05    T    2.00
   3   2   300.00 -12802.60 -12839.79   -0.04    0.00    T    0.00
   4   5   300.00 -12847.41 -12858.37    0.00   -0.78    F    0.00
   5   4   300.00 -12858.19 -12846.63    0.18    0.00    F    0.00
   6   7   300.00 -12859.65 -12833.42    0.00    0.30    T    2.00
   7   6   300.00 -12833.63 -12859.95   -0.21    0.00    T    0.00
   8   1   300.00 -12771.63 -12766.84    0.00   -16.23    F    0.00
# exchange      2
   1   2   300.00 -12825.03 -13147.73    0.00   -0.62    F    0.00
   2   1   300.00 -13148.20 -12824.42   -0.47    0.00    F    1.00
   3   4   300.00 -13136.97 -12823.77    0.00    0.62    T    1.00
   4   3   300.00 -12823.32 -13137.59    0.44    0.00    T    0.00
   5   6   300.00 -12919.25 -13181.18    0.00   -0.41    T    1.00
```

#### 4. Sampling and free energies

6	5	300.00	-13180.48	-12918.84	0.70	0.00	T	1.00
7	8	300.00	-13162.39	-12775.37	0.00	0.16	T	1.00
8	7	300.00	-12775.59	-13162.55	-0.22	0.00	T	0.00

...

The columns, in order, are the replica number, the exchange partner for this attempt, the target temperature, the potential energy of the current structure, the potential energy of the proposed structure, the free energy difference calculated via 4.10 for all exchanges to the 'left' (or 'up' in the Hamiltonian ladder), all free energies for exchanges to the 'right' (or 'down' in the Hamiltonian ladder), whether the exchange attempt succeeded (T) or not (F), and the average success rate. For each step, the only free energy values printed are those between replicas that attempted to exchange. All free energies between non-exchanging pairs are set to 0 for that step. Therefore, the 'final' free energies can be found by summing the respective terms from the last two exchanges in the *remlog* file.

##### 4.7.9.4. An example

When running H-REMD, the format of the groupfile is very similar to that in T-REMD, but specific details depend on the type of simulation being performed. In the case of REFEP, the *groupfile* may look like the following:

```
-O -rem 3 -i FEPRE.mdin -o mdout.rep0 -c inpcrd.rep0 -r restrt.rep0 -x mdcrd.rep0
-O -rem 3 -i FEPRE.mdin -o mdout.rep1 -c inpcrd.rep1 -r restrt.rep1 -x mdcrd.rep1
-O -rem 3 -i FEPRE.mdin -o mdout.rep2 -c inpcrd.rep2 -r restrt.rep2 -x mdcrd.rep2
-O -rem 3 -i FEPRE.mdin -o mdout.rep3 -c inpcrd.rep3 -r restrt.rep3 -x mdcrd.rep3
-O -rem 3 -i FEPRE.mdin -o mdout.rep4 -c inpcrd.rep4 -r restrt.rep4 -x mdcrd.rep4
-O -rem 3 -i FEPRE.mdin -o mdout.rep5 -c inpcrd.rep5 -r restrt.rep5 -x mdcrd.rep5
-O -rem 3 -i FEPRE.mdin -o mdout.rep6 -c inpcrd.rep6 -r restrt.rep6 -x mdcrd.rep6
-O -rem 3 -i FEPRE.mdin -o mdout.rep7 -c inpcrd.rep7 -r restrt.rep7 -x mdcrd.rep7
```

Notice how the topology file differs in each case, but the input file remains the same. An example *groupfile* for umbrella sampling may look like the following:

```
-O -rem 3 -i USRE.mdin.rep0 -o mdout.rep0 -c inpcrd.rep0 -r restrt.rep0 -x mdcrd.rep0
-O -rem 3 -i USRE.mdin.rep1 -o mdout.rep1 -c inpcrd.rep1 -r restrt.rep1 -x mdcrd.rep1
-O -rem 3 -i USRE.mdin.rep2 -o mdout.rep2 -c inpcrd.rep2 -r restrt.rep2 -x mdcrd.rep2
-O -rem 3 -i USRE.mdin.rep3 -o mdout.rep3 -c inpcrd.rep3 -r restrt.rep3 -x mdcrd.rep3
-O -rem 3 -i USRE.mdin.rep4 -o mdout.rep4 -c inpcrd.rep4 -r restrt.rep4 -x mdcrd.rep4
-O -rem 3 -i USRE.mdin.rep5 -o mdout.rep5 -c inpcrd.rep5 -r restrt.rep5 -x mdcrd.rep5
-O -rem 3 -i USRE.mdin.rep6 -o mdout.rep6 -c inpcrd.rep6 -r restrt.rep6 -x mdcrd.rep6
-O -rem 3 -i USRE.mdin.rep7 -o mdout.rep7 -c inpcrd.rep7 -r restrt.rep7 -x mdcrd.rep7
```

Notice in this case how the topology file is the same but the input file differs in each case (which is where the center of the umbrella is defined). Like T-REMD, *sander.MPI* (or *pmemd.MPI*) are executed via the following command:



## 4.7. Replica Exchange Molecular Dynamics (REMD)

```
mpirun -np 16 sander.MPI -ng 8 -groupfile groupfile
```

Note that the particular method for launching an MPI program may depend on your MPI implementation. Also, *pmemd* requires at least 2 threads per replica, whereas *sander* will work with just 1.

### 4.7.10. RXSGLD: Replica exchange using Self-Guided Langevin Dynamics

RXSGLD utilizes the guiding force, *sgft* or *tempsg*, to define replicas. SGLD simulations are performed for replicas. Please refer the SGLD subsection 4.3 about how to set up SGLD simulations. When temperature is the same for all replicas, the replica exchange ratios are high and so is the conformational search efficiency. RXSGLD is an alternative to SGLD or SGLDfp to achieve efficient conformational search while being able to obtain the canonical ensemble distribution. RXSGLD is turned on if *isgld*>0 is set in sander input files when performing replica exchange simulations.

For the convenience of reference, we define replicas as non-interacting identical simulation systems and define stages as simulation conditions between which replicas transit. In REMD, stages are different by temperatures, while in RXSGLD, stages are different by the strength of guiding forces, as defined by *sgld* or *tempsg*. For example, we can set *tempsg*=300, 310, 325, 345, 370, 400, 440, and 500K for stages 1 to 8, respectively, while *temp0*=300K for all stages. In RXSGLD, temperatures in different stages can be same or different from each other, however, it is preferred to keep all temperature the same to achieve high replica exchange efficiency.

Because the temperatures of different stages may be the same, the stages are given a ID from 1 to Nrep. Like REMD, each RXSGLD trajectory file is for each replica. Different from REMD, the frames of RXSGLD trajectories are preceded with the following information:

```
RXSGLD <replica#> <exchange#> <step#> <stage ID>
```

The output from RXSGLD contains the following lines:

```
TEMP0= <temp0> SGFT= <sgft> TEMPSG= <tempsg> STAGE= <stag ID> REPNUM= <rep#> EXCHANG
```

RXSGLD trajectories can be processed with PTRAJ the same way as REMD trajectories, except replace temperatures with stage IDs. For example, to extract the trajectory on stage 1, we can use the following command:

```
ptraj rxsgld.top <<EOF
trajin rxsgld.trj.000 rxsgldtraj rxsgldid 1
trajout rxsgld.trj.stag 1
EOF
```

## 4.8. Adaptively biased MD, steered MD, and umbrella sampling with REMD

### 4.8.1. Overview

The following describes a suite of modules useful for the calculation of the free energy associated with a reaction coordinate  $\sigma(\mathbf{r}_1, \dots, \mathbf{r}_N)$  (which is defined as a smooth function of the atomic positions  $\mathbf{r}_1, \dots, \mathbf{r}_N$ ):

$$f(\xi) = -k_B T \ln \langle \delta[\xi - \sigma(\mathbf{r}_1, \dots, \mathbf{r}_N)] \rangle,$$

(the angular brackets denote an ensemble average,  $k_B$  is the Boltzmann constant and  $T$  is the temperature) that is also frequently referred to as the *potential of mean force*.

Specifically, new frameworks are provided for equilibrium umbrella sampling and steered molecular dynamics that enhance the functionality delivered by earlier implementations (described earlier in this manual), along with a new `Adaptively Biased Molecular Dynamics (ABMD)` method[164] that belongs to the general category of umbrella sampling methods with a time-dependent potential. Such methods were first introduced by Huber, Torda and van Gunsteren (the Local Elevation Method[165]) in the molecular dynamics (MD) context, and by Wang and Landau in the context of Monte Carlo simulations[166]. More recent approaches include the adaptive force bias method[167], and the metadynamics method[168, 169]. All these methods estimate the free energy of a reaction coordinate from an evolving ensemble of realizations, and use that estimate to bias the system dynamics to flatten an effective free energy surface. Collectively, these methods may all be considered to be umbrella sampling methods with an evolving potential.

The `ABMD` method grew out of attempts to speed up and streamline the metadynamics method for free energy calculations with a *controllable* accuracy. It is characterized by a favorable scaling in time, and only a few (two) control parameters. It is formulated in terms of the following equations:

$$m_a \frac{d^2 \mathbf{r}_a}{dt^2} = \mathbf{F}_a + \frac{\partial}{\partial \mathbf{r}_a} U[t|\sigma(\mathbf{r}_1, \dots, \mathbf{r}_N)],$$

$$\frac{\partial U(t|\xi)}{\partial t} = \frac{k_B T}{\tau_F} G[\xi - \sigma(\mathbf{r}_1, \dots, \mathbf{r}_N)],$$

where the first ones represent Newton's equations that govern ordinary MD (temperature and pressure regulation terms are not shown) augmented with an additional force coming from the time dependent biasing potential  $U(t|\xi)$  [ $U(t=0|\xi) = 0$ ], whose time evolution is given by the second equation.  $G(\xi)$  is a positive definite and symmetric kernel, which may be thought of as a smoothed Dirac delta function. For large enough  $\tau_F$  (the flooding timescale) and small enough kernel width, the biasing potential  $U(t|\xi)$  converges towards  $-f(\xi)$  as  $t \rightarrow \infty$ .

Our numerical implementation of the `ABMD` method involves the use of a bi-weight kernel along with the use of cubic B-splines (or products thereof) to discretize the biasing potential  $U(t|\xi)$  w.r.t.  $\xi$ , and an Euler-like scheme for time integration. `ABMD` admits two important extensions, which lead to a more uniform flattening of  $U(t|\xi) + f(\xi)$  due to an improved sampling of the “evolving” canonical distribution. The first extension is identical in spirit to the *multiple*

#### 4.8. Adaptively biased MD, steered MD, and umbrella sampling with REMD

walkers metadynamics [170, 171]. It amounts to carrying out several different MD simulations biased by the same  $U(t|\xi)$ , which evolves via:

$$\frac{\partial U(t|\xi)}{\partial t} = \frac{k_B T}{\tau_F} \sum_{\alpha} G[\xi - \sigma(\mathbf{r}_1^{\alpha}, \dots, \mathbf{r}_N^{\alpha})],$$

where  $\alpha$  labels different MD trajectories. A second extension is to gather several different MD trajectories, each bearing its own biasing potential and, if desired, its own distinct collective variable, into a generalized ensemble for “replica exchange” with modified “exchange” rules[172–174]. Both extensions are advantageous and lead to a more uniform flattening of  $U(t|\xi) + f(\xi)$ .

In order to assess and improve the accuracy of the free energies, the ABMD simulations may need to be followed up with equilibrium umbrella sampling runs, which make use of the biasing potential  $U(t|\xi)$  *as is*. Such a procedure is very much in the spirit of adaptive umbrella sampling. With these runs, one calculates the biased probability density:

$$p^B(\xi) = \langle \delta[\xi - \sigma(\mathbf{r}_1, \dots, \mathbf{r}_N)] \rangle_B.$$

The idea here is that if, as a result of an ABMD run,  $f(\xi) + U(t|\xi) = 0$  exactly, then the biased probability density  $p^B(\xi)$  would be flat (constant). In practice, this is typically not the case, but one can use  $p^B(\xi)$  to “correct” the free energy via:

$$f(\xi) = -U(\xi) - k_B T \ln p^B(\xi).$$

This procedure has previously been successfully used to calculate accurate free energy maps for a number of molecules including several short peptides.

If you find any of these modules useful, we would ask you to kindly consider quoting the following paper: V. Babin, C. Roland, and C. Sagui, “*Adaptively biased molecular dynamics for free energy calculations*”, J. Chem. Phys. **128**, 134101 (2008).

##### 4.8.2. Reaction Coordinates

A reaction coordinate is defined in the `variable` section (see Fig. 4.1). This section must contain a `type` keyword along with a value of type `STRING` and a list of integers `i` (the number of integers vary depending on the variable type). For some types of reaction coordinates the `variable` section must also contain a list of real numbers, `r`, whose length depends on the specific type.

The following reaction coordinates are currently implemented<sup>1</sup>:

- `type = DISTANCE` : distance (in Å) between two atoms whose indexes are read from the list `i`.
- `type = LCOD` : linear combination of distances (in Å) between pairs of atoms listed in `i` with the coefficients read from `r` list. For example, `i = (1, 2, 3, 4)` and `r = (1.0, -1.0)` define the difference between 1-2 and 3-4 distances.

<sup>1</sup>It is really easy to program another one, if desired.

#### 4. Sampling and free energies

```
1 variable
2   type = STRING
3   i = (i1, i2, ..., iN)
4   r = (r1, r2, ..., rM)
5 end variable
```

Figure 4.1.: Syntax of reaction coordinate definition: *type* is a *STRING*, *i* is a list of integer numbers and *r* is a list of real numbers.

- *type* = ANGLE : angle (in radians) between the lines joining atoms with indexes *i*<sub>1</sub> and *i*<sub>2</sub> and atoms with indexes *i*<sub>2</sub> and *i*<sub>3</sub>.
- *type* = TORSION : dihedral angle (in radians) formed by atoms with indexes *i*<sub>1</sub>, *i*<sub>2</sub>, *i*<sub>3</sub> and *i*<sub>4</sub>.
- *type* = COS\_OF\_DIHEDRAL : sum of cosines of dihedral angles formed by atoms with indexes in the list *i*. The number of atoms must be a multiple of four.
- *type* = R\_OF\_GYRATION : radius of gyration (in Å) of atoms with indexes given in the *i* list (mass weighted).

```
1 variable
2   type = MULTI_RMSD
3   i = (1, 2, 3, 4, 0, 3, 4, 5, 0) ! the last zero is optional
4   r = (1.0, 1.0, 1.0, 1.0, ! group #1, atom 1
5       2.0, 2.0, 2.0, 2.0, ! group #1, atom 2
6       3.0, 3.0, 3.0, 3.0, ! group #1, atom 3
7       4.0, 4.0, 4.0, 4.0, ! group #1, atom 4
8       23.0, 23.0, 23.0, ! group #2, atom 3
9       4.0, 4.0, 4.0, ! group #2, atom 4
10      5.0, 5.0, 5.0) ! group #2, atom 5
11 end variable
```

Figure 4.2.: An example of *MULTI\_RMSD* variable definition.

- *type* = MULTI\_RMSD : RMS (in Å, mass weighted) of RMSDs of several groups of atoms w.r.t. reference positions provided in the *r* list. The *i* list is interpreted as a list of indexes of participating atoms. Zeros separate the groups. An atom may enter several groups simultaneously. The *r* array is expected to contain the reference positions (without zero sentinels). The implementation uses the method (and the code) introduced in Ref.[175]. An example of variable of this type is presented in Fig. 4.2. Two groups are defined here: one comprises the atoms with indexes 1, 2, 3, 4 (line 3 in Fig. 4.2, numbers prior to the first zero) and another one of atoms with indexes 3, 4, 5. The code will first compute the (mass weighted) RMSD ( $R_1$ ) of atoms belonging to the first group w.r.t. reference

#### 4.8. Adaptively biased MD, steered MD, and umbrella sampling with REMD

coordinates provided in the  $\mathbf{r}$  array (first  $12 = 4 \times 3$  real numbers of it; lines 4, 5, 6, 7 in Fig. 4.2). Next, the (mass weighted) RMSD ( $R_2$ ) of atoms of the second group w.r.t. the corresponding reference coordinates (last  $9 = 3 \times 3$  elements of the  $\mathbf{r}$  array in Fig. 4.2) will be computed. Finally, the code will compute the value of the variable as follows:

$$\text{value} = \sqrt{\frac{M_1}{M_1 + M_2} R_1^2 + \frac{M_2}{M_1 + M_2} R_2^2},$$

where  $M_1$  and  $M_2$  are the total masses of atoms in the corresponding groups.

- `ttype = N_OF_BONDS :`

$$\text{value} = \sum_p \frac{1 - (r_p/r_0)^6}{1 - (r_p/r_0)^{12}},$$

where the sum runs over pairs of atoms  $p$ ,  $r_p$  denotes distance between the atoms of pair  $p$  and  $r_0$  is a parameter measured in Å. The  $\mathbf{r}$  array must contain exactly one element that is interpreted as  $r_0$ . The  $\mathbf{i}$  array is expected to contain pairs of indexes of participating atoms. For example, if 1 and 2 are the indexes of Oxygen atoms and 3, 4, 5 are the indexes of Hydrogen atoms and one intends to count all possible O-H bonds, the  $\mathbf{i}$  list must be (1, 3, 1, 4, 1, 5, 2, 3, 2, 4, 2, 5), that is, it must explicitly list all the pairs to be counted.

- `ttype = HANDEDNESS :`

$$\text{value} = \sum_a \frac{\mathbf{u}_{a,3} \cdot [\mathbf{u}_{a,1} \times \mathbf{u}_{a,2}]}{|\mathbf{u}_{a,1}| |\mathbf{u}_{a,2}| |\mathbf{u}_{a,3}|},$$

where

$$\begin{aligned} \mathbf{u}_{a,1} &= \mathbf{r}_{a+1} - \mathbf{r}_a \\ \mathbf{u}_{a,2} &= \mathbf{r}_{a+3} - \mathbf{r}_{a+2} \\ \mathbf{u}_{a,3} &= (1-w)(\mathbf{r}_{a+2} - \mathbf{r}_{a+1}) + w(\mathbf{r}_{a+3} - \mathbf{r}_a), \end{aligned}$$

and  $\mathbf{r}_a$  denote the positions of participating atoms. The  $\mathbf{i}$  array is supposed to contain indexes of the atoms and the  $\mathbf{r}$  array may provide the value of  $w$  ( $0 \leq w \leq 1$ , the default is zero).

- `ttype = N_OF_STRUCTURES :`

$$\text{value} = \sum_g \frac{1 - (R_g/R_{0,g})^6}{1 - (R_g/R_{0,g})^{12}},$$

where the sum runs over groups of atoms,  $R_g$  denotes the RMSD of the group  $g$  w.r.t. some reference coordinates and  $R_{0,g}$  are positive parameters measured in Å. The  $\mathbf{i}$  array is expected to contain indexes of participating atoms with zeros separating different groups. The elements of the  $\mathbf{r}$  array are interpreted as the reference coordinates of the first group

## 4. Sampling and free energies

```
1 variable
2   type = N_OF_STRUCTURES
3   i = (1, 2, 3, 4, 0, 3, 4, 5, 0) ! the last zero is optional
4   r = (1.0, 1.0, 1.0, ! group #1, atom 1
5       2.0, 2.0, 2.0, ! group #1, atom 2
6       3.0, 3.0, 3.0, ! group #1, atom 3
7       4.0, 4.0, 4.0, ! group #1, atom 4
8       1.0,           ! R0 for group #1
9       23.0, 23.0, 23.0, ! group #2, atom 3
10      4.0, 4.0, 4.0, ! group #2, atom 4
11      5.0, 5.0, 5.0, ! group #2, atom 5
12      2.0)           ! R0 for group #2
13 end variable
```

Figure 4.3.: An example of `N_OF_STRUCTURES` variable.

followed by their corresponding  $R_0$ ; then followed by the reference coordinates of the atoms of the second group, followed by the second  $R_0$ , and so forth. To make the presentation clearer, let us consider the example presented in Fig. 4.3. The atomic groups and reference coordinates are the same as the ones shown in Fig. 4.2. Lines 7 and 11 in Fig. 4.3 contain additional entries that set the values of the threshold distances  $R_{0,1}$  and  $R_{0,2}$ . To compute the variable, the code first computes the mass weighted RMSD values  $R_1$  and  $R_2$  for both groups –much like in the `MULTI_RMSD` case– and then combines those in a manner similar to that used in the `N_OF_BONDS` variable.

$$\text{value} = \frac{1 - \left(R_1/R_{0,1}\right)^6}{1 - \left(R_1/R_{0,1}\right)^{12}} + \frac{1 - \left(R_2/R_{0,2}\right)^6}{1 - \left(R_2/R_{0,2}\right)^{12}}.$$

In other words, the variable “counts” the number of structures that match (stay close in RMSD sense) with the reference structures.

### 4.8.3. Steered Molecular Dynamics

The `ncsu_smd` section, if present in the `MDIN` file, activates the steered MD code (the method itself is extensively described in the literature: see for example Ref.[176] and references therein). Apart from the `variable` subsection(s), the following is recognized within this section:

- `output_file` = STRING : sets the output file name.
- `output_freq` = INTEGER : sets the output frequency (in MD steps).

There must be at least one reaction coordinate defined within this section (that is, there must be at least one `variable` subsection in the `ncsu_smd` section). The steered MD code requires that additional entries be present in the `variable` subsections:

## 4.8. Adaptively biased MD, steered MD, and umbrella sampling with REMD

- `path = (REAL|X, REAL|X, ..., REAL|X)` : the steering path whose elements must be either real numbers or letter `x`. The latter will be substituted by the value of the reaction coordinate at the beginning of the run. The path must include at least two elements. There is no upper limit on the number of entries. The elements define Catmull-Rom spline used for steering.
- `harm = (REAL, REAL, ..., REAL)` : this variable specifies the harmonic constant. If a single number is provided, e.g., `harm = (10.0)`, then it is constant throughout the run. If two or more numbers are provided, e.g., `harm = (10.0, 20.0)`, then the harmonic constant follows Catmull-Rom spline built upon the provided values.

An example of `MDIN` file for steered MD is shown in Fig. 4.4. The reaction coordinate here is the distance between 5th and 9th atoms. The spring constant is set constant throughout the run in line 14 and the steering path is configured in line 13 (the letter `x` in this context means “take the value of the variable at the beginning of the run”). The values of the reaction coordinate, harmonic constant and the work performed on the system are requested to be dumped to the `smd.txt` file every 50 MD steps. The way steering paths are constructed is controlled by the `path_mode` and `harm_mode` keywords. In `SPLINE` mode (default) the path is approximated by spline that passes through the given points; in `LINES` mode the path is represented by the line segments joining the control points.

```
1 title line
2 &cntrl
3 ...
4 /
5
6 ncsu_smd
7   output_file = 'smd.txt'
8   output_freq = 50
9
10  variable
11    type = DISTANCE
12    i = (5, 9)
13    path = (x, 3.0) path_mode = LINES
14    harm = (10.0)
15  end variable
16 end ncsu_smd
```

Figure 4.4.: An example `MDIN` file for steered MD. Only the relevant part is shown.

### 4.8.4. Umbrella sampling

To activate the umbrella sampling code, the `ncsu_pmd` section must be present in the `MDIN` file. The `ncsu_pmd` section must contain at least one `variable` subsection. Apart from `variable`, `output_file` and `output_freq` entries are recognized like in the steered MD case

## 4. Sampling and free energies

presented earlier. For umbrella sampling, the `variable` section(s) must contain two additional entries:

- `anchor_position = REAL` : real number that sets the position of the minimum of the umbrella (harmonic) potential.
- `anchor_strength = REAL` : non-negative real number that sets the harmonic constant for the umbrella (harmonic) potential.

An example of an `MDIN` file for an umbrella sampling simulation is shown in Fig. 4.5. The first reaction coordinate here is the angle formed by the lines joining the 5th with 9th and 9th with 15th atoms (line 12). It is to be harmonically restrained near 1.0 *rad* (line 13, `anchor_position` keyword) using the spring of strength 10.0 *kcal/mol/rad*<sup>2</sup> (line 14, `anchor_strength` keyword). The second reaction coordinate requested in Fig. 4.5 is a dihedral angle (`type = TORSION`, line 17) formed by the 1st, 2nd, 3rd and 4th atoms (line 18, the `i` array). It is to be restrained near zero with strength 23.8 *kcal/mol/rad*<sup>2</sup> (lines 19, 20 in Fig. 4.5). The values of the reaction coordinate(s) are to be dumped every 50 `MD` steps to the `pmd.txt` file.

The `NCSU` implementation of umbrella sampling works correctly with the Amber standard replica-exchange MD described earlier in this manual. It assumes, however, that the number and type of reaction coordinate(s) are the same in all replicas. On the other hand, both `anchor_position` and `anchor_strength` may be different for different temperatures. For replica-exchange MD the output files (set by the `output_name` keyword on a per-replica basis) are temperature bound (or `MDIN`-bound, since there is one-to-one temperature-`MDIN` correspondence).

### 4.8.5. Adaptively Biased Molecular Dynamics

The implementation has a very simple and intuitive interface: the code is activated if either an `ncsu_abmd` or an `ncsu_bbmd` section is present in the `MDIN` file (the difference between those “flavors” is purely technical and will become clear later). Unlike in the `ncsu_smd` and `ncsu_pmd` cases, the dimensionality of a reaction coordinate (the number of `variable` subsections in a `ncsu_abmd` or `ncsu_bbmd` section) cannot exceed five (though three is already hardly useful due to statistical reasons).

The following entries are recognized within the `ncsu_abmd` (or `ncsu_bbmd`) section:

- `mode = ANALYSIS | UMBRELLA | FLOODING` : sets the execution mode. In `ANALYSIS` mode the dynamics is not altered. The only effect of this mode is that the value(s) of the reaction coordinate(s) is(are) dumped every `monitor_freq` to `monitor_file`. In `UMBRELLA` mode, biasing potential from the `umbrella_file` is used to bias the simulation ( $\tau_F = \infty$ , biasing potential does not change). In `FLOODING` mode the adaptive biasing is enabled.
- `monitor_file = STRING` : sets the name of the file to which value(s) of reaction coordinate(s) (along with the magnitude of biasing potential in `FLOODING` mode) are dumped.
- `monitor_freq = INTEGER` : the frequency of the output to the `monitor_file`.



```

1 title line
2 &ctrl
3 ...
4 /
5
6 ncsu_pmd
7   output_file = 'pmd.txt'
8   output_freq = 50
9
10  variable ! first
11    type = ANGLE
12    i = (5, 9, 15)
13    anchor_position = 1.0
14    anchor_strength = 10.0
15  end variable
16  variable # second
17    type = TORSION
18    i = (1, 2, 3, 4)
19    anchor_position = 0.0
20    anchor_strength = 23.8
21  end variable
22 end ncsu_pmd

```

Figure 4.5.: An example MDIN file for umbrella sampling (only relevant part is presented in full).

- `timescale = REAL :  $\tau_F$` , the flooding timescale in picoseconds (only required in FLOODING mode).
- `umbrella_file = STRING` : biasing potential file name (the file must exist for the UMBRELLA mode).

In FLOODING mode, the `variable` subsections of the `ncsu_abmd` section must also contain the following entries:

- `min = REAL` : smallest desired value of the reaction coordinate (required, unless the reaction coordinate is limited from below).
- `max = REAL` : largest desired value of the reaction coordinate (required, unless the reaction coordinate is limited from above).
- `resolution = REAL` : the “spatial” resolution for the reaction coordinate.

To access the biasing potential files created in the course of FLOODING simulations, the `ncsu-umbrella-slice` utility is provided (it prints a short description of itself if invoked with `--help` option).

An example MDIN file for the `ncsu_abmd` flavor of ABMD is shown in the Fig. 4.6.

#### 4. Sampling and free energies

```
1 title line
2 &cntrl
3 ...
4 /
5
6 ncsu_abmd
7   mode = FLOODING
8
9   monitor_file = 'abmd.txt'
10  monitor_freq = 33
11
12  umbrella_file = 'umbrella.nc'
13
14  timescale = 100.0 ! in ps
15
16  variable
17    type = DISTANCE
18    i = (5, 9)
19    min = -1.0 max = 10.0 ! min is not needed for DISTANCE
20    resolution = 0.5 ! required for mode = FLOODING
21  end variable
22 end ncsu_abmd
```

Figure 4.6.: An example MDIN file for ABMD (only the relevant part is presented in full).

The reaction coordinate is defined in lines 17, 18 as the distance between the 5th and 9th atoms (more than one reaction coordinates might be requested by mere inclusion of additional `variable` subsections). The `mode` is set to `FLOODING` thus enabling the adaptive biasing with flooding timescale  $\tau_F = 100ps$  (line 14). The region of interest of the reaction coordinate is specified to be between  $-1\text{\AA}$  and  $10\text{\AA}$  (line 19) and the resolution is set to  $0.5\text{\AA}$  (line 20). The lower bound ( $-1\text{\AA}$ ) could have been omitted for `DISTANCE` variable: the default value of zero would be used in such case. The code will try to load the biasing potential from the `umbrella.nc` file (line 12) and use it as the value of  $U(t|\xi)$  at the beginning of the run. The biasing potential built in the course of simulation will be saved to the same file (`umbrella.nc`) every time the `RESTART` file is written. The `ncsu-umbrella-slice` utility can then be used to access its content. An MDIN file for the follow up biased run at equilibrium would look much like the one shown in the Fig. 4.6, but with `mode` changed from `FLOODING` to `UMBRELLA`.

The `ncsu_abmd` code works correctly with replica-exchange (that is, for `-rem` flag set to 1). In such case the monitor and umbrella files are temperature-bound (unlike, e.g., `MDOUT` and `MDCRD` files that require post processing). If number of `sander` groups exceeds one (the flag `-ng` is greater than one) and `-rem` flag is set to zero, the code runs *multiple walkers* ABMD. In both cases the number and type(s) of variable(s) must be the same across all replicas.

Finally, the `ncsu_bbmd` flavor allows one to run replica-exchange (AB)MD with different reaction coordinates and different modes (`ANALYSIS`, `UMBRELLA` or `FLOODING`) in different replicas (along with different temperatures, if desired). To this end, the `-rem` flag must be set to zero and

#### 4.8. Adaptively biased MD, steered MD, and umbrella sampling with REMD

the `ncsu_bbmd` sections must be present in all MDIN files. The MDIN file for the replica of rank zero (first line in the group file) is expected to contain additional information as compared to `ncsu_abmd` case (an example of such MDIN file for replica zero is shown in Fig. 4.7). The MDIN files for all other replicas except zero do not need any additional information, and therefore take the same form as in the `ncsu_abmd` flavor (except that the section name is changed from `ncsu_abmd` to `ncsu_bbmd`, thus activating a slightly different code path). Each MDIN file may define its own reaction coordinates, have different `mode` and temperature if desired.

```
1 title line
2 &cntrl
3 ...
4 /
5
6 ncsu_bbmd
7
8     ! 0th replica only
9
10    exchange_freq = 100 ! try for exchange every 100 steps
11
12    exchange_log_file = 'bbmd.log'
13    exchange_log_freq = 25
14
15    mt19937seed = 123455 ! random generator seed
16    mt19937file = 'mt19937.nc' ! file to store/load the PRG
17
18    ! not specific for 0th replica
19
20    mode = ANALYSIS
21
22    monitorfile = 'bbmd.01.txt' ! it is wise to have different
23                                     ! names in different replicas
24    monitor_freq = 123
25
26    variable
27        type = DISTANCE
28        i = (5, 9)
29    end variable
30 end ncsu_bbmd
```

Figure 4.7.: An example MDIN file for `ncsu_bbmd` flavor of ABMD (only the relevant part is presented in full).

Within the first replica `ncsu_bbmd` section the following additional entries are recognized:

- `exchange_freq = INTEGER` : number of MD steps between the exchange attempts.
- `exchange_log_file = STRING` : the name of the file to which exchange statistics is to be reported.

## 4. Sampling and free energies

- `exchange_log_freq = INTEGER` : frequency of `exchange_log_file` updates.
- `mt19937_seed = INTEGER` : seed for the random generator (Mersenne twister [177]).
- `mt19937_file = STRING` : the name of the file to which the state of the Mersenne twister is dumped periodically (for restarts).

The `MDOUT`, `MDCRD`, `RESTR`, `umbrella_file` and `monitor_file` files are `MDIN`-bound in course of the `ncsu_bbmd`-enabled run. An example that uses this kind of replica exchange is presented in Ref.178.

## 4.9. Nudged elastic band calculations

### 4.9.1. Background

In the nudged elastic band method (NEB),[179, 180] the path for a conformational change is approximated with a series of images of the molecule describing the path. Minimization, with the images at the endpoints fixed in space, of the total system energy provides a minimum energy path. Each image in-between is connected to the previous and next image by "springs" along the path that serve to keep each image from sliding down the energy landscape onto adjacent images. NEB is derived from the plain elastic band method, pioneered by Elber and Karplus,[181] which added the spring forces to the potential of energy surface and minimized the energy of the system. The plain elastic band method found low energy paths, but tended to cut corners in the energy landscape. NEB prevents corner cutting by truncating the spring forces in directions perpendicular to the tangent of the path. Furthermore, the forces from the molecular potential are truncated along the path, so that images remain evenly spaced along the path. This leads to:

$$\begin{aligned}\mathbf{F} &= \mathbf{F}^{\perp} + \mathbf{F}^{\parallel} \\ \mathbf{F}^{\perp} &= -\nabla V(\mathbf{P}) + ((\nabla V(\mathbf{P}) \cdot \boldsymbol{\tau}) \boldsymbol{\tau}) \\ \mathbf{F}^{\parallel} &= [(k_{i+1}|\mathbf{P}_{i+1} - \mathbf{P}_i| - k_i|\mathbf{P}_i - \mathbf{P}_{i-1}|) \cdot \boldsymbol{\tau}] \boldsymbol{\tau}\end{aligned}\tag{4.11}$$

where, if  $N$  is the number of atoms per image,  $\mathbf{F}$  is the force on image  $i$ ,  $\mathbf{P}_i$  is the  $3N$  dimensional position vector of image  $i$ ,  $k_i$  is the spring constant between image  $i - 1$  and image  $i$ ,  $V$  is the potential described by the force field, and  $\boldsymbol{\tau}$  is the  $3N$  dimensional tangent unit vector that describes the path.

The simplest definition of  $\boldsymbol{\tau}$  is:

$$\boldsymbol{\tau} = (\mathbf{P}_i - \mathbf{P}_{i-1})/|\mathbf{P}_i - \mathbf{P}_{i-1}|\tag{4.12}$$

This definition leads to instability in the path caused by kinks that occur where the magnitude of  $\mathbf{F}^{\parallel}$  is much larger than the magnitude of  $\mathbf{F}^{\perp}$ . A more stable tangent definition was derived to prevent kinks in the path that depends upon the energies,  $E$ , of adjacent images.[182] The spring constants can be the same between all images or they can be scaled to move the images closer together in the regions of transition states:[183]

$$\begin{aligned} \text{If } (E_i > E_{ref}) \quad & \text{then} \quad k_i = k_{max} - \Delta k (E_{max} - E_i) / (E_{max} - E_{ref}) \\ & \text{otherwise} \quad k_i = k_{max} - \Delta k \end{aligned} \quad (4.13)$$

Here  $E_{max}$  is the highest energy for an image along the path,  $E_{ref}$  is the energy of the higher energy endpoint, and  $k_{max}$  and  $\Delta k$  are parameters with units of force per length. Because the spring force applies only in directions along the path and because the potential of the energy surface is zeroed along the path, the calculation is relatively insensitive to the magnitude of the spring constants. Care must be taken, however, to select a spring constant that does not result in higher frequency motions than those found in the system of interest.[184] At each step, before calculating the spring forces that compose  $\mathbf{F}^{\parallel}$ , each image's neighbor is rotated and translated onto itself to find the RMSD minimum, based on a subset of the system's atoms which the user can define. In this way, each image remains a continuous MD simulation, and the communication of coordinates can be greatly reduced.

Energy minimization of the path is complicated by the fact that the forces are truncated according to the tangent direction, making it impossible to define a Lagrangian.[184] Conjugate gradient minimization, therefore, cannot be used to find the minimum energy path. An algorithm for quenched molecular dynamics has been used to find the minimum.[180] With this method, the component of the velocity parallel to the force is kept, but perpendicular components are scaled:

$$\begin{aligned} \text{If } (\mathbf{v} \cdot \mathbf{f} > 0) \quad & \text{then} \quad \mathbf{v} = (\mathbf{v} \cdot \mathbf{f}) \mathbf{f} \\ & \text{otherwise} \quad \mathbf{v} = x(\mathbf{v} \cdot \mathbf{f}) \mathbf{f} \end{aligned} \quad (4.14)$$

where  $\mathbf{f}$  is the 3N-dimensional unit force vector,  $\mathbf{v}$  is the 3N-dimensional velocity vector, and  $x$  is a scaling factor less than one. Recently, a super-linear minimization method was described using an adopted basis Newton-Raphson minimizer.[184]

A partial NEB (PNEB) implementation is available, and is the only form of NEB that is currently supported [185]. This implementation allows the NEB method to be applied to a user defined subset of the system of interest. It requires users to define the part of the system to apply NEB force decoupling to, as well as the part of the system to RMS fit neighboring images to, to remove rotational and translational motion. This allows NEB to be used efficiently in large systems where a local transition is desired, or in explicitly solvated systems.

As with the previous implementation of NEB in *sander.MPI* [186], minimization of the system energies along the lowest potential energy path is achieved by simulated annealing. This requires no hypothesis for a starting path, but does require careful judgment of the temperature and length of time required to populate the minimum energy path. The initial coordinates can have multiple copies of the structure superimposed on the start and endpoints. When adjacent structures are superimposed, the tangent,  $\tau$  is 0 in every direction. This case is explicitly handled so that the calculation is stable.

## 4. Sampling and free energies

### 4.9.2. Preparing input files for NEB

The NEB capability is implemented inside *sander.MPI* and uses the multisander functionality. Input *prmtop* and *inpcrd* files for NEB should be generated using *Leap*. For NEB you need as a minimum a *prmtop* for a single image of your molecule and two *inpcrd* files representing each end of the pathway.

The following are some notes for preparing NEB input files:

1. Always check that the *prmtop* files generated for the endpoint coordinates are identical. This can be done by diffing the files. One *prmtop* must be used to describe both endpoints' *inpcrd* files.
2. If you have intermediate structures along the path, you must make sure the *prmtop* is appropriate for this structure as well.
3. The endpoint images serve as coordinate reference points, and the first and last images remain fixed in coordinate and energy space along the path. No simulation is performed on these during NEB optimization, so they must initially be well minimized to prevent the rest of the images from migrating to a local minimum before the conformational transition occurs. Take this into consideration when choosing the number of images to connect along the path.

Multisander requires a groupfile input, where each line of the groupfile is the sander command for each individual image's MD simulation. Multiple copies of each endpoint image are used for the initial simulation. If intermediates are available and the user wishes to include them, they should be added sequentially in between the endpoint conformations in the order in which these structures are thought to appear along the transition path.

Notes for running NEB using multisander:

1. The number of CPUs specified must be a multiple of the number of images. You can run this on a standard desktop computer, but it will generally be more efficient to run it on a minimum of one processor per image.
2. If the user has access to parallel computing resources, multiple processors per image may be used. Careful benchmarking should be done to gauge the best balance between computational efficiency in calculating the dynamics of each image and slowdown caused by communications overhead at each step.

### 4.9.3. Input Variables

- |                  |  |
|------------------|--|
| <i>ineb</i>      | Flag for nudged elastic band. A value of 0 (default) means that no nudged elastic band will be used. A value of 1 means that a NEB simulation is being performed.  |
| <i>tgfitmask</i> | Flag which sets atoms to RMS fit each image's neighbor to itself. This must not include solvent, which, due to diffusion, overlapping proves impossible. The more atoms you choose, the more communication has to be done by each bead. Syntax for this is here: <a href="#">C</a> |

- tgtrmsmask** Flag which sets atoms to decouple NEB forces for PNEB. This can be set to all atoms of the solute, or a subset of atoms which best describes the area of the system which undergoes the conformational change you wish to see. Syntax for this is here: **C**
- skmax** Spring constant or **kmax** from above (100 by default).
- skmin** If **skmin** = **skmax**, a fixed spring constant is used. Otherwise, **skmin** is taken from above for scaled spring constants (50 by default).
- tmode** If 1 (default), use the revised tangent definition that prevents kinks. For any other value, use the simple (original) tangent definition.
- vv** If this is 1, use the quenched velocity Verlet minimization; otherwise, do not.
- vfac** Scaling factor for quenched velocity Verlet algorithm. (0.0 by default).

#### Sample input file for running initial heating along the path.

Below is an example input file that can be used to perform the initial heating step of a NEB run. Note that the input and topology files must be identical for each bead; the names of the output, trajectory, restart and info files should not be the same between beads.

```

Alanine NEB initial MD with small K
&cntrl
  imin = 0, irest = 0,
  ntc=1, ntf=1,
  ntp=1, ntwx=500,
  ntb = 0, cut = 999.0, rgbmax=999.0,
  igb = 1, saltcon=0.2,
  nstlim = 40000, nscm=0,
  dt = 0.0005, ig=42,
  ntt = 3, gamma_ln=1000.0,
  tempi=0.0, temp0=300.0,
  tgfitmask=":1,2,3",
  tgtrmsmask=":1,2,3@N,CA,C",
  ineb = 1, skmin = 10, skmax = 10,
  nmropt=1,
  /
  &wt type='TEMP0', istep1=0, istep2=35000,
  value1=0.0, value2=300.0
  /
  &wt type='END'
  /

```

The important NEB specific lines are shown in boldface type. **tgfitmask** variable denotes the atoms that will be used to RMS fit each bead onto its neighbor images at each step. In this case all atoms of residues 1 2 and 3 are specified. The **tgtrmsmask** variable denotes the atoms

#### 4. Sampling and free energies

that the NEB forces will be applied to. In this case the backbone atoms of residues 1, 2 and 3 are specified. In general, the atoms that have NEB forces applied to them should be those involved in the transition of interest. If the specific transition is not known or there are many degrees of freedom involved in the transition, one can simply specify all solute atoms. It is *not* recommended to apply NEB forces to solvent atoms. For more examples, please refer to the runs in the `$AMBERHOME/test/neb-testcases` directory, or see reference [185].

#### 4.9.4. Important Considerations for NEB Simulations

With the implementation of PNEB, it is important to understand some limitations of the method. Only part of the system is simulated with NEB forces, indicating this part of the system is moving along the minimum potential energy landscape of the transition path. However, the part of the system to which NEB is not applied is not necessarily forced along this minimum potential energy path, and attention must be paid to the convergence of this part of the system. The conformational change in this part of the system is no doubt accelerated, since it responds to the part of the system to which NEB forces are applied. Further equilibration of the system may need to be done if the user wishes to examine changes not local to the area the NEB forces are applied to.

Careful attention must be paid to optimization methods, to assure that conformational space is explored for the NEB part of the system, while the integrity of the non-NEB part remains intact. As in all NEB implementations, a general caveat is that as the system size increases, the degrees of freedom increase and conformational changes become more difficult to quantify. While NEB is a method which does not necessitate a reaction coordinate, care should be taken when analyzing the resulting minimum energy path. It is recommended that NEB be run a statistically relevant number of times so reproducibility (and convergence) of the minimum energy path can be studied.

### 4.10. Accelerated Molecular Dynamics

#### 4.10.1. Background

Many systems of interest in chemistry, physics and biology are characterized by the presence of a number of metastable states separated by large barriers. Correctly sampling these systems is challenging for methods based on Molecular Dynamics, Monte Carlo sampling or any other type of dynamic simulation. For most biological systems of interest, the simulation time is limited to the nanosecond-microsecond time scale, so simple molecular dynamics cannot be used to adequately explore portions of the energy landscape separated by high barriers from the initial minimum. Furthermore, for most biological molecules, the energy landscape has multiple minima or potential energy wells with high free energy barriers, and during a molecular dynamics simulation the system is trapped in one or another local minimum for long periods of simulation time. Consequently, thermodynamics and many other properties of interest for large biological systems cannot be simulated directly because of the nonergodic nature of the present state of the molecular dynamics methodology for systems with high free energy barriers.

AMD is a bias potential introduced by the McCammon group at UCSD [187]. It is a modification to the potential that in practice reduces the height of local barriers, allowing the calcula-



tion to evolve much faster. A number of methods have been suggested to aid this problem, like replica exchange, metadynamics, etc. AMD represents an interesting option as it only requires the evolution of a single copy of the system, plus it doesn't require any previous knowledge of the shape of the potential, i.e. AMD doesn't require information of where are the barriers, saddle points or even what type of configuration changes are expected or necessary to traverse through a particular barrier. Moreover, an interesting feature of AMD is that the shape of the added potential conserves the underlying shape of the real one, such that minima are maintained as minima and barriers are preserved as barriers. In result, adding the AMD potential in practice simply modifies the relation between energy differences, so the distribution of sampling of different structures is still related to the original potential distribution and can be recovered exactly by reweighing.

The AMD modification of the potential is defined by the following equation:

$$V(r)* = V(r) + \Delta V(r) \quad (4.15)$$

$$\Delta V(r) = \frac{(E_p - V(r))^2}{(\alpha P + E_p - V(r))} + \frac{(E_d - V_d(r))^2}{(\alpha D + E_d - V_d(r))} \quad (4.16)$$

where  $V(r)$  is the normal potential and  $V_d(r)$  is the normal torsion potential.  $E_p$  and  $E_d$  are average potential and dihedral energies that serve as a reference energy from which to compare the present position of the calculation and therefore the relationship to the boosting factor to be applied. The terms  $\alpha P$  and  $\alpha D$  are factors that determine inversely the strength with which the boost is applied. For large values of alpha, the potential felt at any point will essentially be the same as the true potential. For values of alpha close to zero, the potential felt becomes constant, in this limit, the sampling becomes a random walk. The amount of boost felt at a particular point in the calculation, therefore, depends on the present value of the potential and dihedral energy, which is in direct correlation to how low in the energy surface the configuration is positioned at that moment. The boosting potential will be proportionally bigger for deeper regions of the potential energy surface, while it will be smaller for higher points, which in result conserves the underlying shape of the potential, as previously mentioned.

AMD has been applied to a vast diversity of interesting problems [188–191]. We have recently applied the implementation of AMD in Amber to the Bovine Pancreatic Trypsin Inhibitor and compared with an unbiased millisecond MD simulation, showing AMD is able to recover the right population distribution and shows excellent agreement with the MD simulation as with experimental data [191].

#### 4.10.2. AMD implementation in Amber

AMD has been implemented in both *sander* and *pmemd* by Romelia Salomon-Ferrer. The implementation includes the possibility of boosting independently only the torsional terms of the potential (`iamd=2`) or the whole potential at once (`iamd=1`). It also allows the possibility to boost the whole potential with an extra boost to the torsions (`iamd=3`). All the information generated by AMD, necessary for reweighing is stored at each step into a vector which is flushed to a log file (`amd.log` by default) every time the coordinates are written to disk, i.e. every `ntwx` steps. This is done for performance reasons, since writing to disk is always time consuming and it is not advisable to do it every step. The name of the log file can be set to a user defined name

#### 4. Sampling and free energies

by using the command line option `-amdlog` when running Amber. Our present implementation also allows the user to delay (or lag) the boosting a number of steps, i.e. only boost with a particular frequency defined by the variable `amdlog`. The AMD parameters are specified by the following variables: `EthreshD` ( $E_d$ ), `alphaD` ( $\alpha_D$ ), `EthreshP` ( $E_p$ ) and `alphaP` ( $\alpha_P$ ).

##### 4.10.3. Preparing a system for AMD

As mentioned before, running AMD requires the definition of few parameters. AMD parameters are determined based on previous knowledge of the system, which is easily acquirable by a short regular MD simulation, from which the average values of the potential and torsion energy can be estimated. From there, a given amount of energy per degree of freedom is added to those values, in the form of multiples of alpha, setting the values of  $E_p$  and  $E_d$  to be used. The following example should help clarify this procedure.

```
Average Dihedral : 611.5376 (based on MD simulations)
Average EPtot : -53155.3104 (based on MD simulations)
total ATOMS=16950
protein residues=64
For the dihedral potential:
Approximate energy contribution per degree of freedom.
3.5*64= 224           The value of 3.5 kcal/mol/residue seems to work well
alphaD = (1/5)*224 = 45 The value of .2 seems to work well
EthreshD = 224+611 = 835
For the total potential
alphaP = 16950*(1/5)=3390
For a lower boost you can also use a value between 0.15-0.19 instead of 0.20 (0.16 work)
EthreshP = -53155.3104 + 3390 = -49765.3104
With these parameters, the AMD parameters in the input file should then be set to
iamd=3,EthreshD=835,alphaD=45,EthreshP=-49765,alphaP=3390,
For a higher acceleration it is common to simply add to Eb(dih) multiples of alpha. In
iamd=3,EthreshD=880,alphaD=45,EthreshP=-49765,alphaP=3390,
Two levels higher would be then defined by:
iamd=3,EthreshD=925,alphaD=45,EthreshP=-49765,
```

After the AMD parameters to be used are defined, an MD run with AMD can be set using those parameters. Depending on the progress of the simulation, a higher boost can be applied as specified in the above example.

##### 4.10.4. Sample input file for AMD

An example of an input file would be the following:

```
AVP dt=2.0fs with SHAKE, NPT AMD boost pot and dih
&cntrl
  imin=0, irest=1, ntx=5,
  dt=0.002, ntc=2, ntf=2, tol=0.000001,iwrap=1,
```

```

ntb=2, cut=12.0, ntp=1, igb=0, ntwprt = 3381, ioutfm = 1,
ntt=3, temp0=310.0, gamma_ln=1.0, ig=-1,
ntpr=1000, ntwx=1000, ntwr=1000, nstlim=2000000,
iamd=3, EthreshD=835,
alphaD=45, EthreshP=-49765,
alphaP=3390,
/
&ewald
dsum_tol=0.000001,
/

```

#### 4.10.5. Further information

Test cases have been included into the distribution of Amber, also a tutorial based on a study we performed on BPTI [191], showing the power of AMD and its validation versus a millisecond run on the same system performed on Anton is now present on the Amber website. We encourage the user to read the paper, as well as follow the tutorial for more information.

## 4.11. Constant pH calculations

The constant pH molecular dynamics method has been implemented in *sander* by John Mongan for simulations run with the Generalized Born implicit solvent model.[192] Using the constant pH method requires minor modifications to the process of generating the prmtop file, as well as generation of a second input file from the prmtop file, describing the titrating residues.

### 4.11.1. Background

Traditionally, molecular dynamics simulations have employed constant protonation states for titratable residues. This approach has many drawbacks. First, assigning protonation states requires knowledge of pKa values for the protein's titratable groups. Second, if any of these pKa values are near the solvent pH there may be no single protonation state that adequately represents the ensemble of protonation states appropriate at that pH. Finally, since protonation states are constant, this approach decouples the dynamic dependence of pKa and protonation state on conformation.

The constant pH method implemented in *sander* addresses these issues through Monte Carlo sampling of the Boltzmann distribution of protonation states concurrent with the molecular dynamics simulation. The nature of the distribution is affected by solvent pH, which is set as an external parameter. Residue protonation states are changed by changing the partial charges on the atoms of the protonable residue.

### 4.11.2. Preparing a system for constant pH

Amber provides definitions for titrating side chains of ASP, GLU, HIS, LYS, TYR, and CYS. See below if you need other titrating groups.

#### 4. Sampling and free energies

Begin by preparing your PDB file as you normally would for use with LEaP. Edit the PDB file, replacing all histidine residue names (HIS, HID, or HIE) with HIP. Change all ASP and ASH to AS4 and all GLU and GLH to GL4. The others— LYS, TYR, and CYS— have the same name. This ensures that the prmtop file will have a hydrogen defined at every possible point of protonation. Note that these changes should only be applied to residues that you wish to titrate.

Run LEaP with the leaprc.constph command file. This file loads all parameters that were used for the reference compounds. You can load this file with the following command:

```
source leaprc.constph
```

This loads the ff99SB force field for proteins. In addition, it loads the special carboxylate residue libraries and force field modifications, constph.lib and frcmod.constph, that defines a hydrogen atom at each protonable location; syn- and anti- for both oxygens, along with improper torsions to prevent them from rotating into one another. It also sets the GB solvation radii (PBradii) to mbondi2, which was the set used to parameterize the reference compounds. Now load your edited PDB file and proceed as usual to create the prmtop and prmcrd files. Changing any of these parameters should be closely checked by titrating the reference compounds and ensuring the predicted pKa matches.

Once you have the prmtop file, you need to generate a cpin file. The cpin file describes which residues should titrate, and defines the possible protonation states and their relative energies. A python script, *cpinutil*, is provided to generate this file. It takes a prmtop file as input, on the command line along with the GB model you wish to evaluate protonation transitions in, and writes the cpin file to STDOUT. Since LEaP has inserted extra hydrogens, the atom numbering in your original PDB file will not correspond to the prmtop file. Here is an example of generating the cpin file from your prmtop file, 'prmtop' using the igb=5 GB model:

```
cpinutil.py -p prmtop -igb 5 > cpin
```

The *cpinutil* program accepts a number of flags that modify its behavior. By default, all residues start in protonation state 0: deprotonated for ASP and GLU, protonated for LYS, TYR, and CYS, and doubly protonated for HIS (i.e. HIP). Initial protonation states can be specified using the -states flag followed by a comma and/or whitespace-delimited list of initial protonation states (see below for more about protonation state definitions) as follows:

```
cpinutil.py -p prmtop -igb 5 -states 1,3,0,0,0,1 > cpin
```

Note that if a list of states is provided, it must match exactly the number of residues that cpinutil has found to titrate based on the restrictions put on the command line. The -system flag can be used to provide a name for the titrating system. This is purely cosmetic and has no effect on your simulations.

```
cpinutil.py -p prmtop -igb 5 -system HEWL > cpin
```

A number of flags are available for filtering which residues are included in the cpin file. All residues in the cpin file, and only the residues in the cpin file, will be titrated. In general it is safe to exclude TYR and LYS for acidic simulations and GL4 and AS4 for basic simulations. HIP should be included in all except very acidic simulations. Note that there is currently no

support for titrating N or C terminal residues. If you have an N or C terminal residue with a titratable sidechain, you should explicitly exclude it from the cpin file. The `-resnum` flag may be used to specify which residue numbers should be retained; all others are deleted. Conversely, the `-notresnum` flag can be used to specify which residue numbers are deleted; all others are retained. Residue number refers to the numbering in the PDB file, not the index number among titrating residues. Similarly, `-resname` and `-notresname` can be used to filter by residue type. For instance, `-notresname TYR,LYS` would eliminate basic residues from the cpin file. The `-minpKa` and `-maxpKa` flags can be used to filter out residues whose reference pKas do not satisfy that criteria. For example, `-minpKa 5.0` will exclude all AS4 and GL4 residues from titrating.

### 4.11.3. Running at constant pH

#### 4.11.3.1. Running at constant pH in implicit solvent

Running constant pH under *sander* has few differences from normal operation. In the mdin file, you must set `icnstph=1` to turn on constant pH in implicit solvent. `solvph` is used to set the solvent pH value. You must also specify the period for Monte Carlo steps, `ntcnstph` (for period *n*, a Monte Carlo step is performed every *n* steps). Note that only one residue is examined on each step, so you should decrease the step period as the number of titrating residues increases to maintain a constant effective step period for each residue. We have seen good results with fairly short periods, in the neighborhood of 100 fs effective period for each residue (e.g. `ntcnstph=5`, `dt=0.002` with about 10 residues titrating).

In order to avoid having to calculate non-electrostatic contributions to protonation state transition energies, this method uses correction factors based on the relative energy differences of the different protonation states in the Amber force field. These relative energies were calculated under the following parameters:

```
cut=30.0, igb=#, saltcon=0.1,
ntb=0, dt=0.002, nrespa=1,
ntt=1, temp0=300.0, temp0 = 300., tautp=2.0,
ntc=2, ntf=2, tol=0.000001,
```

where # is the value passed to the *cpinutil* program. Deviations from these parameters, or from the force field or GB radii specified above may affect the relative energies of the protonation states, which will cause erroneous results. If you must deviate from these settings, you can test whether your changes will cause problems by running long (multiple ns) titrations of the model compounds, with solvent pH equal to the model compound pKa value. The model compounds are ACE-X-NME, where X is AS4, GL4, HIP, LYS or TYR. If these titrations predict the model pKa value (4.0, 4.4, 6.5, 10.4 and 9.6, respectively), then the parameter set is probably OK. If not, you must either change the parameter set or recalculate the relative energies (see section below).

Some additional command line flags have been added to *sander* to support constant pH operation. The cpin file must be specified using the `-cpin` option. Additionally, a history of the protonation states sampled is written to the filename specified by `-cpout`. Finally, a constant pH restart file is written to the filename specified by `-cprestrt`. This is used to ensure that titrating residues retain the same protonation state across restarts. The constant pH restart file is a

#### 4. Sampling and free energies

cpin-format file, and should be used as the cpin file when restarting the run. It will generally be longer than the original cpin file, as it contains some amount of zeroed data, due to limitations in the Fortran namelist implementation. The only difference between the cprestrt file created at the end of a simulation and the cpin file used to start it will be the RESSTATES array. Note that due to compiler-dependence of the namelist implementation, cprestrt files written with one version of *sander* compiled on system A with compiler X *may* not be compatible with another version of *sander* compiled on system B with compiler Y.

##### 4.11.4. Analyzing constant pH simulations

As the simulation progresses, the protonation states that are sampled are written to the cpout file. A section of a cpout file is included here:

```
Solvent pH: 2.00000
Monte Carlo step size: 2
Time step: 0
Time: 0.000
Residue 0 State: 1
Residue 1 State: 0
Residue 2 State: 1
Residue 3 State: 0
Residue 4 State: 1
Residue 5 State: 0
Residue 2 State: 0
Residue 4 State: 0
Residue 0 State: 3
Residue 1 State: 0
Residue 0 State: 0
```

One record is written on each Monte Carlo step. Each record is terminated by a blank line. There are two types of records, full records (at the top of the file) and delta records (single or double lines, remainder of file). Full records are written before the run begins and on timesteps where snapshots are written to the trajectory file (assuming these are Monte Carlo steps); delta records are written in all other cases. A delta record that consists of two lines indicates that a two-step Monte Carlo move was attempted involving neighboring titrating residues on the same step. The full record specifies the protonation state of each residue, along with some additional information, while the delta records give only the protonation state for the residue selected on the corresponding Monte Carlo step. Thus, assuming *ntwx* is a multiple of *ntcnstph*, the protonation state of each titratable residue for every frame in the trajectory file is given by the full records in the cpout file. Note that in some cases, the protonation state for a delta record may be the same as that in an earlier record: this indicates that the Monte Carlo protonation move was rejected. The residue numbers in cpout are indices over the titrating residues included in the cpin file; cpout must be analyzed in conjunction with cpin to map these indices back to the original system.

The Perl script *calcpka.pl* is provided as an example parser for the cpout format, and as a utility for calculating predicted pK a values from cpout files. It takes a cpin file as its first

argument and any number of cpout files for its remaining arguments. For instance:

```
calcpka cpin [cpout1 [cpout2 [cpout3 [... ]]]] [-o output] \
          [-t dump_interval] [-ao dump_output] [-po population_output]
```

- Output contains one line for each titrating residue in the system:

*Offset* is the difference between the predicted pK<sub>a</sub> and the system pH.

*Pred* is the predicted pK<sub>a</sub>. Note that predictions are calculated assuming Henderson-Hasselbalch titration curves. Predictions are most accurate when the absolute value of the offset is less than 2.0. If experimental pK<sub>a</sub> values have been defined for the system (see following), then experimental and error values are also printed.

*Frac Prot* is the fraction of time the residue spends protonated and

*Transitions* gives the number of accepted protonation state transitions. Note that transitions between states with the same total protonation (e.g. *syn* and *anti* protonated states of a carboxylic acid) are not included in this total.

*Average total molecular protonation* is the sum of the fractional protonations. It ranges between zero and the number of titrating residues, and gives the average protonation of the molecule as a whole.

- Output can be redirected to a file with the [-o output] flag, but is printed to stdout if this is left blank
- If a dump\_interval is set, the total output printed to stdout or “output” remains unchanged, but additional output is printed to dump\_output (default name “pKa\_evolution.dat”) as well. The simulation is broken up into chunks defined of time whose size is defined by dump\_interval, which is an integer defining how many time steps are to be included in each interval. For each time step, the cumulative data/pK<sub>a</sub>s are printed under a header ===== CUMULATIVE =====, and isolated data strictly for that chunk of time is printed under a header ===== CHUNK =====.
- The populations for each residue for each state is dumped to population\_output (default name “populations.dat”) which tells the user the fraction of snapshots that were present as each state with the number of protons in that state put in parenthesis next to it. An example is shown below:

**Populations:**

<b>Residue Number</b>	<b>State 0</b>	<b>State 1</b>	<b>State 2</b>	<b>-----</b>
<b>Residue: HIP 2</b>	<b>0.002 (2)</b>	<b>0.673 (1)</b>	<b>0.325 (1)</b>	

In this example, a histidine residue was titrated. State 0, the doubly-protonated state (signified by the 2 in parentheses next to it), was populated 0.2% of the time (or 0.002 fraction of the time). State 1, which is singly-protonated, was populated 67.3% of the time (or 0.673 fraction of the time), and state 2, which is also singly-protonated, was populated 32.5% of the time (or 0.325 fraction of the time).

#### 4. Sampling and free energies

##### 4.11.5. Extending constant pH to additional titratable groups

There are two major components to defining a new titrating group for constant pH. First you must define the partial charges for each atom in the residue for each protonation state. Then you must set the relative energies of each state.

###### Defining charge sets

Partial charges are most easily calculated using Antechamber and Gaussian. You must set up a model to calculate charges for each protonation state. If the titrating group you are defining is a polymer subunit (e.g. amino acid residue), you must adjust the charges on atoms that have bonded interactions (including 1-4) with atoms in neighboring residues. The charges on these atoms must be changed so they are constant across all protonation states - otherwise relative energies of protonation states become sequence dependent. For an amino acid, this means that all backbone atoms must have constant charges. For the residues defined here, we arbitrarily selected the backbone charges of the protonated state to be used across all protonation states. The total charge difference between states should remain 1; we achieved this by adjusting the charge on the beta carbon.

###### Calculating relative energies

Relative energies are used to calibrate the method such that when a model compound is titrated at pH equal to its  $pK_a$ , the energies (and thus populations) of the protonated and deprotonated states are equal. Relative energies of the different protonation states are calculated using thermodynamic integration of a model compound between the charge sets defined for the different protonation states. The model compound should be a small molecule that mimics the bonded environment of the titratable group of interest, and for which experimental  $pK_a$  data are available. For instance, the model compound for an amino acid X is generally ACE-X-NME; the model compound for a ligand might be the free ligand. The thermodynamic integration calculations must be performed using exactly the same parameters and force field as you plan to use in your constant pH simulations. Once the relative energies of the states are calculated by thermodynamic integration, the energy difference must be adjusted to account for the  $pK_a$ : the energy of the more protonated states should be increased by  $pK_a RT \ln(10)$ .

For example suppose one were developing a model for an artificial amino acid, ART, with  $pK_a$  3.5 and two protonation states: ARP, having one proton and ARD having zero protons. After calculating partial charges as above, you would construct a model compound having the sequence ACE-ARP-NME and generate a prmtop file where the ARP charges were perturbed to the ARD values. You would then use sander to perform thermodynamic integration between ARP and ARD. Suppose that this showed that the energy of ARD relative to ARP was -6.3 kcal/mol. You would assign a relative energy of -6.3 to ARD and a relative energy of  $3.5RT \ln(10)$  to ARP.

###### Testing the titratable group definitions

Prior to large scale use of your new titratable group definition, it's a good idea to test it by performing a constant pH simulation on your model compound, with pH set to the model  $pK_a$ .



Doing this requires generation of a cpin file, so this is a good point to modify the table of titratable group definitions used by *cpinutil*. These tables are found in `$AMBERHOME/AmberTools/src/etc/cpin_data.py`. The table is a python dictionary of 2D arrays. Each dictionary entry is an array of states that define a titratable group. Each state array consists of the relative energy, the relative protonation, and the partial charges for the state, in that order. An entry for the example given above might look like (charge list shortened for brevity):

```
"ARP" = [
# State 0, ARP
[3.5 * 1.3818, # Relative energy (300K)
1,           # Relative protonation
-0.4157, 0.2719, -0.0014, 0.0876, -0.0152, 0.0295, ], # Partial charges
# State 1, ARD
[-6.3, # Energy
0,     # Protonation
-0.4157, 0.2719, -0.0014, 0.0876, -0.0858, 0.019, ]
]
```

The top of `cpin_data.py` also contains a string of space-delimited residue names with their corresponding pKas. Adding residues to this module requires that these strings be updated so *cpinutil.py* knows that these residues may titrate. Follow the template for existing residues when adding more residues to `cpin_data.py`. After you finish this, you must reinstall the source in `etc/` to update this python module and place it in the path recognized by *cpinutil.py*. Having added your titratable group definition to the table, you should be able to prepare a cpin file as described above, run your simulation and calculate the predicted pKa using *calcpka*. Since the model compound is usually very small, runs of tens of nanoseconds are easily accessible for these tests. In general, the run to run variation of predicted pKa values is a few hundredths of a pKa unit for long runs with pH near pKa. In most cases, the thermodynamic integration procedure described above yields acceptable results, but if your predicted pKa differs significantly from the model pKa, you may want to adjust your relative energies, regenerate your cpin file and rerun the test until you achieve good predictions.

## 4.12. Low-MODE (LMOD) methods

István Kolossváry's LMOD methods for minimization, conformational searching, and flexible docking[193–196] are now fully implemented in Amber. The centerpiece of LMOD is a conformational search algorithm based on eigenvector following of low frequency vibrational modes. It has been applied to a spectrum of computational chemistry domains including protein loop optimization and flexible active site docking.

Details of the LMOD procedure, and hints on getting good performance, are given in the *AmberTools Users' Manual*, which should be consulted before trying the procedures in *sander*. The only difference between the implementation in *sander* and in *NAB* involves details of how the input is specified; the same LMOD code is linked into both. The sections below give input details for *sander*.

## 4. Sampling and free energies

### 4.12.1. XMIN

The XMIN methods for minimization are traditional and manifold in the field of unconstrained optimization: PRCG is a Polak-Ribiere nonlinear Conjugate Gradient algorithm,[197] LBFGS is a Limited-memory Broyden-Fletcher-Goldfarb-Shanno quasi-Newton algorithm,[198] and TNCG is a Truncated Newton linear Conjugate Gradient method with optional LBFGS preconditioning.[199]

Some of the &cntrl namelist variables that control Amber's other minimization facilities also control XMIN. Consequently, non-experts can employ the default XMIN method merely by specifying `ntmin = 3`.

<code>maxcyc</code>	The maximum number of cycles of minimization. Default is 1 to be consistent with Amber's other minimization facilities although it may be unrealistically short.
<code>ntmin</code>	The flag for the method of minimization.  <b>= 3</b> The XMIN method is used. <b>= 4</b> The LMOD method is used. The LMOD procedure employs XMIN for energy relaxation and minimization.
<code>drms</code>	The convergence criterion for the energy gradient: minimization will halt when the root-mean-square of the Cartesian elements of the gradient is less than DRMS. Default is 1.0E-4 kcal/mole Å to be consistent with Amber's other minimization facilities although it may be unrealistically strict.

Other options that control XMIN are in the scope of the &lmod namelist. These parameters enable expert control of XMIN.

<code>lbfgs_memory_depth</code>	The depth of the LBFGS memory for LBFGS minimization, or LBFGS preconditioning in TNCG minimization. Default is 3. Suggested alternate value is 5. The value 0 turns off LBFGS preconditioning in TNCG minimization.
<code>matrix_vector_product_method</code>	The finite difference Hv matrix-vector product method: "forward" = forward difference, "central" = central difference. Default is forward difference.
<code>xmin_method</code>	The minimization method: "PRCG" = Polak-Ribiere Conjugate Gradient, "LBFGS" = Limited-memory Broyden-Fletcher-Goldfarb-Shanno, and "TNCG" = Optionally LBFGS-preconditioned Truncated Newton Conjugate Gradient. Default is LBFGS.
<code>xmin_verbosity</code>	The verbosity of the internal status output from the XMIN package: 0 = none, 1 = minimization details, and 2 = minimization and line search details plus CG details in TNCG. Currently, the XMIN status output may be disordered with respect to Amber's output. Default is 0, no output of the XMIN package internal status. Note that XMIN is also available in AmberTools, in the NAB package. An annotated example output corresponding to <code>XMIN_VERBOSITY=2</code> can be found in the NAB documentation.

### 4.12.2. LMOD

Some of the options that control LMOD have the same names as Amber's other minimization facilities. See the XMIN section immediately above. Other options that control LMOD are in the scope of the &lmod namelist. These parameters enable expert control of LMOD.

**arnoldi\_dimension** The dimension of the ARPACK Arnoldi factorization. Zero specifies the whole space, that is, three times the number of atoms. Default is 0, the whole space. Basically, the ARPACK package used for the eigenvector calculations solves multiple "small" eigenvalue problems instead of a single "large" problem, which is the diagonalization of the three times the number of atoms by three times the number of atoms Hessian matrix. This parameter is the user specified dimension of the "small" problem. The allowed range is  $\text{total\_low\_modes} + 1 \leq \text{arnoldi\_dimension} \leq$  three times the number of atoms. The default means that the "small" problem and the "large" problem are identical. This is the preferred, i.e., fastest, calculation for small to medium size systems, because ARPACK is guaranteed to converge in a single iteration. The ARPACK calculation scales with three times the number of atoms times the arnoldi\_dimension squared and, therefore, for larger molecules there is an optimal arnoldi\_dimension much less than three times the number of atoms that converges much faster in multiple iterations (possibly thousands or tens of thousands of iterations). The key to good performance is to select an arnoldi\_dimension such that all the ARPACK storage fits in memory. For proteins, arnoldi\_dimension=1000 is generally a good value, but often a very small 50-100 Arnoldi dimension provides the fastest net computational cost with very many iterations.

**conflib\_filename** The user-given filename of the LMOD conformational library. The file format is standard Amber trajectory file. The conformations are stored in energetic order (global minimum energy structure first), the number of conformations  $\leq$  conflib\_size. The default filename is *conflib*.

**conflib\_size** The number of conformations to store in conflib. Default is 3.

**energy\_window** The energy window for conformation storage; the energy of a stored structure will be in the interval  $[\text{global\_min}, \text{global\_min} + \text{energy\_window}]$ . Default is 0, only storage of the global minimum structure.

**explored\_low\_modes** The number of low frequency vibrational modes used per LMOD iteration. Default is 3.

**frequency\_eigenvector\_recalc** The frequency, measured in LMOD iterations, of the recalculation of eigenvectors. Default is 3.

**frequency\_ligand\_rotrans** The frequency, measured in LMOD iterations, of the application of rigid-body rotational and translational motions to the ligand(s). At each frequency\_ligand\_rotrans-th LMOD iteration number\_ligand\_rotrans rotations and translations are applied to the ligand(s). Default is 1, ligand(s) are rotated and translated at every LMOD iteration.

#### 4. Sampling and free energies

`lmod_job_title` The user-given title for the job that goes in the first line of the `conflib` and `lmod_trajectory` files. The default job title is "job\_title\_goes\_here".

`lmod_minimize_grms` The gradient RMS convergence criterion of structure minimization. Default is 0.1.

`lmod_relax_grms` The gradient RMS convergence criterion of structure relaxation. Default is 1.0.

`lmod_restart_frequency` The frequency, in LMOD iterations, of `conflib` updating and LMOD restarting with a randomly chosen structure from the pool. Default is 5.

`lmod_step_size_max` The maximum length of a single LMOD ZIG move. Default is 5.0 Å.

`lmod_step_size_min` The minimum length of a single LMOD ZIG move. Default is 2.0 Å.

`lmod_trajectory_filename` The filename of the LMOD pseudo trajectory. The file format is standard Amber trajectory file. The conformations in this file show the progress of the LMOD search. The number of conformations = `number_lmod_iterations` + 1. The default filename is *lmod\_trajectory*.

`lmod_verbosity` The verbosity of the internal status output from the LMOD package: 0 = none, 1 = some details, 2 = more details, 3 = everything including ARPACK information. Currently, the LMOD status output may be disordered with respect to Amber's output. Default is 0, no output of the LMOD package internal status. Note that LMOD is also available in AmberTools, in the NAB package. An annotated example output corresponding to `LMOD_VERBOSITY=2` can be found in the NAB documentation.

`monte_carlo_method` The Monte Carlo method: "Metropolis" = Metropolis Monte Carlo, "Total\_Quench" = the LMOD trajectory always proceeds towards the lowest lying neighbor of a particular energy well found after exhaustive search along all of the low modes, and "Quick\_Quench" = the LMOD trajectory proceeds towards the first neighbor found, which is lower in energy than the current point on the path, without exploring the remaining modes. Default is Metropolis Monte Carlo.

`number_free_rottrans_modes` The number of rotational and translational degrees of freedom. This is related to the number of frozen or tethered atoms in the system: 0 atoms dof=6, 1 atom dof=3, 2 atoms dof=1, >=3 atoms dof=0. Default is 6, no frozen atoms.

`number_ligand_rottrans` The number of rigid-body rotational and translational motions applied to the ligand(s). Such applications occur at each `frequency_ligand_rottrans-th` LMOD iteration. Default is 0, no rigid-body motions applied to the ligand(s).

`number_ligands` The number of ligands for flexible docking. Default is 0, no ligand(s).

`number_lmod_iterations` The number of LMOD iterations. Default is 10. Note that setting `number_lmod_iterations = 0` will result in a single energy minimization.

**number\_lmod\_moves** The number of LMOD ZIG-ZAG moves. Zero means that the number of ZIG-ZAG moves is not pre-defined, instead LMOD will attempt to cross the barrier in as many ZIG-ZAG moves as it is necessary. The criterion of crossing an energy barrier is stated above in the "LMOD Procedure" background section. **number\_lmod\_moves** > 0 means that multiple barriers may be crossed and LMOD can carry the molecule to a large distance on the potential energy surface without severely distorting the geometry. Default is 0, LMOD will determine automatically where to stop the ZIG-ZAG sequence.

**random\_seed** The seed of the random number generator. Default is 314159.

**restart\_pool\_size** The size of the pool of lowest-energy structures to be used for restarting. Default is 3.

**rttemperature** The value of RT in Amber energy units. This is utilized in the Metropolis criterion. Default is 1.5.

**total\_low\_modes** The total number of low frequency vibrational modes to be used. Default is the minimum of 10 and three times the number of atoms minus the number of rotational and translational degrees of freedom (**number\_free\_rotrans\_modes**).

The following commands are part of the `&lmod` namelist. These commands control the way LMOD applies explicit translations and rotations to one or more ligands and take effect only if **number\_ligands** >= 1. All commands are lists in square brackets, separated by commas such as [1, 33, 198], however, the list is read by Sander as a string and, therefore, it should be enclosed in single quotes.

**ligstart\_list, ligend\_list** The serial number(s) of the first/last atom(s) of the ligand(s). Type integer. The number(s) should correspond to the numbering in the Amber input files `prmtop` and `inpcrd/restart`. For example, if there is only one ligand and it starts at atom 193, the command should be `ligstart_list = '[193]'`. If there are three ligands, the command should be, e.g., `'[193, 244, 1435]'`. The same format holds for all of the following commands. Note that the ligand(s) can be anywhere in the atom list, however, a single ligand must have continuous numbering between the corresponding **ligstart\_list** and **ligend\_list** values. For example, `ligstart_list = '[193, 244, 1435]'` and `ligend_list = '[217, 302, 1473]'`.

**ligcent\_list** The serial number(s) of the atom(s) of the ligand(s), which serves as the center of rotation. Type integer. The value zero means that the center of rotation will be the geometric center of gravity of the ligand.

**rotmin\_list, rotmax\_list** The range of random rotation of a particular ligand about the origin defined by the corresponding **ligcent\_list** value is specified by the commands **rotmin\_list** and **rotmax\_list**. The angle is given in +/- degrees. Type float. For example, in case of a single ligand and **ligcent\_list** = '[0]', **rotmin\_list** = '[30.0]' and **rotmax\_list** = '[180.0]' means that random rotations by an angle +/- 30-180 degrees about the center of gravity of the ligand, will be applied. Similarly, with

#### 4. *Sampling and free energies*

`number_ligands = 2, ligcent_list= 120.0]` means that the first ligand will be rotated like in the single ligand example in this paragraph, but a second ligand will be rotated about its atom number 201, by an angle +/- 60-120 degrees.

`trmin_list, trmax_list` The range of random translation(s) of ligand(s) is defined by the same way as rotation. For example, with `number_ligand = 1`, `trmin_list = '[0.1]` and `trmax_list = '[1.0]` means that a single ligand is translated in a random direction by a random distance between 0.1 and 1.0 Angstroms.

# 5. Quantum dynamics

## 5.1. Path-Integral Molecular Dynamics

### 5.1.1. General theory

Based on Feynman's formulation of quantum statistical mechanics in terms of path-integrals, Path-Integral Molecular Dynamics (PIMD) is a computationally efficient method for calculating equilibrium (e.g., thermodynamic and structural) properties of a quantum many-body system. In the following we will briefly illustrate the basic principles, and we will derive the fundamental equations underlying its implementation using standard molecular dynamics methods. The literature should be read for a more rigorous description[105–107].

For the sake of simplicity, we restrict ourselves to a PIMD formulation of the canonical (NVT) ensemble, and we will consider a single quantum particle of mass  $m$ , with momentum  $p$  and coordinate  $x$ , which moves in a one-dimensional potential  $v(x)$ . Generalization to other ensembles and/or to multidimensional many-particle systems is straightforward.

In the NVT ensemble, the canonical partition function  $Z$  is expressed as

$$Z = \sum_i e^{-\beta E_i} \quad (5.1)$$

where  $\beta = 1/k_B T$ , and the corresponding density matrix is defined as

$$\rho = \frac{e^{-\beta E_i}}{Z} \quad (5.2)$$

The expectation value of any operator  $A$  can thus be computed as

$$\langle A \rangle = Tr(\rho A) = \frac{1}{Z} Tr(A e^{-\beta H}) \quad (5.3)$$

with  $H$  being the Hamiltonian for the one-dimensional system:

$$H = \frac{p^2}{2m} + v(x) = T + V \quad (5.4)$$

In Eq. (5.4)  $T$  and  $V$  are the kinetic and potential operators, respectively. Using the coordinate basis set  $\{|x\rangle\}$ , the canonical partition function can be computed as

$$Z = \int dx \langle x | e^{-\beta H} | x \rangle = \int dx \langle x | e^{-\beta(T+V)} | x \rangle \quad (5.5)$$

In general  $T$  and  $V$  do not commute, i.e.  $[T, V] \neq 0$ , and consequently  $e^{-\beta(T+V)}$  cannot be calculated directly. However, using the Trotter formula [200] it is possible to demonstrate that

## 5. Quantum dynamics

$$Z = \lim_{P \rightarrow \infty} \int dx \langle x | \left( e^{-\frac{\beta V}{2P}} e^{-\frac{\beta A}{P}} e^{-\frac{\beta V}{2P}} \right)^P | x \rangle \quad (5.6)$$

After some algebra and using the completeness of the coordinate basis, the quantum canonical partition function can be written as

$$Z = \lim_{P \rightarrow \infty} \int dx_1 dx_2 \dots dx_P \left( \frac{mP}{\hbar^2 \beta} \right)^{\frac{P}{2}} e^{-\sum_{i=1}^P \left[ \frac{mP}{\beta \hbar^2} (x_{i+1} - x_i)^2 + \frac{\beta}{P} v(x_i) \right]}_{x_{P+1}=x_1} \quad (5.7)$$

Defining a "chain" frequency  $\omega_P = \frac{\sqrt{P}}{\beta \hbar}$  and an effective potential as

$$U_{eff}(x_1, \dots, x_P) = \sum_{i=1}^P \left[ \frac{1}{2} m \omega_P^2 (x_{i+1} - x_i)^2 + \frac{\beta}{P} v(x_i) \right]_{x_{P+1}=x_1} \quad (5.8)$$

the canonical partition function is finally expressed as

$$Z = \lim_{P \rightarrow \infty} \int dx_1 dx_2 \dots dx_P \left( \frac{mP}{\hbar^2 \beta} \right)^{\frac{P}{2}} e^{-\beta U_{eff}(x_1, \dots, x_P)} \quad (5.9)$$

In this form, the quantum partition function is isomorphic with a classical configurational partition function for a  $P$ -particle systems, where the  $P$  particles (generally referred to as "beads") are discrete points along a cyclic path[201]. Each bead is coupled to its nearest neighbors by harmonic springs with frequency  $\omega_P$ , and is subject to the external potential  $v(x)$ . It is possible to make the connection between the quantum partition function and a fictitious classical  $P$ -particle system even more manifest by introducing a set of  $P$  Gaussian integrals:

$$Z = \lim_{P \rightarrow \infty} \Lambda \int dp_1 dp_2 \dots dp_P \int dx_1 dx_2 \dots dx_P \left( \frac{mP}{\hbar^2 \beta} \right)^{\frac{P}{2}} e^{-\beta \left[ \sum_{i=1}^P \frac{p_i^2}{2\mu_i} + U_{eff}(x_1, \dots, x_P) \right]} \quad (5.10)$$

The new Gaussian variables are regarded as fictitious classical "momenta" and, consequently, the constants  $\mu_i$  have units of mass and are generally referred to as fictitious masses. Since these Gaussian integrals are uncoupled and can be calculated analytically, the overall constant  $\Lambda$  can be chosen so as to reproduce the correct prefactor. Therefore, one has complete freedom to choose  $\mu_i$ .

>From Eq. (5.5) it follows that the quantum partition function can be evaluated using classical molecular dynamics based on equations of motion derived from a fictitious classical Hamiltonian of the form

$$H(p, x) = \sum_{i=1}^P \frac{p_i^2}{2\mu_i} + U_{eff}(x_1, \dots, x_P) \quad (5.11)$$

However, ordinary MD generates a microcanonical distribution of  $H$ , i.e., a distribution function of the form  $\delta(H(p, x) - E)$ , where  $E$  is the conserved energy. This is clearly not the form appearing in the quantum partition function that requires a canonical distribution of the form  $e^{\beta H}$ . In order to satisfy this condition, the system has to be coupled to a thermostat which



guarantees that the canonical distribution is rigorously obtained.

As shown above, the exact quantum partition function is obtained in the limit of an infinite number of beads  $P$ . In practice this is obviously not possible, and therefore  $P$  must be chosen large enough that all thermodynamic properties are converged. Since  $P$  is directly related to the quantum nature of the system under consideration, a larger number of beads is necessary for systems containing light atoms (e.g., hydrogen and deuterium) and for simulations at low temperatures.

Two different implementations of PIMD are currently available in Amber. The first one corresponds to the so-called primitive approximation (PRIMPIMD) [202] which is directly obtained from the formulation provided above with the fictitious mass of each bead chosen as  $\mu_i = m/P$ , where  $m$  is the particle mass. In PRIMPIMD, the canonical distribution is obtained by either using a Langevin thermostat or Nosé-Hoover chains of thermostats coupled to each degree of freedom of the system according to the algorithm of Ref. [203]. The latter is the recommended option. The second implementation, which is called Normal Mode Path-Integral Molecular Dynamics (NMPIMD) [204], makes use of a normal mode transformation that uncouples the harmonic term in Eq. (5.8). As a consequence the fictitious masses are different. In the current implementation of NMPIMD, the canonical distribution is obtained by using Nosé-Hoover chains of thermostats coupled to each degree of freedom of the system. We note here that NMPIMD is preferred over PRIMPIMD because it guarantees a more efficient sampling of the phase space.

In both PRIMPIMD and NMPIMD, the equations of motion are propagated using the Leapfrog algorithm, and the quantum energies of the system (total, kinetic and potential energy) are computed using the so-called "virial estimator"[202, 205].

All the force fields available for regular MD in Amber can also be used for PRIMPIMD and NMPIMD simulations. However, we note here that the common empirical force fields may require an additional re-parameterization (see Ref. [206] for a more detailed discussion). A simple charge, flexible water model specifically developed in Ref. [206] for investigating nuclear quantum effects is already implemented in the current version of Amber (see Sec. 2.9 of the AmberTools Users' manual) and it is recommended for PRIMPIMD and NMPIMD simulations of aqueous systems.

### 5.1.2. How PIMD works in Amber

#### Implementation and input/output files

The current implementation of PRIMPIMD and NMPIMD allows the "quantization" of either the whole system or just a part of it. In both cases the *mdin* input is the same as for a regular (classical MD) run. However, additional flags are required, which will be described in Section 5.1.2.

For cases where the whole system is quantized, the most efficient way to perform PRIMPIMD and NMPIMD simulations is with *sander.MPI* exploiting the multisander scheme. You must use the same *prmtop* file as in the corresponding classical simulation, while  $P$  separate coordinate files (one for each of the  $P$  beads) are required. The number of beads to get converged results for typical systems at ambient conditions vary between 16 and 32. However, other aspects of quantum behavior may be observed with fewer beads. Therefore, some experimentation on

## 5. Quantum dynamics

your system may be required to find the optimal number. In order to run the simulation you also need a multisander groupfile containing (per line) all the options for each sander job. As output, *sander.MPI* generates the same files as a regular (classical MD) run. The only difference is that there are now  $P$  of such files, one for each bead. Therefore, you will have  $P$  *mdout* files with the bead contributions to the quantum energies,  $P$  *rst* files with the coordinates of each bead for restart, and  $P$  trajectory files (*mdcrd* and *mdvel*) with the bead coordinates and velocities saved during the run. It is important to note that for both PRIMPIMD and NMPIMD the velocities do not correspond to the real-time velocities of the system but are just fictitious velocities needed to solve the integral in Eq. (5.5). *sander.MPI* also writes a general *pimtout* file, which reports the quantum results for the whole system (i.e., total, kinetic and potential energy, pressure, volume, density...). If Nosé-Hoover chains of thermostats are employed, an additional file (*NHC.dat*) is printed with the conserved energy for the extended system. You must carefully check that the timestep used in the simulation is small enough to guarantee conservation of this quantity.

For cases where only a part of the system is quantized, both PRIMPIMD and NMPIMD are implemented within the *LES* scheme (see Chapter 8). Therefore, you must use either *sander.LES* or *sander.LES.MPI*, and prepare the *prmtop* file in a special way. The input files are generated using *addles*. Basically, regular topology and coordinate files are needed, then a control script (usually named *addles.in*) should be written. The necessary input files can then be generated by running "*addles < addles.in*". The following is what a typical *addles.in* will look like (lines start with a "~" are comments):

```
~ designate regular topology file
file rprm name=(input.prmtop) read
~ designate normal coordinate file
file rcrd name=(input.inpcrd) read
~ where to put PIMD topology file
file wprm name=(pimd.prmtop) wovr
~ where to put PIMD coordinate file
file wcrd name=(pimd.inpcrd) wovr
action
~ use original mass(it is required by PIMD)
omas
~ make 4 copies of atom 1-648(should be the whole system)
space numc=4 pick #prt 1 648 done
*EOD
```

Several things should be emphasized here about writing *addles.in* for PRIMPIMD and NMPIMD:

1. If copies of the whole system are made, it means that the whole system is quantized. In this case, *sander.MPI* offers a more efficient way to perform PRIMPIMD and NMPIMD simulations without using *LES* (see above). We note here, that *sander.LES* (and *sander.LES.MPI*) should be used when you are interested in quantizing only a part of your system.
2. The current implementation requires that the "omas" tag must be turned on to make every atom use original mass during the simulation.

3. As mentioned above, how many copies to create is a tradeoff between accuracy and efficiency. To get converged total energies, 16-32 copies may be required; however, other aspects of quantum behavior may be seen with fewer copies. Be prepared to experiment on your system to see what is required.

As output, *sander.LES* (and *sander.LES.MPI*) generates the same files as a regular (classical MD) run. The *mdout* file contains the quantum results for the whole system (i.e., total, kinetic and potential energy, pressure, volume, density...). while the *rst* file contains the coordinates of all beads for restart. The trajectory files (*mdcrd* and *mdvel*) contain the coordinates and velocities of all beads saved during the run. If Nosé-Hoover chains of thermostats are employed, an additional file (*NHC.dat*) is printed with the conserved energy for the extended system. You must carefully check that the timestep used in the simulation is small enough to guarantee conservation of this quantity.

### Input parameters

In order to perform PRIMPIMD and NMPIMD simulations, an additional flag is required in the *mdin* file, which distinguishes among the different methodologies based on the path-integral formalism.

**ipimd** Flag for the different methodologies based on the path-integral formalism. See Sections 5.2.1 and 5.3.1 for the other values.

= 0 defines regular MD (default).

= 1 defines PRIMPIMD.

= 2 defines NMPIMD.

As described above, in order to guarantee a proper canonical sampling of the phase space the quantum system must be coupled to a thermostat. In the current implementation, two schemes are available: Langevin thermostat and Nosé-Hoover chains of thermostats coupled to each degree of freedom of the system. As for any regular MD run, the flag that activates the thermostat is *ntt*. A Langevin thermostat is switched on using *ntt=3*, and defining a collision frequency. To activate the Nosé-Hoover chains of thermostats, you must specify *ntt=4* and provide the number of thermostats (*nchain*) in each chain. Use of Nosé-Hoover chains of thermostats is recommended and is the only option currently available for NMPIMD (*ipimd=2*). The choice of an appropriate number of chains depends on the system. Typically, 4 thermostats (*nchain=4*) are sufficient to guarantee an efficient sampling of the phase space.

In summary:

**ntt** Switch for temperature scaling. See Section 2.5.7 for other options.

= 3 defines a Langevin thermostat and also requires the definition of *gamma\_ln*. Available for PRIMPIMD (*ipimd=1*) only.

= 4 defines Nosé-Hoover chains of thermostats. Available for PRIMPIMD (*ipimd=1*) and NMPIMD (*ipimd=2*). It also requires the number of thermostats in a chain (*nchain*).

## 5. Quantum dynamics

nchain = 2-8 number of thermostats in each Nosé-Hoover chain of thermostats (default 2, recommended  $\geq 4$ ).

Quantum simulations in the isothermic-isobaric (NPT) ensemble are possible only for NMPIMD (*ipimd*=2) and for rectangular periodic boundary conditions (*ntb*=2) with isotropic position scaling (*ntp*=1). All the other flags are identical to those for a classical MD simulation. The current implementation of NMPIMD for the NPT ensemble is based on the derivation of Ref [207].

### Examples

In the following examples of input files for PRIMPIMD and NMPIMD are shown. You are also encouraged to check the test cases in \$AMBERHOME/test/PIMD.

a) PRIMPIMD input for *sander.LES*. No periodic boundary conditions.

Test: \$AMBERHOME/test/PIMD/part\_pimd\_water.

```
ipimd = 1      ! PRIMPIMD
ntb = 0
ntx = 1, irect = 0
cut = 100.
temp0 = 300., tempi = 300., temp0les = -1.
ntt = 3, gamma_ln = 20.      ! Langevin thermostat
dt = 0.0001, nstlim = 1000
ntpr = 100, ntwr = 100, ntwx = 100
```

b) PRIMPIMD input for *sander.LES*. NVT simulation for water with only the hydrogen atoms being quantized.

Test: \$AMBERHOME/test/PIMD/part\_pimd\_spcfw.

```
ipimd = 1      ! PRIMPIMD
ntx = 5, irect = 0
temp0 = 300., tempi = 300., temp0les = -1.
dt = 0.0002, nstlim 10
cut = 7.
ntt = 3, gamma_ln = 20.      ! Langevin thermostat
ntpr = 1, ntwr = 5, ntwx = 1
```

c) NMPIMD input for *sander.LES*. NPT simulation for liquid butane.

Test: \$AMBERHOME/test/PIMD/part\_nmpimd\_ntp.

```
ipimd = 2      ! NMPIMD
ntb = 2, ntp = 1      ! isotropic position scaling
ntx = 5, irect = 0
cut = 8.
```

```

temp0 = 80., tempi = 80., temp0les = -1.
ntt = 4, nchain = 4.      ! Nose'-Hoover chains
dt = 0.0002, nstlim = 50
ntpr = 5, ntwr = 5, ntwx = 1

```

d) NMPIMD input for *sander.MPI*. NPT simulation for liquid water:

Test: *\$AMBERHOME/test/PIMD/full\_pimd\_ntp\_water*.

```

ipimd = 2      ! NMPIMD
ntb = 2, ntp = 1      ! isotropic position scaling
ntx = 5, irest = 1
cut = 7.
temp0 = 298.15
ntt = 4, nchain = 4.      ! Nose'-Hoover chains
dt = 0.0002, nstlim = 10
ntpr = 1, ntwr = 5, ntwx = 5

```

## 5.2. Centroid Molecular Dynamics (CMD)

Two methods based on the path-integral formalism are available to perform approximate quantum dynamical calculations: Centroid Molecular Dynamics (CMD) [208] and Ring Polymer Molecular Dynamics (RPMD) [209].

The CMD method developed by Voth and coworkers draws upon the prescription of quantum distribution functions, in which the exact quantum expressions are cast into a phase space representation leading to a classical-like physical interpretation of the variables of interest. In particular, an approximate quantum dynamics is obtained by propagating the centroid variables (i.e., positions and velocities of the center of mass of the bead polymer) according to classical-like equations of motion. The current implementation is the so-called Adiabatic CMD [210] that makes use of a normal mode representation of path-integrals where the fictitious mass of the zero-frequency mode (i.e., the centroid of the bead polymer) is given the actual mass of the atom and, contrary to NMPIMD, the fictitious masses of all the non-zero frequency modes are scaled by an adiabaticity parameter,  $\gamma < 0$ . This procedure decouples the centroid motion from that of the other normal modes in the same spirit of the Car-Parrinello method. Although the centroid variables move following Newton's equations of motion, Nosé-Hoover chains of thermostats must be attached to each non-zero frequency normal mode. The user is strongly encouraged to refer to the relevant literature (Ref. [208] and references therein) for a more rigorous derivation of the CMD method.

The RPMD method developed by Manolopoulos and coworkers is based on primitive PIMD. However, there are two fundamental differences: 1) each bead is given a fictitious mass equal to the actual mass of the atom (i.e.,  $\mu = m$ ), 2) the dynamics of the system is strictly determined by the fictitious Hamiltonian of Eq. (5.11), i.e., no thermostats are employed. Also in this case, the user is strongly encouraged to refer to the relevant literature for a detailed derivation of this method [209].

Both CMD and RPMD simulations provide an efficient route for the calculation of approximate Kubo transformed correlation functions, which can then be related to the true quantum

## 5. Quantum dynamics

correlation functions. Importantly, running several independent trajectories is required for both CMD and RPMD to guarantee a proper canonical average of the initial conditions and, consequently, to obtain converged results (see Refs. [206] and [211] for examples of CMD and RPMD simulations, respectively).

All the force fields available for regular MD simulations in Amber can be used for CMD and RPMD. However, we also note here that the common empirical force fields may require an additional reparameterization (see Ref. [206] for a more detailed discussion). A simple charge, flexible water model specifically developed in Ref. [206] for investigating nuclear quantum effects is already implemented in the current version of Amber (see Sec. 2.9 of the AmberTools Users' manual) and it is recommended for CMD and RPMD simulations of aqueous systems.

### 5.2.1. Implementation and input/output files

The implementation of CMD and the input/output files are identical to those of NMPIMD (see Section 5.1.2), with few differences. In addition to the NMPIMD output files, two other files are generated for CMD: *CMD\_position.dat* containing the centroid positions, and *CMD\_velocity.dat* containing the centroid velocities saved along the trajectory. The format of these files is identical to that of a classical MD simulation (*mdcrd* and *mdvel*), and the frequency with which these information are saved is determined by *ntpr*. The *mdin* input is the same as for a regular (classical MD) run. However, additional flags are required as described below.

In order to perform CMD simulations the following flags are required in the *mdin* file:

**ipimd** Flag for the different methodologies based on the path-integral formalism. See Section 5.1.2 for the other values.

= 3 defines CMD.

**adiab\_param** This defines the so-called adiabaticity parameter ( $\gamma$ ) used to make the fictitious masses of the non-zero frequency normal modes small enough to decouple their motion from that of the centroid. It has been shown that  $\gamma \leq 1/2P$  (where  $P$  is the total number of beads) is sufficiently small to get converged results. As a consequence of this, a smaller timestep is required. During the equilibration run (see below) you must carefully check that the timestep employed is small enough to guarantee the energy conservation of the extended system reported in the *NHC.dat* file (see Section 5.1.2). Default is 1, but you need to specify this, since default value is not appropriate.

**ntt** Switch for temperature scaling.

= 4 defines Nosé-Hoover chains of thermostats. It also requires the number of thermostats in a chain (*nchain*). For CMD, Nosé-Hoover chains of thermostats must be attached to each non-zero frequency normal mode.

**nchain** = 2-8 number of thermostats in each Nosé-Hoover chain of thermostats (default 2, recommended  $\geq 4$ ).

**eq\_cmd** This flag must be used during the CMD equilibration to generate a canonical distribution of the centroid variables before an actual CMD run. Default is .false.

restart\_cmd Flag necessary for restarting a CMD simulation.

In order to run a CMD simulation, you must first generate an equilibrated quantum configuration of your system using NMPIMD (see Section 5.1.2). A canonical distribution of the centroid variables must then be obtained from a CMD simulation with the *equilib\_cmd* flag on. After this equilibration, the final configuration is then used as initial configuration for the actual CMD simulation. For restarting a CMD run the *restart\_cmd* flag in the *mdin* file is required.

Importantly, for CMD simulations it is necessary that *ntb=1*, which is the default value.

### 5.2.2. Examples

In the following examples of input files for CMD are shown. You are also encouraged to check the test cases in \$AMBERHOME/test/PIMD.

a) *CMD for sander.LES. Equilibration of the centroid variables.*

Test: \$AMBERHOME/test/PIMD/part\_cmd\_water/equilib.

```

ipimd = 3          ! CMD
ntx = 5,  irest = 0
ntb = 1
temp0 = 298.15,  tempi = 298.15,  temp0les = -1.
cut = 7.0
ntt = 4,  nchain = 4.          ! Nose'-Hoover chains
dt = 0.00005,  nstlim = 100
eq_cmd = .true.          ! equilibration for CMD
adiab_param = 0.5      ! adiabaticity parameter
ntpr = 20,  ntwr = 20

```

b) *CMD input for sander.LES. Start of an actual CMD simulation after equilibration.*

Test: \$AMBERHOME/test/PIMD/part\_cmd\_water/start.

```

ipimd = 3          ! CMD
ntx = 5,  irest = 1
ntb = 1
temp0 = 298.15,  tempi = 298.15,  temp0les = -1.
cut = 7.0
ntt = 4,  nchain = 4.          ! Nose'-Hoover chains
dt = 0.00005,  nstlim = 100
eq_cmd = .false.        ! actual CMD
adiab_param = 0.5      ! adiabaticity parameter
ntpr = 20,  ntwr = 20

```

c) *CMD input for sander.LES. Restart of an actual CMD.*

Test: \$AMBERHOME/test/PIMD/part\_cmd\_water/restart.

## 5. Quantum dynamics

```
ipimd = 3          ! CMD
ntx = 5,  irest = 1
ntb = 1
temp0 = 298.15,  tempi = 298.15,  temp0les = -1.
cut = 7.0
ntt = 4,  nchain = 4.          ! Nose'-Hoover chains
dt = 0.00005,  nstlim = 100
eq_cmd = .false.          ! actual CMD
restart_cmd = .true.      ! restart
adiab_param = 0.5        ! adiabaticity parameter
ntpr = 20,  ntwr = 20
```

### 5.3. Ring Polymer Molecular Dynamics (RPMD)

The implementation of RPMD and the necessary input/output files are identical to those of PRIMPIMD (see Section 5.1.2). The *mdin* input is the same as for a PRIMPIMD with only few differences described below.

#### 5.3.1. Input parameters

In order to perform RPMD the following flags are required in the *mdin* file:

**ipimd**      Flag for the different methodologies based on the path-integral formalism. See Section 5.1.2 for the other values.

    = 4 defines RPMD.

**ntt**         Set this to 0, for constant energy dynamics

**nscm**       Set this to 0, to avoid removing translational and rotational center-of-mass motion.

You must first generate an equilibrated quantum configuration of your system using PRIMPIMD (see Section 5.1.2), which is then used as initial configuration for the actual RPMD simulation.

#### 5.3.2. Examples

In the following examples of input files for RPMD are shown. You are also encouraged to check the test cases in \$AMBERHOME/test/PIMD.

a) RPMD input for *sander.LES*.

Test: \$AMBERHOME/test/PIMD/part\_rpmd\_water.

```
ipimd = 4          ! RPMD
ntx = 5,  irest = 0
ntt = 0
nscm = 0
```



## 5.4. Linearized semiclassical initial value representation

```
temp0 = 300., temp0les = -1.
cut = 7.0
dt = 0.0002, nstlim = 10
ntpr = 1, ntwr = 5, ntwx = 1, ntwv = 1
```

## 5.4. Linearized semiclassical initial value representation

### 5.4.1. Experimental observables and thermal correlation functions

Most quantities of interest in the dynamics of complex systems can be expressed in terms of thermal time autocorrelation functions [212], which are of the form

$$C_{AB}(t) = \frac{1}{Z} \text{Tr} \left( \hat{A}^\beta e^{i\hat{H}t/\hbar} \hat{B} e^{-i\hat{H}t/\hbar} \right) \quad (5.12)$$

where  $\hat{A}_{std}^\beta = e^{-\beta\hat{H}}\hat{A}$  for the standard version of the correlation function, or  $\hat{A}_{sym}^\beta = e^{-\beta\hat{H}/2}\hat{A}e^{-\beta\hat{H}/2}$  for the symmetrized version [213], or

$$\hat{A}_{Kubo}^\beta = \frac{1}{\beta} \int_0^\beta d\lambda e^{-(\beta-\lambda)\hat{H}} \hat{A} e^{-\lambda\hat{H}} \quad (5.13)$$

for the Kubo-transformed version [214]. These three versions are related to one another by the following identities between their Fourier transforms,

$$\frac{\beta\hbar\omega}{1 - e^{-\beta\hbar\omega}} I_{AB}^{Kubo}(\omega) = I_{AB}^{std}(\omega) = e^{\beta\hbar\omega/2} I_{AB}^{sym}(\omega) \quad (5.14)$$

where

$$I_{AB}(\omega) = \int_{-\infty}^{\infty} dt e^{-i\omega t} C_{AB}(t) \quad (5.15)$$

is the partition function and  $\hat{H}$  the (time-independent) Hamiltonian of the system, and  $\hat{A}$  and  $\hat{B}$  are operators relevant to the specific property of interest.

### 5.4.2. Linearized semiclassical initial value representation

The Semiclassical initial value representation (SC-IVR) approximates the forward (backward) time evolution operator  $e^{-i\hat{H}t/\hbar}$  ( $e^{i\hat{H}t/\hbar}$ ) by a phase space average over the initial conditions of forward (backward) classical trajectories [215, 216]. By making the approximation that the dominant contribution to the phase space averages comes from forward and backward trajectories that are infinitesimally close to one another, and then linearizing the difference between the forward and backward actions (and other quantities in the integrand), Miller and coworkers [217, 218] obtained the LSC-IVR, or classical Wigner model for the correlation function in Eq. (5.12),

$$C_{AB}^{LSC-IVR}(t) = Z^{-1} (2\pi\hbar)^{-N} \int d\mathbf{x}_0 \int d\mathbf{p}_0 A_w^\beta(\mathbf{x}_0, \mathbf{p}_0) B_w(\mathbf{x}_t, \mathbf{p}_t) \quad (5.16)$$

## 5. Quantum dynamics

where  $A_w^\beta$  and  $B_w$  are the Wigner functions corresponding to these operators,

$$O_w(\mathbf{x}, \mathbf{p}) = \int d\mathbf{x} \langle \mathbf{x} - \Delta\mathbf{x}/2 | \hat{O} | \mathbf{x} + \Delta\mathbf{x}/2 \rangle e^{i\mathbf{p}^T \Delta\mathbf{x}/\hbar} \quad (5.17)$$

for any operator  $\hat{O}$ . Here  $N$  is the number of degrees of freedom in the system, and  $(\mathbf{x}_0, \mathbf{p}_0)$  is the set of initial conditions (i.e., coordinates and momenta) for a classical trajectory,  $(\mathbf{x}(\mathbf{x}_0, \mathbf{p}_0), \mathbf{p}_t(\mathbf{x}_0, \mathbf{p}_0))$  being the phase point at time along this trajectory. It should also be noted that there are other approximate routes which lead to the classical Wigner model for correlation functions (other than simply postulating it). [Please see Section II-A of Ref. [219] or Section III-A of Ref. [220] for more discussion.] The LSC-IVR can be shown to be exact in the classical limit ( $\hbar \rightarrow 0$ ), high temperature limit ( $\beta \rightarrow 0$ ), and harmonic limit [221]. The LSC-IVR can treat both linear and nonlinear operators in a consistent way [222], can be applied to non-equilibrium as well as the above equilibrium correlation functions, and can also be used to describe electronically non-adiabatic dynamics, i.e., processes involving transitions between several potential energy surfaces. These merits of the LSC-IVR make it a versatile tool to study a variety of quantum mechanical effects in chemical dynamics of large molecular systems.

### 5.4.3. Local Gaussian approximation

Calculation of the Wigner function for operator  $\hat{B}$  in Eq. (5.16) is usually straight-forward; in fact, is often a function only of coordinates or only of momenta, in which case its Wigner functions is simply the classical function itself. Calculating the Wigner function for operator  $A^\beta$  however, involves the Boltzmann operator with the total Hamiltonian of the complete system, so that carrying out the multidimensional Fourier transform to obtain it is far from trivial. Furthermore, it is necessary to do this in order to obtain the distribution of initial conditions of momenta for the real time trajectories. To accomplish this task, the local Gaussian approximation (LGA) proposed by Liu and Miller [219], which can be viewed as an improved version of the local harmonic approximation (LHA), [223] and which is able to consistently treat the entire imaginary frequency regime, has been implemented in Amber. Below we briefly summarize the LGA. As in the standard normal-mode analysis, mass-weighted Hessian matrix elements are given by

$$H_{kl} = \frac{1}{\sqrt{m_k m_l}} \frac{\partial^2 V}{\partial x_k \partial x_l} \quad (5.18)$$

where  $m_k$  represent the mass of the  $k$ -th degree of freedom. The eigenvalues of the mass-weighted Hessian matrix produce normal-mode frequencies  $\{\omega_k\}$  i.e.,

$$\mathbf{THT} = \lambda \quad (5.19)$$

with  $\lambda$  a diagonal matrix with the elements  $\{(\omega_k)^2\}$  and  $\mathbf{T}$  an orthogonal matrix. If  $\mathbf{M}$  is the diagonal ‘mass matrix’ with elements  $\{m_k\}$ , then the mass-weighted normal mode coordinates and momenta  $(\mathbf{X}_0, \mathbf{P}_0)$  are given in terms of the Cartesian variables  $(\mathbf{x}_0, \mathbf{p}_0)$  by

$$\mathbf{X}_0 = \mathbf{T}^T \mathbf{M}^{1/2} \mathbf{x}_0 \quad (5.20)$$

and

$$\mathbf{P}_0 = \mathbf{T}^T \mathbf{M}^{-1/2} \mathbf{p}_0 \quad (5.21)$$

The Fourier transform of Eq. (5.17) then gives the Wigner function of as

$$\begin{aligned} A_w^\beta(\mathbf{x}_0, \mathbf{p}_0) &= (2\pi\hbar)^N \langle \mathbf{x}_0 | e^{-\beta\hat{H}} | \mathbf{x}_0 \rangle \\ &\times \prod_{k=1}^N \left[ \left( \frac{\beta}{2\pi Q(u_k)} \right)^{1/2} \exp \left[ -\beta \frac{(P_{0,k})^2}{2Q(u_k)} \right] \right] f_A(\mathbf{x}_0, \mathbf{p}_0) \end{aligned} \quad (5.22)$$

where  $u_k = \beta\hbar\omega_k$ ,  $P_{0,k}$  is the k-th component of the mass-weighted normal-mode momentum in Eq. (5.21) and the quantum correction factor is given by

$$Q(u) = \begin{cases} \frac{u/2}{\tanh(u/2)} & \text{for real } u \\ = \frac{1}{Q(u_i)} = \frac{\tanh(u_i/2)}{u_i/2} & \text{for imaginary } u \ (u = iu_i) \end{cases} \quad (5.23)$$

In Eq. (5.22),

$$f_A(\mathbf{x}_0, \mathbf{p}_0) = \frac{\int d\mathbf{x} \frac{\langle \mathbf{x}_0 - \frac{\Delta\mathbf{x}}{2} | \hat{A}^\beta | \mathbf{x}_0 + \frac{\Delta\mathbf{x}}{2} \rangle}{\langle \mathbf{x}_0 | e^{-\beta\hat{H}} | \mathbf{x}_0 \rangle} e^{i\Delta\mathbf{x}^T \cdot \mathbf{p}_0 / \hbar}}{\int d\Delta\mathbf{x} \frac{\langle \mathbf{x}_0 - \frac{\Delta\mathbf{x}}{2} | e^{-\beta\hat{H}} | \mathbf{x}_0 + \frac{\Delta\mathbf{x}}{2} \rangle}{\langle \mathbf{x}_0 | e^{-\beta\hat{H}} | \mathbf{x}_0 \rangle} e^{i\Delta\mathbf{x}^T \cdot \mathbf{p}_0 / \hbar}} \quad (5.24)$$

is a function depending on the operator  $\hat{A}^\beta$ . For example, when  $\hat{A}^\beta = e^{-\beta\hat{H}} \hat{\mathbf{x}}$ , one has

$$f_A(\mathbf{x}_0, \mathbf{p}_0) = \mathbf{x}_0 + \frac{i\beta\hbar}{2} \mathbf{M}^{-1/2} \mathbf{T} \mathbf{Q}(\mathbf{u})^{-1} \mathbf{P}_0 \quad (5.25)$$

where is the diagonal quantum correction factor matrix with the elements  $\{Q_k \equiv Q(u_k)\}$ . Using Eq. (5.24), one can figure out the quantity  $f_A(\mathbf{x}_0, \mathbf{p}_0)$  for different operators  $\hat{A}^\beta$ .

The explicit form of LSC-IVR correlation function (Eq. (5.16)) with the LGA is thus given by

$$\begin{aligned} C_{AB}^{LSC-IVR}(t) &= \frac{1}{Z} \int d\mathbf{x}_0 \langle \mathbf{x}_0 | e^{-\beta\hat{H}} | \mathbf{x}_0 \rangle \int d\mathbf{P}_0 \prod_{k=1}^N \left[ \left( \frac{\beta}{2\pi Q(u_k)} \right)^{1/2} \exp \left[ -\beta \frac{(P_{0,k})^2}{2Q(u_k)} \right] \right] \\ &\times f_A(\mathbf{x}_0, \mathbf{p}_0) B(\mathbf{x}_t, \mathbf{p}_t) \end{aligned} \quad (5.26)$$

Please refer to Refs. [219] and [220] for more detail about the LSC-IVR and the LGA.

#### 5.4.4. Input parameters for LSC-IVR in Amber

In order to perform LSC-IVR in Amber, two additional flags should be added in the regular input script file for classical molecular dynamics.

## 5. Quantum dynamics

ilscivr      Flag for LSC-IVR  
               =1 defines LSC-IVR

icorf\_lsc    Switch for different kinds of correlation functions. It only affects the output files for LSC-IVR.  
               =1 defines the linear operator  $\hat{A} = \hat{\mathbf{x}}$  or  $\hat{A}^\beta = e^{-\beta\hat{H}}\hat{\mathbf{x}}$  ;  
               =2 defines the linear operator  $\hat{A} = \hat{\mathbf{p}}$  or  $\hat{A}^\beta = e^{-\beta\hat{H}}\hat{\mathbf{p}}$   
               =3 defines any nonlinear operator;  
               =4 defines Kubo-transformed operator  $\hat{\mathbf{p}}_{Kubo}^\beta = \frac{1}{\beta} \int_0^\beta d\lambda e^{-(\beta-\lambda)\hat{H}}\hat{\mathbf{p}}e^{-\lambda\hat{H}}$

Besides the above two parameters, a file ‘LSCrhoa.dat’ is necessary. Put any integer between 0 and 10000 in the file. This parameter (*nrand*) is used for generating the initial random number for LSC-IVR. As the number of trajectories for LSC-IVR is increased, it will automatically be updated. For example, prepare the input file ‘lsc.in’ for running a LSC-IVR trajectory in Amber with liquid water (216 water molecules in a cell with the periodic boundary condition) with the q-SPC/fw model.

```
&cntrl
  ilscivr = 1, icorflsc = 4, ntt = 0, irect = 0, temp0 = 298.15,
  dt = 0.0005, nstlim = 2800, ntb = 1, jfastw = 4, ntpr = 1, cut = 7.0,
  ntwx = 1 ntwv = 1 ntx = 1
/
&ewald skinnb=2.0d0 /
```

As one can see, except the first two parameters for LSC-IVR, all other parameters in the input file ‘lsc.in’ are the same as those in conventional molecular dynamics. Besides ‘lsc.in’, another input file ‘lsc.crd’ for the initial coordinates of the system should be prepared (i.e., from one of the path integral bead). For instance, the command to run a parallel job with 2 processors for LSC-IVR in Amber is

```
mpirun -np 2 sander.MPI -O -i lsc.in -p watqspcfw216.top -c lsc.crd -o lsc.out
```

Here ‘lsc.out’ is the output file to monitor the trajectory as the one for molecular dynamics. After running the above command once, the file ‘LSCrhoa.dat’ will be updated. The first number is *nrand*, which will be increased by one ( $nrand = nrand + 1$ ). Followed are the initial coordinates and momenta for the trajectories. If one sets *icorf\_lsc* =4, then the function  $f_A(\mathbf{x}_0, \mathbf{p}_0)$  for  $\hat{\mathbf{p}}_{Kubo}^\beta$  will also be written into the file ‘LSC-rhoa.dat’. If *icorf\_lsc* =3, then the quantum correction factor and the matrix that diagonalizes the Hessian matrix are recorded in another file ‘LSCtmat.dat’, which allows  $f_A(\mathbf{x}_0, \mathbf{p}_0)B(\mathbf{x}_t, \mathbf{p}_t)$  to be evaluated for any nonlinear operators. 2) Evaluate correlation functions using LSC-IVR in Amber One may summarize the specific procedure for carrying out LSC-IVR calculation for quantum correlation functions (i.e., Eq. (13)) as follows:

1. Use path integral molecular dynamics (PIMD) in Amber to simulate the system at equilibrium.  $\langle \mathbf{x}_0 | e^{-\beta\hat{H}} | \mathbf{x}_0 \rangle / Z$  is evaluated by the PIMD.

## 5.4. Linearized semiclassical initial value representation

Illustration of the LSC-IVR

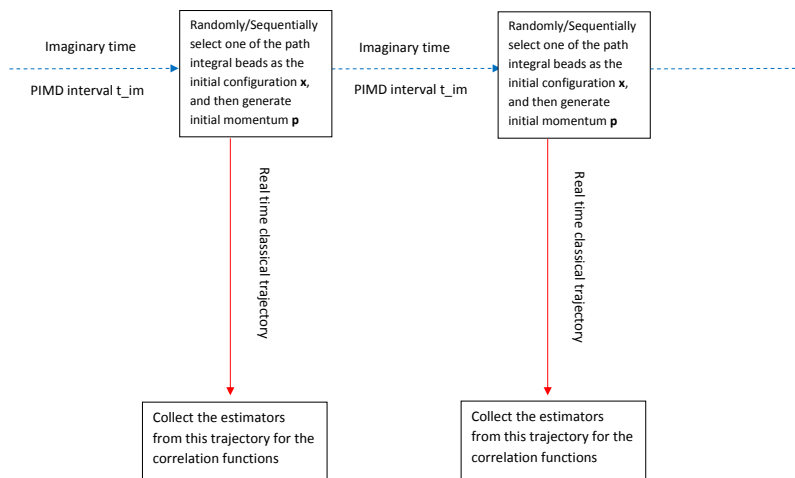


Figure 5.1.: Flow chart for LSC-IVR.

- At specific time steps in the PIMD, randomly select one path integral bead as the initial configuration for the real time dynamics in LSC-IVR.
- LSC-IVR in Amber diagonalizes the mass-weighted Hessian matrix of the potential surface to obtain the local normal mode frequencies and uses the LGA to give the Gaussian distribution for mass-weighted normal mode momenta

$$\prod_{k=1}^N (\beta/2\pi Q(u_k))^{1/2} \exp \left[ -\beta (P_{0,k})^2 / (2Q(u_k)) \right]$$

which is used to randomly sample initial Cartesian momentum  $\mathbf{p}_0 = \mathbf{M}^{1/2} \mathbf{T} \mathbf{P}_0$  for the real time trajectory. Notice the parameter *nrand* in the file ‘LSCrhoa.dat’ is used. LSC-IVR in Amber further runs a trajectory from the phase space point  $(\mathbf{x}_0, \mathbf{p}_0)$ . As in conventional molecular dynamics, the output files ‘mdcrd’ and ‘mdvel’ record the trajectory  $(\mathbf{x}_t(\mathbf{x}_0, \mathbf{p}_0), \mathbf{p}_t(\mathbf{x}_0, \mathbf{p}_0))$ . The parameter *nrand* is updated in the file ‘LSCrhoa.dat’, with the initial phase point  $(\mathbf{x}_0, \mathbf{p}_0)$  the mass, and  $f_A(\mathbf{x}_0, \mathbf{p}_0)$  for  $\hat{\mathbf{p}}_{Kubo}^\beta$ , etc. The file ‘LSCTmat.dat’ may also be created for the quantum correction factor and the matrix.

- The property

$$f_A(\mathbf{x}_0, \mathbf{p}_0) B(\mathbf{x}_t(\mathbf{x}_0, \mathbf{p}_0), \mathbf{p}_t(\mathbf{x}_0, \mathbf{p}_0))$$

for the corresponding time correlation function can be evaluated for the trajectory with the output files (mdcrd, mdvel, LSCrhoa.dat and LSCTmat.dat). One can write a short program in order to do so.

## 5. Quantum dynamics

5. Repeat steps 2)-4) and sum the property

$$f_A(\mathbf{x}_0, \mathbf{p}_0) B(\mathbf{x}_t(\mathbf{x}_0, \mathbf{p}_0), \mathbf{p}_t(\mathbf{x}_0, \mathbf{p}_0))$$

for all real time classical trajectories until a converged result is obtained. It is worth noting that one can also sequentially select one path integral bead as the initial configuration in Step 2) each turn. Also in Step 4), one can simultaneously evaluate different

$$f_A(\mathbf{x}_0, \mathbf{p}_0) B(\mathbf{x}_t(\mathbf{x}_0, \mathbf{p}_0), \mathbf{p}_t(\mathbf{x}_0, \mathbf{p}_0))$$

for different correlation functions.

Here we give an example for the script file to get one real time trajectory in LSC-IVR for the water system already at equilibrium. (216 water molecules in a cell with the periodic boundary condition, 24 path integral beads used for the PIMD).

```
## This is to run PIMD for short time
mpirun -np 24 sander.MPI -ng 24 -groupfile gfpimd > sander.out
## Copy the configuration of one path integral bead
cd ..
cp -p PIMD/pimdbead1.rst LSC/lsc.crd
## This is to run LSC to get a real time trajectory
cd LSC
mpirun -np 2 sander.MPI -O -i lsc.in -p watqspcfw216.top -c lsc.crd -o lsc.out
## a.out is the executable file that the user writes to calculate
## for correlation functions of his/her own interest
./a.out
```

Here the file 'gfpimd' is like

```
-O -i pimd.in -p watqspcfw216.top -c pimdbead1.rst -o pimdbead1.out
-r pimdbead1.rst -pimdout pimd.out
-O -i pimd.in -p watqspcfw216.top -c pimdbead2.rst -o pimdbead2.out
-r pimdbead2.rst -pimdout pimd.out
.....
-O -i pimd.in -p watqspcfw216.top -c pimdbead24.rst -o pimdbead2.out
-r pimdbead2.rst -pimdout pimd.out
```

For collecting many LSC-IVR trajectories, one can repeatedly use the commands in the script file with the only change for sequentially copying a path integral bead for the initial configuration for LSC-IVR, i.e.,

```
cp -p PIMD/pimdbead*.rst LSC/lsc.crd
```

Here '\*' is replaced by one of the numbers 1-24 each time circularly.

All the force fields available for conventional molecular dynamics in Amber can be used for LSC-IVR. However, one should also keep in mind that some empirical force fields may require additional reparameterization (such as q-SPC/fw for SPC/fw) for approximated quantum dynamical methods such as LSC-IVR, CMD and RPMD.

## 5.5. Reactive Dynamics

### 5.5.1. Path integral quantum transition state theory

The path integral quantum transition state theory rate [224] is given by

$$k_{\text{PI-QTST}} = 1/2 \left\langle \left| \dot{\xi} \right| \right\rangle_{\xi^\ddagger} \rho_c(\xi^\ddagger) \quad (5.27)$$

where the centroid density

$$\rho_c(\xi) = \frac{\int d\mathbf{r}^{(1)} d\mathbf{r}^{(2)} \dots d\mathbf{r}^{(P)} \exp[-\beta\Phi(\mathbf{r}^{(1)}, \dots, \mathbf{r}^{(P)})] \delta[\tilde{\xi}_c(\mathbf{r}^{(1)}, \dots, \mathbf{r}^{(P)}) - \xi]}{\int d\mathbf{r}^{(1)} d\mathbf{r}^{(2)} \dots d\mathbf{r}^{(P)} \exp[-\beta\Phi(\mathbf{r}^{(1)}, \dots, \mathbf{r}^{(P)})] h[\xi^\ddagger - \tilde{\xi}_c(\mathbf{r}^{(1)}, \dots, \mathbf{r}^{(P)})]} \quad (5.28)$$

is related to the potential of mean force  $w(\xi)$  as

$$\rho_c(\xi) = \frac{\exp[-\beta w(\xi)]}{\int_{-\infty}^{\xi^\ddagger} d\xi \exp[-\beta w(\xi)]} \quad (5.29)$$

In Eq. (5.28),  $\beta = 1/k_B T$ ,  $\Phi$  is the effective potential (see Eqs. 5.8 and 5.49),  $h$  is the Heaviside step function,  $\xi^\ddagger$  is the location of the dividing surface that partitions the reactant and product regions and  $\tilde{\xi}_c$  is the value of the reaction coordinate as a function of the centroid coordinates  $\mathbf{r}^{(c)} = \frac{1}{P} \sum_{s=1}^P \mathbf{r}^{(s)}$ . As Eq. (5.29) suggests, the centroid density factor can be computed using umbrella sampling approaches to generate a set of biased distributions that then can be combined into a PMF using the WHAM approach [108–110]. The dynamical frequency factor can be approximated by the velocity of a free particle along the reaction coordinate direction

$$\left\langle \left| \dot{\xi} \right| \right\rangle_{\xi^\ddagger} = \left( \frac{2}{\pi\beta} \right)^{1/2} \left\langle \left( \sum_{i=1}^{3N} \frac{1}{m_i} \left( \frac{\partial \tilde{\xi}_c}{\partial r_i^{(c)}} \right)^2 \right)^{1/2} \right\rangle_{\xi^\ddagger} \quad (5.30)$$

where  $\langle \dots \rangle_{\xi^\ddagger}$  denotes the conditional average computed at the dividing surface  $\xi^\ddagger$ . Both factors in the PI-QTST rate expression can be computed using the EVB/LES-PIMD facility in Amber (see Section 3.4.4). The value of the centroid reaction coordinate and the velocity of a free particle along the centroid RC direction are written to the file *evbout* (see Section E). To output  $\left| \dot{\xi} \right|$ , set the variable `out_RCdot = .true.` in the EVB input file.

### 5.5.2. Quantum Instanton

The Quantum Instanton (QI) is a theoretical approach for computing thermal reaction rates in complex molecular systems, which is related to an older semiclassical (SC) theory of reaction rates that came to be known as the “instanton” approximation[225]. The SC instanton approximation is based on a SC approximation for the Boltzmann operator,  $\exp(-\beta H)$ , which involves a classical periodic orbit in pure imaginary time (or equivalently in real time on the

## 5. Quantum dynamics

upside-down potential energy surface) plus harmonic fluctuations about it[225]. The essential feature of the QI rate constant [226] is that it is expressed wholly in terms of the quantum Boltzmann operator, which can be evaluated for complex molecular systems using the path-integral methods described in Sec. 5.1.

In the following we will briefly illustrate the basic principles, and we will derive the fundamentals of the QI approach. We strongly recommend the user to consult the relevant literature for a more rigorous description[226, 227].

The derivation begins with the following formally exact expression of the quantum mechanical thermal rate constant[225]:

$$k(T)Q_r(T) \equiv kQ_r = \frac{1}{2\pi\hbar} \int dE e^{-\beta E} N(E), \quad (5.31)$$

where  $Q_r(T)$  is the reactant partition function per unit volume at temperature  $T$ ,  $\beta$  is the inverse temperature  $1/k_B T$ , and  $N(E)$  is the cumulative reaction probability at total energy  $E$ [213]:

$$N(E) = \frac{(2\pi\hbar)^2}{2} \text{tr} [\hat{F}_a \delta(E - \hat{H}) \hat{F}_b \delta(E - \hat{H})]. \quad (5.32)$$

In Eq. 5.32 the flux operators  $\hat{F}_a$  and  $\hat{F}_b$  are defined by

$$\hat{F}_\gamma = \frac{i}{\hbar} [\hat{H}, h(\xi_\gamma(\mathbf{q}))], \quad (5.33)$$

where  $\gamma = a, b$ ,  $h(\xi_\gamma)$  is the Heaviside function, and  $\hat{H}$  is the Hamiltonian of the system. We note that Eqs. 5.32 and 5.33 involve two dividing surfaces  $\xi_a(\mathbf{q}) = 0$  and  $\xi_b(\mathbf{q}) = 0$ . The microcanonical density operator  $\delta(E - \hat{H})$  in Eq. 5.32 as well as the integral over the total energy in Eq. 5.31 can be computed using a semiclassical approximation, which results in the following quantum instanton expression for the rate constant:

$$k \simeq k_{QI} \equiv \frac{1}{Q_r} C_{ff}(0) \frac{\sqrt{\pi} \hbar}{2 \Delta H}. \quad (5.34)$$

In Eq. 5.34,  $C_{ff}(0)$  is the zero time value of the flux-flux correlation function generalized to the case of two separate dividing surfaces,

$$C_{ff}(t) = \text{tr} \left[ e^{-\beta \hat{H}/2} \hat{F}_a e^{-\beta \hat{H}/2} e^{i\hat{H}t/\hbar} \hat{F}_b e^{-i\hat{H}t/\hbar} \right], \quad (5.35)$$

and  $\Delta H$  is a specific type of energy variance given by

$$\Delta H^2 = \frac{\text{tr} \left[ \hat{\Delta}_a e^{-\beta \hat{H}/2} \hat{H}^2 \hat{\Delta}_b e^{-\beta \hat{H}/2} \right] - \text{tr} \left[ \hat{\Delta}_a e^{-\beta \hat{H}/2} \hat{H} \hat{\Delta}_b e^{-\beta \hat{H}/2} \hat{H} \right]}{\text{tr} \left[ \hat{\Delta}_a e^{-\beta \hat{H}/2} \hat{\Delta}_b e^{-\beta \hat{H}/2} \right]} \quad (5.36)$$

with  $\hat{\Delta}_a$  and  $\hat{\Delta}_b$  being a modified version of the Dirac delta function:

$$\hat{\Delta}_\gamma = \Delta(\xi_\gamma(\hat{\mathbf{q}})) \equiv \delta(\xi_\gamma(\hat{\mathbf{q}})) | m^{-1/2} \nabla \xi_\gamma(\hat{\mathbf{q}}) | \quad (5.37)$$

where  $\gamma = a, b$ . It has been shown that  $\Delta H$  can also be expressed in terms of the ‘‘delta-delta’’



correlation function[227].

The QI rate constant [Eq. (5.34)] can be rewritten in the form [227]

$$k_{QI} = \frac{C_{dd}(0)}{Q_r} \left\{ \frac{C_{ff}(0)}{C_{dd}(0)} \frac{\sqrt{\pi}}{2} \frac{\hbar}{\Delta H} \right\} \quad (5.38)$$

where

$$\frac{C_{dd}(0; \xi_a, \xi_b)}{Q_r} = \frac{\int d\mathbf{r}^{(1)} d\mathbf{r}^{(2)} \dots d\mathbf{r}^{(P)} \exp[-\beta\Phi(\mathbf{r}^{(1)}, \dots, \mathbf{r}^{(P)})] \delta[\tilde{\xi}(\mathbf{r}^{(P)}) - \xi_a] \delta[\tilde{\xi}(\mathbf{r}^{(P/2)}) - \xi_b]}{\int d\mathbf{r}^{(1)} d\mathbf{r}^{(2)} \dots d\mathbf{r}^{(P)} \exp[-\beta\Phi(\mathbf{r}^{(1)}, \dots, \mathbf{r}^{(P)})] h[\xi_a^\ddagger - \tilde{\xi}(\mathbf{r}^{(P)})] h[\xi_b^\ddagger - \tilde{\xi}(\mathbf{r}^{(P/2)})]} \quad (5.39)$$

$$C_{ff}(0)/C_{dd}(0) = \left\langle f_v(\mathbf{r}^{(1)}, \dots, \mathbf{r}^{(P)}) \right\rangle_{\xi_{(P)}^\ddagger, \xi_{(P/2)}^\ddagger} \quad (5.40)$$

$$\Delta H^2 = \frac{1}{2} \left\langle F(\mathbf{r}^{(1)}, \dots, \mathbf{r}^{(P)})^2 + G(\mathbf{r}^{(1)}, \dots, \mathbf{r}^{(P)}) \right\rangle_{\xi_{(P)}^\ddagger, \xi_{(P/2)}^\ddagger} \quad (5.41)$$

The conditional average  $\langle \dots \rangle_{\xi_{(P)}^\ddagger, \xi_{(P/2)}^\ddagger}$  is computed from the ensemble sampled with the  $P$  and  $P/2$  slices constrained to the dividing surface

$$\langle \dots \rangle_{\xi_{(P)}^\ddagger, \xi_{(P/2)}^\ddagger} = \frac{\int d\mathbf{r}^{(1)} d\mathbf{r}^{(2)} \dots d\mathbf{r}^{(P)} \exp[-\beta\Phi(\mathbf{r}^{(1)}, \dots, \mathbf{r}^{(P)})] \delta[\tilde{\xi}(\mathbf{r}^{(P)}) - \xi_a] \delta[\tilde{\xi}(\mathbf{r}^{(P/2)}) - \xi_b] \times (\dots)}{\int d\mathbf{r}^{(1)} d\mathbf{r}^{(2)} \dots d\mathbf{r}^{(P)} \exp[-\beta\Phi(\mathbf{r}^{(1)}, \dots, \mathbf{r}^{(P)})] \delta[\tilde{\xi}(\mathbf{r}^{(P)}) - \xi_a] \delta[\tilde{\xi}(\mathbf{r}^{(P/2)}) - \xi_b]}$$

where the quantities within the average (for the simple case of a single quantized nuclear particle) are defined as follows:

$$f_v(\mathbf{r}^{(1)}, \dots, \mathbf{r}^{(P)}) = m \left( \frac{iP}{2\hbar\beta} \right)^2 \nabla \xi_a(\mathbf{r}^{(P)}) \cdot (\mathbf{r}^{(1)} - \mathbf{r}^{(P-1)}) \times \nabla \xi_b(\mathbf{r}^{(P/2)}) \cdot (\mathbf{r}^{(P/2+1)} - \mathbf{r}^{(P/2-1)}) \quad (5.42)$$

$$F(\mathbf{r}^{(1)}, \dots, \mathbf{r}^{(P)}) = -\frac{mP}{\hbar^2\beta^2} \left\{ \sum_{k=1}^{P/2} - \sum_{k=P/2+1}^P \right\} (\mathbf{r}^{(k)} - \mathbf{r}^{(k-1)})^2 + \frac{2}{P} \left\{ \sum_{k=1}^{P/2-1} - \sum_{k=P/2+1}^{P-1} \right\} V(\mathbf{r}^{(k)}) \quad (5.43)$$

$$G(\mathbf{r}^{(1)}, \dots, \mathbf{r}^{(P)}) = \frac{2dP}{\beta^2} - \frac{4mP}{\hbar^2\beta^3} \sum_{k=1}^P (\mathbf{r}^{(k)} - \mathbf{r}^{(k-1)})^2 \quad (5.44)$$

All factors needed to calculate the QI rate can be obtained from the EVB/LES-PIMD facility in Amber (see Section 3.4.4). For example, the joint distribution function [Eq. (5.39)] is computed using umbrella sampling along the reaction coordinates of the  $P$  and  $P/2$  slices.

## 5. Quantum dynamics

The DG EVB input file of the RS malonaldehyde system may contain the following specifications:

```
&evb nevb = 2, nUFF = 1, nbias = 2, ntw_evb = 50,
dia_type = "ab_initio",
xch_type = "dist_gauss",
evb_dyn = "qi_dbonds_pmf",
dia_shift(1)%st = 1, dia_shift(1)%nrg_offset = 0.0,
dia_shift(2)%st = 2, dia_shift(2)%nrg_offset = 0.0,
dbonds_umb(1)%iatom = 8, dbonds_umb(1)%jatom = 9, dbonds_umb(1)%katom = 7,
dbonds_umb(1)%k = 100.0, dbonds_umb(1)%ezero = -.20,
dbonds_umb(2)%iatom = 8, dbonds_umb(2)%jatom = 9, dbonds_umb(2)%katom = 7,
dbonds_umb(2)%k = 100.0, dbonds_umb(2)%ezero = .40,
dist_gauss%stype = "no_dihedrals",
dist_gauss%lin_solve = "diis",
dist_gauss%xfile_type = "gaussian_fchk",
ts_xfile(1) = "malonaldehydeTS_35.fchk",
min_xfile(1) = "malonaldehydeR_35.fchk",
min_xfile(2) = "malonaldehydeP_35.fchk",
dgpt_alpha(1) = 0.72,
dgpt_alpha(2) = 0.72,
dgpt_alpha(3) = 0.72,
UFF(1)%iatom = 7, UFF(1)%jatom = 9
/
```

where the variable **evb\_dyn = "qi\_dbonds\_pmf"** requests biased sampling along a difference of distances RC on the  $P$  and  $P/2$  slices whose umbrella parameters are specified in **dbonds\_umb(:)**. Input specifications for the PS malonaldehyde system is identical to the above, except that the UFF atom pair has been changed to reflect the product topology (see Section 3.4.5). A set of 2-dimensional (2D) biased simulations, each enhancing the sampling near a particular point of the 2D ( $\xi_P \times \xi_{P/2}$ ) configuration space is required to map out the QI joint distribution. Using the WHAM procedure, the generated biased distributions can be unbiased to form  $C_{dd}(0)/Q_r$  on the EVB ground-state surface  $V_{el0}$ . All remaining factors involve conditional averages of  $f_v$ ,  $F$  and  $G$ . These quantities are computed using umbrella sampling with the  $P$  and  $P/2$  slices constrained to the dividing surface  $\xi^{\ddagger} = 0.0$  and are written to the *evbout* file (see Section E). The corresponding EVB input file is identical to the above, but with the following modifications:

```
:
:
evb_dyn = "qi_dbonds_pmf",
evb_dyn = "qi_dbonds_dyn",
:
:
dbonds_umb(1)%k = 100.0, dbonds_umb(1)%k = -.20,
dbonds_umb(1)%k = 400.0, dbonds_umb(1)%ezero = 0.0,
```

```

:
dbonds_umb(2)%k = 100.0, dbonds_umb(2)%ezero = .40,
dbonds_umb(2)%k = 400.0, dbonds_umb(2)%ezero = 0.0,
:

```

## 5.6. Isotope effects

### 5.6.1. Thermodynamic integration with respect to mass

As mentioned in Section 4.1, the standard implementation of thermodynamic integration in Amber assumes that the potential energy surface (PES) changes, but masses do not. For isotope effects the situation is exactly opposite: Within the Born-Oppenheimer approximation, the PES remains unchanged and it is the masses that change. One is usually interested in the ratio of the partition functions of the system with the heavy isotope ( $Q^{(h)}$ ) and the light isotope ( $Q^{(l)}$ ),

$$Q^{(h)}/Q^{(l)} = e^{-\beta\Delta F},$$

where the change in free energy  $\Delta F$  can be computed by the thermodynamic integration (TI) with respect to mass as

$$\Delta F = \int_0^1 \langle dV_{\text{eff}}(\lambda)/d\lambda \rangle d\lambda. \quad (5.45)$$

The parameter  $\lambda$  interpolates between the masses of the system with the lighter ( $\lambda = 0$ ) and the heavier ( $\lambda = 1$ ) isotopes,

$$m_i(\lambda) = (1 - \lambda)m_i^{(l)} + \lambda m_i^{(h)}, \quad (5.46)$$

and the effective potential  $V_{\text{eff}}$  is defined as

$$V_{\text{eff}}(\lambda) := -\beta^{-1} \log Q(\lambda). \quad (5.47)$$

The TI consists in running several simulations for different values of  $\lambda$ , computing  $\langle dV_{\text{eff}}(\lambda)/d\lambda \rangle$  in each simulation, and performing the simple integral (Eq. 5.45) in the end.

In classical mechanics, the TI w.r.t. mass would be rather trivial, so we assume that the calculation is quantum-mechanical and uses PIMD. Let  $N$  be the number of atoms and  $P$  the number of imaginary time slices in the discretized path integral (PI). ( $P = 1$  gives classical mechanics,  $P \rightarrow \infty$  gives quantum mechanics.) The PI representation of  $Q$  is

$$Q \simeq \left( \frac{P}{2\pi\hbar^2\beta} \right)^{3NP/2} \prod_{i=1}^N m_i^{3P/2} \int d\mathbf{r}^{(1)} \dots \int d\mathbf{r}^{(P)} e^{-\beta\Phi}, \quad (5.48)$$

where  $\Phi$  is given by

$$\Phi = \frac{P}{2\hbar^2\beta^2} \sum_{i=1}^N m_i \sum_{s=1}^P \left( \mathbf{r}_i^{(s)} - \mathbf{r}_i^{(s+1)} \right)^2 + \frac{1}{P} \sum_{s=1}^P V(\mathbf{r}^{(s)}) \quad (5.49)$$

## 5. Quantum dynamics

and  $\mathbf{r}_i^{(s)}$  denotes the  $s$ th slice coordinates of the  $i$ th atom.

The tricky part in PI simulations is finding efficient ways to estimate relevant quantities (in the PI jargon, finding efficient “estimators”) – in our case  $dV_{\text{eff}}(\lambda)/d\lambda$  from Eq. (5.45). For example, direct differentiation of Eq. (5.48) gives the thermodynamic-like estimator (TE), [228]

$$\frac{dV_{\text{eff}}(\lambda)}{d\lambda} \simeq - \sum_{i=1}^N \frac{dm_i}{d\lambda} \left[ \frac{3P}{2m_i\beta} - \frac{P}{2\hbar^2\beta^2} \sum_{s=1}^P \left( \mathbf{r}_i^{(s)} - \mathbf{r}_i^{(s+1)} \right)^2 \right] \quad (\text{TE}). \quad (5.50)$$

The problem with this estimator is that its statistical error grows with  $P$ . If one wishes to go to the quantum limit, one must increase the number of samples enormously. In Ref. [229], this drawback was avoided by subtracting the centroid coordinate

$$\mathbf{r}_i^{(C)} = \frac{1}{P} \sum_{s=0}^{P-1} \mathbf{r}_i^{(s)}$$

and using mass-scaled coordinates in Eq. (5.48). The resulting virial-like estimator (VE),

$$\frac{dV_{\text{eff}}(\lambda)}{d\lambda} \simeq - \sum_{i=1}^N \frac{dm_i/d\lambda}{m_i} \left[ \frac{3}{2\beta} + \frac{1}{2P} \left\langle \sum_{s=1}^P \left( \mathbf{r}_i^{(s)} - \mathbf{r}_i^{(C)} \right) \cdot \frac{\partial V \left( \mathbf{r}_i^{(s)} \right)}{\partial \mathbf{r}_i^{(s)}} \right\rangle \right] \quad (\text{VE}), \quad (5.51)$$

has the advantage that the statistical error is independent of  $P$ . Compared to TE, the virial-like estimator requires the gradient of the potential, but at no additional cost, since the gradient is already needed for the PIMD. Both types of estimators are implemented in Amber in order to provide an independent comparison, but in general the virial estimator is preferred.

Strictly speaking, the preceding derivation was for a system bound in an external potential. In molecular systems with internal interactions only, the partition function can only be defined per unit volume because the center-of-mass coordinate is unbound. However, if the sampling is done in Cartesian coordinates as in Amber, the preceding estimators remain unchanged. This can be justified by considering a finite volume  $V$  and taking a limit  $V \rightarrow \infty$ .

### 5.6.2. Amber implementation

The thermodynamic integration w.r.t. mass is run in Amber as any other PIMD simulation with the following changes.

1. In the *mdin* file, ITIMASS and CLAMBDA must be set.

ITIMASS = 0    No thermodynamic integration w.r.t. mass (default).

ITIMASS = 1    Run TI w.r.t. mass using the efficient virial estimator (5.51). This is the preferred value.

ITIMASS = 2    Run TI w.r.t. mass using the simple thermodynamic estimator (5.50). This option should only be used for testing. The virial estimator (option 1) has much smaller statistical error.

CLAMBDA    Contains the value of  $\lambda$  for TI ( $0.0 \leq \lambda \leq 1.0$ ) from Eq. (5.46).

2. In the *prmtop* (topology) file, a flag `TI_MASS` with the perturbed masses must be added. In other words, the current flag `MASS` includes the masses for the first (unperturbed) isotopic system ( $m_i^{(l)}$ ), and `TI_MASS` includes the masses for the second (perturbed) isotopic system ( $m_i^{(h)}$ ). Note that unlike the standard TI for which the force field changes, the TI w.r.t. mass requires only one topology file.
3. The output  $dV_{\text{eff}}/d\lambda$  from Eqs. (5.50) and (5.51) for the TI is printed as “DV/DL” in the *mdout* file (as for the standard TI).

*Note:* Currently, the TI w.r.t. mass can be used with both implementations of the PIMD (that is the full PIMD and the LES PIMD). There are examples of both in the directory *test/ti\_mass*.

### 5.6.3. Equilibrium isotope effects

Equilibrium (or thermodynamic) isotope effect (EIE) is the effect of isotopic substitution on the equilibrium constant  $K$  of a chemical reaction. Denoting the quantities pertaining to the reaction with the lighter (heavier) isotope by a superscript  $l$  ( $h$ ), the EIE is defined as the ratio of the equilibrium constants

$$\text{EIE} := \frac{K^{(l)}}{K^{(h)}}. \quad (5.52)$$

Within the Born-Oppenheimer approximation, the potential energy surfaces of isotopic molecules are identical, and so the EIE is only due to the effect of the isotopic mass on the nuclear motion of the reactants and products. The EIE can be expressed as the ratio

$$\text{EIE} = \frac{Q_p^{(l)}/Q_p^{(h)}}{Q_r^{(l)}/Q_r^{(h)}}. \quad (5.53)$$

where  $Q_r$  and  $Q_p$  denote the reactant and product partition functions, respectively. Equation (5.52) suggests that the EIE can be found in practice by performing two thermodynamic integrations: for the reactants,  $Q_r^{(l)}/Q_r^{(h)}$ , and for the products,  $Q_p^{(l)}/Q_p^{(h)}$ .

### 5.6.4. Kinetic isotope effects

Similarly, the kinetic isotope effect (KIE) is the effect of isotopic substitution on the rate constant  $k$  of a chemical reaction, and is defined as

$$\text{KIE} := \frac{k^{(l)}}{k^{(h)}}.$$

The exact quantum-mechanical expression for the rate constant is

$$k = Q_r^{-1} \text{tr} \left( e^{-\beta \hat{H}} \hat{F} \hat{P} \right)$$

where  $\hat{H}$  is the Hamiltonian operator and  $\hat{F}\hat{P}$  is the reactive flux operator. Unfortunately, the exact  $k$  cannot be computed even for fairly small molecules. There exists, however, a very

## 5. Quantum dynamics

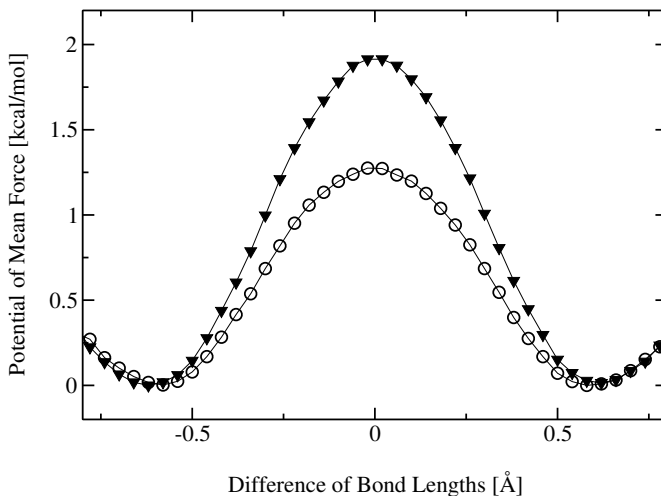


Figure 5.2.: PMFs for proton ( $\odot$  curve) and deuterium ( $\blacktriangledown$  curve) transfer in malonaldehyde using DG EVB/LES-PIMD.

accurate Quantum Instanton (QI) approximation for the rate constant [226], given by

$$k_{\text{QI}} = \frac{1}{2} \sqrt{\pi \hbar} \frac{C_{\text{ff}}(0)}{Q_r \Delta H}. \quad (5.54)$$

In this expression,  $C_{ff}(t)$  is the flux-flux correlation function and  $\Delta H$  is a specific type of energy variance, defined in Ref. [226]. A path-integral implementation of the QI approximation to compute KIEs has been developed in Refs. [228] and [229]. Within this approximation, the KIE is written as a product of several factors,

$$\text{KIE}_{\text{QI}} = \frac{k_{\text{QI}}^{(l)}}{k_{\text{QI}}^{(h)}} = \frac{Q_r^{(l)}}{Q_r^{(h)}} \times \frac{\Delta H^{(h)}}{\Delta H^{(l)}} \times \frac{C_{\text{dd}}^{(l)}(0)}{C_{\text{dd}}^{(h)}(0)} \times \frac{C_{\text{ff}}^{(l)}(0)/C_{\text{dd}}^{(l)}(0)}{C_{\text{ff}}^{(h)}(0)/C_{\text{dd}}^{(h)}(0)}, \quad (5.55)$$

where for convenience we have multiplied and divided by so-called delta-delta correlation function  $C_{\text{dd}}(t)$ . Using the PIMD implementation in Amber, quantities such as  $\Delta H^{(h)}$  or  $C_{\text{ff}}^{(l)}(0)/C_{\text{dd}}^{(l)}(0)$ , can be computed directly in a constrained PIMD simulation because they are thermodynamic averages (see Section 5.5.2 on the QI evaluation of the rate constant). The ratio  $Q_r^{(l)}/Q_r^{(h)}$  must be computed by the TI with respect to mass. Finally, the correlation function  $C_{\text{dd}}(t)$  is defined very similarly to the partition function  $Q$ , with the exception that it is constrained to two dividing surfaces for the reaction. Consequently, the ratio  $C_{\text{dd}}^{(l)}(0)/C_{\text{dd}}^{(h)}(0)$  must be computed by a TI but with a constrained PIMD.

### 5.6.5. Estimating the kinetic isotope effect using EVB/LES-PIMD

The kinetic isotope effect is defined as the ratio of the rate of reaction involving the lighter isotope compared to the rate involving the heavier isotope,  $KIE = k^{(l)}/k^{(h)}$ . Within the PI-QTST approximation, the KIE involves the ratio of dynamical frequency factors and the ratio of centroid densities [see Eqs. (5.27-5.30)]. Each frequency factor can be computed using biased sampling EVB/LES-PIMD, where the umbrella potential constrains the sampling along the dividing surface. The ratio of the centroid densities can be computed by employing biased sampling (see Sections 3.4.3 and 3.4.4) to map out the PMFs for both isotope reactions or by thermodynamic integration with respect to mass (see Sections 5.6.1 and 5.6.2). The former case involves two separate PMF calculations where the respective isotope masses are specified in the `%FLAG MASS` section of the `parmtop` files. Figure 5.2 compares the PMFs for the isotopic substitution of the transferring proton to a deuterium. All simulation parameters used in generating the PMFs are identical, with the exception that the transferring proton mass was changed from 1.008 amu to 2.014 amu in the deuterium `parmtop` file. The ratio of the centroid densities using Eq. (5.29) provide a value of 2.52.

Thermodynamic integration with respect to mass is discussed in detail in Sections 5.6.1 and 5.6.2. The key quantities we need to estimate the ratio of the centroid densities are embodied in the equation [229, 230]

$$\frac{\rho_c^{(l)}(\xi^{\ddagger})}{\rho_c^{(h)}(\xi^{\ddagger})} = \exp \left[ -\beta \int_0^1 d\lambda \left( \left\langle \frac{dV_{\text{eff}}(\lambda)}{d\lambda} \right\rangle_{\text{RS}} - \left\langle \frac{dV_{\text{eff}}(\lambda)}{d\lambda} \right\rangle_{\xi^{\ddagger}} \right) \right] \quad (5.56)$$

Thus two separate TI by mass simulations are required, one that samples  $dV_{\text{eff}}/d\lambda$  in the reactant region and the other which samples along the dividing surface  $\xi^{\ddagger}$ . The former case requires ground-state EVB/LES-PIMD dynamics (i.e., `evb_dyn="groundstate"`) on the reactant surface with TI by mass invoked in the `mdin` file (i.e., `ievb=1`, `ipimd=2`, `ntt=4`, `nchain=4`, `itimass=1`, `clambda=0.2`). A set of simulations with `clambda` ranging from 0 to 1 maps out the derivative along the mass transformation progress variable. Sampling of  $dV_{\text{eff}}/d\lambda$  along the dividing surface is invoked in a similar fashion, but with ground-state dynamics replaced by biased sampling constrained to the dividing surface (i.e., `evb_dyn="dbonds_umb"`, `dbonds_umb(1)%iatom = 8`, `dbonds_umb(1)%jatom = 9`, `dbonds_umb(1)%katom = 7`, `dbonds_umb(1)%k = 400.000`, `dbonds_umb(1)%ezero = 0.0`). Here, the dividing surface  $\xi^{\ddagger}$  is located at 0.0 along the difference of distances RC. Figure 5.3 shows the averages  $-\beta \langle \dots \rangle_{\text{RS}}$  and  $-\beta \langle \dots \rangle_{\xi^{\ddagger}}$  as a parameter of  $\lambda$  for the malonaldehyde system. Using the integration of Eq. (5.56) provides a centroid density ratio of 2.86.

## 5. Quantum dynamics

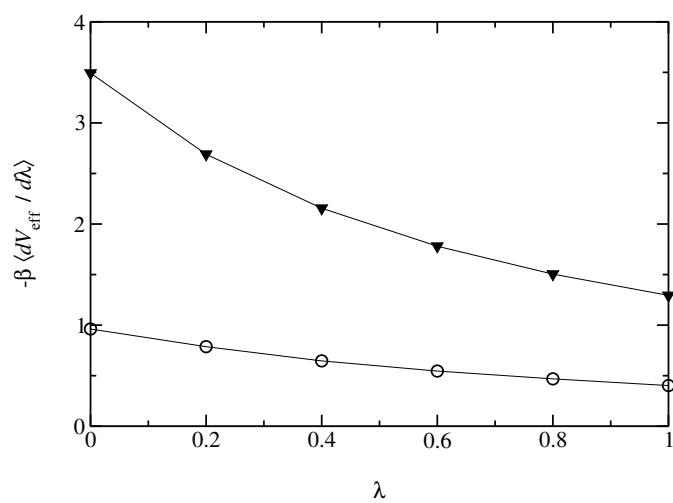


Figure 5.3.: Average value of  $-\beta \langle dV_{\text{eff}} / d\lambda \rangle$  sampled in the RS region (▼ curve) and at the dividing surface  $\xi_{\ddagger}$  (○ curve) as a parameter of  $\lambda$ .



## 6. NMR, X-ray, and cryo-EM/ET refinement

We find the *sander* module to be a flexible way of incorporating a variety of restraints into a optimization procedure that includes energy minimization and dynamical simulated annealing. The "standard" sorts of NMR restraints, derived from NOE and J-coupling data, can be entered in a way very similar to that of programs like DISGEO, DIANA or X-PLOR; an aliasing syntax allows for definitions of pseudo-atoms, connections with peak numbers in spectra, and the use of "ambiguous" constraints from incompletely-assigned spectra. More "advanced" features include the use of time-averaged constraints, use of multiple copies (LES) in conjunction with NMR refinement, and direct refinement against NOESY intensities, paramagnetic and diamagnetic chemical shifts, or residual dipolar couplings. In addition, a key strength of the program is its ability to carry out the refinements (usually near the final stages) using an explicit-solvent representation that incorporates force fields and simulation protocols that are known to give pretty accurate results in many cases for unconstrained simulations; this ability should improve predictions in regions of low constraint density and should help reduce the number of places where the force field and the NMR constraints are in "competition" with one another.

Since there is no generally-accepted "recipe" for obtaining solution structures from NMR data, the comments below are intended to provide a guide to some commonly-used procedures. Generally speaking, the programs that need to be run to obtain NMR structures can be divided into three parts:

1. *front-end* modules, which interact with NMR databases that provide information about assignments, chemical shifts, coupling constants, NOESY intensities, and so on. We have tried to make the general format of the input straightforward enough so that it could be interfaced to a variety of programs. At TSRI, we generally use the FELIX and NMRView codes, but the principles should be similar for other ways of keeping track of a database of NMR spectral information. As the flow-chart on the next page indicates, there are only a few files that need to be created for NMR restraints; these are indicated by the solid rectangles. The primary distance and torsion angle files have a fairly simple format that is largely compatible with the DIANA programs; if one wishes to use information from ambiguous or overlapped peaks, there is an additional "MAP" file that makes a translation from peak identifiers to ambiguous (or partial) assignments. Finally, there are some specialized (but still pretty straightforward) file formats for chemical shift or residual dipolar coupling restraints.

There are a variety of tools, besides the ones described below, that can assist in preparing input for structure refinement in Amber.

- The SANE (Structure Assisted NOE Evaluation) package, <http://ambermd.org/sane.zip>, is widely used at The Scripps Research Institute.[231]
- If you use Bruce Johnson's NmrView package, you might also want to look at the TSRI additions to that:

## 6. NMR, X-ray, and cryo-EM/ET refinement

[http://garbanzo.scripps.edu/nmrgrp/wisdom/pipe/tips\\_scripts.html](http://garbanzo.scripps.edu/nmrgrp/wisdom/pipe/tips_scripts.html). In particular, the *xpkTOupl* and *starTOupl* scripts there convert NmrView peak lists into the "7-column" needed for input to *makeDIST\_RST*.

- Users of the MARDIGRAS programs from UCSF can use the *mardi2amber* program to do conversion to Amber format: <http://picasso.ucsf.edu/mardihome.html>
2. *restrained molecular dynamics*, which is at the heart of the conformational searching procedures. This is the part that *sander* itself handles.
  3. *back-end* routines that do things like compare families of structures, generate statistics, simulate spectra, and the like. For many purposes, such as visualization, or the running of *procheck-NMR*, the "interface" to such programs is just the set of PDB files that contain the family of structures to be analyzed. These general-purpose structure analysis programs are available in many locations and are not discussed here. The principal *sander*-specific tool is *sviol*, which prepares tables and statistics of energies, restraint violations, and the like.

### 6.1. Distance, angle and torsional restraints

Distance, angle, and other restraints are read from the DISANG file if *nmropt* > 0. Namelist *rst* ("&rst") contains the following variables; it is read repeatedly until a namelist &rst statement is found with IAT(1)=0, or until reaching the end of the DISANG file.

If you wish to include weight changes but have no internal constraints, set *nmropt*=1, but do not include a DISANG line in the file redirection section. (Note that, unlike earlier versions of Amber, the &rst namelists must be in the DISANG file, and not in the *mdin* file.)

In many cases, the user will not prepare this section of the input by hand, but will use the auxiliary programs *makeDIST\_RST*, *makeANG\_RST* and *makeCHIR\_RST* to prepare input from simpler files.

There have been several additions made to restraints as of Amber 10. These additions have only been made to *sander* and not to *pmemd*.

#### 6.1.1. Variables in the &rst namelist:

iat(1)→iat(8)

- *If IRESID = 0 (normal operation)*: The atoms defining the restraint. Type of restraint is determined (in order) by:
  1. If IAT(3) = 0, this is a distance restraint.
  2. If IAT(4) = 0, this is an angle restraint.
  3. If IAT(5) = 0, this is a torsional (or J-coupling, if desired) restraint or a generalized distance restraint of 4 atoms, a type of restraint new as of Amber 10 (*sander* only, see below).

## 6.1. Distance, angle and torsional restraints

4. If  $IAT(6) = 0$ , this is a plane-point angle restraint, a second restraint new as of Amber 10 (*sander* only). The angle is measured between the normal of a plane defined by  $IAT(1)..IAT(4)$  and the vector from the center of mass of atoms  $IAT(1)..IAT(4)$  to the position of  $IAT(5)$ . The normal is defined by  $(r_1 - r_2) \times (r_3 - r_4)$ , where  $r_n$  is the position of  $IAT(n)$ .
5. If  $IAT(7) = 0$ , this is a generalized distance restraint of 6 atoms (see below).
6. Otherwise, if  $IAT(1)..IAT(8)$  are all non-zero, this is a plane- plane angle restraint, a third new restraint type as of Amber 10 (*sander* only, or a generalized distance restraint of 8 atoms (see below). For the plane-plane restraint, the angle is measured between the two normals of the two planes, which are defined by  $(r_1 - r_2) \times (r_3 - r_4)$  and  $(r_5 - r_6) \times (r_7 - r_8)$ . In the case of either planar restraint, the plane may be defined using three atoms instead of four simply by using one atom twice.

If any of  $IAT(n)$  are  $< 0$ , then a corresponding group of atoms is defined below, and the coordinate- averaged position of this group will be used in place of atom  $IAT(n)$ . A new feature as of Amber 10, atom groups may be used not only in distance restraints, but also in angle, torsion, the new plane restraints, or the new generalized restraints. If this is a distance restraint, and  $IAT(1) < 0$ , then a group of atoms is defined below, and the coordinate-averaged position of this group will be used in place of the coordinates of atom 1 [ $IAT(1)$ ]. Similarly, if  $IAT(2) < 0$ , a group of atoms will be defined below whose coordinate-averaged position will be used in place of the coordinates for atom 2 [ $IAT(2)$ ].

- If  $IRESID=1$ :  $IAT(1)..IAT(8)$  point to the \*residues\* containing the atoms comprising the internal. Residue numbers are the absolute in the entire system. In this case, the variables  $ATNAM(1)..ATNAM(8)$  must be specified and give the character names of the atoms within the respective residues. If any of  $IAT(n)$  are less than zero, then group input will still be read in place of the corresponding atom, as described below.
- Defaults for  $IAT(1) \rightarrow IAT(8)$  are 0.

$rstwt(1) \rightarrow rstwt(4)$  New as of Amber 10 (*sander* only), users may now define a single restraint that is a function of multiple distance restraints, called a "generalized distance coordinate" restraint. The energy of such a restraint has the following form:

$$U = k(w_1|r_1 - r_2| + w_2|r_3 - r_4| + w_3|r_5 - r_6| + w_4|r_7 - r_8| - r_0)^2$$

where the weights  $w_n$  are given in  $rstwt(1)..rstwt(4)$  and the positions  $r_n$  are the positions of the atoms in  $iat(1)..iat(8)$ .

Generalized distance coordinate restraints must be defined with either 4, 6, or 8 atoms and 2, 3, or 4 corresponding non-zero weights in  $rstwt(1)..rstwt(4)$ . Weights may be any positive or negative real number.

If all the weights in  $rstwt(1)..rstwt(4)$  are zero and four atoms are given in  $iat(1)..iat(4)$  for the restraint, the restraint is a torsional or J-coupling restraint. If eight atoms are given in  $iat(1)..iat(8)$  and all weights are zero, the restraint is a plane-plane angle restraint. However, if the weights are non-zero, the restraint will be a generalized distance coordinate restraint.

Default for  $rstwt(1)..rstwt(4)$  is 0.0

## 6. NMR, X-ray, and cryo-EM/ET refinement

restraint New as of Amber 10 (*sander* only), users may now use a "natural language" system to define restraints by using the RESTRAINT character variable. Valid restraints defined in this manner will begin with a "distance()" "angle()" "torsion()" or "coordinate()" keyword. Within the parentheses, the atoms that make up the restraint are specified. Atoms may be defined either with an explicit atom number or by using ambmask format, namely `:(residue#)@(atom name)`. Atoms may be separated by commas, spaces, or parentheses. Additionally, negative integers may be used if atom groupings are defined in other variables in the namelist as described below. In addition to the principle distance, angle, torsion, and coordinate keywords, Some keywords may be used within the principle keywords to define more complicated restraints. The keyword "plane()" may be used once or twice within the parentheses of the "angle()" keyword to define a planar restraint. Defining one plane grouping plus one other atom in this manner will create a plane-point angle restraint as described above. Defining two plane groupings will create a plane-plane angle restraint. The keyword "plane()" may only be used inside of "angle()," and is necessary to define either a plane-point or plane-plane restraint.

Within the "coordinate()" keyword, the user must use 2 to 4 "distance()" keywords to define a generalized distance coordinate restraint. The "distance()" keyword functions just like it does when used to define a traditional distance restraint. The user may specify any two atom numbers, masks, or negative numbers corresponding to atom groups defined outside of RESTRAINT. Additionally, following each "distance()" keyword inside "coordinate()" the user must specify a real-number weight to be applied to each distance making up the generalized coordinate.

The "com()" keyword may be used within any other keyword to define a center of mass grouping of atoms. Within the parenthesis, the user will enter a list of atom numbers or masks. Negative numbers, which correspond to externally-defined groups, may not be used.

Any type of parenthetical character, i.e., ( ), [ ], or { }, may be used wherever parentheses have been used above.

The following are all examples of valid restraint definitions:

```
restraint = "distance( (45) (49) )"
           = "angle (:21@C5' :21@C4' 108) "
           = "torsion[-1,-1,-1, com(67, 68, 69)] "
           = "angle( -1, plane(81, 85, 87, 90) )"
           = "angle(plane(com(9,10), :5@CA, 31, 32), plane(14,15,15,16) )"
           = "coordinate(distance(:5@C3', :6@O5'), -1.0, distance(134,-1), 1.0) "
```

There is a 256 character limit on RESTRAINT, so if a particularly large atom grouping is desired, it is necessary to specify a negative number instead of "com()" and define the group as described below. RESTRAINT will only be parsed if IAT(1) = 0, otherwise the information in IAT(1) .. IAT(8) will define the restraint. *Default for restraint is ' '.*

atnam If IRESID = 1, then the character names of the atoms defining the internal are

## 6.1. Distance, angle and torsional restraints

contained in ATNAM(1)→ATNAM(8). Residue IAT(1) is searched for atom name ATNAM(1); residue IAT(2) is searched for atom name ATNAM(2); etc. *Defaults for ATNAM(1)→ATNAM(8) are ' '*.

- iresid Indicates whether IAT(I) points to an atom # or a residue #. See descriptions of IAT() and ATNAM() above. If RESTRAINT is used to define the internal instead of IAT(), IRESID has no effect on how RESTRAINT is parsed. However, it will affect the behavior of atom group definitions as described below if negative numbers are specified within RESTRAINT. *Default = 0.*
- nstep1, nstep2 This restraint is applied for steps/iterations NSTEP1 through NSTEP2. If NSTEP2 = 0, the restraint will be applied from NSTEP1 through the end of the run. Note that the first step/iteration is considered step zero (0). *Defaults for NSTEP1, NSTEP2 are both 0.*
- irstyp Normally, the restraint target values defined below (R1→R4) are used directly. If IRSTYP = 1, the values given for R1→R4 define relative displacements from the current value (value determined from the starting coordinates) of the restrained internal. For example, if IRSTYP=1, the current value of a restrained distance is 1.25, and R1 (below) is -0.20, then a value of R1=1.05 will be used. *Default is IRSTYP=0.*
- ialtd Determines what happens when a distance restraint gets very large. If IALTD=1, then the potential "flattens out", and there is no force for large violations; this allows for errors in constraint lists, but might tend to ignore constraints that *should* be included to pull a bad initial structure towards a more correct one. When IALTD=0 the penalty energy continues to rise for large violations. See below for the detailed functional forms that are used for distance restraints. Set IALTD=0 to recover the behavior of earlier versions of *sander*. Default value is 0, or the last value that was explicitly set in a previous restraint. This value is set to 1 if *makeDIST\_RST* is called with the *-altdis* flag.
- ifvari If IFVARI > 0, then the force constants/positions of the restraint will vary with step number. Otherwise, they are constant throughout the run. If IFVARI > 0, then the values R1A→R4A, RK2A, and RK3A must be specified (see below). *Default is IFVARI=0.*
- ninc If IFVARI > and NINC > 0, then the change in the target values of of R1→R4 and K2,K3 is applied as a step function, with NINC steps/ iterations between each change in the target values. If NINC = 0, the change is effected continuously (at every step). *Default for NINC is the value assigned to NINC in the most recent namelist where NINC was specified. If NINC has not been specified in any namelist, it defaults to 0.*
- imult If IMULT=0, and the values of force constants RK2 and RK3 are changing with step number, then the changes in the force constants will be linearly interpolated from rk2→rk2a and rk3→rk3a as the step number changes. If IMULT=1 and the

## 6. NMR, X-ray, and cryo-EM/ET refinement

force constants are changing with step number, then the changes in the force constants will be effected by a series of multiplicative scalings, using a single factor, R, for all scalings. *i.e.*

$$\begin{aligned} \mathbf{rk2a} &= \mathbf{R} \ast \mathbf{INCREMENTS} \ast \mathbf{rk2} \\ \mathbf{rk3a} &= \mathbf{R} \ast \mathbf{INCREMENTS} \ast \mathbf{rk3} . \end{aligned}$$

INCREMENTS is the number of times the target value changes, which is determined by NSTEP1, NSTEP2, and NINC. *Default for IMULT is the value assigned to IMULT in the most recent namelist where IMULT was specified. If IMULT has not been specified in any namelist, it defaults to 0.*

r1→r4, rk2, rk3, r1a→r4a, rk2a, rk3a If IALTD=0, the restraint is a well with a square bottom with parabolic sides out to a defined distance, and then linear sides beyond that. If R is the value of the restraint in question:

- R < r1 Linear, with the slope of the "left-hand" parabola at the point R=r1.
- r1 ≤ R < r2 Parabolic, with restraint energy  $k_2(R - r_2)^2$ .
- r2 ≤ R < r3 E = 0.
- r3 ≤ R < r4 Parabolic, with restraint energy  $k_3(R - r_3)^2$ .
- r4 ≤ R Linear, with the slope of the "right-hand" parabola at the point R=r4.

For torsional restraints, the value of the torsion is translated by  $\pm n \cdot 360$ , if necessary, so that it falls closest to the mean of r2 and r3. Specified distances are in Angstroms. Specified angles are in degrees. Force constants for distances are in kcal/mol-Å<sup>2</sup> Force constants for angles are in kcal/mol-rad<sup>2</sup>. (Note that angle positions are specified in degrees, but force constants are in radians, consistent with typical reporting procedures in the literature).

If IALTD=1, distance restraints are interpreted in a slightly different fashion. Again, If R is the value of the restraint in question:

- R < r2 Parabolic, with restraint energy  $k_2(R - r_2)^2$ .
- r2 ≤ R < r3 E = 0.
- r3 ≤ R < r4 Parabolic, with restraint energy  $k_3(R - r_3)^2$ .
- r4 ≤ R Hyperbolic, with energy  $k_3[b/(R - r_3) + a]$ , where  $a = 3(r_4 - r_3)^2$  and  $b = -2(r_4 - r_3)^3$ . This function matches smoothly to the parabola at  $R = r_4$ , and tends to an asymptote of  $ak_3$  at large R. The functional form is adapted from that suggested by Michael Nilges, *Prot. Eng.* **2**, 27-38 (1988). Note that if *ialtd=1*, the value of r1 is ignored.

ifvari

- = 0 The values of r1→r4, rk2, and rk3 will remain constant throughout the run.
- > 0 The values r1a, r2a, r3a, r4a, r2ka and r3ka are also used. These variables are defined as for r1→r4 and rk2, rk3, but correspond to the values appropriate for NSTEP = NSTEP2: e.g., if IVARI > 0, then the value of r1 will vary between

## 6.1. Distance, angle and torsional restraints

NSTEP1 and NSTEP2, so that, e.g.  $r1(\text{NSTEP1}) = r1$  and  $r1(\text{NSTEP2}) = r1a$ . Note that you *must* specify an explicit value for *nstep1* and *nstep2* if you use this option. *Defaults for  $r1 \rightarrow r4, rk2, rk3, r1a \rightarrow r4a, rk2a$  and  $rk3a$  are the values assigned to them in the most recent namelist where they were specified. They should always be specified in the first &rst namelist.*

$r0, k0, r0a, k0a$  New as of Amber 10 (*sander* only), the user may more easily specify a large parabolic well if desired by using R0 and K0, and then R0A and K0A if IFVARI > 0. The parabolic well will have its zero at  $R = R0$  and a force constant of K0. These variables simply map the desired parabolic well into  $r1 \rightarrow r4, rk2, rk3, r1a \rightarrow r4a, rk2a, \text{ and } rk3a$  in the following manner:

- $R1 = 0$  for distance, angle, and planar restraints,  $R1 = R0 - 180$  for torsion restraints
- $R1A = 0$  for distance, angle, and planar restraints,  $R1A = R0A - 180$  for torsion restraints
- $R2 = R0; R3 = R0$
- $R2A = R0A; R3A = R0A$
- $R4 = R0 + 500$  for distance restraints,  $R4 = 180$  for angle and planar restraints,  $R4 = R0 + 180$  for torsion restraints
- $RK2 = K0; RK3 = K0$
- $RK2A = K0A; RK3A = K0A$

$rjcoef(1) \rightarrow rjcoef(3)$  By default, 4-atom sequences specify torsional restraints. It is also possible to impose restraints on the vicinal 3 J-coupling value related to the underlying torsion. J is related to the torsion  $\tau$  by the approximate Karplus relationship:  $J = A \cos^2(\tau) + B \cos(\tau) + C$ . If you specify a non-zero value for either RJCOEF(1) or RJCOEF(2), then a J-coupling restraint, rather than a torsional restraint, will be imposed. At every MD step, J will be calculated from the Karplus relationship with  $A = \text{RJCOEF}(1)$ ,  $B = \text{RJCOEF}(2)$  and  $C = \text{RJCOEF}(3)$ . In this case, the target values ( $R1 \rightarrow R4, R1A \rightarrow R4A$ ) and force constants ( $RK2, RK3, RK2A, RK3A$ ) refer to J-values for this restraint.  $\text{RJCOEF}(1) \rightarrow \text{RJCOEF}(3)$  must be set individually for each torsion for which you wish to apply a J-coupling restraint, and  $\text{RJCOEF}(1) \rightarrow \text{RJCOEF}(3)$  may be different for each J-coupling restraint. With respect to other options and reporting, J-coupling restraints are treated identically to torsional restraints. This means that if time-averaging is requested for torsional restraints, it will apply to J-coupling restraints as well. The J-coupling restraint contribution to the energy is included in the "torsional" total. And changes in the relative weights of the torsional force constants also change the relative weights of the J-coupling restraint terms. Setting RJCOEF has no effect for distance and angle restraints. *Defaults for  $\text{RJCOEF}(1) \rightarrow \text{RJCOEF}(3)$  are 0.0.*

$igr1(i), i=1 \rightarrow 200, igr2(i), i=1 \rightarrow 200, \dots, igr8(i), i=1 \rightarrow 200$  If  $\text{IAT}(n) < 0$ , then  $\text{IGRn}()$  gives the atoms defining the group whose coordinate averaged position is used to define "atom n" in a restraint. Alternatively, if RESTRAINT is used to define the internal,

## 6. NMR, X-ray, and cryo-EM/ET refinement

then if the *n*th atom specified is a number less than zero, IGR*n*() gives the atoms defining the group whose coordinate averaged position is used to define "atom *n*" in a restraint. If IRESID = 0, absolute atom numbers are specified by the elements of IGR*n*(). If IRESID = 1, then IGR*n*(*I*) specifies the number of the residue containing atom *I*, and the name of atom *I* must be specified using GRNAM*n*(*I*). A maximum of 200 atoms are allowed in any group. Only specify those atoms that are needed. Default value for any unspecified element of IGR*n*(*i*) is 0.

- grnam1(*i*),*i*=1→200, grnam2(*i*),*i*=1→200, ... grnam8(*i*),*i*=1→200 If group input is being specified (IGR*n*(1) > 0), and IRESID = 1, then the character names of the atoms defining the group are contained in GRNAM*n*(*i*), as described above. In the case IAT(1) < 0, each residue IGR1(*i*) is searched for an atom name GRNAM1(*i*) and added to the first group list. In the case IAT(2) < 0, each residue IGR2(*i*) is searched for an atom name GRNAM2(*i*) and added to the second group list. *Defaults for GRNAM*n*(*i*) are ' '.*
- ir6 If a group coordinate-averaged position is being used (see IGR1 and IGR2 above), the average position can be calculated in either of two manners: If IR6 = 0, center-of-mass averaging will be used. If IR6=1, the  $\langle r^{-6} \rangle^{-1/6}$  average of all interaction distances to atoms of the group will be used. *Default for IR6 is the value assigned to IR6 in the most recent namelist where IR6 was specified. If IR6 has not been specified in any namelist, it defaults to 0.*
- ifntyp If time-averaged restraints have been requested (see DISAVE/ANGAVE/TORAVE above), they are, by default, applied to all restraints of the class specified. Time-averaging can be overridden for specific internals of that class by setting IFNTYP for that internal to 1. IFNTYP has no effect if time-averaged restraint are not being used. *Default value is IFNTYP=0.*
- ixpk, nxpk These are user-defined integers than can be set for each constraint. They are typically the "peak number" and "spectrum number" associated with the cross-peak that led to this particular distance restraint. Nothing is ever done with them except to print them out in the "violation summaries", so that NMR people can more easily go from a constraint violation to the corresponding peak in their spectral database. Default values are zero.
- iconstr If *iconstr* > 0, (default is 0) a Lagrangian multiplier is also applied to the two-center internal coordinate defined by IAT(1) and IAT(2). The effect of this Lagrangian multiplier is to maintain the initial orientation of the internal coordinate. The rotation of the vector IAT(1)->IAT(2) is prohibited, though translation is allowed. For each defined two-center internal coordinate, a separate Lagrangian multiplier is used. Therefore, although one can use as many multipliers as needed, defining centers should NOT appear in more than one multiplier. This option is compatible with mass centers (i.e., negative IAT(1) or IAT(2)). ICONSTR can be used together with harmonic restraints. RK2 and RK3 should be set to 0.0 if the two-center internal coordinate is a simple Lagrangian multiplier. An example has been included in \$AMBERHOME/example/lagmul.



Namelist `&rst` is read for each restraint. Restraint input ends when a namelist statement with `iat(1) = 0` (or `iat(1)` not specified) is found. Note that comments can precede or follow any namelist statement, allowing comments and restraint definitions to be freely mixed.

## 6.2. NOESY volume restraints

After the previous section, NOESY volume restraints may be read. This data described in this section is only read if `NMROPT = 2`. The molecule may be broken in overlapping submolecules, in order to reduce time and space requirements. Input for each submolecule consists of namelist `"&noexp"`, followed immediately by standard Amber "group" cards defining the atoms in the submolecule. In addition to the submolecule input (`"&noexp"`), you may also need to specify some additional variables in the `cntrl` namelist; see the "NMR variables" description in that section.

In many cases, the user will not prepare this section of the input by hand, but will use the auxiliary program `makeDIST_RST` to prepare input from simpler files.

### Variables in the `&noexp` namelist:

For each submolecule, the namelist `"&noexp"` is read (either from *stdin* or from the NOESY redirection file) which contains the following variables. There are no effective defaults for `npeak`, `emix`, `ihp`, `jhp`, and `aexp`: you must specify these.

`npeak(imix)` Number of peaks for each of the "imix" mixing times; if the last mixing time is `mxmix`, set `NPEAK(mxmix+1) = -1`. End the input when `NPEAK(1) < 0`.

`emix(imix)` Mixing times (in seconds) for each mixing time.

`ihp(imix,ipeak)`, `jhp(imix,ipeak)` Atom numbers for the atoms involved in cross-peak "ipeak" at mixing time "imix"

`aexp(imix,ipeak)` Experimental target integrated intensity for this cross peak. If `AEXP` is negative, this cross peak is part of a set of overlapped peaks. The computed intensity is added to the peak that follows; the next time a peak with `AEXP > 0` is encountered, the running sum for the calculated peaks will be compared to the value of `AEXP` for that last peak in the list. In other words, a set of overlapped peaks is represented by one or more peaks with `AEXP < 0` followed by a peak with `AEXP > 0`. The computed total intensity for these peaks will be compared to the value of `AEXP` for the final peak.

`arange(imix,ipeak)` "Uncertainty" range for this peak: if the calculated value is within  $\pm$ ARANGE of `AEXP`, then no penalty will be assessed. Default uncertainties are all zero.

`awt(imix,ipeak)` Relative weight for this cross peak. Note that this will be multiplied by the overall weight given by the NOESY weight change cards in the weight changes section (Section 1). Default values are 1.0, unless `INVWT1`, `INVWT2` are set (see below), in which case the input values of `AWT` are ignored.

## 6. NMR, X-ray, and cryo-EM/ET refinement

- invwt1,invwt2* Lower and upper bounds on the weights for the peaks respectively, such that the relative weight for each peak is  $1/\text{intensity}$  if  $1/\text{intensity}$  lies between the lower and upper bounds. This is the intensity after being scaled by *oscale*. The inverse weighing scheme adopted by this option prevents placing too much influence on the strong peaks at the expense of weaker peaks and was previously invoked using the compilation flag "INVWGT". Default values are  $\text{INVWT1}=\text{INVWT2}=1.0$ , placing equal weights on all peaks.
- omega* Spectrometer frequency, in Mhz. Default is 500. It is possible for different sub-molecules to have different frequencies, but *omega* will only change when it is explicitly re-set. Hence, if all of your data is at 600 Mhz, you need only set *omega* to 600. in the first submolecule.
- taurot* Rotational tumbling time of the molecule, in nsec. Default is 1.0 nsec. Like *omega*, this value is "sticky", so that a value set in one submolecule will remain until it is explicitly reset.
- taumet* Correlation time for methyl jump motion, in ns. This is only used in computing the intra-methyl contribution to the rate matrix. The ideas of Woessner are used, specifically as recommended by Kalk & Berendsen.[232] Default is 0.0001 ns, which is effectively the fast motion limit. The default is consistent with the way the rest of the rate matrix elements are determined (also in the fast motion limit,) but probably is not the best value to use, since methyl groups appear to have T1 values that are systematically shorter than other protons, and this is likely to arise from the fact that the methyl correlation time can be near to the inverse of the spectrometer frequency. A value of 0.02 - 0.05 ns is probably better than 0.0001, but this is still an active research area, and you are on your own here, and should consult the literature for further discussion.[233] As with *omega*, *taumet* can be different for different sub-molecules, but will only change when it is explicitly re-set.
- id2o* Flag for determining if exchangeable protons are to be included in the spin-diffusion calculation. If  $\text{ID2O}=0$  (default) then all protons are included. If  $\text{ID2O}=1$ , then all protons bonded to nitrogen or oxygen are assumed to not be present for the purposes of computing the relaxation matrix. No other options exist at present, but they could easily be added to the subroutine *indexn*. Alternatively, you can manually rename hydrogens in the *prmtop* file so that they do not begin with "H": such protons will not be included in the relaxation matrix. (*Note:* for technical reasons, the HOH proton of tyrosine must always be present, so setting  $\text{ID2O}=1$  will not remove it; we hope that this limitation will be of minor importance to most users.) The *id2o* variable retains its value across namelist reads, *i.e.* its value will only change if it is explicitly reset.
- oscale* overall scaling factor between experimental and computed volume units. The experimental intensities are multiplied by *oscale* before being compared to calculated intensities. This means that the weights WNOESY and AWT always refer to "theoretical" intensity scales rather than to the (arbitrary) experimental units. The *oscale*

variable retains its value across namelist reads, *i.e.* its value will only change if it is explicitly reset. The initial (default) value is 1.0.

The atom numbers *ihp* and *jhp* are the absolute atom numbers. For methyl groups, use the number of the last proton of the group; for the delta and epsilon protons of aromatic rings, use the delta-2 or epsilon-2 atom numbers. Since this input requires you to know the absolute atom numbers assigned by Amber to each of the protons, you may wish to use the separate *makeDIST\_RST* program which provides a facility for more turning human-readable input into the required file for *sander*.

Following the `&noexp` namelist, give the Amber "group" cards that identify this sub-molecule. This combination of "`&noexp`" and "group" cards can be repeated as often as needed for many submolecules, subject to the limits described in the *nmr.h* file. As mentioned above, this input section ends when `NPEAK(1) < 0`, or when an end-of-file is reached.

### 6.3. Chemical shift restraints

After reading NOESY restraints above (if any), read the chemical shift restraints in namelist `&shf`, or the pseudocontact restraints in namelist `&pcshift`. Reading this input is triggered by the presence of a SHIFTS line in the I/O redirection section. In many cases, the user will not prepare this section of the input by hand, but will use the auxiliary programs *shifts* or *fantasian* to prepare input from simpler files.

#### Variables in the `&shf` namelist.

(Defaults are only available for *shrang*, *wt*, *nter*, and *shcut*; you must specify the rest.)

nring	Number of rings in the system.
natr( <i>i</i> )	Number of atoms in the <i>i</i> -th ring.
iatr( <i>j</i> , <i>i</i> )	Absolute atom number for the <i>j</i> -th atom of the <i>i</i> -th ring.
namr( <i>i</i> )	Eight-character string that labels the <i>i</i> -th ring. The first three characters give the residue name (in caps); the next three characters contain the residue number (right justified); column 7 is blank; column 8 may optionally contain an extra letter to distinguish the two rings of trp, or the 5 or 8 rings of the heme group.
str( <i>i</i> )	Ring current intensity factor for the <i>i</i> -th ring. Older values are summarized by Cross and Wright; <a href="#">[234]</a> more recent empirical parametrizations seem to give improved results. <a href="#">[235, 236]</a>
nprot	Number of protons for which penalty functions are to be set up.
iprot( <i>i</i> )	Absolute atom number of the <i>i</i> -th proton whose shifts are to be evaluated. For equivalent protons, such as methyl groups or rapidly flipping phenylalanine rings, enter all two or three atom numbers in sequence; averaging will be controlled by the <i>wt</i> parameter, described below.

## 6. NMR, X-ray, and cryo-EM/ET refinement

- `obs(i)` Observed secondary shift for the *i*-th proton. This is typically calculated as the observed value minus a random coil reference value.
- `shrang(i)` "Uncertainty" range for the observed shift: if the calculated shift is within  $\pm$ SHRANG of the observed shift, then no penalty will be imposed. The default value is zero for all shifts.
- `wt(i)` Weight to be assigned to this penalty function. Note that this value will be multiplied by the overall weight (if any) given by the SHIFTS command in the assignment of weights (above). Default values are 1.0. For sets of equivalent protons, give a negative weight for all but the last proton in the group; the last proton gets a normal, positive value. The average computed shift of the group will be compared to *obs* entered for the last proton.
- `shcut` Values of calculated shifts will be printed only if the absolute error between calculated and observed shifts is greater than this value. *Default = 0.3 ppm.*
- `ntr` Residue number of the N-terminus, for protein shift calculations; *default = 1.*
- `cter` Residue number of the C-terminus, for protein shift calculations. Believe it or not, the current code cannot figure this out for itself.

In typical usage, the *shifts* program (<http://casegroup.rutgers.edu/shifts.html>) would be used to create this file, with a typical command line:

```
shifts -readobs -sander ' : :H*' gcg10
```

Sample input and output files are in \$AMBERHOME/test/rdc.

### 6.4. Pseudocontact shift restraints

The PCSHIFT module allows the inclusion of pseudocontact shifts as constraints in energy minimization and molecular dynamics calculations on paramagnetic molecules. The pseudocontact shift depends on the magnetic susceptibility anisotropy of the metal ion and on the location of the resonating nucleus with respect to the axes of the magnetic susceptibility tensor. For the nucleus *i*, it is given by:

$$\delta_{pc}^i = \sum_j \frac{1}{12\pi r_{ij}^3} \left[ \Delta\chi_{ax}^j (3n_{ij}^2 - 1) + (3/2)\Delta\chi_{rh}^j (l_{ij}^2 - m_{ij}^2) \right]$$

where  $l_{ij}$ ,  $m_{ij}$ , and  $n_{ij}$  are the direction cosines of the position vector of atom *i* with respect to the *j*-th magnetic susceptibility tensor coordinate system,  $r_{ij}$  is the distance between the *j*-th paramagnetic center and the proton *i*,  $\Delta\chi_{ax}$  and  $\Delta\chi_{rh}$  are the axial and the equatorial (rhom-bic) anisotropies of the magnetic susceptibility tensor of the *j*-th paramagnetic center. For a discussion, see Ref. [237].

The PCSHIFT module to be used needs a namelist file which includes information on the magnetic susceptibility tensor and on the paramagnetic center, and a line of information for each nucleus. This module allows to include more than one paramagnetic center in the calculations.

To include pseudocontact shifts as constraints in energy minimization and molecular dynamics calculations the NMROPT flag should be set to 2, and a *PCSHIFT=filename* statement entered in the I/O redirection section.

To perform molecular dynamics calculations it is necessary to eliminate the rotational and translational degree of freedom about the center of mass (this because during molecular dynamics calculations the relative orientation between the external reference coordinate system and the magnetic anisotropy tensor coordinate system has to be fixed). This option can be obtained with the NSCM flag of *sander*.

### Variables in the pcshift namelist.

- nprot        number of pseudocontact shift constraints.
- nme         number of paramagnetic centers.
- nmpmc       name of the paramagnetic atom
- optphi(n), opttet(n), optomg(n), opta1(n), opta2(n) the five parameters of the magnetic anisotropy tensor for each paramagnetic center.
- optkon      force constant for the pseudocontact shift constraints

Following this, there is a line for each nucleus for which the pseudocontact shift information is given has to be added. Each line contains :

- iproto(i)    atom number of the i-th proton whose shift is to be used as constraint.
- obs(i)        observed pseudocontact shift value, in ppm
- wt(i)         relative weight
- tolpro(i)    relative tolerance ix mltpro
- mltpro(i)    multiplicity of the NMR signal (for example the protons of a methyl group have mltprot(i)=3)

**Example.** Here is a &pcshf namelist example: a molecule with three paramagnetic centers and 205 pseudocontact shift constraints.

```
&pcshf
nprot=205,
nme=3,
nmpcm='FE ',
optphi(1)=-0.315416,
opttet(1)=0.407499,
optomg(1)=0.0251676,
opta1(1)=-71.233,
opta2(1)=1214.511,
optphi(2)=0.567127,
```

## 6. NMR, X-ray, and cryo-EM/ET refinement

```
opttet (2)=-0.750526,  
optomg (2)=0.355576,  
opta1 (2)=-60.390,  
opta2 (2)=377.459,  
optphi (3)=0.451203,  
opttet (3)=-0.0113097,  
optomg (3)=0.334824,  
opta1 (3)=-8.657,  
opta2 (3)=704.786,  
optkon=30,  
iprot (1)=26, obs (1)=1.140, wt (1)=1.000, tolpro (1)=1.00, mltpro (1)=1,  
iprot (2)=28, obs (2)=2.740, wt (2)=1.000, tolpro (2)=.500, mltpro (2)=1,  
iprot (3)=30, obs (3)=1.170, wt (3)=1.000, tolpro (3)=.500, mltpro (3)=1,  
iprot (4)=32, obs (4)=1.060, wt (4)=1.000, tolpro (4)=.500, mltpro (4)=3,  
iprot (5)=33, obs (5)=1.060, wt (5)=1.000, tolpro (5)=.500, mltpro (5)=3,  
iprot (6)=34, obs (6)=1.060, wt (6)=1.000, tolpro (6)=.500, mltpro (6)=3,  
...  
...  
iprot (205)=1215, obs (205)=.730, wt (205)=1.000, tolpro (205)=.500,  
mltpro (205)=1,  
/  
/
```

An mdin file that might go along with this, to perform a maximum of 5000 minimization cycles, starting with 500 cycles of steepest descent. PCSHIFT=./pcs.in redirects the input from the namelist "pcs.in" which contains the pseudocontact shift information.

Example of minimization including pseudocontact shift constraints

```
&cntrl  
ibelly=0,imin=1,ntpr=100,  
ntr=0,maxcyc=500,  
ncyc=50,ntmin=1,dx0=0.0001,  
drms=.1,cut=10.,  
nmropt=2,pencut=0.1,ipnlty=2,  
/  
&wt type='REST', istep1=0,istep2=1,value1=0.,  
value2=1.0, /  
&wt type='END' /  
DISANG=./noe.in  
PCSHIFT=./pcs.in  
LISTOUT=POUT
```

### 6.5. Direct dipolar coupling restraints

Energy restraints based on direct dipolar coupling constants are entered in this section. All variables are in the namelist &align; reading of this section is triggered by the presence of a

DIPOLE line in the I/O redirection section.

When dipolar coupling restraints are turned on, the five unique elements of the alignment tensor are treated as additional variables, and are optimized along with the structural parameters. Their effective masses are determined by the *scal*m parameter entered in the &cntrl namelist. Unlike some other programs, the variables used are the Cartesian components of the alignment tensor in the axis system defined by the molecule itself: e.g.  $S_{mn} \equiv \langle (3 \cos \theta_m \cos \theta_n - \delta_{mn})/2 \rangle$ , where  $\theta_x$  is the angle between the  $x$  axis and the spectrometer field.[238] The factor of  $10^5$  is just to make the values commensurate with atomic coordinates, since both the coordinates and the alignment tensor values will be updated during the refinement. The calculated dipolar splitting is then

$$D_{calc} = - \left( \frac{10^{-5} \gamma_i \gamma_j h}{2\pi^2 r_{ij}^3} \right) \sum_{m,n=xyz} \cos \phi_m \cdot S_{mn} \cdot \cos \phi_n$$

where  $\phi_x$  is the angle between the internuclear vector and the  $x$  axis. Geometrically, the splitting is proportional to the transformation of the alignment tensor onto the internuclear axis. This is just Eqs. (5) and (13) of the above reference, with any internal motion corrections (which might be a part of  $S_{system}$ ) set to unity. If there is an internal motion correction which is the same for all observations, this can be assimilated into the alignment tensor. The current code does not allow for variable corrections for internal motion. See Ref. [239] for a fuller discussion of these issues.

At the end of the calculation, the alignment tensor is diagonalized to obtain information about its principal components. This allows the alignment tensor to be written in terms of the "axial" and "rhombic" components that are often used to describe alignment.

### Variables in the &align namelist.

- ndip        Number of observed dipolar couplings to be used as restraints.
- id,jd        Atom numbers of the two atoms involved in the dipolar coupling.
- dobsl, dobsu    Limiting values for the observed dipolar splitting, in Hz. If the calculated coupling is less than *dobsl*, the energy penalty is proportional to  $(D_{calc} - D_{obs,l})^2$ ; if it is larger than *dobsu*, the penalty is proportional to  $(D_{calc} - D_{obs,lu})^2$ . Calculated values between *dobsl* and *dobsu* are not penalized. Note that *dobsl* must be less than *dobsu*; for example, if the observed coupling is -6 Hz, and a 1 Hz "buffer" is desired, you could set *dobsl* to -7 and *dobsu* to -5.
- dwt        The relative weight of each observed value. Default is 1.0. The penalty function is thus:
- $$E_{align}^i = D_{wt}^i (D_{calc}^i - D_{obs(u,l)}^i)^2$$
- where  $D_{wt}$  may vary from one observed value to the next. Note that the default value is arbitrary, and a smaller value may be required to avoid overfitting the dipolar coupling data.[239]

## 6. NMR, X-ray, and cryo-EM/ET refinement

- dataset** Each dipolar peak can be associated with a "dataset", and a separate alignment tensor will be computed for each dataset. This is generally used if there are several sets of experiments, each with a different sample or temperature, etc., that would imply a different value for the alignment tensor. By default, there is one dataset to which each observed value is assigned.
- num\_datasets** The number of datasets in the constraint list. Default is 1.
- s11,s12,s13,s22,s23** Initial values for the Cartesian components of the alignment tensor. The tensor is traceless, so S33 is calculated as  $-(S11+S22)$ . In order to have the order of magnitude of the S values be roughly commensurate with coordinates in Angstroms, the alignment tensor values must be multiplied by  $10^5$ .
- gigj** Product of the nuclear "g" factors for this dipolar coupling restraint. These are related to the nuclear gyromagnetic ratios by  $\gamma_N = g_N \beta_N / \hbar$ . Common values are  $^1\text{H} = 5.5856$ ,  $^{13}\text{C} = 1.4048$ ,  $^{15}\text{N} = -0.5663$ ,  $^{31}\text{P} = 2.2632$ .
- dij** The internuclear distance for observed dipolar coupling. If a non-zero value is given, the distance is considered to be fixed at the given value. If a *dij* value is zero, its value is computed from the structure, and it is assumed to be a variable distance. For one-bond couplings, it is usually best to treat the bond distance as "fixed" to an effective zero-point vibration value.[\[240\]](#)
- dcut** Controls printing of calculated and observed dipolar couplings. Only values where  $\text{abs}(\text{dobs}(u,l) - \text{dcalc})$  is greater than *dcut* will be printed. Default is 0.1 Hz. Set to a negative value to print all dipolar restraint information.
- freezemol** If this is set to *.true.*, the molecular coordinates are not allowed to vary during dynamics or minimization: only the elements of the alignment tensor will change. This is useful to fit just an alignment tensor to a given structure. Default is *.false.*

### 6.6. Residual CSA or pseudo-CSA restraints

Resonance positions in partially aligned media will be shifted from their positions in isotropic media, and this can provide information that is very similar to residual dipolar coupling constraints. This section shows how to input these sorts of restraints. The entry of the alignment tensor is done as in Section 6.5, so you must have a DIPOLE file (with an &align namelist) even if you don't have any RDC restraints. Then, if there is a CSA line in I/O redirection section, that file will be read with the following inputs:

#### Variables in the &csa namelist.

- nrsa** Number of observed residual CSA peaks to be used as restraints.
- icsa,jcsa,kcsa** Atom numbers for the csa of interest: *jcsa* is the atom whose  $\Delta\sigma$  value has been measured; *icsa* and *kcsa* are two atoms bonded to it, used to define the local axis frame for the CSA tensor. See *amber12/test/pcsa/RST.csa* for examples of how to set these.



- cobsl, cobsu** Limiting values for the observed residual CSA, in Hz (not ppm or ppb!). If the calculated value of  $\Delta\sigma$  is less than *cobsl*, the energy penalty is proportional to  $(\Delta\sigma_{calc} - \Delta\sigma_{obs,l})^2$ ; if it is larger than *cobsu*, the penalty is proportional to  $(\Delta\sigma_{calc} - \Delta\sigma_{obs,u})^2$ . Calculated values between *cobsl* and *cobsu* are not penalized. Note that *cobsl* must be less than *cobsu*.
- cwt** The relative weight of each observed value. Default is 1.0. The penalty function is thus:
- $$E_{csa}^i = C_{wt}^i (\Delta\sigma_{calc}^i - \Delta\sigma_{obs(u,l)}^i)^2$$
- where  $C_{wt}$  may vary from one observed value to the next. Note that the default value is arbitrary, and a smaller value may be required to avoid overfitting the data.
- datasetc** Each residual CSA can be associated with a "dataset", and a separate alignment tensor will be computed for each dataset. This is generally used if there are several sets of experiments, each with a different sample or temperature, etc., that would imply a different value for the alignment tensor. By default, there is one dataset to which each observed value is assigned. The tensors themselves are entered for each dataset in the DIPOLE file.
- field** Magnetic field (in MHz) for the residual CSA being considered here. This is indexed from 1 to *nrsa*, and is nucleus dependent. For example, if the proton frequency is 600 MHz, then *field* for  $^{13}\text{C}$  would be 150, and that for  $^{15}\text{N}$  would be 60.
- sigma11, sigma22, sigma12, sigma13, sigma23** Values of the CSA tensor (in ppm) for atom *icsa*, in the local coordinate frame defined by atoms *icsa*, *jcsa* and *kcsa*. See *\$AMBERHOME/test/pcsa/RST.csa* for examples of how to set these.
- ccut** Controls printing of calculated and observed residual CSAs. Only values where  $\text{abs}(\text{cobs}(u,l) - \text{ccalc})$  is greater than *ccut* will be printed. Default is 0.1 Hz. Set to a negative value to print all information.

The residual CSA facility is new as of Amber 10, and has not been used as much as other parts of the NMR refinement package. You should study the example files listed above to see how things work. The residual CSA values should closely match those found by the RAMAH package (<http://www-personal.umich.edu/~hashimi/Software.html>), and testing this should be a first step in making sure you have entered the data correctly.

## 6.7. Preparing restraint files for Sander

Fig. 6.1 shows the general information flow for auxiliary programs that help prepare the restraint files. Once the restraint files are made, Fig. 6.2 shows a flow-chart of the general way in which *sander* refinements are carried out.

The basic ideas of this scheme owe a lot to the general experience of the NMR community over the past decade. Several papers outline procedures in the Scripps group, from which a

## 6. NMR, X-ray, and cryo-EM/ET refinement

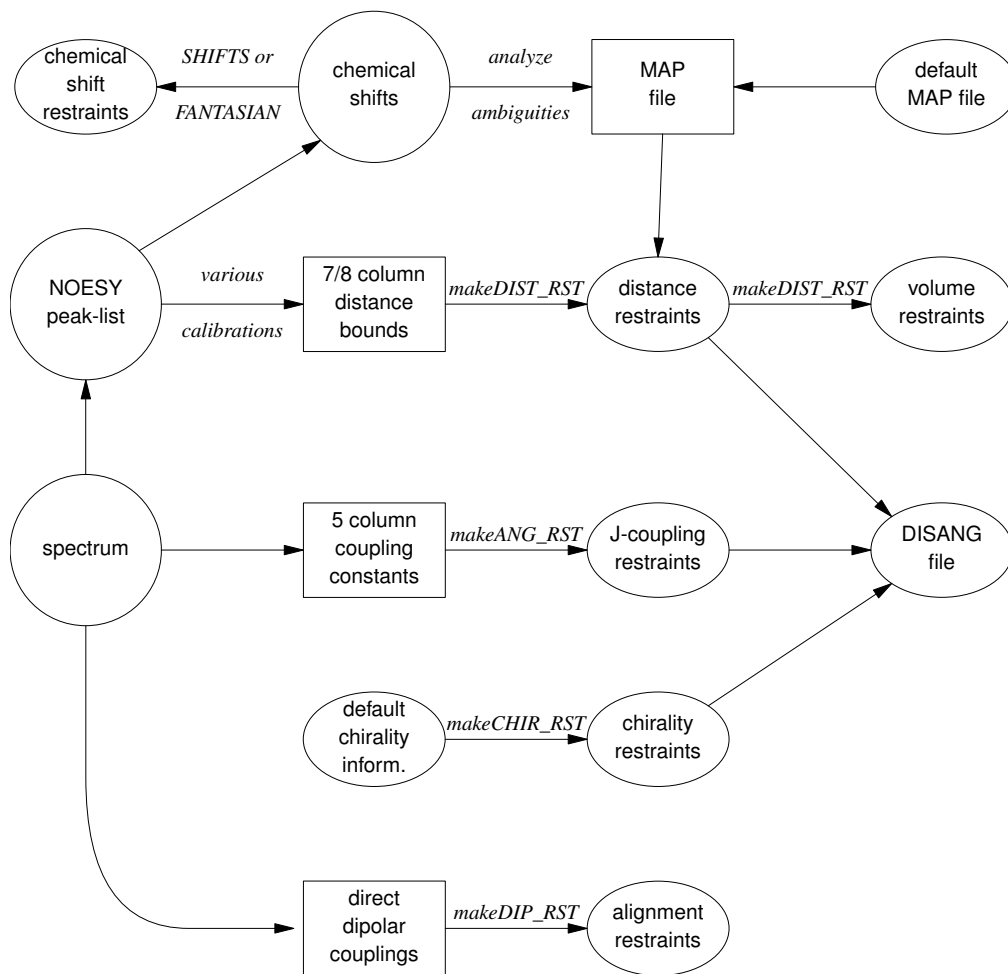


Figure 6.1.: Notation: circles represent logical information, whose format might differ from one project to the next; solid rectangles are in a specific format (largely compatible with DIANA and other programs), and are intended to be read and edited by the user; ellipses are specific to sander, and are generally not intended to be read or edited manually. The conversion of NOESY volumes to distance bounds can be carried out by a variety of programs such as mardigras or xpk2bound that are not included with Amber. Similarly, the analysis and partial assignment of ambiguous or overlapped peaks is a separate task; at TSRI, these are typically carried out using the programs xpkasgn and filter.pl

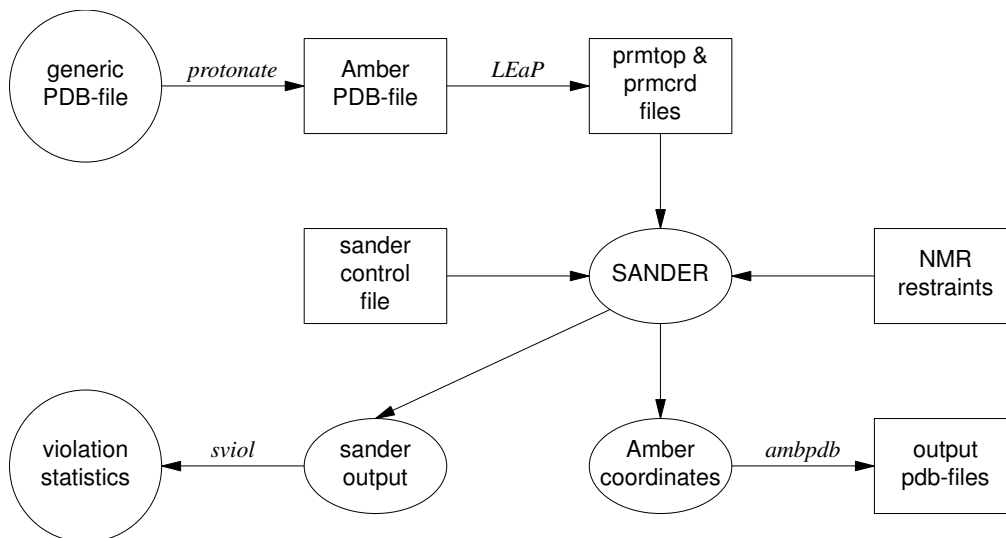


Figure 6.2.: General organization of NMR refinement calculations.

lot of the NMR parts of *sander* are derived.[231, 241–245] They are by no means the only way to proceed. We hope that the flexibility incorporated into *sander* will encourage folks to experiment with refinement protocols.

### 6.7.1. Preparing distance restraints: makeDIST\_RST

The *makeDIST\_RST* program converts a simplified description of distance bounds into a detailed input for *sander*. A variety of input and output filenames may be specified on the command line:

input:

```

-upb <filename> 7-col file of upper distance bounds, OR
-ual <filename> 8-col file of upper and lower bounds, OR
-vol <filename> 7-col file of NOESY volumes
-pdb <filename> Brookhaven format file
-map <filename> MAP file (default:map.DG-AMBER)
-les <filename> LES atom mappings, made by addles

```

output:

```

-dgm <filename> DGEOM95 restraint format
-rst <filename> SANDER restraint format
-svf <filename> Sander Volume Format, for NOESY refinement

```

other options:

```

-help (gives you this explanation, overrides other parameters)

```

## 6. NMR, X-ray, and cryo-EM/ET refinement

```
-report (gives you short runtime diagnostic output)
-nocorr (do not correct upper bound for r*-6 averaging)
-altdis (use alternative form for the distance restraints)
```

The 7/8 column distance bound file is essentially that used by the DIANA or DISGEO programs. It consists of one-line per restraint, which would typically look like the following:

```
23 ALA HA 52 VAL H 3.8 # comments go here
```

The first three columns identify the first proton, the next three the second proton, and the seventh column gives the upper bound. Only the first three letters of the residue name are used, so that DIANA files that contain residues like "ASP-" will be correctly interpreted. An alternate, 8-column, format has both upper and lower bounds as the seventh and eighth columns, respectively. A typical line might in an "8-col" file might look like this:

```
23 ALA HA 52 VAL H 3.2 3.8 # comments go here
```

Here the lower bound is 3.2 Å and the upper bound is 3.8 Å. Comments typically identify the spectrum and peak-number or other identification that allow cross-referencing back to the appropriate spectrum. If the comment contains the pattern "<integer>:<integer>", then the first integer is treated as a peak-identifier, and the second as a spectrum-identifier. These identifiers go into the *ixpk* and *nxpk* variables, and will later be printed out in *sander*, to facilitate going back to the original spectra to track down violations, etc.

The format for the *-vol* option is the same as for the *-upb* option except that the seventh column holds a peak intensity (volume) value, rather than a distance upper bound.

The input PDB file must exactly match the Amber *prmtop* file that will be used; use the *ambpdb -atm* command to create this.

If all peaks involved just single protons, and were fully assigned, this is all that one would need. In general, though, some peaks (especially methyl groups or fast-rotating aromatic rings) represent contributions from more than one proton, and many other peaks may not be fully assigned. *Sander* handles both of these situations in the same way, through the notion of an "ambiguous" peak, that may correspond to several assignments. These peaks are given two types of special names in the 7/8-column format file:

1. Commonly-occurring ambiguities, like the lack of stereospecific assignments to two methylene protons, are given names defined in the default MAP file. These names, also more-or-less consistent with DIANA, are like the names of "pseudo-atoms" that have long been used to identify such partially assigned peaks, e.g. "QB" refers to the (HB2,HB3) combination in most residues, and "MG1" in valine refers collectively to the three methyl protons at position CG1, etc.
2. There are generally also molecule-specific ambiguities, arising from potential overlap in a NOESY spectrum. Here, the user assigns a unique name to each such ambiguity or overlap, and prepares a list of the potential assignments. The names are arbitrary, but might be constructed, for example, from the chemical shifts that identify the peak, e.g. "p\_2.52" might identify the set of protons that could contribute to a peak at 2.52 ppm. The chemical shift list can be used to prepare a list of potential assignments, and these lists can often be pruned by comparison to approximate or initial structures.

The default and molecule-specific MAP files are combined into a single file, which is used, along with the 7-column restraint file, the the program *makeDIST\_RST* to construct the actual *sander* input files. You should consult the help file for *makeDIST\_RST* for more information. For example, here are some lines added to the MAP file for a recent TSRI refinement:

```

AMBIG n2:68 = HE 86 HZ 86
AMBIG n2:72 = HE 24 HD 24 HZ 24
AMBIG n2:73 = HN 81 HZ 13 HE 13 HD 13 HZ 24
AMBIG n2:78 = HN 76 HZ 13 HE 13 HZ 24
AMBIG n2:83 = HN 96 HN 97 HD 97 HD 91
AMBIG n2:86 = HD1 66 HZ2 66
AMBIG n2:87 = HN 71 HH2 66 HZ3 66 HD1 66

```

Here the spectrum name and peak number were used to construct a label for each ambiguous peak. Then, an entry in the restraint file might look like this:

```

123 GLY HN 0 AMB n2:68 5.5

```

indicating a 5.5 Å upper bound between the amide proton of Gly 123 and a second proton, which might be either the HE or HZ protons of residue 86. (The "zero" residue number just serves as a placeholder, so that there will be the same number of columns as for non-ambiguous restraints.) If it is possible that the ambiguous list might not be exhaustive (e.g. if some protons have not been assigned), it is safest to set *ialtd*=1, which will allow "mistakes" to be present in the constraint list. On the other hand, if you want to be sure that every violation is "active", set *ialtd*=0.

If the *-les* flag is set, the program will prepare distance restraints for multiple copies (LES) simulations. In this case, the input PDB file is one *without* LES copies, i.e. with just a single copy of the molecule. The "lesfile" specified by this flag is created by the *addles* program, and contains a mapping from original atom numbers into the copy numbers used in the multiple-copies simulation.

The *-rst* and *-svf* flags specify outputs for *sander*, for distance restraints and NOESY restraints, respectively. In each case, you may need to hand-edit the outputs to add additional parameters. You should make it a habit to compare the outputs with the descriptions given earlier in this chapter to make sure that the restraints are what you want them to be.

It is common to run *makeDIST\_RST* several times, with different inputs that correspond to different spectra, different mixing times, etc. It is then expected that you will manually edit the various output files to combine them into the single file required by *sander*.

### 6.7.2. Preparing torsion angle restraints: *makeANG\_RST*

There are fewer "standards" for representing coupling constant information. We have followed the DIANA convention in the program *makeANG\_RST*. This program takes as input a five-column torsion angle constraint file along with an Amber PDB file of the molecule. It creates as output (to standard out) a list of constraints in RST format that is readable by Amber.

```

Usage: makeANG_RST -help

```

## 6. NMR, X-ray, and cryo-EM/ET refinement

```
makeANG_RST -pdb ambpdb_file [-con constraint] [-lib libfile]
[-les lesfile ]
```

The input torsion angle constraint file can be read from standard in or from a file specified by the `-con` option on the command line. The input constraint file should look something like this:

```
1 GUA PPA 111.5 144.0
2 CYT EPSILN 20.9 100.0
2 CYT PPA 115.9 134.2
3 THY ALPHA 20.4 35.6
4 ADE GAMMA 54.7 78.8
5 GLY PHI 30.5 60.3
6 ALA CHI 20.0 50.0
....
```

Lines beginning with "#" are ignored. The first column is the residue number; the second is the residue name (three letter code, or as defined in your personal torsion library file). Only the first three letters of the residue name are used, so that DIANA files that contain residues like "ASP-" will be correctly interpreted. Third is the angle name (taken from the torsion library described below). The fourth column contains the lower bound, and the fifth column specifies the upper bound. Additional material on the line is (presently) ignored.

*Note:* It is assumed that the lower bound and the upper bound define a region of allowed conformation on the unit circle that is swept out in a clockwise direction from  $lb \rightarrow ub$ . If the number in the  $lb$  column is greater than the number in the  $ub$  column,  $360^\circ$  will successively be subtracted from the  $lb$  until  $lb < ub$ . This preserves the clockwise definition of the allowed conformation space, while also making the number that specifies the lower bound less than the number that specifies the upper bound, as is required by Amber. If this occurs, a warning message will be printed to *stderr* to notify the user that the data has been modified.

The angles that one can constrain in this manner are defined in the library file that can be optionally specified on the command line with the `-lib` flag, or the default library "tordef.lib" (written by Garry P. Gippert) will be used. If you wish to specify your own nomenclature, or add angles that are not already defined in the default file, you should make a copy of this file and modify it to suit your needs. The general format for an entry in the library is:

```
LEU PSI N CA C N+
```

where the first column is the residue name, the second column is the angle name that will appear in the input file when specifying this angle, and the last four columns are the atom names that define the torsion angle. When a torsion angle contains atom(s) from a preceding or succeeding residue in the structure, a "-" or "+" is appended to those atom names in the library, thereby specifying that this is the case. In the example above, the atoms that define PSI for LEU residues are the N, CA, and C atoms of that same LEU and the N atom of the residue after that LEU in the primary structure. Note that the order of atoms in the definition is important and should reflect that the torsion angle rotates about the two central atoms as well as the fact that the four atoms are bonded in the order that is specified in the definition.

If the first letter of the second field is "J", this torsion is assumed to be a J-coupling constraint. In that case, three additional floats are read at the end of the line, giving the A,B and C coefficients for the Karplus relation for this torsion. For example:

```
ALA JHNA H N CA HA 9.5 -1.4 0.3
```

will set up a J-coupling restraint for the HN-HA 3-bond coupling, assuming a Karplus relation with A,B, C as 9.5, -1.4 and 0.3. (These particular values are from Brüschweiler and Case, JACS 116: 11199 (1994).)

This program also supports pseudorotation phase angle constraints for prolines and nucleic acid sugars; each of these will generate restraints for the 5 component angles which correspond to the *lb* and *ub* values of the input pseudorotation constraint. In the torsion library, a pseudorotation definition looks like:

```
PSEUDO CYT PPA NU0 NU1 NU2 NU3 NU4
CYT NU0 C4' O4' C1' C2'
CYT NU1 O4' C1' C2' C3'
CYT NU2 C1' C2' C3' C4'
CYT NU3 C2' C3' C4' O4'
CYT NU4 C3' C4' O4' C1'
```

The first line describes that a PSEUDOrotation angle is to be defined for CYT that is called PPA and is made up of the five angles NU0-NU4. Then the definition for NU0-NU4 should also appear in the file in the same format as the example given above for LEU PSI.

PPA stands for Pseudorotation Phase Angle and is the angle that should appear in the input constraint file when using pseudorotation constraints. The program then uses the definition of that PPA angle in the library file to look for the 5 other angles (NU0-NU4 in this case) which it then generates restraints for. PPA for proline residues is included in the standard library as well as for the DNA nucleotides.

If the *-les* flag is set, the program will prepare torsion angle restraints for multiple copies (LES) simulations. In this case, the input PDB file is one *without* LES copies, i.e. with just a single copy of the molecule. The "lesfile" specified by this flag is created by the *addles* program, and contains a mapping from original atom numbers into the copy numbers used in the multiple-copies simulation.

Torsion angle constraints defined here cannot span two different copy sets, i.e., there cannot be some atoms of a particular torsion that are in one multiple copy set, and other atoms from the same torsion that are in other copy sets. It *is* OK to have some atoms with single copies, and others with multiple copies in the same torsion. The program will create as many duplicate torsions as there are copies.

A good alternative to interpreting J-coupling constants in terms of torsion angle restraints is to refine directly against the coupling constants themselves, using an appropriate Karplus relation. See the discussion of the variable RJCOEF, above.

### 6.7.3. Chirality restraints: makeCHIR\_RST

```
Usage: makeCHIR_RST <pdb-file> <output-constraint-file>
```

## 6. NMR, X-ray, and cryo-EM/ET refinement

We also find it useful to add chirality constraints and *trans*-peptide  $\omega$  constraints (where appropriate) to prevent chirality inversions or peptide bond flips during the high-temperature portions of simulated annealing runs. The program *makeCHIR\_RST* will create these constraints. Note that you may have to edit the output of this program to change *trans* peptide constraints to *cis*, as appropriate.

### 6.7.4. Direct dipolar coupling restraints: *makeDIP\_RST*

For simulations with residual dipolar coupling restraints, the *makeDIP\_RST.protein*, *makeDIP\_RST.dna* and *makeDIP\_RST.diana* are simple codes to prepare the input file. Use *-help* to obtain a more detailed description of the usage. For now, this code only handles backbone NH and C $\alpha$ H data. The header specifying values for various parameters needs to be manually added to the output of *makeDIP\_RST*.

Use of residual dipolar coupling restraints is new both for Amber and for the general NMR community. Refinement against these data should be carried out with care, and the optimal values for the force constant, penalty function, and initial guesses for the alignment tensor components are still under investigation. Here are some suggestions from the experiences so far:

1. Beware of overfitting the dipolar coupling data in the expense of Amber force field energy. These dipolar coupling data are very sensitive to tiny changes in the structure. It is often possible to drastically improve the fitting by making small distortions in the backbone angles. We recommend inclusion of explicit angle restraints to enforce ideal backbone geometry, especially for those residues that have corresponding residual dipolar coupling data.
2. The initial values for the Cartesian components of the alignment tensor can influence the final structure and alignment if the structure is not fixed (*ibelly* = 0). For a fixed structure (*ibelly* = 1), these values do not matter. Therefore, the current "best" strategy is to fit the experimental data to the fixed starting structure, and use the alignment tensor[s] obtained from this fitting as the initial guesses for further refinement.
3. Amber is capable of simultaneously fitting more than one set of alignment data. This allows the use of individually obtained datasets with different alignment tensors. However, if the different sets of data have equal directions of alignment but different magnitudes, using an overall scaling factor for these data with a single alignment tensor could greatly reduce the number of fitting parameters.
4. Because the dipolar coupling splittings depend on the square root of the order parameters ( $0 \leq S_2 \leq 1$ ), these order parameters describing internal motion of individual residues are often neglected (N. Tjandra and A. Bax, *Science* **278**, 1111-1113, 1997). However, the square root of a small number can still be noticeably smaller than 1, so this may introduce undesirable errors in the calculations.

### 6.7.5. *fantasian*

A program to evaluate magnetic anisotropy tensor parameters



Ivano Bertini  
 Depart. of Chemistry, Univ. of Florence, Florence, Italy  
 e-mail: bertini@riscl.lrm.fi.cnr.it

**INPUT FILES:**

*Observed shifts file (pcshifts.in):*

```
1st column --> residue number
2nd column --> residue name
3rd column --> proton name
4th column --> observed pseudocontact shift value
5th column --> multiplicity of the NMR signal (for example it is 3 for of a methyl
6th column --> relative tolerance
7th column --> relative weight
```

*Amber pdb file (parm.pdb):* coordinates file in PDB format. If you need to use a solution NMR family of structures you have to superimpose the structures before to use them.

**OUTPUT FILES:**

*Observed out file (obs.out):* This file is built and read by the program itself, it reports the data read from the input files.

*output file (res.out):* The main output file. In this file the result of the fitting is reported. Using fantasian it is possible to define an internal reference system to visualize the orientation of the tensor axes. Then in this file you can find PDB format lines (ATOM) which can be included in a PDB file to visualize the internal reference system and the tensor axes. In the main output file all the three equivalent permutations of the tensor parameters with respect to the reference system are reported. The summary of the minimum and maximum errors and that of squared errors are also reported.

*Example files:* in the directory example there are all the files necessary to run a fantasian calculation:

```
fantasian.com --> run file
pcshifts.in --> observed shifts file
parm.pdb --> coordinate file in PDB format
obs.out --> data read from input files
res.out --> main output file ~
```

**6.8. Getting summaries of NMR violations**

If you specify LISTOUT=POUT when running *sander*, the output file will contain a lot of detailed information about the remaining restraint violations at the end of the run. When running a family of structures, it can be useful to process these output files with *sviol*, which takes a list of *sander* output files on the command line, and sends a summary of energies and violations to STDOUT. If you have more than 20 or so structures to analyze, the output from *sviol* becomes unwieldy. In this case you may also wish to use *sviol2*, which prints out somewhat less detailed

## 6. NMR, X-ray, and cryo-EM/ET refinement

information, but which can be used on larger families of structures. The *senergy* script gives a more detailed view of force-field energies from a series of structures. (We thank the TSRI NMR community for helping to put these scripts together, and for providing many useful suggestions.)

### 6.9. Time-averaged restraints

The model of the previous sections involves the "single-average-structure" idea, and tries to fit all constraints to a single model, with minimal deviations. A generalization of this model treats distance constraints arising from NOE crosspeaks (for example) as being the average distance determined from a trajectory, rather than as the single distance derived from an average structure.

Time-averaged bonds and angles are calculated as

$$\bar{r} = (1/C) \left\{ \int_0^t e^{(t'-t)/\tau} r(t')^{-i} dt' \right\}^{-1/i} \quad (6.1)$$

where

$\bar{r}$  = time-averaged value of the internal coordinate (distance or angle)

$t$  = the current time

$\tau$  = the exponential decay constant

$r(t')$  = the value of the internal coordinate at time  $t'$

$i$  = average is over internals to the inverse of  $i$ . Usually  $i = 3$  or  $6$  for NOE distances, and  $-1$  (linear averaging) for angles and torsions.

$C$  = a normalization integral.

Time-averaged torsions are calculated as

$$\langle \phi \rangle = \tan^{-1} (\langle \sin(\phi) \rangle / \langle \cos(\phi) \rangle)$$

where  $\phi$  is the torsion, and  $\langle \sin(\phi) \rangle$  and  $\langle \cos(\phi) \rangle$  are calculated using the equation above with  $\sin(\phi(t'))$  or  $\cos(\phi(t'))$  substituted for  $r(t')$ .

Forces for time-averaged restraints can be calculated either of two ways. This option is chosen with the DISAVI / ANGAVI / TORAVI commands. In the first (the default),

$$\partial E / \partial x = (\partial E / \partial \bar{r}) (\partial \bar{r} / \partial r(t)) (\partial r(t) / \partial x) \quad (6.2)$$

(and analogously for  $y$  and  $z$ ). The forces then correspond to the standard flat-bottomed well functional form, with the instantaneous value of the internal replaced by the time-averaged value. For example, when  $r_3 < \bar{r} < r_4$ ,

$$E = k_3 (\bar{r} - r_3)^2$$

and similarly for other ranges of  $\bar{r}$ .

When the second option for calculating forces is chosen (IINC = 1 on a DISAVI, ANGAVI or TORAVI card), forces are calculated as

$$\partial E/\partial x = (\partial E/\partial \bar{r})(\partial r(t)/\partial x) \quad (6.3)$$

For example, when  $r_3 < \bar{r} < r_4$ ,

$$\partial E/\partial x = 2k_3(\bar{r} - r_3)(\partial r(t)/\partial x)$$

Integration of this equation does not give Eq. 6.2, but rather a non-intuitive expression for the energy (although one that still forces the bond to the target range). The reason that it may sometimes be preferable to use this second option is that the term  $\partial \bar{r}/\partial r(t)$ , which occurs in the exact expression [Eq. 6.2], varies as  $(\bar{r}/r(t))^{1+i}$ . When  $i=3$ , this means the forces can be varying with the fourth power the distance, which can possibly lead to very large transient forces and instabilities in the molecular dynamics trajectory. [Note that this will not be the case when linear scaling is performed, i.e. when  $i = -1$ , as is generally the case for valence and torsion angles. Thus, for linear scaling, the default (exact) force calculation should be used].

It should be noted that forces calculated using Eq. 6.3 are not conservative forces, and would cause the system to gradually heat up, if no velocity rescaling were performed. The temperature coupling algorithm should act to maintain the average temperature near the target value. At any rate, this heating tendency should not be a problem in simulations, such as fitting NMR data, where MD is being used to sample conformational space rather than to extract thermodynamic data.

This section has described the methods of time-averaged restraints. For more discussion, the interested user is urged to consult studies where this method has been used.[246–250]

## 6.10. Multiple copies refinement using LES

NMR restraints can be made compatible with the multiple copies (LES) facility; see the following chapter for more information about LES. To use NMR constraints with LES, you need to do two things:

- (1) Add a line like "file wnmr name=(lesnmr) wovr" to your input to *addles*. The filename (lesnmr in this example) may be whatever you wish. This will cause *addles* to output an additional file that is needed at the next step.
- (2) Add "-les lesnmr" to the command line arguments to *makeDIST\_RST*. This will read in the file created by *addles* containing information about the copies. All NMR restraints will then be interpreted as "ambiguous" restraints, so that if any of the copies satisfies the restraint, the penalty goes to zero.

Note that although this scheme has worked well on small peptide test cases, we have yet not used it extensively for larger problems. This should be treated as an experimental option, and users should use caution in applying or interpreting the results.

## 6.11. Some sample input files

The next few pages contain excerpts from some sample NMR refinement files used at TSRI. The first example just sets up a simple (but often effective) simulated annealing run. You may have to adjust the length, temperature maximum, etc. somewhat to fit your problem, but these values work well for many "ordinary" NMR problems.

### 6.11.1. 1. Simulated annealing NMR refinement

```
15ps simulated annealing protocol
&cntrl
  nstlim=15000, ntt=1, (time limit, temp. control)
  ntp=500, pncut=0.1, (control of printout)
  ipnlty=1, nmropt=1, (NMR penalty function options)
  vlimit=10, (prevent bad temp. jumps)
  ntb=0, (non-periodic simulation)
/
&ewald
  eedmeth=5, (use r dielectric)
/
#
# Simple simulated annealing algorithm:
#
# from steps 0 to 1000: raise target temperature 10->1200K
# from steps 1000 to 3000: leave at 1200K
# from steps 3000 to 15000: re-cool to low temperatures
#
&wt type='TEMP0', istep1=0, istep2=1000, value1=10.,
value2=1200., /
&wt type='TEMP0', istep1=1001, istep2=3000, value1=1200.,
value2=1200.0, /
&wt type='TEMP0', istep1=3001, istep2=15000, value1=0.,
value2=0.0, /
#
# Strength of temperature coupling:
# steps 0 to 3000: tight coupling for heating and equilibration
# steps 3000 to 11000: slow cooling phase
# steps 11000 to 13000: somewhat faster cooling
# steps 13000 to 15000: fast cooling, like a minimization
#
&wt type='TAUTP', istep1=0, istep2=3000, value1=0.2,
value2=0.2, /
&wt type='TAUTP', istep1=3001, istep2=11000, value1=4.0,
value2=2.0, /
&wt type='TAUTP', istep1=11001, istep2=13000, value1=1.0,
```

```

value2=1.0, /
&wt type='TAUTP', istep1=13001,istep2=14000,value1=0.5,
value2=0.5, /
&wt type='TAUTP', istep1=14001,istep2=15000,value1=0.05,
value2=0.05, /
#
# "Ramp up" the restraints over the first 3000 steps:
#
&wt type='REST', istep1=0,istep2=3000,value1=0.1,
value2=1.0, /
&wt type='REST', istep1=3001,istep2=15000,value1=1.0,
value2=1.0, /
&wt type='END' /
LISTOUT=POUT (get restraint violation list)
DISANG=RST.f (file containing NMR restraints)

```

The next example just shows some parts of the actual RST file that *sander* would read. This file would ordinarily *not* be made or edited by hand; rather, run the programs *makeDIST\_RST*, *makeANG\_RST* and *makeCHIR\_RST*, combining the three outputs together to construct the RST file.

### 6.11.2. Part of the RST.f file referred to above

```

# first, some distance constraints prepared by makeDIST_RST:
# (comment line is input to makeRST, &rst namelist is output)
#
#( proton 1 proton 2 upper bound)
#-----
#
# 2 ILE HA 3 ALA HN 4.00
#
&rst iat= 23, 40, r3= 4.00, r4= 4.50,
r1 = 1.3, r2 = 1.8, rk2=0.0, rk3=32.0, ir6=1, /
#
# 3 ALA HA 4 GLU HN 4.00
#
&rst iat= 42, 50, r3= 4.00, r4= 4.50, /
#
# 3 ALA HN 3 ALA MB 5.50
#
&rst iat= 40, -1, r3= 6.22, r4= 6.72,
igr1= 0, 0, 0, 0, igr2= 44, 45, 46, 0, /
#
# .....etc.....
#

```

## 6. NMR, X-ray, and cryo-EM/ET refinement

```
# next, some dihedral angle constraints, from makeANG_RST:
#
&rst iat= 213, 215, 217, 233, r1=-190.0,
r2=-160.0, r3= -80.0, r4= -50.0, /
&rst iat= 233, 235, 237, 249, r1=-190.0,
r2=-160.0, r3= -80.0, r4= -50.0, /
# .....etc.....
#
# next, chirality and omega constraints prepared by makeCHIR_RST:
#
#
# chirality for residue 1 atoms: CA CG HB2 HB3
&rst iat= 3 , 8 , 6 , 7 ,
r1=10., r2=60., r3=80., r4=130., rk2 = 10., rk3=10., /
#
# chirality for residue 1 atoms: CB SD HG2 HG3
&rst iat= 5 , 11 , 9 , 10 , /
#
# chirality for residue 1 atoms: N C HA CB
&rst iat= 1 , 18 , 4 , 5 , /
#
# chirality for residue 2 atoms: CA CG2 CG1 HB
&rst iat= 22 , 26 , 30 , 25 , /
#
# .....etc.....
# trans-omega constraint for residue 2
&rst iat= 22 , 20 , 18 , 3 ,
r1=155., r2=175., r3=185., r4=205., rk2 = 80., rk3=80., /
#
# trans-omega constraint for residue 3
&rst iat= 41 , 39 , 37 , 22 , /
#
# trans-omega constraint for residue 4
&rst iat= 51 , 49 , 47 , 41 , /
#
# .....etc.....
#
```

The next example is an input file for volume-based NOE refinement. As with the distance

### 6.11.3. 3. Sample NOESY intensity input file

```
# A part of a NOESY intensity file:
&noexp
id2o=1, (exchangeable protons removed)
oscale=6.21e-4, (scale between exp. and calc. intensity units)
```

```

taumet=0.04, (correlation time for methyl rotation, in ns.)
taurot=4.2, (protein tumbling time, in ns.)
NPEAK = 13*3, (three peaks, each with 13 mixing times)
EMIX = 2.0E-02, 3.0E-02, 4.0E-02, 5.0E-02, 6.0E-02,
8.0E-02, 0.1, 0.126, 0.175, 0.2, 0.25, 0.3, 0.35,
(mixing times, in sec.)
IHP(1,1) = 13*423, IHP(1,2) = 13*1029, IHP(1,3) = 13*421,
(number of the first proton)
JHP(1,1) = 78*568, JHP(1,2) = 65*1057, JHP(1,3) = 13*421,
(number of the second proton)
AEXP(1,1) = 5.7244, 7.6276, 7.7677, 9.3519,
10.733, 15.348, 18.601,
21.314, 26.999, 30.579,
33.57, 37.23, 40.011,
(intensities for the first cross-peak)
AEXP(1,2) = 8.067, 11.095, 13.127, 18.316,
22.19, 26.514, 30.748,
39.438, 44.065, 47.336,
54.467, 56.06, 60.113,
AEXP(1,3) = 7.708, 13.019, 15.943, 19.374,
25.322, 28.118, 35.118,
40.581, 49.054, 53.083,
56.297, 59.326, 62.174,
/
SUBMOL1
RES 27 27 29 29 39 41 57 57 70 70 72 72 82 82 (residues in this submol)
END END

```

Next, we illustrate the form of the file that holds residual dipolar coupling restraints. Again, this would generally be created from a human-readable input using the program *makeDIP\_RST*.

#### 6.11.4. Residual dipolar restraints, prepared by *makeDIP\_RST*:

```

&align
ndip=91, dcut=-1.0, gigj = 37*-3.1631, 54*7.8467,
s11=3.883, s22=53.922, s12=33.855, s13=-4.508, s23=-0.559,
id(1)=188, jd(1)=189, dobsu(1)= 6.24, dobsl(1)= 6.24,
id(2)=208, jd(2)=209, dobsu(2)= -10.39, dobsl(1)= -10.39,
id(3)=243, jd(3)=244, dobsu(3)= -8.12, dobsl(1)= -8.12,
....
id(91)=1393, jd(91)=1394, dobsu(91)= -19.64, dobsl(91) = -19.64,
/

```

Finally, we show how the detailed input to *sander* could be used to generate a more complicated restraint. Here is where the user would have to understand the details of the RST file, since there

## 6. NMR, X-ray, and cryo-EM/ET refinement

are no "canned" programs to create this sort of restraint. This illustrates, though, the potential power of the program.

### 6.11.5. A more complicated constraint

```
# 1) Define two centers of mass. COM1 is defined by
# {C1 in residue 1; C1 in residue 2; N2 in residue 3; C1 in residue 4}.
# COM2 is defined by {C4 in residue 1; O4 in residue 1; N* in residue 1}.
# (These definitions are effected by the igr1/igr2 and grnam1/grnam2
# variables; You can use up to 200 atoms to define a center-of-mass
# group)
#
# 2) Set up a distance restraint between COM1 and COM2 which goes from a
# target value of 5.0A to 2.5A, with a force constant of 1.0, over steps 1-5000.
#
# 3) Set up a distance restraint between COM1 and COM2 which remains fixed
# at the value of 2.5A as the force slowly constant decreases from
# 1.0 to 0.01 over steps 5001-10000.
#
# 4) Sets up no distance restraint past step 10000, so that free (unrestrained)
# dynamics takes place past this step.
#
&rst iat=-1,-1, nstep1=1,nstep2=5000,
iresid=1,irstyp=0,ifvari=1,ninc=0,imult=0,ir6=0,ifntyp=0,
r1=0.00000E+00,r2=5.0000,r3=5.0000, r4=99.000,rk2=1.0000,rk3=1.0000,
r1a=0.00000E+00,r2a=2.5000,r3a=2.5000, r4a=99.000,rk2a=1.0000,rk3a=1.0000,
igr1 = 2,3,4,5,0, grnam1(1)='C1',grnam1(2)='C1',grnam1(3)='N2',
grnam1(4)='C1', igr2 = 1,1,1,0, grnam2(1)='C4',grnam2(2)='O4',grnam2(3)='N*',
/
&rst iat=-1,-1, nstep1=5001,nstep2=10000,
iresid=1,irstyp=0,ifvari=1,ninc=0,imult=0,ir6=0,ifntyp=0,
r1=0.00000E+00,r2=2.5000,r3=2.5000, r4=99.000,rk2=1.0000,rk3=1.0000,
r1a=0.00000E+00,r2a=2.5000,r3a=2.5000, r4a=99.000,rk2a=1.0000,rk3a=0.0100,
igr1 = 2,3,4,5,0, grnam1(1)='C1',grnam1(2)='C1',grnam1(3)='N2',
grnam1(4)='C1', igr2 = 1,1,1,0, grnam2(1)='C4',grnam2(2)='O4',grnam2(3)='N*',
/
```

## 6.12. X-ray Crystallography Refinement using SANDER

An interface program links the SANDER and Crystallography and NMR System (CNS) software packages[251] to run QM/MM refinement on X-ray crystal structures, which in many instances will lead to an improvement of X-ray crystal structure quality for medium to low resolution datasets.[252, 253] The QM calculation is enabled by a linear scaling semi-empirical technique, the divide-and-conquer method, allowing large portions of a protein to be studied at



a quantum mechanical level of theory while still retaining charge effects from the surrounding protein.[254–256]

SANDER computes forces to make an additional call to the interface program, where the atomic coordinates are output to a scratch file, CNS is then invoked via a system call to calculate the X-ray target function and its gradient in Cartesian space based on the coordinates in the scratch file. In practice, this is accomplished by modifying the CNS input script, `minimize.inp`. It does not perform minimization but only evaluates and outputs the X-ray target function and gradient based on the input structure. Next the X-ray target function and the gradient deposited in the scratch files are read into SANDER and added to the physical energy and gradient according to following equations. The QM/MM refinement proceeds by minimizing the total target function.

$$E_{total} = E_{chem} + w_{xray}E_{xray}$$

The QM/MM setup in SANDER is discussed in Chapter 3.6. In order to run QM/MM refinement in Amber, you should have CNS already installed and set up the environment variables for CNS in your shell script. Make sure you can run `"cns_solve < minimize.inp > minimize.out"` directly from your working directory. Convert the PDB structure factors file into CNS format. Generate the input topology and coordinate files for the CNS refinement. If necessary, construct topology and parameter files for unusual ligands as well. The initial coordinates in the SANDER and CNS input files should be consistent with one another. Provide the necessary (and correct) information about crystal structure in the `minimize.inp`, such as crystal data, space group, etc. Change the weighting factor ( $w_{xray}$ ) to balance QM/MM chemical data and the crystallographic data as appropriate.

#### File Usage

```
sander [-help] [-O] -i qmmin -o qmmout -p prmtop -c inpcrd -x qmmcrd -cns
```

	<b>Files for sander</b>
qmmin	Control data for the QM/MM minimization run
prmtop	Molecular topology, force field, periodic box type, atom and residue names
inpcrd	Initial coordinates
	<b>Files for CNS</b>
minimize.inp	Modified minimization input
prote.in	Structure factors file in cns format
xref.in	Link file connected between sander and CNS
generate.mtf	Topology file in CNS format
generate.pdb	Initial coordinates in CNS format

Sample inputs and outputs are in the `$AMBERHOME/test/1vrp_xray` directory.

## 6.13. EMAP constraints using SANDER

EMAP constrained simulation was developed to incorporate electron microscopy (EM) image information into macromolecular structure determination. Different from NMR and X-ray

## 6. NMR, X-ray, and cryo-EM/ET refinement

data, EM images have low resolutions (5~50Å). However, EM images of large molecular assemblies up to millions of atoms and in various biological relevant environments are available. This low resolution images provide precious structure information that can help to determine structures of many molecular assemblies and machineries[257–264].

With EMAP constraints, SANDER can be used to perform rigid fitting of molecules into experimental maps of complexes to obtain complex structures, as well as flexible fittings to obtain conformations agreeing with experimental maps. In addition to experimental map information, homologous structural information can be used by EMAP to perform targeted conformational search (TCS) to induce simulation systems to form structures of interest.

If the constraint map or structure is very different from the starting conformation, SGLD is recommended to induce large conformational change by setting *isgld*=1. This is often used to simulate conformational transition between different states. See Sampling and free energy search section 4.3 for details in setup SGLD runs.

If domain motion is desired while domain structures need to be maintained, each domain is constrained with an EMAP constraint generated from the initial coordinates and set *move*=1 to allow the constraint map moving with the domain.

Each EMAP constraint is defined by a map file and a selection of atoms, as well as related parameters. Multiple EMAP constraints can be defined. The map file can be either an image, or a pdb structure or empty for the starting coordinates. The definition of EMAP constraints are read in from the input file as *emap* namelists. The following are variables in each *emap* namelist.

<i>mapfile</i>	file name of a constraint map or structure. The constraint maps must be in “map” or “ccp4” format. The structure must be in pdb format. The structure need not be the same as the simulation system. A resolution can be specified for the conversion to a density map. When a blank filename is specified, <i>mapfile</i> =”, the input coordinates of the masked atoms will be used to generate a constraint map. (default=”).
<i>atmask</i>	atom mask for selecting atoms to be constrained. (default=’:*)’).
<i>fcons</i>	Constraining constant. (default=0.05).
<i>move</i>	Allow the constraint map to move when <i>move</i> >0. (default=0).
<i>gammamap</i>	friction constant for the constraint map to move. (default=1/ps).
<i>resolution</i>	The resolution used to convert the constraint structure to a constraint map. (default=2 Å).
<i>ifit</i>	Perform rigid fitting between simulation when <i>ifit</i> >0. (default=0).
<i>grids</i>	Grid numbers in x,y,z,phi,psi,theta dimensions for grid-threading rigid fitting[257]. A search for local minimums start from every grid point and the global minimum is identified from all the local minimums. (default=1,1,1,1,1,1) .
<i>mapfit</i>	file name for the final constraint map after rigid fitting and/or moving. The file name must has an extension of .map or .ccp4. (default=”, for no map output).

molfit file name for the final constraint atom coordinates after rigid fitting and/or simulation. The file name must have an extension of .pdb. (default="", for no structure output).

Here is an example input file for an EMAP constrained SGLD simulation:

```

Map Constraint Self-Guided Langevin dynamics
&cntrl ntx=1, ntb=0, nstlim=100000, imin=0, maxcyc=1, ntc=2, ntf=2, cut=9.0,
ntr=1000, ntwr=10000, ntwx=10000, ntt=3, gamma_ln=10.0, nscm=100, dt=0.001,
ntb=0, igb=0, ips=1, isgld=1, tsgavg=1.0, sgft=0.5, tempsg=0, (SGLD)
iemap=1, (turn on EMAP )
/
&emap (EMAP constraint 1 using a map file)
mapfile=' data/lgb1.ccp4', atmask=' :1-20', fcons=0.1, move=1, ifit=1,
mapfit=' scratch/gbln_1.ccp4', molfit=' scratch/gbln_1.pdb', /
&emap (EMAP constraint 2 using a pdb file)
mapfile=' data/lgb1.pdb', atmask=' :22-37', fcons=0.1, move=0, ifit=1,
mapfit=' scratch/gblh_1.ccp4', molfit=' scratch/gblh_1.pdb', /
&emap (EMAP constraint 3 using initial coordinates)
mapfile='', atmask=' :41-56', fcons=0.1, move=1, ifit=1,
mapfit=' scratch/gblc_1.ccp4', molfit=' scratch/gblc_1.pdb', /

```



## 7. PMEMD

### 7.1. Introduction

PMEMD (Particle Mesh Ewald Molecular Dynamics) is a reimplementaion of a subset of sander functionality that has been written with the major goal of improving the performance of the most frequently used methods of sander. PMEMD supports Particle Mesh Ewald simulations, Generalized Born simulations, and ALPB (Analytical Linearized Poisson-Boltzmann) simulations using both the AMBER and CHARMM Force fields. The AMOEBA polarizable force field, is also supported but via a separate pmemd executable, pmemd.amba, which is essentially pmemd v9 with AMOEBA support included.

One of the major additions to PMEMD is the support for acceleration of both PME and GB calculations using NVIDIA GPUs.[265, 266] A detailed overview is provided in section 7.7

For the supported functionality, the input required and output produced are intended to exactly replicate sander within the limits of machine roundoff differences. PMEMD simply runs more rapidly, scales better in parallel using MPI, can be used profitably on significantly higher numbers of processors, can make use of NVIDIA GPUs for acceleration and uses less resident memory. Dynamic memory allocation is used so memory configuration is not required. PMEMD is ideal for molecular dynamics simulations of large solvated systems for long periods of time, especially if supercomputer resources are available. Benchmark data is available on the Amber website, ambermd.org. Given the improvements in performance in both serial and parallel it is adviseable to always use PMEMD in place of sander if the simulation requirements are within the functionality envelope provided by PMEMD.

PMEMD accepts sander input files (*mdin*, *prmtop*, *inpcrd*, *refc*), and is also backward compatible in regard to input to the same extent as sander. All options documented in the sander section of this manual should be properly parsed.

### 7.2. Functionality

New functionality has been added to *pmemd* since the release of Amber 11. These include

- *multi-pmemd* (akin to *multisander*) implemented, using the same *multisander* flags.
- replica exchange MD simulations in both Temperature space and Hamiltonian space
- Atom mask specification option (*restraintmask* and *bellymask* options are available, like in *sander*)
- IPS simulations
- Generalized Born model *igb=8* enabled

## 7. PMEMD

- LCPO surface area potential terms enabled for GB simulations (*gbsa=1*)

As mentioned above, PMEMD is not a complete implementation of sander. Instead, it is intended to be a fast implementation of the functionality most likely to be used by someone doing long time scale explicitly or implicitly solvated systems.

Specifically the following functionality is missing entirely:

- imin=5* In &cntrl. Trajectory analysis is not supported.
- nmropt=2* In &cntrl. A variety of NMR-specific options such as NOESY restraints, chemical shift restraints, pseudocontact restraints, and direct dipolar coupling restraints are not supported.
- idecomp!=0* In &cntrl. Energy decomposition options, used in conjunction with mm\_pbsa, are not supported.
- ipol!=0* In &cntrl. Polarizable force field simulations are not supported, other than amoeba, which is supported in pmemd.amba.
- igb==10* In &cntrl. Poisson-Boltzmann simulations are not supported.
- igb==6* or 8 In &cntrl. Gas phase (*igb==6*) simulations are not supported. IGB model 8 is not supported.
- ntmin>2* In &cntrl. XMIN and LMOD minimization methods are not supported.
- isgld!=0* In &cntrl. Self-guided Langevin dynamics is not supported.
- noshakemask* In &cntrl. The noshakemask string option is not supported.
- Solvent Caps* Solvent cap simulations are not supported.
- icfe!=0* In &cntrl. Calculation of free energies via thermodynamic integration is not supported.
- itgtmd!=0* In &cntrl. Targeted molecular dynamics is not supported.
- ievb!=0* In &cntrl. Empirical Valence Bond methods are not supported.
- ifqnt!=0* In &cntrl. QM/MM methods are not supported.
- icnstph/=0* In &cntrl. Constant pH simulations are not supported.
- &debugf namelist* Use of the &debugf namelist is only supported in a very limited way. Specifically only the do\_charmm\_dump\_gold option is supported.
- ineb!=0* In &cntrl. Nudged elastic band (NEB) calculations are not supported. These calculations are done by sander.MPI.
- LES* The Locally Enhanced Sampling method is not supported.
- REM==2* The partial REMD method (for LES) is not supported

### 7.3. PMEMD-specific namelist variables

*iamoeba!=0* In &cntrl. The amoeba polarizable potentials of Ren and Ponder are not supported in pmemd, but ARE supported in pmemd.amba.

The following &ewald options are supported, but only with the indicated default values:

*ew\_type=0* Only Particle Mesh Ewald calculations are supported. *ew\_type* = 1 (regular Ewald calculations) must be done in sander.

*nbflag=1* The *nbflag* option is ignored for MD, and all nonbonded list updates are scheduled based on "skin" checks. This is more reliable and has little cost. The variable *nsnb* still can be set and has an influence on minimizations. For PME calculations, list building may also be scheduled based on heuristics to suit load balancing requirements in multiprocessor runs.

*nbtell=0* The *nbtell* option is not particularly useful and is ignored.

*eedmeth=1* Only a cubic spline switch function (*eedmeth* = 1) for the direct sum Coulomb interaction is supported. This is the default, and most widely used setting for *eedmeth*. On some machine architectures, energies and forces are actually splined as a function of  $r^{**2}$  to a higher precision than the cubic spline switch. One consequence of only supporting *eedmeth* 1 is that vacuum simulations cannot be done (though generalized Born nonperiodic simulations are available).

*column\_fft=0* This is a sander-specific performance optimization option. PMEMD uses different mechanisms to enhance performance, and ignores this option.

It is suggested that new PMEMD users simply take an existing sander *mdin* file and attempt a short 10-30 step run. The output will indicate whether or not PMEMD will handle the particular problem at hand for all the functionality that is supported by "standard" sander. For functionality that requires special builds of sander or sander-derived executables (LES), there may be failures in namelist parsing.

### 7.3. PMEMD-specific namelist variables

The following namelist options are specific to PMEMD and generally relate to PMEMD specific performance optimizations: default values:

*mdout\_flush\_interval* In &cntrl, this variable can be used to control the minimum time in integer seconds between "flushes" of the *mdout* file. PMEMD DOES NOT use *flush()* calls at all because *flush* functionality does not work for all fortran compilers used in building pmemd. Thus, pmemd does an *open/close* cycle on *mdout* at a default minimum interval of 300 seconds. This interval can be changed with this variable if desired in the range of 0-3600. If *mdout\_flush\_interval* is set to 0, then *mdout* will be reopened and closed for each printed step. This functionality is provided in pmemd because some large systems have such large file i/o buffers that *mdout* will have 0 length on the disk through 100's of psec of simulated time. The default of 300 seconds provides a good compromise between efficiency and being able to observe the progress of the simulation.

## 7. PMEMD

*mdinfo\_flush\_interval* In `&cntrl`, this variable can be used to control the minimum time in integer seconds between "flushes" of the `mdinfo` file. PMEMD DOES NOT use file `flush()` calls at all because flush functionality does not work for all fortran compilers used in building `pmemd`. Thus, `pmemd` does an open/close cycle on `mdinfo` at a default minimum interval of 60 seconds. This interval can be changed with this variable if desired in the range of 0-3600. Note that `mdinfo` under `pmemd` simply serves as a heartbeat for the simulation at *mdinfo\_flush\_interval*, and `mdinfo` probably will not be updated with the last step data at the end of a run. If *mdinfo\_flush\_interval* is set to 0, then `mdinfo` will be reopened and closed for each printed step.

*es\_cutoff*, *vdw\_cutoff* In `&cntrl`, these variables can be used to control the cutoffs used for `vdw` and electrostatic direct force interactions in PME calculations separately. If you specify these variables, you should not specify the `cut` variable, and there is a requirement that *vdw\_cutoff*  $\geq$  *es\_cutoff*. These were introduced anticipating the need to support force fields where the direct force calculations are more expensive. For the current force fields, one can get slightly improved performance and about the same accuracy as one would get using a single cutoff. A good example would be using *vdw\_cutoff*=9.0, *es\_cutoff*=8.0. For this scenario, one gets about the accuracy in calculations associated with 9.0 angstrom cutoffs, but at a cost intermediate between an 8.0 and a 9.0 angstrom cutoff.

*no\_intermolecular\_bonds* In `&cntrl`. New variable controlling molecule definition. If 1, any molecules (ie., molecules as defined by the `prmtop`) joined by a covalent bond are fused to form a single molecule for purposes of pressure and virial-related operations; if 0 then the old behaviour (use `prmtop` molecule definitions) pertains. The default is 1; a value of 0 is not supported with forcefields using extra points. This option was necessitated in order to efficiently parallelize model systems with extra points. This redefinition of molecules actually allows for a more correct treatment of molecules during pressure adjustments and should produce better results with less strain on covalent bonds joining `prmtop`-defined molecules, but if the default value is used for a NTP simulation, results will differ slightly relative to `sander` if any intermolecular bonding was applied in forming the `prmtop` (eg., a `cyx-cyx` bridge was added between two peptides that originated in a PDB file, with each peptide having its own "TER" card). If consistency with `sander` is more important to you, and you are not using extra points, then you may want to set *no\_intermolecular\_bonds* to 0.

*ene\_avg\_sampling* In `&cntrl`. New variable controlling the number of steps between energy samples used in energy averages. If not specified, then `ntr` is used (default). To match the behaviour of `sander` or PMEMD v9 or earlier, this variable should be set to 1. This variable is only used for MD, not minimization and will also effectively be turned off if *ntave* is in use (non-0) or RESPA is in use (`nrespa` > 1). It is a fairly common situation that it is completely unnecessary to sample the energies every step to get a good average during production, and this is costly in terms of performance. Thus, performance can be improved (with greatest improvements for



the ensembles in the order NVE > NVT > NTP) without really losing anything of value by using the new default for energy average sampling (specify nothing).

*use\_axis\_opt* In &ewald. For parallel runs, the most favorable orientation of an orthogonal unit cell is with the longest side in the Z direction. Starting with pmemd 3.00, internal coordinates were actually reoriented to take advantage of this, and in high processor count runs on oblong unit cells, using axis optimization can improve performance on the order of 10%. However, if a system has hotspots, the results produced with axes oriented differently may vary by on the order of 0.05% relatively quickly. This effect has to do with the fact that axis optimization changes the order of LOTS of operations and also the fft slab layout, and under mpi if the system has serious hotspots, shake will come up with slightly different coordinate sets. This is really only a problem in pathological situations, and then it is probably mostly telling you that the situation is pathological, and neither set of results is more correct (typically the ewald error term is also high). In routine regression testing with over a dozen tests, axis reorientation has no effect on results. Nonetheless, the defaults are now selected to be in favor of higher reproducibility of results. Axis optimization is only done for mpi runs in which an orthogonal unit cell has an aspect ratio of at least 3 to 2. It is turned off for all minimization runs and for runs in which velocities are randomized (*ntt* = 2 or 3). If you want to force axis optimization, you may set *use\_axis\_opt* = 1 in the &ewald namelist. If you set it to 0, you will force it off in scenarios where it would otherwise be used.

*fft\_grids\_per\_ang* In &ewald. This variable may be used to set the desired reciprocal space fft grid density in terms of fft grids/angstrom. The nearest grid dimensions, given the prime factors supported by the underlying fft implementation, that meet or exceed this density will be used (ie., *nfft1,2,3* are set based on this specification). The default value is 1.0 grids/angstrom and gives very reasonable accuracy. PMEMD is actually more stringent now than sander in that it will meet or exceed the desired density instead of just approximating it. Thus, to get identical results with sander, one may have to specify grid dimensions to be used with the *nfft1,2,3* variables.

## 7.4. Slightly changed functionality

An I/O optimization has been introduced into PMEMD. The NTWR default value (frequency of writing the restart file) has been modified such that the default minimum is 500 steps, and this value is increased incrementally for multiprocessor runs. In general, frequent writes of *restrt*, especially in runs with a high processor count, is wasteful. Also, if the *mden* file is being written, it is always written as formatted output, regardless of the value of *ioutfm*. SANDER now conforms to this convention regarding *ioutfm* and *mden*.

In addition, there are two command-line options unique to pmemd:

**-l <logfile name>** A name may be assigned to the log file on the command line.

**-suffix <output files suffix>** A suffix may now be appended, following a ".", to all the default output file names for a pmemd run by simply entering the **-suffix** option. The suffix will

## 7. PMEMD

apply to `mdout`, `restrt`, `mdcrd`, `mdvel`, `mden`, `mdinfo`, and `logfile` names. However, if an output file name is explicitly provided on the command line, the provided name takes precedence. Entering "pmemd -suffix foo" will write `mdout` output to `mdout.foo`, and so on. This provides an easy way to group output files with minimal effort.

**-gpes <process\_map\_file>** This option controls the distribution of threads in a *multimemd* simulation and allows you to allocate threads to various processes however you want (rather than dividing up all threads equally between each line of the groupfile). By default, the threads are allocated sequentially (that is, for  $N$  groups given  $M$  threads per group, or  $N*M$  threads total, threads 0 to  $M-1$  will be assigned to the first group, threads  $M$  to  $2M-1$  will be assigned to the second group, etc.). Using the `-ng-nonsequential` flag, threads will be allocated with a one-at-a-time approach. For instance, given the same setup as above, the first group gets threads 0,  $M$ ,  $2M$ ,  $3M$ , ... etc, the second group gets threads 1,  $M+1$ ,  $2M+1$ ,  $3M+1$ , ... etc. The `process_map_file` is a file that contains as many lines as you have groups (although the last line can be omitted, and the remaining unspecified threads will be assigned to the final group). Each line must contain space-delimited integers that correspond to the thread numbers you want assigned to that group. Each group is assigned the threads listed in that line of the `process_map_file`. Every thread must be specified in the `process_map_file`, and no thread can be specified more than once.

### 7.5. Parallel performance tuning and hints

In order to achieve higher scaling, pmemd has implemented several performance algorithms, the most notable of which is the option of using a "block" or pencil fft rather than the usual slab fft algorithm. The block fft algorithm allows the reciprocal space and fft workload to be distributed to more processors, but at a cost of higher communications overhead, both in terms of the distributed fft transpose cost and in terms of communication of the data necessary to set up the fft grids in the first place. A number of variables in the `&ewald` namelist can be used to control whether the slab or block fft algorithm is used, how the block division occurs, whether direct force work is also assigned to tasks doing reciprocal space and fft work, whether the master is given any force and energy computation work to do, as opposed to being reserved strictly for handling output and loadbalancing, and the frequency of atom ownership reassignment, an operation that counteracts rising communications costs caused by diffusion. The various namelist variables involved have all been assigned defaults that adapt to run conditions, and in general it is probably best that the user just use the defaults and not attempt to make adjustments. However, in some instances, fine tuning may yield slightly better performance. The variables involved include `block_fft`, `fft_blk_y_divisor`, `excl_recip`, `excl_master`, and `atm_redist_freq`. These are described further in the README under `pmemd/src` as well as in the sourcecode itself.

Performance depends not only on proper setup of hardware and software, but also on making good choices in simulation configuration. There are many tradeoffs between accuracy and cost, as one might expect, and understanding all of these comes with experience. However, I would like to suggest a couple of good choices for your simulations, if you have facilities where you can routinely run at high processor count, say 32 processors or more. First of all, there is an implementation of binary trajectory files in pmemd and sander, based on the netCDF binary

file format. This is invoked now using `ioutfm == 1`, assuming you have built either `pmemd` or `sander` with "bintraj" support. Using this output format, i/o from the master process will be more efficient and your filesize will be about half what it would otherwise be. In Amber, `ptraj` can read these new netCDF trajectory files and can convert them to ASCII format if needed. At really high processor count using the netCDF format can be on the order of 10% more efficient than using the standard formatted trajectory output. Secondly, other simulation packages typically use multiple timestepping (`respa`) methods as an efficiency measure. These methods typically sample reciprocal space forces for PME less frequently. Due to the limited use of such methods by Amber users this approach has not been optimized in `pmemd` and hence while this can slightly improve performance for `pmemd` at low processor count, at higher processor counts using `respa` typically makes loadbalancing less efficient leading to a net loss of performance. If you wish to use `respa` for pme simulations (done typically by setting `nrespa` to 2 or 4), then you should check whether you actually get better performance. You may well not, and it will be at a cost of a loss in accuracy. Using `respa` for generalized Born simulations is fine in all cases, however.

## 7.6. Installation

Unlike previous versions of PMEMD, the CPU version is now built and tested as part of the standard Amber installation using the Makefile and `config.h` in `$AMBERHOME/src/`. To bring PMEMD inline with other parts of the Amber package the serial executable is `$AMBERHOME/bin/pmemd` while the parallel executable is `$AMBERHOME/bin/pmemd.MPI`.

The choice of compilation parameters as part of the default build has been made to provide good performance across the broadest range of architectures. The most heavily tested of these being Intel and AMD x86\_64 machines using the Intel compiler suite. While one can build PMEMD using other compilers, performance is typically better if the Intel compilers and Intel MKL math libraries are used.

In parallel it is assumed that calculations will be run either within a node or across a high speed interconnect such as Infiniband. The compile time options are chosen with this in mind. However, it is possible that improved serial and parallel performance can be achieved by fine tuning the compiler options and preprocessor flags. This, however, is something that should only be attempted by advanced users. For an overview of the various compile time options and for instructions on using the custom build scripts of earlier versions of PMEMD please refer to the README file in `$AMBERHOME/src/pmemd/`.

## 7.7. GPU Accelerated PMEMD

One of the newer features of PMEMD is the ability to use NVIDIA GPUs to accelerate both explicit solvent PME and implicit solvent GB simulations.[265, 266] This work is by Ross Walker at the San Diego Supercomputer Center in collaboration with NVIDIA. While this GPU acceleration is considered to be production ready it is still very new and thus has not been tested anywhere near as extensively as the CPU code has over the years. It has been in wide use throughout the AMBER community since version 11 but users should still exercise

## 7. PMEMD

caution when using this code. The error checking is not as verbose in the GPU code as it is on the CPU. If you encounter problems during a simulation on the GPU you should first try to run the identical simulation on the CPU to ensure that it is not your simulation setup which is causing problems. Feedback and questions should be posted to the Amber mailing list (see <http://lists.ambermd.org/>).

This section of the manual describes the feature set, installation, performance and accuracy considerations and other aspects of GPUs at the time of Amber's release. However, the rapidly changing nature of this field means that frequent updates are likely. You should refer to the web page <http://ambermd.org/gpus/> for the most up to date information.

### 7.7.1. New Features in AMBER 12

AMBER 12 brings with it a number of enhancements to the GPU accelerated code. Changes include improvements to the way in which specific GPUs are selected when running calculations, support for parallel runs, support for extra points, isotropic periodic sum, accelerated MD, temperature replica exchange, umbrella sampling through  $nmropt=1$ , simulated annealing through  $nmropt=1$ , all GB models, and Jarzynski sampling.

### 7.7.2. Supported Features

The GPU accelerated version of PMEMD supports both explicit solvent PME simulations in all three canonical ensembles (NVE, NVT and NPT) and implicit solvent Generalized Born simulations. It has been designed to support as many of the standard PMEMD features as possible, however, there are some current limitations that are detailed below. Some of these may be addressed in the future, and patches released, with the most up to date list posted on the web page. The following options are **NOT** supported:

1.  $ibelly \neq 0$  Simulations using belly style constraints are not supported.
2. if ( $igb \neq 0$  and  $cut < systemsize$ ) GPU accelerated implicit solvent GB simulations do not support a cutoff.
3.  $nmropt > 1$  Support is not currently available for  $nmropt > 1$ . In addition for  $nmropt = 1$  only features that do not change the underlying force field parameters are supported. For example umbrella sampling restraints are supported as is Jarzynski sampling as well as simulated annealing functions such as variation of Temp0 with simulation step. However, varying the VDW parameters with step is NOT supported.
4.  $nrespa \neq 1$  No multiple time stepping is supported.
5.  $vlimit \neq -1$  For performance reasons the  $vlimit$  function is not implemented on GPUs.
6.  $numextra > 0$  with MPI Extra points are currently only supported for single GPU runs.
7.  $imin = 1$  with MPI Minimization is currently only supported for single GPU runs.
8.  $es\_cutoff \neq vdw\_cutoff$  Independent cutoffs for electrostatics and van der Waals are not supported on GPUs.

9. *order* > 4 PME interpolation orders of greater than 4 are not supported at present.

Additionally there are some minor differences in the output format. For example the Ewald error estimate is NOT calculated when running on a GPU. It is recommended that you first run a short simulation using the CPU code to check the Ewald error estimate is reasonable and that your system is stable. The above limitations are tested for in the code, however, it is possible that there are additional simulation features that have not been implemented or tested on GPUs.

### 7.7.3. Supported GPUs

GPU accelerated PMEMD has been implemented using CUDA and thus will only run on NVIDIA GPUs at present. Due to accuracy concerns with pure single precision the code makes use of double precision in several places. This places the requirement that the GPU hardware supports double precision meaning only GPUs with hardware revision 1.3 or 2.0 and later can be used. At the time of Amber's release this comprises the following NVIDIA cards (\* = untested):

- **Hardware Version 3.0**

- GTX680 and other cards based on revision 3.0, are not currently supported at time of release. These cards severely limit double precision performance compared with version 2.0 cards and thus will require substantial optimization of the underlying code to achieve acceptable performance. It is our intention to release a patch enabling support for these cards in the near future.
- Tesla C2050/C2070/C2075/M2090
- GTX470\*/480/550\*/560\*/570\*/580/590\*

- **Hardware Version 1.3**

- Tesla C1060/S1070
- Quadro FX4800\*/5800\*
- GTX295/285/280\*/275\*/260\*/250\*/240\*/220\*/210\*

Other cards not listed here may also be supported as long as they correctly implement the Hardware Revision 1.3 or 2.0 specifications. Due to the larger graphics memories offered by the Tesla series GPUs these are the recommended models. Additionally you should ensure that all GPUs on which you plan to run PMEMD are connected to PCI-E 2.0 x 16 lane slots or better. If this is not the case then you will likely see significantly degraded performance.

Support is provided for single GPU and multiple GPU runs. Multiple GPU runs work using MPI and require the `pmemd.cuda.MPI` executable to be built. Extensive use of MPI v2 also means that a fully MPI v2 compliant MPI installation is also required. While you might only want to use a single GPU per simulation, since this maximizes efficiency you can still use multiple GPUs in a same node for independent calculations by utilizing the `CUDA_VISIBLE_DEVICES` environment variable. Details are provided in section 7.7.6.

### 7.7.4. Accuracy Considerations

The nature of current generation GPUs is such that single precision arithmetic is considerably faster ( $>8x$  for C1060 and  $>2x$  for C2050) than double precision arithmetic. This poses an issue when trying to obtain good performance from GPUs. Traditionally the CPU code in Amber has always used double precision throughout the calculation. While this full double precision approach has been implemented in the GPU code it gives very poor performance and so the default precision model used when running on GPUs is a combination of single and double precision, termed hybrid precision (SPDP), that is discussed in further detail in references [265, 266]. This approach uses single precision for individual calculations within the simulation but double precision for all accumulations. It also uses double precision for shake calculations and for other parts of the code where loss of precision was deemed to be unacceptable. Tests have shown that energy conservation is equivalent to the full double precision code and specific ensemble properties, such as order parameters, match the full double precision CPU code. However, the user should be aware that such tests at the time of writing are not exhaustive and more indepth validation is being conducted, the results of which will be reported in the literature. Previous acceleration approaches, such as the MDGRAPE accelerated sander, have used similar hybrid precision models and thus we believe that this is a reasonable compromise between accuracy and performance. The user should understand though that this approach leads to rapid divergence between GPU and CPU simulations, similar to that observed when running the CPU code across different processor counts in parallel but occurring much more rapidly. For this reason the GPU test cases are more sensitive to rounding difference caused by hardware and compiler variations and will likely require manual inspection of the test case diff files in order to verify that the installation is providing correct results.

While the default precision model is currently the hybrid SPDP model three different precision models have been implemented within the GPU code to facilitate advanced testing and comparison. The choice of default precision model may change in the future based on the outcome of detailed validation tests of the three different approaches. The precision models supported, and determined at compile time as described later, are:

- **SPSP** - Use single precision for the entire calculation with the exception of SHAKE which is always done in double precision. This provides the highest performance and is probably the most directly comparable model to other GPU MD implementations. However, insufficient testing has been done to know if the use of single precision throughout the simulation is acceptable and so for the moment this precision model should be used for testing and debugging purposes only.
- **SPDP** - (*Default*) Use a combination of single precision for calculation and double precision for accumulation. This approach is believed to provide the optimum tradeoff between accuracy and performance and hence at the time of release is the default model invoked when using the executable *pmemd.cuda*.
- **DPDP** - Use double precision for the entire calculation. This provides for careful regression testing against the CPU code. It makes no additional approximations above and beyond the CPU implementation and would be the model of choice if performance was not a consideration. On v1.3 NVIDIA hardware (e.g. C1060) the performance is approx-

imately a fifth that of the SPDP model while on v2.0 NVIDIA hardware (e.g. C2050) the performance is approximately half that of the SPDP model.

### 7.7.5. Installation and Testing

The GPU version of PMEMD is called `pmemd.cuda` (or `pmemd.cuda.MPI` for the multi GPU version) and must be built separately from the standard serial and parallel installations. Before attempting to build the GPU version of PMEMD you should have built and tested at least the serial version of Amber and preferably the parallel version as well. This will help ensure that basic issues relating to standard compilation on your hardware and operating system do not lead to confusion with GPU related compilation and testing problems. You should also be familiar with Amber's compilation and test procedures.

It is assumed that you have already correctly installed and tested CUDA support on your GPU. Before attempting to build `pmemd.cuda` you should first download and compile the NVIDIA CUDA SDK (available from <http://www.nvidia.com/>). Ensure that you can successfully build and run the `deviceQuery` program provided with this SDK since the output from this will be required if you are seeking help on the Amber mailing list. Additionally the environment variable `CUDA_HOME` should be set to point to your NVIDIA Toolkit installation and `$CUDA_HOME/bin/` should be in your path.

#### Building and Testing the Default SPDP Precision Model

Assuming you have a working CUDA installation you can build `pmemd.cuda` using the default precision model as follows:

```
cd $AMBERHOME
./configure -cuda gnu
make install
```

Next you can run the tests using the default GPU (the one with the largest memory) with:

```
make test.cuda
```

The majority of these tests should pass. However, given the parallel nature of GPUs, meaning the order of operation is not well defined, and the limited precision of the SPDP precision model it is not uncommon for there to be several possible failures. You may also see some tests, particularly the GB nucleosome test, fail on GPUs with limited memory. You should inspect the diff file created in the `$AMBERHOME/logs/test_amber_cuda/` directory to manually verify any possible failures. Differences which occur on only a few lines and are minor in nature can be safely ignored. Any large differences, or if you are unsure, should be posted to the Amber mailing list for comment.

#### Building non-standard Precision Models

You can build different precision models as described below. However, be aware that this is meant largely as a debugging and testing issue and NOT for running production calculations. Please post any questions or comments you may have regarding this to the Amber mailing list.

## 7. PMEMD

You should be aware that the variation in test case results due to rounding differences will be markedly higher when testing the SPSP precision model.

You select which precision model to compile as follows:

```
cd $AMBERHOME
./configure -cuda_DPDP gnu          (use -cuda_SPSP for the SPSP model)
make install
```

This will produce executables named `pmemd.cuda_XXXX` where `XXXX` is the precision model selected at configure time (SPSP or DPDP). You can then test this on the GPU with the most memory as follows:

```
cd $AMBERHOME/test/
./test_amber_cuda.sh DPDP          (to test the DPDP precision model)
```

### Testing Alternative GPUs

Should you wish to run the tests on a GPU different from the one with the most memory (and lowest GPU ID if more than one identical GPU exists) then you should make use of the `CUDA_VISIBLE_DEVICES` environment variable as described below. For example, to test the GPU with ID = 2 and the default SPDP precision model you would run the tests as follows:

```
cd $AMBERHOME
export CUDA_VISIBLE_DEVICES=2
make test.cuda
```

### Building pmemd.cuda.MPI

The GPU version of `pmemd` can be run in parallel on multiple GPUs using the executable (`pmemd.cuda.MPI`). Some simulations, particularly replica exchange simulations, require a parallel executable in order to operate.

Assuming you have a working CUDA installation you can build `pmemd.cuda.MPI` using the default precision model as follows:

```
cd $AMBERHOME
./configure -cuda -mpi gnu
make install
```

Note that `pmemd.cuda.MPI` requires more modern MPI-2 features that are not included with all MPI implementations. In particular, some of the earlier versions of OpenMPI do not support all of the requirements and will therefore not work. OpenMPI versions higher than 1.5 should work, as should most versions of `mpich2`.

Next you can run the tests using the default GPUs (the one with the largest memory in descending order) with:

```
export DO_PARALLEL='mpirun -np 2' # for bash/sh
setenv DO_PARALLEL "mpirun -np 2" # for csh/tcsh
make test.cuda_parallel
```



The majority of these tests should pass. However, as described above it is not uncommon for there to be several possible failures. You should inspect the diff file created in the `$AMBERHOME/logs/test_amber_cuda/` directory to manually verify any possible failures. Differences which occur on only a few lines and are minor in nature can be safely ignored. Any large differences, or if you are unsure, should be posted to the Amber mailing list for comment.

### 7.7.6. Running GPU Accelerated Simulations

In order to run a GPU accelerated MD simulation the only change required is to use the executable `pmemd.cuda` in place of `pmemd`. E.g.

```
$AMBERHOME/bin/pmemd.cuda -O -i mdin -o mdout -p prmtop \  
-c inpcrd -r restrt -x mdcrd
```

This will automatically run the calculation on the GPU with the most memory even if that GPU is already in use. If you have only a single CUDA capable GPU in your machine then this is fine, however if you want to control which GPU is used, or you want to run multiple independent simulations using different GPUs, then you manually need to specify the GPU to use with the `CUDA_VISIBLE_DEVICES` environment variable.

`CUDA_VISIBLE_DEVICES` Specifies which GPU should be used for running a GPU accelerated PMEMD calculation. This is based on the hardware ID of the GPU card which can be obtained by unsetting the variable (`unset CUDA_VISIBLE_DEVICES`) and running the `deviceQuery` command from the NVIDIA CUDA SDK. Valid values are a list of integers from 0 to 32. Multiple GPUs may be listed with commas in between them, and the one with the most memory will be selected. For example:

```
export CUDA_VISIBLE_DEVICES=1,3  
$AMBERHOME/bin/pmemd.cuda -O -i mdin -o mdout -p prmtop \  
-c inpcrd -r restrt -x mdcrd
```

In this way it is possible to make use of multiple GPUs in a single node, such as those provided by a Tesla S1070, for multiple simultaneous calculations. When running a single calculation across multiple GPUs using `pmemd.cuda.MPI` it also allows the selection of specific GPUs on specific nodes. For example running a 2 GPU job with `mpirun -np 2 pmemd.cuda.MPI` with the above listed `CUDA_VISIBLE_DEVICES` would automatically use the second (`id=1`) and fourth (`id=3`) GPU in the node. The multi GPU code will avoid assigning MPI GPU tasks to the same GPU if sufficient GPUs are visible.

### 7.7.7. Considerations for Maximizing GPU Performance

There are a number of considerations above and beyond those typically used on a CPU for maximizing the performance achievable for a GPU accelerated PMEMD simulation. The following provides some tips for ensuring good performance.

1. Avoid using small values of `NTPR`, `NTWX`, `NTWV`, `NTWE` and `NTWR`. Writing to the output, restart and trajectory files too often can hurt performance even on CPU runs,

## 7. PMEMD

however, this is more acute for GPU accelerated simulations because there is a substantial cost in copying data to and from the GPU. Performance is maximized when CPU to GPU memory synchronizations are minimized. This is achieved by computing as much as possible on the GPU and only copying back to CPU memory when absolutely necessary. There is an additional overhead in that performance is boosted by only calculating the energies when absolutely necessary, hence setting NTPR or NTWE to low values will result in excessive energy calculations. You should not set any of these values to less than 100 (except 0 to disable them) and ideally use values of 500 or more. >10000 for NTWR is ideal.

2. Use powers of two for the FFT dimensions (NFFT1,NFFT2,NFFT3) when running PME calculations. This has been addressed with NVIDIA Toolkit (>=4.0), however, better performance can still sometimes be obtained when you set the PME FFT dimensions to be powers of two. This means NFFT1,2,3=64,128 or 256. If this is not feasible then you should attempt to pick dimensions which have the least non-power of 2 prime factors, for example 96 (2x2x2x2x2x3) is better than 100 (2x2x5x5). It is not necessary for the three dimensions to be the same size, for example 64x64x128 will work fine. Additionally 64x128x96 will be better than 64x96x96. It is important, however, when choosing values for NFFT1,2,3 not to use a value that will give a FFT grid spacing of greater than 1 angstrom. If you do not specify FFT grid sizes then the GPU code will attempt to pick a reasonable set of values automatically.
3. Avoid using nmropt=1. Currently there is no CUDA kernel for the nmropt features. Hence simulations using nmropt=1 require additional synchronizations between GPU and CPU on every MD step. Depending on system size this can have a big impact on performance. We are working on developing a CUDA kernel for the nmropt=1 features that will be released as a patch at a later date.
4. Avoid using the NTP ensemble (NTB=2) when it is not required. Performance will generally be NVE~NVT>NPT. However, for explicit solvent simulations it is always necessary to run at least some NPT in order to allow the density to equilibrate. However, once this is done one can typically switch back to NVT or NVE for production
5. Do not assume that for small systems the GPU will always be faster. Typically for GB simulations of less than 150 atoms and PME simulations of less than 9,000 atoms it is not uncommon for the CPU version of the code to outperform the GPU version on a single node. Typically the performance differential between GPU and CPU runs will increase as system size atom count increases. Additionally the larger the non-bond cutoff used the better the GPU to CPU performance gain will be.
6. Avoid using CUDA Toolkit v4.1. At the time of writing the recommended CUDA Toolkit and compiler to use is v4.0. This provides maximum performance. A performance regression bug in v4.1 means that it is about 10 to 15% slower than v4.0. At the time of writing the v4.2 toolkit was not available for testing so it is unknown if this fixes the performance regression caused by v4.1.

## 7.8. Acknowledgements

This code was originally developed by Dr. Robert Duke of Prof. Lee Pedersen's Lab at UNC-Chapel Hill and Dr. Tom Darden's Lab at NIEHS, starting from the version of sander in Amber 6. Extensions have been made by Prof. Walker's lab at the San Diego Supercomputer Center including support for CHARMM force fields[267] and, in collaboration with NVIDIA, a GPU accelerated version of PMEMD.[265, 266]

We thank Prof. Pedersen for his support in the development of this code, and would also like to acknowledge funding support from NIH grant HL-06350 (PPG) and NSF grant 0121361 (ITR/AP) for the original development of PMEMD and UC Lab award 09-LR-06117792 and NSF (SI2-SSE 1047875 and subsequent renewal) for the GPU development and other recent modifications.

We also acknowledge Dr. Lalith Perera and Divi Venkateswarlu in the Pedersen Lab for helpful conversations and a willingness to use early releases of PMEMD. Since Amber 8 shipped, continued support for development has also come from Dr. Tom Darden and his laboratory at NIEHS in the form of intramural NIH funding and from the University of California (UC Lab 09-LR-06-117792) and the DoE SciDAC program (DE-AC36-99G0-10337).

Drs. Tom Darden, Lee Pedersen, Lalith Perera, Coray Colina, Chang Jun Lee, Ping Lin and Vasu Chandrasekaran have all been helpful in providing suggestions and willingness to use early releases of pmemd 9 and 10. This work has required the availability of large piles of processors of many different types. We thank UNC-Chapel Hill, the National Institute of Environmental Health Sciences, the Edinburgh Parallel Computing Centre, the NSF TeraGrid including: the Pittsburgh Supercomputing Center; the National Center for Supercomputing Applications; the San Diego Supercomputer Center at the University of California, San Diego; and the Texas Advanced Computing Center at the University of Texas, Austin; as well as the Center for High Performance Computing at the University of Utah, the Scripps Research Institute, the National Energy Research Scientific Computing Center, the IBM Blue Gene Capacity on Demand Center in Rochester, Minnesota, The Intel and SGI Parallel Application Center, The Microsoft Benchmarking Lab, The NSF Keeneland project at Georgia Tech and NVIDIA for making resources available that were used in the development, test, and benchmarking of this software.

When citing PMEMD (Particle Mesh Ewald Molecular Dynamics) in the literature, please use the Amber Version 12 citation given in the Amber manual. When citing the use of the GPU version of the code please use the Amber Version 12 citation given in the Amber manual along with the corresponding GB-GPU and PME-GPU papers.[265, 266]



## 8. LES

The LES functionality for sander was written by Carlos Simmerling. It basically functions by modifying the *prmtop* file using the program *addles*. The modified *prmtop* file is then used with a slightly modified version of sander called *sander.LES*.

### 8.1. Preparing to use LES with Amber

The first decision that must be made is whether LES is an appropriate technique for the system that you are studying. For further guidance, you may wish to consult published articles to see where LES has proven useful in the past. Several examples will also be given at the end of this section in order to provide models that you may wish to follow.

There are three main issues to consider before running the ADDLES module of Amber.

1. What should be copied?
2. How many copies should be used?
3. How many regions should be defined?

A brief summary of my experience with LES follows.

1. You should make copies of flexible regions of interest. This sounds obvious, and in some cases it is. If you are interested in determining the conformation of a protein loop, copy the loop region. If you need to determine the position of a side chain in a protein after a single point mutation, copy that side chain. If the entire biomolecule needs refinement, then copy the entire molecule. Some other cases may not be obvious- you may need to decide how far away from a particular site structural changes may propagate, and how far to extend the LES region.
2. You should use as few copies as are necessary. While this doesn't sound useful, it illustrates the general point—too few copies and you won't get the full advantages of LES, and too many will not only increase your system size unnecessarily but will also flatten the energy surface to the point where minima are no longer well defined and a wide variety of structures become populated. In addition, remember that LES is an approximation, and more copies make it more approximate. Luckily, published articles that explore the sensitivity of the results to the number of copies show that 3-10 copies are usually reasonable and provide similar results, with 5 copies being a good place to start.
3. Placing the divisions between regions can be the most difficult choice when using LES. This is essentially a compromise between surface smoothing and copy independence. The most effective surface-smoothing in LES takes places between LES regions. This

## 8. LES

is because  $N_a$  copies in region A interact with all  $N_b$  copies in region B, resulting in  $N_a \cdot N_b$  interactions, with each scaled by  $1/(N_a \cdot N_b)$  compared to the original interaction. This is better both from the statistics of how many different versions of this interaction contribute to the LES average, and how much the barriers are reduced. Remember that since the copies of a given region do not interact with different copies of that same region, interactions inside a region are only scaled by  $1/N$ .

The other thing to consider is whether these enhanced statistics are actually helpful. For example, if the copies cannot move apart, you will obtain many copies of the same conformation—obviously not very helpful. This will also result in less effective reduction in barriers, since the average energy barriers will be very similar to the non-average barrier. The independence of the copies is also related to how the copies are attached. For example, different copies of an amino acid side chain are free to rotate independently (at least within restrictions imposed by the surroundings and intrinsic potential) and therefore each side chain in the sequence could be placed into a separate LES region. If you are interested in backbone motion, however, placing each amino acid into a separate region is not the best choice. Each copy of a given amino acid will be bonded to the neighbor residues on each side. This restriction means that the copies are not very independent, since the endpoints for each copy need to be in nearly the same places. A better choice is to use regions of 2-4 amino acids. As the regions get larger, each copy can start to have more variety in conformation— for example, one segment may have some copies in a helical conformation while others are more strand-like or turn-like. The general rule is that larger regions are more independent, though you need to consider what types of motions you expect to see.

The best way to approach the division of the atoms that you wish to copy into regions is to make sure that you have several LES regions (unless you are copying a very small region such as a short loop or a small ligand). This will ensure plenty of inter-copy averaging. Larger regions permit wider variations in structure, but result in less surface smoothing. A subtle point should be addressed here— the statistical improvement available with LES is not a benefit in all cases and care must be taken in the choice of regions. For example, consider a ligand exiting a protein cavity in which a side chain acts as a *gate* and needs to move before the ligand can escape. If we make multiple copies of the gate, and do not copy the ligand, the ligand will interact in an average way with the *gates*. If the gate was so large that even the softer copies can block the exit, then the ligand would have to wait until ALL of the gate copies opened in order to exit. This may be more statistically difficult than waiting for the original, single gate to open despite the reduced barriers. Another way to envision this is to consider the ligand trying to escape against a true probability distribution of the gate— if it was open 50% of the time and closed 50%, then the exit may still be completely blocked. Continuum representations are therefore not always the best choice.

Specific examples will be given later to illustrate how these decisions can be made for a particular system.

### 8.2. Using the ADDLES program

The ADDLES module of Amber is used to prepare input for simulations using LES. A non-LES prmtop and prmcrd file are generated using a program such as LEaP. This prmtop file is

then given to ADDLES and replaced by a new prmtop file corresponding to the LES system. All residues are left intact- copies of atoms are placed in the same residue as the original atom, so that analysis based on sequence is preserved. Atom numbering is changed, but atom names are unchanged, meaning that a given residue may have several atoms with the same name. A different program is available for taking this new topology file and splitting the copies apart into separate residues, if desired. All copies are given the same coordinates as in the input coordinate file for the non-LES system.

Using addles:

```
addles < inputfile > outputfile
```

SAMPLE INPUT FILE:

```

~ a line beginning with ~ is a comment line.
~ all commands are 4 letters.
~ the maximum line length is 80 characters;
~ a trailing hyphen, "-", is the line continuation token.
~ use 'file' to specify an input/output file, then the type of file
' rprm' means this is the file to read the prmtop
~ the 'read' means it is an input file
~
file rprm name=(solv200.topo) read
~
~ 'rcrd' reads the original coordinates- optional, only if you want
~ a set of coords for the new topology
~ you can also use 'rcvd' for coords+velocities, 'rcvb' for coords,
~ velos and box dimensions, 'rcbd' for coords and box dimensions.
~ use "pack=n" option to read in multiple sets of coordinates and
~ assign different coordinates to different copies.
file rcrd name=(501v200.coords) read
~ 'wprm' is the new topology file to be written. the 'wovr' means to
~ write over the file if it exists, 'writ' means don't write over.
file wprm name=(lesparm) wovr
~ 'wcrd is for writing coords, it will automatically write velo and box
~ if they were read in by 'rcvd' or 'rcvb'
file wcrd name=(lescrd) wovr
~ now put 'action' before creating the subspaces
action
~ the default behavior is to scale masses by 1/N.
~ omas leaves all masses at the original values
omas
~ now we specify LES subspaces using the 'spac' keyword, followed
~ by the number of copies to make and then a pick command to tell which
~ atom to copy for this subspace
~ 3 copies of the fragment consisting of monomers 1 and 2
spac numc=3 pick #mon 1 2 done

```

## 8. LES

```
~ 3 copies of the fragment consisting of monomers 3 and 4
spac numc=3 pick #mon 3 4 done
~ 3 copies of the fragment consisting of residues 5 and 6
spac numc=3 pick #mon 5 6 done
~ 2 copies of the side chain on residue 1
~ note that this replaces each of the side chains ON EACH OF THE 3
~ COPIES MADE ABOVE with 2 copies - net 6 copies
~ each of the 3 copies of residue 1-2 has 2 side chain copies.
~ the '#sid' command picks all atoms in the residue except
~ C,O,CA,HA,N,H and HN.
spac numc=2 pick #sid 1 1 done
spac numc=2 pick *sid 2 2 done
spac numc=2 pick #sid 3 3 done
spac numc=2 pick #sid 4 4 done
spac numc=2 pick #sid 5 5 done
~ use the *EOD to end the input
*EOD
```

What this does: all of the force constants are scaled in the new prmtop file by  $1/N$  for  $N$  copies, so that this scaling does not need to be done for each pair during the nonbond calculation. Charges and VDW epsilon values are also scaled. New bond, angle, torsion and atom types are created. Any of the original types that were not used are discarded. Since each LES copy should not interact with other copies of the SAME subspace, the other copies are placed in the exclusion list. If you define very large LES regions, the exclusion list will get large and you may have trouble with the fixed length for this entry in the prmtop file- currently 8 digits.

The coordinates are simply copied - that means that all of the LES copies initially occupy the same positions in space. In this setup, the potential energy should be identical to the original system- this is a good test to make sure everything is functioning properly. Do a single energy evaluation of the LES system and the original system, using the copied coordinate file. All terms should be nearly identical (to within machine precision and roundoff). With PME on non-neutral systems, all charges are slightly modified to neutralize the system. For LES, there are a different number of atoms than in the original system, and therefore this charge modification to each atom will differ from the non-LES system and electrostatic energies will not match perfectly.

**IMPORTANT:** After creating the LES system, the copies will all feel the same forces, and since the coordinates are identical, they will move together unless the initial velocities are different. If you are initializing velocities using `INIT=3` and `TEMPI>0`, this is not a problem. In order to circumvent this problem, addles slightly (and randomly) modifies the copy velocities if they were read from the coordinate input file. If the keyword "nomodv" is specified, the program will leave all of the velocities in the same values as the original file. If you do not read velocities, make sure to assign an initial non-zero temperature to the system. You should think about this and change the behavior to suit your needs. In addition, the program scales the velocities by  $\sqrt{N}$  for  $N$  copies to maintain the correct thermal energy ( $mv^2$ ), but only when the masses are scaled (not using `omas` option). Again, this requires some thought and you may want different behavior. Regardless of what options are used for the velocities, further



### 8.3. More information on the ADDLES commands and options

equilibration should be carried out. These options are simple attempts to keep the system close to the original state.[268]

Sometimes it is critical that different copies can have different initial coordinates (NEB for example), this is why the option "pack" is added to command `rcrd(rcvd,rcvb,rcbd)`. To use this option, user need first concatenate different coordinates into a single file, and use "pack=n" to indicate how many sets of coordinates there are in the file, like the following example:

```
file rcrd name=(input.inpcrd) pack=4 read
```

Then addles will assign coordinates averagely. For example, if 4 sets coordinates exists in input file, and 20 copies are generated, then copy 1-5 will have coordinate set 1, copy 6-10 will have coordinates set 2, and so on. Note this option can't work with multiple copy regions now.

It is important to understand that each subsequent pick command acts on the ORIGINAL particle numbers. Making a copy of a given atom number also makes copies of all copies of that atom that were already created. This was the simplest way to be able to have a hierarchical LES setup, but you can't make extra copies of part of one of the copies already made. I'm not sure why you would want to, or if it is even correct to do so, but you should be warned. Copies can be anything -spanning residues, copies of fragments already copied, non-contiguous fragments, etc. Pay attention to the order in which you make the copies, and look carefully at the output to make sure you get what you had in mind. Addles will provide a list at the end of all atoms, the original parent atom, and how many copies were made.

There are array size limits in the file `SIZE.h`, I apologize in advance for the poor documentation on these. Mail [carlos.simmerling@stonybrook.edu](mailto:carlos.simmerling@stonybrook.edu) if you have any questions or problems.

### 8.3. More information on the ADDLES commands and options

file:	open a file, also use one of
rcrd:	read coords from this file
rcvd:	read coords + velo from file
rcvb:	read coords, velo and box from file
wcrd:	write coords (and more if rcvd, rcvb) to file
wprm:	write new topology file
action:	start run, all of the following options must come AFTER action
nomodv:	do NOT slightly randomize the velocities of the copies
spac:	add a new subspace definition, using a pick command (see below).
follow	with numc=# pickcmd where # is the number of copies to make
and	pickcmd is a pick command that selects the group of atoms to copy.

## 8. LES

omas: leave all masses at original values (otherwise scale 1/N)

pimd: write an prmtop file for PIMD simulation, which contains a much smaller non-bond exclusion list, atoms from other copy will not be included in this non-bond exclusion list.

### *Syntax for 'pick' commands*

Currently, the syntax for picking atoms is somewhat limited. Simple Boolean logic is followed, but operations are carried out in order and parentheses are not allowed.

#prt A B picks the atom range from A to B by atom number

#mon A B picks the residue range from A to B by residue number

#cca A B picks the residue range from A to B by residue number, but dividing the residue between CA and C; the CO for A is included, and the CO for monomer B is not. See Simmerling and Elber, 1994 for an example of where this can be useful.

chem prtc A picks all atoms named A, case sensitive

chem mono A picks all residues named A, case sensitive

Completion wildcards are acceptable for names: H\* picks H, HA, etc. Note that H\*2 will select all atoms starting with H and ignore the 2.

### *Boolean logic:*

| or atoms in either group are selected

& and atoms must be in both groups to be selected

!= not A != B will pick all atoms in A that are NOT in B

The user should carefully check the output file to ensure that the proper atoms were selected.

### *Examples:*

```
pick commandatoms selected
pick #mon 4 19 done all atoms in residues 4 through 19
pick #mon 1 50 & chem mono GLY done only GLY in residues 1 to 50
pick chem mono LYS | chem mono GLU done any GLU or LYS residue
pick #mon 1 5 != #prt 1 3 done residues 1 to 5 but not atoms 1 to 3
```

so, a full command to add a new subspace (LES region) with 4 copies of atoms 15 to 35 is:

```
spac numc=4 pick #prt 15 35 done
```

## 8.4. Using the new topology/coordinate files with SANDER

These topology files are ready to use in Sander with one exception: all of the FF parameters have been scaled by  $1/N$  for  $N$  copies. This is done to provide the energy of the new system as an average of the energies of the individual copies (note that it is an average energy or force, not the energy or force from an average copy coordinate). However, one additional correction is required for interactions between pairs of atoms in the same LES region. Sander will make these corrections for you, and this information is just to explain what is being done. For example, consider a system where you make 2 copies of a sidechain in a protein. Each charge is scaled by  $1/2$ . For these atoms interacting with the rest of the system, each interaction is scaled by  $1/2$  and there are 2 such interactions. For a pair of particles inside the sub-space, however, the interaction is scaled by  $1/2 * 1/2 = 1/4$ , and since the copies do not interact, there are only 2 such interactions and the sum does not correspond to the correct average. Therefore, the interaction must be scaled up by a factor of  $N$ . When the PME technique is requested, this simple scaling cannot be used since the entire charge set is used in the construction of the PME grid and individual charges are not used in the reciprocal space calculation. Therefore, the intra-copy energies and forces are corrected in a separate step for PME calculations. Sander will print out the number of correction interactions that need to be calculated, and very large amounts of these will make the calculation run more slowly. PME also needs to do a separate correction calculation for excluded atom pairs (atoms that should not have a nonbonded interaction, such as those that are connected by a bond). Large LES regions result in large numbers of excluded atoms, and these will result in a larger computational penalty for LES compared to non-LES simulations. For both of these reasons, it is more efficient computationally to use smaller LES regions- but see the discussion above for how region size affects simulation efficiency. These changes are included in the LES version of Sander (sander.LES). Each particle is assigned a LES 'type' (each new set of copies is a new type), and for each pair of types there is a scaling factor for the nonbond interactions between LES particles of those types. Most of the scaling factors are 1.0, but some are not - such as the diagonal terms which correspond to interactions inside a given subspace, and also off-diagonal terms where only some of the copies are in common. An example of this type is the side chain example given above- each of the 3 backbone copies has 2 sidechains, and while interactions inside the side chains need a factor of 6, interactions between the side chain and backbone need a factor of 3. This matrix of scaling factors is stored in the new topology file, along with the type for each atom, and the number of types. The changes made in sander relate to reading and using these scale factors.

## 8.5. Using LES with the Generalized Born solvation model

LES simulations can be performed using the GB solvent model, with some limitations. Compared to LES simulations in explicit water, using GB with LES provides several advantages. The most important is how each of the copies interacts with the solvent. With explicit water, the water is normally not copied and therefore interacts in an average way with all LES copies. This has important consequences for solvation of the copies. If the copies move apart, water cannot overlap any of them and therefore the water cavity will be that defined by the union of the space occupied by the copies. This has two consequences. First, moving the copies apart

## 8. LES

requires creation of a larger solvent cavity and therefore copies have a greater tendency to remain together, reducing the effectiveness of LES. Second, when the copies do move apart, each copy will not be individually solvated.

These effects arise because the water interacts with all of the copies; for each copy to be solvated independently of the other copies would require copying the water molecules. This is normally not a good idea, since copying all of the water would result in very significant computational expense. Copying only water near the solute would be tractable, but one would need to ensure that the copied waters did not exchange with non-LES bulk waters.

Using GB with LES largely overcomes these problems since each copy can be individually solvated with the continuum model. Thus when one copy moves, the solvation of the other copies are not affected. This results in a more reasonable solvation of each copy and also improves the independence of the copies. Of course the resulting simulations do retain all of the limitations that accompany the GB models.

The current code allows `igb` values of 1, 5 or 7 when using LES. Surface area calculations are not yet supported with LES. Only a single LES region is permitted for GB+LES simulations. A new namelist variable was introduced (`RDT`) in `sander` to control the compromise of speed and accuracy for GB+LES simulations. The article referenced below provides more detail on the function of this variable. `RDT` is the effective radii deviation threshold. When using GB+LES, non-LES atoms require multiple effective Born radii for an exact calculation. Using these multiple radii can significantly increase calculation time required for GB calculations. When the difference between the multiple radii for a non-LES atom is less than `RDT`, only a single effective radius will be used. A value of 0.01 has been found to provide a reasonable compromise between speed and accuracy, and is the default value. Before using this method, it is strongly recommended that the user read the article describing the derivation of the GB+LES approach.[269]

## 8.6. Case studies: Examples of application of LES

### 8.6.1. Enhanced sampling for individual functional groups: Glucose

The first example will deal with enhancing sampling for small parts of a molecule, such as individual functional groups or protein side chains. In this case we wanted to carry out separate simulations of  $\alpha$  and  $\beta$  (not converting between anomers, only for conversions involving rotations about bonds) glucose, but the 5 hydroxyl groups and the strong hydrogen bonds between neighboring hydroxyls make conversion between different rotamers slow relative to affordable simulation times. The eventual goal was to carry out free energy simulations converting between anomers, but we need to ensure that each window during the Gibbs calculation would be able to sample all relevant orientations of hydroxyl groups in their proper Boltzmann-weighted populations. We were initially unsure how many different types of structures should be populated and carried out non-LES simulations starting from different conformations. We found that transitions between different conformations were separated by several hundred picoseconds, far too long to expect converged populations during each window of the free energy calculation. We therefore decided to enhance conformational sampling for each hydroxyl group by making 5 copies of each hydroxyl hydrogen and also 5

copies of the entire hydroxymethyl group. Since the hydroxyl rotamer for each copy should be relatively independent, we decided to place each group in a different LES region. This meant that each hydroxyl copy interacted with all copies of the neighboring groups, with a total of  $5*5*5*5*5$  or 3125 structural combinations contributing to the LES average energy at each point in time. The input file is given below.

```
file rprm name=(parm.solv.top) read
file rcvb name=(glucose.solv.equ.crd) read
file wprm name=(les.prmtop) wovr
file wcrd name=(glucose.les.crd) wovr
action
omas
~ 5 copies of each hydroxyl hydrogen- copying oxygen will make no difference
~ since they will not be able to move significantly apart anyway
spac numc=5 pick chem prtc HO1 done
spac numc=5 pick chem prtc HO2 done
spac numc=5 pick chem prtc HO3 done
spac numc=5 pick chem prtc HO4 done
~ take the entire hydroxy methyl group
spac numc=5 pick #prt 20 24 done
*EOD
```

This worked quite well, with transitions now occurring every few ps and populations that were essentially independent of initial conformation.[270]

### 8.6.2. Enhanced sampling for a small region: Application of LES to a nucleic acid loop

In this example, we consider a biomolecule (in this case a single RNA strand) for which part of the structure is reliable and another part is potentially less accurate. This can be the case in a number of different modeling situations, such as with homologous proteins or when the experimental data is incomplete. In this case two different structures were available for the same RNA sequence. While both structures were hairpins with a tetraloop, the loop conformations differed, and one was more accurate. We tested whether MD would be able to show that one structure was not stable and would convert to the other on an affordable timescale.

Standard MD simulations of several ns were not able to undergo any conversion between these two structures (the initial structure was always retained). Since the stem portion of the RNA was considered to be accurate, LES was only applied to the tetraloop region. In this case, both of the ends of the LES region would be attached to the same locations in space, and there was no concern about copies diffusing too far apart to re-converge to the same positions after optimization. The issues that need to be addressed once again are the number of copies to use, and how to place the LES region(s). I usually start with the simplest choices and used 5 LES copies and only a single LES region consisting of the entire loop. If each half of the loop was copied, then it might become too *crowded* with copies near the base-pair hydrogen bonds and conformational changes that required moving a base through this regions could become even more difficult (see the background section for details). Therefore, one region was chosen, and

## 8. LES

the RNA stem, counterions and solvent were not copied. The ADDLES input file is given below.

```
file rprm name=(prm.top) read
file rcvb name=(rna.crd) read
file wprm name=(les.parm) wovr
file wcrd name=(les.crd) wovr
action
omas
~ copy the UUCG loop region- residues 5 to 8.
~ pick by atom number, though #mon 5 8 would work the same way
spac numc=5 pick #prt 131 255 done
*EOD
```

Subsequent LES simulations were able to reproducibly convert from what was known to be the incorrect structure to the correct one, and stay in the correct structure in simulations that started there. Different numbers of LES copies as well as slightly changing the size of the LES region (from 4 residues to 6, extending 1 residue beyond the loop on either side) were not found to affect the results. Fewer copies still converted between structures, but on a slower timescale, consistent with the barrier heights being reduced roughly proportional to the number of copies used. See Simmerling, Miller and Kollman, 1998, for further details.

### 8.6.3. Improving conformational sampling in a small peptide

In this example, we were interested not just in improving sampling of small functional groups or even individual atoms, but in the entire structure of a peptide. The peptide sequence is AVPA, with ACE and NME terminal groups. Copying just the side chains might be helpful, but would not dramatically reduce the barriers to backbone conformational changes, especially in this case with so little conformational variety inherent in the Ala and Pro residues. We therefore apply LES to all atoms. If we copied the entire peptide in 1 LES regions, the copies could float apart. While this would not be a disaster, it would make it difficult to bring all of the copies back together if we were searching for the global energy minimum, as described above. We therefore use more than one LES region, and need to decide where to place the boundaries between regions. A useful rule of thumb is that regions should be at least two amino acids in size, so we pick our two regions as Ace-Ala-Val and Pro-Ala-Nme. If we make five LES copies of each region and each copy does not interact with other copies of the same regions, each half the peptide will be represented by five potentially different conformations at each point in time. In addition, since each copy interacts with all copies of the rest of the system, there are 25 different combinations of the two halves of the peptide that contribute at each point in time. This statistical improvement alone is valuable, but the corresponding barriers are also reduced by approximately the same factors. When we place the peptide in a solvent box the solvent interacts in an average way with each of the copies. The input file is given below, and all of the related files can be found in the test directory for LES.

```
~ all file names are specified at the beginning, before "action"
```

## 8.6. Case studies: Examples of application of LES

```
~ specify input prmtop
file rprm name=(prmtop) read
~ specify input coordinates, velocities and box (this is a restart file)
file rcvb name=(md.solv.crd) read
~ specify LES prmtop
file wprm name=(LES.prmtop) wovr
~ specify LES coordinates (and velocities and box since they were input)
file wcrd name=(LES.crd) wovr
~ now the action command reads the files and tells addles to
~ process commands
action
~ do not scale masses of copied particles
omas
~ divide the peptide into 2 regions.
~ use the CCA option to place the division between carbonyl and
~ alpha carbon
~ use the "or" to make sure all atoms in the terminal residues
~ are included since the CCA option places the region division at C/CA
~ and we want all of the terminal residue included on each end
~
~ make 5 copies of each half
~ "spac" defines a LES subspace (or region)
spac numc=5 pick #cca 1 3 | #mon 1 1 done
spac numc=5 pick #cca 4 6 | #mon 6 6 done
~ the following line is required at the end
+EOD
```

This example brings up several important questions:

1. Should I make LES copies before or after adding solvent? Since LEaP is used to add solvent, and LEaP will not be able to load and understand a LES structure, you must run ADDLES after you have solvated the peptide in LEaP. ADDLES should be the last step before running SANDER.
2. Which structure should be used as input to ADDLES? If you will also be carrying out non-LES simulations, then you can equilibrate the non-LES simulation and carry out any amount of production simulation desired before taking the structure and running ADDLES. At the point you may switch to only LES simulations, or continue both LES and non-LES from the same point (using different versions of SANDER). Typically I equilibrate my system without LES to ensure that it has initial stability and that everything looks OK, then switch to LES afterward. This way I separate any potential problems from incorrect LES setup from those arising from problems with the non-LES setup, such as in initial coordinates, LEaP setup, solvent box dimensions and equilibration protocols.
3. How can I analyze the resulting LES simulation? This is probably the most difficult part of using LES. With all of the extra atoms, most programs will have difficulty. For example, a given amino acid with LES will have multiple phi and psi backbone dihedral

## 8. LES

angles. There are basically two options: first, you can process your trajectory such that you obtain a single structure (non-LES). This might be just extracting one of the copies, or it might be one by taking the average of the LES copies. After that, you can proceed to traditional analysis but must keep in mind that the average structure may be non-physical and may not represent any actual structure being sampled by the copies, especially if they move apart significantly. A better way is to use LES-friendly analysis tools, such as those developed in the group of Carlos Simmerling. The visualization program MOIL-View (<http://morita.chem.sunysb.edu/carlos/moil-view.html>) is one example of these programs, and has many analysis tools that are fully LES compatible. Read the program web page or manual for more details.

### 1.7. Unresolved issues with LES in Amber

1. Sander can't currently maintain groups of particles at different temperatures (important for dynamics, less so for optimization.)[271, 272] Users can set *tempOles* to maintain all LES atoms at a temperature that is different from that for the system as a whole, but all LES atoms are then coupled to the same bath.
2. Initial velocity issues as mentioned above- works properly, user must be careful.
3. Analysis programs may not be compatible. See <http://morita.chem.sunysb.edu/carlos/moil-view.html> for an LES-friendly analysis and visualization program.
4. Visualization can be difficult, especially with programs that use distance-based algorithms to determine bonds. See #3 above.
5. Water should not be copied- the fast water routines have not been modified. For most users this won't matter.
6. Copies should not span different 'molecules' for pressure coupling and periodic imaging issues. Copies of an entire 'molecule' should result in the copies being placed in new, separate molecules- currently this is not done. This would include copying things such as counterions and entire protein or nucleic acid chains.
7. Copies are placed into the same residue as the original atoms- this can make some residues much larger than others, and may result in less efficient parallelization with algorithms that assign nonbond workload based on residue numbers.



## Bibliography

- [1] Pearlman, D.A.; Case, D.A.; Caldwell, J.W.; Ross, W.S.; Cheatham, T.E. III; DeBolt, S.; Ferguson, D.; Seibel, G.; Kollman, P. AMBER, a package of computer programs for applying molecular mechanics, normal mode analysis, molecular dynamics and free energy calculations to simulate the structural and energetic properties of molecules. *Comp. Phys. Commun.*, **1995**, *91*, 1–41.
- [2] Case, D.A.; Cheatham, T.; Darden, T.; Gohlke, H.; Luo, R.; Merz, K.M. Jr.; Onufriev, A.; Simmerling, C.; Wang, B.; Woods, R. The Amber biomolecular simulation programs. *J. Computat. Chem.*, **2005**, *26*, 1668–1688.
- [3] Ponder, J.W.; Case, D.A. Force fields for protein simulations. *Adv. Prot. Chem.*, **2003**, *66*, 27–85.
- [4] Cheatham, T.E. III; Young, M.A. Molecular dynamics simulation of nucleic acids: Successes, limitations and promise. *Biopolymers*, **2001**, *56*, 232–256.
- [5] Harvey, S.; McCammon, J.A. *Dynamics of Proteins and Nucleic Acids*. Cambridge University Press, Cambridge, 1987.
- [6] Leach, A.R. *Molecular Modelling. Principles and Applications, Second Edition*. Prentice-Hall, Harlow, England, 2001.
- [7] Allen, M.P.; Tildesley, D.J. *Computer Simulation of Liquids*. Clarendon Press, Oxford, 1987.
- [8] Frenkel, D.; Smit, B. *Understanding Molecular Simulation: From Algorithms to Applications. Second edition*. Academic Press, San Diego, 2002.
- [9] van Gunsteren, W.F.; Weiner, P.K.; Wilkinson, A.J. eds. *Computer Simulations of Biomolecular Systems, Vol. 3*. ESCOM Science Publishers, Leiden, 1997.
- [10] Pratt, L.R.; Hummer, G. eds. *Simulation and Theory of Electrostatic Interactions in Solution*. American Institute of Physics, Melville, NY, 1999.
- [11] Becker, O.; MacKerell, A.D.; Roux, B.; Watanabe, M. eds. *Computational Biochemistry and Biophysics*. Marcel Dekker, New York, 2001.
- [12] Cheatham, T.E. III; Brooks, B.R.; Kollman, P.A. in *Current Protocols in Nucleic Acid Chemistry*, pp Sections 7.5, 7.8, 7.9, 7.10. Wiley, New York, 1999.
- [13] Kopitz, H.; Zivkovic, A.; Engels, J.W.; Gohlke, H. Determinants of the unexpected stability of RNA fluorobenzene self pairs. *ChemBioChem*, **2008**, *9*, 2619–2622.

## BIBLIOGRAPHY

- [14] Morishita, T. Fluctuation formulas in molecular-dynamics simulations with the weak coupling heat bath. *J. Chem. Phys.*, **2000**, *113*, 2976.
- [15] Mudi, A.; Chakravarty, C. Effect of the Berendsen thermostat on the dynamical properties of water. *Mol. Phys.*, **2004**, *102*, 681–685.
- [16] Berendsen, H.J.C.; Postma, J.P.M.; van Gunsteren, W.F.; DiNola, A.; Haak, J.R. Molecular dynamics with coupling to an external bath. *J. Chem. Phys.*, **1984**, *81*, 3684–3690.
- [17] Harvey, S.C.; Tan, R.K.; Cheatham, T.E. III. The flying ice cube: Velocity rescaling in molecular dynamics leads to violation of energy equipartition. *J. Comput. Chem.*, **1998**, *19*, 726–740.
- [18] Andrea, T.A.; Swope, W.C.; Andersen, H.C. The role of long ranged forces in determining the structure and properties of liquid water. *J. Chem. Phys.*, **1983**, *79*, 4576–4584.
- [19] Andersen, H.C. Molecular dynamics simulations at constant pressure and/or temperature. *J. Chem. Phys.*, **1980**, *72*, 2384–2393.
- [20] Uberuaga, B.P.; Anghel, M.; Voter, A.F. Synchronization of trajectories in canonical molecular-dynamics simulations: Observation, explanation, and exploitation. *J. Chem. Phys.*, **2004**, *120*, 6363–6374.
- [21] Sindhikara, D.J.; Kim, S.; Voter, A.F.; Roitberg, A.E. Bad seeds sprout perilous dynamics: Stochastic thermostat induced trajectory synchronization in biomolecules. *J. Chem. Theory Comput.*, **2009**, *5*, 1624–1631.
- [22] Pastor, R.W.; Brooks, B.R.; Szabo, A. An analysis of the accuracy of Langevin and molecular dynamics algorithms. *Mol. Phys.*, **1988**, *65*, 1409–1419.
- [23] Loncharich, R.J.; Brooks, B.R.; Pastor, R.W. Langevin dynamics of peptides: The frictional dependence of isomerization rates of N-actylananyl-N'-methylamide. *Biopolymers*, **1992**, *32*, 523–535.
- [24] Izaguirre, J.A.; Catarello, D.P.; Wozniak, J.M.; Skeel, R.D. Langevin stabilization of molecular dynamics. *J. Chem. Phys.*, **2001**, *114*, 2090–2098.
- [25] Zhang, Y.; Feller, S.E.; Brooks, B.R.; Pastor, R.W. Computer simulation of liquid/liquid interfaces. I. Theory and application to octane/water. *J. Chem. Phys.*, **1995**, *103*, 10252–10266.
- [26] Ryckaert, J.-P.; Ciccotti, G.; Berendsen, H.J.C. Numerical integration of the cartesian equations of motion of a system with constraints: Molecular dynamics of n-alkanes. *J. Comput. Phys.*, **1977**, *23*, 327–341.
- [27] Miyamoto, S.; Kollman, P.A. SETTLE: An analytical version of the SHAKE and RATTLE algorithm for rigid water models. *J. Comput. Chem.*, **1992**, *13*, 952–962.
- [28] Ren, P.; Ponder, J.W. Consistent treatment of inter- and intramolecular polarization in molecular mechanics calculations. *J. Comput. Chem.*, **2002**, *23*, 1497–1506.

- [29] Ren, P.; Ponder, J.W. Temperature and pressure dependence of the AMOEBA water model. *J. Phys. Chem. B*, **2004**, *108*, 13427–13437.
- [30] Darden, T.; York, D.; Pedersen, L. Particle mesh Ewald—an Nlog(N) method for Ewald sums in large systems. *J. Chem. Phys.*, **1993**, *98*, 10089–10092.
- [31] Essmann, U.; Perera, L.; Berkowitz, M.L.; Darden, T.; Lee, H.; Pedersen, L.G. A smooth particle mesh Ewald method. *J. Chem. Phys.*, **1995**, *103*, 8577–8593.
- [32] Crowley, M.F.; Darden, T.A.; Cheatham, T.E. III; Deerfield, D.W. II. Adventures in improving the scaling and accuracy of a parallel molecular dynamics program. *J. Supercomput.*, **1997**, *11*, 255–278.
- [33] Sagui, C.; Darden, T.A. in *Simulation and Theory of Electrostatic Interactions in Solution*, Pratt, L.R.; Hummer, G., Eds., pp 104–113. American Institute of Physics, Melville, NY, 1999.
- [34] Toukmaji, A.; Sagui, C.; Board, J.; Darden, T. Efficient particle-mesh Ewald based approach to fixed and induced dipolar interactions. *J. Chem. Phys.*, **2000**, *113*, 10913–10927.
- [35] Sagui, C.; Pedersen, L.G.; Darden, T.A. Towards an accurate representation of electrostatics in classical force fields: Efficient implementation of multipolar interactions in biomolecular simulations. *J. Chem. Phys.*, **2004**, *120*, 73–87.
- [36] Wu, X.; Brooks, B.R. Isotropic periodic sum: A method for the calculation of long-range interactions. *J. Chem. Phys.*, **2005**, *122*, 044107.
- [37] Klauda, J.B.; Wu, X.; Pastor, R.W.; Brooks, B.R. Long-Range Lennard-Jones and Electrostatic Interactions in Interfaces. *J. Phys. Chem. B*, **2007**, *111*, 4393–4400.
- [38] Takahashi, K.; Yasuoka, K.; Narumi, T. Cutoff radius effect of isotropic periodic sum method for transport. *J. Chem. Phys.*, **2007**, *127*, 114511.
- [39] Wu, X.; Brooks, B.R. Using the Isotropic Periodic Sum Method to Calculate Long-Range Interactions of Heterogeneous Systems. *J. Chem. Phys.*, **2008**, *129*, 154115.
- [40] Wu, X.; Brooks, B.R. Isotropic periodic sum of electrostatic interactions for polar systems. *J. Chem. Phys.*, **2009**, *131*, 024107.
- [41] Venable, R.M.; Chen, L.E.; Pastor, R.W. Comparison of the Extended Isotropic Periodic Sum and Particle Mesh Ewald Methods for Simulations of Lipid Bilayers and Monolayers. *J. Phys. Chem. B*, **2009**, *113*, 5855–5862.
- [42] Weiser, J.; Shenkin, P.S.; Still, W.C. Approximate Atomic Surfaces from Linear Combinations of Pairwise Overlaps (LCPO). *J. Computat. Chem.*, **1999**, *20*, 217–230.
- [43] Still, W.C.; Tempczyk, A.; Hawley, R.C.; Hendrickson, T. Semianalytical treatment of solvation for molecular mechanics and dynamics. *J. Am. Chem. Soc.*, **1990**, *112*, 6127–6129.

## BIBLIOGRAPHY

- [44] Schaefer, M.; Karplus, M. A comprehensive analytical treatment of continuum electrostatics. *J. Phys. Chem.*, **1996**, *100*, 1578–1599.
- [45] Edinger, S.R.; Cortis, C.; Shenkin, P.S.; Friesner, R.A. Solvation free energies of peptides: Comparison of approximate continuum solvation models with accurate solution of the Poisson-Boltzmann equation. *J. Phys. Chem. B*, **1997**, *101*, 1190–1197.
- [46] Jayaram, B.; Sprous, D.; Beveridge, D.L. Solvation free energy of biomacromolecules: Parameters for a modified generalized Born model consistent with the AMBER force field. *J. Phys. Chem. B*, **1998**, *102*, 9571–9576.
- [47] Cramer, C.J.; Truhlar, D.G. Implicit solvation models: Equilibria, structure, spectra, and dynamics. *Chem. Rev.*, **1999**, *99*, 2161–2200.
- [48] Bashford, D.; Case, D.A. Generalized Born models of macromolecular solvation effects. *Annu. Rev. Phys. Chem.*, **2000**, *51*, 129–152.
- [49] Onufriev, A.; Bashford, D.; Case, D.A. Modification of the generalized Born model suitable for macromolecules. *J. Phys. Chem. B*, **2000**, *104*, 3712–3720.
- [50] Lee, M.S.; Salsbury, F.R. Jr.; Brooks, C.L. III. Novel generalized Born methods. *J. Chem. Phys.*, **2002**, *116*, 10606–10614.
- [51] Dominy, B.N.; Brooks, C.L. III. Development of a generalized Born model parameterization for proteins and nucleic acids. *J. Phys. Chem. B*, **1999**, *103*, 3765–3773.
- [52] Tsui, V.; Case, D.A. Molecular dynamics simulations of nucleic acids using a generalized Born solvation model. *J. Am. Chem. Soc.*, **2000**, *122*, 2489–2498.
- [53] Calimet, N.; Schaefer, M.; Simonson, T. Protein molecular dynamics with the generalized Born/ACE solvent model. *Proteins*, **2001**, *45*, 144–158.
- [54] Onufriev, A.; Bashford, D.; Case, D.A. Exploring protein native states and large-scale conformational changes with a modified generalized Born model. *Proteins*, **2004**, *55*, 383–394.
- [55] Srinivasan, J.; Trevathan, M.W.; Beroza, P.; Case, D.A. Application of a pairwise generalized Born model to proteins and nucleic acids: inclusion of salt effects. *Theor. Chem. Acc.*, **1999**, *101*, 426–434.
- [56] Onufriev, A.; Case, D.A.; Bashford, D. Effective Born radii in the generalized Born approximation: The importance of being perfect. *J. Comput. Chem.*, **2002**, *23*, 1297–1304.
- [57] Hawkins, G.D.; Cramer, C.J.; Truhlar, D.G. Parametrized models of aqueous free energies of solvation based on pairwise descreening of solute atomic charges from a dielectric medium. *J. Phys. Chem.*, **1996**, *100*, 19824–19839.
- [58] Richards, F.M. Areas, volumes, packing, and protein structure. *Ann. Rev. Biophys. Bioeng.*, **1977**, *6*, 151–176.

- [59] Schaefer, M.; Froemmel, C. A precise analytical method for calculating the electrostatic energy of macromolecules in aqueous solution. *J. Mol. Biol.*, **1990**, *216*, 1045–1066.
- [60] Feig, M.; Onufriev, A.; Lee, M.; Im, W.; Case, D.A.; Brooks, C.L. III. Performance comparison of the generalized Born and Poisson methods in the calculation of the electrostatic solvation energies for protein structures. *J. Comput. Chem.*, **2004**, *25*, 265–284.
- [61] Geney, R.; Layten, M.; Gomperts, R.; Simmerling, C. Investigation of salt bridge stability in a generalized Born solvent model. *J. Chem. Theory Comput.*, **2006**, *2*, 115–127.
- [62] Okur, A.; Wickstrom, L.; Simmerling, C. Evaluation of salt bridge structure and energetics in peptides using explicit, implicit and hybrid solvation models. *J. Chem. Theory Comput.*, **2008**, *4*, 488–498.
- [63] Okur, A.; Wickstrom, L.; Layten, M.; Geney, R.; Song, K.; Hornak, V.; Simmerling, C. Improved efficiency of replica exchange simulations through use of a hybrid explicit/implicit solvation model. *J. Chem. Theory Comput.*, **2006**, *2*, 420–433.
- [64] Roe, D.R.; Okur, A.; Wickstrom, L.; Hornak, V.; Simmerling, C. Secondary Structure Bias in Generalized Born Solvent Models: Comparison of Conformational Ensembles and Free Energy of Solvent Polarization from Explicit and Implicit Solvation. *J. Phys. Chem. B*, **2007**, *111*, 1846–1857.
- [65] Gaillard, T.; Case, D.A. Evaluation of DNA Force Fields in Implicit Solvation. *J. Chem. Theory Comput.*, **2011**, *7*, 3181–3198.
- [66] Hawkins, G.D.; Cramer, C.J.; Truhlar, D.G. Pairwise solute descreening of solute charges from a dielectric medium. *Chem. Phys. Lett.*, **1995**, *246*, 122–129.
- [67] Schaefer, M.; Van Vlijmen, H.W.T.; Karplus, M. Electrostatic contributions to molecular free energies in solution. *Adv. Protein Chem.*, **1998**, *51*, 1–57.
- [68] Tsui, V.; Case, D.A. Theory and applications of the generalized Born solvation model in macromolecular simulations. *Biopolymers (Nucl. Acid. Sci.)*, **2001**, *56*, 275–291.
- [69] Sosa, C.P.; Hewitt, T.; Lee, M.S.; Case, D.A. Vectorization of the generalized Born model for molecular dynamics on shared-memory computers. *J. Mol. Struct. (Theochem)*, **2001**, *549*, 193–201.
- [70] Mongan, J.; Simmerling, C.; A. McCammon, J.; A. Case, D.; Onufriev, A. Generalized Born with a simple, robust molecular volume correction. *J. Chem. Theory Comput.*, **2007**, *3*, 156–169.
- [71] Sitkoff, D.; Sharp, K.A.; Honig, B. Accurate calculation of hydration free energies using macroscopic solvent models. *J. Phys. Chem.*, **1994**, *98*, 1978–1988.
- [72] Sigalov, G.; Scheffel, P.; Onufriev, A. Incorporating variable environments into the generalized Born model. *J. Chem. Phys.*, **2005**, *122*, 094511.

## BIBLIOGRAPHY

- [73] Sigalov, G.; Fenley, A.; Onufriev, A. Analytical electrostatics for biomolecules: Beyond the generalized Born approximation. *J. Chem. Phys.*, **2006**, *124*, 124902.
- [74] Luo, R.; David, L.; Gilson, M.K. Accelerated Poisson-Boltzmann calculations for static and dynamic systems. *J. Comput. Chem.*, **2002**, *23*, 1244–1253.
- [75] Wang, J.; Luo, R. Assessment of Linear Finite-Difference Poisson-Boltzmann Solvers. *J. Comput. Chem.*, **2010**, *in press*.
- [76] Cai, Q.; Hsieh, M.-J.; Wang, J.; Luo, R. Performance of Nonlinear Finite-Difference Poisson-Boltzmann Solvers. *J. Chem. Theory Comput.*, **2010**, *6*, 203–211.
- [77] Tan, C. H.; Tan, Y. H.; Luo, R. Implicit nonpolar solvent models. *J. Phys. Chem. B*, **2007**, *111*, 12263–12274.
- [78] Floris, F.; Tomasi, J. Evaluation of the dispersion contribution to the solvation energy. A simple computational model in the continuum approximation. *J. Comput. Chem.*, **1989**, *10*, 616–627.
- [79] Luchko, T.; Gusarov, S.; Roe, D. R.; Simmerling, C.; Case, D. A.; Tuszynski, J.; Kovalenko, A. Three-dimensional molecular theory of solvation coupled with molecular dynamics in Amber. *J. Chem. Theory Comput.*, **2010**, *6*, 607–624.
- [80] Chandler, D.; Andersen, H. C. Optimized cluster expansions for classical fluids. ii. theory of molecular liquids. *J. Chem. Phys.*, **1972**, *57*(5), 1930–1937.
- [81] Hirata, F.; Rossky, P. J. An extended RISM equation for molecular polar fluids. *Chem. Phys. Lett.*, **1981**, pp 329–334.
- [82] Hirata, F.; Pettitt, B. M.; Rossky, P. J. Application of an extended rism equation to dipolar and quadrupolar fluids. *J. Chem. Phys.*, **1982**, *77*(1), 509–520.
- [83] Hirata, F.; Rossky, P. J.; Pettitt, B. M. The interionic potential of mean force in a molecular polar solvent from an extended rism equation. *J. Chem. Phys.*, **1983**, *78*(6), 4133–4144.
- [84] Hirata, F. In *Molecular Theory of Solvation* [541], chapter 1.
- [85] Chandler, D.; McCoy, J.; Singer, S. Density functional theory of nonuniform polyatomic systems. i. general formulation. *J. Chem. Phys.*, **1986**, *85*(10), 5971–5976.
- [86] Chandler, D.; McCoy, J.; Singer, S. Density functional theory of nonuniform polyatomic systems. ii. rational closures for integral equations. *J. Chem. Phys.*, **1986**, *85*(10), 5977–5982.
- [87] Beglov, D.; Roux, B. Numerical solution of the hypernetted chain equation for a solute of arbitrary geometry in three dimensions. *J. Chem. Phys.*, **1995**, *103*(1), 360–364.
- [88] Beglov, D.; Roux, B. An integral equation to describe the solvation of polar molecules in liquid water. *J. Phys. Chem. B*, **1997**, *101*(39), 7821–7826.

- [89] Kovalenko, A.; Hirata, F. Three-dimensional density profiles of water in contact with a solute of arbitrary shape: a RISM approach. *Chem. Phys. Lett.*, **1998**, *290*(1-3), 237–244.
- [90] Kovalenko, A.; Hirata, F. Self-consistent description of a metal–water interface by the Kohn–Sham density functional theory and the three-dimensional reference interaction site model. *J. Chem. Phys.*, **1999**, *110*(20), 10095–10112.
- [91] Kovalenko, A. In Hirata [541], chapter 4.
- [92] Kovalenko, A.; Hirata, F. Potentials of mean force of simple ions in ambient aqueous solution. i: Three-dimensional reference interaction site model approach. *J. Chem. Phys.*, **2000**, *112*, 10391–10402.
- [93] Kovalenko, A.; Hirata, F. Potentials of mean force of simple ions in ambient aqueous solution. ii: Solvation structure from the three-dimensional reference interaction site model approach, and comparison with simulations. *J. Chem. Phys.*, **2000**, *112*, 10403–10417.
- [94] Tuckerman, M.E.; Berne, B.J.; Martyna, G.J. Molecular dynamics algorithm for multiple time scales: Systems with long range forces. *J. Chem. Phys.*, **1991**, *94*, 6811–6815.
- [95] Tuckerman, M.; Berne, B.J.; Martyna, G.J. Reversible multiple time scale molecular dynamics. *J. Chem. Phys.*, **1992**, *97*(3), 1990–2001.
- [96] Grubmüller, H.; Heller, H.; Windemuth, A.; Schulten, K. Generalized Verlet algorithm for efficient molecular dynamics simulations with long-range interactions. *Mol. Simulat.*, **1991**, *6*, 121–142.
- [97] Schlick, T. *Molecular modeling and simulation: an interdisciplinary guide*. Springer-Verlag New York, Inc., Secaucus, NJ, USA, 2002.
- [98] Warshel, A. *Computer Modeling of Chemical Reactions in Enzymes and Solutions*. John Wiley and Sons, New York, 1991.
- [99] Billeter, S.R.; Webb, S.P.; Jordanov, T.; Agarwal, P.K.; Hammes-Schiffer, S. Hybrid approach for including electronic and nuclear quantum effects in molecular dynamics simulations of hydrogen transfer reactions in enzymes. *J. Chem. Phys.*, **2001**, *114*, 6925.
- [100] Schlegel, H.B.; Sonnenberg, J.L. Empirical valence-bond models for reactive potential energy surfaces using distributed Gaussians. *J. Chem. Theory Comput.*, **2006**, *2*, 905.
- [101] Sonnenberg, J.L.; Schlegel, H.B. Empirical valence bond models for reactive potential energy surfaces. II. Intramolecular proton transfer in pyridone and the Claisen reaction of allyl vinyl ether. *Mol. Phys.*, **2007**, *105*, 2719.
- [102] Saad, Y.; Schultz, M.H. GMRES: A generalized minimal residual algorithm for solving nonsymmetric linear systems. *SIAM J. Sci. Stat. Comput.*, **1986**, *7*, 856.
- [103] Pulay, P. Convergence acceleration of iterative sequences. The case of SCF iteration. *Chem. Phys. Lett.*, **1980**, *73*, 393.

## BIBLIOGRAPHY

- [104] Pulay, P. Improved SCF convergence acceleration. *J. Comput. Chem.*, **1982**, *3*, 556.
- [105] Feynman, R.P.; Hibbs, A.R. *Quantum Mechanics and Path Integrals*. McGraw-Hill, New York, 1965.
- [106] Feynman, R.P. *Statistical Mechanics*. Benjamin, Reading, MA, 1972.
- [107] Kleinert, H. *Path Integrals in Quantum Mechanics, Statistics, and Polymer Physics*. World Scientific, Singapore, 1995.
- [108] Kumar, S.; Bouzida, D.; Swendsen, R.H.; Kollman, P.A.; Rosenberg, J.M. The weighted histogram analysis method for free-energy calculations on biomolecules. I. The method. *J. Comput. Chem.*, **1992**, *13*, 1011–1021.
- [109] Kumar, S.; Rosenberg, J.M.; Bouzida, D.; Swendsen, R.H.; Kollman, P.A. Multidimensional free-energy calculations using the weighted histogram analysis method. *J. Comput. Chem.*, **1995**, *16*, 1339–1350.
- [110] Roux, B. The calculation of the potential of mean force using computer simulations. *Comput. Phys. Comm.*, **1995**, *91*, 275–282.
- [111] Frisch, M. J.; Trucks, G. W.; Schlegel, H. B.; Scuseria, G. E.; Robb, M. A.; Cheeseman, J. R.; Montgomery, J. A. Jr.; Vreven, T.; Kudin, K. N.; Burant, J. C.; Millam, J. M.; Iyengar, S. S.; Tomasi, J.; Barone, V.; Mennucci, B.; Cossi, M.; Scalmani, G.; Rega, N.; Petersson, G. A.; Nakatsuji, H.; Hada, M.; Ehara, M.; Toyota, K.; Fukuda, R.; Hasegawa, J.; Ishida, M.; Nakajima, T.; Honda, Y.; Kitao, O.; Nakai, H.; Klene, M.; Li, X.; Knox, J. E.; Hratchian, H. P.; Cross, J. B.; Bakken, V.; Adamo, C.; Jaramillo, J.; Gomperts, R.; Stratmann, R. E.; Yazyev, O.; Austin, A. J.; Cammi, R.; Pomelli, C.; Ochterski, J. W.; Ayala, P. Y.; Morokuma, K.; Voth, G. A.; Salvador, P.; Dannenberg, J. J.; Zakrzewski, V. G.; Dapprich, S.; Daniels, A. D.; Strain, M. C.; Farkas, O.; Malick, D. K.; Rabuck, A. D.; Raghavachari, K.; Foresman, J. B.; Ortiz, J. V.; Cui, Q.; Baboul, A. G.; Clifford, S.; Cioslowski, J.; Stefanov, B. B.; Liu, G.; Liashenko, A.; Piskorz, P.; Komaromi, I.; Martin, R. L.; Fox, D. J.; Keith, T.; Al-Laham, M. A.; Peng, C. Y.; Nanayakkara, A.; Challacombe, M.; Gill, P. M. W.; Johnson, B.; Chen, W.; Wong, M. W.; Gonzalez, C.; Pople, J. A. Gaussian 03, Revision C.02. Gaussian, Inc., Wallingford, CT, 2004.
- [112] Rappe, A.K.; Casewit, C.J.; Colwell, K.S.; Goddard III, W.A.; Skiff, W.M. UFF, a Full Periodic Table Force Field for Molecular Mechanics and Molecular Dynamics Simulations. *J. Am. Chem. Soc.*, **1992**, *114*, 10024–10035.
- [113] Ren, P.Y.; Ponder, J.W. Polarizable atomic multipole water model for molecular mechanics simulation. *J. Phys. Chem. B*, **2003**, *107*, 5933–5947.
- [114] Ren, P.Y.; Ponder, J.W. Tinker polarizable atomic multipole force field for proteins. *to be published.*, **2006**.
- [115] Walker, R.C.; Crowley, M.F.; Case, D.A. The implementation of a fast and efficient hybrid QM/MM potential method within The Amber 9.0 sander module. *J. Computat. Chem.*, **2008**, *29*, 1019–1031.



- [116] Pellegrini, E.; J. Field, M. A generalized-Born solvation model for macromolecular hybrid-potential calculations. *J. Phys. Chem. A.*, **2002**, *106*, 1316–1326.
- [117] Nam, K.; Gao, J.; York, D. An efficient linear-scaling Ewald method for long-range electrostatic interactions in combined QM/MM calculations. *J. Chem. Theory Comput.*, **2005**, *1*, 2–13.
- [118] Seabra, G.M.; Walker, R.C.; Elstner, M.; Case, D.A.; Roitberg, A.E. Implementation of the SCC-DFTB Method for Hybrid QM/MM Simulations within the Amber Molecular Dynamics Package. *J. Phys. Chem. A.*, **2007**, *20*, 5655–5664.
- [119] Elstner, M.; Porezag, D.; Jungnickel, G.; Elsner, J.; Haugk, M.; Frauenheim, T.; Suhai, S.; Seifert, G. Self-consistent charge density functional tight-binding method for simulation of complex material properties. *Phys. Rev. B*, **1998**, *58*, 7260.
- [120] Kruger, T.; Elstner, M.; Schiffels, P.; Frauenheim, T. Validation of the density-functional based tight-binding approximation. *J. Chem. Phys.*, **2005**, *122*, 114110.
- [121] Wang, Q.T.; Bryce, R.A. Improved hydrogen bonding at the NDDO-type semiempirical quantum mechanical/molecular mechanical interface. *J. Chem. Theory Comput.*, **2009**, *5*, 2206–2211.
- [122] te Velde, G.; Bickelhaupt, F. M.; Baerends, E. J.; Guerra, C. Fonseca; van Gisbergen, S. J. A.; Snijders, J. G.; Ziegler, T. Chemistry with ADF. *J. Comp. Chem.*, **2001**, *22*, 931–967.
- [123] ADF2011, SCM, Theoretical Chemistry, Vrije Universiteit, Amsterdam, The Netherlands, <http://www.scm.com>, accessed 02/29/2012.
- [124] Schmidt, Michael W.; Baldridge, Kim K.; Boatz, Jerry A.; Elbert, Steven T.; Gordon, Mark S.; Jensen, Jan H.; Koseki, Shiro; Matsunaga, Nikita; Nguyen, Kiet A.; Su, Shujun; Windus, Theresa L.; Dupuis, Michel; Montgomery, John A. Jr. General atomic and molecular electronic structure system. *J. Comp. Chem.*, **1993**, *14*, 1347–1363.
- [125] Gordon, M. S.; Schmidt, M. W. in *Theory and Applications of Computational Chemistry, the first forty years*, Dykstra, C. E.; Frenking, G.; Kim, K. S.; Scuseria, G. E., Eds., chapter 41, pp 1167–1189. Elsevier, Amsterdam, 2005.
- [126] Valiev, M.; Bylaska, E. J.; Govind, N.; Kowalski, K.; Straatsma, T. P.; van Dam, H. J. J.; Wang, D.; Niepolcha, J.; Apra, E.; Windus, T. L.; de Jong, W. A. Nwchem: a comprehensive and scalable open-source solution for large scale molecular simulations. *Comput. Phys. Commun.*, **2010**, *181*, 1477.
- [127] Frisch, M. J.; Trucks, G. W.; Schlegel, H. B.; Scuseria, G. E.; Robb, M. A.; Cheeseman, J. R.; Scalmani, G.; Barone, V.; Mennucci, B.; Petersson, G. A.; Nakatsuji, H.; Caricato, M.; Li, X.; Hratchian, H. P.; Izmaylov, A. F.; Bloino, J.; Zheng, G.; Sonnenberg, J. L.; Hada, M.; Ehara, M.; Toyota, K.; Fukuda, R.; Hasegawa, J.; Ishida, M.; Nakajima, T.; Honda, Y.; Kitao, O.; Nakai, H.; Vreven, T.; Montgomery, J. A. Jr.; Peralta, J. E.; Ogliaro, F.; Bearpark, M.; Heyd, J. J.; Brothers, E.; Kudin, K. N.; Staroverov, V. N.; Kobayashi,

## BIBLIOGRAPHY

- R.; Normand, J.; Raghavachari, K.; Rendell, A.; Burant, J. C.; Iyengar, S. S.; Tomasi, J.; Cossi, M.; Rega, N.; Millam, J. M.; Klene, M.; Knox, J. E.; Cross, J. B.; Bakken, V.; Adamo, C.; Jaramillo, J.; Gomperts, R.; Stratmann, R. E.; Yazyev, O.; Austin, A. J.; Cammi, R.; Pomelli, C.; Ochterski, J. W.; Martin, R. L.; Morokuma, K.; Zakrzewski, V. G.; Voth, G. A.; Salvador, P.; Dannenberg, J. J.; Dapprich, S.; Daniels, A. D.; Farkas, Ö.; Foresman, J. B.; Ortiz, J. V.; Cioslowski, J.; Fox, D. J. Gaussian 09 Revision A.1. Gaussian Inc. Wallingford CT 2009.
- [128] Neese, F. ORCA - an ab initio, Density Functional and Semiempirical program package, Version 2.8.0, University of Bonn, 2010.
- [129] Ufimtsev, Ivan S.; Martinez, Todd J. Quantum chemistry on graphical processing units. 3. Analytical energy gradients, geometry optimization, and first principles molecular dynamics. *J. Chem. Theory Comput.*, **2009**, *5*, 2619–2628.
- [130] Torras, J.; He, Y.; Cao, C.; Muralidharan, K.; Deumens, E.; Cheng, H.; Trickey, S. PUPIL: A systematic approach to software integration in multi-scale simulations. *Comput. Phys. Comm.*, **2007**, *177*, 265–279.
- [131] Torras, J.; Seabra, G.; Deumens, E.; Trickey, S.B.; Roitberg, A.E. A versatile AMBER-Gaussian QM/MM interface through PUPIL. *J. Comput. Chem.*, **2008**, *29*, 1564–1573.
- [132] Kollman, P. Free energy calculations: Applications to chemical and biochemical phenomena. *Chem. Rev.*, **1993**, *93*, 2395–2417.
- [133] Simonson, T. in *Computational Biochemistry and Biophysics*, Becker, O.; MacKerell, A.D.; Roux, B.; Watanabe, M., Eds. Marcel Dekker, New York, 2001.
- [134] Steinbrecher, T.; Case, D.A.; Labahn, A. A multistep approach to structure-based drug design: Studying ligand binding at the human neutrophil elastase. *J. Med. Chem.*, **2006**, *49*, 1837–1844.
- [135] Steinbrecher, T.; Hrenn, A.; Dormann, K.; Merfort, I.; Labahn, A. Bornyl (3,4,5-trihydroxy)-cinnamate - An optimized human neutrophil elastase inhibitor designed by free energy calculations. *Bioorg. Med. Chem.*, **2008**, *16*, 2385–2390.
- [136] Hummer, G.; Szabo, A. Calculation of free-energy differences from computer simulations of initial and final states. *J. Chem. Phys.*, **1996**, *105*, 2004–2010.
- [137] Steinbrecher, T.; Mobley, D.L.; Case, D.A. Non-linear scaling schemes for Lennard-Jones interactions in free energy calculations. *J. Chem. Phys.*, **2007**, *127*, 214108.
- [138] Deng, Y.; Roux, B. Calculation of standard binding free energies: Aromatic molecules in the T4 lysozyme L99A mutant. *J. Chem. Theor. Comput.*, **2006**, *2*, 1255–1273.
- [139] Steinbrecher, T.; Joung, I.; Case, D.A. Soft-core potentials in thermodynamic integration: Comparing one- and two-step transformations. *J. Comp. Chem.*, **2011**, *32*, 3253–3263.

- [140] Valleau, J.P.; Torrie, G.M. in *Modern Theoretical Chemistry, Vol. 5: Statistical Mechanics, Part A*, Berne, B.J., Ed. Plenum Press, New York, 1977.
- [141] Kottalam, J.; Case, D.A. Dynamics of ligand escape from the heme pocket of myoglobin. *J. Am. Chem. Soc.*, **1988**, *110*, 7690–7697.
- [142] Kästner, J.; Thiel, W. Bridging the gap between thermodynamic integration and umbrella sampling provides a novel analysis method: "Umbrella integration". *J. Chem. Phys.*, **2005**, *123*, 144104.
- [143] Wu, X.; Brooks, B.R. Self-guided Langevin dynamics simulation method. *Chem. Phys. Lett.*, **2003**, *381*, 512–518.
- [144] Wu, X.; Damjanovic, A.; Brooks, B. R. Efficient and unbiased sampling of biomolecular systems in the canonical ensemble: a review of self-guided langevin dynamics. *Adv. Chem. Phys.*, **2012**, *150*, 255–326.
- [145] Wu, X.; Brooks, B.R. Toward canonical ensemble distribution from self-guided Langevin dynamics simulation. *J. Chem. Phys.*, **2011**, *134*, 134108.
- [146] Wu, X.; Brooks, B.R. Force-momentum-based self-guided Langevin dynamics: a rapid sampling method that approaches the canonical ensemble . *J. Chem. Phys.*, **2011**, *135*, 204101.
- [147] Jensen, M.O.; Park, S.; d, E.Tajkhorshi; Schulten, K. Energetics of glycerol conduction through aquaglyceroporin GlpF. *Proc. Natl. Acad. Sci. USA*, **2002**, *99*, 6731–6736.
- [148] Crespo, A.; Marti, M.A.; Estrin, D.A.; Roitberg, A.E. Multiple-steering QM-MM calculation of the free energy profile in chorismate mutase. *J. Am. Chem. Soc.*, **2005**, *127*, 6940–6941.
- [149] Jarzynski, C. Nonequilibrium equality for free energy differences. *Phys. Rev. Lett.*, **1997**, *78*, 2690–2693.
- [150] Hummer, G.; Szabo, A. Free energy reconstruction from nonequilibrium single-molecule pulling experiments. *Proc. Natl. Acad. Sci. USA*, **2001**, *98*, 3658.
- [151] Hummer, G.; Szabo, A. Kinetics from nonequilibrium single-molecule pulling experiments. *Biophys. J.*, **2003**, *85*, 5–15.
- [152] Mitsutake, A.; Sugita, Y.; Okamoto, Y. Generalized-ensemble algorithms for molecular simulations of biopolymers. *Biopolymers*, **2001**, *60*, 96–123.
- [153] Nymeyer, H.; Gnanakaran, S.; García, A.E. Atomic simulations of protein folding using the replica exchange algorithm. *Meth. Enzymol.*, **2004**, *383*, 119–149.
- [154] Cheng, X.; Cui, G.; Hornak, V.; Simmerling, C. Modified replica exchange simulation methods for local structure refinement. *J. Phys. Chem. B*, **2005**, *109*, 8220–8230.

## BIBLIOGRAPHY

- [155] Okur, A.; Roe, D.R.; Cui, G.; Hornak, V.; Simmerling, C. Improving convergence of replica-exchange simulations through coupling to a high-temperature structure reservoir. *J. Chem. Theory comput.*, **2007**, *3*, 557–568.
- [156] Roitberg, A.E.; Okur, A.; Simmerling, C. Coupling of replica exchange simulations to a non-Boltzmann structure reservoir. *J. Phys. Chem. B*, **2007**, *111*, 2415–2418.
- [157] Meng, Yilin; Sabri Dashti, Danial; Roitberg, Adrian E. Computing Alchemical Free Energy Differences with Hamiltonian Replica Exchange Molecular Dynamics (H-REMD) Simulations. *J. Chem. Theory Comput.*, **2011**, *7*(9), 2721–2727.
- [158] Sabri Dashti, Danial; Roitberg, Adrian E. Calculating the pKa Shift of Titratable Group at Position 66 of Staphylococcal Nuclease Mutant with the Replica Exchange Free Energy Perturbation method (REFEP). *In press*, **2012**.
- [159] Sabri Dashti, Danial; Roitberg, Adrian E. Computing the Free Energy Profile for the SN2 Reaction Between Cl<sup>-</sup> and CH<sub>3</sub>Cl Using QM/MM Umbrella Sampling Replica Exchange. *In press*, **2012**.
- [160] Meng, Yilin; Roitberg, Adrian E. Constant pH replica exchange molecular dynamics in biomolecules using a discrete protonation model. *J. Chem. Theory Comput.*, **2010**, *6*(4), 1401–1412.
- [161] Sabri Dashti, Danial; Meng, Yilin; Swails, Jason; Roitberg, Adrian E. pH-Replica Exchange Molecular Dynamics in Proteins Using a Discrete Protonation Method. *In press*, **2012**.
- [162] Shirts, Michael R; Chodera, John D. Statistically optimal analysis of samples from multiple equilibrium states. *J. Chem. Phys.*, **2008**, *129*(12), 124105–124105–10.
- [163] Pohorille, Andrew; Jarzynski, Christopher; Chipot, Christophe. Good practices in Free-Energy calculations. *J. Phys. Chem. B*, **2010**, *114*(32), 10235–10253.
- [164] Babin, V.; Roland, C.; Sagui, C. Adaptively biased molecular dynamics for free energy calculations. *J. Chem. Phys.*, **2008**, *128*, 134101.
- [165] Huber, Thomas; Torda, Andrew E.; van Gunsteren, Wilfred F. Local elevation: a method for improving the searching properties of molecular dynamics simulation. *J. Comput. Aided. Mol. Des.*, **1994**, *8*, 695–708.
- [166] Wang, Fugao; Landau, D. P. Efficient, multiple-range random walk algorithm to calculate the density of states. *Phys. Rev. Lett.*, **2001**, *86*, 2050–2053.
- [167] Darve, Eric; Pohorille, Andrew. Calculating free energies using average force. *J. Chem. Phys.*, **2001**, *115*, 9169–9183.
- [168] Laio, A.; Parrinello, M. Escaping free-energy minima. *Proc. Natl. Acad. Sci.*, **2002**, *99*, 12562–12566.

- [169] Iannuzzi, M.; Laio, A.; Parrinello, M. Efficient exploration of reactive potential energy surfaces using car-parrinello molecular dynamics. *Phys. Rev. Lett.*, **2003**, *90*, 238302–1.
- [170] Lelièvre, Tony; Rousset, Mathias; Stoltz, Gabriel. Computation of free energy profiles with parallel adaptive dynamics. *J. Chem. Phys.*, **2007**, *126*, 134111.
- [171] Raiteri, Paolo; Laio, Alessandro; Gervasio, Francesco Luigi; Micheletti, Cristian; Parrinello, Michele. Efficient reconstruction of complex free energy landscapes by multiple walkers metadynamics. *J. Phys. Chem.*, **2006**, *110*, 3533–3539.
- [172] Sugita, Yuji; Kitao, Akio; Okamoto, Yuko. Multidimensional replica-exchange method for free-energy calculations. *J. Chem. Phys.*, **2000**, *113*, 6042–6051.
- [173] Bussi, Giovanni; Gervasio, Francesco Luigi; Laio, Alessandro; Parrinello, Michele. Free-energy landscape for  $\beta$  hairpin folding from combined parallel tempering and metadynamics. *J. Am. Chem. Soc.*, **2006**, *128*, 13435–13441.
- [174] Piana, S.; Laio, A. A bias-exchange approach to protein folding. *J. Phys. Chem. B*, **2007**, *111*, 4553–4559.
- [175] Coutsias, E. A.; Seok, C.; Dill, K. A. Using quaternions to calculate RMSD. *J. Comput. Chem.*, **2004**, *25*, 1849–1857.
- [176] Park, Sanghyun; Khalili-Araghi, Fatemeh; Tajkhorshid, Emad; Schulten, Klaus. Free energy calculation from steered molecular dynamics simulations using Jarzynski's equality. *J. Chem. Phys.*, **2003**, *119*, 3559–3566.
- [177] Matsumoto, Makoto; Nishimura, Takuji. Mersenne twister: a 623-dimensionally equidistributed uniform pseudo-random number generator. *ACM Trans. Model. Comput. Simul.*, **1998**, *8*, 3–30.
- [178] Babin, Volodymyr; Sagui, Celeste. Conformational free energies of methyl-alpha-l-iduronic and methyl-beta-d-glucuronic acids in water. *J. Chem. Phys.*, **2010**, *132*(10), 104108.
- [179] Mills, G.; Jönsson, H. Quantum and thermal effects in H<sub>2</sub> dissociative adsorption: Evaluation of free energy barriers in multidimensional quantum systems. *Phys. Rev. Lett.*, **1994**, *72*, 1124–1127.
- [180] Jönsson, H.; Mills, G.; Jacobsen, K.W. in *Classical and Quantum Dynamics in Condensed Phase Simulations*, Berne, B.J.; Ciccotti, G.; Coker, D.F., Eds., pp 385–404. World Scientific, Singapore, 1998.
- [181] Elber, R.; Karplus M, M. A method for determining reaction paths in large molecules: Application to myoglobin. *Chem. Phys. Lett.*, **1987**, *139*, 375–380.
- [182] Henkelman, G.; Jönsson, H. Improved tangent estimate in the nudged elastic band method for finding minimum energy paths and saddle points. *J. Chem. Phys.*, **2000**, *113*, 9978–9985.

## BIBLIOGRAPHY

- [183] Henkelman, G.; Uberuaga, B.P.; Jönsson, H. A climbing image nudged elastic band method for finding saddle points and minimum energy paths. *J. Chem. Phys.*, **2000**, *113*, 9901–9904.
- [184] Chu, J.; Trout, B.L.; Brooks, B.R. A super-linear minimization scheme for the nudged elastic band method. *J. Chem. Phys.*, **2003**, *119*, 12708–12717.
- [185] Bergonzo, Christina; Campbell, Arthur J; Walker, Ross C; Simmerling, Carlos. A Partial Nudged Elastic Band Implementation for Use with Large or Explicitly Solvated Systems. *Int J Quantum Chem*, **2009**, *109*(15), 3781.
- [186] Mathews, D.H.; Case, D.A. Nudged Elastic Band calculation of minimal energy pathways for the conformational change of a GG mismatch. *J. Mol. Biol.*, **2006**, *357*, 1683–1693.
- [187] Hamelberg, Donald; Mongan, John; McCammon, J. Andrew. Accelerated molecular dynamics: A promising and efficient simulation method for biomolecules. *J. Chem. Phys.*, **2004**, *120*(24), 11919–11929.
- [188] Hamelberg, Donald; de Oliveira, Cesar Augusto F; McCammon, J. Andrew. Sampling of slow diffusive conformational transitions with accelerated molecular dynamics. *JOURNAL OF PHYSICAL CHEMISTRY*, **2007**, *127*(25), 155102–155109.
- [189] Grant, Barry J.; Gorfe, Alemayehu A.; McCammon, J. Andrew. Ras conformational switching: Simulating nucleotide-dependent conformational transitions with accelerated molecular dynamics. *PLoS Computational Biology*, **2009**, *5*(3), e1000325.
- [190] de Oliveira, Cesar Augusto F; Grant, Barry J.; Zhou, Michelle; McCammon, J. Andrew. Large-scale conformational changes of trypanosoma cruzi proline racemase predicted by accelerated molecular dynamics simulation. *PLoS Computational Biology*, **2011**, *7*(10), e1002178.
- [191] Pierce, Levi C.T.; Salomon-Ferrer, Romelia; de Oliveira, Cesar Augusto F; McCammon, J. Andrew; Walker, Ross C. Routine access to milli-second time scales with accelerated molecular dynamics. *Submitted for publication*, **2012**.
- [192] Mongan, J.; Case, D.A.; McCammon, J.A. Constant pH molecular dynamics in generalized Born implicit solvent. *J. Comput. Chem.*, **2004**, *25*, 2038–2048.
- [193] Kolossváry, I.; Guida, W.C. Low mode search. An efficient, automated computational method for conformational analysis: Application to cyclic and acyclic alkanes and cyclic peptides. *J. Am. Chem. Soc.*, **1996**, *118*, 5011–5019.
- [194] Kolossváry, I.; Guida, W.C. Low-mode conformational search elucidated: Application to C<sub>39</sub>H<sub>80</sub> and flexible docking of 9-deazaguanine inhibitors into PNP. *J. Comput. Chem.*, **1999**, *20*, 1671–1684.
- [195] Kolossváry, I.; Keserü, G.M. Hessian-free low-mode conformational search for large-scale protein loop optimization: Application to c-jun N-terminal kinase JNK3. *J. Comput. Chem.*, **2001**, *22*, 21–30.

- [196] Keserü, G.M.; Kolossváry, I. Fully flexible low-mode docking: Application to induced fit in HIV integrase. *J. Am. Chem. Soc.*, **2001**, *123*, 12708–12709.
- [197] Press, W.H.; Flannery, B.P.; Teukolsky, S.A.; Vetterling, W.T. *Numerical Recipes: The Art of Scientific Computing*. Cambridge University Press, New York, 1989.
- [198] Liu, D.C.; Nocedal, J. On the limited memory method for large scale optimization. *Math. Programming B*, **1989**, *45*, 503–528.
- [199] Nocedal, J.; L. Morales, J. Automatic preconditioning by limited memory quasi-Newton updating. *SIAM J. Opt.*, **2000**, *10*, 1079–1096.
- [200] Schulman, L.S. *Techniques and Applications of Path Integration*. Wiley & Sons, New York, 1996.
- [201] Chandler, D.; Wolynes, P.G. Exploiting the isomorphism between quantum theory and classical statistical mechanics of polyatomic fluids. *J. Chem. Phys.*, **1981**, *74*, 4078–4095.
- [202] Ceperley, D.M. Path integrals in the theory of condensed helium. *Rev. Mod. Phys.*, **1995**, *67*, 279–355.
- [203] Martyna, G.J.; Klein, M.L.; Tuckerman, M. Nosé-Hoover chains: The canonical ensemble via continuous dynamics. *J. Chem. Phys.*, **1992**, *97*, 2635.
- [204] Berne, B.J.; Thirumalai, D. On the simulation of quantum systems: path integral methods. *Annu. Rev. Phys. Chem.*, **1986**, *37*, 401.
- [205] Cao, J.; Berne, B.J. On energy estimators in path integral Monte Carlo simulations: Dependence of accuracy on algorithm. *J. Chem. Phys.*, **1989**, *91*, 6359–6366.
- [206] Paesani, F.; Zhang, W.; Case, D.A.; Cheatham, T.E.; Voth, G.A. An accurate and simple quantum model for liquid water. *J. Chem. Phys.*, **2006**, *125*, 184507.
- [207] Martyna, G.J.; Hughes, A.; Tuckerman, M.E. Molecular dynamics algorithms for path integrals at constant pressure. *J. Chem. Phys.*, **1999**, *110*, 3275.
- [208] Voth, G.A. Path-integral centroid methods in quantum statistical mechanics and dynamics. *Adv. Chem. Phys.*, **1996**, *93*, 135.
- [209] Craig, I.R.; Manolopoulos, D.E. Quantum statistics and classical mechanics: Real time correlation functions from ring polymer molecular dynamics. *J. Chem. Phys.*, **2004**, *121*, 3368.
- [210] Cao, J.; Voth, G.A. The formulation of quantum statistical mechanics based on the Feynman path centroid density. IV. Algorithms for centroid molecular dynamics. *J. Chem. Phys.*, **1994**, *101*, 6168.
- [211] Miller, T.F.; Manolopoulos, D.E. Quantum diffusion in liquid water from ring polymer molecular dynamics. *J. Chem. Phys.*, **2005**, *123*, 154504.

## BIBLIOGRAPHY

- [212] Berne, B.J.; D. Harp, G. *Adv. Chem. Phys.*, **1970**, *17*, 63.
- [213] Miller, W.H.; Schwartz, S.D.; Tromp, J.W. Quantum mechanical rate constants for bimolecular reactions. *J. Chem. Phys.*, **1983**, *79*, 4889–4898.
- [214] Kubo, R.; Toda, M.; Hashitsume, N. *Statistical Physics II: Nonequilibrium Statistical Mechanics*, 2nd ed. Springer-Verlag, Heidelberg, 1991.
- [215] Miller, W.H. *Adv. Chem. Phys.*, **1974**, *25*, 69.
- [216] Miller, W.H. Including quantum effects in the dynamics of complex (i.e., large) molecular systems. *J. Chem. Phys.*, **2006**, *125*, 132305.
- [217] Wang, H.; Sun, X.; Miller, W.H. Semiclassical approximations for the calculation of thermal rate constants for chemical reactions in complex molecular systems. *J. Chem. Phys.*, **1998**, *108*, 9726.
- [218] Sun, X.; Wang, H.; H. Miller, W. Semiclassical theory of electronically nonadiabatic dynamics: Results of a linearized approximation to the initial value representation. *J. Chem. Phys.*, **1998**, *109*, 7064.
- [219] Liu, J.; H. Miller, W. A simple model for the treatment of imaginary frequencies in chemical reaction rates and molecular liquids. *J. Chem. Phys.*, **2009**, *131*, 074113.
- [220] Liu, J.; H. Miller, W.; Paesani, F.; Zhang, W.; A. Case, D. Quantum dynamical effects in liquid water: A semiclassical study on the diffusion and the infrared absorption spectrum. *J. Chem. Phys.*, **2009**, *131*, 164509.
- [221] Liu, J.; Miller, W.H. Real time correlation function in a single phase space integral beyond the linearized semiclassical initial value representation. *J. Chem. Phys.*, **2007**, *126*, 234110.
- [222] Liu, J.; Miller, W.H. Test of the consistency of various linearized semiclassical initial value time correlation functions in application to inelastic neutron scattering from liquid para-hydrogen. *J. Chem. Phys.*, **2008**, *128*, 144511.
- [223] Shi, Q.; Giva, E. *J. Chem. Phys. A*, **2003**, *107*, 9059.
- [224] Voth, G.A.; Chandler, D.; Miller, W.H. Rigorous Formulation of Quantum Transition State Theory and Its Dynamical Corrections. *J. Chem. Phys.*, **1989**, *91*, 7749–7760.
- [225] Miller, W.H. Semiclassical limit of quantum mechanical transition state theory for non-separable systems. *J. Chem. Phys.*, **1975**, *62*, 1899.
- [226] Miller, W.H.; Zhao, Y.; Ceotto, M.; Yang, S. Quantum instanton approximation for thermal rate constants of chemical. *J. Chem. Phys.*, **2003**, *119*, 1329–1342.
- [227] Yamamoto, T.; Miller, W.H. On the efficient path integral evaluation of thermal rate constants with the quantum instanton approximation. *J. Chem. Phys.*, **2004**, *120*, 3086–3099.



- [228] Vaníček, J.; Miller, W.H.; Castillo, J.F.; Aoiz, F.J. Quantum-instanton evaluation of the kinetic isotope effects. *J. Chem. Phys.*, **2005**, *123*, 054108.
- [229] Vaníček, J.; Miller, W.H. Efficient estimators for quantum instanton evaluation of the kinetic isotope effects: application to the intramolecular hydrogen transfer in pentadiene. *J. Chem. Phys.*, **2007**, *127*, 114309.
- [230] Yamamoto, T.; Miller, W.H. Path integral evaluation of the quantum instanton rate constant for proton transfer in a polar solvent. *J. Chem. Phys.*, **2005**, *122*, 044106.
- [231] Duggan, B.M.; Legge, G.B.; Dyson, H.J.; Wright, P.E. SANE (Structure Assisted NOE Evaluation): An automated model-based approach for NOE assignment. *J. Biomol. NMR*, **2001**, *19*, 321–329.
- [232] Kalk, A.; Berendsen, H.J.C. Proton magnetic relaxation and spin diffusion in proteins. *J. Magn. Reson.*, **1976**, *24*, 343–366.
- [233] Olejniczak, E.T.; Weiss, M.A. Are methyl groups relaxation sinks in small proteins? *J. Magn. Reson.*, **1990**, *86*, 148–155.
- [234] Cross, K.J.; Wright, P.E. Calibration of ring-current models for the heme ring. *J. Magn. Reson.*, **1985**, *64*, 220–231.
- [235] Ösapay, K.; Case, D.A. A new analysis of proton chemical shifts in proteins. *J. Am. Chem. Soc.*, **1991**, *113*, 9436–9444.
- [236] Case, D.A. Calibration of ring-current effects in proteins and nucleic acids. *J. Biomol. NMR*, **1995**, *6*, 341–346.
- [237] Banci, L.; Bertini, I.; Gori-Savellini, G.; Romagnoli, A.; Turano, P.; Cremonini, M.A.; Luchinat, C.; Gray, H.B. Pseudocontact shifts as constraints for energy minimization and molecular dynamics calculations on solution structures of paramagnetic metalloproteins. *Proteins*, **1997**, *29*, 68.
- [238] Sanders, C.R. II; Hare, B.J.; Howard, K.P.; Prestegard, J.H. Magnetically-oriented phospholipid micelles as a tool for the study of membrane-associated molecules. *Prog. NMR Spectr.*, **1994**, *26*, 421–444.
- [239] Tsui, V.; Zhu, L.; Huang, T.H.; Wright, P.E.; Case, D.A. Assessment of zinc finger orientations by residual dipolar coupling constants. *J. Biomol. NMR*, **2000**, *16*, 9–21.
- [240] Case, D.A. Calculations of NMR dipolar coupling strengths in model peptides. *J. Biomol. NMR*, **1999**, *15*, 95–102.
- [241] Gippert, G.P.; Yip, P.F.; Wright, P.E.; Case, D.A. Computational methods for determining protein structures from NMR data. *Biochem. Pharm.*, **1990**, *40*, 15–22.
- [242] Case, D.A.; Wright, P.E. in *NMR in Proteins*, Clore, G.M.; Gronenborn, A., Eds., pp 53–91. MacMillan, New York, 1993.

## BIBLIOGRAPHY

- [243] Case, D.A.; Dyson, H.J.; Wright, P.E. Use of chemical shifts and coupling constants in nuclear magnetic resonance structural studies on peptides and proteins. *Meth. Enzymol.*, **1994**, *239*, 392–416.
- [244] Brüschweiler, R.; Case, D.A. Characterization of biomolecular structure and dynamics by NMR cross-relaxation. *Prog. NMR Spectr.*, **1994**, *26*, 27–58.
- [245] Case, D.A. The use of chemical shifts and their anisotropies in biomolecular structure determination. *Curr. Opin. Struct. Biol.*, **1998**, *8*, 624–630.
- [246] Torda, A.E.; Scheek, R.M.; VanGunsteren, W.F. Time-dependent distance restraints in molecular dynamics simulations. *Chem. Phys. Lett.*, **1989**, *157*, 289–294.
- [247] Pearlman, D.A.; Kollman, P.A. Are time-averaged restraints necessary for nuclear magnetic resonance refinement? A model study for DNA. *J. Mol. Biol.*, **1991**, *220*, 457–479.
- [248] Torda, A.E.; Brunne, R.M.; Huber, T.; Kessler, H.; van Gunsteren, W.F. Structure refinement using time-averaged J-coupling constant restraints. *J. Biomol. NMR*, **1993**, *3*, 55–66.
- [249] Pearlman, D.A. How well to time-averaged J-coupling restraints work? *J. Biomol. NMR*, **1994**, *4*, 279–299.
- [250] Pearlman, D.A. How is an NMR structure best defined? An analysis of molecular dynamics distance-based approaches. *J. Biomol. NMR*, **1994**, *4*, 1–16.
- [251] Brünger, A.T.; Adams, P.D.; Clore, G.M.; Delano, W.L.; Gros, P.; Grosse-Kunstleve, R.W.; Jiang, J.-S.; Kuszewski, J.; Nilges, M.; Pannu, N.S.; Read, R.J.; Rice, L.M.; Simonson, T.; Warren, G.L. Crystallography and NMR system (CNS): A new software system for macromolecular structure determination. *Acta Cryst. D*, **1998**, *54*, 905–921.
- [252] Yu, N.; Yennawar, H.P.; Merz, K.M. Jr. Refinement of protein crystal structures using energy restraints derived from linear-scaling quantum mechanics. *Acta Cryst. D*, **2005**, *61*, 322–332.
- [253] Yu, N.; Li, X.; Cui, G.; Hayik, S.; Merz, K.M. Jr. Critical assessment of quantum mechanics based energy restraints in protein crystal structure refinement. *Prot. Sci.*, **2006**, *15*, 2773–2784.
- [254] Yang, W.; Lee, T.-S. A density-matrix divide-and-conquer approach for electronic structure calculations of large molecules. *J. Chem. Phys.*, **1995**, *103*, 5674–5678.
- [255] Dixon, S.L.; Merz, K.M. Jr. Semiempirical molecular orbital calculations with linear system size scaling. *J. Chem. Phys.*, **1996**, *104*, 6643–6649.
- [256] Dixon, S.L.; Merz, K.M. Jr. Fast, accurate semiempirical molecular orbital calculations for macromolecules. *J. Chem. Phys.*, **1997**, *107*, 879–893.
- [257] Wu, X.; Milne, J. L.; Borgnia, M. J.; Rostapshov, A. V.; Subramaniam, S.; Brooks, B. R. A core-weighted fitting method for docking atomic structures into low-resolution maps: application to cryo-electron microscopy. *J Struct Biol*, **2003**, *141*, 63–76.

- [258] Milne, J. L.; Wu, X.; Borgnia, M. J.; Lengyel, J. S.; Brooks, B. R.; Shi, D.; Perham, R. N.; Subramaniam, S. Molecular structure of a 9-MDa icosahedral pyruvate dehydrogenase subcomplex containing the E2 and E3 enzymes using cryoelectron microscopy. *J Biol Chem*, **2006**, *281*, 4364–70.
- [259] Wu, X.; Brooks, B. R. Modeling of Macromolecular assemblies with map objects. *Proc. 2007 Int. Conf. Bioinform. Comput. Biol.*, **2007**, *II*, 411–417.
- [260] Khursigara, C. M.; Wu, X.; Zhang, P.; Lefman, J.; Subramaniam, S. Role of HAMP domains in chemotaxis signaling by bacterial chemoreceptors. *PNAS*, **2008**, *105*, 16555–60.
- [261] Lengyel, J. S.; Stott, K. M.; Wu, X.; Brooks, A. B. R. and Balbo; Schuck, P.; Perham, R. N.; Subramaniam, S.; Milne, J. L. Extended polypeptide linkers establish the spatial architecture of a pyruvate dehydrogenase multi-enzyme complex. *Structure*, **2008**, *16*, 93–103.
- [262] Khursigara, C. M.; Wu, X.; ; Subramaniam, S. Chemoreceptors in *Caulobacter crescentus*: trimers of receptor dimers in a partially ordered hexagonally packed array. *J Bacteriol*, **2008**, *190*, 6805–10.
- [263] Elegheert, J.; Desfosses, A.; Shkumatov, A. V.; Wu, X.; Bracke, N.; Verstraete, K.; Van Craenenbroeck, K.; Brooks, B. R.; Svergun, D. I.; Vergauwen, B.; Gutsche, I.; Savvides, S. N. Extracellular complexes of the hematopoietic human and mouse CSF-1 receptor are driven by common assembly principles. *Structure*, **2011**, *19*, 1762–72.
- [264] Khursigara, C. M.; Lan, G.; Neumann, S.; Wu, X.; Ravindran, S.; Borgnia, M. J.; Sourjik, V.; Milne, J.; Tu, Y.; Subramaniam, S. Lateral density of receptor arrays in the membrane plane influences sensitivity of the *E. coli* chemotaxis response. *Embo J*, **2011**, *30*, 1719–29.
- [265] Goetz, Andreas W; Williamson, Mark J; Xu, Dong; Poole, Duncan; Grand, Scott Le; Walker, Ross C. Routine microsecond molecular dynamics simulations with amber - part i: Generalized born", 2012. *J. Comp. Theo. Chem.*, **2012**, *in press*.
- [266] Salomon-Ferrer, Romelia; Goetz, Andreas W; Poole, Duncan; Grand, Scott Le; Walker, Ross C. Routine microsecond molecular dynamics simulations with amber - part 2: Particle mesh ewald", 2012. *J. Comp. Theo. Chem.*, **2012**, *in preparation*.
- [267] Crowley, M.F.; Williamson, M.J.; Walker, R.C. CHAMBER: Comprehensive support for CHARMM force fields within the AMBER software. *Int. J. Quant. Chem.*, **2009**, *109*, 3767.
- [268] Miranker, A.; Karplus, M. Functionality maps of binding sites: A multiple copy simultaneous search method. *Proteins: Str. Funct. Gen.*, **1991**, *11*, 29–34.
- [269] Cheng, X.; Hornak, V.; Simmerling, C. Improved conformational sampling through an efficient combination of mean-field simulation approaches. *J. Phys. Chem. B*, **2004**, *108*.

## BIBLIOGRAPHY

- [270] Simmerling, C.; Fox, T.; Kollman, P.A. Use of Locally Enhanced Sampling in Free Energy Calculations: Testing and Application of the alpha to beta Anomerization of Glucose. *J. Am. Chem. Soc.*, **1998**, *120*, 5771–5782.
- [271] Straub, J.E.; Karplus, M. Energy partitioning in the classical time-dependent Hartree approximation. *J. Chem. Phys.*, **1991**, *94*, 6737.
- [272] Ulitsky, A.; Elber, R. The thermal equilibrium aspects of the time-dependent Hartree and the locally enhanced sampling approximations: Formal properties, a correction, and computational examples for rare gas clusters. *J. Chem. Phys.*, **1993**, *98*, 3380.
- [273] Hingerty, B.E.; Figueroa, Samuel; L. Hayden, Thomas; Broyde, Suse. Prediction of DNA Structure from Sequence: A Build-up Technique. *Biopolymers*, **1989**, *28*, 1195–1222.
- [274] Jurecka, Petr; Cerný, Jirí; Hobza, Pavel; Salahub, Dennis R. Density functional theory augmented with an empirical dispersion term. Interaction energies and geometries of 80 noncovalent complexes compared with ab initio quantum mechanics calculations. *J. Comp. Chem.*, **2007**, *28*, 555–569.
- [275] Korth, Martin. Third-generation hydrogen-bonding corrections for semiempirical qm methods and force fields. *J. Chem. Theory Comput.*, **2010**, *6*, 3808.
- [276] Korth, Martin; Pitonak, Michal; Rezac, Jan; Hobza, Pavel. A transferable h-bonding correction for semiempirical quantum-chemical methods. *J. Chem. Theory Comput.*, **2010**, *6*, 344–352.
- [277] Thiel, Walter; Voityuk, Alexander A. Extension of the MNDO formalism to d orbitals: Integral approximations and preliminary numerical results. *Theoret. Chim. Acta*, **1992**, *81*, 391–404.
- [278] Thiel, Walter; Voityuk, Alexander A. Erratum: Extension of MNDO to d orbitals: Parameters and results for the second-row elements and for the zinc group. *J. Phys. Chem.*, **1996**, *100*, 616–626.
- [279] Thiel, Walter; Voityuk, Alexander A. Extension of the MNDO formalism to d orbitals: Integral approximations and preliminary numerical results. *Theoret. Chim. Acta*, **1996**, *93*, 315.
- [280] Erie, D.A.; Breslauer, K.J.; Olson, W.K. A Monte Carlo Method for Generating Structures of Short Single-Stranded DNA Sequences. *Biopolymers*, **1993**, *33*, 75–105.
- [281] Pearlman, D.A.; Kim, Sung-Hou. Conformational Studies of Nucleic Acids I. A Rapid and Direct Method for Generating Coordinates from the Pseudorotation Angle. *J. Biomol. Struct. Dyn.*, **1985**, *3*, 85–98.
- [282] Pearlman, D.A.; Kim, Sung-Hou. Conformational Studies of Nucleic Acids II. The Conformational Energetics of Commonly Occurring Nucleosides. *J. Biomol. Struct. Dyn.*, **1985**, *3*, 99–125.

- [283] Pearlman, D.A.; Kim, S.-H. Conformational Studies of Nucleic Acids: III. Empirical Multiple Correlation Functions for Nucleic Acid Torsion Angles. *J. Biomol. Struct. Dyn.*, **1986**, *4*, 49–67.
- [284] Pearlman, D.A.; Kim, S.-H. Conformational Studies of Nucleic Acids: IV. The Conformational Energetics of Oligonucleotides: d(ApApApA) and ApApApA. *J. Biomol. Struct. Dyn.*, **1986**, *4*, 69–98.
- [285] Pearlman, D.A.; Kim, S.-H. Conformational Studies of Nucleic Acids. V. Sequence Specificities of in the Conformational Energetics of Oligonucleotides: The Homo-Tetramers. *Biopolymers*, **1988**, *27*, 59–77.
- [286] Schlick, T. A Modular Strategy for Generating Starting Conformations and Data Structures of Polynucleotide Helices for Potential Energy Calculations. *J. Computat. Chem.*, **1988**, *9*, 861–889.
- [287] Gabarro-Arpa, J.; Cognet, J.A.H.; Le Bret, M. Object Command Language: a formalism to build molecule models and to analyze structural parameters in macromolecules, with applications to nucleic acids. *J. Mol. Graph.*, **1992**, *10*, 166–173.
- [288] Lavery, R. in *Unusual DNA Structures*, Wells, R. D.; Harvey, S. C., Eds. Springer-Verlag, New York, 1988.
- [289] Shen, L.; Tinoco, I. The Structure of an RNA Pseudoknot that Causes Efficient Frameshift in Mouse Mammary Tumor Virus. *J. Mol. Biol.*, **1995**, *247*, 963–978.
- [290] Hubbard, J.M.; Hearst, J.E. Predicting the Three-Dimensional Folding of Transfer RNA with a Computer Modeling Protocol. *Biochemistry*, **1991**, *30*, 5458–5465.
- [291] Chou, S.-H.; Zhu, L.; Reid, B.R. The Unusual Structure of the Human Centromere (GGA)<sub>2</sub> Motif. *J. Mol. Biol.*, **1994**, *244*, 259–268.
- [292] Levitt, M. Detailed Molecular Model for Transfer Ribonucleic Acid. *Nature*, **1969**, *224*, 759–763.
- [293] Babcock, M.S.; Pednault, E.P.D.; Olson, W.K. Nucleic Acid Structure Analysis. *J. Mol. Biol.*, **1994**, *237*, 125–156.
- [294] Hubbard, J.M.; Hearst, J.E. Computer Modeling 16S Ribosomal RNA. *J. Mol. Biol.*, **1991**, *221*, 889–907.
- [295] Major, F.; Turcotte, M.; Gautheret, D.; Lapalme, G.; Fillon, E.; Cedergren, R. The Combination of Symbolic and Numerical Computation for Three-Dimensional Modeling of RNA. *Science*, **1991**, *253*, 1255–1260.
- [296] Schlick, T.; Olson, W.K. Supercoiled DNA Energetics and Dynamics by Computer Simulation. *J. Mol. Biol.*, **1992**, *223*, 1089–1119.
- [297] Dickerson, R.E. Definitions and Nomenclature of Nucleic Acid Structure Parameters. *J. Biomol. Struct. Dyn.*, **1989**, *6*, 627–634.

## BIBLIOGRAPHY

- [298] Holbrook, S.R.; Sussman, J.L.; Warrant, R.W.; Kim, S.-H. Crystal Structure of Yeast Phenylalanine Transfer RNA II. Structural Features and Functional Implications. *J. Mol. Biol.*, **1978**, *123*, 631–660.
- [299] Conner, B.N.; Yoon, C.; Dickerson, J.L.; Dickerson, R.E. Helix Geometry and Hydration in an A-DNA Tetramer: C-C-G-G. *J. Mol. Biol.*, **1984**, *174*, 663–695.
- [300] Le Bret, M.; Gabarro-Arpa, J.; Gilbert, J.C.; Lemarechal, C. MORCAD an object-oriented molecular modeling package. *J. Chim. Phys.*, **1991**, *88*, 2489–2496.
- [301] Zhurkin, V.B.; P. Lysov, Yu.; Ivanov, V.I. Different Families of Double Stranded Conformations of DNA as Revealed by Computer Calculations. *Biopolymers*, **1978**, *17*, 277–312.
- [302] Brünger, A.T. *X-PLOR: A System for Crystallography and NMR, Version 3.1*. Yale University, New Haven, CT, 1992.
- [303] Wyatt, J.R.; Puglisi, J.D.; Tinoco Jr., I. RNA Pseudoknots. Stability and Loop Size Requirements. *J. Mol. Biol.*, **1990**, *214*, 455–470.
- [304] Puglisi, J.D.; Wyatt, J.R.; Tinoco Jr., I. Conformation of an RNA Pseudoknot. *J. Mol. Biol.*, **1990**, *214*, 437–453.
- [305] Kuila, G.; Fee, J.A.; Schoonover, J.R.; Woodruff, W.H. Resonance Raman Spectra of the [2Fe-2S] Clusters of the Rieske Protein from *Thermus* and Phthalate Dioxygenase from *Pseudomonas*. *J. Am. Chem. Soc.*, **1987**, *109*, 1559–1561.
- [306] Lewin, B. in *Genes IV*, pp 409–425. Cell Press, Cambridge, Mass., 1990.
- [307] Press, W.H.; Teukolsky, S.A.; Vetterling, W.T.; Flannery, B.P. in *Numerical Recipes in C*, pp 113–117. Cambridge, New York, 1992.
- [308] Zhurkin, V.B.; Raghunathan, G.; Ulyanov, N.B.; Camerini-Otero, R.D.; Jernigan, R.L. A Parallel DNA Triplex as a Model for the Intermediate in Homologous Recombination. *Journal of Molecular Biology*, **1994**, *239*, 181–200.
- [309] Saenger, W. in *Principles of Nucleic Acid Structure*, p 120. Springer-Verlag, New York, 1984.
- [310] Turcotte, M.; Lapalme, G.; Major, F. Exploring the conformations of nucleic acids. *J. Funct. Program.*, **1995**, *5*, 443–460.
- [311] Tung, C.-S.; Carter, E.S. II. Nucleic acid modeling tool (NAMOT): an interactive graphic tool for modeling nucleic acid structures. *CABIOS*, **1994**, *10*, 427–433.
- [312] Carter, E.S. II; Tung, C.-S. NAMOT2—a redesigned nucleic acid modeling tool: construction of non-canonical DNA structures. *CABIOS*, **1996**, *12*, 25–30.
- [313] Lavery, R.; Zakrzewska, K.; Skelnar, H. JUMNA (junction minimisation of nucleic acids). *Comp. Phys. Commun.*, **1995**, *91*, 135–158.

- [314] Crippen, G.M.; Havel, T.F. *Distance Geometry and Molecular Conformation*. Research Studies Press, Taunton, England, 1988.
- [315] Spellmeyer, D.C.; Wong, A.K.; Bower, M.J.; Blaney, J.M. Conformational analysis using distance geometry methods. *J. Mol. Graph. Model.*, **1997**, *15*, 18–36.
- [316] Hodsdon, M.E.; Ponder, J.W.; Cistola, D.P. The NMR solution structure of intestinal fatty acid-binding protein complexed with palmitate: Application of a novel distance geometry algorithm. *J. Mol. Biol.*, **1996**, *264*, 585–602.
- [317] Macke, T.; Chen, S.-M.; Chazin, W.J. in *Structure and Function, Volume 1: Nucleic Acids*, Sarma, R.H.; Sarma, M.H., Eds., pp 213–227. Adenine Press, Albany, 1992.
- [318] Potts, B.C.M.; Smith, J.; Akke, M.; Macke, T.J.; Okazaki, K.; Hidaka, H.; Case, D.A.; Chazin, W.J. The structure of calyculin reveals a novel homodimeric fold S100 Ca<sup>2+</sup>-binding proteins. *Nature Struct. Biol.*, **1995**, *2*, 790–796.
- [319] Love, J.J.; Li, X.; Case, D.A.; Giese, K.; Grosschedl, R.; Wright, P.E. DNA recognition and bending by the architectural transcription factor LEF-1: NMR structure of the HMG domain complexed with DNA. *Nature*, **1995**, *376*, 791–795.
- [320] Giese, Timothy J.; York, Darrin M. Charge-dependent model for many-body polarization, exchange, and dispersion interactions in hybrid quantum mechanical/molecular mechanical calculations. *J. Chem. Phys.*, **2007**, *127*(19), 194101–194111.
- [321] Gurbiel, R.J.; Doan, P.E.; Gassner, G.T.; Macke, T.J.; Case, D.A.; Ohnishi, T.; Fee, J.A.; Ballou, D.P.; Hoffman, B.M. Active site structure of Rieske-type proteins: Electron nuclear double resonance studies of isotopically labeled phthalate dioxygenase from *Pseudomonas cepacia* and Rieske protein from *Rhodobacter capsulatus* and molecular modeling studies of a Rieske center. *Biochemistry*, **1996**, *35*, 7834–7845.
- [322] Macke, T.J. *NAB, a Language for Molecular Manipulation*. Ph.D. thesis, The Scripps Research Institute, 1996.
- [323] Gautheret, D.; Major, F.; Cedergren, R. Modeling the three-dimensional structure of RNA using discrete nucleotide conformational sets. *J. Mol. Biol.*, **1993**, *229*, 1049–1064.
- [324] Tan, R.; Harvey, S. Molecular Mechanics Model of Supercoiled DNA. *J. Mol. Biol.*, **1989**, *205*, 573–591.
- [325] Havel, T.F. An evaluation of computational strategies for use in the determination of protein structure from distance constraints obtained by nuclear magnetic resonance. *Prog. Biophys. Mol. Biol.*, **1991**, *56*, 43–78.
- [326] Kuszewski, J.; Nilges, M.; Brünger, A.T. Sampling and efficiency of metric matrix distance geometry: A novel partial metrization algorithm. *J. Biomolec. NMR*, **1992**, *2*, 33–56.

## BIBLIOGRAPHY

- [327] deGroot, B.L.; van Aalten, D.M.F.; Scheek, R.M.; Amadei, A.; Vriend, G.; Berendsen, H.J.C. Prediction of protein conformational freedom from distance constraints. *Proteins*, **1997**, *29*, 240–251.
- [328] Havel, T.F.; Kuntz, I.D.; Crippen, G.M. The theory and practice of distance geometry. *Bull. Math. Biol.*, **1983**, *45*, 665–720.
- [329] Agrafiotis, D.K. Stochastic Proximity Embedding. *J. Computat. Chem.*, **2003**, *24*, 1215–1221.
- [330] Brooks, C.; Brünger, A.; Karplus, M. Active site dynamics in protein molecules: A stochastic boundary molecular-dynamics approach. *Biopolymers*, **1985**, *24*, 843–865.
- [331] Nguyen, D.T.; Case, D.A. On finding stationary states on large-molecule potential energy surfaces. *J. Phys. Chem.*, **1985**, *89*, 4020–4026.
- [332] van Gunsteren, W.F.; Weiner, P.K.; Wilkinson, A.J. eds. *Computer Simulations of Biomolecular Systems, Vol. 2*. ESCOM Science Publishers, Leiden, 1993.
- [333] Wang, J.; Cieplak, P.; Kollman, P.A. How well does a restrained electrostatic potential (RESP) model perform in calculating conformational energies of organic and biological molecules? *J. Comput. Chem.*, **2000**, *21*, 1049–1074.
- [334] Dixon, R.W.; Kollman, P.A. Advancing beyond the atom-centered model in additive and nonadditive molecular mechanics. *J. Comput. Chem.*, **1997**, *18*, 1632–1646.
- [335] Cornell, W.D.; Cieplak, P.; Bayly, C.I.; Gould, I.R.; Merz, K.M. Jr.; Ferguson, D.M.; Spellmeyer, D.C.; Fox, T.; Caldwell, J.W.; Kollman, P.A. A second generation force field for the simulation of proteins, nucleic acids, and organic molecules. *J. Am. Chem. Soc.*, **1995**, *117*, 5179–5197.
- [336] Beachy, M.D.; Friesner, R.A. Accurate ab initio quantum chemical determination of the relative energies of peptide conformations and assessment of empirical force fields. *J. Am. Chem. Soc.*, **1997**, *119*, 5908–5920.
- [337] Kollman, P.A.; Dixon, R.; Cornell, W.; Fox, T.; Chipot, C.; Pohorille, A. in *Computer Simulation of Biomolecular Systems, Vol. 3*, Wilkinson, A.; Weiner, P.; van Gunsteren, W.F., Eds., pp 83–96. Elsevier, 1997.
- [338] Higo, J.; Ito, N.; Kuroda, M.; Ono, S.; Nakajima, N.; Nakamura, H. Energy landscape of a peptide consisting of  $\alpha$ -helix,  $3_{10}$  helix,  $\beta$ -turn,  $\beta$ -hairpin and other disordered conformations. *Prot. Sci.*, **2001**, *10*, 1160–1171.
- [339] Wang, L.; Duan, Y.; Shortle, R.; Imperiali, B.; Kollman, P.A. Study of the stability and unfolding mechanism of BBA1 by molecular dynamics simulations at different temperatures. *Prot. Sci.*, **1999**, *8*, 1292–1304.
- [340] Cheatham, T.E. III; Cieplak, P.; Kollman, P.A. A modified version of the Cornell et al. force field with improved sugar pucker phases and helical repeat. *J. Biomol. Struct. Dyn.*, **1999**, *16*, 845–862.



- [341] Weiner, S.J.; Kollman, P.A.; Case, D.A.; Singh, U.C.; Ghio, C.; Alagona, G.; Profeta, S. Jr.; Weiner, P. A new force field for molecular mechanical simulation of nucleic acids and proteins. *J. Am. Chem. Soc.*, **1984**, *106*, 765–784.
- [342] Weiner, S.J.; Kollman, P.A.; Nguyen, D.T.; Case, D.A. An all-atom force field for simulations of proteins and nucleic acids. *J. Comput. Chem.*, **1986**, *7*, 230–252.
- [343] Åqvist, J. Ion-water interaction potentials derived from free energy perturbation simulations. *J. Phys. Chem.*, **1990**, *94*, 8021–8024.
- [344] Åqvist, J.; Warshel, A. Computer simulation of the initial proton-transfer step in human carbonic anhydrase-I. *J. Mol. Biol.*, **1992**, *224*, 7–14.
- [345] Jorgensen, W.L.; Chandrasekhar, J.; Madura, J.; Klein, M.L. Comparison of simple potential functions for simulating liquid water. *J. Chem. Phys.*, **1983**, *79*, 926–935.
- [346] Jorgensen, W.L.; Madura, J.D. Temperature and size dependence for Monte Carlo simulations of TIP4P water. *Mol. Phys.*, **1985**, *56*, 1381–1392.
- [347] Mahoney, M.W.; Jorgensen, W.L. A five-site model for liquid water and the reproduction of the density anomaly by rigid, nonpolarizable potential functions. *J. Chem. Phys.*, **2000**, *112*, 8910–8922.
- [348] Berendsen, H.J.C.; Grigera, J.R.; Straatsma, T.P. The missing term in effective pair potentials. *J. Phys. Chem.*, **1987**, *91*, 6269–6271.
- [349] Bondi, A. van der Waals volumes and radii. *J. Phys. Chem.*, **1964**, *68*, 441–451.
- [350] Berendsen, H.J.C.; Postma, J.P.M.; van Gunsteren, W.F.; DiNola, A.; Haak, J.R. Molecular dynamics with coupling to an external bath. *J. Chem. Phys.*, **1984**, *81*, 3684–3690.
- [351] Wishart, D.S.; Case, D.A. Use of chemical shifts in macromolecular structure determination. *Meth. Enzymol.*, **2001**, *338*, 3–34.
- [352] Caldwell, J.W.; Kollman, P.A. Structure and properties of neat liquids using nonadditive molecular dynamics: Water, methanol and N-methylacetamide. *J. Phys. Chem.*, **1995**, *99*, 6208–6219.
- [353] Honig, B.; Nicholls, A. Classical electrostatics in biology and chemistry. *Science*, **1995**, *268*, 1144–1149.
- [354] Srinivasan, J.; Cheatham, T.E. III; Cieplak, P.; Kollman, P.; Case, D.A. Continuum solvent studies of the stability of DNA, RNA, and phosphoramidate–DNA helices. *J. Am. Chem. Soc.*, **1998**, *120*, 9401–9409.
- [355] Chong, Lillian T.; Duan, Y.; Wang, L.; Massova, I.; Kollman, P.A. Molecular dynamics and free-energy calculations applied to affinity maturation in antibody 48G7. *Proc. Natl. Acad. Sci. USA*, **1999**, *96*, 14330–14335.

## BIBLIOGRAPHY

- [356] Kollman, P.A.; Massova, I.; Reyes, C.; Kuhn, B.; Huo, S.; Chong, L.; Lee, M.; Lee, T.; Duan, Y.; Wang, W.; Donini, O.; Cieplak, P.; Srinivasan, J.; Case, D.A.; Cheatham, T.E. III. Calculating structures and free energies of complex molecules: Combining molecular mechanics and continuum models. *Accts. Chem. Res.*, **2000**, *33*, 889–897.
- [357] Connolly, M.L. Analytical molecular surface calculation. *J. Appl. Cryst.*, **1983**, *16*, 548–558.
- [358] Elber, R.; Karplus, M. Enhanced sampling in molecular dynamics. Use of the time-dependent Hartree approximation for a simulation of carbon monoxide diffusion through myoglobin. *J. Am. Chem. Soc.*, **1990**, *112*, 9161–9175.
- [359] Roitberg, A.; Elber, R. Modeling side chains in peptides and proteins: Application of the locally enhanced sampling and the simulated annealing methods to find minimum energy conformations. *J. Chem. Phys.*, **1991**, *95*, 9277.
- [360] Simmerling, C.; Miller, J.L.; Kollman, P.A. Combined locally enhanced sampling and particle mesh Ewald as a strategy to locate the experimental structure of a nonhelical nucleic acid. *J. Am. Chem. Soc.*, **1998**, *120*, 7149–7155.
- [361] Simmerling, C.; Lee, M.R.; Ortiz, A.R.; Kolinski, A.; Skolnick, J.; Kollman, P.A. Combining MONSSTER and LES/PME to Predict Protein Structure from Amino Acid Sequence: Application to the Small Protein CMTI-1. *J. Am. Chem. Soc.*, **2000**, *122*, 8392–8402.
- [362] Simmerling, C.; Elber, R. Hydrophobic "collapse" in a cyclic hexapeptide: Computer simulations of CHDLFC and CAAAAC in water. *J. Am. Chem. Soc.*, **1994**, *116*, 2534–2547.
- [363] Ross, W.S.; Hardin, C.C. Ion-induced stabilization of the G-DNA quadruplex: Free energy perturbation studies. *J. Am. Chem. Soc.*, **1994**, *116*, 6070–6080.
- [364] Vedani, A.; Huhta, D.W. A new force field for modeling metalloproteins. *J. Am. Chem. Soc.*, **1990**, *112*, 4759–4767.
- [365] Veenstra, D.L.; Ferguson, D.M.; Kollman, P.A. How transferable are hydrogen parameters in molecular mechanics calculations? *J. Comput. Chem.*, **1992**, *13*, 971–978.
- [366] Allen, F.H.; Kennard, O.; Watson, D.G.; Brammer, L.; Orpen, A.G.; Taylor, R. *J. Chem. Soc. Perkin Trans. II*, **1987**, pp S1–S19.
- [367] Harmony, M.D.; Laurie, R.W.; Kuczkowski, R.L.; Schwendemann, R.H.; Ramsay, D.A.; Lovas, F.J.; Lafferty, W.J.; Maki, A.G. *J. Phys. Chem. Ref. Data*, **1979**, *8*, 619.
- [368] Hopfinger, A.J.; Pearlstein, R.A. Molecular mechanics force-field parameterization procedures. *J. Comput. Chem.*, **1985**, *5*, 486–499.
- [369] Cannon, J.F. AMBER force-field parameters for guanosine triphosphate and its imido and methylene analogs. *J. Comput. Chem.*, **1993**, *14*, 995–1005.

- [370] Cieplak, P.; Cornell, W.D.; Bayly, C.; Kollman, P.A. Application of the multimolecule and multiconformational RESP methodology to biopolymers: Charge derivation for DNA, RNA and proteins. *J. Comput. Chem.*, **1995**, *16*, 1357–1377.
- [371] Cornell, W.D.; Cieplak, P.; Bayly, C.I.; Kollman, P.A. Application of RESP charges to calculate conformational energies, hydrogen bond energies and free energies of solvation. *J. Am. Chem. Soc.*, **1993**, *115*, 9620–9631.
- [372] Bayly, C.I.; Cieplak, P.; Cornell, W.D.; Kollman, P.A. A well-Behaved electrostatic potential based method using charge restraints for determining atom-centered charges: The RESP model. *J. Phys. Chem.*, **1993**, *97*, 10269.
- [373] Howard, A.E.; Cieplak, P.; Kollman, P.A. A molecular mechanical model that reproduces the relative energies for chair and twist-boat conformations of 1,3-dioxanes. *J. Comp. Chem.*, **1995**, *16*, 243–261.
- [374] St.-Amant, A.; Cornell, W.D.; Kollman, P.A.; Halgren, T.A. Calculation of molecular geometries, relative conformational energies, dipole moments, and molecular electrostatic potential fitted charges of small organic molecules of biochemical interest by density functional theory. *J. Comput. Chem.*, **1995**, *16*, 1483–1506.
- [375] Halgren, T.A. Merck Molecular Force Field (MMFF94). Part I-V. *J. Comput. Chem.*, **1996**, *17*, 490–641.
- [376] Wang, J.; Morin, P.; Wang, W.; Kollman, P.A. Use of MM-PBSA in reproducing the binding free energies to HIV-1 RT of TIBO derivatives and predicting the binding mode to HIV-1 RT of efavirenz by docking and MM-PBSA. *J. Am. Chem. Soc.*, **2001**, *123*, 5221–5230.
- [377] Wang, W.; Kollman, P. Free energy calculations on dimer stability of the HIV protease using molecular dynamics and a continuum solvent model. *J. Mol. Biol.*, **2000**, *303*, 567.
- [378] Reyes, C.; Kollman, P. Structure and thermodynamics of RNA-protein binding: Using molecular dynamics and free energy analyses to calculate the free energies of binding and conformational change. *J. Mol. Biol.*, **2000**, *297*, 1145–1158.
- [379] Lee, M.R.; Duan, Y.; Kollman, P.A. Use of MM-PB/SA in estimating the free energies of proteins: Application to native, intermediates, and unfolded vilin headpiece. *Proteins*, **2000**, *39*, 309–316.
- [380] Cieplak, P.; Caldwell, J.; Kollman, P. Molecular mechanical models for organic and biological systems going beyond the atom centered two body additive approximation: Aqueous solution free energies of methanol and N-methyl acetamide, nucleic acid base, and amide hydrogen bonding and chloroform/water partition coefficients of the nucleic acid bases. *J. Comput. Chem.*, **2001**, *22*, 1048–1057.
- [381] Meng, E.; Cieplak, P.; Caldwell, J.W.; Kollman, P.A. Accurate solvation free energies of acetate and methylammonium ions calculated with a polarizable water model. *J. Am. Chem. Soc.*, **1994**, *116*, 12061–12062.

## BIBLIOGRAPHY

- [382] Wang, J.; Kollman, P.A. Automatic parameterization of force field by systematic search and genetic algorithms. *J. Comput. Chem.*, **2001**, *22*, 1219–1228.
- [383] Beveridge, D.L.; DiCapua, F.M. Free energy simulation via molecular simulations: Applications to chemical and biomolecular systems. *Annu. Rev. Biophys. Biophys. Chem.*, **1989**, *18*, 431–492.
- [384] Chipot, C.; Kollman, P.A.; Pearlman, D.A. Alternative approaches to potential of mean force calculations: free energy perturbation versus thermodynamics integration. Case study of some representative nonpolar interactions. *J. Comput. Chem.*, **1996**, *17*, 1112–1131.
- [385] Pearlman, D.A.; Kollman, P.A. The overlooked bond-stretching contribution in free energy perturbation calculations. *J. Chem. Phys.*, **1991**, *94*, 4532–4545.
- [386] Pearlman, D.A. Determining the contributions of constraints in free energy calculations: Development, characterization, and recommendations. *J. Chem. Phys.*, **1993**, *98*, 8946–8957.
- [387] Pearlman, D.A. Free energy derivatives: A new method for probing the convergence problem in free energy calculations. *J. Comput. Chem.*, **1994**, *15*, 105–123.
- [388] Pearlman, D.A. A comparison of alternative approaches to free energy calculations. *J. Phys. Chem.*, **1994**, *98*, 1487–1493.
- [389] Pearlman, D.A.; Rao, B.G. in *Encyclopedia of Computational Chemistry*, von R. Schleyer, P.; Allinger, N.L.; Clark, T.; Gasteiger, J.; Kollman, P.A.; H.F. Schaefer, III, Eds., pp 1036–1061. John Wiley, Chichester, 1998.
- [390] Radmer, R.J.; Kollman, P.A. Free energy calculation methods: A theoretical and empirical comparison of numerical errors and a new method for qualitative estimates of free energy changes. *J. Comput. Chem.*, **1997**, *18*, 902–919.
- [391] Pearlman, D.A.; Kollman, P.A. A new method for carrying out free energy perturbation calculations: dynamically modified windows. *J. Chem. Phys.*, **1989**, *90*, 2460–2470.
- [392] Yu, H.-A.; Karplus, M. A thermodynamic analysis of solvation. *J. Chem. Phys.*, **1988**, *89*, 2366–2379.
- [393] Hummer, G. Fast-growth thermodynamic integration: Error and efficiency analysis. *J. Chem. Phys.*, **2001**, *114*, 7330–7337.
- [394] Fleischman, S.H.; Brooks, C.L. III. Thermodynamic calculations on biological systems: Solution properties of alcohols and alkanes. *J. Chem. Phys.*, **1988**, *87*, 221–234.
- [395] Jakalian, A.; Bush, B.L.; Jack, D.B.; Bayly, C.I. Fast, efficient generation of high-quality atomic charges. AM1-BCC model: I. Method. *J. Comput. Chem.*, **2000**, *21*, 132–146.
- [396] Jakalian, A.; Jack, D.B.; Bayly, C.I. Fast, efficient generation of high-quality atomic charges. AM1-BCC model: II. Parameterization and Validation. *J. Comput. Chem.*, **2002**, *23*, 1623–1641.

- [397] Vincent, J.J.; Merz, K.M. Jr. A highly portable parallel implementation of AMBER4 using the message passing interface standard. *J. Comput. Chem.*, **1995**, *16*, 1420–1427.
- [398] Radmer, R.; Kollman, P. The application of three approximate free energy calculations methods to structure based ligand design: Trypsin and its complex with inhibitors. *J. Comput.-Aided Mol. Design*, **1998**, *12*, 215–228.
- [399] Niketic, S.R.; Rasmussen, K. *The Consistent Force Field: A Documentation*. Springer-Verlag, New York, 1977.
- [400] Cerjan, C.; Miller, W.H. On finding transition states. *J. Chem. Phys.*, **1981**, *75*, 2800.
- [401] Nguyen, D.T.; Case, D.A. On finding stationary states on large-molecule potential energy surfaces. *J. Phys. Chem.*, **1985**, *89*, 4020–4026.
- [402] Lamm, G.; Szabo, A. Langevin modes of macromolecules. *J. Chem. Phys.*, **1986**, *85*, 7334–7348.
- [403] Kottalam, J.; Case, D.A. Langevin modes of macromolecules: application to crambin and DNA hexamers. *Biopolymers*, **1990**, *29*, 1409–1421.
- [404] Huo, S.; Massova, I.; Kollman, P.A. Computational Alanine Scanning of the 1:1 Human Growth Hormone-Receptor Complex. *J. Comput. Chem.*, **2002**, *23*, 15–27.
- [405] Darden, T.; Pearlman, D.; Pedersen, L.G. Ionic charging free energies: Spherical versus periodic boundary conditions. *J. Chem. Phys.*, **1998**, *109*, 10921–10935.
- [406] Levy, R.M.; Karplus, M.; Kushick, J.; Perahia, D. Evaluation of the configurational entropy for proteins: Application to molecular dynamics simulations of an  $\alpha$ -helix. *Macromolecules*, **1984**, *17*, 1370–1374.
- [407] Gallicchio, E.; Kubo, M.M.; Levy, R.M. Enthalpy-entropy and cavity decomposition of alkane hydration free energies: Numerical results and implications for theories of hydrophobic solvation. *J. Phys. Chem.*, **2000**, *104*, 6271–6285.
- [408] Arnott, S.; Campbell-Smith, P.J.; Chandrasekaran, R. in *Handbook of Biochemistry and Molecular Biology, 3rd ed. Nucleic*, Fasman, G.P., Ed., pp 411–422. CRC Press, Cleveland, 1976.
- [409] Prompers, J.J.; Brüschweiler, R. Dynamic and structural analysis of isotropically distributed molecular ensembles. *Proteins*, **2002**, *46*, 177–189.
- [410] Prompers, J.J.; Brüschweiler, R. General framework for studying the dynamics of folded and nonfolded proteins by NMR relaxation spectroscopy and MD simulation. *J. Am. Chem. Soc.*, **2002**, *124*, 4522–4534.
- [411] Press, W.H.; Flannery, B.P.; Teukolsky, S.A.; Vetterling, W.T. in *Numerical Recipes: The Art of Scientific Computing*. Cambridge University Press, New York, 1989.
- [412] Beroza, P.; Case, D.A. Calculations of proton-binding thermodynamics in proteins. *Meth. Enzymol.*, **1998**, *295*, 170–189.

## BIBLIOGRAPHY

- [413] Madura, J.D.; Davis, M.E.; Gilson, M.K.; Wade, R.C.; Luty, B.A.; McCammon, J.A. Biological applications of electrostatic calculations and brownian dynamics simulations. *Rev. Computat. Chem.*, **1994**, *5*, 229–267.
- [414] Gilson, M.K. Theory of electrostatic interactions in macromolecules. *Curr. Opin. Struct. Biol.*, **1995**, *5*, 216–23.
- [415] Scarsi, M.; Apostolakis, J.; Cafilisch, A. Continuum electrostatic energies of macromolecules in aqueous solutions. *J. Phys. Chem. A*, **1997**, *101*, 8098–8106.
- [416] Li, Z.; K., Ito. *The Immersed Interface Method: numerical solutions of PDEs involving interfaces and irregular domains*. SIAM Frontiers in Applied Mathematics, Philadelphia, 2006.
- [417] Wang, J.; Cai, Q.; Li, Z.; Zhao, H.; Luo, R. Achieving Energy Conservation in Poisson-Boltzmann Molecular Dynamics: Accuracy and Precision with Finite-difference Algorithms. *Chem. Phys. Lett.*, **2009**, *468*, 112.
- [418] Cai, Q.; Wang, J.; Zhao, H.; Luo, R. On removal of charge singularity in Poisson-Boltzmann equation. *J. Chem. Phys.*, **2009**, *130*, 145101.
- [419] Cai, Q.; Ye, X.; Wang, J.; Luo, R. Dielectric boundary force in numerical Poisson-Boltzmann methods: Theory and numerical strategies. *Chem. Phys. Lett.*, **2011**, *514*, 368–373.
- [420] Cai, Q.; Ye, X.; Wang, J.; Luo, R. On-the-Fly Numerical Surface Integration for Finite-Difference Poisson-Boltzmann Methods. *J. Chem. Theory Comput.*, **2011**, *7*, 3608–3619.
- [421] Ye, X.; Wang, J.; Luo, R. A Revised Density Function for Molecular Surface Calculation in Continuum Solvent Models. *J. Chem. Theory Comput.*, **2010**, *6*, 1157–1169.
- [422] Simonson, T. Electrostatics and dynamics of proteins. *Rep. Prog. Phys.*, **2003**, *66*, 737–787.
- [423] Bashford, D.; Karplus, M. pK sub a's of ionizable groups in proteins: Atomic detail from a continuum electrostatic model. *Biochemistry*, **1990**, *29*, 10219–10225.
- [424] Ghosh, A.; Rapp, C.S.; Friesner, R.A. Generalized Born model based on a surface integral formulation. *J. Phys. Chem. B*, **1998**, *102*, 10983–10990.
- [425] Duan, Y.; Wu, C.; Chowdhury, S.; Lee, M.C.; Xiong, G.; Zhang, W.; Yang, R.; Cieplak, P.; Luo, R.; Lee, T. A point-charge force field for molecular mechanics simulations of proteins based on condensed-phase quantum mechanical calculations. *J. Comput. Chem.*, **2003**, *24*, 1999–2012.
- [426] Jackson, J.D. *Classical Electrodynamics*. Wiley and Sons, New York, 1975.
- [427] Lu, Q.; Luo, R. A Poisson-Boltzmann dynamics method with nonperiodic boundary condition. *J. Chem. Phys.*, **2003**, *119*, 11035–11047.

- [428] Tan, C. H.; Yang, L. J.; Luo, R. How well does Poisson-Boltzmann implicit solvent agree with explicit solvent? A quantitative analysis. *J. Phys. Chem. B*, **2006**, *110*, 18680–18687.
- [429] Feig, M.; Karanicolas, J.; Brooks, C.L. III. MMTSB Tool Set: Enhanced sampling and multiscale modeling methods for application in structural biology. *J. Mol. Graphics Mod.*, **2004**, *22*, 377–395.
- [430] Simmerling, C.; Strockbine, B.; Roitberg, A.E. All-atom structure prediction and folding simulations of a stable protein. *J. Am. Chem. Soc.*, **2002**, *124*, 11258–11259.
- [431] García, A.E.; Sanbonmatsu, K.Y.  $\alpha$ -helical stabilization by side chain shielding of backbone hydrogen bonds. *Proc. Natl. Acad. Sci. USA*, **2002**, *99*, 2782–2787.
- [432] Wang, J.; Wolf, R.M.; Caldwell, J.W.; Kollman, P.A.; Case, D.A. Development and testing of a general Amber force field. *J. Comput. Chem.*, **2004**, *25*, 1157–1174.
- [433] Kirschner, K.N.; Woods, R.J. Solvent interactions determine carbohydrate conformation. *Proc. Natl. Acad. Sci. USA*, **2001**, *98*, 10541–10545.
- [434] Basma, M.; Sundara, S.; Calgan, D.; Venali, T.; Woods, R.J. Solvated ensemble averaging in the calculation of partial atomic charges. *J. Comput. Chem.*, **2001**, *22*, 1125–1137.
- [435] Kirschner, K.N.; Woods, R.J. Quantum mechanical study of the nonbonded forces in water-methanol complexes. *J. Phys. Chem. A*, **2001**, *105*, 4150–4155.
- [436] Sharp, K.A.; Honig, B. Electrostatic interactions in macromolecules: Theory and experiment. *Annu. Rev. Biophys. Biophys. Chem.*, **1990**, *19*, 301–332.
- [437] Gilson, M.K.; Sharp, K.A.; Honig, B.H. Calculating the electrostatic potential of molecules in solution: method. *J. Comput. Chem.*, **1988**, *9*, 327–35.
- [438] Warwicker, J.; Watson, H.C. Calculation of the electric potential in the active site cleft due to. *J. Mol. Biol.*, **1982**, *157*, 671–679.
- [439] Klapper, I.; Hagstrom, R.; Fine, R.; Sharp, K.; Honig, B. Focussing of electric fields in the active site of Cu, Zn superoxide dismutase. *Proteins*, **1986**, *1*, 47–59.
- [440] Nicholls, A.; Honig, B. A rapid finite difference algorithm, utilizing successive over-relaxation to solve the Poisson-Boltzmann equation. *J. Comput. Chem.*, **1991**, *12*, 435–445.
- [441] Davis, M.E.; McCammon, J.A. Dielectric boundary smoothing in finite difference solutions of the Poisson equation: An approach to improve accuracy and convergence. *J. Comput. Chem.*, **1991**, *12*, 909–912.
- [442] Davis, M.E.; McCammon, J.A. Electrostatics in biomolecular structure and dynamics. *Chem. Rev.*, **1990**, *90*, 509–521.

## BIBLIOGRAPHY

- [443] Davis, M.E.; McCammon, J.A. Solving the finite-difference linearized Poisson-Boltzmann equation – a comparison of relaxation and conjugate gradient methods. *J. Comput. Chem.*, **1989**, *10*, 386–391.
- [444] Bashford, D. An object-oriented programming suite for electrostatic effects in biological molecules. *Lect. Notes Comput. Sci.*, **1997**, *1343*, 233–240.
- [445] Luty, B.A.; Davis, M.E.; McCammon, J.A. Electrostatic energy calculations by a finite-difference method: Rapid calculation of charge-solvent interaction energies. *J. Comput. Chem.*, **1992**, *13*, 768–771.
- [446] Singh, U.C.; Weiner, S.J.; Kollman, P.A. Molecular dynamics simulations of d(C-G-C-G-A).d(T-C-G-C-G) with and without "hydrated" counterions. *Proc. Nat. Acad. Sci.*, **1985**, *82*, 755–759.
- [447] Gao, J. Absolute free energy of solvation from Monte Carlo simulations using combined quantum and molecular mechanical potentials. *J. Phys. Chem.*, **1992**, *96*, 537–540.
- [448] Warshel, A.; Levitt, M. Theoretical studies of enzymic reactions: Dielectric, electrostatic and steric stabilization of the carbonium ion in the reaction of lysozyme. *J. Mol. Biol.*, **1976**, *103*, 227–249.
- [449] Field, M.J.; Bash, P.A.; Karplus, M. A combined quantum mechanical and molecular mechanical potential for molecular dynamics simulations. *J. Comput. Chem.*, **1990**, *11*, 700–733.
- [450] Stanton, R.V.; Hartsough, D.S.; Merz, K.M. Jr. An examination of a density functional/molecular mechanical coupled potential. *J. Comput. Chem.*, **1994**, *16*, 113–128.
- [451] Stanton, R.V.; Little, L.R.; Merz, K.M. Jr. An examination of a Hartree-Fock/molecular mechanical coupled potential. *J. Phys. Chem.*, **1995**, *99*, 17344–17348.
- [452] Stanton, R.V.; Hartsough, D.S.; Merz, K.M. Jr. Calculations of solvation free energies using a density functional/molecular dynamics coupled potential. *J. Phys. Chem.*, **1993**, *97*, 11868–11870.
- [453] Nocedal, J.; Wright, S.J. *Numerical Optimization*. Springer-Verlag, New York, 1999.
- [454] Nash, S.G. A survey of truncated-Newton methods. *J. of Computational and Applied Mathematics*, **2000**, *124*, 45–59.
- [455] Lee, M.C.; Duan, Y. Distinguish protein decoys by using a scoring function based on a new Amber force field, short molecular dynamics simulations, and the generalized Born solvent model. *Proteins*, **2004**, *55*, 620–634.
- [456] Sorin, E.J.; Pande, V.S. Exploring the helix-coil transition via all-atom equilibrium ensemble simulations. *Biophys. J.*, **2005**, *88*, 2472–2493.
- [457] Yang, L.; Tan, C.; Hsieh, M.-J.; Wang, J.; Duan, Y.; Cieplak, P.; Caldwell, J.; Kollman, P.A.; Luo, R. New-generation Amber united-atom force field. *J. Phys. Chem. B*, **2006**, *110*, 13166–13176.



- [458] Wang, B.; Merz, K.M. Jr. A fast QM/MM (quantum mechanical/molecular mechanical) approach to calculate nuclear magnetic resonance chemical shifts for macromolecules. *J. Chem. Theory Comput.*, **2006**, *2*, 209–215.
- [459] Rizzo, R.C.; Aynechi, T.; Case, D.A.; Kuntz, I.D. Estimation of absolute free energies of hydration using continuum methods: Accuracy of partial charge models and optimization of nonpolar contributions. *J. Chem. Theory Comput.*, **2006**, *2*, 128–139.
- [460] Wang, Z.-X.; Zhang, W.; Wu, C.; Lei, H.; Cieplak, P.; Duan, Y. Strike a Balance: Optimization of backbone torsion parameters of AMBER polarizable force field for simulations of proteins and peptides. *J. Comput. Chem.*, **2006**, *27*, 781–790.
- [461] Nam, Kwangho; Cui, Qiang; Gao, Jiali; York, Darrin M. Specific Reaction Parametrization of the AM1/d Hamiltonian for Phosphoryl Transfer Reactions: H, O, and P Atoms. *J. Chem. Theory Comput.*, **2007**, *3*, 486–504.
- [462] Porezag, D.; Frauenheim, T.; Kohler, T.; Seifert, G.; Kaschner, R. Construction of tight-binding-like potentials on the basis of density-functional-theory: Applications to carbon. *Phys. Rev. B*, **1995**, *51*, 12947.
- [463] Seifert, G.; Porezag, D.; Frauenheim, T. Calculations of molecules, clusters and solids with a simplified LCAO-DFT-LDA scheme. *Int. J. Quantum Chem.*, **1996**, *58*, 185.
- [464] Elstner, M.; Hobza, P.; Frauenheim, T.; Suhai, S.; Kaxiras, E. Hydrogen bonding and stacking interactions of nucleic acid base pairs: a density-functional-theory based treatment. *J. Chem. Phys.*, **2001**, *114*, 5149.
- [465] Messiah, A. *Quantum Mechanics*. Wiley & Sons, New York, 1958.
- [466] Dewar, M.J.S.; Thiel, W. Ground states of molecules. 38. The MNDO method, approximations and parameters. *J. Am. Chem. Soc.*, **1977**, *99*, 4899–4907.
- [467] Dewar, M.J.S.; Zoebisch, E.G.; Healy, E.F.; Stewart, J.J.P. AM1: A new general purpose quantum mechanical molecular model. *J. Am. Chem. Soc.*, **1985**, *107*, 3902–3909.
- [468] Stewart, J.J.P. Optimization of parameters for semiempirical methods I. Method. *J. Comput. Chem.*, **1989**, *10*, 209–220.
- [469] Storer, J.W.; Giesen, D.J.; Cramer, C.J.; Truhlar, D.G. Class IV charge models: A new semiempirical approach in quantum chemistry. *J. Comput.-Aided Mol. Design*, **1995**, *9*, 87–110.
- [470] Li, J.; Cramer, C.J.; Truhlar, D.G. New class IV charge model for extracting accurate partial charges from Wave Functions. *J. Phys. Chem. A*, **1998**, *102*, 1820–1831.
- [471] Imhof, Petra; Noé, Frank; Fischer, Stefan; Smith, Jeremy C. AM1/d Parameters for Magnesium in Metalloenzymes. *J. Chem. Theory Comput.*, **2006**, *2*, 1050–1056.
- [472] van der Vaart, A.; Merz, K.M. Jr. Divide and conquer interaction energy decomposition. *J. Phys. Chem. A*, **1999**, *103*, 3321–3329.

## BIBLIOGRAPHY

- [473] Mitin, A.V. The dynamic level shift method for improving the convergence of the SCF procedure. *J. Comput. Chem.*, **1988**, *9*, 107–110.
- [474] Ermolaeva, M.D.; van der Vaart, A.; Merz, K.M. Jr. Implementation and testing of a frozen density matrix - divide and conquer algorithm. *J. Phys. Chem.*, **1999**, *103*, 1868–1875.
- [475] Wang, B.; Brothers, E.N.; van der Vaart, A.; Merz Jr., K.M. Fast semiempirical calculations for nuclear magnetic resonance chemical shifts: A divide-and-conquer approach. *J. Chem. Phys.*, **2004**, *120*, 11392–11400.
- [476] Wang, B.; Raha, K.; Merz Jr., K.M. Pose scoring by NMR. *J. Am. Chem. Soc.*, **2004**, *126*, 11430–11431.
- [477] Raha, K.; van der Vaart, A.; E. Riley, K.; B. Peters, M.; M. Westerhoff, L.; Kim, H.; Merz Jr., K.M. Pairwise decomposition of residue interaction energies using semiempirical quantum mechanical methods in studies of protein-ligand interaction. *J. Am. Chem. Soc.*, **2005**, *127*, 6583–6594.
- [478] Repasky, M.P.; Chandrasekhar, J.; Jorgensen, W.L. PDDG/PM3 and PDDG/MNDO: Improved semiempirical methods. *J. Comput. Chem.*, **2002**, *23*, 1601–1622.
- [479] McNamara, J.P.; Muslim, A.M.; Abdel-Aal, H.; Wang, H.; Mohr, M.; Hillier, I.H.; Bryce, R.A. Towards a quantum mechanical force field for carbohydrates: A reparameterized semiempirical MO approach. *Chem. Phys. Lett.*, **2004**, *394*, 429–436.
- [480] Stewart, J.J.P. Optimization of parameters for semiempirical methods V: Modification of NDDO approximations and application to 70 elements. *J. Mol. Mod.*, **2007**, *13*, 1173–1213.
- [481] Luzhkov, A.; Warshel, A. Microscopic models for quantum-mechanical calculations of chemical processes in solutions - Ld/Ampac and Scaas/Ampac calculations of solvation energies. *J. Comp. Chem.*, **1992**, *13*, 199–213.
- [482] Singh, U.C.; Kollman, P.A. A combined Ab initio quantum-mechanical and molecular mechanical method for carrying out simulations on complex molecular systems - Applications to the  $\text{CH}_3\text{Cl} + \text{Cl}$ - exchange-reaction and gas-phase protonation of polyethers. *J. Comp. Chem.*, **1986**, *7*, 718–730.
- [483] Bersuker, I.B.; Leong, M.K.; Boggs, J.E.; Pearlman, R.S. A method of combined quantum mechanical (QM) molecular mechanics (MM) treatment of large polyatomic systems with charge transfer between the QM and MM fragments. *Int. J. Quant. Chem.*, **1997**, *63*, 1051–1063.
- [484] Maseras, F.; Morokuma, K. Imomm - a new integrated ab-initio plus molecular geometry optimization scheme of equilibrium structures and transition-states. *J. Comp. Chem.*, **1995**, *16*, 1170–1179.
- [485] Zhang, Y.K.; Lee, T.S.; Yang, W.T. A pseudobond approach to combining quantum mechanical and molecular mechanical methods. *J. Chem. Phys.*, **1999**, *110*, 46–54.

- [486] Gao, J.L.; Amara, P.; Alhambra, C.; Field, M.J. A generalized hybrid orbital (GHO) method for the treatment of boundary atoms in combined QM/MM calculations. *J Phys Chem A*, **1998**, *102*, 4714–4721.
- [487] Philipp, D.M.; Friesner, R.A. Mixed ab initio QM/MM modeling using frozen orbitals and tests with alanine dipeptide and tetrapeptide. *J. Comp. Chem.*, **1999**, *20*, 1468–1494.
- [488] Field, M.J.; Albe, M.; Bret, C.; Proust-De Martin, F.; Thomas, A. The Dynamo library for molecular simulations using hybrid quantum mechanical and molecular mechanical potentials. *J. Comp. Chem.*, **2000**, *21*, 1088–1100.
- [489] Hornak, V.; Abel, R.; Okur, A.; Strockbine, B.; Roitberg, A.; Simmerling, C. Comparison of multiple Amber force fields and development of improved. *Proteins*, **2006**, *65*, 712–725.
- [490] Levy, R.M.; Gallicchio, E. Computer simulations with explicit solvent: recent progress in the thermodynamic decomposition of free energies and in modeling electrostatic effects. *Annu. Rev. Phys. Chem.*, **1999**, *49*, 531–567.
- [491] Wang, J.; Wang, W.; Kollman, P.A.; Case, D.A. Automatic atom type and bond type perception in molecular mechanical. *J. Mol. Graphics Model.*, **2006**, *25*, 247–260.
- [492] Hornak, V.; Okur, A.; Rizzo, R.; Simmerling, C. HIV-1 protease flaps spontaneously open and reclose in molecular dynamics simulations. *Proc. Nat. Acad. Sci. USA*, **2006**, *103*, 915–920.
- [493] Hornak, V.; Okur, A.; Rizzo, R.; Simmerling, C. HIV-1 protease flaps spontaneously close when an inhibitor binds to the open state. *J. Am. Chem. Soc.*, **2006**, *128*, 2812–2813.
- [494] Wollacott, A.M.; Merz, K.M. Jr. Development of a parameterized force field to reproduce semiempirical geometries. *J. Chem. Theory Comput.*, **2006**, *2*, 1070–1077.
- [495] Simmerling, C.; Elber, R. Hydrophobic "collapse" in a cyclic hexapeptide: Computer simulations of CHDLFC and CAAAAC in water. *J. Am. Chem. Soc.*, **1994**, *116*, 2534–2547.
- [496] Kabsch, W.; Sander, C. Dictionary of protein secondary structure: pattern recognition of hydrogen-bonded and geometrical features. *Biopolymers*, **1983**, *22*, 2577–2637.
- [497] Rocha, G.B.; Freire, R.O.; Simas, A.M.; Stewart, J.J.P. RM1: A Reparameterization of AM1 for H, C, N, O, P, S, F, Cl, Br and I. *J. Comp. Chem.*, **2006**, *27*, 1101–1111.
- [498] Marinelli, L.; Cosconati, S.; Steinbrecher, T.; Limongelli, V.; Bertamino, A.; Novellino, E.; Case, D.A. Homology Modeling of NR2B Modulatory Domain of NMDA Receptor and Analysis of Ifenprodil Binding. *ChemMedChem*, **2007**, *2*, 1498–1510.
- [499] Kirschner, K.N.; Yongye, A.B.; Tschampel, S.M.; González-Outeiriño, J.; Daniels, C.R.; Foley, B.L.; Woods, R.J. GLYCAM06: A generalizable biomolecular force field. Carbohydrates. *J. Comput. Chem.*, **2008**, *29*, 622–655.

## BIBLIOGRAPHY

- [500] Tschampel, S.M.; Kennerty, M.R.; Woods, R.J. TIP5P-consistent treatment of electrostatics for biomolecular simulations. *J. Chem. Theory Comput.*, **2007**, *3*, 1721–1733.
- [501] Tessier, M.B.; DeMarco, M.L.; Yongye, A.B.; Woods, R.J. Extension of the GLYCAM06 biomolecular force field to lipids, lipid bilayers and glycolipids. *Mol. Simul.*, **2008**, *34*, 349–363.
- [502] Kalinowski, J.A.; Lesyng, B.; Thompson, J.D.; Cramer, C.J.; Truhlar, D.G. Class IV charge model for the self-consistent charge density-functional tight-binding method. *J. Phys. Chem. A*, **2004**, *108*, 2545–2549.
- [503] Fulle, S.; Gohlke, H. Analyzing the flexibility of RNA structures by constraint counting. *Biophys. J.*, **2008**, DOI:10.1529/biophysj.107.113415.
- [504] Gohlke, H.; Kuhn, L. A.; Case, D. A. Change in protein flexibility upon complex formation: Analysis of Ras-Raf using molecular dynamics and a molecular framework approach. *Proteins*, **2004**, *56*, 322–327.
- [505] Ahmed, A.; Gohlke, H. Multiscale modeling of macromolecular conformational changes combining concepts from rigidity and elastic network theory. *Proteins*, **2006**, *63*, 1038–1051.
- [506] Wu, Y.; Tepper, H.L.; Voth, G.A. Flexible simple point-charge water model with improved liquid-state properties. *J. Chem. Phys.*, **2006**, *124*, 024503.
- [507] Price, D.J.; Brooks, C.L. A modified TIP3P water potential for simulation with Ewald summation. *J. Chem. Phys.*, **2004**, *121*, 10096–10103.
- [508] Horn, H.W.; Swope, W.C.; Pitara, J.W.; Madura, J.D.; Dick, T.J.; Hura, G.L.; Head-Gordon, T. Development of an improved four-site water model for biomolecular simulations: TIP4P-Ew. *J. Chem. Phys.*, **2004**, *120*, 9665–9678.
- [509] Horn, H.W.; Swope, W.C.; Pitara, J.W. Characterization of the TIP4P-Ew water model: Vapor pressure and boiling point. *J. Chem. Phys.*, **2005**, *123*, 194504.
- [510] Woods, R.J. Derivation of net atomic charges from molecular electrostatic potentials. *J. Comput. Chem.*, **1990**, *11*, 29–310.
- [511] DeMarco, M.L.; Woods, R.J. Bridging computational biology and glycobiology: A game of snakes and ladders. *Glycobiology, in press*, **2008**.
- [512] Woods, R.J. Restrained electrostatic potential charges for condensed phase simulations of carbohydrates. *J. Mol. Struct (Theochem)*, **2000**, *527*, 149–156.
- [513] Pettersen, E.F.; Goddard, T.D.; Huang, C.C.; Couch, G.S.; Greenblatt, D.M.; Meng, E.C.; Ferrin, T.E. UCSF Chimera - A visualization system for exploratory research and analysis. *J. Comput. Chem.*, **2004**, *25*, 1605–1612.
- [514] Sasaki, H.; Ochi, N.; Del, A.; Fukuda, M. Site-specific glycosylation of human recombinant erythropoietin: Analysis of glycopeptides or peptides at each glycosylation site by fast atom bombardment mass spectrometry. *Biochemistry*, **1988**, *27*, 8618–8626.

- [515] Dube, S.; Fisher, J.W.; Powell, J.S. Glycosylation at specific sites of erythropoietin is essential for biosynthesis, secretion, and biological function. *J. Biol. Chem.*, **1988**, *263*, 17516–17521.
- [516] Darling, R.J.; Kuchibhotla, U.; Glaesner, W.; Micanovic, R.; Witcher, D.R.; Beals, J.M. Glycosylation of erythropoietin effects receptor binding kinetics: Role of electrostatic interactions. *Biochemistry*, **2002**, *41*, 14524–14531.
- [517] Cheetham, J.C.; Smith, D.M.; Aoki, K.H.; Stevenson, J.L.; Hoeffel, T.J.; Syed, R.S.; Egrie, J.; Harvey, T.S. NMR structure of human erythropoietin and a comparison with its receptor bound conformation. *Nat. Struct. Biol.*, **1998**, *5*, 861–866.
- [518] Dormann, K.L.; Steinbrecher, T.; Grond, S.; Labahn, A.; Brueckner, R. Undecided. *Chemistry (in preparation)*, **2008**.
- [519] Dormann, K.L.; Brueckner, R. Variable Synthesis of the Optically Active Thiotetronic Acid Antibiotics Thiolactomycin, Thiotetromycin, and 834-B1. *Angew. Chem. Int. Ed.*, **2007**, *46*, 1160–1163.
- [520] Jojart, B.; Martinek, T.A. Performance of the general amber force field in modeling aqueous POPC membrane bilayers. *J. Comput. Chem.*, **2007**, *28*, 2051–2058.
- [521] Rosso, L.; Gould, I.R. Structure and dynamics of phospholipid bilayers using recently developed general all-atom force fields. *J. Comput. Chem.*, **2008**, *29*, 24–37.
- [522] Graves, A.P.; Shivakumar, D.M.; Boyce, S.E.; Jacobson, M.P.; Case, D.A.; Shoichet, B.K. Rescoring docking hit lists for model cavity sites: Predictions and experimental testing. *J. Mol. Biol.*, **2008**, *377*, 914–934.
- [523] Perez, A.; Marchan, I.; Svozil, D.; Sponer, J.; Cheatham, T.E.; Loughton, C.A.; Orozco, M. Refinement of the AMBER Force Field for Nucleic Acids: Improving the Description of alpha/gamma Conformers. *Biophys. J.*, **2007**, *92*, 3817–3829.
- [524] Dang, L. Mechanism and thermodynamics of ion selectivity in aqueous solutions of 18-crown-6 ether: A molecular dynamics study. *J. Am. Chem. Soc.*, **1995**, *117*, 6954–6960.
- [525] Joung, S.; Cheatham, T.E. III. Determination of alkali and halide monovalent ion parameters for use in explicitly solvated biomolecular simulations. *J. Phys. Chem. B*, **2008**, *112*, 9020–9041.
- [526] Aduri, R.; Psciuk, B.T.; Saro, P.; Taniga, H.; Schlegel, H.B.; SantaLucia, J. Jr. AMBER force field parameters for the naturally occurring modified nucleosides in RNA. *J. Chem. Theory Comput.*, **2007**, *3*, 1465–1475.
- [527] Shao, J.; Tanner, S.W.; Thompson, N.; Cheatham, T.E. III. Clustering molecular dynamics trajectories: 1. Characterizing the performance of different clustering algorithms. *J. Chem. Theory Comput.*, **2007**, *3*, 2312–2334.

## BIBLIOGRAPHY

- [528] Auffinger, P.; Cheatham, T.E. III; Vaiana, A.C. Spontaneous formation of KCl aggregates in biomolecular simulations: a force field issue? *J. Chem. Theory Comput.*, **2007**, *3*, 1851–1859.
- [529] Cieplak, P.; Dupradeau, F.-Y.; Duan, Y.; Wang, J. Polarization effects in molecular mechanical force fields. *J. Phys.: Condens. Matter*, **2009**, *21*, 333102.
- [530] Shi, Z.J.; Shen, J. New inexact line search method for unconstrained optimization. *J. Optim. Theory Appl.*, **2005**, *127*, 425–446.
- [531] Yang, Y.; Yu, H.; York, D.M.; Cui, Q.; Elstner, M. Extension of the self-consistent charge density-functional tight-binding method: Third-order expansion of the density functional theory total energy and introduction of a modified effective Coulomb interaction. *J. Phys. Chem. A*, **2007**, *111*, 10861–10873.
- [532] MacKerell Jr., A.D.; Bashford, D.; Bellott, M.; Dunbrack, R.L.; Evanseck, J.D.; Field, M.J.; Fischer, S.; Gao, J.; Guo, H.; Ha, S.; Joseph-McCarthy, D.; Kuchnir, L.; Kuczera, K.; Lau, F.T.K.; Mattos, C.; Michnick, S.; Ngo, T.; Nguyen, D.T.; Prodhom, B.; Reiher, W.E.; Roux, B.; Schlenkrich, M.; Smith, J.C.; Stote, R.; Straub, J.; Watanabe, M.; Wiorkiewicz-Kuczera, J.; Yin, D.; Karplus, M. All-Atom Empirical Potential for Molecular Modeling and Dynamics Studies of Proteins. *J. Phys. Chem. B*, **1998**, *102*, 3586–3616.
- [533] MacKerell Jr., A.D.; Banavali, N.; Foloppe, N. Development and current status of the CHARMM force field for nucleic acids. *Biopolymers*, **2000**, *56*, 257–265.
- [534] Brooks, B.R.; Brucoleri, R.E.; Olafson, D.J.; States, D.J.; Swaminathan, S.; Karplus, M. CHARMM: A Program for Macromolecular Energy, Minimization, and Dynamics Calculations. *J. Computat. Chem.*, **1983**, *4*, 187–217.
- [535] Brooks, B. R.; Brooks, C. L.; Mackerell, A. D.; Nilsson, L.; Petrella, R. J.; Roux, B.; Won, Y.; Archontis, G.; Bartels, C.; Boresch, S.; Caffisch, A.; Caves, L.; Cui, Q.; Dinner, A. R.; Feig, M.; Fischer, S.; Gao, J.; Hodoseck, M.; Im, W.; Kuczera, K.; Lazaridis, T.; Ma, J.; Ovchinnikov, V.; Paci, E.; Pastor, R. W.; Post, C. B.; Pu, J. Z.; Schaefer, M.; Tidor, B.; Venable, R. M.; Woodcock, H. L.; Wu, X.; Yang, W.; York, D. M.; Karplus, M. CHARMM: the biomolecular simulation program. *J. Comput. Chem.*, **2009**, *30*, 1545–1614.
- [536] MacKerell, A.D. Jr.; Feig, M.; Brooks III, C.L. Improved Treatment of the Protein Backbone in Empirical Force Fields. *J. Am. Chem. Soc.*, **2004**, *126*, 698–699.
- [537] MacKerell, A.D. Jr.; Feig, M.; Brooks III, C.L. Extending the treatment of backbone energetics in protein force fields: Limitations of gas-phase quantum mechanics in reproducing protein conformational distributions in molecular dynamics simulations. *J. Computat. Chem.*, **2004**, *25*, 1400–1415.
- [538] Ponder, J.W.; Wu, C.; Ren, P.; Pande, V.S.; Chodera, J.D.; Schieders, M.J.; Haque, I.; Mobley, D.L.; Lambrecht, D.S.; DiStasio, R.A. Jr.; Head-Gordon, M.; Clark, G.N.I.;

- Johnson, M.E.; Head-Gordon, T. Current status of the AMOEBA polarizable force field. *J. Phys. Chem. B*, **2010**, *114*, 2549–2564.
- [539] Wickstrom, L.; Okur, A.; Simmerling, C. Evaluating the performance of the ff99SB force field based on NMR scalar coupling data. *Biophys. J.*, **2009**, *97*, 853–856.
- [540] Hsieh, M.-J.; Luo, R. Balancing simulation accuracy and efficiency with the Amber united atom force field. *J. Phys. Chem. B*, **2010**, *114*, 2886–2893.
- [541] Hirata, F., Ed. *Molecular Theory of Solvation*. Kluwer Academic Publishers, 2003.
- [542] Kovalenko, A.; Ten-No, S.; Hirata, F. Solution of three-dimensional reference interaction site model and hypernetted chain equations for simple point charge water by modified method of direct inversion in iterative subspace. *J. Comput. Chem.*, **1999**, *20*(9), 928–936.
- [543] Hansen, J.-P.; McDonald, I. R. *Theory of simple liquids*. Academic Press, London, 1990.
- [544] Frigo, M. A fast Fourier transform compiler. in *Proc. 1999 ACM SIGPLAN Conf. on Programming Language Design and Implementation*, volume 34, pp 169–180. ACM, May 1999.
- [545] Frigo, M.; Johnson, S. G. FFTW: An adaptive software architecture for the FFT. in *Proc. 1998 IEEE Intl. Conf. Acoustics Speech and Signal Processing*, volume 3, pp 1381–1384. IEEE, 1998.
- [546] Gusarov, S.; Ziegler, T.; Kovalenko, A. Self-consistent combination of the three-dimensional RISM theory of molecular solvation with analytical gradients and the amsterdam density functional package. *J. Phys. Chem. A*, **2006**, *110*(18), 6083–6090.
- [547] Miyata, T.; Hirata, F. Combination of molecular dynamics method and 3D-RISM theory for conformational sampling of large flexible molecules in solution. *J. Comput. Chem.*, Oct 2007, *29*, 871–882.
- [548] Genheden, S.; Luchko, T.; Gusarov, S.; Kovalenko, A.; Ryde, U. An MM/3D-RISM approach for ligand-binding affinities. *J. Phys. Chem.*, **2010**. Accepted.
- [549] Kaminski, J. W.; Gusarov, S.; Wesolowski, T. A.; Kovalenko, Andiry. Modeling solvatochromic shifts using the orbital-free embedding potential at statistically mechanically averaged solvent density. *J. Phys. Chem. A*, **2010**, *in press*.
- [550] Perkyns, J. S.; Pettitt, B. M. A site-site theory for finite concentration saline solutions. *J. Chem. Phys.*, **1992**, *97*(10), 7656–7666.
- [551] Gilson, M.K.; Davis, M.E.; Luty, B.A.; McCammon, J.A. Computation of electrostatic forces on solvated molecules using the Poisson-Boltzmann equation. *J Phys Chem*, **1993**, *97*(14), 3591–3600.
- [552] Li, D.W.; Brüschweiler, R. NMR-based protein potentials. *Angew. Chem. Int. Ed.*, **2010**, *49*, 6778–6780.

## BIBLIOGRAPHY

- [553] Lindorff-Larsen, K.; Piana, S.; Palmo, K.; Maragakis, P.; Klepeis, J.; Dror, R.O.; Shaw, D.E. Improved side-chain torsion potentials for the Amber ff99SB protein force field. *Proteins*, **2010**, *78*, 1950–1958.
- [554] Banáš, P.; Hollas, D.; Zgarbová, M.; Jurecka, P.; Orozco, M.; Cheatham, T.E. III; Šponer, J.; Otyepka, M. Performance of molecular mechanics force fields for RNA simulations: Stability of UUCG and GNRA hairpins. *J. Chem. Theory. Comput.*, **2010**, *6*, 3836–3849.
- [555] Anandakrishnan, Ramu; Onufriev, Alexey V. An N log N approximation based on the natural organization of biomolecules for speeding up the computation of long range interactions. *J. Comput. Chem.*, **2010**, *31*(4), 691–706.
- [556] Anandakrishnan, R.; Daga, M.; Onufriev, A.V. An n log n Generalized Born Approximation. *J. Chem. Theory Comput.*, **2011**, *7*, 544–559.
- [557] Kast, Stefan M.; Kloss, Thomas. Closed-form expressions of the chemical potential for integral equation closures with certain bridge functions. *J. Chem. Phys.*, **2008**, *129*, 236101.
- [558] Olson, Wilma K.; Bansal, Manju; Burley, Stephen K.; Dickerson, Richard E.; Gerstein, Mark; Harvey, Stephen C.; Heinemann, Udo; Lu, Xiang-Jun; Neidle, Stephen; Shakked, Zippora; Sklenar, Heinz; Suzuki, Masashi; Tung, Chang-Shung; Westhof, Eric; Wolberger, Cynthia; Berman, Helen M. A standard reference frame for the description of nucleic acid base-pair geometry. *J. Mol. Biol.*, **2001**, *313*, 229–237.
- [559] Cerutti, D.S.; Duke, R.E.; Darden, T.A.; Lybrand, T.P. Staggered Mesh Ewald: An Extension of the Smooth Particle-Mesh Ewald Method Adding Great Versatility. *J. Chem. Theory Computat.*, **2009**, *5*, 2322–2338.
- [560] Cerutti, D.S.; Case, D.A. Multi-Level Ewald: A Hybrid Multigrid/Fast Fourier Transform Approach to the Electrostatic Particle-Mesh Problem. *J. Chem. Theory Comput.*, **2010**, *6*, 443–458.
- [561] Cerutti, D.S.; Freddolino, P.L.; Duke, R.E. Jr.; Case, D.A. Simulations of a Protein Crystal with a High Resolution X-ray Structure: Evaluation of Force Fields and Water Models. *J. Phys. Chem. B*, **2010**, pp 12811–12824.
- [562] Peters, M.B.; Yang, Y.; Wang, B.; Fusti-Molnar, L.; Weaver, M.N.; Merz, K.M. Structural Survey of Zinc-Containing Proteins and Development of the Zinc AMBER Force Field (ZAFF). *J. Chem. Theor. Comput.*, **2010**, *6*, 2935–2947.
- [563] Hsieh, M.-J.; Luo, R. Exploring a coarse-grained distributive strategy for finite-difference poisson-boltzmann calculations. *Journal of Molecular Modeling*, **2011**.
- [564] Yildirim, I.; Stern, H.A.; Kennedy, S.D.; Tubbs, J.D.; Turner, D.H. Reparameterization of RNA chi Torsion Parameters for the AMBER Force Field and Comparison to NMR Spectra for Cytidine and Uridine. *J. Chem. Theory Comput.*, **2010**, *6*, 1520–1531.



- [565] Joung, I.S.; Cheatham, T.E. III. Molecular dynamics simulations of the dynamic and energetic properties of alkali and halide ions using water-model-specific ion parameters. *J. Phys. Chem. B*, **2009**, *113*, 13279–13290.
- [566] Yildirim, I.; Stern, H.A.; Tubbs, J.D.; Kennedy, S.D.; Turner, D.H. Benchmarking AMBER Force Fields for RNA: Comparisons to NMR Spectra for Single-Stranded r(GACC) Are Improved by Revised chi Torsions. *J. Phys. Chem. B*, **2011**, *115*, 9261–9270.
- [567] Wang, J.; Hou, T. Application of Molecular Dynamics Simulations in Molecular Property Prediction. 1. Density and Heat of Vaporization. *J. Chem. Theory Comput.*, **2011**, *7*, 2151–2165.
- [568] Palmer, David S; Frolov, Andrey I; Ratkova, Ekaterina L; Fedorov, Maxim V. Towards a universal method for calculating hydration free energies: a 3D reference interaction site model with partial molar volume correction. *J. Phys.: Condens. Matter*, **2010**, *22*(49), 492101.
- [569] Chandler, David; Singh, Yashwant; Richardson, Diane M. Excess electrons in simple fluids. I. General equilibrium theory for classical hard sphere solvents. *J. Chem. Phys.*, **1984**, *81*(4), 1975–1982.
- [570] Ichiye, Toshiko; Chandler, David. Hypernetted chain closure reference interaction site method theory of structure and thermodynamics for alkanes in water. *J. Phys. Chem.*, **1988**, *92*(18), 5257–5261.
- [571] Lee, Pil H.; Maggiora, Gerald M. Solvation thermodynamics of polar molecules in aqueous solution by the XRISM method. *J. Phys. Chem.*, **1993**, *97*(39), 10175–10185.
- [572] Zgarbova, M.; Otyepka, M.; Sponer, J.; Mladek, A.; Banas, P.; Cheatham, T.E.; Jurecka, P. Refinement of the Cornell et al. Nucleic Acids Force Field Based on Reference Quantum Chemical Calculations of Glycosidic Torsion Profiles. *J. Chem. Theory Comput.*, **2011**, *7*, 2886–2902.
- [573] Perez, C.; Lohr, F.; Ruterjans, H.; Schmidt, J.M. Self-Consistent Karplus Parameterization of (3)J couplings depending on the polypeptide side-chain torsion chi(1). *J. Am. Chem. Soc.*, **2001**, *123*, 7081–7093.
- [574] Chou, J.J.; Case, D.A.; Bax, A. Insights into the mobility of methyl-bearing side chains in proteins. *J. Am. Chem. Soc.*, **2003**, *125*, 8959–8966.
- [575] Yu, Hsiang-Ai; Roux, Benoit; Karplus, Martin. Solvation thermodynamics: An approach from analytic temperature derivatives. *J. Chem. Phys.*, **1990**, *92*(8), 5020–5033.
- [576] Yamazaki, Takeshi; Blinov, Nikolay; Wishart, David; Kovalenko, Andriy. Hydration effects on the HET-s prion and amyloid- $\beta$ 2 fibrillous aggregates, studied with three-dimensional molecular theory of solvation. *Biophys. J.*, **2008**, *95*, 4540–4548.
- [577] Yamazaki, T.; Kovalenko, A.; Murashov, V.V.; Patey, G.N. Ion solvation in a water-urea mixture. *J. Phys. Chem. B*, **2010**, *114*(1), 613–619.

## BIBLIOGRAPHY

- [578] Homeyer, N.; Gohlke, H. Free energy calculations by the molecular mechanics poisson-boltzmann surface area method. *Mol. Informatics*, **2012**, DOI: 10.1002/minf.201100135.
- [579] Wong, V.; Case, D.A. Evaluating rotational diffusion from protein md simulations. *J. Phys. Chem. B*, **2008**, 112(19), 6013–6024.
- [580] Lu, XJ; Olson, WK. 3dna: a software package for the analysis, rebuilding and visualization of three-dimensional nucleic acid structures. *NUCLEIC ACIDS RESEARCH*, **2003**, 31(17), 5108–5121.
- [581] Altona, C; Sundaralingam, M. Conformational analysis of the sugar ring in nucleosides and nucleotides. a new description using the concept of pseudorotation. *J Am Chem Soc*, **1972**, 94, 8205–8212.
- [582] Harvey, SC; Prabhakaran, M. Ribose puckering - structure, dynamics, energetics, and the pseudorotation cycle. *J Am Chem Soc*, **1986**, 108, 6128–6136.
- [583] Cremer, D; Pople, JA. A general definition of ring puckering coordinates. *J Am Chem Soc*, **1975**, 97, 1354–1358.
- [584] Skjevik, Åge A.; Madej, Benjamin D.; Walker, R.C.; Teigen, K. Lipid11: A comprehensive modular lipid force field for amber. *In press*, **2012**.
- [585] Mobley, David L.; Bayly, Christopher I.; Cooper, Matthew D.; Shirts, Michael R.; Dill, Ken A. Small Molecule Hydration Free Energies in Explicit Solvent: An Extensive Test of Fixed-Charge Atomistic Simulations. *J. Chem. Theory Comput.*, **2009**, 5, 350–358.
- [586] Bernal-Uruchurtu, M. I.; Ruiz-López, M. F. Basic ideas for the correction of semiempirical methods describing H-bonded systems. *Chem. Phys. Lett.*, **2000**, 330, 118–124.
- [587] Arillo-Flores, O. I.; Ruiz-López, M. F.; Bernal-Uruchurtu, M. I. Can semi-empirical models describe HCl dissociation in water? *Theoret. Chem. Acc.*, **2007**, 118, 425–435.

# Index

1D-RISM, 55

3D-RISM, 55

## A

adjust\_q, 91

aexp, 207

alpb, 54

alpha, 119

amoeba\_verbose, 79

apply\_rism\_force, 60

arad, 54

arange, 207

arnoldi\_dimension, 169

asympcorr, 59

atmask, 232

atnam, 202

atomn, 43

awt, 207

## B

bar\_intervall, 120

bar\_l\_incr, 120

bar\_l\_max, 120

bar\_l\_min, 120

basis, 97, 99, 101, 103, 104

beeman\_integrator, 78

bellymask, 22

bond\_umb, 76

buffer, 59

## C

cbasis, 103

ccut, 215

centering, 60

charge, 97, 99, 101, 103, 105

charge density, 58

charge distribution, 58

chelpg, 99

chkvir, 43

chnghmask, 35

clambda, 114

closure, 58

cobsl, 215

column\_fft, 33

comp, 25

conflib\_filename, 169

conflib\_size, 169

convkey, 103

convthre, 105

core, 97

crcut, 107

crgmask, 119

crin, 106

crprintcharges, 107

crskin, 107

csurften, 26

cter, 210

cut, 30

cutcap, 28

cuv, 58

cwt, 215

## D

dataset, 214

datasetc, 215

dbonds\_umb, 76

dcut, 214

del, 59

dftb\_3rd\_order, 90

dftb\_chg, 90

dftb\_maxiter, 90

dftb\_telec, 90

dftd, 105

dftgrid, 105

dgpt\_alpha, 77

## INDEX

diag\_routine, 90  
dia\_shift, 74  
dielc, 30  
dij, 214  
dipmass, 36  
dipole, 98, 100, 102, 103, 105  
dipole\_scf\_iter\_max, 79  
dipole\_scf\_tol, 79  
diptau, 36  
diptol, 36  
dist\_gauss, 77  
dobs1, 213  
do\_debugf, 43  
do\_vdw\_longrange, 80  
do\_vdw\_taper, 79  
drms, 22, 168  
dsum\_tol, 32  
dt, 23  
dtfb\_disper, 90  
dumpfrc, 43  
dvbips, 35  
dvd1\_norest, 119  
dwt, 213  
dx0, 22  
dynamicgrid, 105  
dynlmb, 119

### E

ee\_damped\_cut, 79  
eedmeth, 33  
ee\_dsum\_cut, 79  
eedtdns, 33  
egap\_umb, 76  
emap, 76  
emix, 207  
ene\_avg\_sampling, 238  
energy\_window, 169  
eq\_cmd, 180  
es\_cutoff, 238  
evb\_dyn, 74  
ew\_coeff, 32  
exactdensity, 98  
executable, 105  
explored\_low\_modes, 169  
extdiel, 52

### F

fcap, 28  
FCE, 56  
fcedrd, 61  
fcentbasis, 61  
fcestride, 61  
fcons, 232  
fft\_grids\_per\_ang, 239  
finalgrid, 103  
fit\_type, 97  
fixcom, 123  
frameon, 35  
freezemol, 214  
frequency\_eigenvector\_recalc, 169  
frequency\_ligand\_rottrans, 169

### G

gamma\_ten, 26  
gamma\_ln, 24  
gammamap, 232  
gbsa, 53  
gigj, 214  
gms\_version, 100  
gpu, 247  
gpuids, 105  
grdspc, 59  
grid, 103  
gridips, 34  
grids, 232  
grnam1, 206  
guv, 57

### H

huv, 58  
hybridgb, 137

### I

ialtd, 203  
iamoeba, 31  
iat, 200  
iatr, 209  
ibelly, 21  
icfe, 114  
iconstr, 206  
icsa, 214

id, 213  
 id2o, 208  
 idecomp, 21, 114  
 iemap, 29  
 ievb, 31, 65  
 ifcr, 106  
 ifit, 232  
 ifmbar, 120  
 ifntyp, 206  
 ifqnt, 31  
 ifsc, 118  
 ifvari, 203, 204  
 ig, 24  
 igb, 31, 50  
 igr1, 205  
 ihp, 207  
 imin, 17  
 imult, 203  
 indmeth, 35  
 ineb, 156  
 inp, 55  
 intdiel, 52  
 integration, 98  
 invwt1, 208  
 ioutfm, 20  
 ipimd, 177, 180, 182  
 ipnlty, 28  
 ipol, 31  
 iprot, 209, 211  
 ips, 34  
 iqmatoms, 87  
 ir6, 206  
 iresid, 203  
 irest, 19  
**irism**, 31, 58  
 irstdip, 36  
 irstyp, 203  
 iscale, 28  
 isgend, 123  
 isgld, 122  
 isgsta, 123  
 itgetmd, 125  
 itrmax, 90  
 ivcap, 27  
 iwrap, 20

ixpk, 206

## J

jbasis, 103  
 jfastw, 27

## K

klambda, 114  
 kmaxqx, 88  
 ksqmaxq, 88

## L

lbfgs\_memory\_depth, 168  
 ligcent\_list, 171  
 ligstart\_list, 171  
 lmod\_job\_title, 170  
 lmod\_minimize\_grms, 170  
 lmod\_relax\_grms, 170  
 lmod\_restart\_frequency, 170  
 lmod\_step\_size\_max, 170  
 lmod\_step\_size\_min, 170  
 lmod\_trajectory\_filename, 170  
 lmod\_verbosity, 170  
 lnk\_atomic\_no, 91  
 lnk\_dis, 90  
 lnk\_method, 90  
 logdvd1, 119  
 long-range asymptotics, 58

## M

mapfile, 232  
 mapfit, 232  
 matrix\_vector\_product\_method, 168  
 maxcore, 103  
 maxcyc, 22, 168  
 maxit, 100, 105  
 maxiter, 36, 103  
 maxstep, 60  
 mdiis\_method, 60  
 mdiis\_nvec, 60  
 mdinfo\_flush\_interval, 238  
 mdout\_flush\_interval, 237  
 method, 99, 101, 103, 104  
 min\_xfile, 77  
 mipso, 34  
 mipsx, 34

## INDEX

mlimit, 32  
mltpro, 211  
modvdw, 76  
molfit, 233  
monte\_carlo\_method, 170  
morsify, 75  
move, 232  
mtmdforce, 127  
mtmdform, 126  
mtmdmask, 127  
mtmdmult, 127  
mtmdninc, 127  
mtmdrmsd, 127  
mtmdstep1, 126  
mtmdvari, 126  
MTS, 56  
mwords, 100  
mxsub, 29

**N**  
namr, 209  
natr, 209  
nbflag, 32  
nbias, 73  
nbtell, 33  
nchain, 180  
ncyc, 22  
ndip, 213, 214  
neglgdel, 43  
netfrc, 33  
nevb, 73  
nfft3, 31  
ng3, 59  
ngpus, 105  
ninc, 203  
ninterface, 26  
nleb, 100  
nme, 211  
nmodvdw, 73  
nmorse, 73  
nmpmc, 211  
nmropt, 18  
noeskp, 28  
no\_intermolecular\_bonds, 238  
noshakemask, 27, 117

npeak, 207  
npropagate, 60  
nprot, 209, 211  
nrad, 99  
nranatm, 43  
nrespa, 23  
nring, 209  
nscm, 22, 182  
nsnb, 31  
nstep1, 203  
nstlim, 22, 133  
ntave, 19  
ntb, 30  
ntc, 26  
nter, 210  
ntf, 29  
ntmin, 22, 168  
ntp, 25  
ntpr, 19, 98, 100, 102, 103, 105  
ntr, 21  
ntrx, 19  
ntt, 23, 177, 180, 182  
ntwe, 20  
ntw\_evb, 73  
ntwprt, 20  
ntwr, 20  
ntwrism, 61  
ntwv, 20  
ntwx, 20  
ntx, 18  
ntxo, 19  
nuff, 73  
num\_threads, 98, 100, 101, 103  
number\_free\_rottrans\_modes, 170  
number\_ligand\_rottrans, 170  
number\_ligands, 170  
number\_lmod\_iterations, 170  
number\_lmod\_moves, 171  
num\_datasets, 214  
numexchg, 133  
numwatkeep, 137  
nxpk, 206

## O

obs, 210, 211

offset, 52  
 omega, 208  
 optkon, 211  
 optphi, 211  
 order, 32  
 oscale, 208  
 out\_RCdot, 77

**P**

param, 180  
 parameter\_file, 90  
 pencut, 29  
 peptide\_corr, 90  
 polarDecomp, 62  
 precision, 105  
 pres0, 25  
 printcharges, 90  
 printdipole, 90  
 profile\_mpi, 37  
 progress, 62  
 pseudo\_diag, 90  
 pseudo\_diag\_criteria, 90

**Q**

qmcharge, 90  
 qmcut, 87  
 qm\_ewald, 87  
 qmgb, 88  
 qmmask, 87  
 qmmm\_int, 89  
 qmmm\_switch, 88  
 qm\_pme, 88  
 qmqmdx, 90  
 qmshake, 90  
 qm\_theory, 89, 90  
 qxd, 90

**R**

r0, 205  
 raips, 34  
 random\_seed, 171  
 ranseed, 43  
 rbornstat, 52  
 rdt, 53  
 refin, 126

repcrd, 133  
 resolution, 232  
 restart\_pool\_size, 171  
 restraint, 202  
 restraintmask, 21  
 restraint\_wt, 21  
 restrt\_cmd, 181  
 rgbmax, 52  
 RISM, 55, 56  
 rismld, 55  
 RISMnRESPA, 56  
 rismnrespa, 61  
 rjcoef, 205  
 rmsfrc, 43  
 rotmin\_list, 171  
 rstwt, 201  
 rsum\_tol, 32  
 r\_switch\_hi, 88  
 r\_switch\_lo, 88  
 rtemperature, 171

**S**

s11, 214  
 saltcon, 52  
 scaldip, 36  
 scalm, 29  
 scf\_conv, 98, 100, 101  
 scf\_iter, 98  
 scfconv, 90, 103  
 scmask, 119  
 sgft, 123  
 shcut, 210  
 shrang, 210  
 skinnb, 33  
 skmax, 157  
 skmin, 157  
 smoothopt, 54, 55  
 solvbox, 59  
**solvcut**, 59  
 sor\_coefficient, 79  
 spin, 90, 97  
 spinmult, 99, 101, 103, 105  
 str, 209  
 surfTEN, 53

## INDEX

### T

t, 23  
taumet, 208  
taup, 26  
taurot, 208  
tausw, 29  
tautp, 24  
temp0, 24  
temp0les, 24  
tempi, 24  
tempsg, 123  
tgtfitmask, 125, 156  
tgtmdfrc, 125  
tgtrmsd, 125  
tgtrmsmask, 125, 157  
threall, 105  
tight\_p\_conv, 90  
tmode, 157  
tol, 27  
tolerance, 59  
tolpro, 211  
total\_low\_modes, 171  
treff, 123  
trmin\_list, 172  
tsgavg, 122  
ts\_xfile, 77  
type, 32

### U

uff, 78  
use\_dftb, 98  
use\_template, 98, 100, 101, 103, 105  
use\_axis\_opt, 239

### V

vdw\_cutoff, 238  
vdwmeth, 33  
verbose, 32, 61  
verbosity, 90  
vfac, 157  
vlimit, 25  
volfmt, 61  
vrand, 25  
vv, 157

### W

write\_thermo, 61  
writepdb, 90  
wt, 210, 211

### X

xc, 97  
xch\_cnst, 74  
xch\_exp, 75  
xch\_gauss, 75  
xch\_type, 73  
xdg\_xfile, 77  
xmin\_method, 168  
xmin\_verbosity, 168  
xvv, 57

### Z

zcap, 28  
zerochg, 43  
zerodip, 43  
zerofrc, 60  
zerovdw, 43



# **Amber12 Reference Manual Appendices**



## A. Namelist Input Syntax

Namelist provides list-directed input, and convenient specification of default values. It dates back to the early 1960's on the IBM 709, but was regrettably not part of Fortran 77. It is a part of the Fortran 90 standard, and is supported as well by most Fortran 77 compilers (including g77).

Namelist input groups take the form:

```
&name  
var1=value, var2=value, var3(sub)=value,  
var4(sub,sub,sub)=value,value,  
var5=repeat*value,value,  
/
```

The variables must be names in the Namelist variable list. The order of the variables in the input list is of no significance, except that if a variable is specified more than once, later assignments may overwrite earlier ones. Blanks may occur anywhere in the input, except embedded in constants (other than string constants, where they count as ordinary characters).

It is common in older inputs for the ending "/" to be replaced by "&end"; this is non-standard-conforming.

Letter case is ignored in all character comparisons, but case is preserved in string constants. String constants must be enclosed by single quotes (''). If the text string itself contains single quotes, indicate them by two consecutive single quotes, e.g. C1' becomes 'C1'' as a character string constant.

Array variables may be subscripted or unsubscripted. An unsubscripted array variable is the same as if the subscript (1) had been specified. If a subscript list is given, it must have either one constant, or exactly as many as the number in the declared dimension of the array. Bounds checking is performed for ALL subscript positions, although if only one is given for a multi-dimension array, the check is against the entire array size, not against the first dimension. If more than one constant appears after an array assignment, the values go into successive locations of the array. It is NOT necessary to input all elements of an array.

Any constant may optionally be preceded by a positive (1,2,3,...) integer repeat factor, so that, for example, 25\*3.1415 is equivalent to twenty-five successive values 3.1415. The repeat count separator, \*, may be preceded and followed by 0 or more blanks. Valid LOGICAL constants are 0, F, .F., .FALSE., 1, T, .T., and .TRUE.; lower case versions of these also work.



## B. GROUP Specification

This section describes the format used to define groups of atoms in various Amber programs. In *sander*, a group can be specified as a movable "belly" while the other atoms are fixed absolutely in space (aside from scaling caused by constant pressure simulation), and/or a group of movable atoms can independently be restrained (held by a potential) at their positions. In *anal*, groups can be defined for energy analysis.

Except in the analysis module where different groups of atoms are considered with different group numbers for energy decomposition, in all other places the groups of atoms defined are considered as marked atoms to be included for certain types of calculations. In the case of constrained minimization or dynamics, the atoms to be constrained are read as groups with a different weight for each group.

Reading of groups is performed by the routine RGROUP, and you are advised to consult it if there is still some ambiguity in the documentation.

### Input description:

- 1 - Title *format(20a4)*

ITITL Group title for identification.

Setting ITITL = 'END' ends group input.

---

- 1A - Weight *format(f)*

This line is only provided/read when using GROUP input to define restrained atoms.

WT The harmonic force constants in kcal/mol-Å\*\*2 for the group of atoms for restraining to a reference position.

---

- 1B - Control to define the group

KTYPG , (IGRP(I) , JGRP(I) , I = 1,7) *format(a,14i)*

KTYPG Type of atom selection performed. A molecule can be defined by using only 'ATOM' or 'RES', or part of the molecule can be defined by 'ATOM' and part by 'RES'.

'ATOM' The group is defined in terms of atom numbers. The atom number list is given in igrp and jgrp.

'RES' The group is defined in terms of residue numbers. The residue number list is given in igrp and jgrp.

'FIND' This control is used to make additional conditions (apart from the 'ATOM' and 'RES' controls) which a given atom must satisfy to be included in the current group. The conditions are read in the next section (1C) and are terminated by a SEARCH card.

Note that the conditions defined by FIND filter any set(s) of atoms defined by the following ATOM/RES instructions. For example,

-- group input: select main chain atoms --

## B. GROUP Specification

```
FIND
* * M *
SEARCH
RES 1 999
END
END
'END' End input for the current group. Followed by either another
group definition (starting again with line 1 above), or by a second
'END' "card", which terminates all group input.
```

```
IGRP(I) , JGRP(I)
```

The atom or residue pointers. If ktypg .eq. 'ATOM' all atoms numbered from igrp(i) to jgrp(i) will be put into the current group. If ktypg .eq. 'RES' all atoms in the residues numbered from igrp(i) to jgrp(i) will be put into the current group. If igrp(i) = 0 the next control card is read.

It is not necessary to fill groups according to the numerical order of the residues. In other words, Group 1 could contain residues 40-95 of a protein, Group 2 could contain residues 1-40 and Group 3 could contain residues 96-105.

If ktypg .eq. 'RES', then associating a minus sign with igrp(i) will cause all residues igrp(i) through jgrp(i) to be placed in separate groups.

In the analysis modules, all atoms not explicitly defined as members of a group will be combined as a unit in the (n + 1) group, where the (n) group in the last defined group.

---

- 1C - Section to read atom characteristics

\*\*\*\*\* Read only if KTYPG = 'FIND' \*\*\*\*\*

```
JGRAPH(I) , JSYMBL(I) , JTREE(I) , JRESNM(I) format(4a)
```

A series of filter specifications are read. Each filter consists of four fields (JGRAPH,JSYMBL,JTREE,JRESNM), and each filter is placed on a separate line. Filter specification is terminated by a line with JGRAPH = 'SEARCH'. A maximum of 10 filters may be specified for a single 'FIND' command.

The union of the filter specifications is applied to the atoms defined by the following ATOM/RES cards. I.e. if an atom satisfies any of the filters, it will be included in the current group. Otherwise, it is not included. For example, to select all non main chain atoms from residues 1 through 999:

```
-- group input: select non main chain atoms --
```

```
FIND
* * S *
* * B *
* * 3 *
* * E *
SEARCH
```

```

RES 1 999
END
END
'END' End input for the current group. Followed by either another
The four fields for each filter line are:
JGRAPH(I) The atom name of atom to be included. If this and the
following three characteristics are satisfied the atom is
included in the group. The wild card '*' may be used to
to indicate that any atom name will satisfy the search.
JSYMBL(I) Amber atom type of atom to be included. The wild card
'*' may be used to indicate that any atom type will
satisfy the search.
JTREE(I) The tree name (M, S, B, 3, E) of the atom to be included.
The wild card '*' may be used to indicate that any tree
name will satisfy the search.
JRESNM(I) The residue name to which the atom has to belong to be
included in the group. The wild card '*' may be used to
indicate that any residue name will satisfy the search.
-----

```

### Examples:

The molecule 18-crown-6 will be used to illustrate the group options. This molecule is composed of six repeating (-CH<sub>2</sub>-O-CH<sub>2</sub>-) units. Let us suppose that one created three residues in the PREP unit: CRA, CRB, CRC. Each of these is a (-CH<sub>2</sub>-O-CH<sub>2</sub>-) moiety and they differ by their dihedral angles. In order to construct 18-crown-6, the residues CRA, CRB, CRC, CRB, CRC, CRB are linked together during the LINK module with the ring closure being between CRA(residue 1) and CRB(residue 6).

#### Input 1:

```

Title one
RES 1 5
END
Title two
RES 6
END
END

```

**Output 1:** Group 1 will contain residues 1 through 5 (CRA, CRB, CRC, CRB, CRC) and Group 2 will contain residue 6 (CRB).

#### Input 2:

```

Title one
RES 1 5
END
Title two
ATOM 36 42
END
END

```

## B. GROUP Specification

**Output 2:** Group 1 will contain residues 1 through 5 (CRA, CRB, CRC, CRB, CRC) and Group 2 will contain atoms 36 through 42. Coincidentally, atoms 36 through 42 are also all the atoms in residue 6.

### Input 3:

```
Title one
RES -1 6
END
END
```

**Output 3:** Six groups will be created; Group 1: CRA, Group 2: CRB,..., Group 6: CRB.

### Input 4:

```
Title one
FIND
O2 OS M CRA
SEARCH
RES 1 6
END
END
```

**Output 4:** Group 1 will contain those atoms with the atom name 'O2', atom type 'OS', tree name 'M' and residue name 'CRA'.

### Input 5:

```
Title one
FIND
O2 OS * *
SEARCH
RES 1 6
END
END
```

**Output 5:** Group 1 will contain those atoms with the atom name 'O2', atom type 'OS', any tree name and any residue name.



## C. ambmask

### NAME

ambmask - test group input FIND mask (or mask string given in the &cntrl section) and dump the resulting atom selection in a given format

### SYNOPSIS

```
ambmask -p prmtop -c inpcrd -prnlev [0-3] -out [short|pdb|amber] -find [maskstr]
```

### DESCRIPTION

**ambmask** acts as a filter which takes Amber topology and coordinate "restart" file and applies the "maskstr" selection string (similar syntactically to UCSF Chimera/Midas) to select specific atoms or residues. Residues can be selected by their numbers or names. Atoms can be selected by numbers, names, or Amber (forcefield) type. Selections are case insensitive. The selected atoms are printed to **stdout** (by default, in Amber-style PDB format). Atom and residue names and numbers are taken from Amber topology. Beware that selection string works on those names and not the ones from the original PDB file. If you are not sure how atoms or residues are named or numbered in the Amber topology, use **ambmask** with a selection string ".\*" (which is the default) to dump the whole PDB file with corresponding Amber atom/residue names and numbers.

The "maskstr" selection expression is composed of "elementary selections". These start with ":" to select by residues, or "@" to select by atoms. Residues can be selected by numbers (given as numbers separated by commas, or as ranges separated by a dash) or by names (given as a list of residue names separated by commas). The same holds true for atom selections by atom numbers or atom names. In addition, atoms can be selected by Amber atom type, in which case "@" must be immediately followed by "%". ".\*" means all residues and "@\*" means all atoms. The following examples show the usage of this syntax. Square brackets should not be used in actual expressions, they are only used for clarity here:

```
:{residue numlist} [:1-10] [:1,3,5] [:1-3,5,7-9]
:{residue namelist} [:LYS] [:ARG,ALA,GLY]
@{atom numlist} [@12,17] [@54-85] [@12,54-85,90]
@{atom namelist} [@CA] [@CA,C,O,N,H]
@%{atom typelist} [%CT] [%N*,N3]
```

These "elementary selections" can be combined into more complex selections using binary operators "&" (and) and "|" (or), unary operator "!" (negation), distance binary operators "<:", ">:", "<@", ">@", and parentheses. Spaces around operators are irrelevant. Parentheses have

### C. *ambmask*

the highest priority, followed by distance operators (" $<$ ", " $>$ ", " $<$ @", " $>$ @"), "!" (negation), "&" (and) and "|" (or) in order of descending priority. A wildcard "=" in an atom or residue name matches any name starting with a given character (or characters). For example, [AS=] would match all aspartic acid residues (ASP), and asparagines (ASN); [H=] would match all atom names starting with H (which are effectively all hydrogens). It cannot be used to match the end part of names (such as [A]). Some examples of more complex selections follow:

```
[@C= & !@CA,C]
```

.. all carbons except backbone alpha and carbonyl carbon

```
[ (:1-3@CA | :5-7@CB) ]
```

.. alpha carbons in residues 1-3 and beta carbons in residues 5-7

```
[ :CYS,ARG & ! (:1-10 | @CA,CB) ]
```

.. all CYS and ARG atoms except those which are in residues 1-10 and which are CA or CB

```
[ :* & !@H= ] or [ !@H= ]
```

.. all heavy atoms (i.e. except hydrogens)

```
[ :5 <@4.5 ]
```

.. all atoms within 4.5A from residue 5

```
[ (:1-55 <:3.0) & :WAT ]
```

.. all water molecules within 3A from residues 1-55

Compound expressions of the following type are also allowed:

```
:{residue numlist|namelist}@{atom numlist|namelist|typelist}
```

```
[ :1-10@CA ] is equivalent to [ :1-10 & @CA ]
```

```
[ :LYS@H= ] is equivalent to [ :LYS & @H= ]
```

### OPTIONS

The program needs an Amber topology file and coordinates (restrt format). The filename specified with the *-p* option is Amber topology, while the filename given with the *-c* option is a coordinate file. If *-p* or *-c* options are not given, the program expects that files "prmtop" and/or "inpcrd" exist in the current directory, which will be taken as topology and coordinate files correspondingly. If no command line options are given, the program prints the usage statement.

The option *-prnlev* specifies how much (debugging) information is printed to **stdout**. If it is 0, only selected atoms are printed. More verbose output (which might be useful for debugging purposes) is achieved with higher values: 1 prints original "maskstr" in its tokenized (with operands enclosed in square brackets) and postfix (or Reverse Polish Notation) forms; number of atoms and residues in the topology file and number of selected atoms are also printed to **stdout**. 2 prints the resulting mask array, which is an array of integer values, with '1' representing a selected atom, and '0' an unselected one. Value of 3, in addition, prints mask arrays

as they are pushed or popped from the stack (this is really only useful for tracing the problems occurring during stack operations). The *-prnlev* values of 0 or 1 should suffice for most uses.

The option *-out* specifies the format of printed atoms. "short" means a condensed output using residue (:) and atom (@) designators followed by residue ranges and atom names. "pdb" (default) prints atoms in Amber-style PDB format with the original "maskstr" printed as a REMARK at the top of the PDB file, and "amber" prints atom/residue ranges in the format suitable for copying into group input section of Amber input file.

The option *-find* is followed by "maskstr" expression. This is a string where some characters have a special meaning and thus express what parts (atoms/residues) of the molecule will get selected. The syntax of this string is explained in the section above (DESCRIPTION). If this option is left out, it defaults to ":\*", which selects all atoms in the given topology file. The length of "maskstr" is limited to 80 characters. If the "maskstr" contains spaces or special characters (which would be expanded by the shell), it should be protected by single or double quotes (depending on the shell). In addition, for C-shells even a quoted exclamation character may be expanded for history substitution. Thus, it is recommended that the operand of the negation operator always be enclosed in parentheses so that "!" is always followed by a "(" to produce "!((" which disables the special history interpretation. For example, [*@C= & !(@CA,C)*] selects all carbons except backbone alpha and carbonyl carbon; the parentheses are redundant but shell safe. The man page indicates further ways to disable history substitution.

## FILES

Assumes that *prmtop* and *inpcrd* files exist in the current directory if they are not specified with *-p* and *-c* options. Resulting (i.e. selected) atoms are written to **stdout**.

## BUGS

Because all atom names are left justified in Amber topology and the selections are case insensitive, there is no way to distinguish some atom names: alpha carbon CA and a calcium ion Ca are a notorious example of that.



## D. MM\_PBSA

(*Note:* The recommended version of MM/PBSA to use is MMPBSA.py, described in the AmberTools manual.)

The MM\_PBSA approach represents the postprocessing method to evaluate free energies of binding or to calculate absolute free energies of molecules in solution. The sets of structures are usually collected with molecular dynamics or Monte Carlo methods. However, the collections of structures should be stored in the format of an Amber trajectory file. The MM\_PBSA/GBSA method combines the molecular mechanical energies with the continuum solvent approaches. The molecular mechanical energies are determined with the *sander* program from Amber and represent the internal energy (bond, angle and dihedral), and van der Waals and electrostatic interactions. An infinite cutoff for all interactions is used. The electrostatic contribution to the solvation free energy is calculated with a numerical solver for the Poisson-Boltzmann (PB) method, for example, as implemented in the *pbsa* program[74] or by generalized Born (GB) methods implemented in *sander*. Previous MM\_PBSA applications were mostly performed with a numerical PB solver in the widely used *DelPhi* program,[353] which has been shown by Amber developers to be numerically consistent with the *pbsa* program. The nonpolar contribution to the solvation free energy has been determined with solvent-accessible-surface-area-dependent terms.[71] The surface area is computed with Paul Beroza's *molsurf* program, which is based on analytical ideas primarily developed by Mike Connolly.[357] An alternative method for nonpolar solvation energy is also included here. [77] The new method separates nonpolar contribution into two terms: the attractive (dispersion) and repulsive (cavity) interactions. Doing so significantly improves the correlation between the cavity free energies and solvent accessible surface areas for branched and cyclic organic molecules.[407] This is in contrast to the commonly used strategy that correlates total nonpolar solvation energies with solvent accessible surface areas, which only correlates well for linear aliphatic molecules.[71] In the new method, the attractive interaction is computed by a numerical integration over the solvent accessible surface area that accounts for solute solvent attractive interactions with an infinite cutoff.[78] Finally, estimates of conformational entropies can be made with the *nmode* or *NAB* module from Amber.

Although the basic ideas here have many precedents, the first application of this model in its present form was to the A- and B-forms of RNA and DNA, where many details of the basic method are given.[354] You may also wish to refer to reviews summarizing many of the applications of this model,[356, 578] as well as to papers describing more recent applications.[376–379, 498]

The initial MM\_PBSA scripts were written by Irina Massova. These were later modified and mostly turned into Perl scripts by Holger Gohlke, who also added GB/SA (generalized Born/surface area) options, and techniques to decompose energies into pairwise contributions from groups (where possible).

## D.1. General instructions

The general procedure is to edit the *mm\_pbsa.in* file (see below), and then to run the code as follows:

```
mm_pbsa.pl mm_pbsa.in > mm_pbsa.log
```

The *mm\_pbsa.in* file refers to "receptor", "ligand" and "complex", but the chemical nature of these is up to the user, and these could equally well be referred to as "A", "B", and "AB". The procedure can also be used to estimate the free energy of a single species, and this is usually considered to be the "receptor".

The user also needs to prepare *prmtop* files for receptor, ligand, and complex using LEaP; if you are just doing "stability" calculations, only one of the *prmtop* files is required. Note that the *prmtop* files usually should only include the solutes, i.e., solvent molecules and counter ions should not be present. A sample LEaP command file for how to prepare *prmtop* files for solvated systems for the initial molecular dynamics runs and *prmtop* files for the systems in vacuum for the subsequent MM\_PBSA calculations can be found in the *\$AMBERHOME/src/mm\_pbsa/Examples* directory.

The output files are labeled ".out", and the most useful summaries are in the "statistics.out" files. These give averages and standard deviations for various quantities, using the following labeling scheme:

```
*** Abbreviations for mm_pbsa output ***
ELE - non-bonded electrostatic energy + 1,4-electrostatic energy
VDW - non-bonded van der Waals energy + 1,4-van der Waals energy
INT - bond, angle, dihedral energies
GAS - ELE + VDW + INT
PBSUR - hydrophobic contrib. to solv. free energy for PB calculations
PBCAL - reaction field energy calculated by PB
PBSOL - PBSUR + PBCAL
PBELE - PBCAL + ELE
PBTOT - PBSOL + GAS
GBSUR - hydrophobic contrib. to solv. free energy for GB calculations
GB - reaction field energy calculated by GB
GBSOL - GBSUR + GB
GBELE - GB + ELE
GBTOT - GBSOL + GAS
TSTRA - translational entropy (as calculated by nmode) times temperature
TSROT - rotational entropy (as calculated by nmode) times temperature
TSVIB - vibrational entropy (as calculated by nmode) times temperature
*** Prefixes in front of abbreviations for energy decomposition ***
"T" - energy part due to _T_otal residue
"S" - energy part due to _S_idechain atoms
"B" - energy part due to _B_ackbone atoms
```

The *\$AMBERHOME/src/mm\_pbsa/Examples* directory shows examples of running a "Stability" calculation (i.e., estimating the free energy of one species), a "Binding" calculation (estimating  $\Delta G$  for  $A + B \rightarrow AB$ ), an "Nmode" calculation (to estimate entropies), and examples

of how total energies (either by residue, or pair-wise by residue) and vibrational entropies (by residue only) can be decomposed. You should study the inputs and outputs in these directories to see how the program is typically used.

## D.2. Input explanations

Below is a description of the input parameters for MM-PB/SA. A sample file can be found at `$AMBERHOME/src/mm_pbsa/Examples/mm_pbsa.in`. Further template files for variants of the implicit solvent models can be found in `$AMBERHOME/src/mm_pbsa/Examples/TEMPLATE_INPUT_SCRIPTS`. There, the file `SURFTEN_SURFOFF_Recommendations.pdf` describes in detail recommended combinations of parameters for the implicit solvent models. The input file is structured into sections for different purposes. The parameters in the general section control which kind of operations are executed. Additional parameters for the chosen operations have to be defined in the later sections.

### D.2.1. General

**VERBOSE** If set to 1, input and output files are not removed. This is useful for debugging purposes.

**PARALLEL** If set to values  $> 1$ , energy calculations for snapshots are done in parallel, using **PARALLEL** number of threads.

#### specifying snapshot location and naming

**PREFIX** To the prefix of the snapshots, "{\_com, \_rec, \_lig}.crd.Number" is added during generation of snapshots as well as during `mm_pbsa` calculations.

**PATH** Specifies the location where to store or get snapshots.

#### selecting subsets of snapshots

**START** Specifies the first snapshot to be used in energy calculations (optional, default is 1).

**STOP** Specifies the last snapshot to be used in energy calculations (optional, default is  $10e10$ ).

**OFFSET** Specifies the offset between snapshots in energy calculations (optional, default is 1). This may be interesting for entropy calculations via `nmode` or `NAB` to cut down on the number of snapshots to save computational time.

#### calculation of energy differences or absolute energies

**COMPLEX** Set to 1 if free energy difference is calculated.

**RECEPTOR** Set to 1 if either (absolute) free energy or free energy difference are calculated.

## D. MM\_PBSA

LIGAND Set to 1 if free energy difference is calculated.

### selection of parameter and topology files

COMPT Parmtop file for the complex (not necessary for option GC).

RECPT Parmtop file for the receptor (not necessary for option GC).

LIGPT Parmtop file for the ligand (not necessary for option GC).

### specification of operations/calculations

GC Snapshots are generated from trajectories (see below).

AS Residues are mutated during generation of snapshots from trajectories.

DC Decompose the free energies into individual contributions (only works with MM, nmode, GB, and PB with the pbsa program of Amber).

MM Calculation of gas phase energies using sander.

GB Calculation of desolvation free energies using the GB models in sander (see below).

PB Calculation of desolvation free energies using delphi (see below). Calculation of nonpolar solvation free energies according to the NPOPT option in pbsa (see below).

MS Calculation of nonpolar contributions to desolvation using molsurf (see below). If MS = 0 and GB = 1, nonpolar contributions are calculated with the LCPO method in sander. If MS = 0 and PB = 1, nonpolar contributions are calculated according to the NPOPT option in pbsa (see below).

NM Calculation of entropies with nmode or NAB.

## D.2.2. Energy Decomposition Parameters

Energy decomposition is performed for gasphase energies, desolvation free energies calculated with GB or PB (using the pbsa program of Amber), nonpolar contributions to desolvation using the ICOSA method, and vibrational entropies using nmode. For amino acids and nucleotides, decomposition is also performed with respect to backbone and sidechain atoms. When doing a pairwise decomposition of the PB reaction field energy, one should note that for each included residue the PB equation has to be solved once per snapshot. Also a further decomposition into backbone and sidechain contributions has not been implemented for a pairwise PB decomposition.



### specification of decomposition modus

- DCTYPE Values of 1 or 2 yield a decomposition on a per-residue basis.  
Values of 3 or 4 yield a decomposition on a pairwise basis. So far the number of pairs must not exceed the number of residues in the molecule considered.  
Values 1 or 3 add 1-4 interactions to bond contributions.  
Values 2 or 4 add 1-4 interactions to either electrostatic or vdW contributions.

### residue assignment

- COMREC Residues belonging to the receptor molecule IN THE COMPLEX.  
COMLIG Residues belonging to the ligand molecule IN THE COMPLEX.  
RECRES Residues in the receptor molecule.  
LIGRES Residues in the ligand molecule.  
{REC,LIG}MAP Residues in the complex which are equivalent to the residues in the receptor molecule or the ligand molecule.

### output filter

- {COM,REC,LIG}PRI Residues considered for output.

### D.2.3. Poisson-Boltzmann Parameters

The following parameters are passed to the PB solver. Additional input parameters may also be added here. See the sander PB documentation for more options.

- PROC Determines which method is used for solving the PB equation. By default (PROC = 2) the pbsa program of the Amber suite is used.
- REFE Determines which reference state is taken for the PB calculation. By default (REFE = 0) reaction field energy is calculated with EXDI/INDI. Here, INDI must agree with DIELC from the MM section.
- INDI Dielectric constant for the solute.
- EXDI Dielectric constant for the surrounding solvent.
- ISTRNG Ionic strength (in mM) for the Poisson-Boltzmann solvent.
- PRBRAD Solvent probe radius in Angstrom:  
**1.4** with the radii in the prmtop files (default);  
**1.6** with the radii optimized by Tan and Luo (in preparation).  
See RADIOPT on how to choose a cavity radii set.

## D. MM\_PBSA

RADIOPT Option to set up radii for PB calc:

**0** uses the radii from the prmtop file (default);

**1** uses the radii optimized by Tan and Luo (in preparation) with respect to the reaction field energies computed in the TIP3P explicit solvents. Note that these optimized radii are based on Amber atom types (upper case) and charges. Radii from the ~.prmtop files are used if the atom types are defined by antechamber (lower case).

SCALE Lattice spacing in number of grids per Angstrom.

LINIT Number of iterations with the linear PB equation.

### hybrid solvation model

IVCAP If set to 1, a solvent sphere (specified by CUTCAP, XCAP, YCAP, and ZCAP) is excised from a box of water.

If set to 5, a solvent shell is excised, specified by CUTCAP (the thickness of the shell in Å). The electrostatic part of the solvation free energy is estimated from a linear response approximation using the explicit water plus a reaction field contribution from outside the sphere (i.e., a hybrid solvation approach is pursued).

In addition, the nonpolar contribution is estimated from a sum of (attractive) dispersion interactions calculated between the solute and the solvent molecules plus a (repulsive) cavity contribution. For the latter, the surface calculation must be done with MS = 1 and the PROBE should be set to 1.4 to get the solvent excluded surface.

CUTCAP Radius of the water sphere or thickness of the water shell. Note that the sphere must enclose the whole solute.

XCAP/YCAP/ZCAP Location of the center of the water sphere.

### nonpolar solvation

*Parameters for nonpolar solvation energies if MS = 0*

INP Option for modeling nonpolar solvation free energy. See sander PB documentation for more information on the implementations by Tan and Luo (in preparation).

**1:** uses the solvent-accessible-surface area to correlate total nonpolar solvation free energy:  $G_{np} = SURFTEN * SASA + SURFOFF$ . Default.

**2:** uses the solvent-accessible-surface area to correlate the repulsive (cavity) term only, and uses a surface-integration approach to compute the attractive (dispersion) term:  $G_{np} = G_{disp} + G_{cavity} = G_{disp} + SURFTEN * SASA + SURFOFF$ . When this option is used, RADIOPT has to be set to 1, i.e. the radii set optimized by Tan and Luo to mimic  $G_{np}$  in TIP3P explicit solvents. Otherwise, there is no guarantee that  $G_{np}$  matches that in explicit solvents.

**SURFTEN/SURFOFF**

Values used to compute the nonpolar solvation free energy  $G_{np}$  according to INP. If  $INP = 1$  and  $RADIOPT = 0$  (default, see above), use SURFTEN/SURFOFF parameters that fit with the radii from the prmtop file, e.g., use SURFTEN: 0.00542; SURFOFF: 0.92 for PARSE radii. If  $INP = 2$  and  $RADIOPT = 1$ , these two lines can be removed, i.e., use the default values set in pbsa for this nonpolar solvation model. Otherwise, set these to the following: SURFTEN: 0.04356; OFFSET: -1.008

*Parameters for nonpolar solvation energies if  $MS = 1$*

**SURFTEN/SURFOFF** Values used to compute the nonpolar contribution  $G_{np}$  to the desolvation according to either

(I)  $G_{np} = SURFTEN * SASA + SURFOFF$  (if  $IVCAP = 0$ ) or

(II)  $G_{np} = G_{disp} + G_{cavity} = G_{disp} + SURFTEN * SASA + SURFOFF$  (if  $IVCAP > 0$ ).

In the case of (I), use parameters that fit with the radii from the reaction field calculation. E.g., use SURFTEN: 0.00542, SURFOFF: 0.92 for PARSE radii or use SURFTEN: 0.005, SURFOFF: 0.86 for Tan & Luo radii. In the case of (II), use SURFTEN: 0.069; SURFOFF: 0.00 for calculating the  $G_{cavity}$  contribution.

**D.2.4. Molecular Mechanics Parameters**

The following parameters are passed to sander. For further details see the sander documentation.

**DIELC** Dielectric constant for electrostatic interactions. Note: This is not related to GB calculations.

**D.2.5. Generalized Born Parameters**

**IGB** Switches between Tsui's GB (1) and Onufriev's GB (2, 5).

**GBSA** Switches between LCPO (1) and ICOSA (2) method for SASA calculation. Decomposition only works with ICOSA.

**SALTCON** Concentration (in M) of 1-1 mobile counterions in solution.

**EXTDIEL** Dielectric constant for the solvent.

**INTDIEL** Dielectric constant for the solute.

**SURFTEN/SURFOFF** Values used to compute the nonpolar contribution  $G_{np}$  to the desolvation free energy according to  $G_{np} = SURFTEN * SASA + SURFOFF$ .

### D.2.6. Molsurf Parameters

**PROBE** Radius of the probe sphere used to calculate the SAS. In general, since Bondi radii are already augmented by 1.4A, PROBE should be 0.0 In IVCAP = 1 or 5, the solvent excluded surface is required for calculating the cavity contribution. Bondi radii are not augmented in this case and PROBE should be 1.4.

### D.2.7. NMODE Parameters

The following parameters are passed either to NAB (for minimization and entropy calculation using gasphase statistical mechanics) or to sander (for minimization) and nmode (for entropy calculation using gasphase statistical mechanics). For further details see documentation.

**PROC** Determines which method is used for the calculations: By default, PROC = 1, the NAB implementation of nmode is used. This allows using either a GB model or a distance-dependent dielectric for electrostatic energies. No entropy decomposition is possible, however. If PROC = 2, the "original" nmode implementation is used. Here, only a distance-dependent dielectric is available for electrostatic energies. Entropy decomposition is possible here, too.

**MAXCYC** Maximum number of cycles of minimization.

**DRMS** Convergence criterion for the energy gradient.

**IGB** Switches between no GB (i.e., vacuum electrostatics) (0) or Tsui's GB (1).

**SALTCON** Concentration (in M) of 1-1 mobile counterions in solution.

**EXTDIEL** Dielectricity constant for the solvent.

**SURFTEN** Value used to compute the nonpolar contribution  $G_{np}$  to the desolvation according to  $G_{np} = SURFTEN * SASA$ .

**DIELC** (Distance-dependent) dielectric constant.

### D.2.8. Parameters for Snapshot Generation

**BOX** "YES": means that periodic boundary conditions were used during MD simulation and that box information has been printed in the trajectory files; "NO": means opposite.

**NTOTAL** Total number of atoms per snapshot printed in the trajectory file (including water, ions, ...).

**NSTART** Start structure extraction from NSTART snapshot.

**NSTOP** Stop structure extraction at NSTOP snapshot.

**NFREQ** Every NFREQ structure will be extracted from the trajectory.

NUMBER\_LIG\_GROUPS Number of subsequent LSTART/LSTOP combinations to extract atoms belonging to the ligand.

LSTART Number of first ligand atom in the trajectory entry.

LSTOP Number of last ligand atom in the trajectory entry.

NUMBER\_REC\_GROUPS Number of subsequent RSTART/RSTOP combinations to extract atoms belonging to the receptor.

RSTART Number of first receptor atom in the trajectory entry.

RSTOP Number of last receptor atom in the trajectory entry.

Note: If only one molecular species is extracted, use only the receptor parameters (NUMBER\_REC\_GROUPS, RSTART, RSTOP).

### D.2.9. Parameters for Alanine Scanning

The following parameters are additionally passed to `make_crd_hg` in conjunction with the ones from the snapshot generation section if "alanine scanning" is requested. The description of the parameters is taken from Irina Massova.

NUMBER\_MUTANT\_GROUPS Total number of mutated residues. For each mutated residue, the following four parameters must be given subsequently.

MUTANT\_ATOM1 If residue is mutated to Ala then this is: a pointer on the CG atom of the mutated residue for all residues except Thr, Ile and Val; a pointer to CG2 if Thr, Ile or Val residue is mutated to Ala; or a pointer to OG if Ser residue is mutated to Ala. If residue is mutated to Gly then this is a pointer on CB.

MUTANT\_ATOM2 If residue is mutated to Ala then this is: zero for all mutated residues except Thr, Val, and Ile; a pointer on OG1 if Thr residue is mutated to Ala; or a pointer on CG1 if Val or Ile residue is mutated to Ala. If residue is mutated to Gly then this should be always zero.

MUTANT\_KEEP A pointer on the C atom (carbonyl atom) for the mutated residue.

MUTANT\_REFERENCE If residue is mutated to Ala then this is a pointer on CB atom for the mutated residue. If residue is mutated to Gly then this is a pointer on CA atom for the mutated residue.

Note: The method will not work for a smaller residue mutation to a bigger for example Gly -> Ala mutation. Note: Maximum number of the simultaneously mutated residues is 40.

### D.2.10. Trajectory Specification

The specified trajectories are used to extract snapshots with "make\_crd\_hg"

TRAJECTORY Each trajectory file name must be preceded by the TRAJECTORY card. Subsequent trajectories are considered together. Trajectories may be in ascii as well as in .gz format. To be able to identify the title line, it must be identical in all files.

### D.3. Auxiliary programs used by MM\_PBSA

Several programs can be used to compute numerical solutions to the Poisson-Boltzmann equation. The default is a *pbsa* implementation in *sander*. Please see *sander* PB pages in Section 6.2 for detailed description. Other programs for computing numerical Poisson-Boltzmann results are also available, such as *Delphi*, *MEAD*, and *UHBD*. These could be merged into the Perl scripts developed here with a little work. See:

- <http://honiglab.cpmc.columbia.edu/> (for *DELPHI*)
- <http://www.scripps.edu/bashford/> (for *MEAD*)
- <http://adrik.bchs.uh.edu/uhbd.html> (for *UHBD*)

### D.4. APBS as an alternate PB solver in Sander

APBS is a robust, numerical Poisson-Boltzmann solver with many features (for more details see <http://apbs.sourceforge.net/>). APBS can be used as an alternative PB solver in *sander* when compiled with *sander* using *iAPBS*. *sander.APBS* can be then used for implicit solvent MD simulations, calculation of solvation energies and electrostatic properties and to generate electrostatic potential maps for visualization. It can also be used in the *MM\_PBSA* approach to estimate solvation and apolar ( $\text{GAMMA} * \text{SASA}$ ) energy contributions to free energies of binding.

Please see APBS documentation (<http://apbs.sourceforge.net/doc/user-guide/index.html>) for definition of APBS input parameters and *iAPBS* documentation (<http://mccammon.ucsd.edu/iapbs/>) on how to build *sander.APBS* and how to use it.

To use *mm\_pbsa.pl* script with *sander.APBS* the following is necessary:

- - *sander.APBS* must be installed in  $\$AMBERHOME/bin$  directory.
- - `@GENERAL` and `@PB` sections in input file need to be modified.
- - PQR files for ligand, receptor and complex need to be prepared if an
- alternate charge/radius scheme is used (which is recommended).

#### Input file description

The *mm\_pbsa.in* input file which is included in the Amber distribution can be used with the following modifications:

(1) Turn on PB and turn off GB and MS calculations in the `@GENERAL` section of the input file:

```
@GENERAL
MM 1
GB 0
PB 1
MS 0
```

(2) Input file @PB section:

```

#
@PB
#
#
# PROC = 3 uses sander.APBS as the PB solver
# REFE - REFE = 0 is always used with sander.APBS
# INDI and EXDI are solute and solvent dielectric constants
# SCALE - grid spacing in number of grid points per A
# LINIT - no effect
# PRBRAD - solvent probe radius in A
# ISTRNG - ionic strength in mM
#
# RADIOPT - option to set up radii and charges for PB calculation:
# 0: uses the radii from prmtop files
# 2: reads in PQR files with radii/charges information from
# lig.pqr, rec.pqr and com.pqr PQR files
#
# APBS options:
# BCFL, SRFM, CHGM, SWIN, GAMMA - see APBS and iAPBS documentation for details
# GAMMA is surface tension for apolar energies (in kJ/mol/A**2),
# defaults to 0.105 (Please note the units!)
#
PROC 3
REFE 0
INDI 1.0
EXDI 80.0
SCALE 2
LINIT 1000
PRBRAD 1.4
ISTRNG 0.0
#
RADIOPT 0
#
BCFL 2
SRFM 1
CHGM 1
SWIN 0.3
GAMMA 0.105
#

```

### PQR files

With RADIOPT=2 three PQR files are required: lig.pqr, rec.pqr and com.pqr with charge/radius information for the ligand, receptor and complex, respectively. This is the recommended

#### D. MM\_PBSA

option to get better estimates of solvation energies.

The PQR files can be created with `pdb2pqr` utility:

```
pdb2pqr.py --assign-only --ff=amber com.pdb com.pqr
pdb2pqr.py --assign-only --ff=amber rec.pdb rec.pqr
pdb2pqr.py --assign-only --ff=amber lig.pdb lig.pqr
```

where `-ff=amber` is the requested force field charge/radius parameters. Several options are available (Amber, CHARMM, PARSE, etc.) and also a user defined charge/radius scheme is supported (with `-ff=myff` option).

`pdb2pqr.py` can be obtained from <http://pdb2pqr.sourceforge.net/>. PDB2PQR service is also available on the web at <http://nbc.net/pdb2pqr/>. The PDB files (`com.pdb`, `rec.pdb` and `lig.pdb`) can be generated using `ambpdb` utility.



## E. EVB output file specifications

This section describes the contents of the EVB output file *evbout*. The data type of each variable is enclosed in  $\{\dots\}$ , while the size of each array variable is enclosed in  $[\dots]$ . Below are the formatting specifications for the output data:

```
100 format( A/, A )
200 format( A/, I8 )
300 format( A/, 3(2X,I8), 2X, F14.8 )
400 format( A/, 2I8, F14.8 )
500 format( A/, 2I8, F14.8, 2X, F14.8 )
600 format( A/, 3I8, F14.8, 2X, F14.8 )
888 format( A, 2X, I10, 2X, A, 2X, F20.8 )
1000 format( A/, (5(2X,F20.8)) )
```

The EVB output file begins with the following header information:

```
write(evb_unit, '/')
write(evb_unit, 100) ' [DYNAMICS TYPE]: ', trim( adjustl(evb_dyn) )
write(evb_unit, '/')
write(evb_unit, 200) ' [NBEAD]: ', ncopy
write(evb_unit, '/')
write(evb_unit, 300) ' [NEVB] [NBIAS] [NTW_EVB] [DT]: ' &
    , nevb, nbias, ntw_evb, dt
write(evb_unit, '/')
```

```
evb_dyn      : {character*512} EVB dynamics specification.
ncopy        : {integer} No. of PIMD slices. Classical EVB  $\Rightarrow$  ncopy = 1.
nevb         : {integer} No. of diabatic states.
nbias        : {integer} No. of biasing potentials included in  $V_{el0}$ .
ntw_evb      : {integer} No. of MD steps between output to evbout file.
dt           : {real} MD time step size (ps).
```

```
! Output ONLY if performing mapping potential dynamics.
do n = 1, nbias
    write(evb_unit, 400) ' [MAPPING POTENTIAL]: ni, nf, lambda ' &
        , bias_ndx(n,1), bias_ndx(n,2), lambda(n)
enddo

! Output ONLY if performing umbrella sampling on an energy gap RC.
do n = 1, nbias
    write(evb_unit, 500) ' [NRG_GAP UMBRELLA]: ni, nf, k, ezero ' &
        , bias_ndx(n,1), bias_ndx(n,2), k_umb(n), r0_umb(n)
enddo
```

## E. EVB output file specifications

```

bias_ndx(:, :) : {integer}, [nbias,2]. Valence bond state index.
lambda(:)      : {real}, [nbias].  $V_\lambda = (1 - \lambda)V_{ii} + \lambda V_{ff}$ .
k0_umb(:)      : {real}, [nbias]. Umbrella force constant.
r0_umb(:)      : {real}, [nbias]. RC anchor point for umbrella sampling.

```

```

! Output ONLY if sampling involves the difference of distances RC.
do n = 1, nbias
  write(evb_unit,600) &
    ' [DBONDS UMBRELLA]: iatom, jatom, katom, k, ezero ' &
    , dbonds_RC(n)%iatom, dbonds_RC(n)%jatom &
    , dbonds_RC(n)%katom, k_umb(n), r0_umb(n)
enddo

! Output ONLY if sampling involves a distance RC.
do n = 1, nbias
  write(evb_unit,500) ' [BOND UMBRELLA]: iatom, jatom, k, ezero ' &
    , bond_RC(n)%iatom, bond_RC(n)%jatom, k_umb(n), r0_umb(n)
enddo

```

```

dbonds_RC(:) : {derived type}, [nbias].
              %iatom {integer} index of atom involved in  $r_{ij}$ .
              %jatom {integer} index of atom involved in  $r_{ij}$ .
              %katom {integer} index of atom involved in  $r_{kj}$ .
bond_RC(:)   : {derived type}, [nbias].
              %iatom {integer} index of atom involved in  $r_{ij}$ .
              %jatom {integer} index of atom involved in  $r_{ij}$ .
k0_umb(:)    : {real}, [nbias]. Umbrella force constant.
r0_umb(:)    : {real}, [nbias]. RC anchor point for umbrella sampling.

```

The following data is output every `ntw_evb` steps:

```

write(evb_unit,' (/)')
write(evb_unit,888) ' {NSTEP}: ', nstep, ' {TIME}: ', nstep*dt

nstep      : {integer}. MD step counter.
nstep*dt   : {real}. Time (ps).

```

```

! Output ONLY if the nuclei are NOT quantized.
write(evb_unit,' (A)')
write(evb_unit,1000) ' [EVB MATRIX]', evb_Hmat%evb_mat(:, :)
write(evb_unit,' (A)')
write(evb_unit,1000) ' [EVB VEC_0]', evb_Hmat%evb_vec0(:)

```

```

evb_Hmat%evb_mat(:, :) : {real}, [nevb,nevb]. EVB matrix elements.
evb_Hmat%evb_vec0(:)  : {real}, [nevb]. ground-state EVB vector.

```

```

! Output ONLY if the nuclei are quantized.
write(evb_unit,' (A)')
write(evb_unit,1000) ' [EVB MATRIX]', evb_matrix(:, :) write(evb_unit,' (A)')
write(evb_unit,1000) ' [EVB VEC_0^2]', evb_pop(:) * nbead_inv

```

```

evb_matrix(:, :)      : {real}, [nevb, nevb].  $\frac{1}{P} \sum_1^P \begin{bmatrix} V_{11} & \dots & V_{1n} \\ \vdots & \ddots & \vdots \\ V_{n1} & \dots & V_{nn} \end{bmatrix}_P$ .

```

```

evb_pop(:)*nbead_inv  : {real}, [nevb].  $\frac{1}{P} \sum_1^P [C_0^2]_P$ .

```

```

! Output if performing ground-state dynamics.
write(evb_unit, ' (A)')
write(evb_unit, 1000) '{VELO_PIMD}: ', ( nrg_frc(n), n = 1, 3 )

```

```

nrg_frc(:)           : {real}, [3]. KE +  $V_{el0}$ , KE,  $V_{el0}$  in kcal/mol.

```

```

! Output if performing umbrella sampling
write(evb_unit, ' (A)')
write(evb_unit, 1000) ' [RC EVB]', ( evb_bias%RC(n), n = 1, nbias )

! Output if performing umbrella sampling with nuclear quantization
write(evb_unit, ' (A)')
write(evb_unit, 999) '{VELO_PIMD}: ', ( nrg_frc(n), n = 1, 3 )

```

```

evb_bias%RC(:)       : {real}, [nbias]. RC value.
nrg_frc(:)           : {real}, [3]. KE +  $V_{el0}$ , KE,  $V_{el0}$  in kcal/mol.

```

```

! Output if performing TI by mass
write(evb_unit, ' (A)')
write(evb_unit, 1000) '{TI MASS: (d/dl) v_eff}: ', dV_dl

```

```

dV_dl                : {real}.  $dV_{eff}/d\lambda$  [Eq. (5.51)].

```

```

! Output only if out_RCdot = .true.
write(evb_unit, ' (A)')
write(evb_unit, 1000) '{TST: (d/dt) RC}: ', RCdot

```

```

RCdot                : {real}.  $\left| \dot{\xi} \right|$  [Eq. (5.30)].

```

```

! Output if performing qi_bond_dyn or qi_dbonds_dyn
write(evb_unit, ' (A)')
write(evb_unit, 1000) '{QI rate: f_v, F, G}: ', f_v, F, G

```

```

f_v                  : {real}.  $f_v$  [Eq. (5.42)].

```

```

F                    : {real}.  $F$  [Eq. (5.43)].

```

```

G                    : {real}.  $G$  [Eq. (5.44)].

```



## F. Distributed Gaussian EVB format specifications

The distributed Gaussian EVB method in Amber provides native support for the *Gaussian* [111] formatted checkpoint file. Support for other electronic structure packages is provided via the Amber EVB format. The user will need to write a script that converts outputs from these other electronic structure packages to the Amber EVB format. While the DG EVB method utilizes the internal coordinate representation of the molecular system by default, Cartesian gradient and Hessian information can be used for the DG fitting procedure. Amber has the machinery to automatically transform from Cartesians to internals based on the specified internal coordinate definitions. Both flavors of the EVB formatted ab initio data files utilize the following fixed formatting where applicable (see the **read** statements below and examples in the test/evb directory):

```
1000 format( 5( 1PE16.8 ) )
3000 format( 4I12 )
```

### F.1. Cartesian coordinate representation

```
[coordinate type]
use_cartesians
```

```
read( ioe, ' (A)' ) coord_type
```

```
coord_type == "use_cartesians" => gradient & Hessian in Cartesians
```

```
[external evb data dimension]
```

```
56      12      13      19      24
```

```
read( ioe, ' (5I12)' ) ncoord, natm, nbond, nangle, ndihed
```

```
ncoord      : total No. of internal coordinates
natm        : No. of atoms
nbond       : No. of bonds
nangle      : No. of angles
ndihed     : No. of proper dihedrals
```

## F. Distributed Gaussian *EVB* format specifications

[redundant internal indices]

```

      :
      1      2      0      0
      :
      2      1      6      0
      :
      6      1      2      3
      :
  
```

do n = 1, nbond + nangle + ndihed

read( ioe, 3000 ) i, j, k, l

:

enddo

```

i j 0 0      : bond between atoms i & j
i j k 0      : angle between atoms i, j, & k, with j at apex
i j k l      : proper dihedral, with j & k forming the inner bond
  
```

[cartesian coordinates]

```

-2.10145193E+00  3.72231492E-01  0.00000000E+00  0.00000000E+00  1.86063791E+00
      :
  
```

read( ioe, 1000 ) ( xdat%qcart(n), n = 1, natm\*3)

read( ioe, \* )

[electronic energy]

```

-3.226440399344254E+02
  
```

read( ioe, \* ) xdat%v

read( ioe, \* )

[cartesian gradient]

```

3.17848421E-07  1.39797188E-07  6.11516832E-31  -2.06822408E-07  -2.80165145E-07
      :
  
```

read( ioe, 1000 ) ( grad\_cart(n), n = 1, natm\*3)

read( ioe, \* )

[cartesian hessian]

```

4.65149270E-01  1.00394244E-01  7.54852119E-01  -4.82566443E-17  6.87529647E-17
      :
  
```

read( ioe, 1000 ) ( ch(n), n = 1, natm\*3\*(natm\*3+1)/2 )

read( ioe, \* )

ch(:) : lower triangle of Cartesian Hessian.

## F.2. Internal coordinate representation

```
[coordinate type]
```

```
use_internals
```

```
read( ioe, ' (A)' ) coord_type
```

```
coord_type == "use_internals"    => gradient & Hessian in internals
```

```
[external evb data dimension]
```

```
56          12          13          19          24
```

```
read( ioe, ' (5I12)' ) ncoord, natm, nbond, nangle, ndihed
```

```
ncoord      : total No. of internal coordinates
```

```
natm        : No. of atoms
```

```
nbond       : No. of bonds
```

```
nangle      : No. of angles
```

```
ndihed      : No. of proper dihedrals
```

```
[redundant internal indices]
```

```
      :
      :
      1      2      0      0
      :
      :
      2      1      6      0
      :
      :
      6      1      2      3
      :
      :
```

```
do n = 1, nbond + nangle + ndihed
```

```
  read( ioe, 3000 ) i, j, k, l
```

```
  :
```

```
  :
```

```
enddo
```

```
i j 0 0      : bond between atoms i & j
```

```
i j k 0      : angle between atoms i, j, & k, with j at apex
```

```
i j k l      : proper dihedral, with j & k forming the inner bond
```

```
[cartesian coordinates]
```

```
-2.10145193E+00 3.72231492E-01 0.00000000E+00 0.00000000E+00 1.86063791E+00
```

```
:
```

```
:
```

```
read( ioe, 1000 ) ( xdat%qcart(n), n = 1, natm*3)
```

```
read( ioe, * )
```

## F. Distributed Gaussian *EVB* format specifications

```
[redundant internal coordinates]
  2.57516094E+00  2.54225222E+00  2.41077005E+00  2.67027840E+00  2.43908613E+00
  :
```

```
read( ioe, 1000 ) ( xdat%q(n), n = 1, ncoord )
read( ioe, * )
read_qint = .true.
```

```
[electronic energy]
-3.226440399344254E+02
```

```
read( ioe, * ) xdat%v
read( ioe, * )
```

```
[redundant internal gradient]
-3.16984808E-07 -1.14744500E-07 -2.60042682E-08 -5.64233681E-08  3.56746392E-08
  :
```

```
read( ioe, 1000 ) ( xdat%d(n), n = 1, ncoord )
read( ioe, * )
```

```
[redundant internal hessian]
  2.75181669E-01  9.43369526E-03  4.31679400E-01  5.40885192E-02  1.51723420E-03
  :
```

```
read( ioe, 1000 ) ( ih(n), n = 1, ncoord*(ncoord+1)/2 )
read( ioe, * )
```

ih(:) : lower triangle of internal coordinate Hessian.



# G. AMBER Trajectory NetCDF Format

*John Mongan (jmongan@mccammon.ucsd.edu)*

The file format described in this document was developed for storing data generated by molecular dynamics simulations. It was introduced in version 9 of the AMBER suite of programs (<http://amber.scripps.edu>).

The primary design goals of this format are:

- Efficient input and output
- Compact, high-precision representation of data
- Portability of data files across different machine architectures
- Extensibility of the format (ability to add additional data without re-writing parsers)
- Compatibility with existing tools and formats

The file format is based on the NetCDF (Network Common Data Form) developed by Unidata (<http://www.unidata.ucar.edu/software/netcdf/>). NetCDF is designed for representation of arbitrary array-based data. Unidata provides libraries with bindings in C, C++, Fortran (F77 and F90), Java, Python, Perl, Ruby and MATLAB for reading and writing NetCDF files. The design goals above are largely met by NetCDF and the libraries that implement it. It is expected that all I/O of the format described here will occur through these libraries; this specification describes the file format at a high level in terms of the API implemented by version 3.6 of these libraries. In NetCDF terms, this document is a “Convention,” describing the names, dimensions and attributes of the arrays that may be present in the file.

## G.0.1. Program behavior

Programs creating trajectory files (“creators”) shall adhere strictly to the requirements of this document. Programs reading trajectory files (“readers”) shall be as permissive as possible in applying the requirements of this document. Readers may emit warnings if out-of-spec files are encountered; these warnings should include information about the program that originally created the file (see Global attributes, section G.0.3). Readers shall not fail to read a file unless the required information cannot be located or interpreted. In particular, to ensure forward compatibility with later extensions of the format, readers shall not fail or emit warnings if elements not described in this document are present in the file.

### G.0.2. NetCDF file encoding

- Trajectory files shall be encoded in the manner employed by NetCDF version 3.x.  
Those using NetCDF versions 4 or later should take care to ensure that files are read and written using this encoding, and not the HDF5 encoding.
- Trajectory files shall use 64 bit offsets  
This can be accomplished by setting a flag during file creation; refer to API docs for details.

### G.0.3. Global attributes

Global attributes shall have type character string. Spelling and capitalization of attribute names shall be exactly as appears below. Creators shall include all attributes marked required and may include attributes marked optional. Creators shall not write an attribute string having a length greater than 80 characters. Readers may warn about missing required attributes, but shall not fail, except in the case of a missing or unexpected *Conventions* or *ConventionVersion* attributes.

- Conventions (required)  
Contents of this attribute are a comma or space delimited list of tokens representing all of the conventions to which the file conforms. Creators shall include the string *AMBER* as one of the tokens in this list. In the usual case, where the file conforms only to this convention, the value of the attribute will simply be “AMBER”. Readers may fail if this attribute is not present or none of the tokens in the list are *AMBER*. Optionally, if the reader does not expect NetCDF files other than those conforming to the AMBER convention, it may emit a warning and attempt to read the file even when the Conventions attribute is missing.
- ConventionVersion (required)  
Contents are a string representation of the version number of this convention. Future revisions of this convention having the same version number may include definitions of additional variables, dimensions or attributes, but are guaranteed to have no incompatible changes to variables, dimensions or attributes specified in previous revisions. Creators shall set this attribute to “1.0”. If this attribute is present and has a value other than “1.0”, readers may fail or may emit a warning and continue. It is expected that the version of this convention will change rarely, if ever.
- application (optional)  
If the creator is part of a suite of programs or modules, this attribute shall be set to the name of the suite.
- program (required)  
Creators shall set this attribute to the name of the creating program or module.

- programVersion (required)

Creators shall set this attribute to the preferred textual formatting of the current version number of the creating program or module.

- title (optional)

Creators may set use this attribute to represent a user-defined title for the data represented in the file. Absence of a title may be indicated by omitting the attribute or by including it with an empty string value.

#### **G.0.4. Dimensions**

- frame (required, length unlimited)

Coordinates along the frame dimension will generally represent data taken from different time steps, but may represent arbitrary conformation numbers when the trajectory file does not represent a true trajectory but rather a collection of conformations (e.g. from clustering).

- spatial (required, length 3)

This dimension represents the three spatial dimensions (X,Y,Z), in that order.

- atom (required, length set as appropriate)

Coordinates along this dimension are the indices of particles for which data is stored in the file. The length of this dimension may be different (generally smaller) than the actual number of particles in the simulation if the user chooses to store data for only a subset of particles.

- cell\_spatial (optional, length 3)

This dimension represents the three lengths (a,b,c) that define the size of the unit cell.

- cell\_angular (optional, length 3)

This dimension represents the three angles (alpha,beta,gamma) that define the shape of the unit cell.

- label (optional, length set as appropriate)

This dimension is used for character strings in label variables where the label is longer than a single character. The length of this dimension is equal to the length of the longest label string.

#### **G.0.5. Label variables**

Label variables shall be written by creators whenever their corresponding dimension is present. These variables are for self-description purposes, so readers may generally ignore them. Labels requiring more than one character per coordinate shall use the label dimension. Individual coordinate labels that are shorter than the length of the label dimension shall be space padded to the length of the label dimension.

## G. AMBER Trajectory NetCDF Format

- char spatial(spatial)  
Creators shall write the string “xyz” to this variable, indicating the labels for coordinates along the spatial dimension.
- char cell\_spatial(cell\_spatial)  
Creators shall write the string “abc” to this variable, indicating the labels for the three lengths defining the size of the unit cell.
- char cell\_angular(cell\_angular, label)  
Creators shall write the strings “alpha”, “beta”, “gamma” to this variable, naming the angles defining the shape of the unit cell.

### G.0.6. Data variables

All data variables are optional. Some data variables have dependencies on other data variables, as described below. Creators shall define a *units* attribute of type character string for each variable as described below. Creators may define a *scale\_factor* attribute of type float for each variable. Creators shall ensure that the units of data values, after being multiplied by the value of *scale\_factor* (if it exists) are equal to that described by the *units* attribute. If a *scale\_factor* attribute exists for a variable, readers shall multiply data values by the value of the *scale\_factor* attribute before interpreting the data. This scaling burden is placed on the reader rather than the creator, as writing data is expected to be a more time-sensitive operation than reading it.

It is left as an implementation detail whether creators create a separate file for each variable grouping (e.g. coordinates and velocities) or a single file containing all variables. Some creators may allow the user to select the approach. Readers should support reading both styles, that is, combining data from multiple files or reading it all from a single file.

- float time(frame) units = "picosecond"  
When coordinates on the frame dimension have a temporal sequence (e.g. they form a molecular dynamics trajectory), creators shall define this dimension and write a float for each frame coordinate representing the number of picoseconds of simulated time elapsed since the start of the trajectory. When the file stores a collection of conformations having no temporal sequence, creators shall omit this variable.
- float coordinates(frame, atom, spatial) units = "angstrom"  
This variable shall contain the Cartesian coordinates of the specified particle for the specified frame.
- float cell\_lengths(frame, cell\_spatial) units = "angstrom"  
When the *coordinates* variable is included *and* the data in the coordinates variable come from a simulation with periodic boundaries, creators shall include this variable. This variable shall represent the lengths (a,b,c) of the unit cell for each frame. When each of the angles in *cell\_angles* is 90, a, b and c are parallel to the x, y and z axes, respectively. If the simulation has one or two dimensional periodicity, then the length(s) corresponding to spatial dimensions in which there is no periodicity shall be set to zero.

- float cell\_angles(frame, cell\_angular) units = "degree"

Creators shall include this variable if and only if they include the *cell\_lengths* variable. This variable shall represent the angles ( $\alpha, \beta, \gamma$ ) defining the unit cell for each frame.  $\alpha$  defines the angle between the a-b and a-c planes,  $\beta$  defines the angle between the a-b and b-c planes and  $\gamma$  defines the angle between the a-c and b-c planes. Angles that are undefined due to less than three dimensional periodicity shall be set to zero.

- float velocities(frame, atom, spatial) units = "angstrom/picosecond"

When the *velocities* variable is present, it shall represent the cartesian components of the velocity for the specified particle and frame. It is recognized that due to the nature of commonly used integrators in molecular dynamics, it may not be possible for the creator to write a set of velocities corresponding to exactly the same point in time as defined by the *time* variable and represented in the *coordinates* variable. In such cases, the creator shall write a set of velocities from the nearest point in time to that represented by the specified frame.

### G.0.7. Example

The following is an example of the CDL for a trajectory file conforming to the preceding specification and containing most of the elements described in this document. This CDL was generated using `ncdump -h <trajectory file>`.

```
netcdf mdtrj {
dimensions:
    frame = UNLIMITED ; // (10 currently)
    spatial = 3 ;
    atom = 28 ;
    cell_spatial = 3 ;
    cell_angular = 3 ;
    label = 5 ;
variables:
    char spatial(spatial) ;
    char cell_spatial(cell_spatial) ;
    char cell_angular(cell_angular, label) ;
    float time(frame) ;
        time:units = "picosecond" ;
    float coordinates(frame, atom, spatial) ;
        coordinates:units = "angstrom" ;
    float cell_lengths(frame, cell_spatial) ;
        cell_lengths:units = "angstrom" ;
    float cell_angles(frame, cell_angular) ;
        cell_angles:units = "degree" ;
    float velocities(frame, atom, spatial) ;
        velocities:units = "angstrom/picosecond" ;
        velocities:scale_factor = 20.455f ;
```

### G. AMBER Trajectory NetCDF Format

```
// global attributes:  
    :title = "netCDF output test" ;  
    :application = "AMBER" ;  
    :program = "sander" ;  
    :programVersion = "9.0" ;  
    :Conventions = "AMBER" ;  
    :ConventionVersion = "1.0" ;  
}
```